

The chemistry of radical ions

Guest editor: Paul E. Floreancig

Department of Chemistry, University of Pittsburgh, Pittsburgh, PA 15260, USA

Contents

Announcement: Tetrahedron Symposia-in-Print
Preface

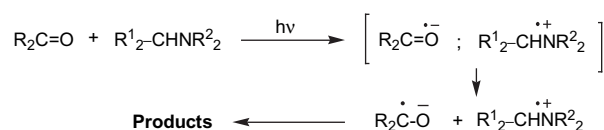
pp 6453–6455
p 6457

ARTICLES

Generation of ketyl radical anions by photoinduced electron transfer (PET) between ketones and amines. Synthetic applications

Janine Cossy* and Damien Belotti

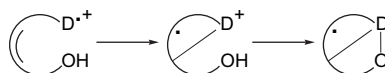
pp 6459–6470



Intramolecular nucleophilic capture of radical cations by tethered hydroxy functions

Heinz D. Roth,* Torsten Herbertz, Ronald R. Sauers* and Hengxin Weng

pp 6471–6489

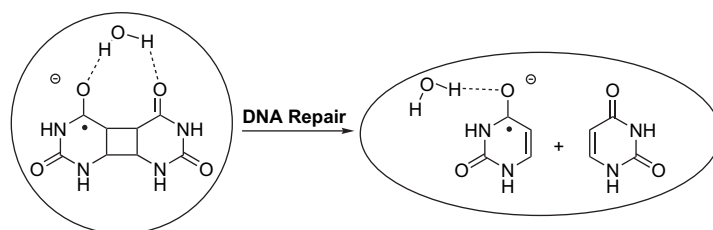


Electron donor systems bearing tethered hydroxy functions are converted upon photo-induced electron transfer to mono-, bi-, or tricyclic ethers by intramolecular nucleophilic substitution or capture via four- to seven-membered transition states. Geraniol and nerol undergo tandem-cyclizations as 1,5- and/or 1,6-C–C cyclizations precede nucleophilic capture.

Explicit and implicit solvation of radical ions: the cycloreversion of CPD dimers

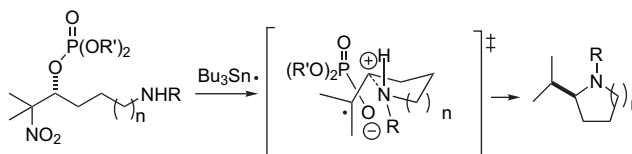
pp 6490–6500

Nicolas J. Saettel and Olaf Wiest*

**Enantioselective alkene radical cations reactions**

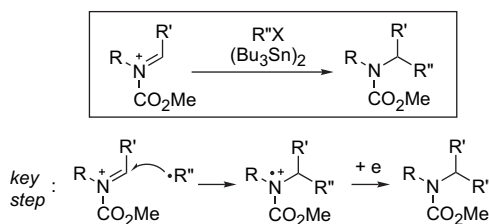
pp 6501–6518

David Crich,* Michio Shirai, Franck Brebion and Sochanchingwung Rumthao

**Distannane mediated reaction of *N*-acyliminium ion pools with alkyl halides. A chain mechanism involving radical addition followed by electron transfer**

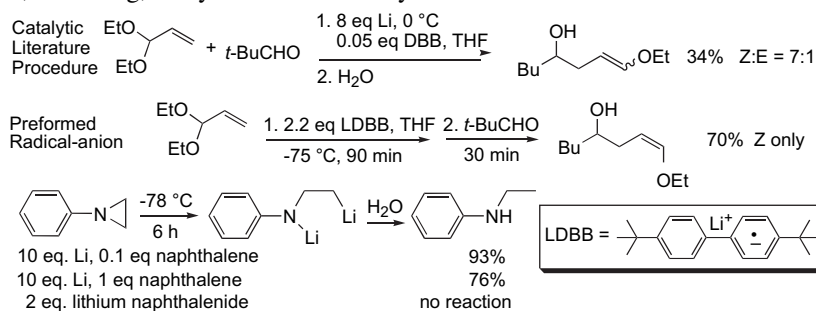
pp 6519–6525

Tomokazu Maruyama, Seiji Suga* and Jun-ichi Yoshida*

**Organolithiums by reductive lithiation: the catalytic aromatic method versus the use of preformed aromatic radical-anions. Naphthalene can behave as a catalyst or an inhibitor**

pp 6526–6535

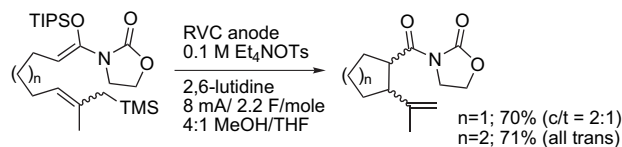
Ao Yang, Heather Butela, Kai Deng, Mary Dosch Doubleday and Theodore Cohen*



Anodic cyclization reactions: probing the chemistry of *N,O*-ketene acetal derived radical cations

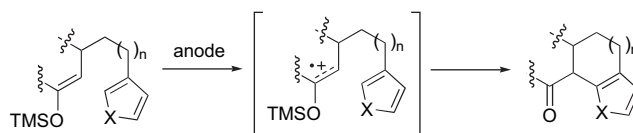
pp 6536–6550

Yung-tzung Huang and Kevin D. Moeller*

**Annulated heterocycles through a radical-cation cyclization: synthetic and mechanistic studies**

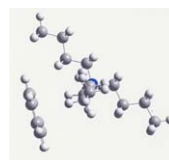
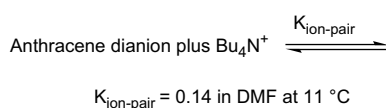
pp 6551–6557

Jeffrey B. Sperry and Dennis L. Wright*

**A computational study of solution effects on the disproportionation of electrochemically generated polycyclic aromatic hydrocarbon radical anions. Thermodynamics and structure**

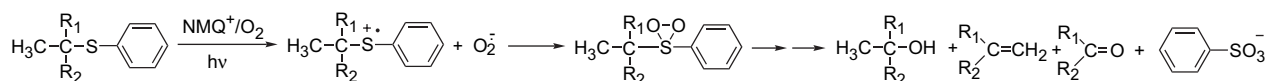
pp 6558–6565

Albert J. Fry

**C–S bond cleavage in the sensitized photooxygenation of *tert*-alkyl phenyl sulfides. The role of superoxide anion**

pp 6566–6573

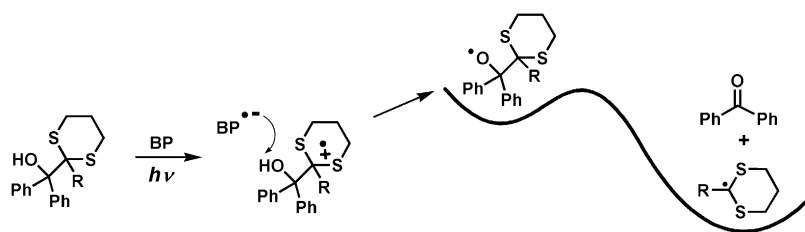
Enrico Baciocchi,* Tiziana Del Giacco,* Paolo Giombolini and Osvaldo Lanzalunga*



Externally sensitized mesolytic fragmentations in dithiane–ketone adducts

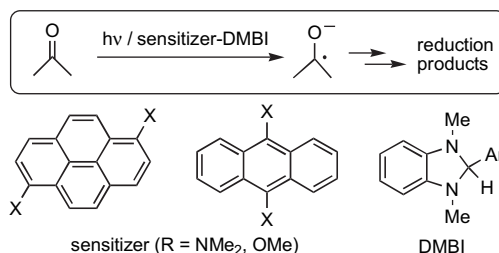
pp 6574–6580

Tiffany P. Gustafson, Alexei N. Kurchan and Andrei G. Kutateladze*

**Photoinduced electron-transfer systems consisting of electron-donating pyrenes or anthracenes and benzimidazolines for reductive transformation of carbonyl compounds**

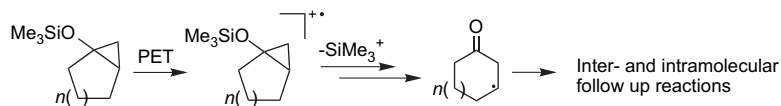
pp 6581–6588

Eietsu Hasegawa,* Shinya Takizawa, Takayuki Seida, Akira Yamaguchi, Naoto Yamaguchi, Naoki Chiba, Tomoya Takahashi, Hiroshi Ikeda and Kimio Akiyama

**Facile ring opening of siloxy cyclopropanes by photoinduced electron transfer. A new way to β -keto radicals**

pp 6589–6593

Heiko Rinderhagen, Prashant A. Waske and Jochen Mattay*



OTHER CONTENT**Calendar****pp I–II**

*Corresponding author

①⁺ Supplementary data available via ScienceDirect**COVER**

The cover illustrates an electron transfer from a donor molecule to an acceptor molecule to form a radical cation and a radical anion, which are the featured reactive intermediates in this Symposium-in-Print. Numerous downstream processes can occur upon forming these species. The structures illustrate a subset of the intermediates that are accessed in the work described in this issue, en route to a wealth of unique reactivity.

© 2006 P. E. Floreancig. Published by Elsevier Ltd.



Full text of this journal is available, on-line from **ScienceDirect**. Visit www.sciencedirect.com for more information.

Indexed/Abstracted in: AGRICOLA, Beilstein, BIOSIS Previews, CAB Abstracts, Chemical Abstracts. Current Contents: Life Sciences, Current Contents: Physical, Chemical and Earth Sciences, Current Contents Search, Derwent Drug File, Ei compendex, EMBASE/Excerpta Medica, Medline, PASCAL, Research Alert, Science Citation Index, SciSearch

**ELSEVIER**

ISSN 0040-4020

Tetrahedron Symposia-in-Print

Series Editor

Professor H. H. Wasserman, Department of Chemistry, Yale University, P.O. Box 208107, New Haven, CT 06520-8107, U.S.A.

Tetrahedron Symposia-in-Print comprise collections of original research papers covering timely areas of organic chemistry.

Each symposium is organized by a Symposium Editor who will invite authors, active in the selected field, to submit original articles covering current research, complete with experimental sections. These papers will be rapidly reviewed and processed for publication by the Symposium Editor under the usual refereeing system.

Authors who have not already been invited, and who may have obtained recent significant results in the area of the announced symposium, may also submit contributions for Editorial consideration and possible inclusion. Before submitting such papers authors should send an abstract to the Symposium Editor for preliminary evaluation. Firm deadlines for receipt of papers will allow sufficient time for completion and presentation of ongoing work without loss of the freshness and timeliness of the research results.

Symposia-in-Print—already published

1. Recent trends in organic photochemistry, Albert Padwa, Ed. *Tetrahedron* **1981**, *37*, 3227–3420.
2. New general synthetic methods, E. J. Corey, Ed. *Tetrahedron* **1981**, *37*, 3871–4119.
3. Recent developments in polycyclopentanoid chemistry, Leo A. Paquette, Ed. *Tetrahedron* **1981**, *37*, 4357–4559.
4. Biradicals, Josef Michl, Ed. *Tetrahedron* **1982**, *38*, 733–867.
5. Electron-transfer initiated reactions, Gary B. Schuster, Ed. *Tetrahedron* **1982**, *38*, 1025–1122.
6. The organic chemistry of animal defense mechanisms, Jerrold Meinwald, Ed. *Tetrahedron* **1982**, *38*, 1853–1970.
7. Recent developments in the use of silicon in organic synthesis, Hans Reich, Ed. *Tetrahedron* **1983**, *39*, 839–1009.
8. Linear tetrapyrroles, Ray Bonnett, Ed. *Tetrahedron* **1983**, *39*, 1837–1954.
9. Heteroatom-directed metallations in heterocyclic synthesis, George R. Newkome, Ed. *Tetrahedron* **1983**, *39*, 1955–2091.
10. Recent aspects of the chemistry of β -lactams, J. E. Baldwin, Ed. *Tetrahedron* **1983**, *39*, 2445–2608.
11. New spectroscopic techniques for studying metabolic processes, A. I. Scott, Ed. *Tetrahedron* **1983**, *39*, 3441–3626.
12. New developments in indole alkaloids, Martin E. Kuehne, Ed. *Tetrahedron* **1983**, *39*, 3627–3780.
13. Recent aspects of the chemistry of nucleosides, nucleotides and nucleic acids, Colin B. Reese, Ed. *Tetrahedron* **1984**, *40*, 1–164.
14. Bioorganic studies on receptor sites, Koji Nakanishi, Ed. *Tetrahedron* **1984**, *40*, 455–592.
15. Synthesis of chiral non-racemic compounds, A. I. Meyers, Ed. *Tetrahedron* **1984**, *40*, 1213–1418.
16. Control of acyclic stereochemistry, Teruaki Mukaiyama, Ed. *Tetrahedron* **1984**, *40*, 2197–2344.
17. Recent aspects of anthracycline chemistry, T. Ross Kelly, Ed. *Tetrahedron* **1984**, *40*, 4537–4794.
18. The organic chemistry of marine products, Paul J. Scheuer, Ed. *Tetrahedron* **1985**, *41*, 979–1108.
19. Recent aspects of carbene chemistry, Matthew Platz, Ed. *Tetrahedron* **1985**, *41*, 1423–1612.
20. Recent aspects of singlet oxygen chemistry of photooxidation, Isao Saito and Teruo Matsuura, Eds. *Tetrahedron* **1985**, *41*, 2037–2236.
21. Synthetic applications of dipolar cycloaddition reactions, Wolfgang Oppolzer, Ed. *Tetrahedron* **1985**, *41*, 3447–3568.
22. Selectivity and synthetic applications of radical reactions, Bernd Giese, Ed. *Tetrahedron* **1985**, *41*, 3887–4302.
23. Recent aspects of organoselenium chemistry, Dennis Liotta, Ed. *Tetrahedron* **1985**, *41*, 4727–4890.
24. Application of newer organometallic reagents to the total synthesis of natural products, Martin Semmelhack, Ed. *Tetrahedron* **1985**, *41*, 5741–5900.
25. Formal transfers of hydride from carbon–hydrogen bonds, James D. Wuest, Ed. *Tetrahedron* **1986**, *42*, 941–1208.
26. Synthesis of non-natural products: challenge and reward, Philip E. Eaton, Ed. *Tetrahedron* **1986**, *42*, 1549–1916.
27. New synthetic methods—II, F. E. Ziegler, Ed. *Tetrahedron* **1986**, *42*, 2777–3028.
28. Structure and reactivity of organic radical ions, Heinz D. Roth, Ed. *Tetrahedron* **1986**, *42*, 6097–6350.
29. Organic chemistry in anisotropic media, V. Ramamurthy, J. R. Scheffer and N. J. Turro, Eds. *Tetrahedron* **1987**, *43*, 1197–1746.
30. Current topics in sesquiterpene synthesis, John W. Huffman, Ed. *Tetrahedron* **1987**, *43*, 5467–5722.
31. Peptide chemistry: design and synthesis of peptides, conformational analysis and biological functions, Victor J. Hruby and Robert Schwyzer, Eds. *Tetrahedron* **1988**, *44*, 661–1006.
32. Organosilicon chemistry in organic synthesis, Ian Fleming, Ed. *Tetrahedron* **1988**, *44*, 3761–4292.
33. α -Amino acid synthesis, Martin J. O'Donnell, Ed. *Tetrahedron* **1988**, *44*, 5253–5614.
34. Physical-organic/theoretical chemistry: the Dewar interface, Nathan L. Bauld, Ed. *Tetrahedron* **1988**, *44*, 7335–7626.
35. Recent developments in organocopper chemistry, Bruce H. Lipshutz, Ed. *Tetrahedron* **1989**, *45*, 349–578.
36. Organotin compounds in organic synthesis, Yoshinori Yamamoto, Ed. *Tetrahedron* **1989**, *45*, 909–1230.

37. Mycotoxins, Pieter S. Steyn, Ed. *Tetrahedron* **1989**, *45*, 2237–2464.
38. Strain-assisted syntheses, Léon Ghosez, Ed. *Tetrahedron* **1989**, *45*, 2875–3232.
39. Covalently linked donor-acceptor species for mimicry of photosynthetic electron and energy transfer, Devens Gust and Thomas A. Moore, Eds. *Tetrahedron* **1989**, *45*, 4669–4912.
40. Aspects of modern carbohydrate chemistry, S. Hanessian, Ed. *Tetrahedron* **1990**, *46*, 1–290.
41. Nitroalkanes and nitroalkenes in synthesis, Anthony G. M. Barrett, Ed. *Tetrahedron* **1990**, *46*, 7313–7598.
42. Synthetic applications of anodic oxidations, John S. Swenton and Gary W. Morrow, Eds. *Tetrahedron* **1991**, *47*, 531–906.
43. Recent advances in bioorganic chemistry, Dale L. Boger, Ed. *Tetrahedron* **1991**, *47*, 2351–2682.
44. Natural product structure determination, R. B. Bates, Ed. *Tetrahedron* **1991**, *47*, 3511–3664.
45. Frontiers in natural products biosynthesis. Enzymological and molecular genetic advances, D. E. Cane, Ed. *Tetrahedron* **1991**, *47*, 5919–6078.
46. New synthetic methods—III, S. E. Denmark, Ed. *Tetrahedron* **1992**, *48*, 1959–2222.
47. Organotitanium reagents in organic chemistry, M. T. Reetz, Ed. *Tetrahedron* **1992**, *48*, 5557–5754.
48. Total and semi-synthetic approaches to taxol, J. D. Winkler, Ed. *Tetrahedron* **1992**, *48*, 6953–7056.
49. Synthesis of optically active compounds—prospects for the 21st century, Kenji Koga and Takayuki Shioiri, Eds. *Tetrahedron* **1993**, *49*, 1711–1924.
50. Peptide secondary structure mimetics, Michael Kahn, Ed. *Tetrahedron* **1993**, *49*, 3433–3689.
51. Transition metal organometallics in organic synthesis, Anthony J. Pearson, Ed. *Tetrahedron* **1993**, *49*, 5415–5682.
52. Palladium in organic synthesis, Jan-E. Bäckvall, Ed. *Tetrahedron* **1994**, *50*, 285–572.
53. Recent progress in the chemistry of enediyne antibiotics, Terrence W. Doyle and John F. Kadow, Eds. *Tetrahedron* **1994**, *50*, 1311–1538.
54. Catalytic asymmetric addition reactions, Stephen F. Martin, Ed. *Tetrahedron* **1994**, *50*, 4235–4574.
55. Mechanistic aspects of polar organometallic chemistry, Manfred Schlosser, Ed. *Tetrahedron* **1994**, *50*, 5845–6128.
56. Molecular recognition, Andrew D. Hamilton, Ed. *Tetrahedron* **1995**, *51*, 343–648.
57. Recent advances in the chemistry of zirconocene and related compounds, Ei-ichi Negishi, Ed. *Tetrahedron* **1995**, *51*, 4255–4570.
58. Fluoroorganic chemistry: synthetic challenges and biomedical rewards, Giuseppe Resnati and Vadim A. Soloshonok, Eds. *Tetrahedron* **1996**, *52*, 1–330.
59. Novel applications of heterocycles in synthesis, A. R. Katritzky, Ed. *Tetrahedron* **1996**, *52*, 3057–3374.
60. Fullerene chemistry, Amos B. Smith III, Ed. *Tetrahedron* **1996**, *52*, 4925–5262.
61. New synthetic methods—IV. Organometallics in organic chemistry, István E. Markó, Ed. *Tetrahedron* **1996**, *52*, 7201–7598.
62. Cascade reactions, Ron Grigg, Ed. *Tetrahedron* **1996**, *52*, 11385–11664.
63. Applications of solid-supported organic synthesis in combinatorial chemistry, James A. Bristol, Ed. *Tetrahedron* **1997**, *53*, 6573–6706.
64. Recent applications of synthetic organic chemistry, Stephen F. Martin, Ed. *Tetrahedron* **1997**, *53*, 8689–9006.
65. Chemical biology, Gregory L. Verdine and Julian Simon, Eds. *Tetrahedron* **1997**, *53*, 11937–12066.
66. Recent aspects of S, Se, and Te chemistry, Richard S. Glass and Renji Okazaki, Eds. *Tetrahedron* **1997**, *53*, 12067–12318.
67. Modern organic chemistry of polymerization, H. K. Hall Jr., Ed. *Tetrahedron* **1997**, *53*, 15157–15616.
68. New synthetic methods—V, John L. Wood, Ed. *Tetrahedron* **1997**, *53*, 16213–16606.
69. New developments in organonickel chemistry, Bruce H. Lipshutz and Tien-Yau Luh, Eds. *Tetrahedron* **1998**, *54*, 1021–1316.
70. Solution phase combinatorial chemistry, David L. Coffen, Ed. *Tetrahedron* **1998**, *54*, 3955–4150.
71. Heterocycles in asymmetric synthesis, Alexandre Alexakis, Ed. *Tetrahedron* **1998**, *54*, 10239–10554.
72. Recent advances of phase-transfer catalysis, Takayuki Shioiri, Ed. *Tetrahedron* **1999**, *55*, 6261–6402.
73. Olefin metathesis in organic synthesis, Marc L. Snapper and Amir H. Hoveyda, Eds. *Tetrahedron* **1999**, *55*, 8141–8262.
74. Stereoselective carbon–carbon bond forming reactions, Harry H. Wasserman, Stephen F. Martin and Yoshinori Yamamoto, Eds. *Tetrahedron* **1999**, *55*, 8589–9006.
75. Applications of combinatorial chemistry, Miles G. Siegel and Stephen W. Kaldor, Eds. *Tetrahedron* **1999**, *55*, 11609–11710.
76. Advances in carbon–phosphorus heterocyclic chemistry, François Mathey, Ed. *Tetrahedron* **2000**, *56*, 1–164.
77. Transition metal organometallics in organic synthesis, Kenneth M. Nicholas, Ed. *Tetrahedron* **2000**, *56*, 2103–2338.
78. Organocopper chemistry II, Norbert Krause, Ed. *Tetrahedron* **2000**, *56*, 2727–2904.
79. Carbene complexes in organic chemistry, James W. Herndon, Ed. *Tetrahedron* **2000**, *56*, 4847–5044.
80. Recent aspects of the chemistry of β -lactams—II, Marvin J. Miller, Ed. *Tetrahedron* **2000**, *56*, 5553–5742.
81. Molecular assembly and reactivity of organic crystals and related structures, Miguel A. Garcia-Garibay, Vaidhyanathan Ramamurthy and John R. Scheffer, Eds. *Tetrahedron* **2000**, *56*, 6595–7050.
82. Protein engineering, Richard Chamberlin, Ed. *Tetrahedron* **2000**, *56*, 9401–9526.
83. Recent advances in peptidomimetics, Jeffrey Aubé, Ed. *Tetrahedron* **2000**, *56*, 9725–9842.
84. New synthetic methods—VI, George A. Kraus, Ed. *Tetrahedron* **2000**, *56*, 10101–10282.
85. Oxidative activation of aromatic rings: an efficient strategy for arene functionalization, Stéphane Quideau and Ken S. Feldman, Eds. *Tetrahedron* **2001**, *57*, 265–424.
86. Lewis acid control of asymmetric synthesis, Keiji Maruoka, Ed. *Tetrahedron* **2001**, *57*, 805–914.
87. Novel aromatic compounds, Lawrence T. Scott and Jay S. Siegel, Eds. *Tetrahedron* **2001**, *57*, 3507–3808.
88. Asymmetric synthesis of novel sterically constrained amino acids, Victor J. Hruby and Vadim A. Soloshonok, Eds. *Tetrahedron* **2001**, *57*, 6329–6650.
89. Recognition-mediated self-assembly of organic systems, Vincent M. Rotello, Ed. *Tetrahedron* **2002**, *58*, 621–844.
90. Synthesis of marine natural products containing polycyclic ethers, Masahiro Hirama and Jon D. Rainier, Eds. *Tetrahedron* **2002**, *58*, 1779–2040.

91. Fluorous chemistry, John A. Gladysz and Dennis P. Curran, Eds. *Tetrahedron* **2002**, 58, 3823–4132.
92. Recent developments in chiral lithium amide base chemistry, Peter O'Brien, Ed. *Tetrahedron* **2002**, 58, 4567–4734.
93. Beyond natural product synthesis (Tetrahedron Prize for Creativity in Organic Chemistry 2001 – Yoshito Kishi), Harry H. Wasserman and Stephen F. Martin, Eds. *Tetrahedron* **2002**, 58, 6223–6602.
94. Strained heterocycles as intermediates in organic synthesis, Amy R. Howell, Ed. *Tetrahedron* **2002**, 58, 6979–7194.
95. Molecular design of Lewis and Brønsted acid catalysts—the key to environmentally benign reagents (Tetrahedron Chair 2002), Hisashi Yamamoto, Ed. *Tetrahedron* **2002**, 58, 8153–8364.
96. Recent developments in dendrimer chemistry, David K. Smith, Ed. *Tetrahedron* **2003**, 59, 3787–4024.
97. Art, science and technology in total synthesis (Tetrahedron Prize for Creativity in Organic Chemistry 2002 – K. C. Nicolaou), Stephen F. Martin and Harry H. Wasserman, Eds. *Tetrahedron* **2003**, 59, 6667–7070.
98. New synthetic methods—VII, Brian M. Stoltz, Ed. *Tetrahedron* **2003**, 59, 8843–9030.
99. Oxiranyl and aziridinyl anions as reactive intermediates in synthetic organic chemistry, S. Florio, Ed. *Tetrahedron* **2003**, 59, 9683–9864.
100. Recent advances in rare earth chemistry, Shū Kobayashi, Ed. *Tetrahedron* **2003**, 59, 10339–10598.
101. Biocatalysts in synthetic organic chemistry, S. M. Roberts, Ed. *Tetrahedron* **2004**, 60, 483–806.
102. Recent advances in the chemistry of zirconocenes, Keisuke Suzuki and Peter Wipf, Eds. *Tetrahedron* **2004**, 60, 1257–1424.
103. Atropisomerism, Jonathan Clayden, Ed. *Tetrahedron* **2004**, 60, 4325–4558.
104. Chemistry of biologically and physiologically intriguing phenomena, Daisuke Uemura, Ed. *Tetrahedron* **2004**, 60, 6959–7098.
105. Olefin metathesis: a powerful and versatile instrument for organic synthesis (Tetrahedron prize for creativity in organic chemistry 2003 – R. H. Grubbs), Stephen F. Martin and Harry H. Wasserman, Eds. *Tetrahedron* **2004**, 60, 7099–7438.
106. From synthetic methodology to biomimetic target assembly (Tetrahedron prize for creativity in organic chemistry 2003 – D. Seebach), Léon A. Ghosez, Ed. *Tetrahedron* **2004**, 60, 7439–7794.
107. Solid and solution phase combinatorial chemistry, Rolf Breinbauer and Herbert Waldmann, Eds. *Tetrahedron* **2004**, 60, 8579–8738.
108. Catalytic tools enabling total synthesis (Tetrahedron Chair 2004), Alois Fürstner, Ed. *Tetrahedron* **2004**, 60, 9529–9784.
109. Synthesis and applications of non-racemic cyanohydrins and α -amino nitriles, Michael North, Ed. *Tetrahedron* **2004**, 60, 10371–10568.
110. Synthetic receptors as sensors, Eric V. Anslyn, Ed. *Tetrahedron* **2004**, 60, 11041–11316.
111. Functionalised organolithium compounds, Carmen Nájera and Miguel Yus, Eds. *Tetrahedron* **2005**, 61, 3125–3450.
112. Applications of catalysis in academia and industry, Michael J. Krische, Ed. *Tetrahedron* **2005**, 61, 6155–6472.
113. Development and application of highly active and selective palladium catalysts, Ian J. S. Fairlamb, Ed. *Tetrahedron* **2005**, 61, 9647–9918.
114. Multicomponent reactions, Ilan Marek, Ed. *Tetrahedron* **2005**, 61, 11299–11520.
115. Polymer-supported reagents and catalysts: increasingly important tools for organic synthesis, Patrick Toy and Min Shi, Eds. *Tetrahedron* **2005**, 61, 12013–12192.
116. Organocatalysis in organic synthesis, Pavel Kočovský and Andri V. Malkov, Eds. *Tetrahedron* **2006**, 62, 243–502.
117. Supramolecular chemistry of fullerenes, Nazario Martín and Jean-François Nierengarten, Eds. *Tetrahedron* **2006**, 62, 1905–2132.
118. Chemistry of electron-deficient ynamines and ynamides, Richard P. Hsung, Ed. *Tetrahedron* **2006**, 62, 3771–3938.
119. Microwave assisted organic synthesis, Nicholas E. Leadbeater, Ed. *Tetrahedron* **2006**, 62, 4623–4732.
120. Nature-inspired approaches to chemical synthesis, Erik J. Sorensen and Emmanuel A. Theodorakis, Eds. *Tetrahedron* **2006**, 62, 5159–5354.
121. The chemistry of radical ions, Paul E. Floreancig, Ed. *Tetrahedron* **2006**, 62, 6447–6594.



ELSEVIER

Preface

The chemistry of radical ions

The impact that adding or removing an electron from a molecule can have on accessible reaction pathways is genuinely remarkable. Stable bonds fragment. Electron-rich alkenes and arenes react with nucleophiles. Electron-poor alkenes react with electrophiles. Super acids and potent bases are formed. Highly reactive intermediates are formed in downstream processes. The abundance of unusual pathways is perhaps the reason that radical ion chemistry is often viewed as being somewhat esoteric. Of course, this wealth of reactivity creates ample opportunities for new reaction development, provided that a particular pathway can be predictably accessed. Indeed biological systems make extensive use of radical ion intermediates to lower activation energies for a range of processes. Substantial progress toward understanding the reactivity patterns of radical ions has been reported over the years, leading to a level of predictive capacity that allows for efficient new processes to be developed on complex substrates that yield integral components of important materials.

The purpose of the *Symposium-in-Print* is to highlight advances in design and theory for processes that proceed through radical ion intermediates. Several elements of the manuscripts should be noted. The structural features that make a molecule susceptible to single electron oxidation or reduction are often unique relative to those that lead to reactivity through other manifolds such as acid/base association. For example, alkenes, arenes, strained rings, and sulfides are common precursors to electrophiles, and ethers can be used as precursors to nucleophiles. Methods of accessing radical ions are also diverse. Radical cations can be formed through oxidation under electrochemical conditions, electron transfer to ground state or photoexcited oxidants, or radical

solvolysis. Radical anions can be generated by electron transfer from other radical anions or photoexcited neutral molecules, or by electrochemical reduction. Substrates that contain an electron donor and an electron acceptor can undergo intramolecular electron transfer to yield a radical cation and a radical anion in the same molecule, creating the potential for truly unique transformations. Reaction pathways can be controlled through rational substitution. Fragmentation processes can be promoted by installing a group that either stabilizes a reactive intermediate or releases strain adjacent to the radical ion. Otherwise electrophilic character will dominate for radical cations and nucleophilic/basic character will dominate for radical anions.

As editor of this *Symposium-in-Print*, I owe a debt of gratitude to those who contributed to this endeavor. They have done an outstanding job of illustrating the versatility and power of radical ion intermediates at a level that is enjoyable for both those who work with these species routinely and those who are looking to develop a greater understanding of this chemistry. My underlying personal objective is for this issue to stimulate new creative applications for radical ion intermediates, allowing electron transfer reactions to be considered as attractive options for routine applications in synthesis design.

Paul E. Floreancig
Department of Chemistry,
University of Pittsburgh,
Pittsburgh, PA 15260, USA
E-mail address: floean@pitt.edu

Available online 19 May 2006



Generation of ketyl radical anions by photoinduced electron transfer (PET) between ketones and amines. Synthetic applications

Janine Cossy* and Damien Belotti

Laboratoire de Chimie Organique associé au CNRS, ESPCI, 10 Rue Vauquelin, 75231—Paris Cedex 05, France

Received 25 March 2005; accepted 18 May 2005

Available online 24 April 2006

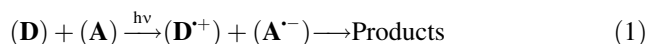
Abstract—Photoreduction of ketones in the presence of amines led to ketyl radicals through photoinduced electron transfer (PET). Tertiary amines, such as triethylamine (Et_3N) have frequently been used in these reactions. Different reactions can occur from ketyl radicals such as photoreduction, coupling reactions, additions on activated double bonds, cyclizations, bond cleavage of strained rings, tandem reactions such as cyclization–ring opening or ring opening–cyclization.

© 2006 Elsevier Ltd. All rights reserved.

1. Introduction

Electron-transfer reactions are extensively studied in chemistry¹ and the photochemical approach of reactions of this type has become familiar to most organic chemists as the result of a better understanding of primary processes. Recognition of charge transfer processes in photochemical reactions, direct characterization and determination of kinetic and thermodynamic properties of radical ion intermediates, has induced a renewed interest in applications of photochemical reactions to organic synthesis.²

Photoinduced electron transfer (PET) processes involve two neutral molecules, a donor (**D**) and an acceptor (**A**) and an electronic excitation (Eq. 1).



Production of radical ions ($\mathbf{D}^{+\bullet}$) and ($\mathbf{A}^{\bullet-}$) depends on the oxidation potential $E_{\text{ox}1/2}(\mathbf{D})$, the reduction potential $E_{\text{red}1/2}(\mathbf{A})$ of the starting molecules and on the electronic excitation energy E_{00} , according to the Rehm–Weller equation (Eq. 2) where the coulombic interaction term in polar solvents, such as acetonitrile, can be neglected in the first approximation.³

$$\Delta G_{\text{set}} = E_{\text{ox}1/2}(\mathbf{D}) - E_{\text{red}1/2}(\mathbf{A}) - \Delta E_{00} + \Delta E_c \quad (2)$$

When the PET is thermodynamically favourable ($\Delta G < 0$), electron transfer proceeds close to a diffusion controlled rate. However, the behaviour of the formed radical ion pair

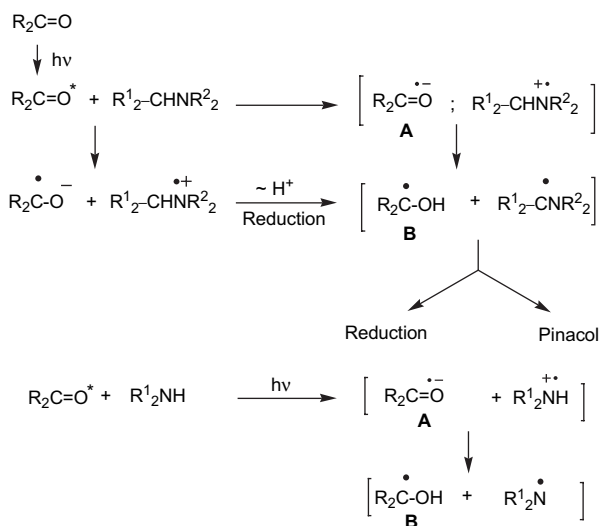
depends strongly on the nature of the solvent and on the rate of the reverse electron transfer to molecules (**A**) and (**D**) in their ground state. Use of polar solvents favours the formation of solvent separated ion pairs and limits this reverse electron-transfer process. Furthermore, the selective transformation of one of the radical ion often promotes efficient chemical transformations.

PET processes between a carbonyl derivative considered as an acceptor (**A**) and an amine considered as a donor (**D**) have received considerable attention⁴ since the pioneering studies on photoreduction of aromatic ketones with tertiary amines.⁵ Numerous developments have appeared during the last 30 years. In this review, we will focus our attention only on the behaviour of the ketyl radical anion generated by photoreduction of ketones by amines and we will not consider the reactivity of enones and quinones. Five different processes can occur from the ketyl radical anion, e.g., abstraction of hydrogen from the reaction media to produce alcohols, coupling of two ketyl radical anions and/or coupling of the ketyl radical anion with the radical cation formed from the donor, intermolecular addition of the ketyl radical anion to an activated double bond, cyclization as in the case of ω -unsaturated ketyl radical anions, fragmentation when a $C\alpha$ –X bond (X=O, C) is present. Tandem reactions can also take place such as opening of strained rings followed by cyclization or cyclization followed by opening of strained rings.

Photoreduction of ketones in the presence of amines involves charge transfer interactions between amines and ketones excited states.^{5a} Kinetic studies indicate that for a given ketone, the rate constants increase when the oxidation potential of the amine is lowered [$\text{DABCO} > \text{R}_3\text{N} > \text{R}_2\text{NH} > \text{RNH}_2$] and the products are derived from an initial electron transfer

* Corresponding author. Tel.: +33 1 40 79 44 29; fax: +33 1 40 79 46 60; e-mail: janine.cossy@espci.fr

rather than from a direct hydrogen atom transfer.⁶ Early studies by Cohen and co-workers⁷ as well as more recent studies,⁸ have demonstrated that a radical ion pair is generated through electron transfer from the ground state of the amine to the photoexcited ketone, followed by proton transfer from the amine radical cation to the ketyl species. Tertiary amines, such as triethylamine (Et₃N) have frequently been used in these reactions.⁹ Electron transfer can also occur to the ground state of the ketone when the amine is excited (Scheme 1).

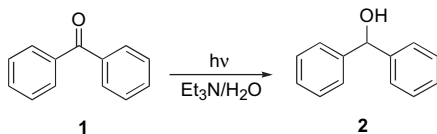


Scheme 1.

Depending on the nature of the amine, either C–H or N–H bond intervenes in the hydrogen atom transfer with the formation of the hemipinacol radical and an aminyl or α -amino radical. Furthermore, depending on the conditions and on the substrate, the abstraction of a proton by the radical anion **A** can be faster than the reactivity of the radical anion **A** itself and products can come from radical **A** or **B**.

2. Photoreduction

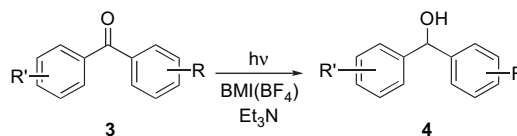
The photoreduction of aromatic ketones by aliphatic amines has been the subject of extensive investigation.⁵ In aqueous media, it was found that the reduction of aromatic ketones by amines proceeds rapidly to form secondary alcohols via a ketyl radical anion rather than a pinacol type product^{5a,10} (Scheme 2).



Scheme 2.

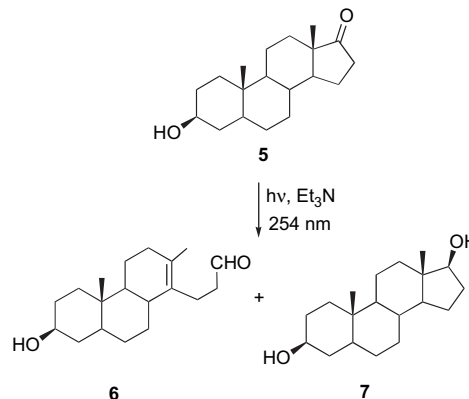
In polar solvents, as well as in ionic liquids,¹¹ benzhydrols can be obtained from amine-mediated photoreduction of benzophenones **3** at room temperature. In ionic liquids, because the reaction consumes only 1 equiv of amine and the solvent can be easily recycled, the photoreduction allows a very

clean process for the conversion of benzophenones to benzhydrols (Scheme 3).



Scheme 3.

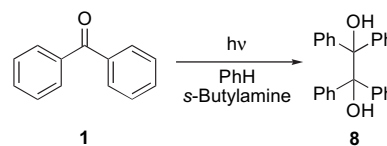
When 3 β -hydroxy-5 α -androstan-17-one and Et₃N were irradiated at 254 nm, such as Et₃N absorbs 99% of the incident light, one obtains products resulting from Norrish type I product, **6**, and alcohol **7** coming from the reduction of the ketone. The product ratio depends strongly on the solvent. In ether and THF, compound **6** (Norrish type I product) and alcohol **7** are observed in a ratio of 1/1 but in acetonitrile only the 5 α -androstan-3 β ,17 β -diol **7** is formed¹² (Scheme 4).



Scheme 4.

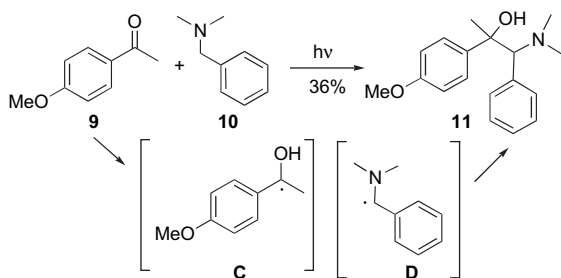
3. Coupling reactions

Coupling reactions between a radical cation and a radical anion or between two radical anions can occur. The proportion of the different products is very sensitive to the solvent and additives. For example, the irradiation of benzophenone **1** in benzene in the presence of *s*-butylamine produces the benzopinacol **8** in quantitative yield¹¹ (Scheme 5).



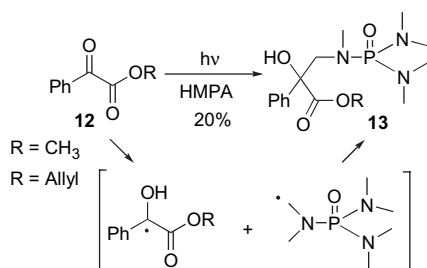
Scheme 5.

A mixed coupling product **11** is obtained when the aromatic ketone **9** is irradiated in the presence of a tertiary amine such as *N,N*-dimethyl *N*-benzylamine in acetonitrile. Compound **11** corresponds to the coupling of the α -amino-alkyl radical **C** with radical **D**. Both radicals possess an aromatic and an electron-donating substituent and this structure resemblance favoured the photopinacolization type reaction¹³ (Scheme 6).



Scheme 6.

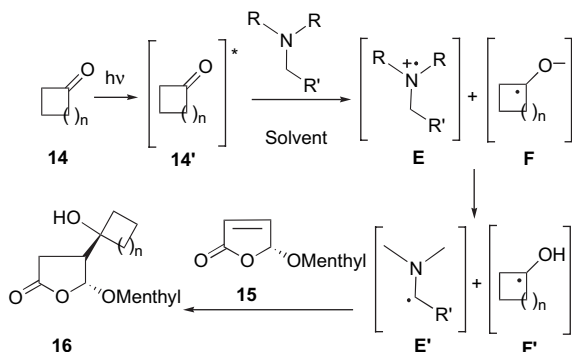
Another example of cross-coupling reaction is observed when α -ketoester **12** is irradiated in HMPA.¹⁴ The irradiation resulted in the cross-coupling of the ketyl radical with the generation of a HMPA-derived radical according to Scheme 7.



Scheme 7.

4. Addition

A third process that can take place is an intermolecular addition of a radical onto an activated olefin. When ketones **14** are photoreduced by a tertiary amine in the presence of an activated olefin such as (5*R*)-5-(–)-menthyloxy-2[5*H*]-furanone **15**, a ketyl radical anion is formed and after a subsequent proton transfer from the tertiary amine, a stereoselective addition of the ketyl radical to olefin **15** is observed.^{13,15} It is worth noting that, due to their low reactivity, α -amino alkyl radicals, which are generated at the same time than the hydroxy radicals, do not add to **15** (Scheme 8).

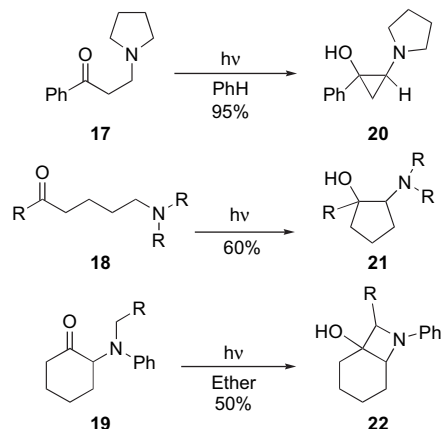


Scheme 8. Amine: Et₃N; yield in **16** ($n=1-9$): 12–38%. Amine: (CH₃)₂NBn; yield in **16** ($n=1-9$): 37–69%.

5. Cyclization

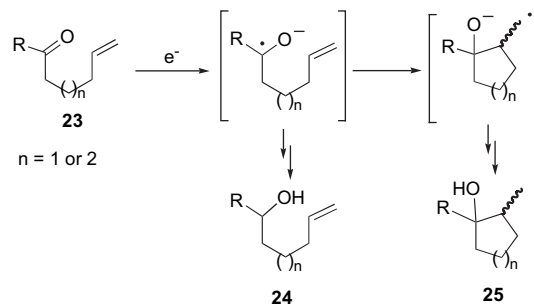
Before the 1980s, intermolecular photoreduction of ketones by amines has not provided much synthetic utility except

for the production of alcohols, aminoalcohols, pinacols and polymers. More interestingly, the amino group can belong to the same molecule without disturbing the charge transfer process. Depending on the structure of the starting amino-ketones **17**, **18** and **19**, α -aminocyclopropanols **20**, α -aminocyclopentanols **21** and hydroxyazetidines **22** can be, respectively, obtained in high yields¹⁶ (Scheme 9).



Scheme 9.

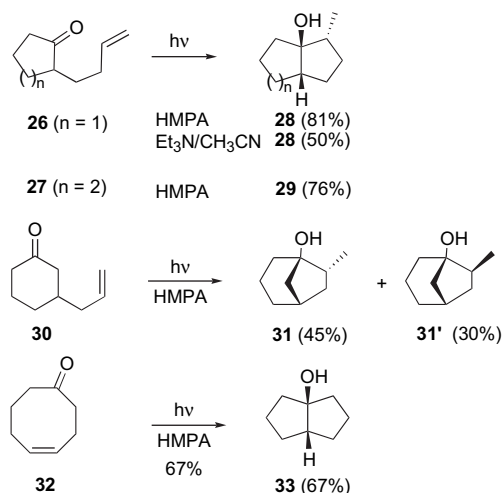
The most useful process in synthesis is probably the cyclization of ω -unsaturated ketyl radical anions, which produces functionalized substituted carbo- and heterocyclic compounds. Cyclization of δ,ϵ -unsaturated radicals is a very fast process,¹⁷ which leads to cyclopentylmethyl or cyclohexyl radicals. Formation of the cyclopentane ring is highly favoured according to the literature data¹⁸ and the Baldwin's rules.¹⁹ According to the very fast cyclization process δ,ϵ -unsaturated ketyl radical anion, produced by photoinduced electron donor such as HMPA or tertiary amines such Et₃N, leads to cyclopentanol or cyclohexanol derivatives²⁰ rather than δ,ϵ -unsaturated alcohols or pinacols just as observed in the ground-state reduction^{21–24} (Scheme 10).



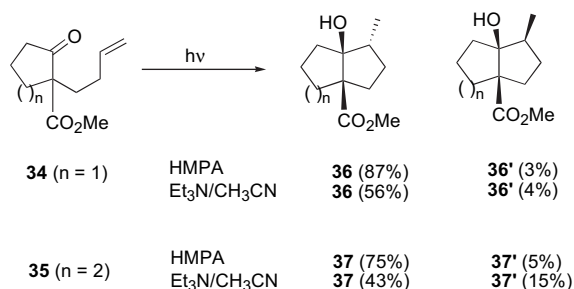
Scheme 10.

Irradiation of δ,ϵ -olefinic cyclopentanone **26** and cyclohexanone **27** in HMPA with low pressure mercury lamps ($\lambda=254$ nm) produced the bicyclic cyclopentanols **28** and **29**, respectively, in high yields. Analysis of the reaction mixture did not reveal any reduction compound such as ω -olefinic alcohol, other than the cyclized one. Furthermore, only one stereoisomer having the methyl and the hydroxy groups in a *trans* relationship was obtained (Scheme 11). Using Et₃N as the donor, in a polar solvent such as acetonitrile, the same reaction occurred but in lower yield. Due to the

high regio- and stereoselectivity as well as the high yield obtained in HMPA, the synthetic usefulness of the reaction toward various bicyclic cyclopentanol was tested. When 3-allylcyclohexanone **30** is irradiated in HMPA, a mixture of cyclized isomers **31** and **31'** is obtained in 45% and 30% yields, respectively. Similarly, 4-cyclooctenone **32** produced bicyclo[3.3.0]cyclooctan-1-ol **33** in 67% yield. When several functional groups are present in the starting molecule, the electron transfer from the donor occurred selectively to the most reducible group. Indeed, ketoesters **34** and **35** are transformed to the cyclized products **36/36'** and **37/37'**, respectively. In contrast to **26** and **27**, two stereoisomers were isolated, although the cyclization remains very stereoselective. A better stereoselectivity is observed in HMPA than in $\text{Et}_3\text{N}/\text{CH}_3\text{CN}$ ²⁰ (Scheme 12).



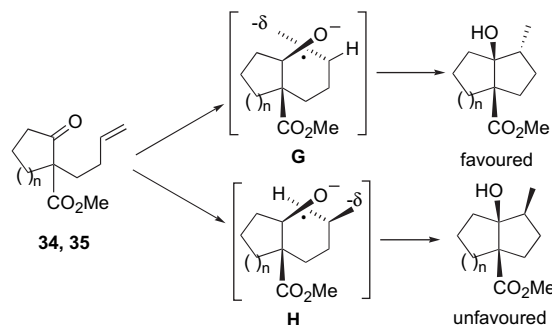
Scheme 11.



Scheme 12.

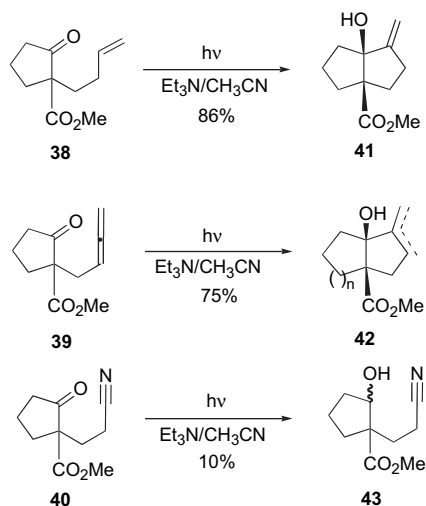
Good regioselectivities and stereoselectivities are observed and can be explained by a repulsive electrostatic interaction, which can take place between the negatively charged oxygen centre and the terminal sp^2 carbon atom in one of the two diastereomeric cyclic and polar transition states²¹ (Scheme 13).

Even if HMPA gives better yields in the cyclization of unsaturated ketones than Et_3N , it is preferable to use Et_3N since this compound is less hazardous, more volatile and allows a simpler work-up (only requiring evaporation of the solvent).²⁵ From a preparative point of view, it was found that the procedure using Et_3N tolerates various substituents such as carbonitriles, esters, ethers, alkenes and alkynes.



Scheme 13.

For example, compounds **38** and **39**, when irradiated in acetonitrile in the presence of Et_3N , leads, respectively, to the cyclized products **41** and **42** in good yields. It is worth of note that no cyclized product was observed when ketone **40** was irradiated in the presence of Et_3N , alcohol **43** was the only isolated product²⁰ (Scheme 14).

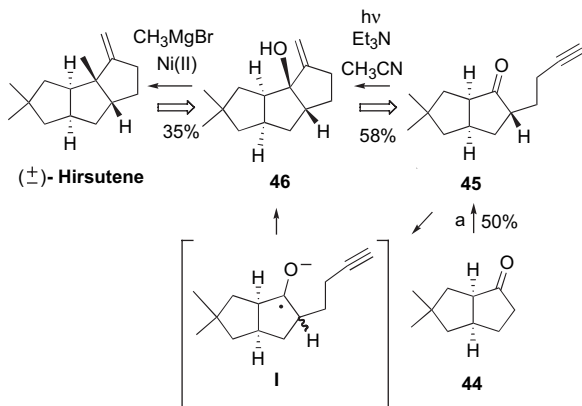


Scheme 14.

The behaviour of the intermediate radical formed from δ,ϵ -unsaturated ketones does not depend strongly on the method used to produce its chemical reduction, electroreduction or photoreduction. However, the latter method presents the advantage of being carried out under very mild and homogeneous conditions with few problems of reproducibility constituting a complementary and advantageous approach to cyclic compounds. For this reason, the photoreductive cyclization was applied successfully to the synthesis of cyclopentanoids, alkaloids, iridoids and sesquiterpenes.

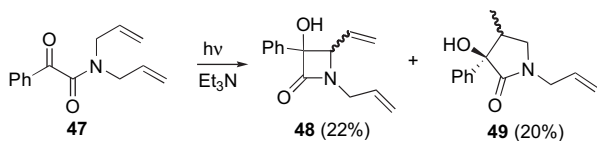
One of the first achievements based on this method was a short synthesis of (\pm)-hirsutene.²⁶ The retrosynthetic analysis shows that the tricyclic skeleton of hirsutene should come from an acetylenic ketyl radical anion cyclization, which will be issued from the photochemical reduction of ketone **45**. After the stereoselective replacement of the angular hydroxy group by a methyl group, hirsutene should be obtained. Thus, the photochemical reduction applied to compound **45**, obtained by alkylation of the bicyclic ketone **44**, afforded **46** as the only tricyclic product, which possesses the desired

cis-anti-cis stereochemistry. The highly regio-, stereo- and chemoselective replacement of the tertiary allylic alcohol in **46** with methylmagnesium bromide in the presence of a Ni(II) catalyst²⁷ completed the synthesis of (±)-hirsutene (Scheme 15).



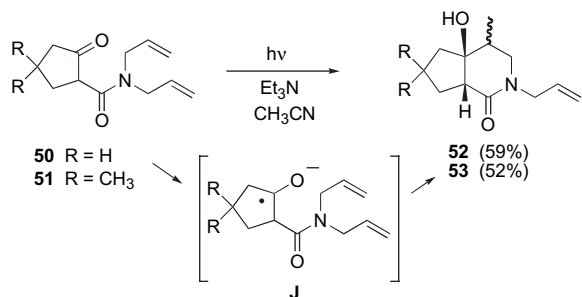
Scheme 15. (a) (1) KH/DME, $\text{ICH}_2\text{CH}=\text{C}(\text{CH}_3)\text{Cl}$, -78°C ; (2) LiAlH_4 , ether, 0°C ; (3) KAPA, APA, 0°C ; (4) PCC, MS 3A, CH_2Cl_2 .

Straightforward access to heterocyclic compounds can be obtained using the photoreductive cyclization of ω -unsaturated ketones. However, when *N,N'*-dialkyloxamides are irradiated under reducing conditions, competition between PET and γ -hydrogen abstraction products can be observed as compounds **48** and **49** were isolated²⁸ (Scheme 16).



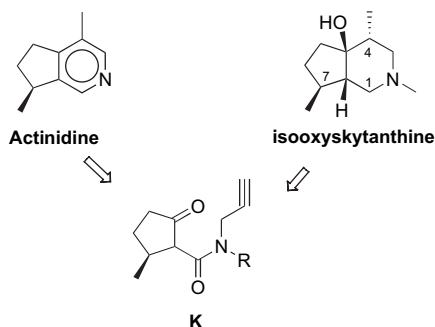
Scheme 16.

On the contrary, the photoreduction of *N,N*-unsaturated dialkyl β -oxamides **50** and **51** afforded only substituted 3-azabicyclo[4.3.0]nonanes, which are issued from the ketyl radical anion **J**²⁹ (Scheme 17).



Scheme 17.

This photoreductive cyclization is of great synthetic utility as illustrated below in the synthesis of actinidine^{30,31} and isooskytanthine,^{31,32} two rare monoterpenic alkaloids, which contain a 3-azabicyclo[4.3.0]nonane skeleton substituted by methyl groups at C4 and C7 (Scheme 18).



Scheme 18.

The synthesis of the skeleton of these two monoterpenic alkaloids and the control of the relative stereochemistry at C7 and C7a was achieved by relying on a Wolff rearrangement applied to a diazodiketone, followed by a photoreductive cyclization of unsaturated *N*-alkyl-2-oxocyclopentane carboxamides of type **K**.

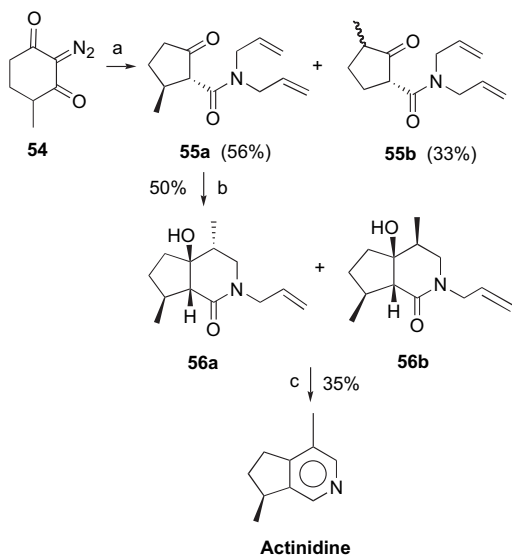
A Wolff rearrangement³³ applied to the diazodiketone **54** in the presence of diallylamine gave a 1.6/1 mixture of two regioisomeric amides **55a** and **55b**. The major product **55a**, which is the precursor of actinidine, was isolated in 56% yield. Similarly, photolysis of **54** in the presence of *N*-methyl,*N*-propargylamine gave almost quantitatively a mixture **57a** and **57b** (1.5/1). The photoreductive cyclization of **55a** carried out in the presence of Et_3N led to a 1.7/1 mixture of **56a** and **56b**, which was transformed to actinidine. Irradiation of **57a** under the same conditions led to a single product **58**, which could be converted to isooskytanthine (Scheme 19).

Iridoids represent a class of highly oxygenated monoterpenes characterized by a *cis*-fused cyclopentapyran ring system. In principle, synthesis of such systems could be achieved by a photoreductive cyclization of δ,ϵ -unsaturated β -ketoesters. Unfortunately, unsaturated β -ketoester **59** did not lead to the expected bicyclic compound **60** because of an unfavourable conformation of the ester group of **59** (Scheme 20).³⁴

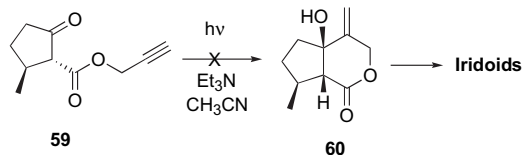
In order to overcome this conformational effect, annulation of the unsaturated β -ketoacetal **62** was investigated as a model for the synthesis of C5 oxygenated iridoids.³⁵ The β -ketoester, readily available from the irradiation of the diazodiketone **54** in the presence of MeOH through a Wolff rearrangement was transformed into the ketoketal **62** in a few steps. As expected, irradiation of **62** at 254 nm in acetonitrile with Et_3N led to the formation of the desired bicyclic compound **63** with a yield of 80% (Scheme 21).

The photoreductive cyclization process has been extended to unsaturated alkoxyketones to attain the furofuranic system present in antifeedant substances such as azadirachtin.³⁶ Ketone **65**, obtained from dihydrofuran **64**, was irradiated in the presence of Et_3N to furnish the bicyclic compound **66**. Its transformation to **68** was then achieved in five steps by using a Bamford–Stevens reaction^{37,38} as a key step (Scheme 22).

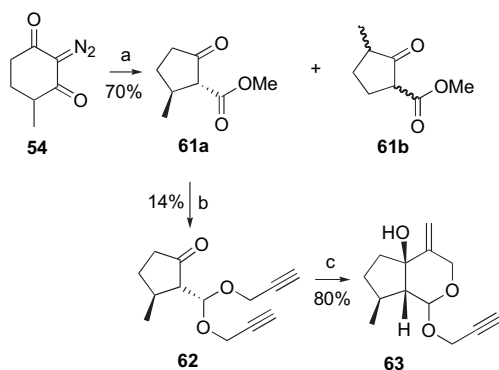
The photoreductive cyclization is very reproducible and produces stereoselectively substituted carbocyclic or heterocyclic compounds in high yields.



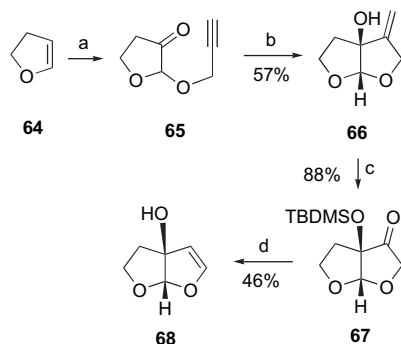
Scheme 19. Synthesis of actinidine: (a) hv, 254 nm, *N,N*-diallylamine, CH₃CN; (b) hv, Et₃N, 254 nm, CH₃CN; (c) i. LiAlH₄, ii. 10% Pd/C, xylene, nitrobenzene, MS 3A. Synthesis of isooxyskylanthine: (a) hv, 254 nm, *N*-methyl-*N*-propargylamine, CH₃CN; (b) hv, 254 nm, Et₃N, CH₃CN; (c) i. LiAlH₄, ii. 10% Pd/C, H₂, MeOH.



Scheme 20.



Scheme 21. (a) hv, CH₃CN, MeOH; (b) i. LiAlH₄, ether, 0 °C, ii. HMDS, TMSCl, CH₂Cl₂, 0 °C, iii. CrO₃, pyridine, CH₂Cl₂, iv. TMSCl, propargylic alcohol, CH₂Cl₂, v. PCC, MS 3A, CH₂Cl₂; (c) hv, Et₃N, CH₃CN.

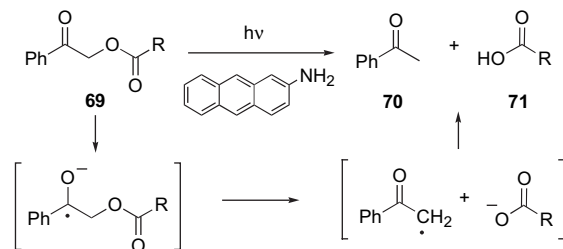


Scheme 22. (a) i. *m*-CPBA, CH₂Cl₂, 0 °C, ii. Propargylic alcohol, TsOH, iii. CrO₃, H₂SO₄, acetone; (b) hv, Et₃N, 254 nm; (c) i. *t*-BuMe₂SiCl, imidazole, ii. O₃; (d) i. H₂NNHTs, MeOH, H₂O, ii. Ethyleneglycol, Na, 140 °C, iii. Bu₄NF, THF.

6. Bond cleavage

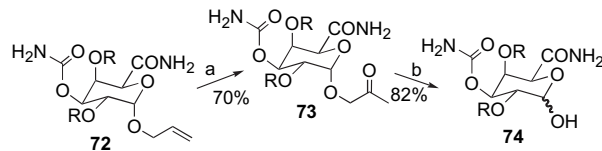
While most of the work related to PET reactions has focused on the formation of C–C bonds, the cleavage of C–O and C–C bonds has gained interest. One synthetic application of the cleavage of a C–O bond is the release of carboxylic acids upon photolysis of phenacyl esters using photosensitizers such as *N,N,N',N'*-tetramethylphenylene diamine, *N*-methylcarbazole, 2-aminoanthracene or *N,N*-dimethyl-aniline.³⁹

It is argued that this reaction is initiated by a photoinduced electron transfer from the excited state sensitizer to the phenacyl ester. The latter process forms the ketyl anion radical of the phenacyl ester, which in turn undergoes a rapid C–O bond scission leading to the phenacyl radical and to the corresponding carboxylate anion (Scheme 23).



Scheme 23.

A second synthetic application of the C–O bond cleavage is the elimination of an allyl protection at the anomeric position of a carboxylate, which is sometimes problematic. In the case of compound **72**, the deprotection problem was solved by using a Wacker oxidation⁴⁰ followed by photolysis of **73** in the presence of Et₃N⁴¹ (Scheme 24).

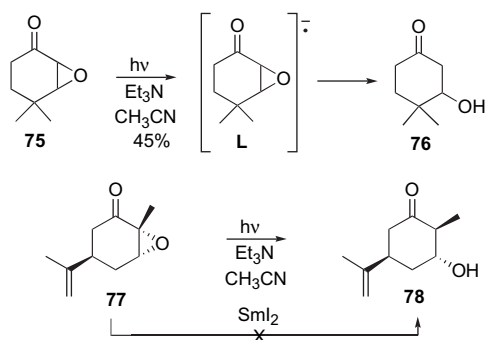


Scheme 24. (a) PdCl₂, CuCl, O₂, DMF/H₂O; (b) hv, Et₃N, CH₃CN, 254 nm.

The cleavage of heterocyclic strained rings can also be achieved by using a PET process. Irradiation of α -epoxyketones in acetonitrile in the presence of tertiary amine

[Et₃N, tribenzylamine, *N,N*-dimethyl,*N*-(trimethylsilylmethyl)amine, 2-phenyl-*N,N*-dimethylbenzimidazole] produces the cleavage of the epoxide ring of the α -epoxyketone and leads to 3-hydroxyketone⁴² (Scheme 25).

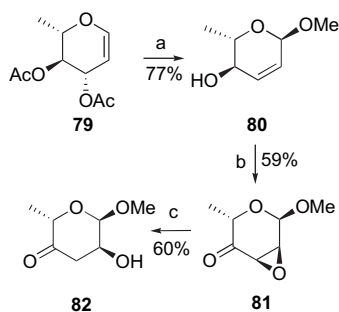
Although the exact mechanism of the epoxide ring opening from intermediate **L** has not yet been determined, a PET process seems to be involved. The observed cleavage of the C α –O bond of an epoxyketone is similar to the reductive cleavage of the same bond using lithium in liquid ammonia,⁴³ Bu₃SnH⁴⁴ or by cathodic reduction.⁴⁵ Surprisingly, SmI₂ did not cleave the epoxide ring of carvone oxide⁴⁶ (Scheme 25).



Scheme 25.

The photoinduced epoxy ring opening of an α -epoxyketone, allowing stereospecific formation of a β -hydroxy ketone, has also been used in the synthesis of the methyl glycoside of cinerulose **82**, a rare sugar present in the antibiotic cinerubine B.⁴⁷

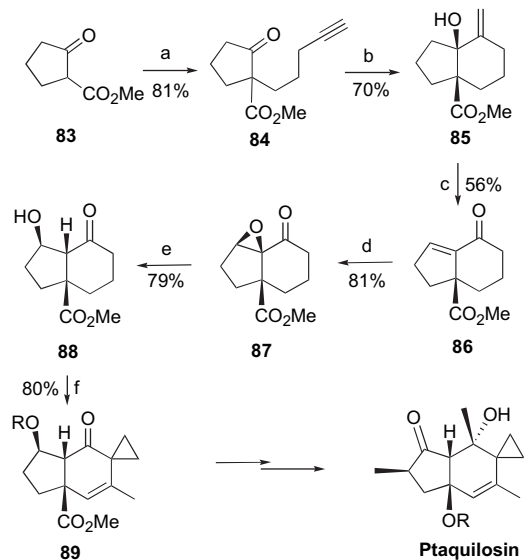
Irradiation of the epoxyketone **81**, prepared from the commercially available di-*O*-acetyl-*L*-rhamnamin, affords the methyl glycoside **82**. The transformation of **81** to **82** considerably shortens the synthesis of this rare sugar as compared with the previous synthesis⁴⁸ (Scheme 26).

Scheme 26. (a) i. BF₃·OEt, MeOH, ii. Resin OH[−]; (b) i. *m*-CPBA CH₂Cl₂, ii. PCC, CH₂Cl₂, MS 3A; (c) hv, Et₃N, CH₃CN, 254 nm.

Ptaquilosin is the aglycone of ptaquilosine, which has been evaluated for its antitumor activity at the National Cancer Institute (NCI).⁴⁹ The photoreductive cyclization and photoreductive opening of an epoxide, which are two highly chemo-, regio- and stereoselective processes, were used to control the configurations at C5 and C9 and consequently at C1 and C7 in a total synthesis of ptaquilosin.⁵⁰ The photoreductive cyclization applied to compound **84** allows the formation of the bicyclic compound **85** (70%) in which the ester

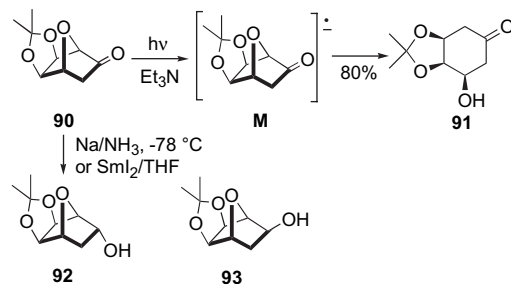
group is the precursor of the C5 hydroxy group present in ptaquilosin. Compound **85** was transformed to the enone **86**, which was epoxidized in a very stereoselective way using H₂O₂ in a methanolic potassium carbonate solution. The thus formed epoxide **87** was transformed under photoreductive conditions and hydroxy ketone **88** was isolated with a yield of 79%. In this compound all the functionalities needed are present to complete the synthesis of ptaquilosin.

As compound **84** can be prepared in its two enantiomeric forms,^{51,52} both (+)-ptaquilosin and (−)-ptaquilosin have been synthesized using this approach (Scheme 27).

Scheme 27. (a) KOH, EtOH, 1-iodopent-4-yne; (b) hv, Et₃N, CH₃CN, 254 nm; (c) i. O₃, MeOH, Me₂S, ii. Ac₂O, H₃PO₄ cat, iii. Resin OH[−], MeOH; (d) H₂O₂, K₂CO₃; (e) hv, Et₃N, CH₃CN, 254 nm; (f) i. TBDMSCl, imidazole, ii. TMSOTf, 2,6-lutidine, iii. Pd(OAc)₂, *p*-benzoquinone, CH₃CN, iv. CuBr·Me₂S, CH₃Li, TMSCl, v. Pd(OAc)₂, *p*-benzoquinone, vi. *t*-BuOK/*t*-BuOH, ICHCH₂SMe₂I, KI.

Oxonorbomanones, which possess a strained oxabridge can be cleaved under PET conditions.^{42,53} When these compounds are indeed irradiated in the presence of Et₃N, 3-hydroxycyclohexanones are obtained in moderate to good yields, depending on the nature of the substituents at C5 and C6. This reaction was applied to the synthesis of 3-hydroxycyclohexanones with excellent stereocontrol (transformation of **90** to **91**) (Scheme 28).

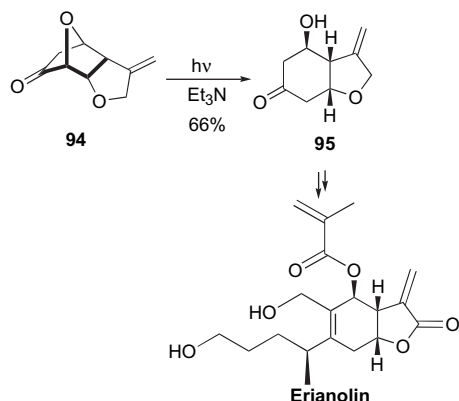
Interestingly, the treatment of **90** with Na in liquid NH₃ (−78 °C) did not induce the required C–O bond cleavage but gave a 10/1 mixture of the *endo* and *exo* alcohols **92**



Scheme 28.

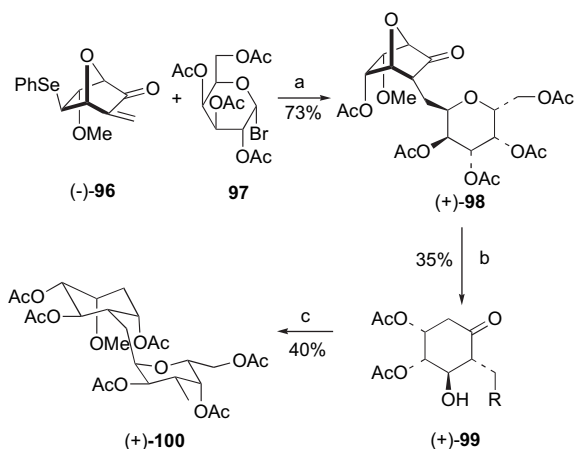
and **93**.⁵³ Furthermore, the treatment of **90** with 3 equiv of SmI₂ in THF led to the exclusive formation of the *endo*-alcohol **92**. These experiments show the difference in reactivity of intermediates produced by photochemistry and ground-state chemistry (Scheme 28).

The photoreductive 7-oxa ring opening method has allowed the synthesis of the erianolin skeleton from ketone **94**.⁵⁴ A new class of disaccharide mimics⁵⁵ that are α -C-galactopyranosides of carbo-pentopyranols⁵⁶ have been synthesized using the same approach (Scheme 29).



Scheme 29.

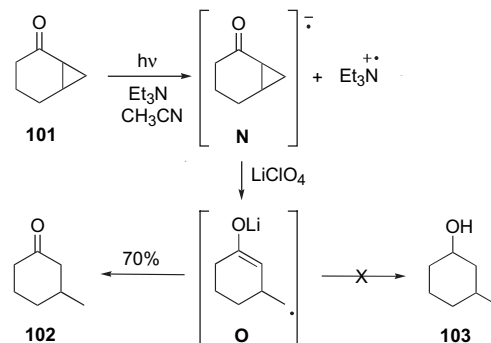
Photoinduced electron transfer from Et₃N to the all-*endo* 7-oxanorbornanone derivative (+)-**98** prepared by radical C–C bond formation between enone **96**⁵⁷ and acetobromogalactone **97**⁵⁸ led as expected to the reductive ring opening of the oxabridge and provided the tetrasubstituted cyclohexanone (+)-**99** without epimerization in the position α of the ketone. Compound (+)-**99** was then converted into **100**, a dicarba analogue of 2-*O*-(α -*O*-galactopyranosyl)-xylopyranodialdehyde (Scheme 30).



Scheme 30. (a) i. Bu₃SnH, AIBN, PhH, ii. *m*-CPBA, –78 °C, iii. Ac₂O/AcOH, iv. Bu₃SnH; AIBN; (b) hv, Et₃N, CH₃CN, 254 nm; (c) i. NaBH₄, MeOH, ii. Ac₂O, pyridine, DMAP.

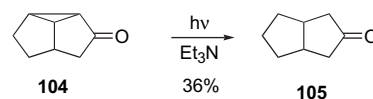
The PET induced opening of oxygenated strained rings can be extended to carbocyclic strained rings such as cyclopropanes^{42a,59} or cyclobutanes. Irradiation of bicyclo[4.1.0]heptanone **101** at 254 nm in acetonitrile in the presence of Et₃N led to cyclohexanone **102** according to Scheme 31.⁶⁰

Interestingly, the addition of LiClO₄ avoids further reduction of the ketone **102** to the alcohol **103** (Scheme 31).



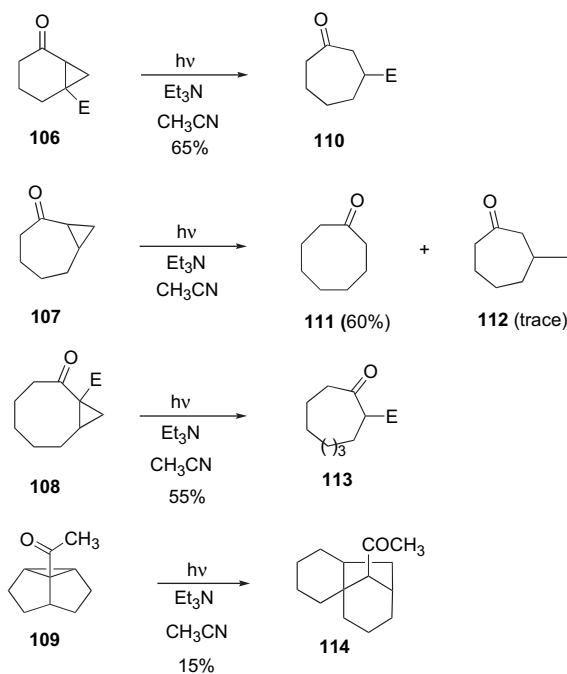
Scheme 31.

In the rigid tricyclic octanone system represented by **104**, the major product comes from the cleavage of the C2–C8 bond, arising from a better overlapping of this bond with the neighbouring carbonyl π -orbital⁶¹ (Scheme 32).



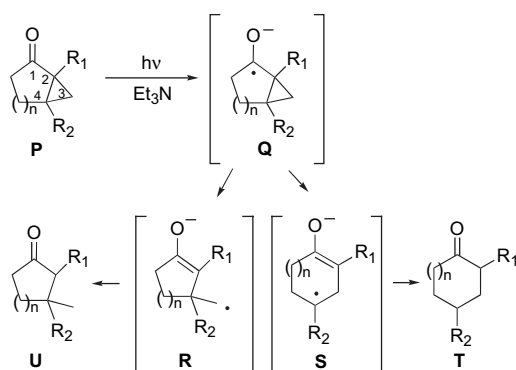
Scheme 32.

The preferred regioselectivity of the ring opening (*exo* vs *endo*) depends on the substitution pattern of the bicycloalkanes and on their ring size⁶² (Scheme 33). When the bicyclo[3.1.0]hexanone and bicyclo[4.1.0]heptanone are substituted by electron-withdrawing groups at C β , ring-expanded products are formed. Similarly, the irradiation of bicyclo[5.1.0]octanone and bicyclo[6.1.0]nonane in the presence of Et₃N led to the ring-expanded products⁶² (Scheme 33).



Scheme 33.

The radical-enolate intermediates of type **S** arising from the cleavage of the bond C2–C4 (ring enlargement process) are more stable (3.4 kcal/mol if R₂=H and 11–14 kcal/mol if R₂=CO₂Me)^{62,63} than the corresponding intermediate **R** (Scheme 34). The former intermediate is a secondary radical either substituted or not by an ester moiety and the latter is a primary radical. The ring enlargement can be explained by the fact that the C2–C4 bond of the bicyclo[*n*.1.0]alkan-2-ones is weaker than that of bond C2–C3. In the case of compound **101**, the C2–C3 bond is cleaved preferentially due to stereoelectronic factors, the latter bond being better aligned with the π-system of the ketyl radical anion than bond C2–C4. In the case of compounds **106–108** the kinetic stereoelectronic factor does not compete with the highly favourable factor, which makes the ring-enlarged radical-anion intermediates highly stabilized by the carbonyl group. In compound **107**, the flexibility of the bicyclic carbon skeleton makes both the C2–C3 and C2–C4 bonds capable of proper alignment with the π-system of the ketyl radical anion, thus leading to mixtures of the corresponding methylcycloheptanones and ring-enlarged cyclooctanones. (Scheme 34).

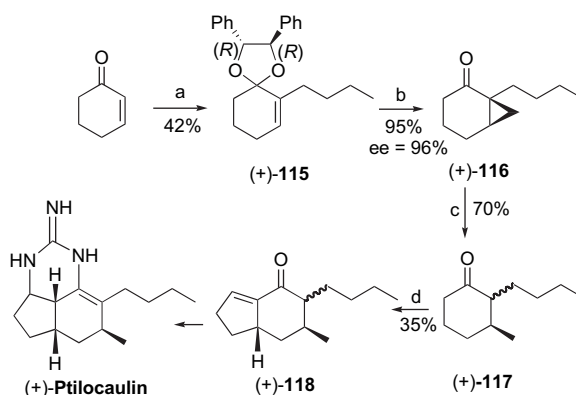


Scheme 34.

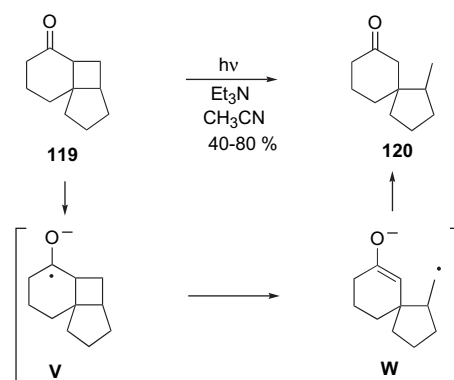
The ring cleavage of the cyclopropane ring of a chiral bicyclo[4.1.0]heptanone has been used as the key step in the synthesis of an antifungal agent, (+)-ptilocaulin.⁶⁴ Thus the chiral 2-butylbicyclo[4.1.0]heptanone was obtained by the cyclopropanation⁶⁵ of the chiral unsaturated ketal **115**⁶⁶ with high enantiomeric excess (96%). After deprotection, ketone **116** was irradiated in the presence of Et₃N and LiClO₄ to give the desired ketone **117**, which is the key molecule in the synthesis of (+)-ptilocaulin. The stereocontrol at C3 using this ring opening of a bicycloalkanone is much better than the addition of Me₂CuLi in the presence of a chiral inductor to the corresponding cyclohexenone.⁶⁷ Intermediate **117** was then transformed to ptilocaulin using a Sakurai reaction,⁶⁸ a hydroboration⁶⁹ an aldolisation and a treatment of **118** by guanidine (Scheme 35).⁷⁰

Ketyl radical anion can also induced the cleavage of a cyclobutane ring. Irradiation of compound **119** in the presence of Et₃N results in the formation of the spiroproduct **120**^{59,71} (Scheme 36).

A PET mechanism was postulated for this reaction, since the cleavage of the cyclobutane ring was not observed in the absence of Et₃N. Similarly, various cyclobutylketones have been subjected to PET conditions with Et₃N. For example,

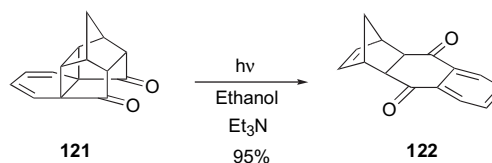


Scheme 35. (a) i. KF, Al₂O₃, *t*-BuOOH, ii. LDA, *n*-BuLi, TsOH, iii. Chiral diol, TsOH; (b) i. CH₂I₂, ZnEt₂, ii. TsOH; (c) hv, Et₃N, LiClO₄, CH₃CN, 254 nm; (d) i. LDA, NBS, ii. NaOH, iii. allylsilane, TiCl₄, iv. RhCl₃, catecholborane, v. PCC, CH₂Cl₂, MS 4A, vi. HCl, 2 N.



Scheme 36.

the irradiation of an ethanolic solution of **121** in the presence of Et₃N led to its quantitative conversion to **122**⁷² (Scheme 37).

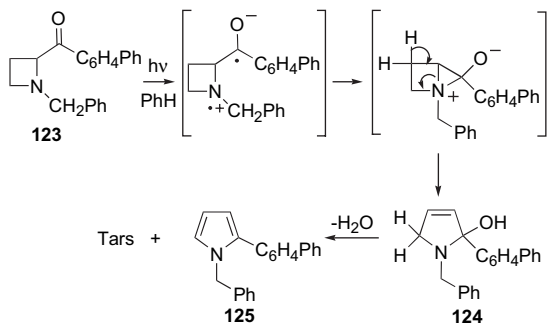


Scheme 37.

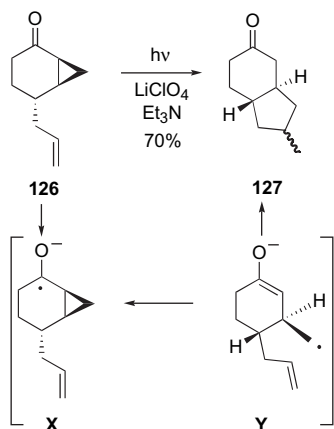
7. Tandem reactions: cyclization–ring opening and ring opening–cyclization

An intramolecular PET process in α-ketoazetidines induces an interesting rearrangement and formation of bicyclic hydroxy azetidines. These hydroxyaziridines rearrange quickly into 2-hydroxy-3,4-dihydropyrrole derivatives that aromatize through water elimination⁷³ (Scheme 38).

The radical intermediate **Y** induced by the PET fragmentation of bicyclo[*n*.1.0]alkanones can be trapped intramolecularly as shown by irradiation of the bicycloalkanone **126**^{59,62} (Scheme 39).

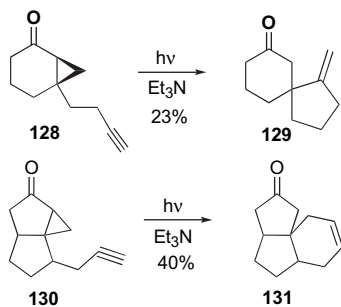


Scheme 38.

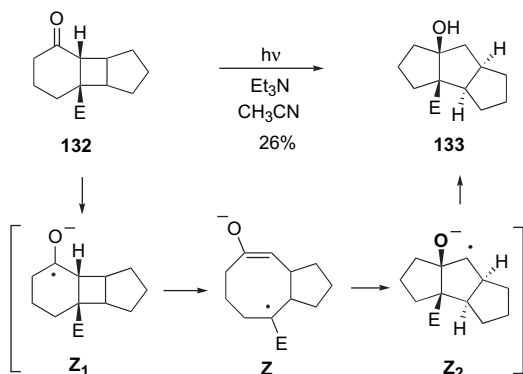


Scheme 39.

Spiro compounds can be obtained by applying a PET to compound of type **128**. Tricyclic compound **131** can also be obtained from compound **130**⁷⁴ (Scheme 40).

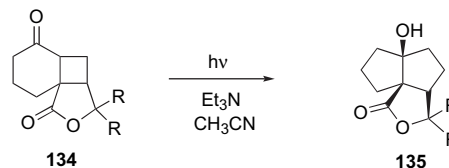


Scheme 40.



Scheme 41.

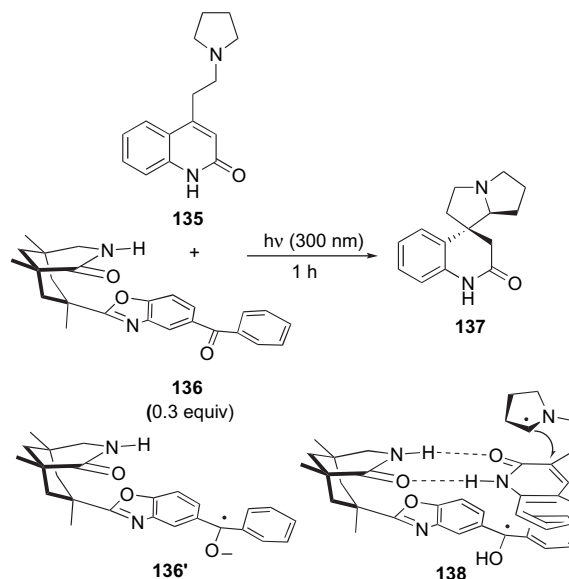
The skeleton of linear triquinanes is easily accessible from the methyl 8-oxotricyclo[5.4.0.0]^{2,6}undecan-1-carboxylate **132**.⁷¹ Photoreduction of **132** implied the formation of a ring-expanded intermediate **Z**, which cyclized to produce the linearly fused triquinane **133** (Scheme 41). An extension of this reaction to heterocyclic angular tricyclic compounds has been achieved⁷⁵ (Scheme 42).



Scheme 42.

8. Miscellaneous

Even, if it is not a direct reactivity of a ketyl radical anion, and based on previously reported catalyzed conjugate additions of α -amino alkyl radicals to enones in a non-enantioselective process,⁷⁶ it is worth to point out that catalytic enantioselective reactions driven by photoinduced electron transfer can take place. Compound **137** can be obtained in 70% enantiomeric excess and in 64% yield when compound **135** is irradiated in the presence of **136**. The facial differentiation in the PET-catalyzed cyclization of the prochiral substrate is probably due to the ketyl radical anion **136'**, which can produce intermediate **138** and, it is assumed, that the facial differentiation is due to this intermediate (Scheme 43).⁷⁷



Scheme 43.

9. Conclusion

Reactions involving PET processes are usually chemio-regio- and diastereoselective. For this reason, numerous synthetic developments have appeared during the last 30 years. At present and in spite of the interest of these

reactions, the photoreduction of ketones by tertiary amines is probably one of the most useful processes from a synthetic point of view. In the field of natural products, carbocyclic and heterocyclic molecules can be easily prepared from unsaturated ketones and PET processes cannot be neglected in synthetic schemes. The mild conditions and the high selectivity involving PET processes, make these reactions very attractive for further synthetic applications.

References and notes

- (a) Fox, M. A.; Chanon, M. *Photoinduced Electron Transfer*; Elsevier: Amsterdam, 1988; (b) Julliard, M.; Chanon, M. *Chem. Rev.* **1983**, *83*, 425.
- (a) Mattay, J. *Synthesis* **1989**, 233; (b) Cossy, J. *Bull. Soc. Chim. Fr.* **1994**, *131*, 344; (c) Ebersson, L. *Electron Transfer Reactions in Organic Chemistry*; Springer: Berlin, 1987.
- Rehm, D.; Weller, A. *Isr. J. Chem.* **1970**, *8*, 259.
- (a) Yoon, U. C.; Mariano, P. S.; Givens, R. S.; Atwater, B. W., III. *Advances in Electron Transfer Chemistry*; Mariano, P. S., Ed.; JAI: Greenwich, CT, 1994; Vol. 4, p 117; (b) Cossy, J.; Pète, J.-P. *Advances in Electron Transfer Chemistry*; Mariano, P. S., Ed.; JAI: Greenwich, CT, 1996; Vol. 5, p 141; (c) Hasegawa, E. *J. Photochemistry* **2003**, *10*, 61.
- (a) Cohen, S. G.; Parola, A.; Parsons, G. H., Jr. *Chem. Rev.* **1973**, *73*, 141; (b) Wagner, P. *Top. Curr. Chem.* **1976**, *66*, 1; (c) Kavarnos, G. J.; Turro, N. J. *Chem. Rev.* **1986**, *86*, 428.
- Simon, J. D.; Peters, K. S. *J. Am. Chem. Soc.* **1983**, *105*, 4875.
- (a) Cohen, S. G.; Chao, H. M. *J. Am. Chem. Soc.* **1968**, *90*, 165; (b) Cohen, S. G.; Stein, N. *J. Am. Chem. Soc.* **1969**, *91*, 3690; (c) Inbar, S.; Linschitz, H.; Cohen, S. G. *J. Am. Chem. Soc.* **1981**, *103*, 1048.
- (a) Peters, K. S.; Freilich, S. C.; Schaeffer, C. G. *J. Am. Chem. Soc.* **1980**, *102*, 5701; (b) Simon, J. D.; Peters, K. S. *J. Am. Chem. Soc.* **1981**, *103*, 6403; (c) Schanze, K. S.; Lee, L. Y. C.; Giannotti, C.; Whitten, D. G. *J. Am. Chem. Soc.* **1986**, *108*, 2646; (d) Setsune, J.; Fujiwara, T.; Murakami, K.; Mizuta, Y.; Kitao, T. *Chem. Lett.* **1986**, 1393.
- For example, see: (a) Ci, X.; Silveira da Silva, R.; Nicodem, D.; Whitten, D. G. *J. Am. Chem. Soc.* **1989**, *111*, 1337; (b) Ci, X.; da Silva, R. S.; Goodman, J. L.; Nicodem, D. E.; Whitten, D. G. *J. Am. Chem. Soc.* **1988**, *110*, 8548; (c) Shuster, D. I.; Insogna, A. M. *J. Org. Chem.* **1991**, *56*, 1879.
- Cohen, S. G.; Stein, N. M. *J. Am. Chem. Soc.* **1971**, *93*, 6542.
- Reynolds, J. L.; Erdner, K. R.; Jones, P. B. *Org. Lett.* **2002**, *4*, 917.
- Wu, Z.-Z.; Hug, G. L.; Morrison, H. *J. Am. Chem. Soc.* **1992**, *114*, 1812.
- Brulé, C.; Hoffmann, N. *Tetrahedron Lett.* **2002**, *43*, 69.
- Kohmoto, S.; Kreber, T.; Yamamoto, H.; Yamada, K. *Bull. Chem. Soc. Jpn.* **1990**, *63*, 3698.
- Hoffmann, N.; Görner, H. *Chem. Phys. Lett.* **2004**, *383*, 451.
- (a) Wagner, P. J.; Truman, R. J.; Puchalski, A. E.; Wake, R. *J. Am. Chem. Soc.* **1986**, *108*, 7727; (b) Wagner, P. J.; Park, B. S. *Organic Photochemistry*; Padwa, A., Ed.; Marcel Dekker: New York, NY, 1991; Vol. 11, p 227; (c) Cossy, J.; Guha, M. Unpublished results.
- (a) Griller, D.; Ingold, K. U. *Acc. Chem. Res.* **1980**, *13*, 317; (b) Beckwith, A. L. J.; Ingold, K. U. *Rearrangements in Ground and Excited States*; De Mayo, P., Ed.; Academic: New York, NY, 1980; Vol. 1, p 161.
- (a) Julia, M. *Acc. Chem. Res.* **1971**, *4*, 386; (b) Beckwith, A. L. J. *Tetrahedron* **1981**, *37*, 3073; (c) Surzur, J. M. *Reactive Intermediates*; Abramovitch, R. A., Ed.; Plenum: New York, NY, 1983; Vol. 2, p 164.
- Baldwin, J. E. *J. Chem. Soc., Chem. Commun.* **1976**, 734.
- (a) Belotti, D.; Cossy, J.; Pète, J. P.; Portella, C. *Tetrahedron Lett.* **1985**, *26*, 4591; (b) Belotti, D.; Cossy, J.; Pète, J. P.; Portella, C. *J. Org. Chem.* **1986**, *51*, 4196.
- Shono, T.; Nishigushi, I.; Ohmizu, H.; Mitami, M. *J. Am. Chem. Soc.* **1978**, *100*, 545.
- Corey, E. J.; Pyne, S. G. *Tetrahedron Lett.* **1983**, *24*, 2821.
- (a) Pradhan, S. K.; Radhakrishnan, T. V.; Subramanian, R. *J. Org. Chem.* **1976**, *41*, 1943; (b) Stork, G.; Malhotra, S.; Thomson, H.; Uchibayashi, M. *J. Am. Chem. Soc.* **1965**, *87*, 1148.
- Molander, G. A.; Etter, J. B.; Zinke, P. W. *J. Am. Chem. Soc.* **1987**, *109*, 453.
- Typical procedure: a solution of ketone (5×10^{-2} M) in acetonitrile in the presence of Et₃N (5 equiv) was irradiated at 254 nm by using a 12 TUV 15 Philips lamps merry-go-round system.
- (a) Cossy, J.; Belotti, D.; Pète, J. P. *Tetrahedron Lett.* **1987**, *28*, 4547; (b) Cossy, J.; Belotti, D.; Pète, J. P. *Tetrahedron* **1990**, *46*, 1859.
- Cherest, M.; Felkin, H.; Umpleby, J. D. *J. Chem. Soc., Chem. Commun.* **1981**, 681.
- (a) Cossy, J.; Madaci, A.; Pète, J. P. *Tetrahedron Lett.* **1994**, *35*, 1541; (b) Chesta, C. A.; Whitten, D. G. *J. Am. Chem. Soc.* **1992**, *114*, 2188.
- Cossy, J.; Belotti, D.; Pète, J. P. *Tetrahedron Lett.* **1987**, *28*, 4545.
- Cossy, J.; Belotti, D. *Tetrahedron Lett.* **1988**, *29*, 6113.
- Cossy, J.; Belotti, D.; Leblanc, C. *J. Org. Chem.* **1993**, *58*, 2351.
- Cossy, J.; Leblanc, C. *Tetrahedron Lett.* **1991**, *32*, 3051.
- (a) Wittaker, B. *The Chemistry of Diazonium and Diazo Groups*; Wiley-Interscience: New York, NY, 1978; p 593; (b) Froborg, J.; Magnusson, G. *J. Am. Chem. Soc.* **1978**, *100*, 6728; (c) Kunish, F.; Hobert, K.; Welzel, P. *Tetrahedron Lett.* **1985**, 5433; (d) Cossy, J.; Bouzide, A.; Thellend, A.; Belotti, D. *Bull. Soc. Chim. Fr.* **1994**, 723.
- (a) Oppolzer, W.; Robbani, C.; Bättig, K. *Helv. Chim. Acta* **1980**, *63*, 2015; (b) Oppolzer, W.; Kurth, M.; Reichlin, D.; Chapuis, C.; Mohnhaupt, M.; Moffat, F. *Helv. Chim. Acta* **1981**, *64*, 2803.
- Cossy, J. *Tetrahedron Lett.* **1989**, *30*, 4113.
- Brunetière, A. P.; Leclaire, M.; Bhatnagar, S.; Lallemand, J. M.; Cossy, J. *Tetrahedron Lett.* **1989**, *30*, 341.
- (a) Bamford, W. R.; Stevens, T. S. *J. Chem. Soc.* **1952**, 4735; (b) Shapiro, R. H. *Org. React.* **1976**, *23*, 405.
- Gianturco, M. A.; Friedel, D.; Flanagan, V. *Tetrahedron Lett.* **1965**, 1847.
- (a) Banerjee, A.; Falvey, D. E. *J. Org. Chem.* **1997**, *62*, 6245; (b) Banerjee, A.; Falvey, D. E. *J. Am. Chem. Soc.* **1998**, *120*, 2965; (c) Banerjee, A.; Lee, K.; Yu, Q.; Fang, A. G.; Falvey, D. E. *Tetrahedron Lett.* **1998**, *39*, 4635; Bochet, C. G. *J. Chem. Soc., Perkin Trans. 1* **2002**, 125.
- (a) Tsuji, J. *Synthesis* **1984**, 369 and references therein; (b) Gouedard, M. *Bull. Soc. Chim. Fr.* **1973**, 577.
- Lüning, J.; Möller, U.; Debski, N.; Welzel, P. *Tetrahedron Lett.* **1993**, *34*, 5871.
- (a) Cossy, J.; Aclinou, P.; Bellosta, V.; Furet, N.; Baranne-Lafont, J.; Sparfel, D.; Souchaud, C. *Tetrahedron Lett.* **1991**,

- 32, 1315; (b) Hasegawa, E.; Ishiyama, K.; Horaguchi, T.; Shimizu, T. *J. Org. Chem.* **1991**, *56*, 1631; (c) Hasegawa, E.; Ishiyama, K.; Fujita, T.; Kato, T.; Abe, T. *J. Org. Chem.* **1997**, *62*, 2396; (d) Hasegawa, E.; Yoneoka, A.; Suzuki, K.; Kato, T.; Kitazume, T.; Yanagi, K. *Tetrahedron* **1999**, *55*, 12957; (e) Hasegawa, E.; Chiba, N.; Nakajima, A.; Suzuki, K.; Yoneoka, A.; Iwaya, K. *Synthesis* **2001**, 1248; (f) Hasegawa, E.; Kamata, M. *CRC Handbook of Organic Photochemistry and Photobiology*; Horspool, W. M., Lenci, F., Eds.; CRC: Boca Raton, FL, 2004; Chapter 53, p 1; (g) Hasegawa, E.; Chiba, N.; Takahashi, T.; Takizawa, S.; Kitayama, T.; Suzuki, T. *Chem. Lett.* **2004**, *33*, 18.
43. (a) Caine, D. *Organic Reaction*; Dauben, W. G., Ed.; John Wiley: New York, NY, 1976; (b) Mc Chesney, J. D.; Thompson, T. N. *J. Org. Chem.* **1985**, *50*, 3473.
44. Hasegawa, E.; Ishiyama, K.; Kato, T.; Horaguchi, T.; Shimizu, T.; Tanaka, S.; Yamashita, Y. *J. Org. Chem.* **1992**, *57*, 5352.
45. Shapiro, E. L.; Gentles, M. J. *J. Org. Chem.* **1981**, *46*, 5017.
46. Molander, G. A.; Hahn, G. *J. Org. Chem.* **1986**, *51*, 1135.
47. Cossy, J.; Ibhi, S. *Carbohydr. Res.* **1994**, *259*, 141.
48. Stevens, C. L.; Schultz, K. W.; Smith, D. J.; Pillai, P. M.; Rubenstein, P.; Strominger, J. L. *J. Am. Chem. Soc.* **1973**, *95*, 5767.
49. Hirono, I.; Ogino, H.; Fujimoto, M.; Yamada, K. J.; Yoshida, Y.; Ikagawa, M.; Okumura, M. *J. Natl. Cancer Inst.* **1987**, *79*, 1143.
50. Cossy, J.; Ibhi, S.; Kahn, P. H.; Tacchini, L. *Tetrahedron Lett.* **1995**, *36*, 7877.
51. (a) Buisson, D.; Azerad, R. *Tetrahedron Lett.* **1986**, *23*, 2631; (b) Genêt, J. P.; Pfister, X.; Ratovelomanana-Vidal, V.; Pinel, C.; Laffitte, J. A. *Tetrahedron: Asymmetry* **1994**, *5*, 4559.
52. (a) Frater, G. *Helv. Chim. Acta* **1979**, *62*, 2825; (b) Frater, G. *Helv. Chim. Acta* **1980**, *63*, 1383.
53. Cossy, J.; Ranaivosata, J. L.; Bellosta, V.; Ancerewicz, J.; Ferritto, R.; Vogel, P. *J. Org. Chem.* **1995**, *60*, 8351.
54. Cossy, J.; Ranaivosata, J. L.; Bellosta, V. *Tetrahedron Lett.* **1995**, *36*, 2067.
55. Postema, M. H. D. *Tetrahedron* **1992**, *48*, 8545.
56. Ferritto, R.; Vogel, P. *Tetrahedron Lett.* **1995**, *36*, 3517.
57. Arval, G.; Fattori, D.; Vogel, P. *Tetrahedron* **1992**, *48*, 10621.
58. (a) Martin, O. R.; Lai, W. *J. Org. Chem.* **1990**, *55*, 5188; (b) Martin, O. R.; Lai, W. *J. Org. Chem.* **1993**, *58*, 176; (c) Lopez-Herrera, F. J.; Pino-Gonzalez, M. S.; Planas-Ruiz, F. *Tetrahedron: Asymmetry* **1990**, *1*, 465.
59. Kirschberg, T.; Mattay, J. *Tetrahedron Lett.* **1994**, *35*, 7217.
60. Cossy, J.; Furet, N. *Tetrahedron Lett.* **1993**, *34*, 8107.
61. (a) Pandey, B.; Bal, S. Y.; Khire, U. R. *Tetrahedron Lett.* **1989**, *30*, 4007; (b) Pandey, B.; Rao, A. T.; Dalvi, P. V.; Kumar, P. *Tetrahedron* **1994**, *50*, 3848; (c) Maiti, B. C.; Lahiri, S. *Tetrahedron* **1998**, *54*, 9111.
62. Cossy, J.; Furet, N.; Bouzbouz, S. *Tetrahedron* **1995**, *51*, 11751.
63. Mc Millen, D. F.; Golden, D. M. *Annu. Rev. Phys. Chem.* **1982**, *33*, 493.
64. Cossy, J.; Bouzbouz, S. *Tetrahedron Lett.* **1996**, *37*, 5721.
65. Sugimura, T.; Yoshikawa, M.; Furagawa, T. *Tetrahedron* **1990**, *46*, 5955.
66. Mash, E. A.; Torok, D. S. *J. Org. Chem.* **1989**, *54*, 250.
67. Corey, E. J.; Naef, R.; Hannon, F. J. *J. Am. Chem. Soc.* **1986**, *108*, 7115.
68. Hosomi, A.; Sakurai, H. *J. Am. Chem. Soc.* **1977**, *99*, 1673.
69. Männig, D.; Nöth, H. *Angew. Chem., Int. Ed. Engl.* **1985**, 879.
70. Snider, B. B.; Faith, W. C. *J. Am. Chem. Soc.* **1984**, *106*, 1443.
71. (a) Mattay, J.; Banning, A.; Bischof, E. W.; Heibreder, A.; Runsink, J. *Chem. Ber.* **1992**, *125*, 2119; (b) Kirschberg, T.; Mattay, J. *J. Org. Chem.* **1996**, *6*, 18885.
72. Pandey, B.; Rao, A. T.; Dalvi, P. V.; Kumar, P. *Tetrahedron* **1994**, *50*, 3835.
73. Padwa, A.; Albrecht, F.; Singh, P.; Vega, E. *J. Am. Chem. Soc.* **1971**, *93*, 2928.
74. (a) Fagnoni, M.; Schmoldt, P.; Kirschberg, T.; Mattay, J. *Tetrahedron* **1998**, *54*, 6427; (b) Tzvetkov, N.; Schmidtman, M.; Müller, A.; Mattay, J. *Tetrahedron Lett.* **2003**, *44*, 5979.
75. Le Blanc-Piva, S.; Piva, O.; Pete, J. P. Unpublished results.
76. (a) Jeon, Y. T.; Lee, C.-P.; Mariano, P. S. *J. Am. Chem. Soc.* **1991**, *113*, 8847; (b) Bertrand, S.; Hoffmann, N.; Pete, J.-P. *Eur. J. Org. Chem.* **2000**, 2227.
77. Bauer, A.; Westkämper, F.; Grimme, S.; Bach, T. *Nature* **2005**, *436*, 1139.



ELSEVIER

Available online at www.sciencedirect.com

SCIENCE @ DIRECT®

Tetrahedron 62 (2006) 6471–6489

Tetrahedron

Intramolecular nucleophilic capture of radical cations by tethered hydroxy functions

Heinz D. Roth,* Torsten Herbertz, Ronald R. Sauers* and Hengxin Weng

Department of Chemistry and Chemical Biology, Rutgers University, Wright-Rieman Laboratories,
New Brunswick, NJ 08854-8087, USA

Received 28 September 2005; accepted 6 December 2005

Available online 24 April 2006

Abstract—A range of systems bearing hydroxy functions tethered to the molecular framework gives rise to a family of interesting radical cations, 5^{+} – 11^{+} , upon electron transfer to photo-excited cyanoaromatics. Geraniol (**5**), nerol (**6**), citronellol (**7**), chrysanthemol (**8**), homochrysanthemol (**9**), *trans*-1-*o*-hydroxyphenyl-2-phenylcyclopropane (**10**), and *endo*-5-hydroxymethylnorbornene (**11**), generate a series of mono-, bi-, or tricyclic ethers via a series of four- to seven-membered transition states. Two of the radical cations, 5^{+} and 6^{+} , undergo tandem cyclizations where 1,5- and/or 1,6-C–C cyclizations precede nucleophilic capture.

© 2006 Elsevier Ltd. All rights reserved.

1. Introduction

The structures of organic radical cations and their reactions have attracted much attention during recent decades and continue to be the focus of intense interest.^{1–13} Because of their dual nature, radical cations contain an unpaired spin and a positive charge, they may undergo a wide range of diverse reactions, including rearrangements^{3–6} and sigmatropic shifts,⁷ nucleophilic substitution or ‘capture’,^{8,9} cycloadditions,^{2d,10} as well as fragmentations¹¹ and cycloreversions.¹² Compared to the analogous reactions of the parent molecules, many radical cation reactions show a dramatic decrease in activation barriers,^{11,13} one of the most striking aspects of radical cation chemistry.³ Among the plethora of reactions the capture by nucleophiles has been investigated in detail.

As a result of their electron deficient nature radical cations are strong acids and are excellent targets for nucleophilic substitution or capture. A wide range of strained ring radical cations undergo nucleophilic substitution, i.e., backside attack with inversion of configuration.^{8,9} The stereochemical requirements for this reaction are considered rigorous; molecular orbital calculations indicate that a trajectory close to 180° is critical.¹⁴ Many of these substitutions occur at sterically encumbered carbons,^{7,13} apparently, relief of ring strain significantly increases the driving force; this increase more than compensates for the steric hindrance.

The various factors governing regio- and stereochemistry of nucleophilic substitution on radical cations have been evaluated in a series of substrates that offer regiochemical competition within the target molecule. Not surprisingly, molecular orbital (MO) factors, particularly the nature of the singly occupied molecular orbital (SOMO) and the lowest unoccupied molecular orbital (LUMO), are of major importance. If MO factors allow more than one reaction, the thermodynamic stability of the resulting free radicals determines the outcome.^{7b,c,15} Steric factors typically do not play a major role; in fact, several radical cations are captured by attack on highly congested centers.^{7,13} However, at least one radical cation is captured selectively at the less encumbered site.¹⁵ We illustrate the major factors in the following examples, which were chosen to differentiate unambiguously between potentially governing factors.

A simple system illustrating the role of molecular orbital effects is the radical cation of *trans*-1,2-dimethylcyclopropane. The unpaired spin density, SOMO and LUMO of this species are shown in Figure 1; both HOMO and LUMO have a node at C-3. Accordingly, this radical cation and likewise other 1,2-disubstituted cyclopropane radical cations are unreactive at C-3.^{3b,16}

The radical cation of sabinene, 1^{+} , contains a rigidly arranged vinylcyclopropane system; unpaired electron spin and charge are delocalized over four atoms, C-5, C-1, C-4, and C-4'; however, only two centers, C-1 and C-4' have significant orbital coefficients in both HOMO and LUMO. Thus, nucleophiles should be able to attack 1^{+} either at the exocyclic alkene position or at the cyclopropane ring. In fact, nucleophilic attack occurs exclusively at the highly congested

Keywords: Electron transfer; Radical cation; Photochemistry; Intramolecular nucleophilic substitution; Tandem cyclization.

* Corresponding authors. Tel.: +1 732 445 5664; fax: +1 732 445 5312 (H.D.R.); tel.: +1 732 445 2626 (R.R.S.); e-mail addresses: roth@rutchem.rutgers.edu; sauers@rutchem.rutgers.edu

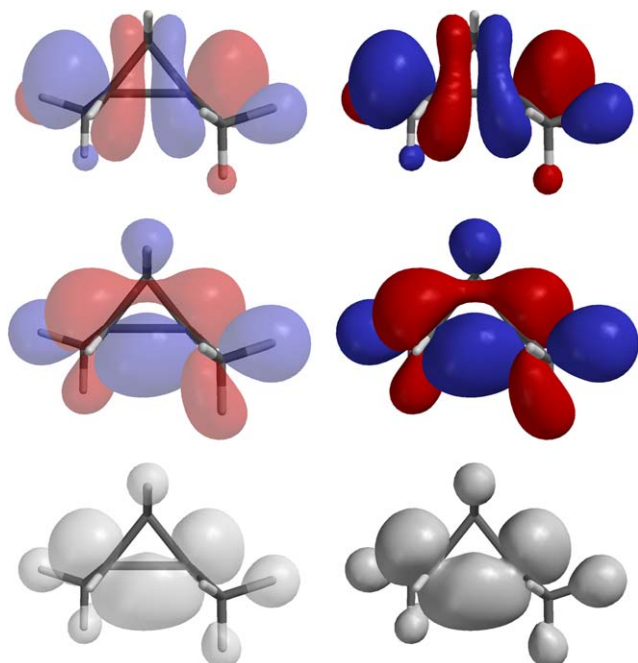
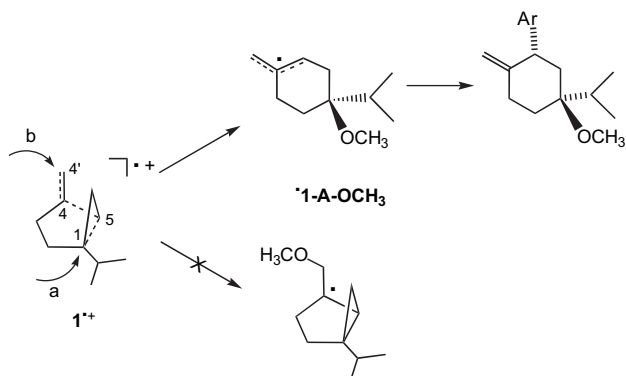


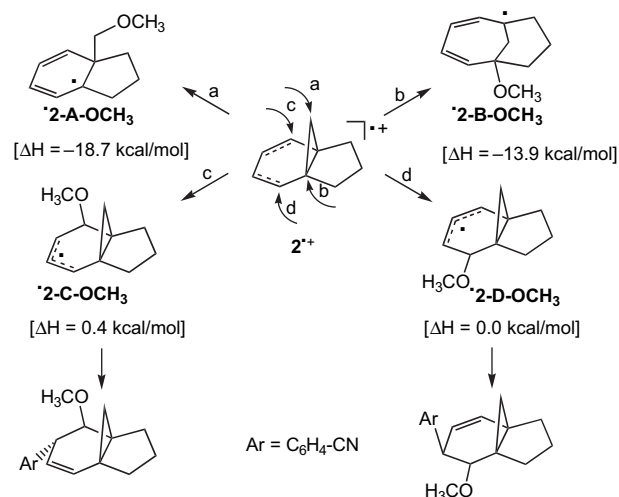
Figure 1. Stereoview of unpaired spin density (bottom), singly occupied molecular orbital (SOMO, center), and lowest unoccupied molecular orbital (LUMO, top) for the radical cation of *trans*-1,2-dimethylcyclopropane.¹⁶

quaternary cyclopropane carbon; this reaction is favored because (1) it gives rise to a more stable allylic free radical (\rightarrow **1-A-OCH₃**) and (2) it occurs with complete release of ring strain.^{7b}



In contrast, tricyclo[4.3.1.0^{1,6}]deca-2,4-triene radical cation, **2⁺**, which formally has two pathways of nucleophilic substitution with relief of ring strain (a,b), fails to utilize either. The species has spin and charge density at C-2, C-5, and C-10 but is attacked exclusively at C-2/C-5 (c,d), retaining the significant ring strain in the products. The course of this substitution is determined by the large LUMO coefficients at C-2, C-5 in contrast to the absence of major LUMO coefficients at C-10 or at the bridgehead carbons, C-1 and C-6 (Scheme 1; Fig. 2).¹⁷

The role of steric factors is illustrated unambiguously by comparison of two tricyclane isomers, 2,3,3-trimethyltricyclo[2.2.1.0^{2,6}]heptane,¹⁸ **3**, and 1,3,3-trimethyltricyclo[2.2.1.0^{2,6}]heptane,¹⁵ **4**. Nucleophiles attack **3⁺** and **4⁺** exclusively at tertiary carbons, not the quaternary ones; this finding is ascribed to the formation of the more stable



Scheme 1. Potential regioisomeric free radicals generated by nucleophilic addition/capture of tricyclo[4.3.1.0^{1,6}]deca-2,4-triene radical cation, **2⁺**, by methanol. The enthalpies of the corresponding truncated norcaradiene system are given in brackets.

tertiary radicals, **3-A-OCH₃** and **4-A-OCH₃**. The symmetrical tricyclane, **3**, does not offer an unambiguous conclusion: attack at C-1/C-6 is unencumbered from either face. On the other hand, the chiral isomer, **4**, clearly illustrates the role of steric hindrance. One of the tertiary cyclopropane centers

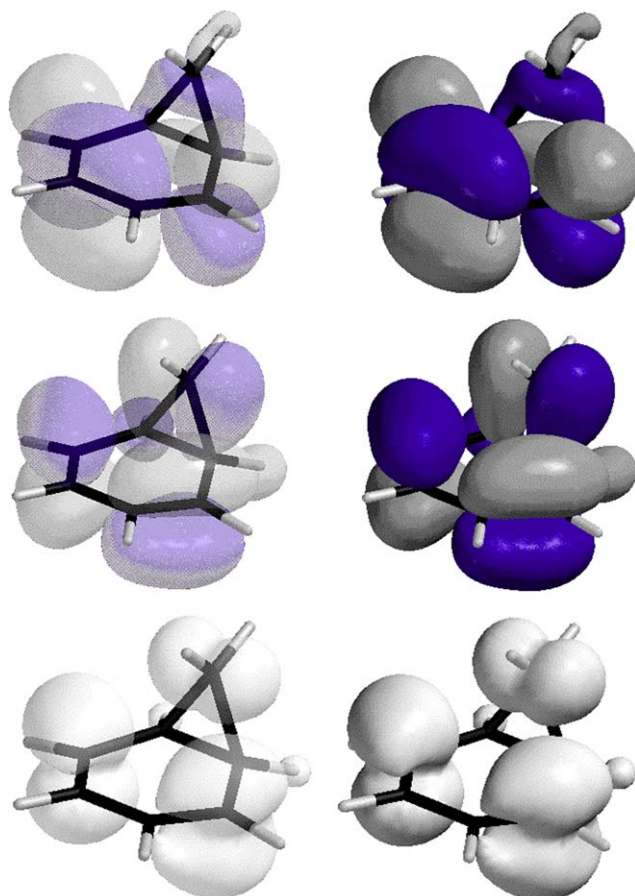
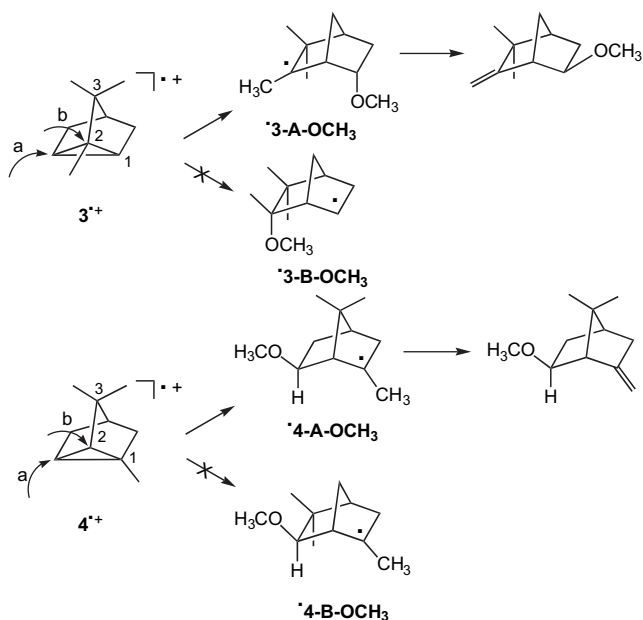


Figure 2. Stereoview of unpaired spin density (bottom), SOMO (center) and LUMO (top) for the radical cation of norcaradiene.¹⁷

of **4**, C-2, is a neopentyl type carbon whereas C-6 is sterically unencumbered. The result, exclusive attack at C-6, clearly establishes a significant role of steric hindrance in this system.¹⁵ The intermediates of both reactions, **3-A-OCH₃** and **3-B-OCH₃** respectively, form the final product by hydrogen, respectively, form the final product by hydrogen atom transfer to an adventitious acceptor.



Three of the reactions discussed above, those of **1⁺**, **3⁺**, and **4⁺**, are ‘genuine’ substitution reactions, akin to an S_N2 reaction, albeit on substrates that are one electron shy of the diamagnetic prototype. These reactions involve backside attack with release of a leaving group, in each case a free radical that remains attached to the molecule. For these reactions, the trajectory of approach may be important.¹⁴ The reaction of **2⁺** is different as the nucleophile adds to, or is ‘captured’ by an ‘empty p-orbital’ or an electron deficient π -system. This reaction is akin to the second, product-forming step of an S_N1 reaction. The stereochemical requirements for this type of reaction may be less demanding.

We have an interest in the intramolecular variant of these reactions, i.e., nucleophilic substitution or capture of radical cations by hydroxy groups tethered to the centers bearing spin and charge. Compared to the more general case of capture by an external nucleophile the intramolecular case offers some intriguing features. Steric features, including conformational preferences, may play a significant role in the substitution by or capture of an intramolecular nucleophile. Particularly, introduction of ring strain is seen as a major potential impediment for the cyclization of such systems. In general, the factors may be similar to those governing other ring-forming reactions such as the Dieckman condensation¹⁹ or intramolecular nucleophilic substitution of bifunctional compounds.²⁰ For example, the Dieckman condensation works well for five-, six-, and seven-membered rings, whereas larger rings require high-dilution techniques, a direct reflection of the conformationally encumbered transition states of such ring systems. Similarly, intramolecular S_N2 reactions proceed optimally via five- and six-membered transition states.

In order to probe various features of intramolecular reactions of radical cations with nucleophiles, we selected a series of substrates designed to cover a range of cases that would allow us to elucidate the principles governing this reaction type. For several of these species the tethered nucleophile has only a single possibility to react whereas in others it has the ‘option’ of attacking two or three different centers via different transition states with different driving forces and different barriers.

The systems chosen provide the opportunity to evaluate reactions proceeding via four- to eight-membered transition states, in several cases with intra-species competition. A four-membered transition state is actually realized in one system. Not surprisingly, several substrates utilize five- and six-membered transition states; both substitution and capture readily proceed via these common transition states. Three of our systems have the potential of reacting via seven-membered transition states; two radical cations react in this fashion, one actually in competition with other cyclizations. Finally, two radical cations offer the possibility of reaction via an eight-membered transition state without, however, using this pathway. Three of the systems studied contain three-membered rings; they were chosen for the additional driving force which relief of ring strain might provide.

The seven target molecules chosen for our investigation are listed in **Chart 1**; geraniol (**5**), nerol (**6**), citronellol (**7**), chrysanthemol (**8**), homochrysanthemol (**9**), *trans*-1-*o*-hydroxyphenyl-2-phenylcyclopropane (**10**), and *endo*-5-hydroxymethylnorbornene (**11**), generate a family of mono-, bi-, or tricyclic ethers via a series of four- to seven-membered transition states.

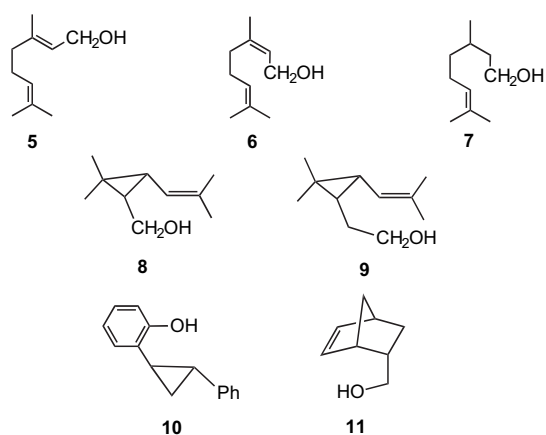


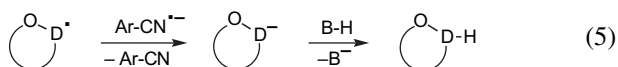
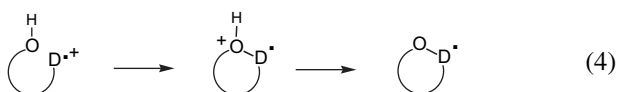
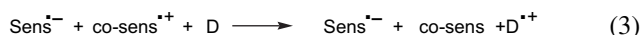
Chart 1. Target systems chosen for this study.

In all these systems the hydroxyl function serves as the nucleophile. This moiety is not a potent nucleophile in S_N2 reactions; for example, OH or COOH functions only undergo intramolecular substitution after being deprotonated. However, in reactions with radical cations, as well as carbocations, which are superacids as well as ‘super electrophiles’, the OH function is an efficient nucleophile. This is borne out by rates of nucleophilic capture, e.g., $k \sim 10^8 \text{ l mol}^{-1} \text{ s}^{-1}$, for the capture of phenylcyclopropane radical cation by methanol.^{13d}

In selected cases, these experimental findings are viewed in the light of molecular orbital calculations with *ab initio* or density functional theory (DFT) methods (*vide infra*). In addition to the geometries of selected intermediates, especially key bond lengths, we have generated pictorial representations of unpaired spin densities (ρ), the singly occupied molecular orbitals (SOMOs), and the lowest unoccupied (LU) MOs. The unpaired spin densities on carbon determine the hyperfine coupling constants (hfcc) of free radicals and radical ions; in most cases the signs and magnitudes of hfccs provide the only available *experimental* evidence for the structures of these intermediates.

2. Method of generation

The radical cations of the target molecules, **5**–**11**, were generated by electron transfer to a photo-excited sensitizer or a sensitizer/co-sensitizer system (e.g., Scheme 2, Eq. 1–3). The intramolecular nucleophilic substitution or capture of radical cations, **5**^{•+}–**11**^{•+}, give rise initially to bifunctional radical cations containing an oxonium ion and a localized or delocalized free radical. Rapid deprotonation of the oxonium ions leaves free radicals (Eq. 4), which have several potential reactions available, including aromatic substitution on the sensitizer radical anion (Eq. 6); reduction by return electron transfer (RET) from the sensitizer radical anion, followed by protonation (Eq. 5); or hydrogen abstraction from an adventitious hydrogen atom donor (Eq. 7). In some cases, the neutral radicals may form alkenes by hydrogen transfer to a suitable hydrogen atom acceptor (Eq. 8).



Scheme 2. Photo-induced electron transfer reactions of donor molecules bearing a tethered hydroxyl function.

The free energy of formation of radical ion pairs generated by electron transfer between a donor and an acceptor (Scheme 2; Eq. 3) is determined by the excited state energy, ($E_{0,0}$), the reduction potential of the acceptor, $E_{(A^-/A)}^0$, the oxidation potential of the donor, $E_{(D/D^+)}^0$, and a term accounting for ion pairing (Eqs. 9 and 10).²¹ In a modified formulation

of the Rehm–Weller equation (Eq. 10), $[2.6 \text{ eV}/\epsilon - 0.13 \text{ eV}]$ is an empirical term accounting for solvents of different polarity,^{21a} when the excitation energy and redox potentials are measured in acetonitrile; in polar solvents, $e^2/\epsilon a$ has a value of $\sim 0.06 \text{ eV}$. Typically, a driving force, $-\Delta G_{\text{ET}} \geq 0.5 \text{ eV}$, is sufficient to generate solvent separated radical ion pairs (SSRIP).

$$-\Delta G^0 = E_{(0,0)} - E_{(D/D^+)}^0 + E_{(A^-/A)}^0 - e^2/\epsilon a; \quad (9)$$

$$-\Delta G_{\text{SSRIP}}^0 = E_{(0,0)} - E_{(D/D^+)}^0 + E_{(A^-/A)}^0 - [2.6 \text{ eV}/\epsilon - 0.13 \text{ eV}] \quad (10)$$

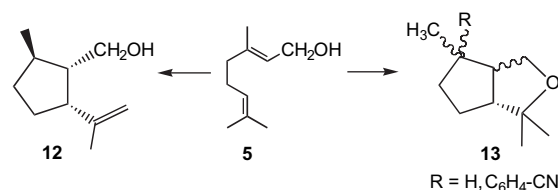
The oxidative power of an acceptor/sensitizer can be gauged by its excited state reduction potential,

$${}^*E_{(A^-/A)}^0 = E_{(0,0)}^0 + E_{(A^-/A)}^0 \quad (11)$$

Photosensitizers used in this study include 1,4-dicyanobenzene (**DCB**; $E_{(0,0)}^0 = 4.29 \text{ eV}$, $E_{(A^-/A)}^0 = -1.6 \text{ V}$; ${}^*E_{(A^-/A)}^0 = 2.7 \text{ V}$), 9,10-dicyanoanthracene (**DCA**; $E_{(0,0)}^0 = 2.88 \text{ eV}$, $E_{(A^-/A)}^0 = -0.9 \text{ V}$; ${}^*E_{(A^-/A)}^0 = 2.0 \text{ V}$), and triphenylpyrylium tetrafluoroborate (**TTP**; ${}^1E_{(0,0)}^0 = 2.8 \text{ eV}$, $E_{(A^-/A)}^0 = -0.29 \text{ V}$; ${}^1E_{(A^-/A)}^0 = 2.5 \text{ V}$; ${}^3E_{(A^-/A)}^0 = 2.0 \text{ V}$). Their oxidative strength should be sufficient to oxidize all electron donors studied. Accordingly, all photoreactions discussed here can be viewed as radical cation reactions. Details will be given as appropriate.

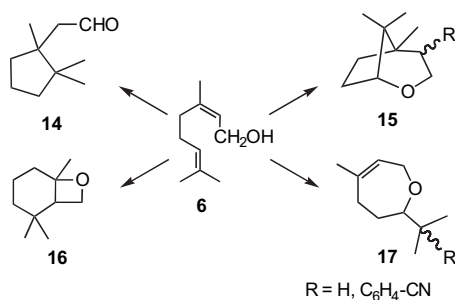
3. Results

Photo-induced one-electron transfer causes the terpene geraniol, **5**, to undergo an interesting five-center C–C cyclization. With 1,4-dicyanoanthracene/biphenyl (**DCA/BP**) as sensitizer/co-sensitizer, a primary stereoselective C–C cyclization is followed by intramolecular hydrogen transfer yielding **12**. With 9,10-dicyanobenzene/phenanthrene (**DCB/Ph**) the C–C cyclization is less selective and is followed by a second five-center cyclization, capture of C₇ by the alcohol function. Overall, this reaction generates a series of *cis*- and *trans*-fused 3-oxabicyclo[3.3.0]octanes, **13**.^{22a}

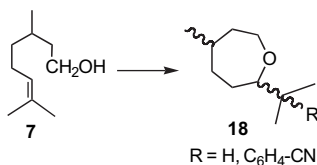


The *Z*-isomer of **5**, nerol, **6**, undergoes a range of significantly different reactions. Irradiation of **DCA/BP** in the presence of **6** gives rise to two monocyclic and two bicyclic ring systems, **14**–**17**. The formation of two products, 1,2,2-cyclopentylacetaldehyde, **14**, and 4-cyanophenyl-5,7,7-trimethyl-2-oxabicyclo[3.2.1]octane, **15**, appears compatible with a five-center C–C cyclization; one product, 2,2,6-trimethyl-7-oxabicyclo[4.2.0]octane, **16**, arises by a ‘tandem’

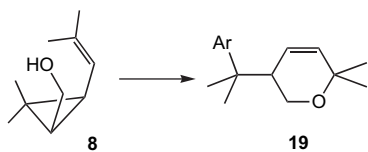
cyclization, initiated by a six-center C–C ring closure, which is followed by a four-center nucleophilic capture. Finally, the oxepene, 4-methyl-7-isopropyl-3-oxepene, **17**, requires a seven-center intramolecular nucleophilic capture. With the **DCB/Ph** pair, **6** undergoes *Z*-to-*E* isomerization, and forms aldehyde, **14**, in addition to traces of **17** and tandem cyclization product, **15**.^{22b}



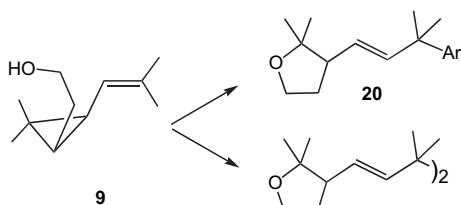
Irradiation of **DCA/BP** as sensitizer/co-sensitizer in acetonitrile in the presence of citronellol, **7**, which has only one olefinic function (i.e., dihydro-**6**), gives rise to the oxepane derivative **18** (i.e., dihydro-**17**) in good yield, confirming the dimethylethene function as a suitable electron donor under these conditions. This reaction requires a seven-center intramolecular nucleophilic capture.^{22b}



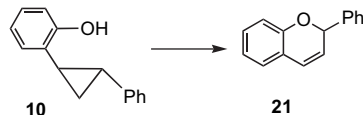
The OH function of chrysanthemol [1-(2-hydroxy-ethyl)-2,2-dimethyl-3-(2-methyl-1-propenyl)-cyclopropane] radical cation, **8**⁺, could attack the three-membered ring by nucleophilic substitution or the olefinic side chain by nucleophilic capture. Only the capture reaction is observed forming ring-expanded aryl-substituted products of type **19**.²³



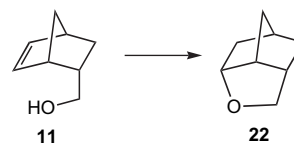
Homochrysanthemol [1-(3-hydroxy-propyl)-2,2-dimethyl-3-(2-methyl-1-propenyl)-cyclopropane] radical cation, **9**⁺, like the lower homolog **8**⁺, has two possible pathways for the OH function to react with the electron deficient moiety. The extended tether diverts the point of attack completely to the three-membered ring, giving rise to aryl-substituted products of type **20**, as well as a free radical dimer.²⁴



The electron transfer photochemistry of *trans*-**10** was carried out with triphenylpyrylium tetrafluoroborate (**TPT**). Sensitized irradiation of *trans*-**1** through Pyrex in methylene chloride under argon gave rise to 2-phenyl-2*H*-benzopyran, **21**, as the sole product (15% conversion after 5 h, 97% material balance).²⁵



Finally, irradiation of **DCA/BP** as sensitizer/co-sensitizer in acetonitrile in the presence of *endo*-5-hydroxymethylnorbornene, **11**, generated the tricyclic ether, 4-oxatricyclo[4.2.1.03,7]nonane, **22**, in moderate yield.²²



4. Discussion

We will discuss the radical cations whose reactions are being treated here in three groups. First we consider the terpene radical cations, **5**⁺, **6**⁺, and **7**⁺; they are of particular interest because **5**⁺ and **6**⁺ provide a competition between C–C and C–O bond formations. The second group, comprised of chrysanthemol and homochrysanthemol radical cations, **8**⁺ and **9**⁺, offers two different competing pathways involving nucleophilic substitution and capture. Finally, we discuss two radical cations that undergo 1,5-cyclizations, at least formally. The diarylcyclopropane radical cation, **10**⁺, poses an intriguing structure/reactivity problem whereas **11**⁺ probes the interesting aspect of *endo* attack on a norbornene radical cation.

4.1. Geraniol and nerol radical cations—competing C–C and C–O cyclizations

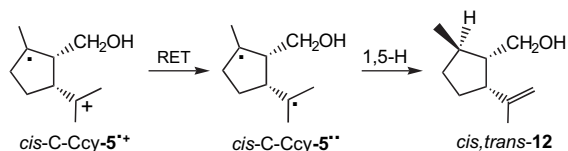
The radical ions of geraniol and nerol undergo both C–C and C–O cyclizations. Both processes generate bifunctional radical cations. The difference lies in the fact that the C–O closures generate a ‘product’ containing an oxonium ion, which is readily deprotonated, and is not suitable for further cyclization. In contrast, the species resulting from C–C closure contain a carbocationic site; intermediates of this type are less easily deprotonated and are still suitable/susceptible for nucleophilic capture. These species have the potential for tandem cyclization: both **5**⁺ and **6**⁺ undergo 1,5- and/or 1,6-C–C cyclizations, which are followed by nucleophilic capture.

Because of the *E*-geometry of geraniol the nucleophilic center of its radical cation, **5**⁺, can only serve in this capacity after having been ‘released’ or ‘unlocked’, for example, by an addition at C-2. Accordingly, it was not surprising that **5**⁺ reacted by bond formation between C-2 and C-6, i.e., via a five-membered transition state; the resulting

bifunctional radical cation, *cis*-5-C-Ccy-5⁺, is a ditertiary species and should be relatively stable. Indeed, with **DCA**/**BP** as sensitizer/co-sensitizer, the reaction was arrested at the stage of the monocyclic intermediate. The high stereospecificity observed with **DCA**/**BP** was unexpected: only the *cis*-fused ring was formed and only one stereoisomer of **12** was generated.^{22a}

In order to explain the (unexpected) stereospecificity of ring closure, we note the limited driving force for electron transfer. The reduction potential of **DCA** ($E_{(A^-/A)} = -0.9$ V), and its low excited state energy ($E_{0,0} = 2.88$ eV) render the oxidation of **5** by ¹**DCB*** mildly exergonic ($\Delta G_{ET} \sim -0.1$ eV) in CH₃CN and slightly endergonic ($\Delta G_{ET} \sim +0.2$ eV) in CH₂Cl₂. Accordingly, the radical ions **DCA**^{•-} and **5**^{•+} can be generated only as tight ('sandwich') ion pairs, causing the substituents at the developing bonds to move 'outward', away from the counter ion, resulting in the observed *cis*-stereochemistry. The orientation of the methyl group *trans* to the isopropenyl function was explained via triplet return electron transfer, generating a biradical, *cis*-5-C-Ccy-5^{••}; a 1,5-intramolecular (suprafacial) hydrogen shift readily accounts for the *trans*-stereochemistry.^{22a}

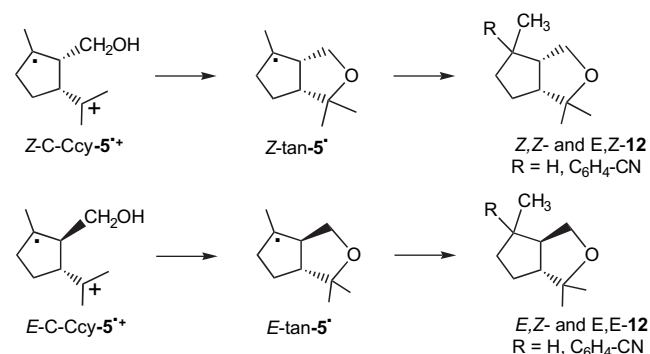
Return electron transfer in triplet radical ion pairs has been of great interest for several decades.²⁶ Of special interest are systems that undergo rearrangement during the consecutive lifetimes of radical ions and triplet states or biradicals.²⁷ Geraniol belongs to a group of systems where the radical cation undergoes a major structure change, **5**^{•+} to *cis*-5-C-Ccy-5^{•+}, a species corresponding to a non-Kekule structure in the ground state.²⁷ The reorganized structure is retained upon electron return (*cis*-5-C-Ccy-5^{•+} to *cis*-5-C-Ccy-5^{••}), then reverts to a Kekule structure with a minor change in structure, a 1,5-H shift forming *cis,trans*-**12**.²⁷ Details of this interesting topic go beyond the scope of this article.



For the reaction of **5** with the **DCB**/**Ph** pair, electron transfer from the donor substrates to ¹**DCB*** dicyanobenzene ($E_{(0,0)}^0 = 4.29$ eV, $E_{(A^-/A)}^0 = -1.6$ V; $*E_{(A^-/A)}^0 = 2.7$ V) should be efficient, regardless of the solvent. Under these conditions the reaction takes a different course in two respects: (a) the C-C ring closure is much less stereospecific and (b) the reaction proceeds past the stage of 5-C-Ccy-5^{•+}, as the partial positive charge at C-7 is captured by the hydroxy function, completing a tandem cyclization.

Because the electron transfer reaction is comfortably exergonic ($-\Delta G_{ET} \sim 0.8$ eV), the ion pair, **DCA**^{•-}-**5**^{•+}, is generated as a solvent separated radical ion pair without intra-pair interactions that would affect the stereochemistry of C-C closure. The resulting bicyclic free radicals, *Z*- or *E*-**5**[•], react by aromatic substitution²⁸ (Scheme 2, Eq. 6) as well as by hydrogen abstraction (Scheme 2, Eq. 7)—neither reaction has any pronounced stereochemical preference. The lack of specificity in this reaction turned product separation

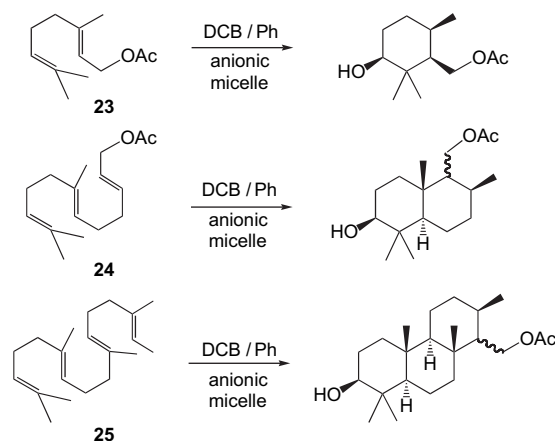
into a challenge and has precluded synthetic utility, at least to date.^{22a}



The structural features of the three key radical cations, **5**^{•+}, *cis*-5-C-Ccy-5^{•+}, and 5,5-tan-5^{•+}, were calculated using density functional theory (DFT) methods (Fig. 3); in order to allow a comparison of their calculated enthalpies the proton on the oxonium ion, 5,5-tan-5^{•+} was not allowed to dissociate. The first (C-C) cyclization is endergonic by 2.5 kcal mol⁻¹, whereas the second (O-C) cyclization is exergonic by 4.3 kcal mol⁻¹. The deprotonation of the oxonium function lowers the enthalpy further, rendering the tandem cyclization irreversible.

A comparison of the spin and charge density distributions in the three species is illuminating. The parent radical cation, **5**^{•+}, has unpaired spin density in both alkene groups; the dimethylethylene carbons bear similar spin densities ($\rho_6 = 0.212$, $\rho_7 = 0.213$), whereas the hydroxyl group apparently polarizes the partial double bond between C-2 and C-3 ($\rho_2 = 0.272$, $\rho_3 = 0.096$). In the first cyclization product, *cis*-5-C-Ccy-5^{•+}, the spin is distributed between C-3 ($\rho = 0.461$) and C-7 ($\rho = 0.542$). Upon closing the second ring, forming 5,5-tan-5^{•+}, the unpaired spin becomes localized on C-7 ($\rho = 0.958$) whereas the charge is placed on the oxygen, polarizing the bonds to the adjacent atoms ($C_1 = 0.339$, $C_7 = 0.265$, $O-H = 0.474$).

Interestingly, under different reaction conditions, using 1,4-**DCB**/**Ph** in anionic micellar solution, the acetate of **5** (**23**) as well as the sesquiterpene and diterpene acetates, farnesyl (**24**) and geranylgeraniol acetate (**25**), undergo 1,6-cyclizations, generating six-membered mono-, bi-, and tricyclic



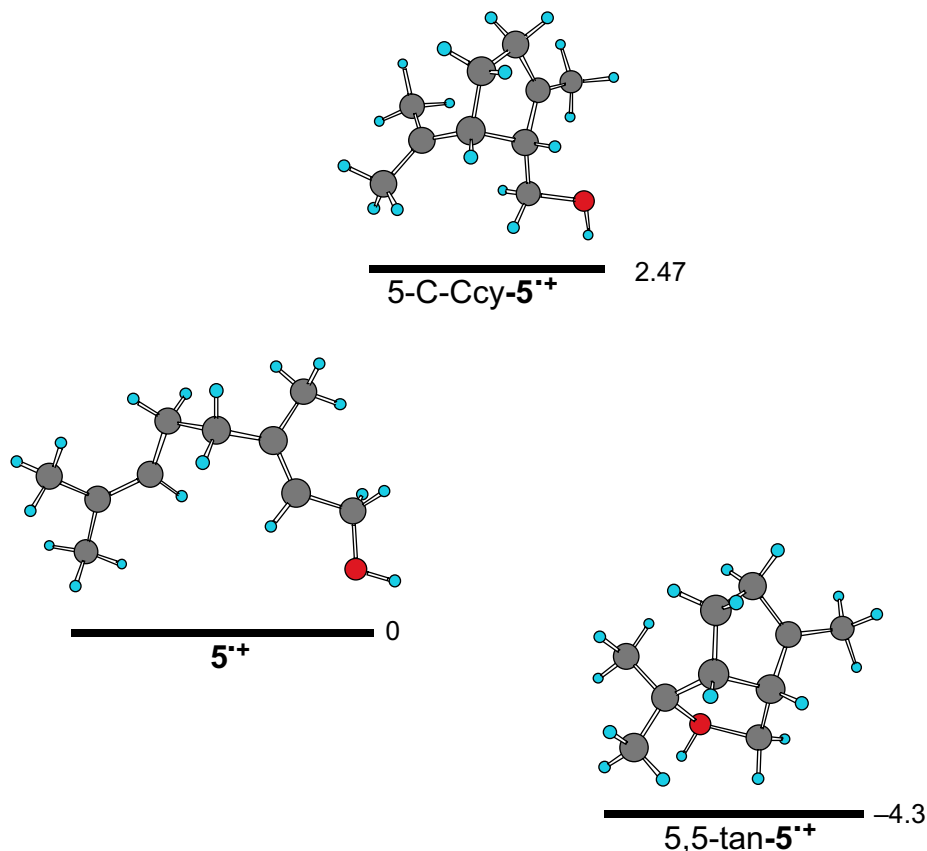


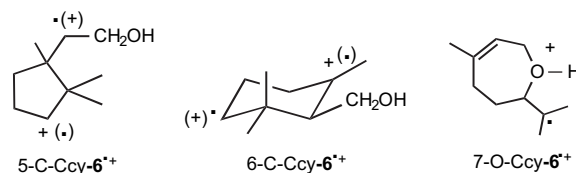
Figure 3. Chem-3D models of geraniol radical cation, $5^{\bullet+}$, and two isomers generated by C–C cyclization, *cis*-5-C-Ccy- $5^{\bullet+}$, and tandem cyclization, 5,5-tan- $5^{\bullet+}$, respectively. The geometries were calculated by DFT methods using the 6-31G* basis set; relative enthalpies (kcal mol⁻¹) are indicated.

products, respectively.²⁹ The bi- and tricyclic products are trans-fused and all are hydroxylated in anti-Markovnikov fashion; apparently the radical ions are terminated by water. These reactions are the first examples of photochemically initiated biomimetic terpenoid cyclizations.

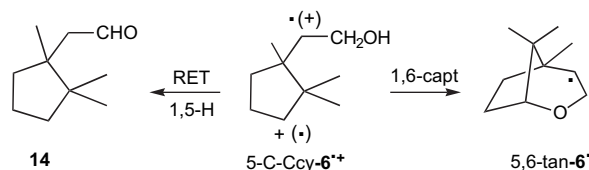
The *Z*-isomer of $5^{\bullet+}$, nerol radical cation, $6^{\bullet+}$, cannot be expected to undergo cyclization between C-2 and C-6 because the conformer required for this conversion appears to be seriously hindered by the steric repulsion between the hydroxymethyl group and the terminal dimethylethylene moiety. For $5^{\bullet+}$, a helical arrangement can relieve the less severe steric repulsion between the hydrogens at C₂ and C₆ without compromising their required proximity. However, the helical conformer of $6^{\bullet+}$ is still severely hindered, so that alternative reactions must be expected. Indeed, **6** does not generate any product derived by bond formation between C-2 and C-6.^{22b}

However, other cyclizations also have steric challenges. For example, products **14** and **15** result from five-carbon C–C cyclization between C-3 and C-7, yielding 5-C-Ccy- $6^{\bullet+}$. Although this approach avoids the C-2–C-6 crowding, the C-3 onto C-7 approach does not appear significantly less crowded. Perhaps as a result of this steric impediment $6^{\bullet+}$ undergoes the most varied ring formations of any system discussed here. The various reactions of $6^{\bullet+}$ result in the formation of five-, six-, and seven-membered rings and support nucleophilic capture via four-, six-, and seven-membered transition states. These products are compatible with primary cyclizations yielding 5-C-Ccy- $6^{\bullet+}$, 6-C-Ccy- $6^{\bullet+}$, and

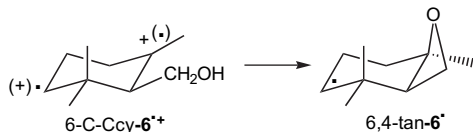
7-O-Ccy- $6^{\bullet+}$, respectively; the latter would be deprotonated readily to 7-O-Ccy- 6^{\bullet} .^{22b}



With DCB/Ph as sensitizer/co-sensitizer, **6** forms aldehyde **14** as the major product and undergoes *Z*-to-*E* isomerization. This cyclization is not only sterically disadvantaged, but it places spin and charge on two secondary carbons in the putative intermediate. For the conversion of 5-C-Ccy- $6^{\bullet+}$ to **14** we consider triplet electron return and an intramolecular (suprafacial) 1,5-hydrogen shift from the β-carbon of the side chain (C₂) to the cyclopentyl ring (C₆) in the resulting biradical, 5-C-Ccy- $6^{\bullet\bullet}$; this species also explains the observed *Z*-to-*E* isomerization.^{26,27} The bicyclic ether, **15**, suggests that 5-C-Ccy- $6^{\bullet+}$, in analogy to 5-C-Ccy- $5^{\bullet+}$, undergoes intramolecular nucleophilic capture completing a tandem cyclization. The resulting 5,6-tan- 6^{\bullet} generates **15** by hydrogen abstraction (cf., Scheme 2, Eq. 7).^{22b}



With the **DCA/BP** as sensitizer/co-sensitizer, **6** is converted to **14**, **16**, and **17**. The intermediate leading to **16** is a cyclohexane-1,4-diyl system, 6-C-Ccy-6⁺, formed by bond formation between C₂ and C₇; spin and charge are localized on a secondary and tertiary carbon, respectively. This type of system contains spin and charge in two parallel p-orbitals; this arrangement allows ready delocalization, thereby stabilizing the species.³⁰ Interestingly, 6-C-Ccy-6⁺ undergoes nucleophilic capture of the tertiary carbon by the alcohol function via a four-membered transition state. The conversion of the 7-oxabicyclo[4.2.0]octan-4-yl radical, 6,4-tan-6[•], to **16** by hydrogen abstraction (cf., Scheme 2, Eq. 7) is unexceptional. The formation of 6,4-tan-6[•] from 6-C-Ccy-6⁺ is significant as the only example of oxetane formation from a radical cation.²² The reason for the general lack of specificity observed for 6⁺ may well lie in the sterically less demanding nature of nucleophilic capture and C–C bond formations between two trisubstituted, sp² hybridized carbons.^{22b}



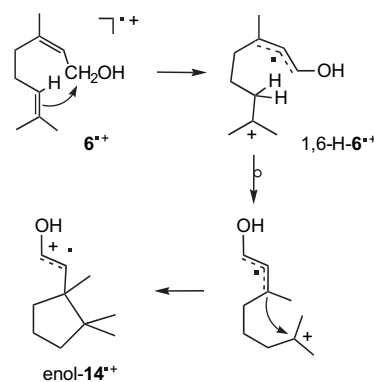
Finally, the hydroxymethyl group of 6⁺ interacts with the dimethylethylene function by forming the oxepene system, apparently by nucleophilic capture of C₆. The *Z*-arrangement of 6⁺ causes the hydroxy function to reside in the general vicinity of the molecule's 'tail end', allowing nucleophilic capture with formation of 7-O-Ccy-6⁺. The transition state appears sterically congested, but it may be possible to arrange the seven centers C₆ through O in a quasi-boat that will reduce steric repulsion yet facilitate capture of C₆ by the OH function.²² Formally, 6⁺ also has the potential to form an eight-membered ring system, but no product of this structure type was observed.^{22b}

These results show that the potential hypersurface of nerol radical cation is significantly more complicated than that of 5⁺. The products suggest three primary cyclized species, 5-C-Ccy-6⁺, 6-C-Ccy-6⁺, and 7-O-Ccy-6⁺, and two species resulting from tandem cyclization, 5,5-tan-6⁺ and 6,4-tan-6⁺, in addition to the parent radical cation, 6⁺. In order to gain additional insight into this potential surface, the key radical cations were probed using density functional theory (DFT) methods. As was the case for the intermediates derived from **5**, the oxonium protons were not 'allowed' to dissociate.

The calculations yielded five of the radical cations considered as likely intermediates. The cyclized species, 6-C-Ccy-6⁺ and 7-O-Ccy-6⁺, lie 9.96 kcal mol⁻¹ and 8.85 kcal mol⁻¹, respectively, above 6⁺ ($\Delta H=0$) and, thus, should be accessible during its lifetime. The products of tandem cyclization, 5,5-tan-6⁺ ($\Delta H=7.97$ kcal mol⁻¹) and 6,4-tan-6⁺ ($\Delta H=11.70$ kcal mol⁻¹), appear likewise accessible; deprotonation of the oxonium functions should lower the free enthalpies further, rendering the second cyclizations essentially irreversible. However, the calculations revealed one irreconcilable discrepancy with the simple mechanism considered: the putative precursor, 5-C-Ccy-6⁺, for the major product (**14**) proved to be elusive. The approach of

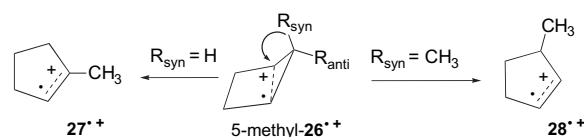
carbon atoms C-3 and C-7 is connected with a steep rise in energy due to the interference of the alkyl groups, rendering the formation of 5-C-Ccy-6⁺ highly unfavorable. Accordingly, we searched for additional pathways leading from 6⁺ to **14**.

We noted that in the lowest energy conformer of 6⁺ one of the H atoms attached to C-1 is pointing inward, quasi poised for a hydride shift to C-6. This shift would lead to an intermediate, 6,1-H-6⁺, containing an allylic free radical tethered to a tertiary carbocation. Rotational reorganization of the tether would allow cyclization between C-3 and C-7, yielding enol-14⁺. Return electron transfer from the counter ion followed by tautomerization would complete a pathway to the major product, **14**, which potentially is lower in energy. In contrast to the conversion of 6⁺ to 5-C-Ccy-6⁺, the hydride shift precedes the cyclization step in the newly considered pathway.



An examination of the proposed pathway by density functional calculations revealed the hydride shift to be exergonic; the corresponding transition state lies only 2.7 kcal mol⁻¹ above 6⁺. Furthermore, the cyclization of 6,1-H-6⁺ to enol-14⁺ is endergonic by only 0.13 kcal mol⁻¹. These energetic features readily explain why **14** is obtained as the major product. The pertinent structures delineating the hydride shift are shown in Figure 4.

The hydride shift revealed by the calculations is interesting because it converts a bifunctional ('distic') species in which spin and charge occupy separate regions of the molecular framework into a species in which spin and charge share the same pi system. In general, hydride shifts in radical cations are not without precedent; several rigid radical cations undergo stereospecific sigmatropic shifts. For example, the puckered ion, *anti*- and *syn*-5-methyl-26⁺, undergo stereospecific hydride or methyl migration, respectively, forming 1-methylcyclopentene radical cation, 27⁺, as well as the 3-methyl isomer, 28⁺.³¹



Similarly, sabinene radical cation, 1⁺, undergoes a stereospecific [1,3] shift to β -phellandrene radical cation, 29⁺, with high retention of optical purity whereas α -thujene

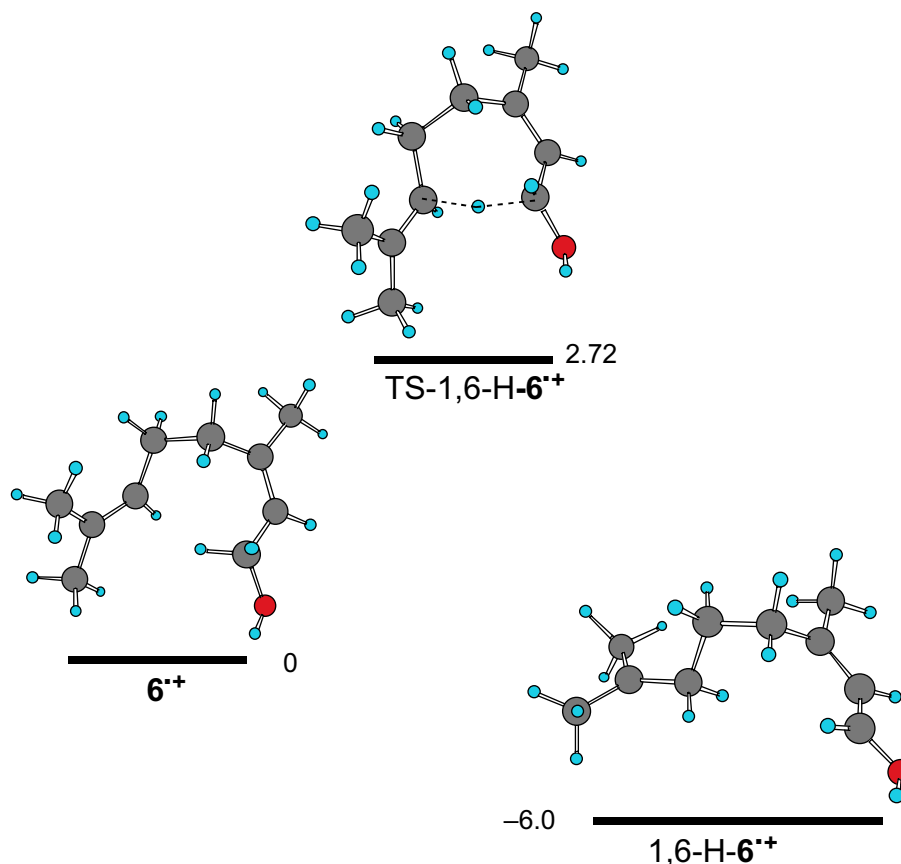
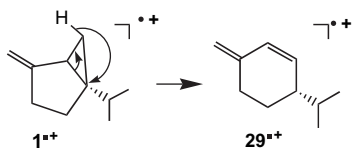


Figure 4. Chem-3D models of nerol radical cation, 6^{+} , an isomer generated by H-shift, $1,6\text{-H-}6^{+}$, and the transition state for the H-shift, $\text{TS-}1,6\text{-H-}6^{+}$. The geometries were calculated by DFT methods (6-31G* basis set); relative enthalpies (kcal mol^{-1}) are indicated.

radical cation (not shown) undergoes competing [1,3] and home-[1,5] shifts to α -phellandrene radical cation.^{7c} In these examples radical cations containing spin and charge in a lengthened cyclopropane ‘sigma’ bond are converted into species in which spin and charge share the same pi system.



The high barrier connected with the putative ring closure of 6^{+} to $5\text{-C-Ccy-}6^{+}$ affects the overall mechanism further as it eliminates the ‘logical’ precursor for the tandem cyclization product, $5,6\text{-tan-}6^{+}$. The newly uncovered species is not bifunctional and, therefore, cannot undergo a second ring closure. The possibility of yet another hydride shift, generating $5,6\text{-tan-}6^{+}$ from $\text{enol-}14^{+}$, is remote because of the prohibitive enthalpy ($\Delta H=+13.84 \text{ kcal mol}^{-1}$) of this reaction.

A comparison of the spin and charge density distributions in 6^{+} and the diverse radical cations derived from it provides additional insights. The parent radical cation, 6^{+} , has unpaired spin density in both the alkene groups; the spin densities of both the groups are slightly polarized ($\rho_6=0.167$, $\rho_7=0.212$; $\rho_2=0.232$, $\rho_3=0.137$); the hydroxyl group affects

the spin density to a lesser degree than for 5^{+} . The product generated by hydride shift, $1,6\text{-H-}6^{+}$, has an unusual distribution of spin and charge; the spin is located mainly on C-7 ($\rho_7=0.632$) and to a lesser extent on C-1 ($\rho_1=0.214$) and C-3 ($\rho_3=0.210$) whereas the charge is distributed between C-1 (0.156) and C-3 (0.205) and C-7 (0.211). Cyclization product $6\text{-C-Ccy-}6^{+}$ bears spin density mainly at C-6 ($\rho_6=0.758$) and C-3 ($\rho_3=0.322$) whereas the charge has its greatest density at C-3 (0.273), which interacts with the hydrogen atoms at C-2, C-4, and the adjacent methyl group; finally, $7\text{-O-Ccy-}6^{+}$ has the unpaired spin essentially localized at C-7 ($\rho_7=0.667$) and the charge is placed on the oxygen, polarizing the bonds to the adjacent atoms, C-6 (0.175), C-1 (0.266), C-3 (0.197), and O-H (0.447). Tandem cyclization product $5,6\text{-tan-}6^{+}$ has the unpaired spin localized on C-2 ($\rho_2=0.944$) whereas the charge on the oxygen atom polarizes the bonds to the adjacent atoms, C-1 (0.323), C-6 (0.265), and O-H (0.473). Finally, $6,4\text{-tan-}6^{+}$ has the unpaired spin localized on C-6 ($\rho_6=1.019$) whereas the charge on the oxygen atom polarizes the bonds to the adjacent atoms, C-1 (0.398), C-3 (0.277) and the adjacent methyl carbon (0.142), and O-H (0.471). The relative enthalpies of the key intermediates are summarized in Figure 5.

Our interest in citronellol, **7**, a terpene with only one double bond, not likely to be an excellent electron donor, arose from the unusual reaction of 6^{+} . This reaction might suggest that the terminal dimethylethylene group serves as the primary electron donor. This possibility can be probed by

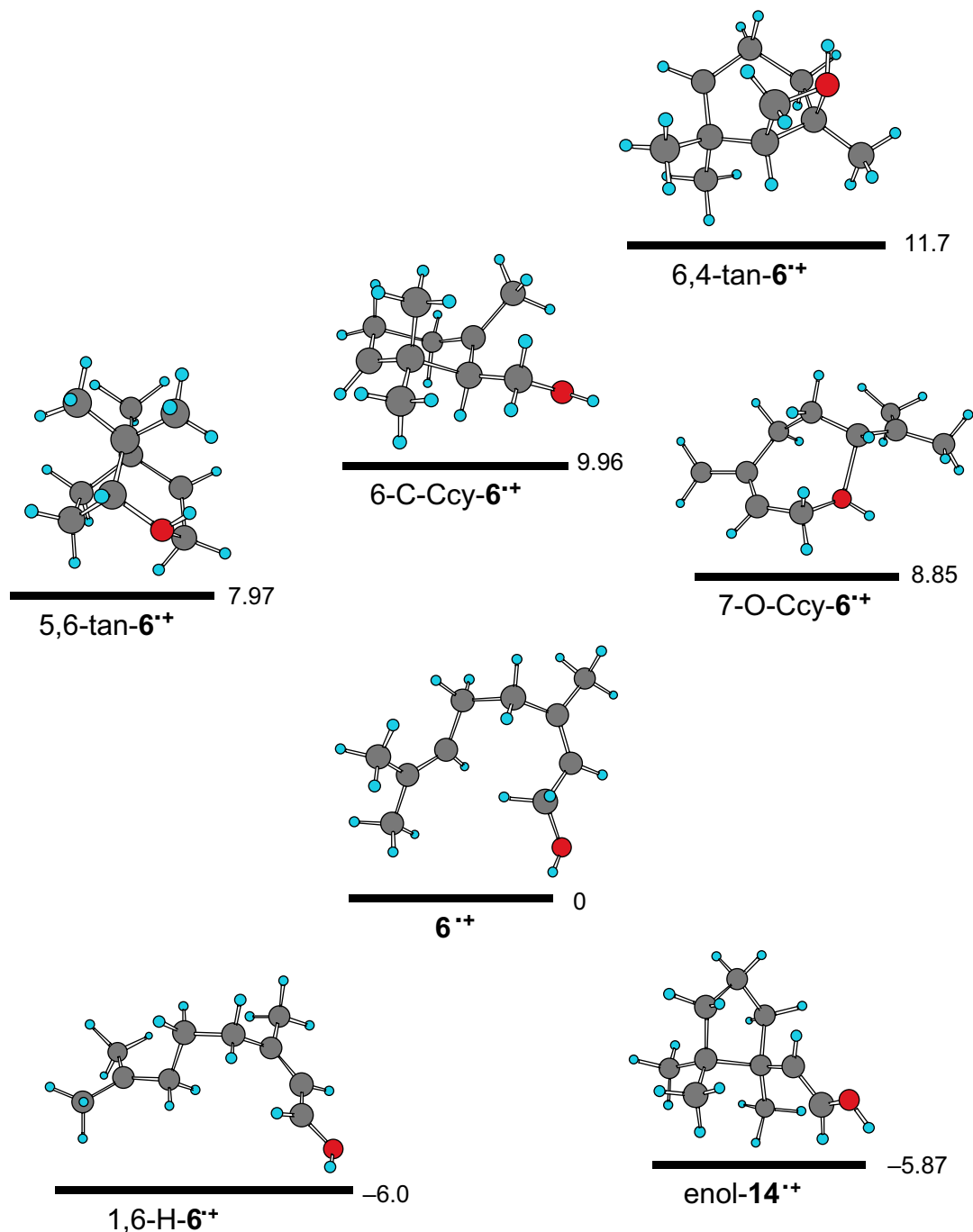
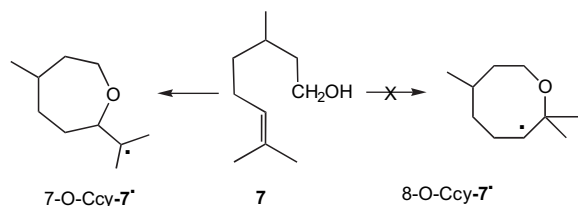


Figure 5. Chem-3D models of nerol radical cation, $6^{+\bullet}$, and isomers: (i) generated by C–C or O–C cyclization, $6\text{-C-Ccy-}6^{+\bullet}$ and $7\text{-O-Ccy-}6^{+\bullet}$, (ii) resulting from tandem cyclization, $5,6\text{-tan-}6^{+\bullet}$ and $6,4\text{-tan-}6^{+\bullet}$, and (iii) formed by a H-shift, $1,6\text{-H-}6^{+\bullet}$, and subsequent cyclization, $\text{enol-}14^{+\bullet}$, respectively. The geometries were calculated by DFT methods with the 6-31G* basis set; relative enthalpies (kcal mol⁻¹) are indicated.

investigating the electron transfer photochemistry of citronellol, **7**, in essence the dihydro-derivative of **6**. Irradiation of **DCA/BP** in the presence of **7** gives rise to oxepane **18** (i.e., dihydro-**17**) in good yield, confirming the dimethylethene function as a suitable electron donor.²²

However, $7^{+\bullet}$ is of interest also because it offers a less biased test for a seven-membered transition state than the formation of **17** from $6^{+\bullet}$. Radical ion $7^{+\bullet}$ lacks the *Z*-arrangement of $6^{+\bullet}$, which limits the hydroxy function to the same hemisphere as the dimethylethene target. In contrast, the reac-

tive groups of $7^{+\bullet}$ have a full complement of conformers accessible and have to meet by conformational diffusion. Again, $7^{+\bullet}$ has the potential to form, in addition, an eight-membered ring system. The fact that this was not realized has thermodynamic as well as kinetic reasons. Energetic reasons favor the product formed via $7\text{-O-C-cy-}7$, because it has a tertiary free radical site compared to the secondary site of $8\text{-O-Ccy-}7^{+\bullet}$. Conformational/kinetic reasons, such as the precedent of the Dieckmann condensation,¹⁹ further argue against the eight-membered transition state as a viable option.



We note, however, that a nucleophilic substitution via an eight-membered transition state has been achieved by Floreancig and co-workers. In this reaction a benzyl group is being replaced by a tethered hydroxy function (vide infra).³² The intramolecular substitution in the system studied does not have the option of a competing pathway, which may be more favorable for either energetic or kinetic reasons.

4.2. Chrysanthemol and homochrysanthemol radical cations—nucleophilic substitution versus nucleophilic capture

The second group of target molecules is comprised of chrysanthemol and homochrysanthemol, whose radical cations, **8⁺** and **9⁺**, offer two different cases of competing pathways between nucleophilic substitution and capture. As derivatives of vinylcyclopropane, the distribution of spin and charge in these species is of special interest. The radical cation of the parent system is of a very special structure type: spin and charge are delocalized between the vinyl group and the tertiary cyclopropane carbon (Fig. 6).³³ This radical cation is one of the few cyclopropane species with two lengthened ring bonds.^{3a,c,d,17,33}

The additional substituents in **8⁺** and **9⁺** distort the symmetry and affect the distribution of spin and charge. The nature of **8⁺** was probed by chemically induced dynamic nuclear polarization (CIDNP), an NMR technique that allows one to derive patterns of hyperfine coupling constants of free

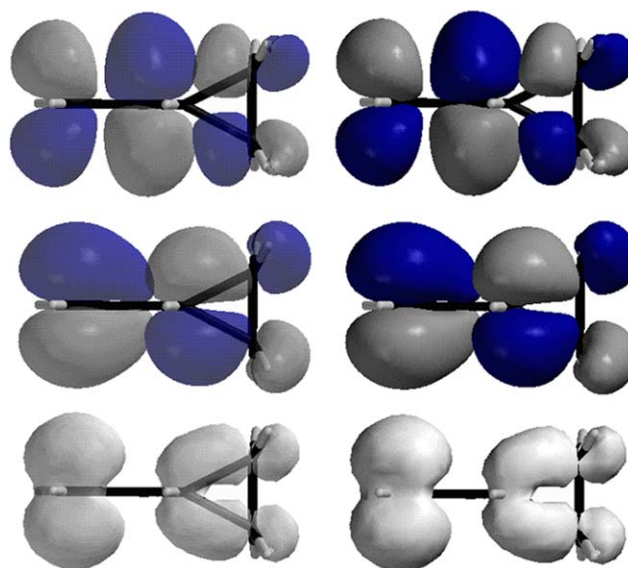


Figure 6. Stereoview of unpaired spin density (bottom), SOMO (center) and LUMO (top) for the radical cation of vinylcyclopropane.³²

radicals and radical ions from enhanced NMR spectra, observed in emission and/or absorption, during radical (ion) pair reactions.³⁴ The CIDNP spectrum of the electron transfer reaction from **8** to photo-excited chloranil (Fig. 7) shows that the spin density of **8⁺** is extended to C-1. This assignment is confirmed by the HOMO and LUMO coefficients of **8⁺** (Fig. 8).²³

The SOMO and LUMO coefficients of **8⁺** and the distribution of spin and charge are such that nucleophilic substitution is possible at two cyclopropane carbons, C-2 and C-3. In addition, nucleophilic capture of the β -carbon in the 2-methylpropenyl side chain is feasible. We evaluate the probability of the potential pathways by considering steric

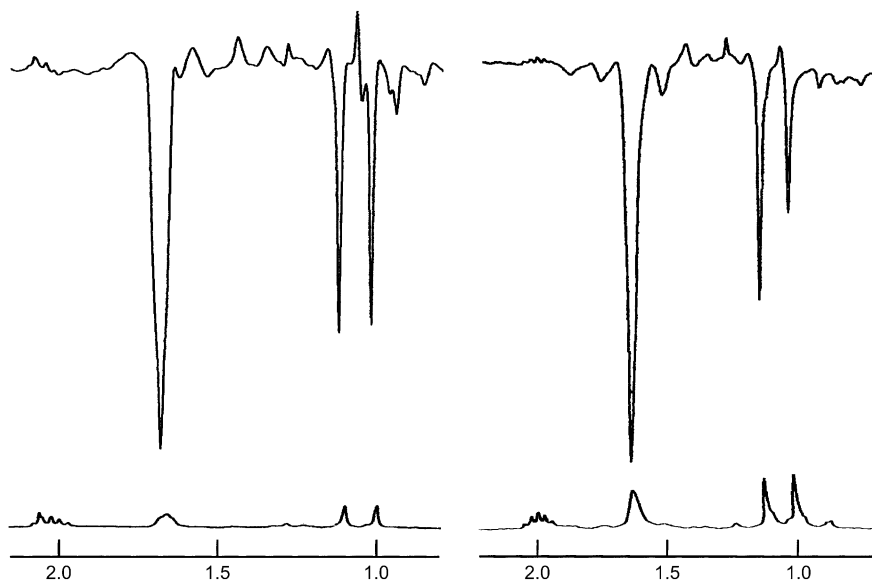


Figure 7. ¹H CIDNP spectra observed during irradiation of chloranil solutions in acetonitrile in the presence of *cis*- (left) and *trans*-chrysanthemol, **8** (right).²³ The spectra support radical cations of very similar spin density distributions. The signals representing the two pairs of non-equivalent methyl groups at ~1.6 and at 1.1 and 1.0 ppm, respectively, show strong emission; the single olefinic resonance appears in weak emission (not shown). The allylic cyclopropane proton (1.25 ppm) and the proton adjacent to the hydroxymethyl group show negligible polarization.

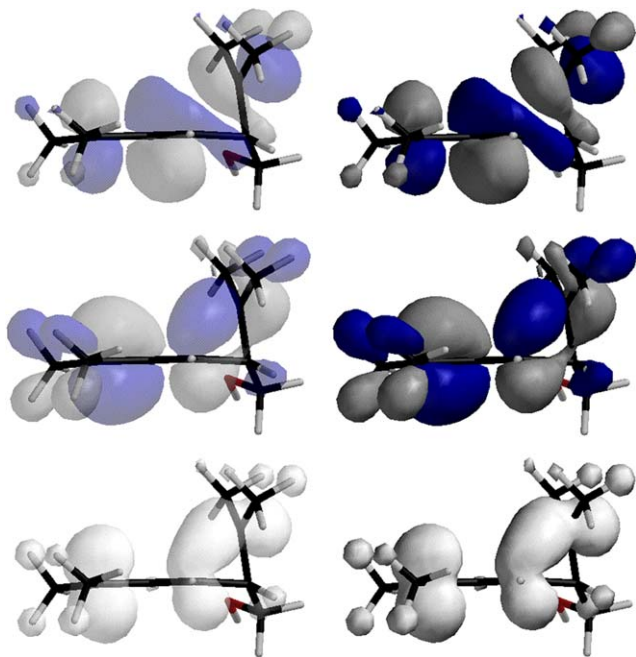
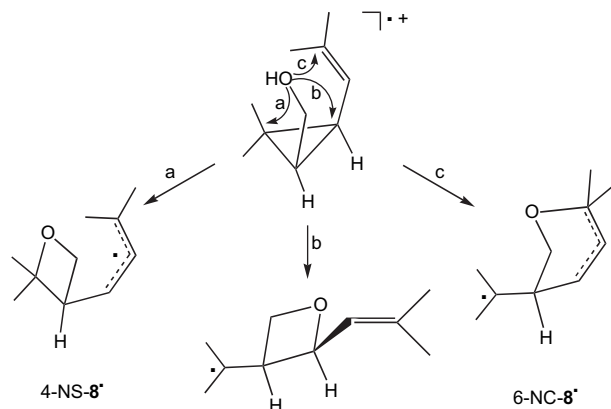


Figure 8. Stereoview of unpaired spin density (bottom), SOMO (center) and LUMO (top) for *cis*-chrysanthemol radical cation, 8^{++} .

and energetic factors. Substitution at C-2 generates 4-NuS- 8^* ; substitution at C-3 generates 4'-NuS- 8^* with inversion of configuration at C-3; finally, nucleophilic capture at the β -carbon forms 6-NuC- 8^* ; the configuration at C-1 is retained in all three reactions.²³

The two pathways leading to oxetane formation do not appear favorable, because they involve replacing a three-membered ring by a four-membered one with negligible change in strain energy. The pathway leading to 4'-NuS- 8^* is particularly unfavorable, because it generates an isolated radical site, albeit a tertiary one, and a double bond rather than an allylic radical, as in 4-NuS- 8^* . For both reactions, the trajectory of approach is far from the ideal 180° . On the other hand, the nucleophilic capture at the β -carbon offers an unencumbered six-membered transition state, which has an additional opportunity of stabilization by subsequent ring

opening with formation of a tertiary free radical as an intramolecular leaving group. Formally, the overall mechanism belongs to the elusive S_N2' type. In view of these considerations, it is hardly surprising that 8^{++} , exclusively forms 6-NC- 8^* .²³ The final product, **19**, once again is formed by aromatic substitution (cf., Scheme 2, Eq. 7).



We illustrate the conformational challenges to intramolecular nucleophilic substitution by exploring the conformational hypersurface of 8^{++} using density functional theory (DFT) methods. The lowest energy conformer of radical cation 8^{++} is one in which the hydroxyl function is deployed far from either electron deficient center, C-2 or C β (Fig. 9). Rotation of the 2-methylpropenyl function around the C-3–C-1' bond results in a complex conformational profile; for comparison, the distance between the oxygen atom and C-2 is shown for selected conformers (Fig. 10).

The case of homochrysanthemol radical cation, 9^{++} , is different because the two reaction types, substitution and capture, now proceed via five- and seven-membered transition states, respectively. This changes the energetic and conformational features for both. Nucleophilic substitution now becomes favorable because of a five-membered transition state in which an allyl radical is an intramolecular leaving group.²⁴ On the other hand, capture of the β -carbon, generating 7-NuC- 9^* , now is encumbered by the presumably less favorable seven-membered transition state.²⁴ As a consequence of

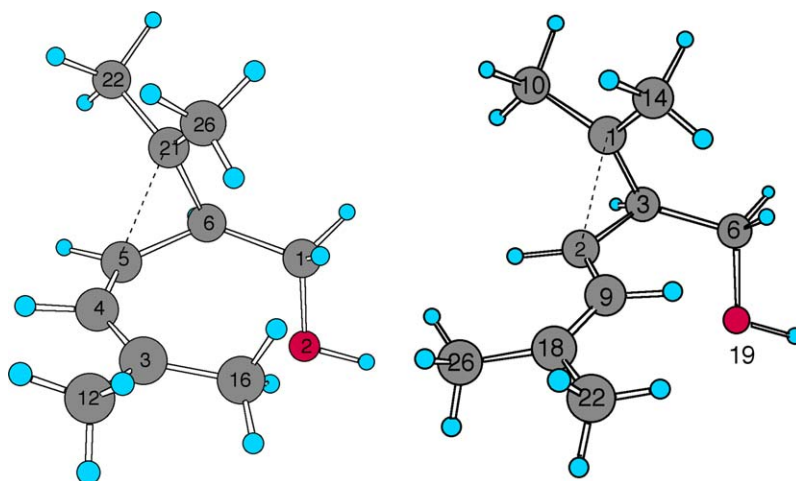


Figure 9. *cis,syn,syn*-Conformer (left) and *cis,syn,anti*-conformer of *cis*-chrysanthemol radical cation, *cis*- 8^{++} (right) calculated by DFT methods (6-31G* basis set).

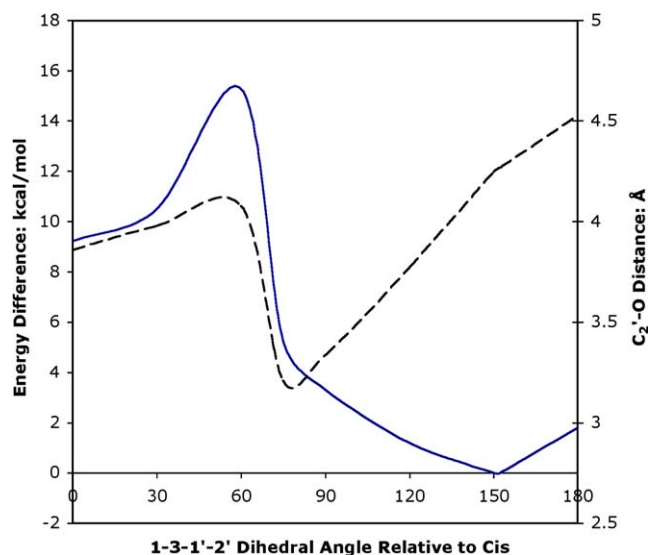
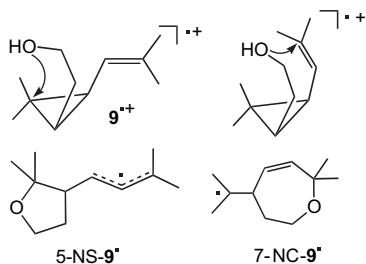


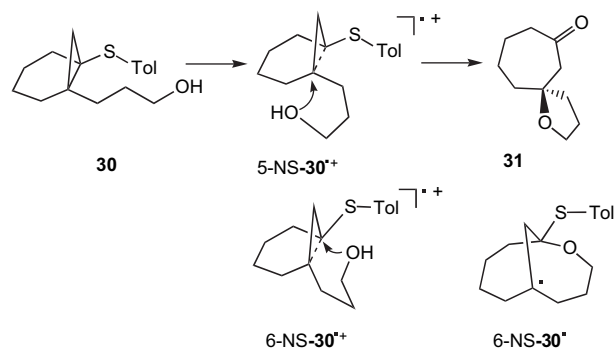
Figure 10. Conformational profile of *cis,syn*-**8⁺⁺**, for rotation around the bond between C-3 and C-1' (—, solid curve) and C-2'-O distance as a function of dihedral angle (---, dashed curve). The geometries of seven individual conformers were calculated by DFT methods (6-31G* basis set).

the changed energetics compared to **8⁺⁺**, the reaction of **9⁺⁺** takes a different course: it proceeds exclusively via the five-membered transition state, producing 5-NuS-**9⁺**. The final product, **20**, once again is formed by aromatic substitution (Scheme 2, Eq. 7).



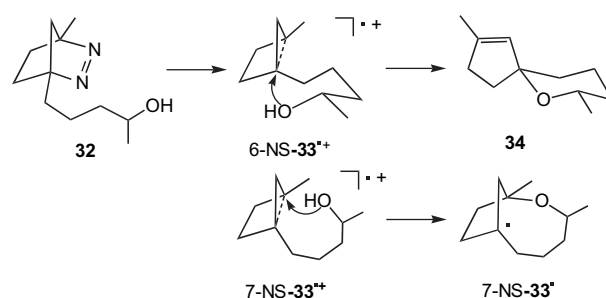
The intramolecular nucleophilic substitution of **9⁺⁺** was not without precedent. A bicyclic system, 1-(3-hydroxypropyl)-bicyclo[4.1.0]heptane radical cation, **30⁺⁺**, was known to form the spiro-fused ether, **31**. This reaction also involves a five-membered transition state, 5-NuS-**30⁺⁺**; it proceeds by backside attack with inversion of configuration and retention of chirality.³⁵ In principle, **30⁺⁺** could also react via a six-membered transition state, viz. 6-NuS-**30⁺⁺**, but the approach of the OH function would have to follow a trajectory far from the ideal 180°. Furthermore, this pathway does not benefit from the favorable loss of benzyl radical (Scheme 3).

Results observed in the photo-induced electron transfer reaction of 1-(4-hydroxypentyl)-4-methyl-2,3-diazabicyclo[2.2.1]hept-2-ene, **32**, provide an interesting complement to those observed for **30**. Radical cation, **32⁺⁺**, yields a [6.4]spiro-fused six-membered ether, **34**, via the deazetized radical cation **33⁺⁺**.³⁶ This product arises by backside attack, via a six-membered transition state, 6-NuS-**33⁺⁺**, with a trajectory near 180°. The rigid steric requirements for intramolecular nucleophilic substitution (as well as for nucleophilic



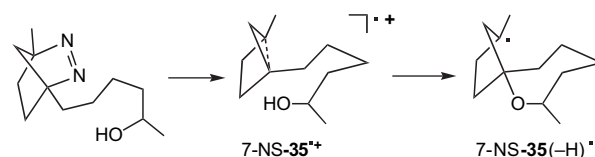
Scheme 3.

substitution in general) are further illustrated by the failure of **33⁺⁺** to yield products that could arise via the seven-membered transition state, 7-NuS-**33⁺⁺** (Scheme 4).

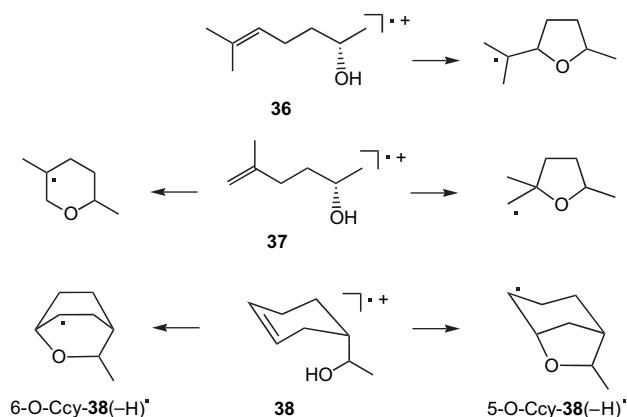


Scheme 4.

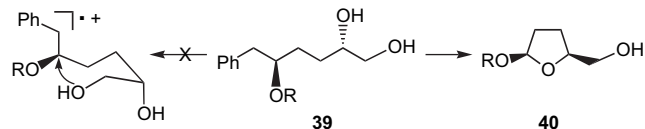
A system similar to **32**, but with a side chain extended by one methylene group, might be useful to probe the feasibility of nucleophilic substitution via a seven-membered transition state, although the approach of the OH function generating the bridgehead free radical 7-NuS-**35⁺** might have a trajectory deviating from the ideal 180°. A reaction of this type was realized by Floreancig (vide infra).



Arnold and co-workers evaluated the intramolecular nucleophilic capture of 6-methyl-5-hepten-2-ol, **36⁺⁺**, 6-methyl-6-hepten-2-ol, **37⁺⁺**, and terpineol [4-(1-hydroxy-1-methyl-ethyl)cyclohexene] radical cations, **38⁺⁺**.³⁷ Their results were published essentially simultaneously³⁸ with our work on geraniol^{22a} and chrysanthemol.²³ The systems studied can form tetrahydrofuran or pyran rings via five- or six-membered transition states, respectively. The five-membered transition state is favored significantly: the internal alkene, **36⁺⁺**, exclusively forms the tetrahydrofuran; the terminal alkene, **37⁺⁺**, preferentially forms the tetrahydrofuran ring, even though this reaction requires formation of a primary radical (!); finally, the terpene, **38⁺⁺**, prefers the five-membered transition state by a ratio of 10:1.

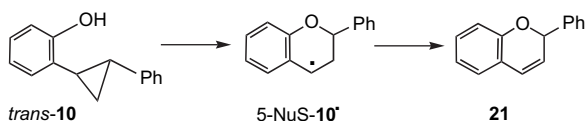


More recently, O–C cyclizations yielding five- through eight-membered rings have been accomplished, in which benzyl groups, the primary seat of spin and charge, act as leaving groups for the tethered hydroxyl function; an alkoxy group at the electrophilic center serves to further weaken the benzylic bond.³² These studies included one case of an intramolecular competition between five- and six-membered transition states. Substrate **39**, which has hydroxyl functions in both γ - and δ -positions, clearly prefers the formation of the tetrahydrofuran derivative, **40**, compared to the cyclization leading to the pyran derivative. In these reactions the promise of synthetic utility is fulfilled.³²



4.3. Electron transfer photosensitized cyclization of *trans*-1-(*o*-hydroxyphenyl)-2-phenylcyclopropane

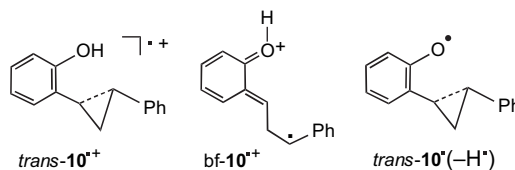
In the light of the preceding discussion, the formation of the dehydrogenated cyclic ether, **21**, upon triphenylpyrylium tetrafluoroborate (TPT) sensitized irradiation of *trans*-**10** poses a highly interesting mechanistic problem. The potential intramolecular capture of *trans*-**10**^{•+} is of special interest because it would amount to an unprecedented front-side substitution with retention of configuration. Formally, the required five-membered transition state has precedence (*vide supra*), but the trajectory is far from the suggested ideal one for nucleophilic substitution.¹⁴



The available evidence supports the intermediacy of the radical cation, *trans*-**10**^{•+}. Thus, the oxidation potential of *trans*-**10** is assumed to lie near that of 1,2-diphenylcyclopropane, $E_{\text{ox}}=1.17$ V versus Ag/Ag⁺,³⁹ given the reduction potential of TPT ($E_{\text{red}}=-0.29$ V vs SCE),⁴⁰ electron transfer is energetically feasible to both the excited singlet state, ¹TPT*

($E_{0,0}=65$ kcal mol⁻¹; $\Delta G\sim-1.0$ eV), and the triplet state, ³TPT* ($E_{\text{T}}=53$ kcal mol⁻¹; $\Delta G\sim-0.5$ eV).⁴¹ In addition, the formal product of intramolecular capture, the benzylic free radical, 5-NuC-**10**[•], is the likely immediate precursor for **21**.

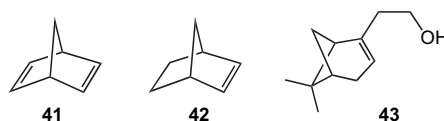
This leaves the question whether *trans*-**10**^{•+} is the direct precursor for 5-NuC-**10**[•], or whether the conversion of *trans*-**10**^{•+} into 5-NuC-**10**[•] proceeds via an additional intermediate and, thus, involves a mechanism other than intramolecular nucleophilic substitution. The electronic structure of *trans*-**10**^{•+} is of major importance in determining its reactivity. Typically, disubstituted cyclopropane radical cations adopt a 'trimethylene' structure in which significant spin and charge reside in one lengthened C–C bond.^{2e,3a,d} However, the presence of the *o*-OH function in conjugation with charge and unpaired spin, may change the structure of *trans*-**10**^{•+} to a bifunctional one, e.g., bf-**10**^{•+}. The details of this interesting conversion go beyond the scope of this paper. Approaches to gain further insight into the mechanism of this reaction will be reported in a separate paper, including the results of density functional theory (DFT) calculations, laser flash photolysis (LFP), and an evaluation of the reactivity of a related phenoxyl radical, *trans*-**10**[•] (–H[•]).



Laser flash photolysis has proved to be an exceedingly valuable tool to probe fast photo-induced conversions. This technique has yielded a wealth of information about free radicals, carbocations, carbenes, or nitrenes.⁴² Molecular orbital calculations, either using *ab initio* or density functional theory (DFT) methods are well suited to elucidate this problem. Structural features such as spin and charge density distribution will delineate the preferred structure type and provide the key to the reactivity of the prevailing species.

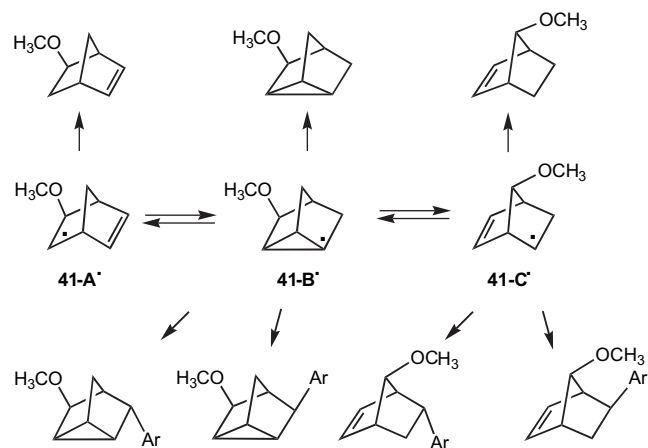
4.4. Electron transfer photosensitized cyclization of *endo*-2-hydroxymethylbicyclo[2.2.1]heptene and related compounds

The final intramolecular reaction to be discussed is the intramolecular capture of radical cation, **11**^{•+}, derived from *endo*-5-norbornene-2-methanol, which forms the tricyclic ether **22**. Compared to the complex structural and mechanistic problem posed by the reaction of *trans*-**10** this system may appear trivial, but it does command some interest in its own right. We selected this target because of its relationship with norbornadiene and norbornene radical cations, **41**^{•+} and **42**^{•+}, respectively, and to the radical cation, **43**^{•+},

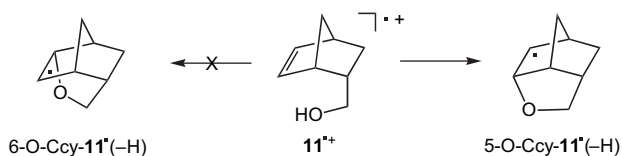


derived from 6,6-dimethylbicyclo[3.1.1]hept-2-ene-2-ethanol (nopol).

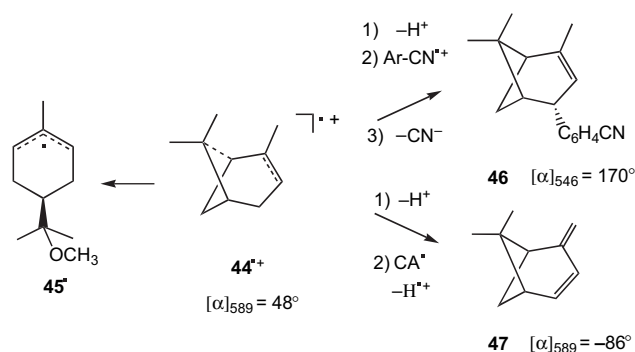
Norbornadiene radical cation, **41**^{•+}, and its valence isomer, quadricyclane radical cation, undergo a rich variety of reactions with nucleophiles.⁴³ Interestingly, **41**^{•+} is captured exclusively from the *exo* face,^{43a,b} but forms a molecular complex with cyanoaromatic radical anions from the *endo* side.^{43c,d} For example, addition of methanol forms a free radical, **41-A**[•], which is in equilibrium with two isomeric radicals, **41-B**[•] and **41-C**[•], by cyclopropylcarbinyl–butenylcarbinyl rearrangements.^{43a,b} The free radicals form products by reduction/protonation^{43b} (Eq. 5, Scheme 2), hydrogen abstraction^{43b} (Eq. 7, Scheme 2), or aromatic substitution (Eq. 6, Scheme 2).^{43b}



Since norbornene, **42**, on the other hand, is attacked from *endo* and *exo* face,^{8c} **11**^{•+} was expected to readily undergo nucleophilic capture. An interesting question concerned the regiochemistry of capture, whether a six-membered transition state might give rise to a tricyclic pyran derivative. The only product isolated from this reaction, **22**, shows that nucleophilic capture via a five-membered transition state prevails; product **22** arises from the tricyclic radical intermediate 5-O-Ccy-**11**(-H)[•] either by hydrogen abstraction (Eq. 7, Scheme 2) or reduction/protonation (Eq. 5, Scheme 2).^{22b}

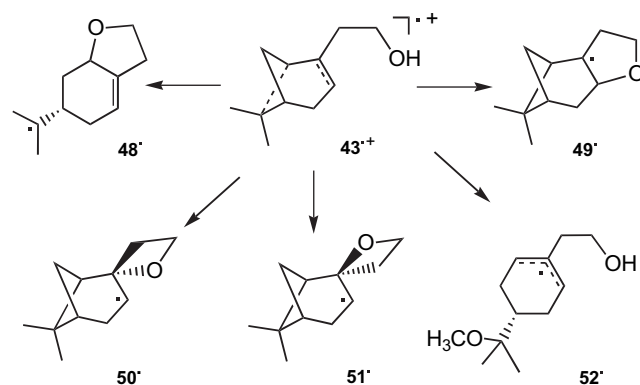


Nopol is one of several vinylcyclobutane systems whose radical cations have attracted attention.^{18,44} As was demonstrated particularly clearly for α -pinene radical cation, **44**^{•+}, these intermediates delocalize spin and charge between the vinyl group and the cyclobutane ring while retaining their chirality.⁴⁵ They are captured by nucleophilic attack on C-6 (\rightarrow **45**[•]) or give rise to unusual ‘substitution’ products, e.g., **46**, which are initiated by deprotonation.^{44,45} The dehydrogenation product, verbenene, **47**, also can be rationalized via deprotonation (Scheme 5).^{44,45}



Scheme 5.

Nopol radical cation, **43**^{•+}, has two potential pathways for intramolecular nucleophilic reaction, capture at C-3 (\rightarrow **49**[•]) and substitution at C-1 (\rightarrow **48**[•]). Given the fact that significant charge density is removed from the alkene function, it may not be too surprising that **43**^{•+} fails to undergo capture. In addition, this reaction will reintroduce any ring strain partially relieved by delocalizing spin and charge into the C-1–C-6 bond. The failure to undergo intramolecular substitution may have steric reasons; the required transition state is different from 5-NuS-**30**^{•+} (vide supra), because three atoms are fixed leaving only rotations around two bonds to align the nucleophile for the required trajectory. Given the relatively high energy calculated for intermediate 5-NuS-**10**^{•+} in the analogous reaction of **10**, it is understandable that **43**^{•+} only reacts with intermolecular nucleophiles (\rightarrow **52**[•]; Scheme 6).¹⁸



Scheme 6.

Concerning the relationship of **11**^{•+} to **43**^{•+}, the analogy is but a formal one, a hydroxyl function attached in a fashion that would allow a five-membered transition state for nucleophilic capture or substitution. The difference in reactivity can be ascribed to the steric and electronic features that set the reactions of **43**^{•+} apart from those of **11**^{•+}. One significant difference that might contribute to the eventual outcome of the reactions, lies in the fact that **11**^{•+} reacts by a Baldwin-5-*exo-trig* process, whereas the conversion of **43**^{•+} to **49**[•] proceeds via a 5-*endo-trig* process. We ignore the 4-*exo-trig* closure, which would generate a spiro-fused system. There is only one analog for this reaction, the formation of 6,4-tan-**6**[•] from 6-C-C-cy-**6**^{•+} (vide supra), where the OH function is captured by an empty p orbital. However, the analogy is remote, as it does not involve a nucleophilic substitution.

5. Conclusion

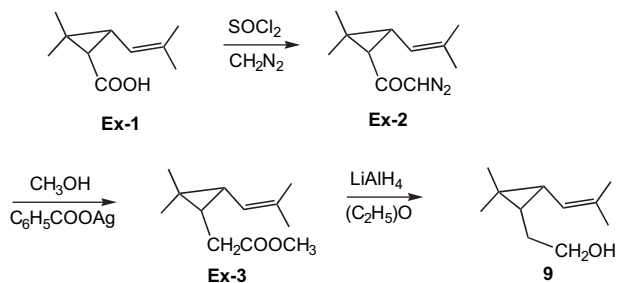
The seven systems, **5–11**, investigated in our laboratory and additional systems, **30, 32, 36–39**, and **43**, reported in the literature, provide a consistent framework for the understanding of intramolecular nucleophilic substitution and capture of alkene and strained ring systems and offer guidelines for further studies. The target molecules form mono-, di-, and tricyclic ethers via four to seven-membered transition states. Not surprisingly, the majority of cyclizations proceed via five- and six-membered transition states for both substitution and capture. A four-membered transition state is realized only in one system: the bicyclic oxetane, **16**, is formed following the C–C cyclization of nerol radical cation, **6⁺**, which places a hydroxy group in close proximity to a carbocationic site with no alternative cyclization accessible.

Two of the systems studied react via seven-membered transition states; in both cases competing reactions via eight-membered transition states are avoided. The outcome of the competition does not reflect kinetic factors alone; the formation of the eight-membered ethers is also unfavorable thermodynamically. Nerol radical cation, **6⁺**, forms a seven-membered ether in competition with C–C cyclizations forming five- and six-membered rings. For homochrysanthemol radical cation, **8⁺**, nucleophilic substitution via a five-membered transition state is preferred over nucleophilic capture via a seven-membered transition state. Finally the formation of dihydropyran, **21**, from *trans*-1-(*o*-hydroxyphenyl)-2-phenylcyclopropane, *trans*-**10**, poses an intriguing mechanistic puzzle.

6. Experimental

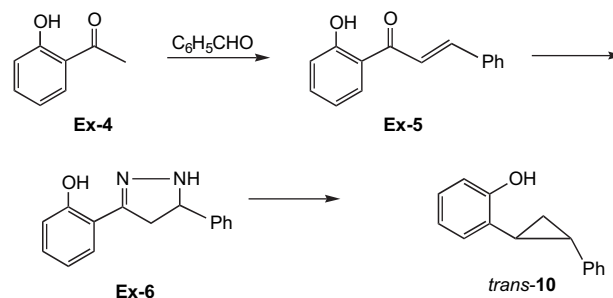
6.1. Materials

Three hydroxy-substituted substrates, **5–7**, are available commercially (Aldrich). Chrysanthemol, **8**, was prepared by LiAlH reduction of the methyl chrysanthemate prepared from a commercially available mixture of *cis*- and *trans*-chrysanthemic acid (Aldrich). Homochrysanthemol, **9**, was prepared by LiAlH reduction of the methyl ester of homochrysanthemic acid, which was prepared by Arndt–Eistert homologation of chrysanthemic acid, **Ex-1**.⁴⁶ The crude diazoketone, **Ex-2**, obtained by treatment of **Ex-3** with thionyl chloride, followed by reaction with diazomethane⁴⁷ was heated in methanol solution in the presence of silver benzoate.⁴⁸



Diarylcyclopropane *trans*-**10** was prepared by a sequence of reactions, initiated by Claisen–Schmidt condensation of benzaldehyde with *o*-hydroxy-acetophenone; condensation

of the resulting chalcone with hydrazine hydrate generated a pyrazoline,^{49,50} which was deacetylated under basic conditions.⁵¹ A mixture of *endo*- and *exo*-5-norbornene-2-methanol (Aldrich) was used without separation because the presence of the *exo*-isomer was not expected to interfere with the chemistry of *endo*-**11⁺**.



The electron acceptor/sensitizers, 1,4-dicyanobenzene (Aldrich; 98%) and phenanthrene (Aldrich; 98%) were purified by recrystallization. 9,10-Dicyanoanthracene (Eastman Kodak) was purified by recrystallization from acetonitrile. Acetonitrile (Fischer), methanol (Fischer), and methylene chloride (Fischer; Spectranalyzed[®]) were distilled from calcium hydride and stored over 4A molecular sieves in brown bottles under argon atmosphere.

6.2. Electron transfer photosensitized reactions—irradiation procedures

Solutions containing 0.1 M of donors **1–5** or **7** and either 0.1 M of 1,4-dicyanobenzene/0.02 M phenanthrene or 0.1 M of 9,10-dicyanoanthracene/0.02 M biphenyl as sensitizer/co-sensitizer in acetonitrile or methylene chloride were deoxygenated by purging with argon for 15 min and irradiated in a Rayonet RPR-100 photoreactor equipped with 16 RPR-3500 lamps. The progress of the reaction was monitored by gas chromatography on a GC/MS system (HP 5890 series II GC interfaced with an HP 5971 mass selective detector), using a 12 m×0.2 mm×0.33 μm HP-1 capillary column (cross-linked methyl silicone on fused silica). Exploratory runs were carried out in 4-mm ID NMR tubes capped with latex stoppers, preparative runs in 30-mm ID tubes with central cooling fingers (water-cooling).

For donor **6** exploratory experiments were carried out by irradiating solutions of 0.02 g substrate in 20 mL methylene chloride with triphenylpyrilium tetrafluoroborate in 10% molar ratio under argon for 1 h in Pyrex tubes surrounding a central quartz cooling jacket with a 125-W medium-pressure mercury lamp. For preparative runs solutions of 1.0 g of the substrate in 400 mL freshly distilled methylene chloride were irradiated at ambient temperature with a 125-W medium-pressure mercury lamp inside a quartz immersion well.

6.3. Isolation of reaction products

Reaction products obtained in yields >5% were isolated by chromatography on columns, 1 cm < ID < 5 cm, packed with ~15-cm of TLC standard grade silica gel (Aldrich; without

binder), and eluted with solvent gradients, usually from light petroleum ether (bp < 65 °C) to mixtures with either methylene chloride or ethyl acetate. Several passes were required to isolate the products.

The product resulting from *trans*-**10** was isolated and purified by conventional column chromatography on silica gel Merck 60 (0.063–0.200 mm), by preparative layer chromatography on silica gel Merck 60 PF₂₅₄, using dichloromethane as eluent, or by means of isocratic HPLC equipment fitted with a semi-preparative Microporasil column, using hexane/ethyl acetate as eluent.

6.4. Characterization/identification of products

Structure assignments of isolated products rest on MS and NMR data, including DEPT, two-dimensional COSY, and HETCOR experiments, where appropriate. NOE difference spectra were recorded to elucidate the substituent stereochemistry and the spatial relationship between the various functional groups. ¹H NMR spectra (CDCl₃; δ, ppm downfield of TMS) were recorded on a Varian XL-400, a 300 MHz Varian Gemini instrument, or a Varian VXR-200 spectrometer. ¹³C and HETCOR spectra were recorded on the Varian VXR-200 spectrometer operating at 50.3 MHz. IR spectra were recorded on a GC-FTIR Hewlett-Packard 5965; the major bands are characterized by their ν_{max} (cm⁻¹). Mass spectra were obtained using a Hewlett-Packard 5988 A spectrometer.

6.5. Computational details

Density functional theory (DFT) and/or ab initio calculations⁵² were carried out with the GAUSSIAN 03 series of electronic structure programs,⁵³ in some cases with earlier versions, using extended basis sets, including p-type polarization functions on carbon (6-31G*). The geometries of the neutral parent molecules and radical cations were optimized at the unrestricted Hartree-Fock (UHF/6-31G**/UHF/6-31G*) and UB3LYP/6-31G* levels, respectively. Previous experience suggests that this level of theory will reproduce the major geometric features of the systems under study. Some radical cations were also calculated to include higher degrees of electron correlation at the MP2 level of theory (MP2/6-31G**/MP2/6-31G*). Wavefunction analyses for charge and spin density distributions used the conventional Mulliken partitioning scheme.⁵²

Møller–Plesset perturbation theory (MP2) reproduces positive ¹H hyperfine coupling constants satisfactorily, but overestimates spin densities on carbon and negative hfc's significantly, often by factors > 2.^{54–57} On the other hand, density functional theory methods⁵⁹ give satisfactory agreement with experimental results.^{58–60} Indeed, positive and negative hfc's of norbornadiene, quadricyclane, and bicyclobutane radical cations are reproduced accurately with either the (B3LYP/6-31G**/MP2/6-31G*) or the (B3LYP/6-31G**/B3LYP/6-31G*) method.^{58–60} In selected cases, including the radical cations of 1,2-dimethylcyclopropane, norcaradiene, vinylcyclopropane, and chrysanthemol, pictorial representations of spin density, SOMO and LUMO were derived with the program SPARTAN.⁶¹ The previously optimized MP2/6-31G* geometries were imported into

SPARTAN, an HF/6-31G* single point calculation was carried out followed by a surface analysis for spin density, SOMO and LUMO.

Acknowledgements

H. D. Roth thanks NSF (Grant NSF-97-14850) and gratefully acknowledges an IBERDROLA Award. R. R. Sauers thanks the National Center for Supercomputer Applications for an allocation of time on the IBM P Series 690 (Grant CHE030060).

References and notes

- (a) *Radical Ions*; Kaiser, E. T., Kevan, L., Eds.; Interscience: New York, NY, 1968; (b) Forrester, R. A.; Ishizu, K.; Kothe, G.; Nelsen, S. F.; Ohya-Nishiguchi, H.; Watanabe, K.; Wilker, W. *Organic Cation Radicals and Polyradicals*. In *Landolt-Börnstein, Numerical Data and Functional Relationships in Science and Technology*; Springer: Heidelberg, 1980; Vol. IX, Part d2; (c) Yoshida, K. *Electrooxidation in Organic Chemistry: The Role of Cation Radicals as Synthetic Intermediates*; Wiley: New York, NY, 1984; (d) Shida, T. *Electronic Absorption Spectra of Radical Ions*; Elsevier: Amsterdam, 1988; (e) *Radical Ionic Systems*; Lund, A., Shiotani, M., Eds.; Kluwer Academics: Dordrecht, The Netherlands, 1991; In addition, SciFinder Scholar retrieves 2352 papers on the chemistry, spectroscopy, and physics of radical cations in the first four years of the current millennium alone.
- (a) Ledwith, A. *Acc. Chem. Res.* **1972**, *5*, 133–139; (b) Shida, T.; Haselbach, E.; Bally, T. *Acc. Chem. Res.* **1984**, *17*, 180–186; (c) Nelsen, S. F. *Acc. Chem. Res.* **1987**, *20*, 269–276; (d) Bauld, N.; Bellville, D. J.; Harirchian, B.; Lorenz, K. T.; Pabon, R. A., Jr.; Reynolds, D. W.; Wirth, D. D.; Chiou, H.-S.; Marsh, B. K. *Acc. Chem. Res.* **1987**, *20*, 180–186; (e) Roth, H. D. *Acc. Chem. Res.* **1987**, *20*, 343–370; (f) Mangione, D.; Arnold, D. R. *Acc. Chem. Res.* **2002**, *35*, 297–304.
- (a) Makosza, M. *Pure Appl. Chem.* **1997**, *69*, 559; (b) Makosza, M.; Wojciechowski, K. *Liebigs Ann.-Rcl.* **1997**, *9*, 1805; (c) Makosza, M.; Wojciechowski, K. *Heterocycles* **2001**, *54*, 445; (d) Makosza, M.; Wojciechowski, K. *Chem. Rev.* **2004**, *104*, 2631.
- (a) Takahashi, Y.; Mukai, T.; Miyashi, T. *J. Am. Chem. Soc.* **1983**, *105*, 6511–6513; (b) Miyashi, T.; Takahashi, Y.; Mukai, T.; Roth, H. D.; Schilling, M. L. M. *J. Am. Chem. Soc.* **1985**, *107*, 1079–1080; (c) Gassman, P. G.; Hay, B. A. *J. Am. Chem. Soc.* **1985**, *107*, 4075–4076; (d) Gassman, P. G.; Hay, B. A. *J. Am. Chem. Soc.* **1986**, *108*, 4227–4228; (e) Arnold, A.; Burger, U.; Gerson, F.; Kloster-Jensen, E.; Schmidlin, S. P. *J. Am. Chem. Soc.* **1993**, *115*, 4271–4281.
- (a) Gassman, P. G.; Hay, B. A. *J. Am. Chem. Soc.* **1985**, *107*, 4075; (b) Gassman, P. G.; Hay, B. A. *J. Am. Chem. Soc.* **1986**, *108*, 4227.
- Arnold, A.; Burger, U.; Gerson, F.; Kloster-Jensen, E.; Schmidlin, S. P. *J. Am. Chem. Soc.* **1993**, *115*, 4271–4281.
- (a) Adam, W.; Walter, H.; Chen, G.-F.; Williams, F. J. *Am. Chem. Soc.* **1992**, *114*, 3007–3014; (b) Weng, H.; Sethuraman, V.; Roth, H. D. *J. Am. Chem. Soc.* **1994**, *116*, 7021–7025; (c) Weng, H.; Sheik, Q.; Roth, H. D. *J. Am. Chem. Soc.* **1995**, *117*, 10655–10661.

8. (a) Neunteufel, R. A.; Arnold, D. R. *J. Am. Chem. Soc.* **1973**, *95*, 4080–4081; (b) Maroulis, A. J.; Shigemitsu, Y.; Arnold, D. R. *J. Am. Chem. Soc.* **1978**, *100*, 535–541; (c) Arnold, D. R.; Snow, M. S. *Can. J. Chem.* **1988**, *66*, 3012–3026; (d) Arnold, D. R.; Du, X. *J. Am. Chem. Soc.* **1989**, *111*, 7666–7667.
9. (a) Klett, M.; Johnson, R. P. *J. Am. Chem. Soc.* **1985**, *107*, 6615–6620; (b) Rao, V. R.; Hixson, S. S. *J. Am. Chem. Soc.* **1979**, *101*, 6458–6459; (c) Mizuno, K.; Ogawa, J.; Otsuji, Y. *Chem. Lett.* **1981**, 742–744; (d) Hixson, S. S.; Xing, Y. *Tetrahedron Lett.* **1991**, *32*, 173–174.
10. (a) Mattes, S. L.; Farid, S. *Org. Photochem.* **1983**, *6*, 233–326; (b) Lewis, F. D. *Photoinduced Electron Transfer*; Fox, M. A., Chanon, M., Eds.; Elsevier: Amsterdam, 1988; Part C, Chapter 4.1; (c) Bauld, N. L. *Adv. Electron Transfer Chem.* **1992**, *2*, 1.
11. (a) Maslak, P.; Asel, S. A. *J. Am. Chem. Soc.* **1988**, *110*, 8260–8261; (b) Maslak, P.; Asel, S. A. *Angew. Chem., Int. Ed. Engl.* **1990**, *29*, 8260–8261.
12. (a) Lorenz, K.; Bauld, N. L. *J. Catal.* **1985**, *95*, 613–616; (b) Roth, H. D.; Schilling, M. L. M. *J. Am. Chem. Soc.* **1985**, *107*, 716–718; (c) Roth, H. D.; Schilling, M. L. M.; Abelt, C. J. *Tetrahedron* **1986**, *42*, 6157–6166; (d) Roth, H. D.; Schilling, M. L. M.; Abelt, C. J. *J. Am. Chem. Soc.* **1986**, *108*, 6098–6099; (e) Miyashi, T.; Konno, A.; Takahashi, Y. *J. Am. Chem. Soc.* **1988**, *110*, 3676–3677.
13. (a) Dinnocenzo, J. P.; Schmittel, M. *J. Am. Chem. Soc.* **1987**, *109*, 1561–1562; (b) Dinnocenzo, J. P.; Conlon, D. A. *J. Am. Chem. Soc.* **1988**, *110*, 2324–2326; (c) Dinnocenzo, J. P.; Todd, W. P.; Simpson, T. R.; Gould, I. R. *J. Am. Chem. Soc.* **1987**, *109*, 1561–1562; (d) Dinnocenzo, J. P.; Todd, W. P.; Simpson, T. R.; Gould, I. R. *J. Am. Chem. Soc.* **1990**, *112*, 2462–2464.
14. (a) Shaik, S. S.; Dinnocenzo, J. P. *J. Org. Chem.* **1990**, *55*, 3434–3436; (b) Shaik, S. S.; Reddy, A. C.; Ioffe, A.; Dinnocenzo, J. P.; Danovich, D.; Cho, J. K. *J. Am. Chem. Soc.* **1995**, *117*, 3205–3222.
15. Wlostowski, M.; Roth, H. D. Unpublished results, cited in Roth, H.D., Ref. 3d.
16. Herberzt, T.; Roth, H. D. Unpublished results, cited in Roth, H.D., Ref. 3d.
17. Herberzt, T.; Blume, F.; Roth, H. D. *J. Am. Chem. Soc.* **1998**, *120*, 4591–4599.
18. Arnold, D. R.; Du, X. *Can. J. Chem.* **1994**, *72*, 403–414.
19. Schaefer, J. P.; Bloomfield, J. J. *Org. React.* **1967**, *15*, 1–203.
20. Makosza, M.; Owczarczyk, Z. *J. Org. Chem.* **1989**, *54*, 5094.
21. (a) Makosza, M.; Goliński, J.; Baran, J. *J. Org. Chem.* **1984**, *49*, 1488; (b) RajanBabu, T. V.; Reddy, G. S.; Fukunaga, T. *J. Am. Chem. Soc.* **1985**, *107*, 5473; (c) Makosza, M.; Bialecki, M. *J. Org. Chem.* **1998**, *63*, 4878.
22. (a) Weng, H.; Scarlata, C.; Roth, H. D. *J. Am. Chem. Soc.* **1996**, *118*, 10947–10953; (b) Weng, H. Ph.D. Thesis, Rutgers University, 1996.
23. Herberzt, T.; Roth, H. D. *J. Am. Chem. Soc.* **1996**, *118*, 10954–10962.
24. Herberzt, T.; Roth, H. D. *J. Org. Chem.* **1999**, *64*, 3708–3713.
25. Delgado, J.; Espinós, A.; Jiménez, M. C.; Miranda, M. A.; Roth, H. D.; Tormos, R., unpublished results.
26. (a) Goldschmidt, C. R.; Potashnik, R.; Ottolenghi, M. *J. Phys. Chem.* **1971**, *75*, 1025–1031; (b) Ottolenghi, M. *Acc. Chem. Res.* **1973**, *6*, 153–160; (c) Schomburg, H.; Staerk, H.; Weller, A. *Chem. Phys. Lett.* **1973**, *21*, 433; (d) Taylor, G. N. Unpublished results, cited in Roth H.D. *Mol. Photochem.* 1973, *5*, 91–126. (e) Schulden, K.; Staerk, H.; Weller, A.; Werner, H. J.; Nickel, H. Z. *Phys. Chem. NF* **1976**, *101*, 371–390; (f) Roth, H. D.; Schilling, M. L. M. *J. Am. Chem. Soc.* **1980**, *102*, 6805–6811; (g) Karki, S. B.; Dinnocenzo, J. P.; Farid, S.; Goodman, J. C.; Gould, I.; Zona, T. A. *J. Am. Chem. Soc.* **1997**, *119*, 431–432.
27. (a) Roth, H. D. *J. Photochem. Photobiol., C: Photochem. Rev.* **2001**, *2*, 93–116; (b) Roth, H. D. *Pure Appl. Chem.* **2005**, *77*, 1075–1085.
28. The aromatic substitution products, *E,E*-, *E,Z*-, *Z,E*-, and *Z,Z*-**12** (R=C₆H₄-CN), are the first of several examples for this product type in this paper. For simple systems, the overall reaction sequence generating them has been dubbed NOCAS, for Nucleophile-Olefin-Combination-Aromatic-Substitution. In French NOCAS is converted to its mirror image, SACON, for Substitution Aromatique avec Combinaison d'une Oléfine et d'une Nucléophile. In the spirit of this acronym, the above reaction is a Tandem-Cyclization-Intramolecular-Nucleophilic-Capture-Aromatic-Substitution or TCINCAS (a creative mind has no limits designing awkward acronyms).
29. Hoffmann, U.; Gao, Y.; Pandey, B.; Klinge, S.; Warzecha, K. D.; Krueger, C.; Roth, H. D.; Demuth, M. *J. Am. Chem. Soc.* **1993**, *115*, 10358–10359.
30. (a) Guo, Q.-X.; Qin, X.-Z.; Wang, J. T.; Williams, F. *J. Am. Chem. Soc.* **1988**, *110*, 1974–1976; (b) Ikeda, H.; Minegishi, T.; Miyashi, T.; Lakkaraju, P. S.; Sauer, R. R.; Roth, H. D. *J. Phys. Chem. B* **2005**, *109*, 2504–2511.
31. Williams, F.; Guo, Q.-X.; Kolb, T. M.; Nelsen, S. F. *J. Chem. Soc., Chem. Commun.* **1989**, 1835–1836.
32. (a) Kumar, V. S.; Floreancig, P. E. *J. Am. Chem. Soc.* **2001**, *123*, 3842–3843; (b) Wang, L.; Seiders, J. R., II; Floreancig, P. E. *J. Am. Chem. Soc.* **2004**, *126*, 12596–12603.
33. Herberzt, T.; Roth, H. D. *J. Am. Chem. Soc.* **1998**, *120*, 11904–11911.
34. (a) Closs, G. L. *Adv. Magn. Reson.* **1974**, *7*, 157–229; (b) Kaptein, R. *Adv. Free Radical Chem.* **1975**, *5*, 319–380; (c) Roth, H. D. *Encyclopedia of Nuclear Magnetic Resonance*, Vol. 2; Grant, D. M., Harris, R. K., Eds.; 1996, pp 1337–1350.
35. Takemoto, Y.; Ohra, T.; Koike, H.; Furuse, S.-i.; Iwata, Ch.; Ohishi, H. *J. Org. Chem.* **1994**, *59*, 4727–4729.
36. Adam, W.; Sendelbach, J. *J. Org. Chem.* **1993**, *58*, 5316–5322.
37. (a) McManus, K. A.; Arnold, D. R. *Can. J. Chem.* **1995**, *73*, 2158–2169; (b) Arnold, D. R.; Connor, D. A.; McManus, K. A.; Bakshi, P. K.; Cameron, T. S. *Can. J. Chem.* **1996**, *74*, 602–612.
38. The independent pursuit of these topics is borne out by the dates of submission of the respective publications, June 20 (Ref. 37a) and November 29, 1995 (Ref. 37b), and July 31 (Ref. 22) and October 26, 1995 (Ref. 23). Of course, all four papers were submitted long after Ref. 29 (May 24, 1993).
39. Wong, P. C.; Arnold, D. R. *Tetrahedron Lett.* **1979**, 2101–2104.
40. Saeva, F. D.; Olin, G. R. *J. Am. Chem. Soc.* **1980**, *102*, 299–303.
41. García, H.; Miranda, M. A. *Chem. Rev.* **1994**, *94*, 1063–1089.
42. (a) Johnston, L. J.; Scaiano, J. C.; Sheppard, J. W.; Bays, J. P. *Chem. Phys. Lett.* **1986**, *124*, 493–498; (b) Das, P. K. *Chem. Rev.* **1993**, *93*, 119–144; (c) Hadel, L. M.; Maloney, V. M.; Platz, M. S.; McGimpsey, W. G.; Scaiano, J. C. *J. Phys. Chem.* **1986**, *90*, 2488–2491; (d) Ford, F.; Yazawa, T.; Platz, M. S.; Ratzinger, S.; Fülischer, M. *J. Am. Chem. Soc.* **1998**, *120*, 4430–4438; (e) Pandurangi, R. S.; Lustak, P.; Kuntz, R. R.; Volkert, W. A.; Rogowski, J.; Platz, M. S. *J. Org. Chem.* **1998**, *63*, 9019–9030.
43. (a) Gassman, P. G.; Olsen, K. D. *Tetrahedron Lett.* **1983**, *1*, 19–22; (b) Weng, H.; Roth, H. D. *J. Org. Chem.* **1995**, *60*, 4136–4145; (c) Weng, H.; Roth, H. D. *Tetrahedron Lett.* **1996**, *37*,

- 4895–4898; (d) Weng, H.; Roth, H. D. *J. Phys. Org. Chem.* **1998**, *11*, 101–108.
44. Zhou, D.; Sheik, M.; Roth, H. D. *Tetrahedron Lett.* **1996**, *37*, 2385–2388.
45. (a) Roth, H. D.; Weng, H.; Zhou, D.; Lakkaraju, P. S. *Acta Chem. Scand.* **1997**, *51*, 626–635; (b) Zhou, D.; Chou, J.; Roth, H. D. *J. Phys. Org. Chem.* **1999**, *12*, 867–874.
46. Crombie, L.; Crossley, J.; Mitchard, D. A. *J. Chem. Soc.* **1963**, 4957–4969.
47. Black, T. H. *Aldrichim. Acta* **1983**, *16*, 3–10.
48. Wiberg, K. B.; Hutton, T. W. *J. Am. Chem. Soc.* **1956**, *78*, 1640–1645.
49. Chattree, N. S.; Sharma, T. C. *Asian J. Chem.* **1994**, *6*, 405–407.
50. Iksanova, S. V. *Geterosikl. Soedin.* **1991**, 1131–1136; *Chem. Abstr.* **1992**, *116*, 194239s.
51. Gao, C.; Hay, A. S. *Polymer* **1995**, *36*, 5051.
52. Hehre, W. J.; Radom, L.; Schleyer, P. v. R.; Pople, J. A. *Ab Initio Molecular Orbital Theory*; Wiley Interscience: New York, NY, 1986; presents a detailed description of the theoretical methods used in this work.
53. Frisch, M. J.; Trucks, G. W.; Schlegel, H. B.; Scuseria, G. E.; Robb, M. A.; Cheeseman, J. R.; Montgomery, J. A., Jr.; Vreven, T.; Kudin, K. N.; Burant, J. C.; Millam, J. M.; Iyengar, S. S.; Tomasi, J.; Barone, V.; Mennucci, B.; Cossi, M.; Scalmani, G.; Rega, N.; Petersson, G. A.; Nakatsuji, H.; Hada, M.; Ehara, M.; Toyota, K.; Fukuda, R.; Hasegawa, J.; Ishida, M.; Nakajima, T.; Honda, Y.; Kitao, O.; Nakai, H.; Klene, M.; Li, X.; Knox, J. E.; Hratchian, H. P.; Cross, J. B.; Adamo, C.; Jaramillo, J.; Gomperts, R.; Stratmann, R. E.; Yazyev, O.; Austin, A. J.; Cammi, R.; Pomelli, C.; Ochterski, J. W.; Ayala, P. Y.; Morokuma, K.; Voth, G. A.; Salvador, P.; Dannenberg, J. J.; Zakrzewski, V. G.; Dapprich, S.; Daniels, A. D.; Strain, M. C.; Farkas, O.; Malick, D. K.; Rabuck, A. D.; Raghavachari, K.; Foresman, J. B.; Ortiz, J. V.; Cui, Q.; Baboul, A. G.; Clifford, S.; Cioslowski, J.; Stefanov, B. B.; Liu, G.; Liashenko, A.; Piskorz, P.; Komaromi, I.; Martin, R. L.; Fox, D. J.; Keith, T.; Al-Laham, M. A.; Peng, C. Y.; Nanayakkara, A.; Challacombe, M.; Gill, P. M. W.; Johnson, B.; Chen, W.; Wong, M. W.; Gonzalez, C.; Pople, J. A. *Gaussian 03, Revision B.02*; Gaussian: Pittsburgh, PA, 2003.
54. Raghavachari, K.; Haddon, R. C.; Roth, H. D. *J. Am. Chem. Soc.* **1983**, *105*, 3110–3114.
55. Raghavachari, K.; Roth, H. D. *J. Am. Chem. Soc.* **1989**, *111*, 7132–7136.
56. Roth, H. D.; Schilling, M. L. M.; Raghavachari, K. *J. Am. Chem. Soc.* **1984**, *106*, 253–255.
57. Krogh-Jespersen, K.; Roth, H. D. *J. Am. Chem. Soc.* **1992**, *114*, 8388–8394.
58. (a) Eriksson, L. A.; Malkin, V. G.; Malkina, O. L.; Salahub, D. R. *J. Chem. Phys.* **1993**, *99*, 9756–9763; (b) Eriksson, L. A.; Malkin, V. G.; Malkina, O. L.; Salahub, D. R. *Int. J. Quant. Chem.* **1994**, *52*, 879–901.
59. Batra, R.; Giese, B.; Spichty, M.; Gescheidt, G.; Houk, K. N. *J. Phys. Chem.* **1996**, *100*, 18371–18379.
60. Roth, H. D.; Herberz, T. 1996, unpublished results.
61. *SPARTAN, SGI Version 4.0.4 GL*; Wavefunction: Irvine, CA, 1991–1995; Deppmeier, B. J.; Driessen, A. J.; Hehre, W. J.; Johnson, H. C.; Leonard, J. M.; Yu, J.; Lou, L., Development Staff; Baker, J.; Carpenter, J. E.; Dixon, R. W.; Fielder, S. S.; Kahn, S. D.; Pietro, W. J., Contributors.

Explicit and implicit solvation of radical ions: the cycloreversion of CPD dimers

 Nicolas J. Saettel^a and Olaf Wiest^{b,*}
^a*C.E.R.M.N., University of Caen, 5, rue Vaubénard, 14032 Caen Cedex, France*
^b*Department of Chemistry and Biochemistry, University of Notre Dame, Notre Dame, IN 46556, United States*

Received 24 August 2005; accepted 1 November 2005

Available online 25 April 2006

Abstract—The electron transfer catalyzed cycloreversion of cyclobutane pyrimidine dimers is the key step in repair of light-induced DNA lesions catalyzed by the enzyme CPD photolyase. The formation of the CPD radical anion was found to be strongly solvent dependent due to a specific hydrogen bond that stabilizes the valence bound state over the dipole bound state of the additional electron. The effect of solvation on the vertical and adiabatic electron affinity of uracil and uracil dimers as well as on the mechanism of the cycloreversion of the uracil dimer radical anion is explored for three model systems that include explicit solvent molecules at the B3LYP/6-311++G**/B3LYP/6-31+G* level of theory. The second solvation shell is described using the implicit C-PCM solvation model. These calculations indicate an effectively barrierless mechanism. These results are in agreement with the available experimental data for the reaction energies and isotope effects. It is also shown that a single hydrogen bond donor is a sufficient minimal model for the first solvation shell by adequately describing the stabilization of the valence bound state of the radical anion through hydrogen bonding. The relationship of these model systems with the enzymatic reaction catalyzed by DNA photolyase is also discussed.

© 2006 Elsevier Ltd. All rights reserved.

1. Introduction

UV irradiation of DNA with wavelengths around 280 nm induces the [2+2] cycloaddition between adjacent thymine bases to form cyclobutane-like *cis*, *syn* thymine dimer **TT**, or cyclobutane pyrimidine dimer (CPD), as the major product (Fig. 1). This lesion is the principal cause for skin cancer as it blocks cell replication and transcription. The enzyme CPD photolyase is capable of reversing this process by using near-UV and visible light (300–500 nm) and has been the subject of a number of reviews.^{1–11} The cycloreversion of

the neutral cyclobutane moiety is thermally forbidden according to the Woodward–Hoffman rules of orbital symmetry.¹² From the same rules, a photo-induced cycloreversion is symmetry allowed, but the system lacks the conjugated π system necessary for absorption of visible light.

To circumvent this problem, CPD photolyase uses electron transfer catalysis to promote the cycloreversion of the CPD lesion. The now commonly accepted pathway is shown in Scheme 1 for the example of the most simple CPD, the uracil pyrimidine dimer **UU**. The first step of the repair is the

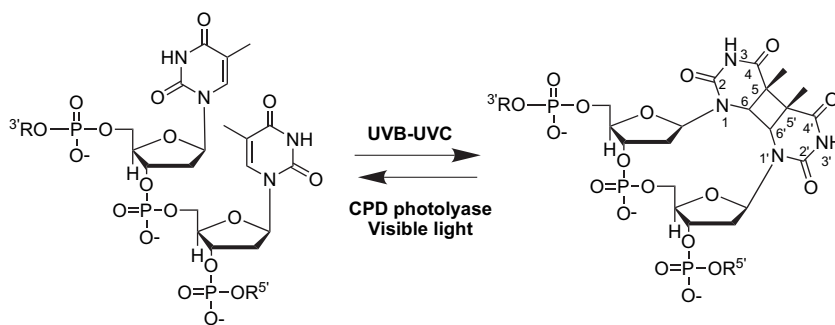
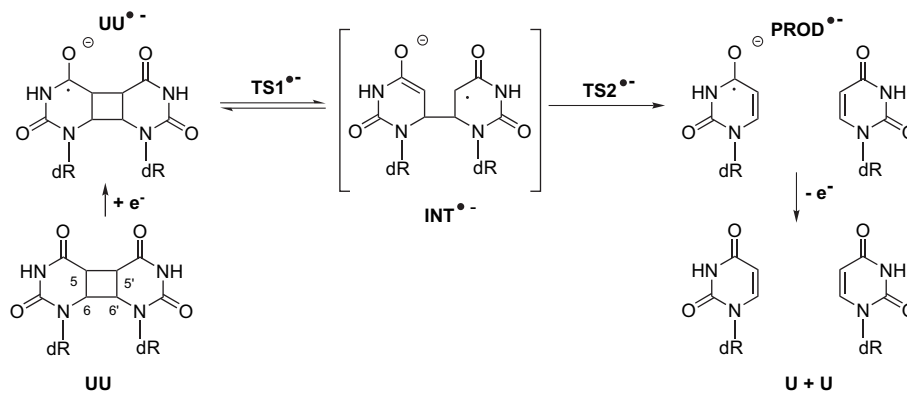


Figure 1. Formation and cycloreversion of the *cis*, *syn*-thymine dimer **TT**.

* Corresponding author. Tel.: +1 574 631 5876; fax: +1 574 631 6652; e-mail: owiest@nd.edu



Scheme 1. Radical anionic pathway for the cycloreversion of uracil dimer **UU**.

one-electron reduction to form the radical anion $UU^{\bullet-}$. This electron transfer (ET) is induced by the absorption of a photon by a light-harvesting cofactor, followed by a Förster-type transfer of the excitation energy to the catalytic cofactor $FADH^-$. The S_1 state of the flavin then acts as the donor in the ET for $UU^{\bullet-}$. Upon addition of the electron to the uracil dimer (**UU**), the [2+2] cycloreversion of the cyclobutane moiety is accelerated greatly by weakening the C5–C5' bond. In a stepwise mechanism, after C5–C5' bond breaking through the transition state $TS1^{\bullet-}$, $UU^{\bullet-}$ leads to the intermediate $INT^{\bullet-}$, which may or may not exist as a distinct, short-lived reactive intermediate with an enolate on one moiety and an α -carbonyl radical on the other. Subsequent breaking of the C6–C6' bond via $TS2^{\bullet-}$ leads to the complex ion-molecule $PROD^{\bullet-}$, which gives the two pyrimidine bases **U+U** upon back electron transfer (BET) to the $FADH^-$.

Despite the importance of this reaction for DNA repair and maintaining the genetic integrity of the living cell, there are relatively little reliable experimental data available for this reaction due to the inherently complex mechanism and the short lifetime of the species involved. The anionic cycloreversion was found to be exothermic by 21 kcal/mol using photothermal beam deflection calorimetry for the neutral reaction and fluorescence quenching experiments.¹⁴

In contrast to the radical cationic pathway, which has been shown to be stepwise by trapping the corresponding 5,5'-singly linked radical cation intermediate $INT^{\bullet+}$,¹⁵ the presence of an intermediate in the radical anionic pathway could not be proven experimentally, by either trapping through a cyclopropylcarbinyl rearrangement,¹⁶ cleavage of a 5-CH₂OMs substituted photodimer¹⁷ or observation by low-temperature EPR.¹⁸ These results make the existence of INT doubtful and a concerted mechanism was postulated based on kinetic isotope effect studies,² even though the interpretation of isotope effects ET catalyzed reactions in complex.^{19,20} More recently, potential evidence for a distinct stepwise pathway has been observed by ultrafast spectroscopy.²¹

Computational investigations of the radical anionic reaction mechanism have been ambiguous too. As discussed in more detail in a recent review,²² calculations of the reaction pathway in the gas phase using a variety of methods yielded very

different results for electron affinity, reaction mechanism, and overall reaction energetics. This indicates that the underlying physical model, i.e., the calculation of a single molecule in the gas phase, might not be appropriate and needs to be evaluated carefully. First, unless large basis sets incorporating diffuse functions are used, the Electron Affinity (EA) of pyrimidine dimers is endothermic with *ab initio* methods. Second, the relationship between the dipole and valence bond states and its dependence on the computational method used is unclear. Finally, gas phase calculations neither reproduce the thermodynamics nor give a clear picture of the mechanism of the reaction. In a previous communication,²³ we addressed these points and presented the first reconciliation between theory and experiment, based on calculations of hydrogen bonded uracil dimers.

In this contribution, an investigation of the effects of solvation on the electron affinities and the reaction mechanism of the cycloreversion of the cyclobutane uracil dimer radical anion $UU^{\bullet-}$ is presented. Besides providing a more detailed picture of how the environment affects the reaction mechanism, the unique dependence of the properties of the radical anions involved in the environment make them an interesting test case for the performance evaluation of solvent models. To address these questions, the previously published model involving three water molecules and $UU^{\bullet-}$ will be compared to simpler models using a single hydrogen bond donor with and without implicit description of solvation by a cavity model. Finally, we will discuss some technical issues in the application of implicit solvent models for the calculation of radical anions.

2. Computational methodology

Because of the close energy spacing of the orbitals, an adequate treatment of electron correlation is crucial for accurate calculation of radical ions. The best way to treat electron correlation for these systems, however, has been a matter of current discussion.^{24–35} We adopted a computational strategy in which all structures were fully optimized at the B3LYP level of theory with the 6-31+G* basis set, followed by harmonic frequency analysis to ensure that all species have the correct number of negative eigenvalues. The G98 and G03 series of programs³⁶ has been used for all calculations and the one negative eigenfrequency of the transition structures was

animated using MOLDEN³⁷ to ensure that the optimized stationary point corresponds to the transition structure of the desired reaction. In cases where the imaginary normal mode in the transition structure was not unambiguous or the localization of intermediates was difficult, intrinsic reaction path calculations (IRC) were performed. Final energies were evaluated using the 6-311++G** basis set.

The description of solvation beyond the first solvent shell, which is described *explicitly* in the hydrogen bonded systems, can be achieved by a number of popular *implicit* solvation models derived from statistically averaged information on the solvent effects. The different methods within this model differ in the size and shape of the solute cavity, the method of calculating the cavity creation and the dispersion contributions, how the charge distribution of the solute is represented, and how the dielectric medium is described. A number of reviews of this field appeared over the past few years.^{38–42} In general, the cavity models available in electronic structure calculation programs can reproduce the behavior of a solvent from averaged descriptions, but lack the description of specific interactions on a solute, such as hydrogen bonds. In our case, where the effect of such an interaction has already been addressed, implicit solvation calculations can provide additional information.

We investigated the solvent effects using the C-PCM model⁴³ implemented in the Gaussian³⁶ series of programs. It derives from the original Polarizable Continuum Model^{44–46} where the surrounding medium is modeled as a conductor instead of a dielectric, based on Klamt's concept (the COSMO model).⁴⁷ The most important practical aspect is that the procedure replaces the normal component of the electric field on the cavity tesserae with the electrostatic potential, making the surface-charge solving process non-iterative since it is included directly in the SCF procedure, with a noticeable reduction in computational costs. Also the problems of the solvent outlying charge are noticeably reduced.

3. Results and discussion

3.1. Dipole versus valence bound states

The electronic structure of the radical anions of nucleobases has been a topic of intense interest in the last decade.⁴⁸ Two distinct states can be distinguished upon electron attachment to a molecule. The valence bound (VB) state has the extra electron localized in a valence shell of the molecule corresponding to its LUMO. It is the most common way for a molecule to localize an extra electron. In addition, the dipole bound (DB) state is characterized by having its electron localized outside the molecular frame and towards the attractive field of the permanent molecular dipole moment.⁴⁹ This state is energetically accessible, provided the dipole moment of the molecule is above 2.5 D.⁵⁰ Their relevance to DNA and RNA bases attracted some attention both experimentally and theoretically over the past decade.⁵¹

A DB state in the gas phase for the bases uracil and/or thymine has been observed experimentally using negative ion photoelectron spectroscopy (PES),⁵² charge exchange with

laser-excited Rydberg atoms,^{49,53–57} and photodetachment-photoelectron (PD-PE) spectroscopy.⁵⁸ Using very diffuse functions, several groups were able to calculate DB states with positive electron affinities close to the experimental values.^{56,57,59–64} Since thymine and thymine dimer have dipole moments of 4.5 D and 7 D, respectively,⁶⁵ the importance in the gas phase of such a state for the study of the DNA lesion is non-negligible.

The stabilization of the VB state by hydrogen bonding has been first postulated by Adamowicz. The complexes of uracil with water,^{66–69} and with uracil,⁷⁰ thymine⁷¹ or adenine⁷² have been investigated computationally with as high as the MP2/6-311++G** level of theory. The transformation from DB to VB state was later observed experimentally by negative ion photoelectron spectroscopy⁷³ and photodetachment-photoelectron spectroscopy.⁵⁸ Bonding with water stabilizes the valence state of the radical anion more than the dipole state, because the stabilizing interaction of the hydrogen-bonded water is greater with the localized electron density in the molecular frame.

An agreement between the calculated and experimental EAs has been elusive because of the problems associated with the description of weakly bound electrons in the VB versus DB states, and the uncertainties found in the experimental values. In particular, only negative or small EAs were obtained by calculations. Sevilla and co-workers scaled *ab initio* results to fit experimental results.^{74–78} More recent calculations critically evaluated the experimental data and compared them with highly correlated methods and diffuse basis sets and bracketing techniques, giving very low VB AEAs of approximately 0.2 eV.^{51,79–82}

In general, the C2 carbonyl is considered as the strongest binding site and most of the studies mentioned above are focused on that site. However, the C4 position is more accessible in the case of a thymine base. In addition, a water molecule can bridge the two C4 carbonyls in the case of the dimer, which is thus more relevant in this case. Lastly, the C4 carbonyl is the relevant position in the active site, since it is the position because of which a radical anion is stabilized by hydrogen bonding. Thus, bonding of water to the C4 carbonyl was investigated first.

Table 1 summarizes calculations at the B3LYP/6-31++G**//B3LYP/6-31+G* level of theory and structures are shown in Figures 2–4. On the basis of the gas phase calculations of electron affinities, these results allow one to dissect how incorporation of hydrogen bonded water molecules stabilizes

Table 1. Vertical (VEA) and adiabatic (AEA) electron affinities of uracil and uracil dimer with different numbers of water (in kcal/mol)

		U/ 0·H ₂ O	U/ 1·H ₂ O	U/ 2·H ₂ O	U/ 3·H ₂ O	UU/ 1·H ₂ O	UU/ 3·H ₂ O
Gas phase	VEA	−6.3	−2.5	−2.4	−0.3	8.7	7.9
	AEA ^a	4.9	18.6	15.7	16.5	29.1	32.6
Ether	VEA	27.5	29.8	29.6	30.0	30.2	30.5
	AEA ^a	38.6	48.9	45.4	46.4	53.6	47.8
Water	VEA	37.1	39.0	39.4	40.2	37.4	38.9
	AEA ^a	48.2	57.5	54.6	55.3	60.1	58.6

^a Zero-point corrected using B3LYP/6-31+G* frequencies.

the uracil anion valence state and provides a reasonable model for the study of the subsequent reaction. In particular, it is clear that the stabilization of the VB state of the radical anion by one or more water molecules is even more pronounced for the case of $\text{UU}^{\cdot-}$. Direct comparison of the values reported in Table 1 with experimental data is not straightforward. The reduction potential of uracil in water is reported to be -1.1 eV versus NHE.⁸³ Taking into account the absolute potential of NHE of 4.44 ± 0.02 eV,⁸⁴ it is clear that the combination of implicit and explicit water models underestimates the stability of the uracil radical anion by as much as 1 eV. Nevertheless, the application of the implicit solvation model beyond the first solvent shell does improve agreement with experiment considerably, demonstrating that the long-range stabilization of the negative charge by the solvent is important. The performance of the C-PCM model for the relative electron affinities of U and UU is much better. Although experimental values for the direct comparison of the redox potentials of U and UU in water are not available, the energy difference for the three water models of 1.4 and 3.3 kcal/mol in ether and water, respectively, is in good agreement with the experimental value of 1.4 kcal/mol measured for 1,3-dimethyl thymine and its dimer in acetonitrile.⁸⁵ Thus, the relative reduction potentials can be predicted quite well, while the absolute stabilities are consistently too low, most likely due to an underestimation of the solvent stabilization of the radical anions. It is not only clear that the calculation of systems like the ones discussed here remains a significant challenge for cavity-type solvation models, but also that they could also serve as useful benchmarks in the development of new methods for the implicit treatment of solvation. Figure 2 shows the structures of uracil with and without a water molecule and its corresponding anion. One can observe a distortion from planarity upon electron uptake, with a deformation of the C4 carbonyl function due to the initial ketyl radical anion formation. Pyramidalization of the C6 center can be rationalized in terms of involvement of the β -radical enolate resonance form.

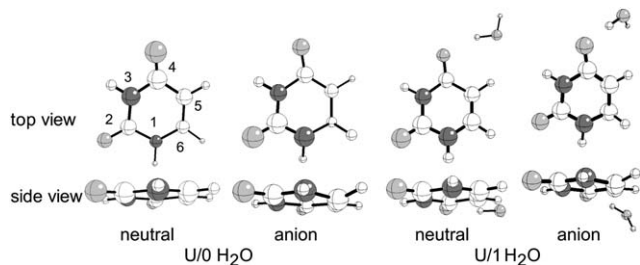


Figure 2. Two views of neutral and radical anion uracil with and without water.

Figure 3 shows uracil with three water molecules. Due to a very flat hypersurface, several minima, all less than 1 kcal/mol, with different orientations of water can be found. There were several other orientations of the water molecules found. These are all within 1 kcal/mol of each other, indicating a very flat hypersurface with multiple minima. In all cases, the hydrogen-bonding distances are shortened from 1.9–2.0 Å in the neutral form to 1.7–1.8 Å in the radical anion. These stronger hydrogen bonds are reflected in the energetics; the VEA is negative, and the AEA does not change substantially from the one- or two-water model.

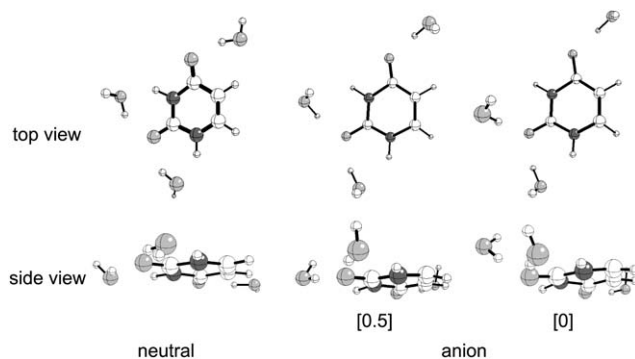


Figure 3. Uracil with three water molecules. Values in brackets are relative energies in kcal/mol.

This indicates that the specific interactions occurring in the first solvation shell are well reproduced with three water molecules.

The hydrogen-bonding effect is more important in the case of uracil dimer. UHF or MP2/6-31G* calculations of uracil give a negative EA of about -28 kcal/mol.⁸⁶ Introduction of one bridging H_2O across the C4 carbonyl groups of UU increases the EA to $+29.1$ kcal/mol. Three water molecules do not change the adiabatic EA significantly from the one-water model, indicating that a single specific interaction is responsible for the bulk of the effect. This indicates that the introduction of one or more water molecules is a reasonable model for studying the reaction in solution. Hydrogen bonding is also important for substrate recognition in the active site. Previously, *Escherichia coli* CPD photolyase was found to interact through Trp³⁸⁴ with the C4 carbonyl of a thymine dimer lesion in DNA.^{87–89} More recently, the crystal structures of CPD photolyase from *Thermus thermophilus* with thymine in its active site⁹⁰ and a DNA duplex containing a model of CPD, bound to *Aspergillus nidulans* photolyase⁹¹ were solved. In the first structure, the C2 carbonyl is hydrogen bonded to Asn³⁴⁰, and the second part of the dimer is postulated to interact with Glu²⁴⁴, while in the second, the model of CPD is hydrogen bonded to the amino group of the adenine in the FADH cofactor.

3.2. Effects of explicit solvation on the mechanism of the cycloreversion

Previously, we have shown that hydrogen bonding to the radical anion has a dramatic effect not only on the electron affinity of the CPD, but also on the reaction mechanism for the cycloreversion of the CPD radical anion. The results for a test system surrounded by three explicit water molecules were found to be in good agreement with the available experimental data.²³ In the complex interplay of the hydrogen bonding and charge distribution between the CPD radical anion and the three explicit water molecules, it is less clear what influence the individual components has and what the minimal model for an adequate description of the reaction is. We have therefore studied several other model systems to elucidate the effect of hydrogen bonding on the reaction mechanism.

Figure 4 summarizes the results of the cycloreversion for a model system where a single water molecule bridges the

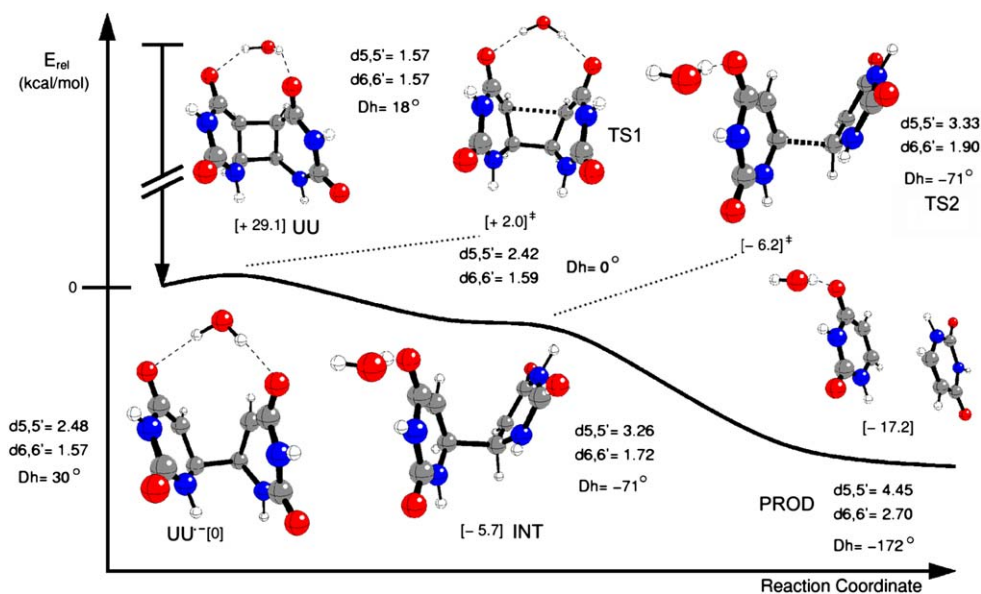


Figure 4. Reaction pathway for the one-water system. All energies are zero-point corrected B3LYP/6-311++G**//B3LYP/6-31+G*.

two C4 carbonyl groups. Dh represents the dihedral angle formed by the atoms C5–C6–C6′–C5′.

As mentioned before, the AEA of uracil dimer is exothermic by 29 kcal/mol because the hydrogen bonding stabilizes significantly the radical anion formed by electron transfer. This is in contrast to the value of -20.3 kcal/mol calculated at the same level of theory for thymine dimers in the gas phase⁶⁵ and demonstrates again the importance of specific interactions with water. During the UU radical anion cycloreversion, the cyclobutane framework undergoes distinctive changes. Upon ionization, the C5–C5′ bond length is considerably increased, going from 1.6 Å to 2.5 Å, with a concomitant twisting of the initial cyclobutane ring (Dh increases) and a deformation similar to the parent uracil radical anion. This can be rationalized in terms of delocalization of the singly occupied C4–O π^* orbital into the C5–C5′ σ^* orbital.⁹² Then, Dh changes from $+30^\circ$ in the anion to -71° in the intermediate. The transition state is characterized by an essentially planar C5–C6–C6′–C5′ framework, and the associated imaginary frequency corresponding to a rotation having for axis the C6–C6′ bond. The activation energy for this process is with 2 kcal/mol very small. In the intermediate, which is 5.7 kcal/mol lesser in energy than $\text{UU}^{\cdot-} \cdot \text{H}_2\text{O}$, the water can no longer bridge the two C4 carbonyls due to the large Dh, and stays with the moiety where the negative charge is localized. The C6–C6′ bond is already elongated, and further increases its bond length in the second transition state, while the other geometric parameters resemble the intermediate. After zero-point correction, the barrier disappears. On the way to the final complex, the two uracil molecules orient themselves in an opposite direction to minimize the total dipole moment of the model. The overall exothermicity is calculated to be -17.2 kcal/mol.

The overall reaction mechanism predicted for this model system is very similar to the one reported earlier for the model system containing three explicit water molecules.²³ This shows that a single hydrogen bond is sufficient to

achieve the stabilization of the valence bound state as a ketyl radical anion and gives an effectively concerted reaction pathway. Even though a formally stepwise pathway is found, it is downhill and barrierless after the first transition state, which is only slightly higher in energy than $\text{UU}^{\cdot-} \cdot \text{H}_2\text{O}$ and easily accessible at ambient temperature. The differences with the previous studies at the same level of theory, which predicted the intermediate to be separated from the product by a 14 kcal/mol barrier,⁹³ can be rationalized in terms of localization of spin and charge through the hydrogen bonded water molecule. The assumption of a destabilization of the gas phase intermediate by the geometry-constraining enzyme, proposed previously,⁹⁴ is not necessary to rationalize the concerted reaction mechanism. However, the one-water system does not reproduce the experimentally observed overall thermochemistry of the reaction. The value of 17.2 kcal/mol is too low by 4 kcal/mol compared to the experimental value^{14,13} when only one water molecule is explicitly included in the calculation. This is due to the fact that in this model system, the water molecule can only bind to the product radical anion. The neutral uracil remains unsolvated, which is not a good model for the experimental conditions.

In light of the finding that a single water molecule constitutes a sufficient minimal model, it is interesting to investigate the role of the other two water molecules in the previous system. As discussed above, the main differences between the three-water model and the one-water model are in the values of the EA and the overall thermochemistry. We thus revisited the structures for the neutral uracil dimer UU and its radical anion as well as the product ion–molecule complex in the presence of the water molecules.

Figure 5 shows two different orientations of the water molecules around the neutral uracil dimer within 1 kcal/mol. With three coordinating water molecules around UU, other water orientations and slightly higher energy structures were found. Due to the flatness of the hypersurface, they

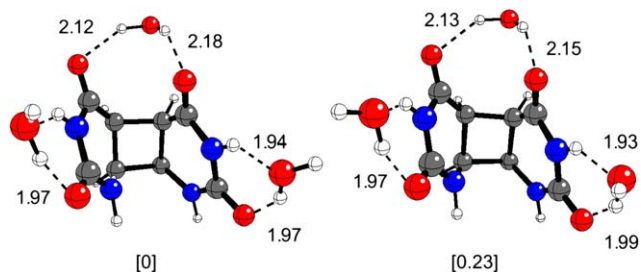


Figure 5. Different orientations of three water molecules bound to uracil dimer. Relative energies are shown in kcal/mol and distances in Å.

are virtually identical in energy. This suggests that the interactions between **UU** and water are relatively weak and the exact position of the water molecules does not have a large energetic effect. **Figure 6** shows three different conformations of the water molecules around the **UU^{•-}** radical anion, with energy differences as high as 5.6 kcal/mol. It can thus be concluded that the exact position of the water molecules is much more important in this case. The lowest energy species is the one where hydrogen bonding is maximized in a network of hydrogen bonds with the C-4 oxygen that localizes the negative charge of the radical anion acting as an acceptor in two hydrogen bonds. It is noteworthy that this structure is also the one where C6–C6' bond length is 1.57 Å, the shortest of all the **UU^{•-}** considered. This is most likely because of an additional bridging water molecule holding the C5–C6–C6'–C5' moiety in a well-defined conformation.

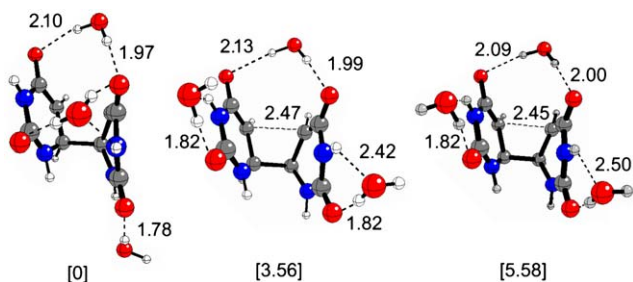


Figure 6. Different orientations of three water molecules bound to uracil dimer radical anion. Relative energies are shown in kcal/mol and distances in Å.

The reaction pathway of this three-water system was already reported in a communication²³ and will only be reviewed briefly here. The first step of the cycloreversion reaction has an activation energy of 1.1 kcal/mol, only 0.9 kcal/mol smaller than the one-water system. Subsequent bond breaking is barrierless, with an exothermicity of 21.5 kcal/mol, in accordance with the experimental results. In the final complex, a network of water molecules holds the two molecules together in a π -stacking fashion. The importance of this network is demonstrated by the fact that another structure with an energy 8.7 kcal/mol higher than the stacked structure was also calculated (**Fig. 7**). The orientation of the dipoles opposite to each other found in the gas phase calculation, is now overcome by the hydrogen-bonding network. This structure is also reminiscent to a restrained active site where radical substrate movement like in the one-water systems is restricted by the residues.

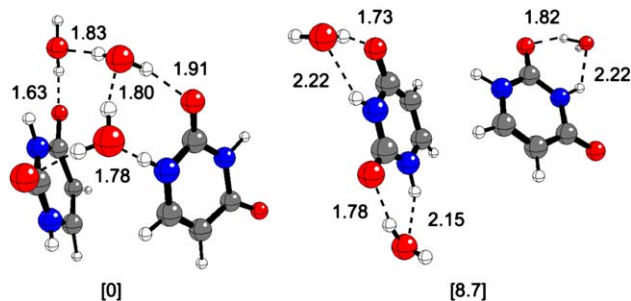


Figure 7. Different conformers of the product of cycloreversion. Relative energies are shown in kcal/mol and distances in Å.

3.3. Amine system

In the available computational models of the enzyme–substrate complex^{87–89} as well as in the recent X-ray structure of a DNA duplex containing a model of CPD, bound to *A. nidulans* photolyase,⁹¹ the C4 carbonyl oxygen of CPD is hydrogen bonded to an NH, either in the indole ring of a tryptophane residue or in the amino group of the adenine in the FADH cofactor. This raises the question whether there will be significant differences between the hydrogen bonding to the water molecules in our model systems, which could lead to partial protonation, and the hydrogen bonding to N–H bonds in the enzyme, which will be based on the relative pK_a 's of the ketyl radical anion and the amine. Hydrogen-bonded methyl vinyl amine (MVA) was thus introduced in our calculations as a model for specific interactions in the active site of CPD photolyase.

The resulting reaction pathway is very similar to the one-water pathway with some noticeable differences (**Fig. 8**). In the initial ionization, the C5–C5' bond elongates more than that in the one-water system. Because methyl vinyl amine can only provide one hydrogen bond, and a weaker one, it cannot provide the restraint that the bridging water does. Thus, the localization of spin and charge is more pronounced and the EA of the amine-bonded system is thus lower than the water-bonded one. The second significant difference is the disappearance of the barrier for C5–C6–C6'–C5' rotation after zero-point correction (even at the B3LYP/6-31+G* level, it is a negligible 0.3 kcal/mol) since no hydrogen bond needs to be broken. Since the C6–C6' bond breaking is identical to the one-water system, the process is barrierless.

The overall exothermicity of the reaction is 16.9 kcal/mol. This value is the first estimate of the energetics of the reaction taking place in the enzyme as the MVA bonding models the tryptophan bonding in the active site. As in the one-water system, the product complex has the two uracil molecules aligning their dipole moments in opposite directions. This geometry is almost certainly not present in the active site of the enzyme for the residues create a pocket where steric interactions would hold the two uracil molecules close to their initial position. A large change in Dh would not be feasible. It can therefore be expected that a bridged hydrogen bonding as indicated by the bifurcated interaction observed in the experimental X-ray structure⁹¹ and modeled by a water in our calculations, or a single hydrogen bonding as predicted by our model of the enzyme–substrate complex⁸⁷

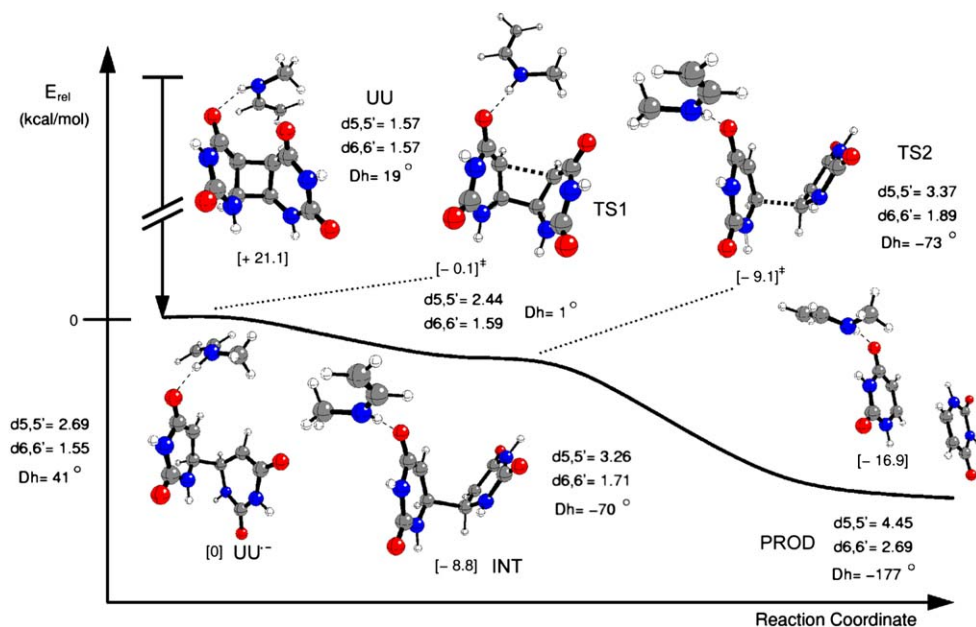


Figure 8. Reaction pathway for the amine system. All energies are zero-point corrected B3LYP/6-311++G**//B3LYP/6-31+G*.

and represented by the MVA in this model system, will lead to very similar results. This is indeed found in our calculations where the change from a water to an amine system showed little changes. In both cases, the reaction is essentially barrierless and strongly exothermic. Kinetic isotope effects in solution, in CPD photolyase and in an antibody all gave similar results that led the authors to conclude a concerted mechanism.^{95,96} It is demonstrated that hydrogen-bond interaction either with solvent or an active site model renders the cycloreversion concerted and non-synchronous.

3.4. Summary of the systems

Table 2 gives an overview of the three systems considered, with the energies of the optimized B3LYP/6-31+G* structures and the zero-point corrected B3LYP/6-311++G** single point calculations. Using the larger basis set with more diffuse and polarized basis functions influences the EA and the overall exothermicity of the cycloreversion, but not the relative energies of the transition states and intermediates. They are necessary to account for those systems, however, since they describe hydrogen bonding and anionic species more accurately. The good agreement between the energies obtained from the two basis sets also shows that the smaller basis set gives reasonable results based on error

cancellation between similar species along the reaction pathway.

The EA of the uracil dimer increases when stronger hydrogen bonds are formed, and when the system can form several of them. A complexed amine or a water molecule does not change significantly the exothermicity of the reversion; however, a hydrogen-bond network can stabilize the complex uracil–uracil radical anion complex.

When introducing only one hydrogen-bonded molecule to the cycloreversion of the uracil dimer radical anion, a plausible mechanism for this process can be described. Through an amine hydrogen bond, a model for the splitting in CPD photolyase is achieved. An arrangement of three water molecules is sufficient to account for the first solvation shell and reproduce experimental results for the reaction thermodynamics of model systems in the condensed phase. Because specific hydrogen bonds stabilize the valence states of the radical anion species, the effect of the first solvation shell is well reproduced in these systems: a non-synchronous concerted pathway with a low to no activation barrier for cycloreversion after the initial ionization. The effect of a surrounding medium as an averaged property in the second solvation shell can now be addressed. This is the subject of the next section.

Table 2. Comparison of hydrogen bonded systems with different basis sets

	1H ₂ O		MVA		3H ₂ O	
	6-31+G* ^a	6-311++G** ^b	6-31+G* ^a	6-311++G** ^b	6-31+G* ^a	6-311++G** ^b
UU	+28.1	+29.1	+26.2	+21.1	+31.8	+24.8
UU ⁻	0	0	0	0	0	0
TS1	+2.1	+2.0	+0.3	-0.1	+1.4	+1.1
INT	-5.4	-5.7	-8.4	-8.8	-5.1	-5.6
TS2	-5.5	-6.2	-8.5	-9.1	-5.2	-6.0
PROD	-15.3	-17.2	-15.1	-16.9	-20.9	-21.5

All values are zero-point corrected at the B3LYP/6-31+G* level.

^a Optimized geometries.

^b Single-point calculations at the 6-31+G* geometry.

3.5. Solvent effects

The one-water and amine systems, which model the initial interaction of a solvation shell and a specific active site, respectively, were analyzed in the presence of solvent to account for the second solvation shell effects. Apart from being a biologically important study, it can also constitute a test case for the performance of implicit solvation models due to the difficulties encountered in calculations of radical anions. The cycloreversion was studied with the C-PCM method in two solvents. Water ($\epsilon=78.39$) was used to account for further effects in solution other than the specific hydrogen bonding to the C4 carbonyl. Since the active site has no averaged macroscopic properties but discrete interactions (van der Waals, hydrogen bonds...), the assignment of an average dielectric constant for a protein active site is an open question. Honig has evaluated the electrostatic effect of active sites and suggested a value of $\epsilon=4$.^{97–99} Thus, the characteristics of the solvent ether ($\epsilon=4.335$) were introduced in the second calculation. However, the effect of the dielectric constant in the PCM model is largest for low values of ϵ due to the functional form of the underlying Onsager equation. Therefore, little changes are expected between water and ether.

In the course of these studies, several interesting technical issues arose. First, the combination of the solvation model and diffuse basis functions led to problems in converging the wavefunctions. Second, the amount of charge escape obtained by using the default parameters was found unacceptably high (in some cases larger than 10%). The C-PCM parameters radii, number of tesserae, and scaling factor were thus adjusted for the species **INT** in the amine system to minimize the amount of charge escape from the solute cavity (3–4%) and used throughout the calculations, except for the calculation of the **INT**–**MVA** complex in a water cavity, where 80 tesserae were necessary to obtain a converged wavefunction. The results of these calculations are shown in Table 3.

As expected, **UU**^{•−} is much more stabilized by the solvent cavity than the neutral **UU**, increasing the electron affinity in water by 32 kcal/mol in the case of the one-water system. This effect is even more pronounced in the case of the amine system, where only one weaker hydrogen bond is formed between the C4 carbonyl of one uracil moiety and the amine

Table 3. Comparison of gas phase and C-PCM energies

	1H ₂ O			MVA		
	Gas phase	Water	Ether	Gas phase	Water	Ether
UU	+29.1	+61.4	+53.9	+21.1	+57.1	+50.2
UU ^{•−}	0	0	0	0	0	0
TS1	+2.0	+1.0	+1.3	−0.1	−1.0	−0.7
INT	−5.7	−4.5	−4.8	−8.8	−8.3 ^a	−8.8
TS2	−6.2	−4.8	−5.1	−9.1	−8.5	−8.2
PROD	−17.2	−10.7	−11.9	−16.9	−12.1	−12.9

All values are zero-point corrected at the B3LYP/6-31+G* level. Parameters: RADII=PAULING (Merz–Kollman atomic radii), ALPHA (scaling factor for the definition of the solvent accessible surface)=1.5, TSNUM (number of tesserae for each sphere)=70. Values optimized based on the least amount of charge diffusion in the case of **INT**.

^a TSNUM=80.

hydrogen. Thus, the initial stabilization by MVA complexation is less, as can be seen by EA comparison of the two systems in the gas phase. This plays again a role in the exothermicity of the reaction. In water, the one-water system is less exothermic by 6.5 kcal/mol compared to the gas phase. This is explained by the fact that the bridging water molecule in **UU**^{•−} delocalizes the extra electron on the whole system, making the two uracil units equivalent with respect to their charge. However, in **PROD** the charge is localized on one uracil and only one hydrogen bond can be achieved by the water. The effect of the solvent on the whole system is thus less important. This charge delocalization through the water molecule is best illustrated by the electrostatic surface potential (ESP) mapped onto the electron density surface rendered by the program ArgusLab 3.0¹⁰⁰ and is shown in Figure 9. Whereas the ESP charge is spread over the whole dimer **UU**^{•−} through the bridging water, a neutral uracil with little extra charge density accounts for half of the complex **PROD**.

In analogy to the above argument, the magnitude of the solvent effect on the exothermicity of the amine system is only 4.8 kcal/mol in water. This is again represented by Figure 10, where the smaller extent of a delocalization through the amine hydrogen bond is clearly visible.

Compared to the large change in exothermicity, no significant changes in the relative energies of **TS1**, **INT** and **TS2** are observed in the cavity compared to the gas phase calculations. Finally, the changes between water and ether cavity

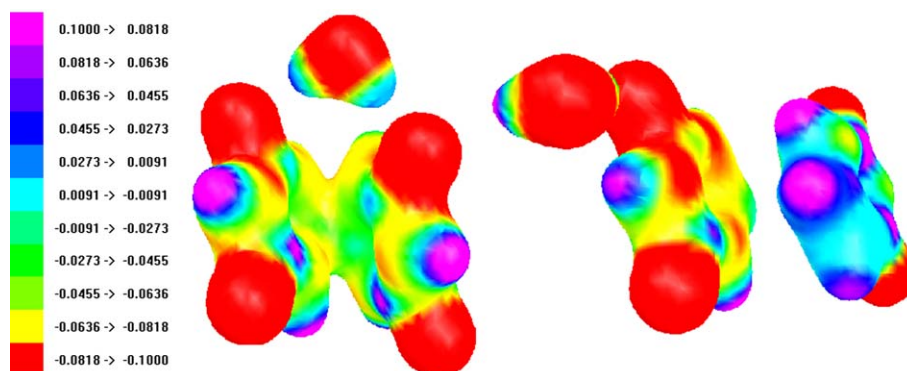


Figure 9. ESP mapped on electron density for **UU**^{•−} (left) and **PROD** (right) for the one-water system.

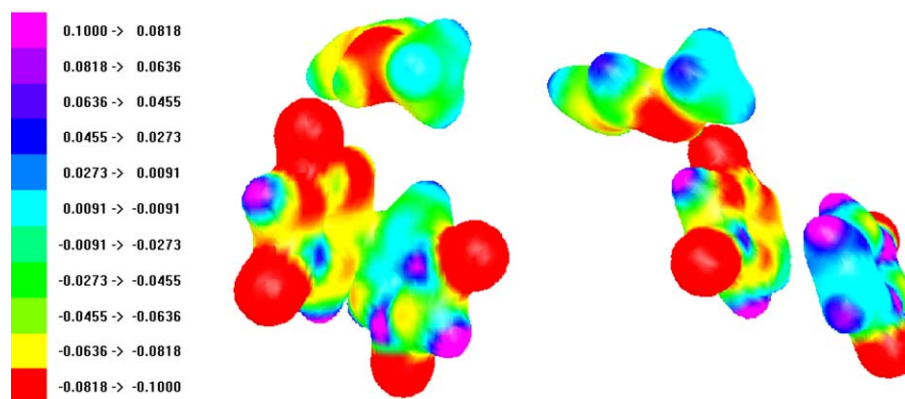


Figure 10. ESP mapped on electron density for UU^- (left) and **PROD** (right) for the amine system.

are minimal, either having a lesser influence of approximately 7 and 1 kcal/mol on the EA and the exothermicity, respectively.

4. Conclusions

Since the discovery of DNA repair by the enzyme CPD photolyase, much effort has been deployed toward a better understanding of its mode of action. Whereas energy and charge transfer have been successfully studied, theory could not be reconciled with experimental results on the key process, the splitting of the thymine dimer radical anion. In our study, the mechanism of the anionic cycloreversion of the DNA UV lesions was elucidated by the introduction of one hydrogen bond responsible for the reversal of the relative energies of dipole and valence states. Several systems accounting for behavior in solution or in the active site were investigated, and solvent effects were evaluated by means of dielectric continuum theory.

The electron transfer catalyzed cycloreversion of pyrimidine dimers is strongly influenced by specific hydrogen-bonding interactions that stabilized the radical anion. A single hydrogen bond to one of the C4 carbonyl group is sufficient to stabilize the valence bond state of the radical anion, resulting in an exothermic electron affinity and an effectively barrierless cycloreversion. A water molecule, which represents a minimal model of the reaction in aqueous solution, bridges between the two C4 carbonyls of the dimer. The results for a complex, with a methyl vinyl amine, designed to represent the previously described hydrogen bond of the pyrimidine dimer in the active site of CPD photolyase are very similar, indicating again that the bulk of the interactions is caused by a single hydrogen bond. The structure of intermediates along the pathway shows an immediate C5–C5' bond breaking followed by a twisting of the cyclobutane framework on the way to the final complex, which can adopt a stacking or *anti* conformation depending on its surroundings. The effect of a solvent environment is rationalized in terms of further stabilization of the initial radical anion. Although the reaction pathway is described qualitatively correct by these minimum models, a more complex model involving explicit consideration of the first solvent shell is necessary to correctly describe the thermochemistry of the reaction.²³

The solvation interactions in the product complexes responsible for the accurate description of the overall reaction thermochemistry cannot be satisfactorily described by the C-PCM cavity solvation model alone. As a result, absolute electron affinities in solution are consistently underestimated by as much as 1 eV. Relative electron affinities between compounds and model systems are described much more accurately, allowing the dissection of the influence of different interactions in the model systems. Computed electron affinities and plots of the electrostatic surfaces indicate that the localized reactant complex is strongly stabilized, lowering the computed reaction energies. In comparison, the relative energies of the stationary points along the reaction pathways are not affected strongly because the degree of delocalization of the additional electron over the molecule is very similar in all cases.

Acknowledgements

We gratefully acknowledge financial support of our work on the chemistry of radical ions by the National Institutes of Health (CA073775), the National Science Foundation (CHE-9733050 and CHE-0415344) as well as the Dreyfus Foundation for a Camille Dreyfus Teacher-Scholar Award to O.W. We would also like to thank the Office of Information Technology at the University of Notre Dame for the generous allocation of computing resources.

Supplementary data

All coordinates, energies, zero-point corrections, and solvation energies of the species discussed, along with negative frequencies of transition states. Supplementary data associated with this article can be found in the online version, at doi:10.1016/j.tet.2006.03.059.

References and notes

1. Sancar, A. *Biochemistry* **1994**, *33*, 2–9.
2. Begley, T. P. *Acc. Chem. Res.* **1994**, *27*, 394–401.
3. Heelis, P. F.; Hartman, R. F.; Rose, S. D. *Chem. Soc. Rev.* **1995**, *24*, 289–297.

4. Heelis, P. F.; Hartman, R. F.; Rose, S. D. *J. Photochem. Photobiol.*, A **1996**, 95, 89–98.
5. Carell, T.; Burgdorf, L.; Butenandt, J.; Epple, R.; Schwogler, A. *Bioorganic Chemistry*; Diederichsen, U., Lindhorst, T. K., Westermann, B., Wessjohann, L. A., Eds.; Wiley-VCH: Weinheim, 1999; pp 337–345.
6. Sancar, G. B. *Mutat. Res.* **2000**, 451, 25–37.
7. Deisenhofer, J. *Mutat. Res.* **2000**, 460, 143–149.
8. Carell, T.; Burgdorf, L. T.; Kundu, L. M.; Cichon, M. *Curr. Opin. Chem. Biol.* **2001**, 5, 491–498.
9. Sancar, A. *Chem. Rev.* **2003**, 103, 2203–2238.
10. Sancar, A. *Adv. Protein Chem.* **2004**, 69, 73–100.
11. Weber, S. *Biochim. Biophys. Acta* **2005**, 1707, 1–23.
12. Woodward, R. B.; Hoffmann, R. *The Conservation of Orbital Symmetry*; Academic: New York, NY, 1970.
13. Scannell, M. P.; Yeh, S. R.; Falvey, D. E. *Photochem. Photobiol.* **1996**, 64, 764–768.
14. Scannell, M. P.; Fenick, D. J.; Yeh, S.-R.; Falvey, D. E. *J. Am. Chem. Soc.* **1997**, 119, 1971–1977.
15. Burdi, D.; Begley, T. P. *J. Am. Chem. Soc.* **1991**, 113, 7768–7770.
16. Fenick, D. J.; Falvey, D. E. *J. Org. Chem.* **1994**, 59, 4791–4799.
17. McMordie, R. A. S.; Altmann, E.; Begley, T. P. *J. Am. Chem. Soc.* **1993**, 115, 10370–10371.
18. Pezeshk, A.; Podmore, I. D.; Heelis, P. F.; Symons, M. C. R. *J. Phys. Chem.* **1996**, 100, 19714–19718.
19. Reddy, G. D.; Wiest, O.; Hudlicky, T.; Schapiro, V.; Gonzalez, D. *J. Org. Chem.* **1999**, 64, 2860–2863.
20. Saettel, N. J.; Wiest, O.; Singleton, D. A.; Meyer, M. P. *J. Am. Chem. Soc.* **2002**, 124, 11552–11559.
21. MacFarlane, A. W. I. V.; Stanley, R. J. *Biochemistry* **2003**, 42, 8558–8568.
22. Harrison, C. B.; O’Neil, L. L.; Wiest, O. *J. Phys. Chem.* **2005**, 109, 7001–7012.
23. Saettel, N. J.; Wiest, O. *J. Am. Chem. Soc.* **2001**, 123, 2693–2694.
24. Bally, T.; Borden, W. T. *Calculations on Open-Shell Molecules: A Beginner’s Guide*; Lipkowitz, K. B., Boyd, D. B., Eds.; Reviews in Computational Chemistry; Wiley: New York, NY, 1999; Vol. 13, pp 1–97.
25. Hrouda, V.; Roeselova, M.; Bally, T. *J. Phys. Chem.* **1997**, 101, 3925–3935.
26. Hrouda, V.; Carsky, P.; Ingr, M.; Chval, Z.; Sastry, G. N.; Bally, T. *J. Phys. Chem.* **1998**, 102, 9297–9307.
27. Wiest, O. *Theochem* **1996**, 368, 39–48.
28. Ma, N. L.; Smith, B. J.; Radom, L. *Chem. Phys. Lett.* **1992**, 193, 386–394.
29. Nobes, R. H.; Moncrieff, D.; Wong, M. W.; Radom, L.; Gill, P. M. W.; Pople, J. A. *Chem. Phys. Lett.* **1991**, 182, 216–224.
30. Mayer, P. M.; Parkinson, C. J.; Smith, D. M.; Radom, L. *J. Chem. Phys.* **1998**, 108, 604–615.
31. Sastry, G. N.; Bally, T.; Hrouda, V.; Carsky, P. *J. Am. Chem. Soc.* **1998**, 120, 9323–9334.
32. Bally, T.; Sastry, G. N. *J. Phys. Chem.* **1997**, 101, 7923–7925.
33. Noodleman, L.; Post, D.; Baerends, E. J. *Chem. Phys.* **1982**, 64, 159–166.
34. Sodupe, M.; Bertran, J.; Rodriguez-Santiago, L.; Baerends, E. J. *J. Phys. Chem.* **1999**, 103, 166–170.
35. Braid, B.; Hiberty, P. C.; Savin, A. *J. Phys. Chem.* **1998**, 102, 7872–7877.
36. (a) Frisch, M. J.; Trucks, G. W.; Schlegel, H. B.; Scuseria, G. E.; Robb, M. A.; Cheeseman, J. R.; Zakrzewski, V. G.; Montgomery, J. A., Jr.; Stratmann, R. E.; Burant, J. C.; Dapprich, S.; Millam, J. M.; Daniels, A. D.; Kudin, K. N.; Strain, M. C.; Farkas, O.; Tomasi, J.; Barone, V.; Cossi, M.; Cammi, R.; Mennucci, B.; Pomelli, C.; Adamo, C.; Clifford, S.; Ochterski, J.; Petersson, G. A.; Ayala, P. Y.; Cui, Q.; Morokuma, K.; Malick, D. K.; Rabuck, A. D.; Raghavachari, K.; Foresman, J. B.; Cioslowski, J.; Ortiz, J. V.; Baboul, A. G.; Stefanov, B. B.; Liu, G.; Liashenko, A.; Piskorz, P.; Komaromi, I.; Gomperts, R.; Martin, R. L.; Fox, D. J.; Keith, T.; Al-Laham, M. A.; Peng, C. Y.; Nanayakkara, A.; Challacombe, M.; Gill, P. M. W.; Johnson, B.; Chen, W.; Wong, M. W.; Andres, J. L.; Gonzalez, C.; Head-Gordon, M.; Replogle, E. S.; Pople, J. A. *G98; Gaussian: Pittsburgh, PA, 1998*; (b) Frisch, M. J.; Trucks, G. W.; Schlegel, H. B.; Scuseria, G. E.; Robb, M. A.; Cheeseman, J. R.; Montgomery, J. A., Jr.; Vreven, T.; Kudin, K. N.; Burant, J. C.; Millam, J. M.; Iyengar, S. S.; Tomasi, J.; Barone, V.; Mennucci, B.; Cossi, M.; Scalmani, G.; Rega, N.; Petersson, G. A.; Nakatsuji, H.; Hada, M.; Ehara, M.; Toyota, K.; Fukuda, R.; Hasegawa, J.; Ishida, M.; Nakajima, T.; Honda, Y.; Kitao, O.; Nakai, H.; Klene, M.; Li, X.; Knox, J. E.; Hratchian, H. P.; Cross, J. B.; Adamo, C.; Jaramillo, J.; Gomperts, R.; Stratmann, R. E.; Yazyev, O.; Austin, A. J.; Cammi, R.; Pomelli, C.; Ochterski, J. W.; Ayala, P. Y.; Morokuma, K.; Voth, G. A.; Salvador, P.; Dannenberg, J. J.; Zakrzewski, V. G.; Dapprich, S.; Daniels, A. D.; Strain, M. C.; Farkas, O.; Malick, D. K.; Rabuck, A. D.; Raghavachari, K.; Foresman, J. B.; Ortiz, J. V.; Cui, Q.; Baboul, A. G.; Clifford, S.; Cioslowski, J.; Stefanov, B. B.; Liu, G.; Liashenko, A.; Piskorz, P.; Komaromi, I.; Martin, R. L.; Fox, D. J.; Keith, T.; Al-Laham, M. A.; Peng, C. Y.; Nanayakkara, A.; Challacombe, M.; Gill, P. M. W.; Johnson, B.; Chen, W.; Wong, M. W.; Gonzalez, C.; Pople, J. A. *G03 Gaussian 03, Revision C.01*; Gaussian: Wallingford, CT, 2004.
37. Schaftenaar, G. Molden; Centre for Molecular and Biomolecular Informatics: Nijmegen, The Netherlands.
38. Amovilla, C.; Barone, V.; Cammi, R.; Cancès, E.; Cossi, M.; Mennucci, B.; Pomelli, C. S.; Tomasi, J. *Adv. Quantum Chem.* **1998**, 32, 227–261.
39. Cramer, C. J.; Truhlar, D. G. *Chem. Rev.* **1999**, 99, 2161–2200.
40. Javier Luque, F.; Curutchet, C.; Muñoz-Muriedas, J.; Bidon-Chanal, A.; Soteras, I.; Morreale, A.; Gelpi, J. L.; Orozco, M. *Phys. Chem. Chem. Phys.* **2003**, 5, 3827–3836.
41. Tomasi, J. *Theor. Chem. Acc.* **2004**, 112, 184–203.
42. Tomasi, J.; Mennucci, B.; Cammi, R. *Chem. Rev.* **2005**, 105, 2999–3094.
43. Barone, V.; Cossi, M.; Tomasi, J. *J. Comput. Chem.* **1998**, 19, 404–417.
44. Miertus, S.; Scrocco, E.; Tomasi, J. *Chem. Phys.* **1981**, 55, 117–129.
45. Miertus, S.; Tomasi, J. *Chem. Phys.* **1982**, 65, 239–245.
46. Cossi, M.; Barone, V.; Cammi, R.; Tomasi, J. *Chem. Phys. Lett.* **1996**, 255, 327–335.
47. (a) Klamt, A.; Schueuermann, G. *J. Chem. Soc., Perkin Trans. 2* **1993**, 799–805; (b) Klamt, A. *J. Phys. Chem.* **1995**, 99, 2224–2235.
48. Svozil, D.; Jungwirth, P.; Havlas, Z. *Collect. Czech. Chem. Commun.* **2004**, 69, 1395–1428.
49. Desfrancois, C.; Abdoul-Carime, H.; Schermann, J. P. *Int. J. Mod. Phys. B* **1996**, 10, 1339–1395.
50. Crawford, O. H.; Garrett, W. R. *J. Chem. Phys.* **1977**, 66, 4968–4970.

51. Wesolowski, S. S.; Leininger, M. L.; Pentchev, P. N.; Schaefer, H. F. *J. Am. Chem. Soc.* **2001**, *123*, 4023–4028.
52. Hendricks, J. H.; Lyapustina, S. A.; de Clercq, H. L.; Snodgrass, J. T.; Bowen, K. H. *J. Chem. Phys.* **1996**, *104*, 7788–7791.
53. Desfrancois, C.; Abdoul-Carime, H.; Khelifa, N.; Schermann, J. P. *Phys. Rev. Lett.* **1994**, *73*, 2436–2439.
54. Desfrancois, C.; Abdoul-Carime, H.; Schulz, C. P.; Schermann, J. P. *Science* **1995**, *269*, 1707–1709.
55. Desfrancois, C.; Abdoul-Carime, H.; Schermann, J. P. *J. Chem. Phys.* **1996**, *104*, 7792–7794.
56. Desfrancois, C.; Periquet, V.; Bouteiller, Y.; Schermann, J. P. *J. Phys. Chem.* **1998**, *102*, 1274–1278.
57. Desfrancois, C.; Abdoul-Carime, H.; Carles, S.; Periquet, V.; Schermann, J. P.; Smith, D. M. A.; Adamowicz, L. *J. Chem. Phys.* **1999**, *110*, 11876–11883.
58. Schiedt, J.; Weinkauff, R.; Neumark, D. M.; Schlag, E. W. *Chem. Phys.* **1998**, *239*, 511–524.
59. Oyler, N. A.; Adamowicz, L. *J. Phys. Chem.* **1993**, *97*, 11122–11123.
60. Oyler, N. A.; Adamowicz, L. *Chem. Phys. Lett.* **1994**, *219*, 223–227.
61. Roehrig, G. H.; Oyler, N. A.; Adamowicz, L. *Chem. Phys. Lett.* **1994**, *225*, 265–272.
62. Roehrig, G. H.; Oyler, N. A.; Adamowicz, L. *J. Phys. Chem.* **1995**, *99*, 14285–14289.
63. Smith, D. M. A.; Smets, J.; Elkadi, Y.; Adamowicz, L. *J. Phys. Chem.* **1997**, *101*, 8123–8127.
64. Dolgounitcheva, O.; Zakrzewski, V. G.; Ortiz, J. V. *Chem. Phys. Lett.* **1999**, *307*, 220–226.
65. Durbeej, B.; Eriksson, L. A. *J. Am. Chem. Soc.* **2000**, *122*, 10126–10132.
66. Smets, J.; McCarthy, W. J.; Adamowicz, L. *Chem. Phys. Lett.* **1996**, *256*, 360–369.
67. Smets, J.; McCarthy, W. J.; Adamowicz, L. *J. Phys. Chem.* **1996**, *100*, 14655–14660.
68. Smets, J.; Smith, D. M. A.; Elkadi, Y.; Adamowicz, L. *J. Phys. Chem.* **1997**, *101*, 9152–9156.
69. Dolgounitcheva, O.; Zakrzewski, V. G.; Ortiz, J. V. *J. Phys. Chem.* **1999**, *103*, 7912–7917.
70. Smith, D. M. A.; Smets, J.; Adamowicz, L. *J. Phys. Chem.* **1999**, *103*, 5784–5790.
71. Smith, D. M. A.; Smets, J.; Adamowicz, L. *J. Phys. Chem.* **1999**, *103*, 4309–4312.
72. Al-Jihad, I.; Smets, J.; Adamowicz, L. *J. Phys. Chem.* **2000**, *104*, 2994–2998.
73. Hendricks, J. H.; Lyapustina, S. A.; de Clercq, H. L.; Bowen, K. H. *J. Chem. Phys.* **1998**, *108*, 8–11.
74. Colson, A. O.; Besler, B.; Close, D. M.; Sevilla, M. D. *J. Phys. Chem.* **1992**, *96*, 661–668.
75. Colson, A. O.; Besler, B.; Sevilla, M. D. *J. Phys. Chem.* **1992**, *96*, 9787–9794.
76. Colson, A. O.; Besler, B.; Sevilla, M. D. *J. Phys. Chem.* **1993**, *97*, 13852–13859.
77. Sevilla, M. D.; Besler, B.; Colson, A. O. *J. Phys. Chem.* **1994**, *98*, 2215.
78. Sevilla, M. D.; Besler, B.; Colson, A. O. *J. Phys. Chem.* **1995**, *99*, 1060–1063.
79. Russo, N.; Toscano, M.; Grand, A. *J. Comput. Chem.* **2000**, *21*, 1243–1250.
80. Wetmore, S. D.; Boyd, R. J.; Eriksson, L. A. *Chem. Phys. Lett.* **2000**, *322*, 129–135.
81. Turecek, F.; Wolken, J. K. *J. Phys. Chem.* **2001**, *105*, 8740–8747.
82. Li, X.; Cai, Z.; Sevilla, M. D. *J. Phys. Chem.* **2002**, *106*, 1596–1603.
83. Steenken, S.; Telo, J. P.; Novais, H. M.; Candelas, L. P. *J. Am. Chem. Soc.* **1992**, *114*, 4701–4709.
84. Trasatti, S. *Pure Appl. Chem.* **1986**, *58*, 955–966. Note that there are some unresolved questions regarding the potentials at the electrode interface and the standard state of the electron. For a more detailed discussion, see: Pearson, R. G. *J. Am. Chem. Soc.* **1986**, *108*, 6109–6114; Jonsson, M.; Houmam, A.; Jocys, G.; Wayner, D. D. M. *J. Chem. Soc., Perkin Trans. 2* **1999**, 425–429.
85. Scannell, M. P.; Prakash, G.; Falvey, D. E. *J. Phys. Chem.* **1997**, *101*, 4332–4337.
86. Voityuk, A. A.; Rösch, N. *J. Phys. Chem.* **1997**, *101*, 8335–8338.
87. Sanders, D. B.; Wiest, O. *J. Am. Chem. Soc.* **1999**, *121*, 5127–5134.
88. Hahn, J.; Michel-Beyerle, M. E.; Rösch, N. *J. Phys. Chem.* **1999**, *103*, 2001–2007.
89. Antony, J.; Medvedev, D. M.; Stuchebrukhov, A. A. *J. Am. Chem. Soc.* **2000**, *122*, 1057–1065.
90. Komori, H.; Masui, R.; Kuramitsu, S.; Yokoyama, S.; Shibata, T.; Inoue, Y.; Miki, K. *Proc. Natl. Acad. Sci. U.S.A.* **2001**, *98*, 13560–13565.
91. Mees, A.; Klar, T.; Gnau, P.; Hennecke, U.; Eker, A. P. M.; Carell, T.; Essen, L.-O. *Science* **2004**, *306*, 1789–1793.
92. Hartman, R. F.; Van Camp, J. R.; Rose, S. D. *J. Org. Chem.* **1987**, *52*, 2684–2689.
93. Wiest, O. Unpublished results.
94. Voityuk, A. A.; Michel-Beyerle, M. E.; Rösch, N. *J. Am. Chem. Soc.* **1996**, *118*, 9750–9758.
95. Witmer, M. R.; Altmann, E.; Young, H.; Begley, T. P. *J. Am. Chem. Soc.* **1989**, *111*, 9264–9265.
96. Jacobsen, J. R.; Cochran, A. G.; Stephans, J. C.; King, D. S.; Schultz, P. G. *J. Am. Chem. Soc.* **1995**, *117*, 5453–5461.
97. Honig, B.; Gilson, M.; Fine, R.; Rashin, A. *Biophys. J.* **1984**, *45*, A129.
98. Gilson, M. K.; Honig, B. H. *Biopolymers* **1986**, *25*, 2097–2119.
99. Honig, B.; Sharp, K.; Yang, A. S. *J. Phys. Chem.* **1993**, *97*, 1101–1109.
100. Thompson, M. *Planaria Software*; ArgusLab: Seattle, Washington, 2001.

Enantioselective alkene radical cations reactions

David Crich,* Michio Shirai, Franck Brebion and Sochanchingwung Rumthao

Department of Chemistry, University of Illinois at Chicago, 845 West Taylor Street, Chicago, IL 60607-7061, USA

Received 6 September 2005; accepted 12 November 2005

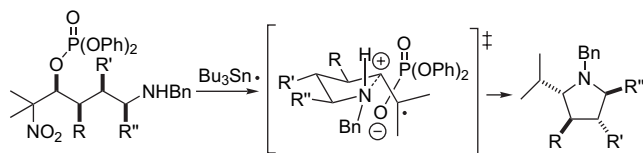
Available online 2 May 2006

Abstract—The reaction of enantiomerically enriched 2-methyl-2-nitro-3-(diphenylphosphatoxy)alkyl radicals with tributyltin hydride and AIBN in benzene at reflux results in the formation of alkene radical cation/anion pairs, which are trapped intramolecularly by amine nucleophiles, leading to pyrrolidine and piperidine systems with memory of stereochemistry. The scope and limitations of the system are explored with respect to nucleophile, leaving group, and substituents within the substrate backbone.

© 2006 Elsevier Ltd. All rights reserved.

1. Introduction

Alkene radical cations generated within the confines of contact ion pairs by the expulsion of leaving groups from the β -position of radicals participate in stereoselective cyclization reactions with suitably placed amines. This concept was demonstrated (Scheme 1) with an extensive series of substrates carrying methyl groups on the carbon backbone, with the results best accommodated by a chair-like transition state for cyclization with the maximum number of substituents pseudo-equatorial.¹



Scheme 1. Preferred model for diastereoselective alkene radical cation cyclizations.¹

In this paper we report in full on a parallel series of experiments in which all stereogenic centers are destroyed on formation of the alkene radical cation, leaving the operation of a memory effect as the only explanation for the observed enantioselectivity.²

2. Results and discussion

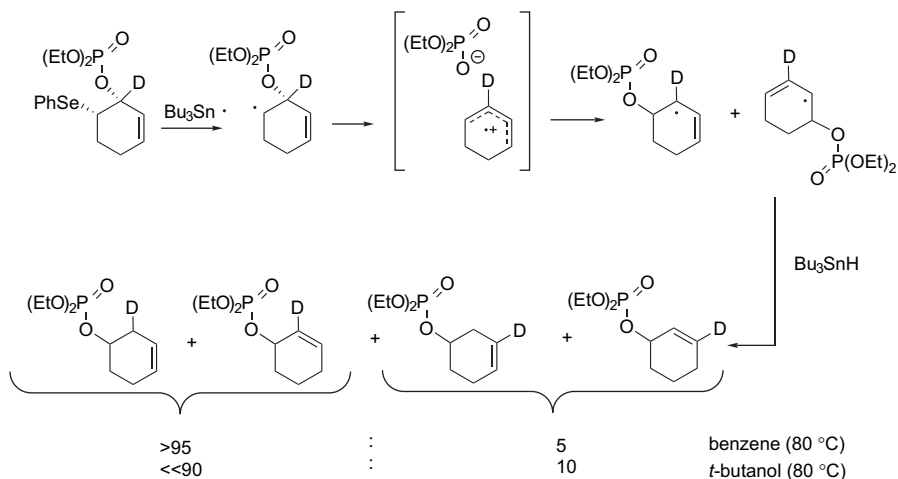
Working in collaboration with Newcomb we have established, using time resolved laser flash photolytic techniques,

that alkyl radicals substituted with a leaving group in the β -position expel the leaving group to afford contact alkene radical cation/anion pairs even in nonpolar solvents.³ In polar solvents supporting charge separation these contact ion pairs undergo equilibration with the medium leading to solvent separated ion pairs and even free radical cations and the corresponding anions. This type of behavior is seen under anaerobic conditions with DNA C'4 radicals when the C'3-phosphate group is expelled leading to the C3'C4' alkene radical cation, such as has been so productively employed as a 'hole' source in the study of charge transfer through DNA by Giese.⁴ In nonpolar solvents collapse of the contact alkene radical cation/anion pair to either the original radical or a rearranged radical is extremely rapid, typically out competing equilibration of the components of the contact ion pair. This extremely rapid recombination is now seen as the basis for a number of regio-⁵ and stereoselective^{5a,6} rearrangements that were originally interpreted as open-shell concerted processes (Schemes 2 and 3).⁷ Computational work in this area, while originally supportive of the concerted mechanisms, has evolved and now points to the fragmentation/recombination mechanisms for these rearrangements.⁸

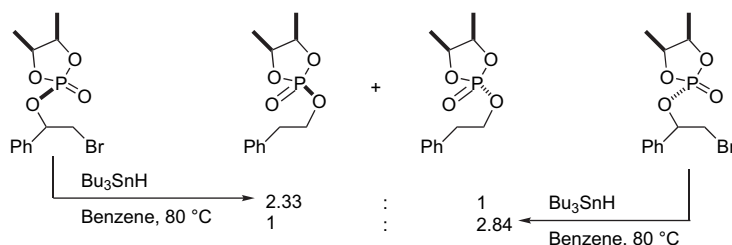
In parallel with the mechanistic studies we have developed a series of preparative methods in which nucleophilic attack, inter- or intramolecular, on the contact radical ion pair takes place in competition with collapse to a rearranged radical in nonpolar solvents. When this nucleophilic trapping is followed up by a radical cyclization the overall tandem polar/radical crossover sequence affords diverse bicyclic systems depending on the substitution pattern (Scheme 4).⁹

The combination of the stereoselectivity of the rearrangement reactions (Schemes 2 and 3), which implies rapid collapse of a highly ordered contact radical ion pair, coupled

* Corresponding author. Tel.: +1 312 996 5189; fax: +1 312 996 0431; e-mail: dcrich@uic.edu

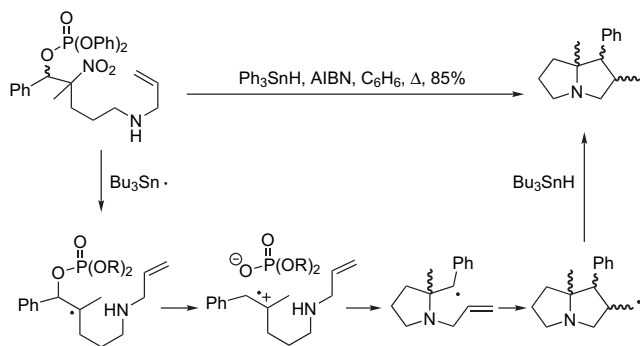


Scheme 2. Changing regioselectivity of a β -phosphatoxyalkyl radical rearrangement as a function of solvent.^{5,6}



Scheme 3. Stereoselective rearrangement with predominant retention of configuration at phosphorus.⁵

with the polar/radical crossover reactions (**Scheme 4**), and the implicit faster rates of nucleophilic trapping than ion pair collapse, lead directly to the hypothesis of stereoselective nucleophilic trapping reactions in which the order of the contact radical ion pair is reflected in the stereochemistry of the product.

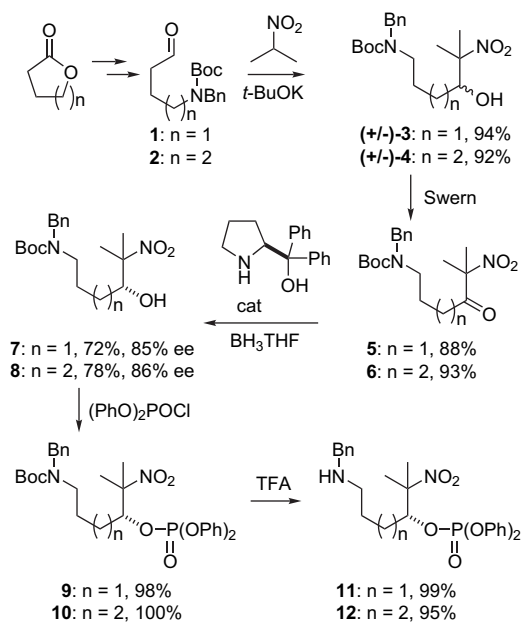


Scheme 4. Example of a polar/radical crossover sequence.^{9c,d}

As discussed above, the hypothesis of memory effects in alkene radical cation reactions was first put to the test at the level of diastereoselectivity leading to the model of **Scheme 1**. In this system the amine attacks the face of the alkene radical cation opposite to that shielded by the just departed leaving group through a chair-like transition state with a maximum number of substituents pseudo-equatorial. The second generation system described here is enantioselective and requires the synthesis of a series of enantiomerically

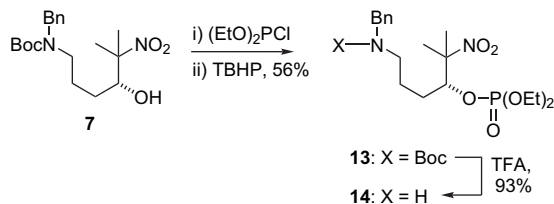
enriched β -(phosphatoxy)nitroalkanes, the precursors of choice in these tin hydride mediated polar radical crossover sequences, which we accessed by Corey oxazaborolidine-catalyzed reduction of α -nitroketones.¹⁰

The synthesis of a first pair of substrates, **11** and **12**, was accomplished as set out in **Scheme 5**.



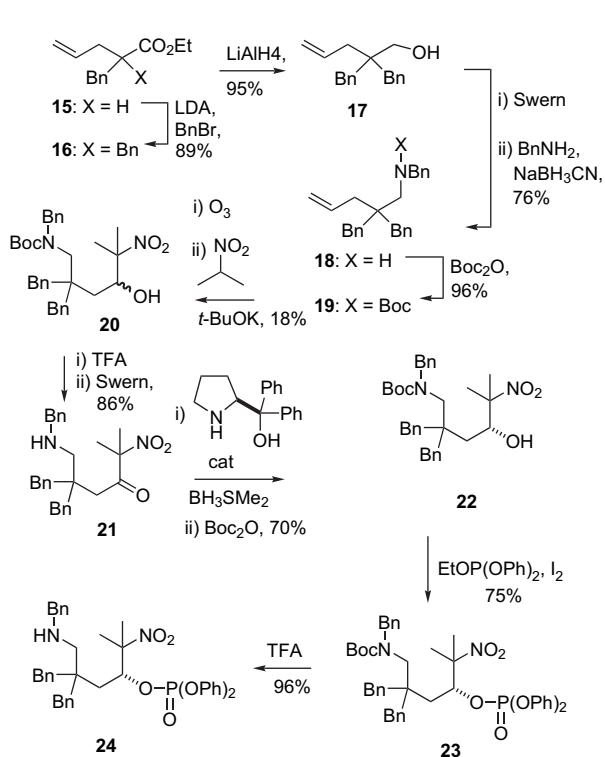
Scheme 5. Synthesis of substrates **11** and **12**.

In order to compare the effect of the leaving group the diethylphosphate analog **14** of one of these substrates was also prepared (Scheme 6).



Scheme 6. Synthesis of a diethylphosphate **14**.

With a view to determining the influence of the ‘gem-disubstituent’ effect¹¹ on the diastereoselectivity substrate **24**, bearing a quaternary carbon center, was synthesized by the route outlined in Scheme 7.

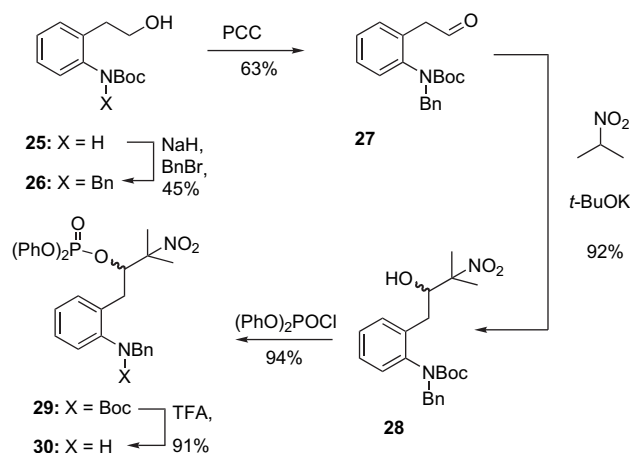


Scheme 7. Synthesis of substrate **24**.

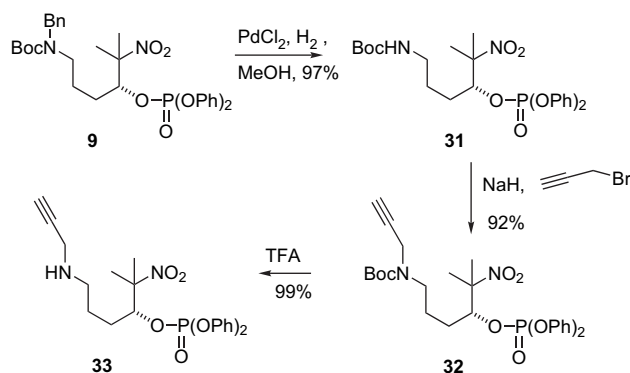
Yet another substrate, conformationally biased **30**, was obtained from the aniline derivative **25** (Scheme 8).¹² Substrate **30** was prepared only in racemic form, as a control experiment indicated that it did not undergo cyclization on treatment with tributyltin hydride under the usual conditions, as discussed below.

A substrate for a tandem polar/radical process in which the nucleophilic cyclization is followed by a radical cyclization was prepared from **9** by a process in which a benzyl group was exchanged for a propargylic moiety (Scheme 9).

Two substrates incorporating alcohol rather than amine nucleophiles were accessed as described in Schemes 10 and 11. Whereas the synthesis of the simple substrate **41** was straightforward (Scheme 10), that of the *gem*-dialkyl



Scheme 8. Preparation of an aniline-base substrate **30**.

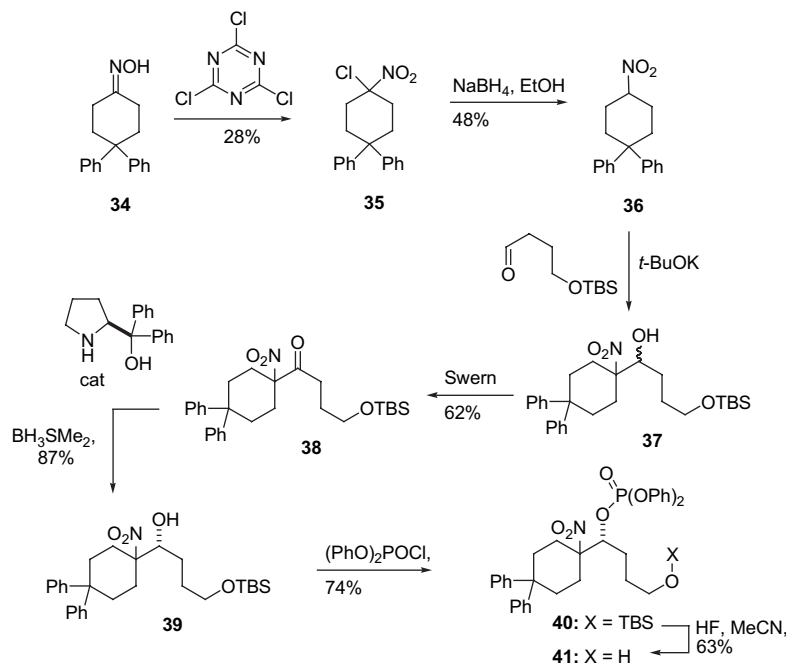


Scheme 9. Synthesis of a propargylic substrate.

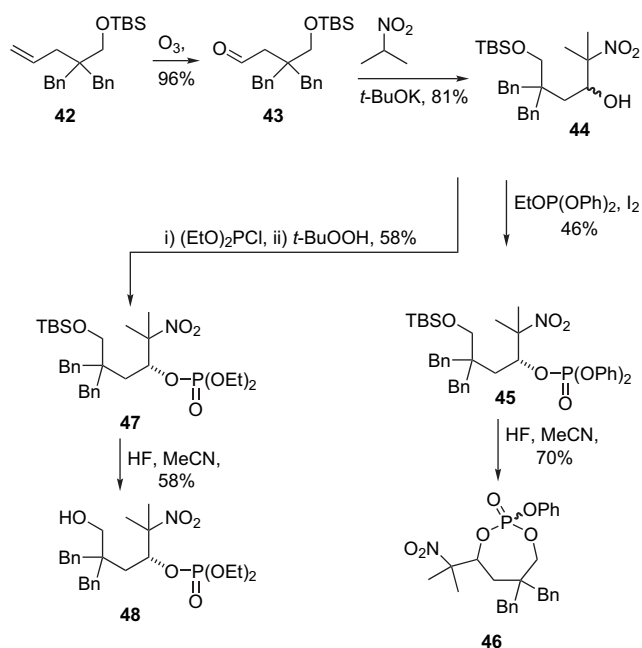
substituted variant proved more problematic owing to cyclization of the newly revealed alcohol onto the phosphate in the course of the final desilylation, with isolation of the 1,3,2-dioxaphosphepane **46** (Scheme 11). This problem, which could only be overcome by switching to the less electrophilic diethylphosphate, also reared its head in the attempted polar/radical cyclization of racemic **48**, as discussed below, and consequently no attempt was made to obtain this compound in enantiomerically enriched form.

A common feature of the above syntheses is the borane reduction of α -nitroketones catalyzed by the Corey oxazaborolidine catalyst. For ease of comparison the various reductions are presented in Table 1. The absolute stereochemistry of the nitroalcohols obtained from these reductions is assigned according to the standard model of Corey for the oxazaborolidine reduction of disymmetrically substituted ketones,¹³ with the 1-methyl-1-nitroethyl group playing the role of the most bulky substituent. The applicability of this model to the α -nitroketones was rigorously established in our earlier model studies.¹⁰ It is noteworthy that moderate to good enantioselectivities were obtained in all instances, with only a minor reduction due to the presence of the quaternary center in **21**.

The polar/radical crossover reactions were conducted with tributylstannane and AIBN in benzene at 80 °C leading to the results presented in Table 2. The enantioselectivities were determined by either chiral GC or HPLC as appropriate.



Scheme 10. Synthesis of substrate 41.



Scheme 11. Preparation of substrate 48.

The absolute configuration of pyrrolidine **49** was established by hydrogenolytic debenzoylation and subsequent tosylation to give the sulfonamide **57**, whose specific rotation was compared to the literature value (Scheme 12).^{14,15} As all successful cyclizations in Table 2, with the exception of alcohol **41**, gave comparable enantioselectivities it was not considered necessary to rigorously establish the configuration of all products, which consequently were assigned by analogy with **49**.

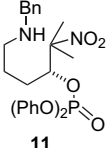
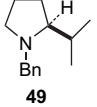
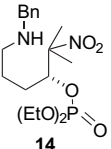
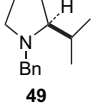
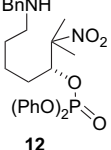
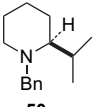
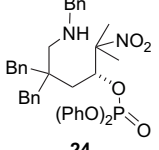
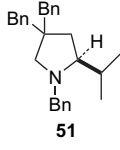
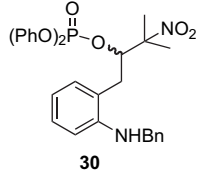
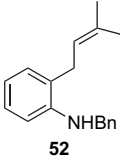
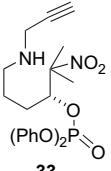
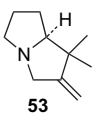
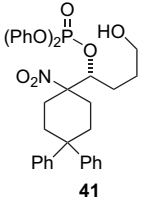
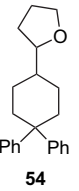
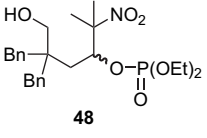
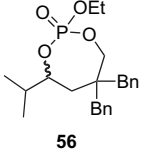
Comparison of entries 1–4 and 6 in Table 2 indicates that in the case of a secondary amine as nucleophile neither ring

Table 1. Enantiomerically enriched nitro alcohols obtained by CBS reduction of α -nitroketones

Nitro alcohol	% Yield	% ee
	72	85
	78	86
	70	79
	87	96

size (five or six), leaving group (diphenyl or diethylphosphate), nor the presence of a normally rate enhancing quaternary center has major significance on the enantioselectivity of these cyclizations. We interpret this result as arising from an extremely rapid trapping of the contact radical cation/anion pair once it is formed in what is probably the rate limiting radical ionic fragmentation step. This observation is consistent with the earlier study based on diastereoselectivity (Scheme 1) and the general rationale presented above. This is entirely reasonable given the intramolecular nature of the attack on a simple trialkyl substituted alkene radical

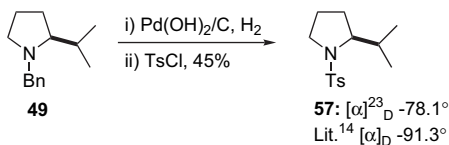
Table 2. Enantioselective alkene radical cation cyclizations

Entry	Substrate	Substrate % ee	Product	% Yield	% ee ^a
1	 11	85	 49	43	61 (71)
2	 14	85	 49	45	62
3	 12	86	 50	41	60 (70)
4	 24	79	 51	44	60 (76)
5	 30	(+/-) ^b	 52	50	—
6	 33	85	 53	64	60 (71)
7	 41	94	 54	54: 25 55: 52	0
8	 48	(+/-) ^b	 56	67	—

^a Actual ee (ee predicated on enantiomerically pure substrate).^b Reactions conducted with racemic material.

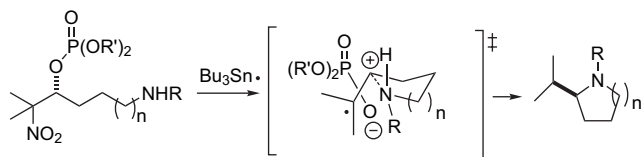
cation in a nonpolar solvent, in view of the $2.5 \times 10^9 \text{ M}^{-1} \text{ s}^{-1}$ rate constant determined for the intermolecular rate constant for the attack of butylamine on the stabilized *p*-methoxystyrene radical cation in the polar solvent acetonitrile at 25 °C.¹⁶ Taking into account the absolute configurations of the

substrates and products, we are led to propose a model for these cyclizations (Scheme 13) that is directly comparable to the one advanced earlier for the diastereoselective cyclizations. Thus, the initial radical undergoes rate determining fragmentation to give an ordered contact alkyl radical



Scheme 12. Establishment of absolute configuration.

cation/anion pair that suffers extremely rapid collapse to the cyclized radical with attack of the nucleophile on the opposite face of the alkene radical cation to the one shielded by the counter-ion (Scheme 13). While this model bears some resemblance to the widespread Beckwith/Houk model for radical cyclization,¹⁷ it differs fundamentally in one key aspect. The Beckwith/Houk model requires full conformational equilibration before cyclization through the most-favored chair-like transition state, while the model of Schemes 1 and 13 implies very rapid cyclization before solvation of the contact radical ion pair and conformational equilibration.¹⁸

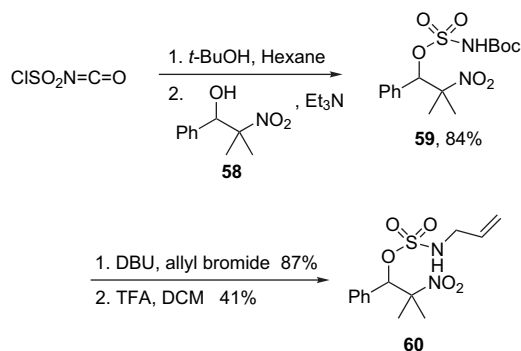


Scheme 13. Preferred model for enantioselective alkene radical cation cyclizations.

The remaining entries of Table 2 serve to illustrate the limitations of the method. Thus, with the much weaker aniline-based nucleophile (entry 5) no cyclization was seen, leading to decomposition of the alkene radical cation and the formation of a complex reaction mixture from which only the alkene **52** was isolated. Alcohols are generally much poorer nucleophiles than amines as is known to hold with alkene radical cations as electrophiles, with the rate constants for the attack of alcohols being slower than those of amines.¹⁶ This leads to a reduced rate of cyclization, enabling solvation of the contact ion pair and conformational equilibration to become competitive, leading overall to a reduction in enantioselectivity (Table 2, entry 7). Finally, a significant limitation to the use of alcohols as nucleophiles in these cyclizations, at least when conducted under refluxing conditions in benzene, is seen in the formation of the 1,3,2-dioxaphosphepanes **55** and **56** (Table 2, entries 7 and 8). Given the reaction protocol, with dropwise addition of the stannane to a solution of the substrate in benzene at reflux, these cyclizations involving nucleophilic attack at phosphorus presumably take place before the radical reaction. The formation of the cyclic phosphepane ring should not prevent fragmentation to the alkene radical cation, as we have previously demonstrated that suitably substituted phosphepanes undergo a rearrangement analogous to the one in Scheme 3 with rate constants of 10^5 – 10^6 s⁻¹ in benzene at 80 °C with a very high degree of retention of configuration at phosphorus.¹⁹ However, the intramolecular nature of the contact radical cation/anion pair generated from expulsion of the phosphepane leaving group presumably accelerates internal return and thereby reduces the possibility of nucleophilic attack by the alcohol.

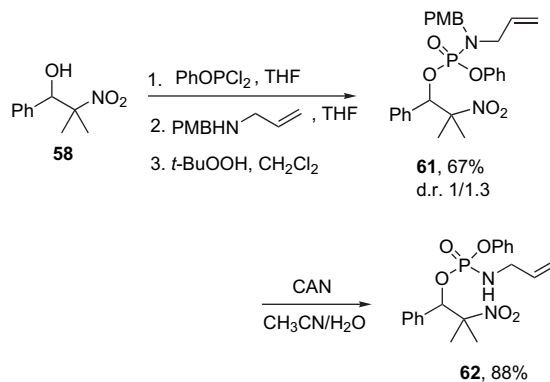
We considered an alternative approach to enantioselective alkene radical cation reactions in which the leaving group

in the fragmentation step serves as source of chirality, thereby eliminating the need for the synthesis of enantiomerically enriched phosphorals. This approach, employing a stereogenic phosphorus or sulfur center, may be viewed as an extension of the diastereoselective probes of mechanism reported in Scheme 3. Before undertaking the synthesis of any enantiomerically enriched compounds a series of simple models were prepared to test the viability of such an approach in the context of a tandem polar/radical reaction. Thus, reaction of chlorosulfonyl isocyanate with nitroalcohol **58**^{9b,20} afforded the sulfamate **59** which, following N-alkylation²¹ and subsequent removal of the carbamate group, gave the radical precursor **60** (Scheme 14).



Scheme 14. Synthesis of an *N*-allyl sulfamate.

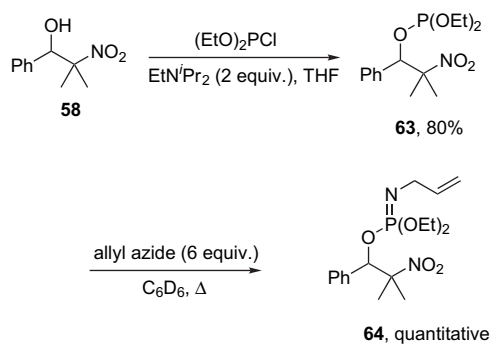
In the phosphorus series an *N*-allyl phosphoramidate **62** was prepared in straightforward manner as outlined in Scheme 15.



Scheme 15. Synthesis of an *N*-allyl phosphoramidate.

The synthesis of an *N*-allyl phosphorimidate **64**, after some experimentation, was also achieved in a straightforward manner employing the Staudinger reaction²² of phosphite **63** with allyl azide (Scheme 16). In accordance with the precedent for the Staudinger reaction with phosphites,²³ as opposed to the more common phosphines, reaction of allyl azide with the diethylphosphite **63** proceeded according to plan to give the unstable **64**. However, reaction of allyl azide with the corresponding diphenylphosphite corresponding to **63** was prohibitively slow.

Compounds **60**, **62**, and **64** were treated with tin hydride and AIBN in benzene at reflux in the usual manner, unfortunately, no evidence was found for any of the anticipated



Scheme 16. Synthesis of an *N*-allyl phosphorimidate.

rearrangements. Nevertheless, as seen in Table 3, the results obtained are of more general interest in the context of the compartment of contact alkene radical cation/anion pairs. Blank experiments in benzene at reflux demonstrated the thermal stability of **60**, **62**, and **64**, in the absence of air and water.

With the sulfamate **60** the only isolated product was *N*-allyl sulfamic acid **65**, which was obtained in 48% yield (Table 3, entry 1). This material obviously derives from radical ionic fragmentation followed by cage escape and reflects the poor nucleophilicity of the sulfamate anion. With the phosphoramidate **62**, the main product **66** was that of a 1,2-shift of the initial radical (Table 3, entry 2). This reflects the predominant 1,2-shift identified with simple phosphate esters either by stereochemical or isotopic labeling (Scheme 3).^{5a} Aside from the simple reduction product **67**, which was isolated in 7% yield from this reaction, the phosphoramidate **62** also gave rise to a very interesting minor product in the form of the 1,3,2-azoxaphosphocane **68** in 8% yield (Table 3, entry 2). This product, which appears to be the first example of its class,²⁴ and which was isolated as a single but unassigned diastereomer, is the apparent result of an 8-*endo-trig* cyclization of the initial radical. 8-*endo-trig* Cyclizations are relatively uncommon, usually involve conformationally constrained systems,²⁵ and have low rate constants,²⁶ and

thus, the formation of **68** was somewhat unexpected as the 1,1-dimethyl-2-diphenylphosphatoxy-2-phenylethyl radical is known to rearrange in benzene at 20 °C with a rate constant of $1.2 \times 10^6 \text{ s}^{-1}$.^{3a} However, it should be noted that the rates of β -phosphatoxyalkyl rearrangement are severely influenced by substituents on phosphorus. For example, the 1,1-dimethyl-2-diethylphosphatoxy-2-phenylethyl radical rearranges too slowly to measure by time resolved laser flash photolysis in benzene ($k < 10^4 \text{ s}^{-1}$).^{3a,k,27} The failure of **62** to rearrange in a formal 2,3-manner, preferring instead the 1,2-mode, led us to the phosphorimidate **64** with the hope that the exchange of a P=N double bond for a P=O would force the rearrangement into the formal 2,3-mode of rearrangement needed for the tandem polar/radical crossover process. We were encouraged in this direction by recent publication of the 3,3-sigmatropic rearrangements of *O*-allyl phosphorimidates by the Mapp group^{23f,g} and by the formal analogy between open-shell 2,3-rearrangements and closed shell 3,3-sigmatropic rearrangements recognized by Zipse in his methyleneology principle.²⁸ Unfortunately, the major product isolated from this reaction was the simple phosphoramidate **69**. This suggests that recombination within the ion pair formed on radical ionic fragmentation was not a viable reaction path. Two other minor products isolated, **70** and **71**, suggest that decomposition of the phosphorimidate is competitive with the radical ionic fragmentation under the reaction conditions employed, discouraging us from further work with this class of substrate.

3. Conclusion

The fragmentation of β -(phosphatoxy)alkyl radicals in benzene at reflux results in the formation of alkene radical cation/phosphate anion pairs. Amines trap these ion pairs intramolecularly to form five- and six-membered rings on a time scale that competes with equilibration of the ion pair with solvent, resulting in the observation of significant stereochemical memory effects. A chair-like transition state is proposed as a model for these cyclizations. Oxygen

Table 3. Radical reactions of sulfamates, phosphoramides, and phosphorimidates

Entry	Substrate	Products	% Yield
1			~48%
2		 + +	66: 42% 67: 7% 68: 8%
3		 + +	69: 40% 70: 6% 71: 5%

nucleophiles, on the other hand, are not sufficiently nucleophilic to achieve cyclization before solvent equilibration of the ion pair. Sulfamates, phosphoramides, and phosphorimidates were also explored as leaving groups for alkene radical formation and appear to function as such. However, it was not possible to achieve rearrangements akin to the β -(phosphatoxy)alkyl and β -(acetoxy)alkyl rearrangements with these groups.

4. Experimental

4.1. General

Unless otherwise stated, ^1H , ^{13}C and, ^{31}P NMR spectra were recorded in CDCl_3 solution. Specific rotations were recorded in CHCl_3 solution, unless otherwise stated. All solvents were dried and distilled by standard protocols. All reactions were conducted under a blanket of dry nitrogen or argon. All organic extracts were dried over sodium sulfate, and concentrated under aspirator vacuum at room temperature. Chromatographic purifications were carried out over silica gel. Room temperature is referred to as rt.

4.1.1. Typical protocol for the Henry reaction.

4.1.1.1. *N*-Benzyl-*N*-(*tert*-butyloxycarbonyl)-4-hydroxy-5-methyl-5-nitrohexylamine (3).¹ 2-Nitropropane (1.97 g, 22.1 mmol) and aldehyde **1** (3.01 g, 10.9 mmol) were dissolved in a 1:1 mixture of acetonitrile and *tert*-BuOH (20 mL). To this solution was added potassium *tert*-butoxide (597 mg, 5.32 mmol) and the reaction mixture was stirred overnight. Satd aq NH_4Cl and ether were then added. The organic layer was separated and the aqueous layer was extracted with ether. The combined organic layer was washed with water and brine, then dried, and concentrated to dryness. Purification by column chromatography afforded the respective nitroaldol product **3**¹ (3.74 g, 94%).

4.1.2. Typical protocol for the Swern oxidation of nitroaldol adducts.

4.1.2.1. *N*-Benzyl-*N*-(*tert*-butyloxycarbonyl)-5-methyl-5-nitro-4-oxo-hexylamine (5).¹ A solution of oxalyl chloride (1.3 mL, 14.9 mmol) in CH_2Cl_2 (50 mL) was cooled to -78°C under N_2 followed by the dropwise addition of a solution of DMSO (1.5 mL, 21.1 mmol) in CH_2Cl_2 (7 mL), then the reaction mixture was stirred for 15 min. To this mixture was added dropwise a solution of nitroaldol adduct **3** (2.58 g, 7.04 mmol) in CH_2Cl_2 (17 mL) and stirred at -78°C for 1 h. Triethylamine (7.4 mL, 53.1 mmol) was added dropwise. After stirring for 20 min, the reaction mixture was allowed to warm up to rt. Satd aq NH_4Cl was then added and the separated organic layer was washed with H_2O and brine, then dried and concentrated to dryness. Purification by column chromatography afforded **5**¹ (2.26 g, 88%).

4.1.3. Typical protocol for the CBS reduction of nitroketones.

4.1.3.1. (4*R*)-*N*-Benzyl-*N*-(*tert*-butyloxycarbonyl)-4-hydroxy-5-methyl-5-nitrohexylamine (7). To a solution of (*S*)-(-)- α,α -diphenyl-2-pyrrolidinemethanol (135 mg, 0.533 mmol, 9 mol %) in THF (4 mL) was added borane/dimethyl sulfide (2 M in THF, 7.20 mL, 14.4 mmol) under

Ar. The mixture was stirred at $45\text{--}50^\circ\text{C}$ overnight. Ketone **5** (2.23 g, 6.12 mmol) in THF (35 mL) was added dropwise to the solution of the catalyst for 30 min at $45\text{--}50^\circ\text{C}$, then the reaction mixture was stirred for 20 min. Then the reaction solution was cooled to rt and quenched by dropwise addition of satd aq NH_4Cl until the vigor of the reaction subsided. The aqueous layer was extracted with ethyl acetate and the combined organic layer was washed with water and brine, then dried and concentrated to dryness. Purification by column chromatography gave **7** (1.57 g, 72%, 85% ee) as colorless oil, $[\alpha]_{\text{D}}^{23} +12.2$ (*c* 1.0) with spectral data identical to those of the racemate (**3**).¹

4.1.4. Typical protocol for the phosphorylation of nitroaldols.

4.1.4.1. (4*R*)-*N*-Benzyl-*N*-(*tert*-butyloxycarbonyl)-4-diphenylphosphatoxy-5-methyl-5-nitrohexylamine (9). Diphenyl chlorophosphate (179 mg, 0.67 mmol) was added to nitroalcohol **7** (207 mg, 0.565 mmol) in CH_2Cl_2 (5 mL) followed by the addition of DMAP (91 mg, 0.74 mmol) in one portion at rt. The reaction mixture was stirred overnight, then quenched by satd aq NH_4Cl . The aqueous layer was extracted with CH_2Cl_2 , the combined organic layer was washed with water and brine, then dried and concentrated to dryness. Purification by column chromatography afforded the corresponding phosphate **9** (331 mg, 98%) as colorless oil. $[\alpha]_{\text{D}}^{23} +0.16$ (*c* 2.5); ^1H NMR: δ 7.34–7.14 (m, 15H), 5.10 (br t, *J*=6.9 Hz, 1H), 4.37 (d, *J*=15.6 Hz, 1H), 4.29 (d, *J*=15.6 Hz, 1H), 3.18 (m, 2H), 1.80 (m, 1H), 1.75–1.45 (m, 3H), 1.59 (s, 3H), 1.53 (s, 3H), 1.44 (s, 9H); ^{13}C NMR: δ 155.9, 138.5, 129.8, 128.5, 127.5, 127.2, 125.5, 120.2, 90.3, 83.6, 79.9, 50.2, 45.9, 28.8, 28.5, 24.7, 22.7; ^{31}P NMR: δ -12.2; ESIHRMS: Calcd for $\text{C}_{31}\text{H}_{39}\text{N}_2\text{O}_8\text{PNa}$ [*M*+*Na*]⁺ 621.2342. Found 621.2344.

4.1.5. Typical protocol for the removal of Boc group.

4.1.5.1. (4*R*)-*N*-Benzyl-4-diphenylphosphatoxy-5-methyl-5-nitrohexylamine (11). Phosphate **9** (257 mg, 0.43 mmol) was stirred in 10% TFA/ CH_2Cl_2 (10 mL) under N_2 at rt overnight. NaOH (15%) was then added to pH 11 and the aqueous layer was extracted with ethyl acetate. The combined organic layer was washed with water and brine, then dried and concentrated to dryness. Column chromatography afforded the respective radical precursor **11** (207 mg, 99%) as colorless oil. $[\alpha]_{\text{D}}^{23} +3.2$ (*c* 2.0); ^1H NMR: δ 7.37–7.14 (m, 15H), 5.19 (m, 1H), 3.69 (s, 2H), 2.58 (m, 2H), 1.74–1.64 (m, 4H), 1.61 (s, 3H), 1.56 (s, 3H); ^{13}C NMR: δ 150.5, 140.5, 131.0, 129.9, 128.5, 128.2, 127.0, 125.6, 120.4, 120.3, 120.2, 90.5, 83.9, 54.0, 48.6, 29.2, 26.3, 22.9, 21.8; ^{31}P NMR: δ -11.9; ESIHRMS: Calcd for $\text{C}_{26}\text{H}_{32}\text{N}_2\text{O}_6\text{P}$ [*M*+*H*]⁺ 499.1998. Found 499.1991.

4.1.6. Determination of enantiomeric excess. The ee's of nitroalcohols and nitrophosphates were determined by chiral HPLC, whereas the ee's of the radical cyclization products were obtained by chiral GC. HPLC conditions: Chiralcel OD (250×4.6 mm) column; eluent: 0.5, 1.7 or 2.0% 2-propanol/hexanes with a flow rate 0.5 or 1.0 mL/min. UV Detector: 254 nm. GC conditions: Supelco ALPHA DEX 120 Capillary Column (α -cyclodextrin) (30 m×0.25 μm) or Supelco GAMMA DEX 120 Capillary Column (γ -cyclodextrin) (30 m×0.25 μm), with He as carrier gas, a flow rate of 20 or 30 cm/s, and FID detection.

4.1.6.1. *N*-Benzyl-*N*-(*tert*-butyloxycarbonyl)-5-hydroxy-6-methyl-6-nitroheptylamine (4). Following the general procedure for Henry reaction, **2** (1.98 g, 6.79 mmol) was converted to **4** (2.37 g, 92%) as colorless oil. ^1H NMR: δ 7.32–7.19 (m, 5H), 4.41 (s, 2H), 3.91 (m, 1H), 3.18 (m, 2H), 1.61–1.47 (m, 6H), 1.54 (s, 3H), 1.51 (s, 3H), 1.45 (s, 9H); ^{13}C NMR: δ 156.1, 138.7, 128.5, 127.5, 1127.2, 92.2, 79.9, 77.3, 75.9, 50.6, 46.3, 31.3, 31.1, 28.5, 23.2, 20.8; ESIHRMS: Calcd for $\text{C}_{20}\text{H}_{32}\text{N}_2\text{O}_5$ [M+H] $^+$ 403.2209. Found 403.2227.

4.1.6.2. *N*-Benzyl-*N*-(*tert*-butyloxycarbonyl)-6-methyl-6-nitro-5-oxo-heptylamine (6). Following the general procedure for Swern oxidation, **4** (1.26 g, 3.32 mmol) was converted to **6** (1.17 g, 93%) as colorless oil. ^1H NMR: δ 7.30–7.19 (m, 5H), 4.41 (s, 2H), 3.17 (t, $J=6.6$ Hz, 2H), 2.46 (t, $J=6.8$ Hz, 2H), 1.70 (s, 6H), 1.57 (m, 4H), 1.46 (s, 9H); ^{13}C NMR: δ 206.7, 188.5, 138.7, 128.5, 127.5, 127.20, 127.17, 94.1, 79.8, 77.3, 50.5, 46.2, 35.8, 28.5, 23.3, 21.0; ESIHRMS: Calcd for $\text{C}_{20}\text{H}_{30}\text{N}_2\text{O}_5$ Na [M+Na] $^+$ 401.2052. Found 401.2037.

4.1.6.3. (5*R*)-*N*-Benzyl-*N*-(*tert*-butyloxycarbonyl)-5-hydroxy-6-methyl-6-nitroheptylamine (8). Following the general procedure for CBS reduction, **6** (313 mg, 0.827 mmol) was converted to **8** (245 mg, 78%) as colorless oil. $[\alpha]_{\text{D}}^{23} +1.6$ (c 1.0). Enantiomeric excess was determined by chiral HPLC after the derivatization to the phosphate **10**. The spectral data for this compound corresponded with those of the racemate (**4**).

4.1.6.4. (5*R*)-*N*-Benzyl-*N*-(*tert*-butyloxycarbonyl)-5-diphenylphosphatoxy-6-methyl-6-nitroheptylamine (10). Following the general procedure for phosphorylation, **8** (192 mg, 0.51 mmol) was converted to **10** (306 mg, 99%, 86% ee) as colorless oil. $[\alpha]_{\text{D}}^{23} +4.0$ (c 1.0); ^1H NMR: δ 7.33–7.10 (m, 15H), 5.10 (m, 1H), 4.36 (s, 2H), 3.05 (m, 2H), 1.65–1.46 (m, 6H), 1.61 (s, 3H), 1.54 (s, 3H), 1.44 (s, 9H); ^{13}C NMR: δ 172.2, 138.7, 129.8, 129.4, 128.5, 127.4, 127.2, 125.4, 120.2, 100.2, 90.3, 83.7, 79.7, 77.3, 50.5, 46.3, 31.2, 28.5, 23.2, 22.6; ^{31}P NMR: δ –12.2; ESIHRMS: Calcd for $\text{C}_{32}\text{H}_{41}\text{N}_2\text{O}_8\text{PNa}$ [M+Na] $^+$ 635.2498. Found 635.2489.

4.1.6.5. (5*R*)-*N*-Benzyl-5-diphenylphosphatoxy-6-methyl-6-nitroheptylamine (12). Following the general procedure for removal of Boc group, **10** (231 mg, 0.38 mmol) was converted to **12** (183 mg, 95%) as colorless oil. $[\alpha]_{\text{D}}^{23} +3.1$ (c 0.9); ^1H NMR: δ 7.35–7.12 (m, 15H), 5.14 (br t, $J=9.0$ Hz, 1H), 3.72 (s, 2H), 2.50 (m, 2H), 2.07 (m, 2H), 1.78–1.40 (m, 4H), 1.60 (s, 3H), 1.54 (s, 3H); ^{13}C NMR: δ 150.6, 129.9, 128.6, 128.3, 128.2, 127.1, 125.6, 120.32, 120.26, 120.2, 120.1, 90.3, 83.8, 54.0, 48.8, 31.3, 29.8, 29.6, 23.7, 22.8; ^{31}P NMR: δ –11.9; ESIHRMS: Calcd for $\text{C}_{27}\text{H}_{34}\text{N}_2\text{O}_6\text{P}$ [M+H] $^+$ 513.2155. Found 513.2167.

4.1.6.6. (4*R*)-*N*-Benzyl-*N*-(*tert*-butyloxycarbonyl)-4-diethylphosphatoxy-5-methyl-5-nitrohexylamine (13). Enantioenriched nitroalcohol **7** (385 mg, 1.05 mmol) and pyridine (0.2 mL, 2.5 mmol) were dissolved in dry CH_2Cl_2 (20 mL) and the solution was cooled to 0 °C. Chlorodiethylphosphite (0.30 mL, 2.1 mmol) was added dropwise. The reaction was stirred for 50 min, then *tert*-butyl hydroperoxide

in decane (0.45 mL, 2.25 mmol) was added dropwise. After stirring overnight, the reaction was quenched with satd aq NH_4Cl , then separated and the aqueous layer was extracted with CH_2Cl_2 . The combined organic layer was washed with water and brine, then dried, and concentrated. Chromatographic purification gave the colorless oil **13** (294 mg, 56%) ^1H NMR: δ 7.33–7.22 (m, 5H), 4.83 (m, 1H), 4.46 (d, $J=15.6$ Hz, 1H), 4.38 (d, $J=15.6$ Hz, 1H), 4.09 (m, 4H), 3.23 (m, 2H), 1.86 (m, 1H), 1.66–1.40 (m, 3H), 1.60 (s, 3H), 1.52 (s, 3H), 1.46 (s, 9H), 1.32 (m, 6H); ^{13}C NMR (CDCl_3): δ 155.8, 138.4, 128.5, 127.7, 127.2, 90.4, 81.8, 80.5, 79.8, 64.1, 61.8, 50.2, 45.8, 29.8, 28.4, 25.8, 22.9, 16.3, 16.1; ESIHRMS: Calcd for $\text{C}_{23}\text{H}_{39}\text{N}_2\text{O}_8\text{PNa}$ [M+Na] $^+$ 525.2342. Found 525.2350.

4.1.6.7. (4*R*)-*N*-Benzyl-4-diethylphosphatoxy-5-methyl-5-nitrohexylamine (14). Following the general procedure for Boc group removal, **13** (258 mg, 0.513 mmol) afforded **14** (193 mg, 93%) as a colorless oil. ^1H NMR: δ 7.33–7.24 (m, 5H), 4.91 (m, 1H), 4.10 (m, 4H), 3.82 (s, 2H), 2.71 (br s, 2H), 1.95–1.69 (m, 4H), 1.63 (s, 3H), 1.56 (s, 3H), 1.32 (t, $J=7.2$ Hz, 6H); ^{13}C NMR (CDCl_3): δ 130.1, 130.0, 129.5, 129.3, 127.3, 90.3, 81.9, 65.6, 65.4, 63.1, 52.3, 46.9, 30.3, 27.9, 23.4, 22.5, 19.6, 15.7; ESIHRMS: Calcd for $\text{C}_{18}\text{H}_{32}\text{N}_2\text{O}_6\text{P}$ [M+H] $^+$ 403.1998. Found 403.2002.

4.1.6.8. Ethyl 2,2-dibenzylpent-4-enoate (16). *n*-BuLi (2.4 M in hexanes, 1.0 mL, 2.4 mmol) was added dropwise to diisopropylamine (30 mg, 2.3 mmol) in THF (3 mL) over 5 min at –78 °C under N_2 followed by stirring for 30 min. To this LDA solution was added 2-benzyl-3-phenylpropionate³ (406 mg, 1.86 mmol) in THF (3 mL) dropwise for 5 min. The reaction mixture was stirred for 45 min at –78 °C followed by dropwise addition of allyl bromide in THF (3 mL) at –78 °C. The reaction was slowly warmed up to 0 °C over a period of 2.5 h and quenched with satd aq NH_4Cl . The aqueous mixture was extracted with EtOAc, combined organic layer was washed with brine and dried and concentrated to dryness. Purification by column chromatography (hexanes/EtOAc, 9:1) provided **16** (510 mg, 89%). ^1H NMR: δ 7.31–7.17 (m, 10H), 6.08–5.94 (m, 1H), 5.28–5.16 (m, 2H), 4.09 (q, $J=7.2$, 2H), 3.13 (d, $J=14.1$ Hz, 2H), 2.92 (d, $J=13.2$ Hz, 2H), 2.35 (dd, $J=7.2$, 7.2 Hz, 2H), 1.190 (t, $J=7.5$ Hz, 3H); ^{13}C NMR: δ 175.4, 137.6, 134.4, 130.3, 128.2, 126.7, 119.1, 60.6, 51.8, 42.2, 36.0, 14.2; ESIHRMS: Calcd for $\text{C}_{21}\text{H}_{24}\text{O}_2\text{Na}$ [M+Na] $^+$ 331.1674. Found 331.1669.

4.1.6.9. 2,2-Dibenzylpent-4-en-1-ol (17). Ester **16** (51 mg, 0.17 mmol) in dry ether (2 mL) was added to a solution of LiAlH_4 (75 mg, 0.20 mmol) in dry ether (20 mL) at 0 °C under Ar. The resulting mixture was refluxed for 12 h and quenched by dropwise addition of 10% NaOH (1 mL) at rt. The organic layer was decanted off and the residue was washed with EtOAc. The combined organic layer was washed with water and brine and dried. Concentration and purification of the crude mixture by column chromatography (hexanes/EtOAc, 4:1) afforded the alcohol **17** (41 mg, 95%). ^1H NMR: δ 7.32–7.20 (m, 10H), 6.04 (m, 1H), 5.15 (m, 2H), 3.35 (s, 2H), 2.76 (d, $J=13.2$ Hz, 2H), 2.68 (d, $J=13.2$ Hz, 2H), 2.01 (d, $J=6.9$ Hz, 2H); ^{13}C NMR: δ 138.4, 135.0, 130.8, 128.2, 126.3, 118.3, 66.5, 43.0, 41.3, 38.2; ESIHRMS: Calcd for $\text{C}_{19}\text{H}_{22}\text{O}$ [M] $^+$ 266.1671. Found 266.1688.

4.1.6.10. 5-Benzylamino-4,4-dibenzylpent-1-ene (18).

Following the general procedure for Swern oxidation, alcohol **17** (4.77 g, 17.9 mmol) was converted to the corresponding aldehyde (5.23 g) as colorless oil, which was directly taken to the next reaction after the extraction. $^1\text{H NMR}$: δ 9.71 (s, 1H), 7.33–7.12 (m, 10H), 5.91 (m, 1H), 5.22 (m, 2H), 3.02 (d, $J=13.8$ Hz, 2H), 2.85 (d, $J=13.8$ Hz, 2H), 2.29 (d, $J=7.5$ Hz, 2H); $^{13}\text{C NMR}$: δ 206.6, 136.6, 133.4, 130.6, 128.5, 126.9, 119.5, 53.7, 40.3, 35.6; ESIHRMS: Calcd for $\text{C}_{19}\text{H}_{20}\text{ONa}$ $[\text{M}+\text{Na}]^+$ 287.1412. Found 287.1424. To a CH_3OH (50 mL) solution of crude aldehyde (5.23 g), benzylamine (3.86 g, 36.0 mmol) and $\text{CH}_3\text{CO}_2\text{H}$ (1.10 mL, 18.5 mmol) was added sodium cyanoborohydride (1.48 g, 22.4 mmol) in portions at 0 °C under N_2 . The reaction was stirred at rt for 2 h. Satd aq NaHCO_3 was added, then CH_3OH was removed by the evaporation. The aqueous layer was extracted with ether, the combined organic layer was washed with satd aq NH_4Cl , satd aq NaHCO_3 , H_2O , and brine then dried. Concentration gave yellow oil which was purified by column chromatography giving amine **18** (4.84 g, 76% from alcohol) as a colorless oil. $^1\text{H NMR}$: δ 7.42–7.12 (m, 15H), 6.03 (m, 1H), 5.13 (m, 2H), 3.70 (s, 2H), 2.77 (d, $J=6.0$ Hz, 2H), 2.70 (d, $J=7.5$ Hz, 2H), 2.34 (s, 2H), 2.03 (d, $J=6.9$ Hz, 2H); $^{13}\text{C NMR}$: δ 138.7, 135.2, 130.9, 129.4, 128.8, 128.2, 128.0, 127.1, 126.2, 118.1, 68.1, 54.7, 54.3, 51.5, 42.1, 39.4; ESIHRMS: Calcd for $\text{C}_{26}\text{H}_{30}\text{N}$ $[\text{M}+\text{H}]^+$ 356.2378. Found 356.2376.

4.1.6.11. 5-[*N*-Benzyl-*N*-(*tert*-butyloxycarbonyl)amino-4,4-dibenzyl-pent-1-ene (19).

To the CH_2Cl_2 (50 mL) solution of **18** (4.552 g, 12.80 mmol) and TEA (2.8 mL, 20.1 mmol) was added Boc_2O (3.781 g, 17.32 mmol) in CH_2Cl_2 (7 mL) at 0 °C under N_2 , then it was stirred for 19 h at rt. The reaction was quenched with satd aq NH_4Cl , then aqueous layer was extracted with CH_2Cl_2 . The combined organic layer was washed with satd aq NH_4Cl , H_2O , and brine, then dried and concentrated to dryness. Purification by column chromatography then afforded Boc-protected amine **19** (5.62 g, 96%) as a colorless oil. $^1\text{H NMR}$: δ 7.31–7.04 (m, 15H), 5.99 (m, 1H), 5.09 (m, 2H), 4.49 (s, 2H), 3.42 (s, 2H), 2.82 (d, $J=13.8$ Hz, 2H), 2.74 (d, $J=13.8$ Hz, 2H), 2.19 (d, $J=6.9$ Hz, 2H), 1.39 (s, 9H); $^{13}\text{C NMR}$: δ 157.1, 138.5, 135.5, 131.2, 130.8, 129.1, 128.5, 128.0, 127.1, 126.9, 126.2, 117.8, 80.1, 57.5, 43.0, 42.6, 40.1, 28.6, 28.4; ESIHRMS: Calcd for $\text{C}_{31}\text{H}_{37}\text{NO}_2\text{Na}$ $[\text{M}+\text{Na}]^+$ 478.2722. Found 478.2716.

4.1.6.12. *N*-Benzyl-*N*-(*tert*-butyloxycarbonyl)-2,2-dibenzyl-4-hydroxy-5-methyl-5-nitrohexylamine (20). A solution of alkene **19** (5.05 g, 11.1 mmol) in CH_2Cl_2 (50 mL) was bubbled with O_3 at -78 °C until the solution turned blue. On complete disappearance of the starting material, N_2 gas was bubbled through the reaction mixture for 15 min at -78 °C. To the resulting mixture was added Ph_3P (3.33 g, 12.7 mmol) at -78 °C and the reaction was allowed to warm up to rt. After stirring the reaction mixture overnight, it was concentrated and purified by column chromatography to afford an aldehyde (1.74 g, 34%). $^1\text{H NMR}$: δ 9.69 (t, $J=1.5$ Hz, 1H), 7.34–7.09 (m, 15H), 4.43 (s, 2H), 3.51 (s, 2H), 3.00 (d, $J=13.8$ Hz, 2H), 2.84 (d, $J=13.8$ Hz, 2H), 2.37 (d, $J=1.5$ Hz, 2H), 1.36 (s, 9H); $^{13}\text{C NMR}$: δ 202.2, 157.0, 138.4, 137.3, 131.20, 131.15, 128.7, 128.6, 128.4, 128.3, 127.2, 126.7, 106.2, 80.6, 54.3, 53.5, 48.0,

43.9, 43.8, 28.3; ESIHRMS: Calcd for $\text{C}_{30}\text{H}_{35}\text{NO}_3\text{Na}$ $[\text{M}+\text{Na}]^+$ 480.2515. Found 480.2500. To a mixture of this aldehyde (1.30 g, 2.84 mmol) and 2-nitropropane (20 mL, 22 mmol) was added *t*-BuOK (177 mg, 1.58 mmol) at rt. After stirring for 12 h, the reaction was quenched with satd aq NH_4Cl , diluted with water, and the aqueous layer was extracted with Et_2O . The combined organic layer was washed with H_2O and brine, then dried and concentrated to dryness. Purification of the residue by column chromatography ($\text{Et}_2\text{O}/\text{CH}_2\text{Cl}_2$, 0.5:99.5) afforded nitroalcohol **20** (838 mg, 54%). $^1\text{H NMR}$: δ 7.33–7.13 (m, 13H), 7.01 (m, 2H), 4.67 (d, $J=15.9$ Hz, 1H), 4.30 (br t, $J=8.7$ Hz, 1H), 4.10 (d, $J=15.0$ Hz, 1H), 4.03 (d, $J=15.0$ Hz, 1H), 3.03–2.07 (m, 5H), 1.64 (dd, $J=12.0$, 11.4 Hz, 1H), 1.55 (s, 3H), 1.49–1.41 (m, 1H), 1.38 (s, 12H); $^{13}\text{C NMR}$: δ 158.4, 138.3, 138.1, 137.8, 131.2, 131.1, 128.6, 128.3, 128.24, 128.17, 127.3, 126.9, 126.6, 126.5, 92.8, 81.4, 77.2, 73.6, 43.0, 42.1, 28.3, 22.2, 21.8; ESIHRMS: Calcd for $\text{C}_{33}\text{H}_{42}\text{N}_2\text{O}_5\text{Na}$ $[\text{M}+\text{Na}]^+$ 569.2991. Found 569.2997.

4.1.6.13. *N*-Benzyl-2,2-dibenzyl-5-methyl-5-nitro-4-oxo-hexylamine (21).

Following the general procedure for removal of Boc group, **20** (140 mg, 0.26 mmol) afforded the crude secondary amine, which was directly taken to the next step after the extraction. Following the general procedure for Swern oxidation, ketone **21** (97 mg, 86%) was obtained as colorless oil. $^1\text{H NMR}$: δ 8.32 (br s, 1H), 7.47–7.06 (m, 15H), 4.05 (s, 2H), 3.35 (s, 2H), 3.11 (d, $J=13.5$ Hz, 2H), 3.00 (d, $J=13.5$ Hz, 2H), 2.37 (s, 2H), 1.67 (s, 6H); $^{13}\text{C NMR}$: δ 202.1, 162.2, 138.2, 130.92, 130.90, 130.7, 130.6, 130.1, 129.0, 128.4, 128.3, 126.5, 94.9, 63.6, 57.5, 42.0, 40.5, 39.2, 23.8.

4.1.6.14. (4*R*)-*N*-Benzyl-*N*-(*tert*-butyloxycarbonyl)-2,2-dibenzyl-4-hydroxy-5-methyl-5-nitrohexylamine (22).

Following the general procedure for CBS reduction, ketone **21** (95 mg, 0.21 mmol) was converted to alcohol. The colorless oil was obtained by the extraction, then Boc protection was directly accomplished. To the CH_2Cl_2 solution (15 mL) of obtained alcohol, Boc_2O (160 mg, 0.73 mmol) and TEA (0.5 mL, 3.6 mmol) were added. The reaction was stirred overnight and the solvent was removed by evaporation. Purification by column chromatography gave enantiomerically enriched alcohol **22** (80 mg, 70%) as colorless oil, which showed similar spectra to racemate **20**. The enantiomeric excess was determined after the derivatization to **24**.

4.1.6.15. (4*R*)-*N*-Benzyl-*N*-(*tert*-butyloxycarbonyl)-2,2-dibenzyl-4-diphenylphosphatoxy-5-methyl-5-nitrohexylamine (23).

I_2 (306 mg, 1.21 mmol) was added to a stirred solution of ethyldiphenylphosphite (250 mg, 0.95 mmol) in CH_2Cl_2 (2 mL) at 0 °C under N_2 . After 15 min, this solution was added to a mixture of nitroalcohol **22** (345 mg, 0.63 mmol), pyridine (0.120 mL, 1.48 mmol) in CH_2Cl_2 (3 mL) under N_2 at 0 °C. The reaction mixture was stirred at 0 °C for 1 h, then NH_4Cl was added. The aqueous layer was extracted with CH_2Cl_2 , the combined organic layer was washed with 10% $\text{Na}_2\text{S}_2\text{O}_3$, H_2O , and brine, then dried and concentrated to dryness. Purification by column chromatography afforded phosphorylated product **23** (371 mg, 75%). $^1\text{H NMR}$: δ 7.36–7.03 (m, 25H), 5.78 (t, $J=9.0$ Hz, 1H), 4.45 (d, $J=16.2$ Hz, 1H), 4.29 (d, $J=16.2$ Hz, 1H), 3.71 (d, $J=14.7$ Hz, 1H), 3.45 (d, $J=14.7$ Hz, 1H),

3.11 (d, $J=14.7$ Hz, 1H), 3.02 (d, $J=14.4$ Hz, 1H), 2.99 (d, $J=14.7$ Hz, 1H), 2.83 (d, $J=14.4$ Hz, 1H), 1.91 (dd, $J=15.3, 10.8$ Hz, 1H), 1.75 (dd, $J=15.3, 4.5$ Hz, 1H), 1.61 (s, 3H), 1.42 (s, 3H), 1.33 (s, 9H); ^{13}C NMR: δ 157.3, 138.8, 138.1, 131.5, 130.1, 129.7, 128.7, 128.5, 128.3, 128.2, 126.8, 126.4, 125.3, 120.2, 91.7, 82.1, 80.2, 53.2, 53.0, 42.3, 41.7, 41.3, 35.8, 28.4, 27.7, 24.4, 21.3; ^{31}P NMR: δ -12.9; ESIHRMS: Calcd for $\text{C}_{45}\text{H}_{51}\text{N}_2\text{O}_8\text{PNa}$ $[\text{M}+\text{Na}]^+$ 801.3281. Found 801.3263.

4.1.6.16. (4R)-N-Benzyl-2,2-dibenzyl-4-diphenylphosphoxy-5-methyl-5-nitrohexylamine (24). Following the general procedure for removal of Boc group, phosphate **23** (294 mg, 0.38 mmol) gave the secondary amine **24** (245 mg, 96%, 79% ee). ^1H NMR: δ 7.33–7.09 (m, 25H), 5.96 (t, $J=8.4$ Hz, 1H), 3.67 (d, $J=13.5$ Hz, 1H), 3.61 (d, $J=13.5$ Hz, 1H), 3.01 (s, 2H), 2.77 (s, 2H), 2.73 (d, $J=12.3$ Hz, 1H), 2.63 (d, $J=12.3$ Hz, 1H), 1.76 (m, 2H), 1.65 (s, 3H), 1.46 (s, 3H); ^{13}C NMR: δ 150.7, 138.4, 138.0, 131.1, 131.0, 129.9, 128.8, 128.7, 128.2, 128.1, 127.7, 126.6, 126.4, 125.5, 120.2, 91.7, 82.2, 54.9, 54.6, 43.3, 42.4, 41.0, 35.7, 24.7, 20.8; ^{31}P NMR: δ -12.8; ESIHRMS: Calcd for $\text{C}_{40}\text{H}_{44}\text{N}_2\text{O}_6\text{P}$ $[\text{M}+\text{H}]^+$ 679.2937. Found 679.2943.

4.1.6.17. 2-{2-[N-Benzyl-N-(tert-butyloxycarbonyl)-amino]phenyl}ethanol (26). Carbamate **25**¹² (2.00 g, 8.45 mmol) was treated with NaH (60% in oil, 433 mg, 10.8 mmol) in DMF (80 mL) at 0 °C followed by dropwise addition of BnBr (1.10 mL, 9.25 mmol). After stirring overnight, the reaction was quenched with NH_4Cl and the separated aqueous layer was extracted with ether. The combined organic layer was washed with water and brine then dried. Purification by column chromatography gave **26** (1.39 g, 50%). ^1H NMR: δ 7.27–7.19 (m, 7H), 7.12 (m, 1H), 6.89 (br s, 1H), 4.91 (d, $J=14.5$ Hz, 1H), 4.50 (d, $J=14.5$ Hz, 1H), 3.75 (br s, 2H), 2.72 (m, 1H), 2.59 (m, 1H), 1.44 (s, 9H); ^{13}C NMR: δ 155.4, 141.3, 138.0, 136.8, 130.0, 129.1, 128.9, 128.3, 127.6, 127.4, 127.1, 80.6, 62.6, 54.3, 34.1, 28.3. Anal. Calcd for $\text{C}_{20}\text{H}_{25}\text{NO}_3$: C, 73.37; H, 7.70. Found: C, 73.27; H, 7.69.

4.1.6.18. 2-{2-[N-Benzyl-N-(tert-butyloxycarbonyl)-amino]phenyl}ethanal (27). Alcohol **26** (2.14 g, 6.52 mmol) was stirred in CH_2Cl_2 (40 mL) with PCC (98%, 1.74 g, 7.92 mmol) and 4 Å molecular sieves overnight. The resulting black suspension was filtered through silica gel pre-wetted by hexanes, eluting with Et_2O . Chromatographic purification gave **27** (1.326 g, 63%) as a colorless oil. ^1H NMR: δ 9.38 (s, 1H), 7.26–7.04 (m, 9H), 4.72 (m, 2H), 3.38 (d, $J=16.5$ Hz, 1H), 3.27 (d, $J=16.5$ Hz, 1H), 1.41 (s, 9H); ^{13}C NMR: δ 199.0, 154.7, 141.5, 137.6, 131.4, 130.7, 128.8, 128.4, 128.3, 127.6, 80.7, 54.2, 45.8, 28.3. Anal. Calcd for $\text{C}_{20}\text{H}_{23}\text{NO}_3$: C, 73.82; H, 7.12. Found C, 73.65; H, 7.11.

4.1.6.19. 1-[2-[N-Benzyl-N-(tert-butyloxycarbonyl)-amino]phenyl]-3-methyl-3-nitrobutan-2-ol (28). Following the general Henry reaction procedure, **27** (1.39 g, 4.28 mmol) afforded **28** (1.63 g, 92%). ^1H NMR: δ 7.32–6.90 (m, 9H), 4.79 (m, 1H), 4.60 (m, 1H), 4.37 (d, $J=11$ Hz, 0.5H), 4.24 (d, $J=11$ Hz, 0.5H), 2.58 (br s, 1H), 2.27–2.10 (m, 2H), 1.57 (s, 3H), 1.53 (s, 3H), 1.47 (s, 9H);

^{13}C NMR: δ 155.3, 141.3, 137.8, 137.4, 135.5, 131.0, 129.8, 129.5, 128.8, 128.4, 128.38, 128.2, 128.0, 127.8, 127.6, 91.6, 91.4, 81.9, 80.9, 74.4, 55.2, 54.3, 33.6, 32.1, 28.4, 28.3, 23.1, 20.9; ESIHRMS: Calcd for $\text{C}_{23}\text{H}_{30}\text{N}_2\text{O}_5\text{Na}$ $[\text{M}+\text{Na}]^+$ 437.2052. Found 437.2054.

4.1.6.20. 1-[2-[N-Benzyl-N-(tert-butyloxycarbonyl)-amino]phenyl]-3-methyl-3-nitro-2-(diphenylphosphoxy)butane (29). Following the general procedure for phosphorylation, **28** (198 mg, 0.48 mmol) afforded colorless oil **29** (291 mg, 94%). ^1H NMR: δ 7.50–6.80 (m, 19H), 5.61 (br s, 0.6H), 5.49 (m, 0.4H), 5.25 (m, 0.6H), 4.99 (d, $J=14.5$ Hz, 0.4H), 4.49 (d, $J=15$ Hz, 0.4H), 4.31 (d, $J=14.5$ Hz, 0.6H), 3.05 (d, $J=15$ Hz, 0.4H), 2.87 (m, 1.6H), 1.68 (s, 3H), 1.57 (s, 1H), 1.55 (s, 2H), 1.44 (s, 9H), 1.44; ^{13}C NMR: δ 155.1, 154.7, 150.52, 150.46, 150.4, 142.0, 141.6, 138.7, 138.0, 133.6, 133.4, 131.9, 130.1, 129.8, 129.6, 129.5, 129.49, 129.3, 128.8, 128.6, 128.4, 128.3, 128.1, 127.7, 127.6, 127.4, 127.3, 125.4, 125.3, 125.1, 120.2, 120.16, 120.1, 120.0, 90.5, 90.46, 90.38, 83.0, 82.98, 82.63, 82.6, 80.8, 80.7, 54.2, 53.3, 34.2, 32.3, 28.3, 23.4, 23.1, 21.8, 21.6; ^{31}P NMR: δ -12.4, -12.6; ESIHRMS: Calcd for $\text{C}_{35}\text{H}_{39}\text{N}_2\text{O}_8\text{PNa}$ $[\text{M}+\text{Na}]^+$ 669.2342. Found 669.2322.

4.1.6.21. 1-[2-Benzylaminophenyl]-3-methyl-3-nitro-2-(diphenylphosphoxy)butane (30). Removal of the Boc group from **29** (685 mg, 1.06 mmol) according to the general procedure gave **30** (568 mg, 98%). ^1H NMR: δ 7.42–6.90 (m, 17H), 6.58 (m, 2H), 5.65 (m, 1H), 5.11 (br s, 1H), 4.41 (d, $J=15$ Hz, 1H), 4.35 (d, $J=15$ Hz, 1H), 3.15 (dd, $J=15, 6$ Hz, 1H), 2.86 (dd, $J=15, 6$ Hz, 1H), 1.68 (s, 3H), 1.42 (s, 3H); ^{13}C NMR: δ 150.4, 150.37, 150.3, 150.2, 146.4, 139.7, 131.5, 129.9, 129.0, 128.6, 127.3, 127.0, 125.6, 120.3, 120.2, 120.19, 119.1, 117.1, 111.6, 90.8, 90.75, 80.44, 80.40, 47.8, 35.5, 23.1, 21.7; ^{31}P NMR: δ -11.1; ESIHRMS: Calcd for $\text{C}_{30}\text{H}_{31}\text{N}_2\text{O}_6\text{PNa}$ $[\text{M}+\text{Na}]^+$ 569.1817. Found 569.1819.

4.1.6.22. (4R)-N-(tert-Butyloxycarbonyl)-4-diphenylphosphoxy-5-methyl-5-nitrohexylamine (31). Phosphate **9** (103 mg, 0.17 mmol) was treated with PdCl_2 (64 mg, 0.36 mmol) in methanol (10 mL) under hydrogen atmosphere for 4 h. Satd aq NaHCO_3 was added, then it was extracted with EtOAc. The organic layer was washed with H_2O and brine, then dried and concentrated to dryness. Purification by column chromatography gave the secondary amine **31** (84 mg, 97%) as colorless oil. $[\alpha]_D^{23} +0.3$ (c 0.94); ^1H NMR: δ 7.36–7.14 (m, 10H), 5.15 (m, 1H), 4.43 (br s, 1H), 3.06 (m, 2H), 1.75–1.48 (m, 4H), 1.61 (s, 3H), 1.56 (s, 3H), 1.43 (s, 9H); ^{13}C NMR: δ 155.6, 129.9, 129.3, 125.6, 120.4, 120.1, 90.3, 83.5, 39.8, 28.5, 26.5, 23.0, 21.5; ^{31}P NMR: δ -12.0; ESIHRMS: Calcd for $\text{C}_{24}\text{H}_{33}\text{N}_2\text{O}_8\text{PNa}$ $[\text{M}+\text{Na}]^+$ 531.1872. Found 531.1859.

4.1.6.23. (4R)-N-(tert-Butyloxycarbonyl)-N-prop-2-ynyl-4-diphenylphosphoxy-5-methyl-5-nitrohexylamine (32). Secondary amine **31** (161 mg, 0.317 mmol) was treated with NaH (60% in oil, 37 mg, 0.93 mmol) in DMF (15 mL) at 0 °C under N_2 for 20 min, then propargyl bromide (75 mg, 0.63 mmol) was added dropwise. The reaction was stirred for 1 h, then quenched with H_2O . It was extracted with EtOAc then washed with H_2O and brine. It was dried

over Na₂SO₄ followed by the evaporation, which gave a brown oil. Purification by column chromatography gave **32** (160 mg, 92%) as a colorless oil. ¹H NMR: δ 7.34–7.18 (m, 10H), 5.15 (m, 1H), 3.92 (m, 2H), 3.31 (t, *J*=7.2 Hz, 2H), 2.13 (t, *J*=2.1 Hz, 1H), 1.90–1.78 (m, 2H), 1.75–1.65 (m, 2H), 1.62 (s, 3H), 1.57 (s, 3H), 1.45 (s, 9H); ¹³C NMR: δ 155.1, 129.8, 125.5, 120.2, 83.6, 80.4, 71.7, 46.1, 36.3, 28.8, 28.4, 24.7, 23.8, 22.7, 22.2; ³¹P NMR: δ –12.1; ESIHRMS: Calcd for C₂₇H₃₅N₂O₈PNa [M+Na]⁺ 569.2029. Found 569.2036.

4.1.6.24. (4*R*)-4-Diphenylphosphatoxy-*N*-prop-2-ynyl-5-methyl-5-nitrohexylamine (33). Following the general procedure for removal of Boc group, **32** (211 mg, 0.386 mmol) gave the precursor of radical cyclization **33** (170 mg, 99%). ¹H NMR: δ 7.33–7.17 (m, 10H), 5.17 (m, 1H), 3.36 (s, 2H), 2.66 (m, 2H), 2.52 (br s, 1H), 2.21 (s, 1H), 1.66–1.64 (m, 4H), 1.61 (s, 3H), 1.56 (s, 3H); ¹³C NMR: δ 129.8, 125.5, 120.2, 106.2, 90.4, 83.7, 71.8, 47.7, 37.9, 29.2, 25.7, 22.7, 22.0; ³¹P NMR: δ –11.9; ESIHRMS: Calcd for C₂₂H₂₈N₂O₆P [M+H]⁺ 447.1685. Found 447.1677.

4.1.6.25. 4,4-Diphenylcyclohexanone oxime (34). 4,4-Diphenylcyclohexanone²⁹ (4.70 g, 18.8 mmol) in EtOH (94 mL) was added to a stirred solution of hydroxylamine hydrochloride (6.25 g, 90.0 mmol) and sodium acetate (12.63 g, 154 mmol) in water (25 mL) at rt. The resulting milky white solution was stirred for 2 h and concentrated under rotary evaporation. The residue was extracted with EtOAc, dried by Na₂SO₄, and concentrated. Purification of the crude mixture by column chromatography (EtOAc/hexanes, 1:5) afforded oxime **34** (4.85 g, 97%). IR (film): 3243, 1446 cm⁻¹; ¹H NMR: δ 7.31–7.26 (m, 10H), 2.66 (t, *J*=6.9 Hz, 2H), 2.50–2.34 (m, 6H); ¹³C NMR: δ 159.8, 146.6, 128.6, 127.0, 126.1, 46.3, 36.5, 35.5, 28.5, 21.4; ESIHRMS: Calcd for C₁₈H₁₉NONa [M+Na]⁺ 288.1364. Found 288.1360.

4.1.6.26. 1-Chloro-1-nitro-4,4-diphenylcyclohexane (35). Trichloroisocyanuric acid (20.41 g, 88 mmol) was added in five portions at 5 min intervals to a well stirred two phase mixture of EtOAc/H₂O (1:1, 1534 mL), oxime **34** (4.60 g, 17.5 mmol), and NaHCO₃ (36.4 g, 434 mmol). The reaction mixture developed a distinct blue color after 20 min and stirring was continued at rt until the organic layer became colorless for 24 h. The reaction mixture was transferred into a separatory funnel and 0.2 M aq NaOH solution (230 mL) was added. The aqueous layer was extracted with EtOAc. The combined organic layer was washed with water and brine and concentrated to dryness. Purification by column chromatography (EtOAc/hexanes, 1:5) afforded **35** (1.54 g, 28%). IR (film): 1555, 698 cm⁻¹; ¹H NMR: δ 7.38–7.18 (m, 10 H), 2.67–2.43 (m, 8H); ¹³C NMR: δ 129.0, 128.84, 128.77, 126.9, 126.63, 126.60, 126.52, 126.49, 126.44, 35.8, 35.2, 33.2; ESIHRMS: Calcd for C₁₈H₁₈NO₂Cl [M]⁺ 315.1.26. Found 315.1025.

4.1.6.27. 1-Nitro-4,4-diphenylcyclohexane (36). Ten percent Pd/C (106 mg, 5%) and NaBH₄ (337 mg, 8.9 mmol) were added to a solution of **35** (2.00 g, 6.3 mmol) in EtOH (33 mL) at rt. The reaction was stirred for 1 h after which it was filtered and concentrated. The

residue was diluted with water and the aqueous layer was extracted with EtOAc. The combined organic layer was washed with brine, dried and concentrated. Purification of the crude mixture by column chromatography (EtOAc/hexanes, 1:4) afforded **36** (850 mg, 48%). IR (film): 1543 cm⁻¹; ¹H NMR: δ 7.38–7.14 (m, 10H), 4.52–4.48 (m, 1H), 2.78–2.71 (m, 2H), 2.26–2.14 (m, 6H); ¹³C NMR: δ 149.6, 144.0, 128.9, 128.6, 127.3, 126.4, 126.3, 126.2, 83.8, 34.0, 27.2; ESIHRMS: Calcd for C₁₈H₁₉NO₂ [M]⁺ 281.1415. Found 281.1414.

4.1.6.28. 4-(*tert*-Butyldimethylsiloxy)-1-(1'-nitro-4',4'-diphenylcyclohexyl)butan-1-ol (37). To a stirred solution of **36** (166 mg, 0.59 mmol) in THF (1 mL) was added 0.025 M aqueous NaOH (0.87 mL) at rt and further stirred for 2 min. 4-(*tert*-Butyldimethylsiloxy)butan-1-ol (107 mg, 0.53 mmol) was added followed by cetyl ammonium bromide (21 mg, 0.059 mmol) at rt. After stirring the reaction for 12 h at ambient temperature, the reaction was quenched with satd aq NH₄Cl solution (5 mL) and the aqueous layer was extracted with EtOAc. The organic layer was washed with water and brine and dried. Concentration and purification of the residue by column chromatography (EtOAc/hexanes, 1:9) afforded nitro alcohol **37** (0.142 g, 50%) as a colorless oil. ¹H NMR: δ 7.38–7.10 (m, 10H), 3.68–3.57 (m, 3H), 3.39 (d, *J*=4.8 Hz, 1H), 2.67–2.53 (m, 4H), 2.09–1.60 (m, 8H), 0.87 (s, 9H), 0.03 (s, 6H); ¹³C NMR: δ 149.6, 144.0, 128.8, 128.4, 127.5, 126.2, 126.1, 126.0, 94.9, 76.4, 63.2, 45.3, 32.4, 29.1, 28.8, 27.5, 27.1, 26.0, 18.4, –5.3; ESIHRMS: Calcd for C₂₈H₄₁NO₄SiK [M+K]⁺ 522.2442. Found 522.2437. Anal. Calcd for C₂₈H₄₁NO₄Si: C, 69.52; H, 8.54. Found: C, 69.78; H, 8.45.

4.1.6.29. 4-(*tert*-Butyldimethylsiloxy)-1-(1'-nitro-4',4'-diphenylcyclohexyl)butan-1-one (38). Following the general procedure for Swern oxidation, nitroalcohol **37** (629 mg, 1.3 mmol) provided ketone **38** (388 mg, 62%). IR (film) 1725, 1542 cm⁻¹; ¹H NMR: δ 7.34–7.12 (m, 10H), 3.54 (t, *J*=6.3 Hz, 2H), 2.62 (d, *J*=11.4 Hz, 4H), 2.53 (t, *J*=6.9 Hz, 2H), 2.16 (d, *J*=10.5 Hz, 4H), 1.73 (quint, *J*=6.0 Hz, 2H), 0.87 (s, 9H), 0.01 (s, 6H); ¹³C NMR: δ 201.7, 148.3, 144.1, 129.0, 128.5, 127.1, 126.5, 126.2, 98.4, 61.4, 44.9, 32.4, 32.1, 28.3, 26.4, 26.0, 18.4, –5.2. Anal. Calcd for C₂₈H₃₉NO₄Si: C, 69.82; H, 8.16. Found C, 69.74; H, 8.25.

4.1.6.30. (1*R*)-4-(*tert*-Butyldimethylsiloxy)-1-(1'-nitro-4',4'-diphenylcyclohexyl)butan-1-ol (39). Following the general procedure for CBS reduction, ketone **38** (563 mg, 1.0 mmol) afforded alcohol **39** (420 mg, 87%, 96% ee). [α]_D²³ +9.0 (*c* 1.0); with spectral data matching those of the racemate (**37**).

4.1.6.31. (1*R*)-4-(*tert*-Butyldimethylsilyloxy)-1-(1'-nitro-4',4'-diphenylcyclohexyl)-1-diphenylphosphatoxy butane (40). Following general procedure for phosphorylation, alcohol **39** (104 mg, 0.21 mmol) afforded phosphate **40** (109 mg, 74%). ¹H NMR: δ 7.37–7.08 (m, 20H), 4.73 (m, 1H), 3.64–3.48 (m, 2H), 2.69–2.60 (m, 4H), 2.05–1.82 (m, 5H), 1.63–1.51 (m, 3H), 0.86 (s, 9H), 0.00 (s, 6H); ¹³C NMR: δ 150.5, 149.3, 143.5, 129.9, 129.8, 129.0, 128.8, 128.4, 127.5, 127.3, 126.4, 126.2, 126.1, 126.0, 125.5, 120.3, 120.2, 120.1, 93.5, 93.4, 84.4, 84.3, 76.4, 63.2, 61.9, 45.0,

32.2, 32.1, 29.2, 28.7, 27.8, 27.7, 27.5, 27.2, 27.1, 26.0, 18.4, –5.2; ^{31}P NMR: δ –11.80; ESIHRMS: Calcd for $\text{C}_{40}\text{H}_{50}\text{NO}_7\text{PSiNa}$ $[\text{M}+\text{Na}]^+$ 738.2992. Found 738.2984.

4.1.6.32. (4R)-4-Diphenylphosphatoxy-4-(1'-nitro-4', 4'-diphenylcyclohexyl)butan-1-ol (41). To a solution of **40** (100 mg, 0.15 mmol) in acetonitrile (6 mL) at rt was added aqueous solution of HF (49%, 0.15 mmol, 4 mL). The reaction was further stirred for 5 min and diluted with EtOAc. The organic layer was washed with water and brine and dried over Na_2SO_4 . Concentration and purification of the residue by column chromatography (EtOAc/hexanes, 1:1) afforded alcohol **41** (55 mg, 63%, 94% ee). ^1H NMR: δ 7.35–7.06 (m, 20H), 4.76 (t, $J=7.6$ Hz, 1H), 3.54–3.47 (m, 2H), 2.69–2.61 (m, 4H), 2.03–1.55 (m, 8H); ^{13}C NMR: δ 149.2, 143.4, 129.9, 129.0, 128.4, 127.4, 126.4, 126.1, 125.6, 120.2, 120.1, 93.5, 93.4, 84.2, 84.1, 62.0, 45.0, 32.1, 28.4, 27.8, 27.7, 27.5, 27.4; ^{31}P NMR: δ –11.72; ESIHRMS: Calcd for $\text{C}_{34}\text{H}_{38}\text{NO}_7\text{P}$ $[\text{M}+\text{H}]^+$ 602.2308. Found 602.2335.

4.1.6.33. 2,2-Dibenzyl-1-(tert-butyldimethylsiloxy)-pent-4-ene (42). Alcohol **17** (0.50 g, 1.87 mmol) in DMF (2 mL) was added slowly to a stirred solution of TBDMSCl (0.338 g, 2.24 mmol) and imidazole (0.317 g, 4.6 mmol) in DMF (15 mL) at 0 °C under Ar. The resulting mixture was warmed to rt and stirred for 2 h. Water (15 mL) was added and the aqueous layer was extracted with hexane (3 \times 15 mL). The combined organic layer was washed with water and brine and dried. Concentration and purification of the crude mixture by column chromatography (hexanes/EtOAc, 9:1) afforded **42** (0.60 g, 79%). ^1H NMR: δ 7.28–7.17 (m, 10H), 6.08–5.99 (m, 1H), 5.17–5.03 (m, 2H), 3.18 (s, 2H), 2.69 (ABq, $J=13.2$, 13.2 Hz, 4H), 1.93 (d, $J=7.2$ Hz, 2H), 1.00 (s, 9H), 0.06 (s, 6H); ^{13}C NMR: δ 138.7, 134.9, 131.0, 127.8, 126.0, 117.9, 65.5, 42.9, 40.4, 37.1, 26.1, –5.3; ESIHRMS: Calcd for $\text{C}_{25}\text{H}_{36}\text{OSiNa}$ $[\text{M}+\text{Na}]^+$ 403.2433. Found 403.2452.

4.1.6.34. 3-Benzyl-3-(tert-butyldimethylsilyloxymethyl)-4-phenylbutanal (43). A solution of olefin (6.0 g, 15.8 mmol) in DCM (180 mL) cooled to –78 °C was bubbled O_3 until the solution turned light blue. On complete disappearance of the starting material, N_2 gas was bubbled through the reaction mixture for 10 min at –78 °C. The resulting mixture was treated with Me_2S (4.89 g, 79 mmol) at –78 °C and slowly warmed to rt. After stirring for 6 h at rt, it was concentrated and purified by column chromatography (hexanes/EtOAc, 9:1) to afford **43** (5.77 g, 96%). IR (film): 1718, 1085 cm^{-1} ; ^1H NMR: δ 9.86 (br s, 1H), 7.33–7.21 (m, 10H), 3.42 (s, 2H), 2.92 (s, 4H), 2.23 (d, $J=2.1$ Hz, 2H), 1.04 (s, 9H), 0.14 (s, 6H); ^{13}C NMR δ 202.6, 137.7, 130.9, 128.2, 126.6, 65.5, 47.6, 43.7, 41.1, 26.1, 18.4, –5.2; ESIHRMS: Calcd for $\text{C}_{24}\text{H}_{34}\text{NO}_2\text{SiNa}$ $[\text{M}+\text{Na}]^+$ 405.2226. Found 405.2224.

4.1.6.35. 5-Benzyl-5-(tert-butyldimethylsilyloxy-methyl)-2-methyl-2-nitro-6-phenylhexan-3-ol (44). To a stirred solution of **43** (70 mg, 0.18 mmol) and 2-nitropropane (0.77 g, 2.6 mmol) was added *t*-BuOK (0.77 g, 2.6 mmol) at 0 °C. After stirring for 12 h at rt the reaction was quenched with satd solution of NH_4Cl , diluted with water and the aqueous layer was extracted with EtOAc. Concentration

and purification of the residue by column chromatography (EtOAc/hexanes, 3:7) afforded **44** (70 mg, 81%). IR (film) 3394, 1543, 1082 cm^{-1} . ^1H NMR: δ 7.32–7.12 (m, 10H), 4.42–4.39 (m, 1H), 4.13 (d, $J=3.0$ Hz, 1H), 3.56 (d, $J=9.9$ Hz, 1H), 3.41 (d, $J=9.9$ Hz, 1H), 2.86 (d, $J=13.5$ Hz, 1H), 2.73 (m, 2H), 2.63 (d, $J=13.5$ Hz, 1H), 1.51 (s, 3H), 1.49–1.39 (m, 2H), 1.40 (s, 3H), 0.93 (s, 9H), 0.09 (s, 3H), 0.08 (s, 3H); ^{13}C NMR: δ 137.6, 137.4, 131.0, 130.9, 128.2, 128.1, 126.6, 126.5, 92.4, 71.9, 68.5, 43.8, 40.8, 37.5, 26.0, 23.0, 20.8, 0.16, –5.3; ESIHRMS: Calcd for $\text{C}_{27}\text{H}_{41}\text{NO}_4\text{SiNa}$ $[\text{M}+\text{Na}]^+$ 494.2703. Found 494.2709.

4.1.6.36. 2,2-Dibenzyl-1-(tert-butyldimethylsiloxy)-5-methyl-5-nitro-4-(diphenylphosphatoxy)hexane (45). I_2 (0.0812 g, 0.32 mmol) was added to a stirred solution of ethyldiphenylphosphite (0.08 g, 0.31 mmol) in dichloromethane (9 mL) at –30 to –20 °C under Ar. After 15 min this solution was added to a mixture of **44** (0.15 g, 0.32 mmol), pyridine (0.10 g, 1.28 mmol) in dichloromethane (15 mL) under Ar at –30 to –20 °C. The reaction mixture was allowed to warm to 0 °C, diluted with dichloromethane, subsequently washed with NH_4Cl , satd $\text{Na}_2\text{S}_2\text{O}_3$, brine and dried. Concentration and purification by column chromatography (hexanes/EtOAc, 4:1) afforded **45** (100 mg, 46%). IR (film): 1548, 1010, 956 cm^{-1} ; ^1H NMR: δ 7.29–7.12 (m, 20H), 5.78 (t, $J=9.0$ Hz, 1H), 3.42 (d, $J=9.9$ Hz, 1H), 3.19 (d, $J=9.9$ Hz, 1H), 2.99 (s, 2H), 2.94 (d, $J=13.5$ Hz, 1H), 2.65 (d, $J=13.5$ Hz, 1H), 1.65 (s, 3H), 1.47–1.68 (m, 2H), 1.25 (s, 3H), 0.94 (s, 9H), 0.25 (s, 3H), 0.21 (s, 3H); ^{31}P NMR: δ –13.07; ^{13}C NMR: δ 156.4, 150.6, 150.5, 138.0, 137.9, 131.3, 129.9, 129.5, 128.1, 128.0, 126.3, 125.6, 125.5, 120.2, 120.1, 120.0, 115.6, 91.5, 82.0, 66.0, 41.6, 40.1, 39.5, 33.2, 33.1, 26.1, 24.3, 21.2, 18.3, –5.2, –5.3; ESIHRMS: Calcd for $\text{C}_{39}\text{H}_{50}\text{NO}_7\text{SiPNa}$ $[\text{M}+\text{Na}]^+$ 726.2992. Found 726.2986.

4.1.6.37. 6,6-Dibenzyl-4-(1-methyl-1-nitroethyl)-2-phenoxy-[1,3,2]dioxaphosphepane 2-oxide (46). Forty-nine percent aqueous HF solution (2 mL) was added to a solution of **45** (0.086 g, 0.08 mmol) in CH_3CN (2 mL) at 0 °C. The reaction mixture was stirred for 5 min at rt followed by quenching with water (5 mL) at rt. The aqueous layer was extracted with EtOAc, washed with brine, and dried. Concentration and purification by column chromatography (EtOAc/hexanes, 1:1) provided **46** (0.049 g, 70%). IR (film): 1546 cm^{-1} ; ^1H NMR: δ 7.36–6.89 (m, 15H), 5.26–5.19 (m, 1H), 3.94 (d, $J=9.6$ Hz, 1H), 3.44 (d, $J=13.5$ Hz, 1H), 2.61–2.45 (m, 4H), 1.90 (dd, $J=11.1$, 10.8 Hz, 1H), 1.68 (s, 3H), 1.54 (s, 3H), 1.53–1.46 (m, 1H); ^{31}P NMR: δ –4.48; ^{13}C NMR: δ 135.8, 135.4, 131.2, 131.0, 130.5, 129.9, 128.7, 128.6, 128.6, 128.5, 127.1, 127.0, 125.6, 120.0, 120.0, 89.8, 89.7, 75.9, 75.8, 72.1, 43.5, 40.75, 40.73, 40.6, 38.4, 24.5, 20.3; ESIHRMS: Calcd for $\text{C}_{27}\text{H}_{30}\text{NO}_6\text{PNa}$ $[\text{M}+\text{Na}]^+$ 518.1708. Found 518.1689.

4.1.6.38. 2,2-Dibenzyl-1-(tert-butyldimethylsiloxy)-4-(diethylphosphatoxy)-5-methyl-5-nitrohexane (47). To a solution of **44** (0.370 g, 0.79 mmol), pyridine (0.312 g, 3.95 mmol) in dichloromethane (11 mL) at 10 °C was added diethylchlorophosphite (0.37 g, 2.37 mmol) and stirred for 30 min at rt. When the starting material was consumed, *t*-BuOOH (0.79 mL, 3.95 mmol) was added into the reaction

flask at 10 °C over 5 min and continued stirring for 20 min at rt. EtOAc (20 mL) was added and the organic layer was washed with 5% Na₂S₂O₃, and dried. Concentration and purification of the crude mixture by column chromatography (EtOAc/hexanes, 3:2) gave **47** (0.233 g, 58%). IR (film): 1549, 1031, 1004 cm⁻¹; ¹H NMR: δ 7.37–7.18 (m, 10H), 5.51 (t, *J*=9.0 Hz, 1H), 4.20–4.13 (m, 4H), 3.41 (d, *J*=9.9 Hz, 1H), 3.19 (d, *J*=9.9 Hz, 1H), 3.07 (d, *J*=13.5 Hz, 1H), 2.98 (m, 1H), 2.93 (m, 1H), 2.69 (d, *J*=13.5 Hz, 1H), 1.61 (s, 3H), 1.57–1.40 (m, 2H), 1.42 (s, 3H), 1.39–1.28 (m, 6H), 0.98 (s, 9H), 0.10 (s, 3H), 0.04 (s, 3H); ³¹P NMR: δ -1.99; ¹³C NMR: δ 138.1, 131.2, 131.0, 127.8, 126.1, 91.5, 79.9, 79.8, 65.7, 64.4, 64.3, 64.2, 41.5, 39.8, 39.2, 32.6, 32.5, 26.0, 24.4, 20.7, 18.2, 16.2, 16.1, -5.3, -5.4; ESIHRMS: Calcd for C₃₁H₅₀NO₇SiPNa [M+Na]⁺ 630.2992. Found 630.2987.

4.1.6.39. 2,2-Dibenzyl-4-(diethylphosphoxy)-5-methyl-5-nitrohexanol (48). To a solution of **47** (0.18 g, 0.29 mmol) in acetonitrile (2 mL) was added aq HF (49%, 1.02 mL, 29 mmol) at rt. After stirring for 5 min at rt, water (4 mL) was added and the aqueous mixture was extracted with EtOAc. The organic layer was washed with water and brine and dried. Concentration and purification of the crude mixture by column chromatography (EtOAc/hexanes, 3:2) afforded **48** (82 mg, 58%). ¹H NMR: δ 7.29–7.18 (m, 10H), 5.56 (m, 1H), 4.09 (m, 2H), 3.98 (m, 2H), 3.50 (s, 2H), 2.94 (d, *J*=13.2, 1H), 2.90 (m, 2H), 2.54 (d, *J*=13.2 Hz, 1H), 1.76 (dd, *J*=15.3, 8.4 Hz, 1H), 1.58 (s, 3H), 1.58–1.48 (m, 1H), 1.42 (s, 3H), 1.32 (t, *J*=6.0 Hz, 3H), 1.22 (t, *J*=6.0 Hz, 3H); ³¹P NMR: δ -2.09; ¹³C NMR: δ 138.0, 137.9, 131.1, 131.0, 128.3, 128.2, 126.5, 126.4, 91.7, 79.8, 65.6, 64.7, 64.3, 41.7, 41.6, 41.4, 36.9, 24.3, 20.4, 16.2, 16.1; ESIHRMS: Calcd for C₂₅H₃₆NO₇PNa [M+Na]⁺ 516.2127. Found 516.2113.

4.1.7. Typical protocol for the radical cyclization.

4.1.7.1. (S)-1-Benzyl-2-isopropylpyrrolidine (49). To the solution of the radical precursor **11** (200 mg, 0.40 mmol) and AIBN (14 mg, 0.085 mmol) in deoxygenated benzene (30 mL) was added tributyltin hydride (0.173 mL, 0.643 mmol). The reaction mixture was heated to reflux for 30 h with addition of further AIBN (8 mg, 0.05 mmol) twice in 12 h intervals. The reaction mixture was then cooled to rt, 2 M HCl (12 mL) was added, and the biphasic mixture was stirred for 20 min. The organic layer was washed with aq 2 M HCl and the combined aqueous layer was washed with hexane, then basified to pH 11 with 15% NaOH and extracted with ethyl ether. The combined organic layer was washed with water and brine then dried. Concentration under reduced pressure followed by chromatographic purification afforded **49** (35 mg, 43%, 61% ee) as colorless oil. [α]_D²³ -32.4 (*c* 1.0); ¹H NMR: δ 7.38–7.22 (m, 5H), 4.04 (d, *J*=13.2 Hz, 1H), 3.10 (d, *J*=13.2 Hz, 1H), 2.88 (m, 1H), 2.34 (m, 1H), 2.03 (m, 1H), 1.95 (m, 1H), 1.61 (m, 4H), 0.94 (s, 3H), 0.92 (s, 3H); ¹³C NMR: δ 131.4, 129.9, 129.2, 127.9, 78.2, 71.6, 52.3, 29.7, 28.7, 26.1, 22.1, 21.1; ESIHRMS: Calcd for C₁₄H₂₂N [M+H]⁺ 204.1752. Found 204.1747.

4.1.7.2. (S)-1-Benzyl-2-isopropylpiperidine (50). Following the general procedure for radical cyclization, **12** (180 mg, 0.351 mmol) afforded **50** (31 mg, 41%, 60% ee)

as colorless oil. [α]_D²³ -23.7 (*c* 0.27); ¹H NMR: δ 7.39–7.19 (m, 5H), 4.10 (d, *J*=13.5 Hz, 1H), 3.09 (d, *J*=13.5 Hz, 1H), 2.81 (m, 1H), 2.26 (m, 1H), 2.00 (m, 1H), 1.92 (m, 1H), 1.73 (m, 1H), 1.60 (m, 2H), 1.42 (m, 1H), 1.23 (m, 2H), 0.94 (d, *J*=3.0 Hz, 3H), 0.91 (d, *J*=3.0 Hz, 3H); ¹³C NMR: δ 129.0, 128.2, 126.6, 124.4, 77.4, 66.6, 56.6, 27.7, 24.9, 24.7, 23.6, 20.3, 16.1; ESIHRMS: Calcd for C₁₅H₂₄N [M+H]⁺ 218.1909. Found 218.1911.

4.1.7.3. (S)-1,4,4-Tribenzyl-2-isopropylpyrrolidine (51). Following the general procedure for radical cyclization, **24** (205 mg, 0.30 mmol) afforded **51** (51 mg, 44%, 60% ee) as colorless oil. [α]_D²³ -24.4 (*c* 1.0); ¹H NMR: δ 7.35–7.00 (m, 15H), 3.96 (d, *J*=13.5 Hz, 1H), 2.90–2.75 (m, 3H), 2.66–2.62 (m, 3H), 2.20 (td, *J*=8.6, 4.5 Hz, 1H), 2.02–1.88 (m, 2H), 1.70 (dd, *J*=12.6, 8.6 Hz, 1H), 1.57 (dd, *J*=12.6, 9.0 Hz, 1H), 0.91 (d, *J*=6.9 Hz, 3H), 0.85 (d, *J*=7.2 Hz, 3H); ¹³C NMR: δ 140.1, 139.3, 131.0, 131.0, 128.8, 128.2, 128.0, 127.8, 126.7, 126.0, 125.9, 69.1, 62.8, 58.0, 46.1, 44.0, 35.0, 30.4, 27.8, 20.3, 15.3; ESIHRMS: Calcd for C₂₈H₃₄N [M+H]⁺ 384.2691. Found 384.2691.

4.1.7.4. N-Benzyl-2-(3-methyl-2-butenyl)aniline (52). Following the general procedure for radical cyclization, **30** (409 mg, 0.62 mmol) afforded **52** (80 mg, 50%) as a colorless oil. ¹H NMR: δ 7.38–7.34 (m, 3H), 7.31–7.26 (m, 2H), 7.14–7.08 (m, 2H), 6.73–6.67 (m, 2H), 5.21 (t, *J*=6.9 Hz, 1H), 4.33 (s, 2H), 3.22 (d, *J*=6.9 Hz, 2H), 1.69 (s, 3H), 1.58 (s, 3H); ¹³C NMR (CDCl₃): δ 133.7, 130.5, 129.3, 129.1, 128.6, 127.8, 127.3, 121.9, 117.5, 111.0, 48.6, 31.2, 25.7, 17.7; ESIHRMS: Calcd for C₁₈H₂₁N [M]⁺ 251.1674. Found 251.1670.

4.1.7.5. (7S)-1,1-Dimethyl-2-methylenepyrrolizidine (53). The general procedure for radical cyclization was followed but extraction method was changed. On complete consumption of **33** (144 mg, 0.32 mmol) the reaction mixture was cooled to rt, then 2 M HCl (12 mL) was added, and stirred for 20 min. The aqueous layer was washed with hexane, then basified to pH 11 with 15% aq NaOH and extracted with ethyl ether. The combined organic layer washed with water and 2 M HCl (12 mL) was added again. After stirring for 30 min, aqueous layer was separated and concentrated to give the pure HCl salt of pyrrolizidine **53** (39 mg, 64%, 60% ee). [α]_D²³ -9.2 (*c* 1.0); ¹H NMR: δ 12.8 (br s, 1H), 5.08 (br s, 1H), 5.06 (br s, 1H), 4.51 (dd, *J*=14.1, 6.3 Hz, 1H), 3.90 (m, 2H), 3.42 (d, *J*=15.6 Hz, 1H), 2.84 (m, 1H), 2.05 (m, 3H), 1.61 (m, 1H), 1.33 (s, 3H), 1.17 (s, 3H); ¹³C NMR: δ 108.9, 100.2, 76.9, 57.9, 56.2, 33.0, 28.8, 27.4, 25.2, 21.5; ESIHRMS: Calcd for C₁₀H₁₈N [M+H]⁺ 152.1439. Found 152.1439.

4.1.7.6. 2-(4',4'-Diphenylcyclohexyl)-tetrahydrofuran (54) and (7R)-7-(4',4'-diphenylcyclohexyl)-2-phenoxy-[1,3,2]dioxaphosphepane-2-oxide (55). To the mixture of **41** (158 mg, 0.26 mmol), AIBN (22 mg, 0.14 mmol), and tributyltin hydride (169 mg, 0.58 mmol) was added deoxygenated benzene (6.5 mL) and refluxed for 12 h. The reaction mixture was cooled, concentrated, and purified by column chromatography to provide tetrahydrofuran **54** (20 mg, 25%) and the cyclic phosphate **55** (68 mg, 52%). **54:** ¹H NMR: δ 7.38–7.16 (m, 10H), 3.81–3.79 (m, 1H), 3.67–3.65

(m, 1H), 3.40–3.35 (m, 2H), 2.72 (d, $J=12.4$ Hz, 1H), 1.97–1.80 (m, 5H), 1.59–0.98 (m, 6H); ^{13}C NMR: δ 151.3, 146.1, 128.5, 128.2, 128.1, 126.3, 125.6, 125.5, 83.8, 67.8, 46.1, 43.1, 36.3, 29.4, 26.6, 25.9, 25.4; ESIHRMS: Calcd for $\text{C}_{22}\text{H}_{26}\text{ONa}$ $[\text{M}+\text{Na}]^+$ 329.1881. Found 329.1886. **55**: ^1H NMR: δ 7.37–7.06 (m, 15H), 4.23–4.05 (m, 3H), 2.79–2.74 (m, 2H), 1.95–1.91 (m, 5H), 1.73–1.67 (m, 4H), 1.41–1.36 (m, 2H); ^{13}C NMR: δ 151.1, 144.8, 129.8, 128.7, 128.3, 128.0, 126.3, 125.8, 125.7, 125.1, 120.2, 83.0, 82.9, 68.9, 68.8, 45.9, 43.0, 36.3, 36.2, 31.8, 29.2, 25.5, 24.5; ^{31}P NMR: δ -2.92; ESIHRMS: Calcd for $\text{C}_{28}\text{H}_{31}\text{O}_4\text{PNa}$ $[\text{M}+\text{Na}]^+$ 485.1858. Found 485.1838.

4.1.7.7. 6,6-Dibenzyl-2-ethoxy-4-(1-methyl-1-nitroethyl)[1,3,2]dioxaphosphepane 2-oxide (56). In a one necked 25 mL flask fitted with a condenser, and a septum was placed nitrophosphate **48** (0.082 g, 0.177 mmol), tributyltin hydride (0.77 g, 0.27 mmol), and AIBN (0.012 g, 0.071 mmol). Degassed benzene (18 mL) was added to the reaction mixture, which was then heated to reflux in an oil bath preheated at 100 °C for 15 h. The reaction mixture was cooled to rt and concentrated. Chromatographic purification (EtOAc/hexanes, 3:7) provided cyclic phosphates **56** (44 mg, 67%). IR (film): 1026, 992 cm^{-1} ; ^1H NMR: δ 7.32–7.20 (m, 8H), 6.94 (d, $J=6.9$ Hz, 2H), 4.50–4.46 (m, 1H), 4.19–4.09 (m, 2H), 3.82–3.77 (m, 2H), 3.26 (d, $J=13.8$ Hz, 1H), 2.64 (d, $J=13.8$ Hz, 1H), 2.58 (d, $J=13.5$, 1H), 2.48 (d, $J=13.5$ Hz, 1H), 1.87–1.77 (m, 2H), 1.51 (d, $J=15.1$ Hz, 1H), 1.29 (t, $J=7.2$ Hz, 3H), 0.97 (d, $J=6.9$ Hz, 3H), 0.94 (d, $J=6.6$ Hz, 3H); ^{31}P NMR: δ 2.71; ^{13}C NMR: δ 136.7, 136.2, 131.3, 130.7, 128.4, 126.8, 126.7, 77.9, 71.4, 64.2, 43.7, 41.0, 40.8, 40.4, 33.8, 33.7, 19.0, 17.4, 16.3; ESIHRMS: Calcd for $\text{C}_{23}\text{H}_{32}\text{O}_2\text{PNa}$ $[\text{M}+\text{Na}]^+$ 425.1775. Found 425.1773.

4.1.7.8. (S)-1-*p*-Toluenesulfonyl-2-isopropylpyrrolidine (57). Pyrrolidine **49** (15 mg, 0.074 mmol) was treated in EtOAc (10 mL) with 20% Pd(OH)₂/C (18 mg) under a H₂ atmosphere for 4 h. The reaction mixture was carefully filtered through Celite and residue was washed with EtOAc (10 mL). The filtrate was treated with diisopropylethylamine (0.1 mL, 0.57 mmol) and TsCl (45 mg, 0.24 mmol), then stirred overnight at rt. The reaction was quenched with satd aq NaHCO₃ and aqueous layer was extracted with EtOAc. The combined organic layer was washed with H₂O and brine then dried. After the evaporation, the residue was purified by silica gel chromatography. The sulfonamide **57** (9 mg, 45%) was obtained as a colorless solid, $[\alpha]_{\text{D}}^{23}$ -78.1 (*c* 0.9), lit.¹⁴ $[\alpha]_{\text{D}}^{23}$ -91.3 (*c* 1.0).

4.1.7.9. *N*-tert-Butyloxycarbonyl *O*-(2-methyl-2-nitro-1-phenylpropyl) sulfamate (59). A solution of chlorosulfonyl isocyanate (0.8 mL, 9.1 mmol) in hexanes (8 mL) was added dropwise to a solution of 2-methylpropan-2-ol (675 mg, 9.1 mmol) in hexane (17 mL) and the solution was stirred at rt for 45 min. Then a solution of alcohol **58**²⁰ (1.2 g, 6.07 mmol) and triethylamine (1.35 mL, 9.7 mmol) in THF (20 mL) was added dropwise. After 2 h, the reaction was quenched with water and extracted with CH₂Cl₂. The organic layer was washed with brine, dried, and concentrated. Chromatographic purification (hexanes/EA from 90:10 to 70:30) afforded **59** (1.914 g, 84%) as a colorless oil. IR (neat): 3255, 2987, 1757, 1550, 1456, 1147,

923 cm^{-1} ; ^1H NMR: δ 7.39 (s, 5H), 7.30 (br s, 1H), 6.18 (s, 1H), 1.70 (s, 3H), 1.45 (s, 3H), 1.42 (s, 9H); ^{13}C NMR: δ 148.6, 133.1, 129.9, 128.8, 128.0, 90.5, 87.3, 84.9, 27.9, 23.9, 20.2.

4.1.7.10. *N*-Allyl *O*-(2-methyl-2-nitro-1-phenylpropyl) sulfamate (60). To a solution of **59** (1.0 g, 2.7 mmol) and allyl bromide (10 mL) in acetonitrile (16 mL) was added dropwise 1,8-diazabicyclo[5.4.0]undec-7-ene (0.52 mL, 3.5 mmol) at rt. The reaction mixture was stirred overnight and quenched with a satd aq NH₄Cl. The aqueous layer was extracted twice with CH₂Cl₂ and the resulting organic layer was washed with brine, dried, and concentrated. The residue was purified by flash chromatography (hexanes/EA from 95:5 to 85:15) to afford *N*-allyl *N*-tert-butyloxycarbonyl *O*-(2-methyl-2-nitro-1-phenylpropyl) sulfamate (962 mg, 87%) as a white solid. mp 68–70 °C; IR (neat): 3069, 2983, 1742, 1550, 1401, 1191, 1149, 958, 857, 843 cm^{-1} ; ^1H NMR: δ 7.35–7.40 (s, 5H), 6.13 (s, 1H), 5.76 (m, 1H), 5.22 (d, $J=18.1$ Hz, 1H), 5.18 (d, $J=11.1$ Hz, 1H), 3.97–4.07 (ABX, $J=16.5$ Hz, 4H), 1.70 (s, 3H), 1.48 (s, 9H), 1.44 (s, 3H); ^{13}C NMR: δ 150.1, 133.3, 132.5, 130.0, 128.8, 128.0, 118.6, 90.4, 87.2, 85.2, 51.4, 28.1, 24.1, 20.3. Anal. Calcd for C₁₈H₂₆N₂O₇S: C, 52.16; H, 6.32. Found: C, 52.07; H, 6.29. To a solution of this sulfamate (207 mg, 0.5 mmol) in CH₂Cl₂ (5 mL) was added at 0 °C trifluoroacetic acid (0.39 mL, 5 mmol). The reaction mixture was stirred at rt for 2 h and quenched with a 1 N NaOH solution. The aqueous layer was extracted with CH₂Cl₂ and the combined organic layer was washed with brine, dried, and concentrated. Chromatographic purification (hexanes/EA from 100:0 to 80: 10) afforded **60** (64 mg, 41%) as a colorless oil. IR (neat): 3317, 3067, 1647, 1547, 1456, 1349, 1180, 963 cm^{-1} ; ^1H NMR: δ 7.40 (s, 5H), 5.96 (s, 1H), 5.66 (ddt, $J=16.9, 10.5, 5.0$ Hz, 1H), 5.11–5.18 (m, 2H), 4.51 (t, $J=5.9$ Hz, 1H), 3.57–3.43 (m, 2H), 1.67 (s, 3H), 1.47 (s, 3H); ^{13}C NMR: δ 133.9, 132.5, 129.9, 128.8, 128.1, 118.6, 90.8, 85.7, 46.5, 24.3, 19.9. Anal. Calcd for C₁₃H₁₈N₂O₅S: C, 49.67; H, 5.77. Found: C, 49.77; H, 5.74.

4.1.7.11. *N*-Allyl *N*-(4-methoxybenzyl) *O*-(2-methyl-2-nitro-1-phenylpropyl) *O*-phenyl phosphoramidate (61). To a solution of phenylphosphorodichloridite (2.87 mL, 20.0 mmol) and *N,N*-diisopropylethylamine (11.6 mL, 66.8 mmol) in THF (40 mL) was added dropwise, at -78 °C, a solution of alcohol **58**²⁰ (3.26 g, 16.7 mmol) in THF (15 mL). The reaction mixture was warmed up to rt and stirred for 1 h. Then the solution was cooled to -78 °C and a solution of allyl-(4-methoxybenzyl)amine (5.33 g, 30.1 mmol) in THF (10 mL) was added dropwise. The reaction mixture was warmed up to rt and stirred for 2 h. The solid was filtrated and washed with EtOAc. The filtrate was concentrated in vacuo to give the phosphoramidite as oil. The crude reaction mixture was dissolved in CH₂Cl₂ (80 mL) and a solution of *tert*-butyl hydroperoxide (5–6 M in decane, 8 mL, 40 mmol) was added at 0 °C and the reaction mixture was stirred at rt for 1 h. The reaction was quenched with satd aq NaHCO₃, extracted with CH₂Cl₂, washed with water and brine, dried, and concentrated. Chromatographic purification (CH₂Cl₂/EA from 100:0 to 90:10) afforded the phosphate **61** (5.55 g, 67%) as a viscous oil. IR (neat): 3066, 1612, 1591, 1545, 1491, 1266, 1210, 1025,

926 cm^{-1} ; ^1H NMR: δ 7.39–7.10 (m, 20H, two diast), 6.97 (m, 2H, one diast), 6.91 (m, 2H, one diast), 6.82 (m, 2H, one diast), 6.74 (m, 2H, one diast), 5.95 (d, $J=8.5$ Hz, 1H, one diast), 5.93 (d, $J=8.6$ Hz, 1H, one diast), 5.66 (m, 1H, one diast), 5.30 (m, 1H, one diast), 5.19–4.95 (m, 4H, two diast), 4.20–4.08 (m, 3H, two diast), 3.96 (dd, $J=14.8$, 10.1 Hz, 1H, one diast), 3.79 (s, 3H, one diast), 3.77 (s, 3H, one diast), 3.52 (m, 2H), 3.45 (m, 1H), 3.26 (m, 1H), 1.62 (s, 3H, one diast), 1.57 (s, 3H, one diast), 1.45 (s, 3H, one diast), 1.38 (s, 3H, one diast); ^{13}C NMR: δ 159.2, 159.1, 151.0 (d, $J_{\text{PC}}=7.0$ Hz), 150.9 (d, $J_{\text{PC}}=6.8$ Hz), 135.1, 135.0, 134.0, 133.8, 130.1 (2C), 129.8, 129.7, 129.5, 129.2, 129.0 (d, $J_{\text{PC}}=3.4$ Hz), 128.6, 128.3, 128.2, 128.1, 125.0, 124.8, 120.5 (d, $J_{\text{PC}}=4.6$ Hz), 120.3 (d, $J_{\text{PC}}=4.9$ Hz), 119.0, 118.9, 114.0, 113.9, 91.2 (d, $J_{\text{PC}}=4.7$ Hz), 91.1 (d, $J_{\text{PC}}=4.7$ Hz), 82.6 (d, $J_{\text{PC}}=5.2$ Hz), 82.5 (d, $J_{\text{PC}}=5.1$ Hz), 60.6, 55.5, 48.2 (d, $J_{\text{PC}}=3.5$ Hz), 48.1 (d, $J_{\text{PC}}=3.7$ Hz), 47.7 (d, $J_{\text{PC}}=2.7$ Hz), 47.4 (d, $J_{\text{PC}}=2.7$ Hz), 24.1, 23.6, 20.4, 20.0; ^{31}P NMR: δ 4.78, 2.39. Anal. Calcd for $\text{C}_{27}\text{H}_{31}\text{N}_2\text{O}_6\text{P}$: C, 63.52; H, 6.12. Found: C, 63.40; H, 6.14.

4.1.7.12. *N*-Allyl *O*-(2-methyl-2-nitro-1-phenylpropyl) *O*-phenyl phosphoramidate (62). To a solution of phosphoramidate **61** (two diast ratio 1.7:1) (1 g, 1.96 mmol) in $\text{CH}_3\text{CN}/\text{H}_2\text{O}$ (6:1, 19 mL) was added at rt cerium ammonium nitrate (3.22 g, 7.84 mmol). The mixture was stirred at rt for 1 h and then diluted with CH_2Cl_2 and quenched with satd aq NaHCO_3 . The organic layer was washed with brine, dried and concentrated. Chromatographic purification ($\text{CH}_2\text{Cl}_2/\text{EA}$ from 100:0 to 90:10) afforded **62** as an unassigned mixture of two diastereomers (670 mg, 88%) as a white solid. IR (neat): 3223, 1593, 1545, 1491, 1261, 1212, 1041, 1025, 934 cm^{-1} ; ^1H NMR: δ 7.40–7.08 (m, 18H, major and minor), 7.00 (d, $J=8.7$ Hz, 2H, major), 5.95 (d, $J=8.5$ Hz, 1H, major), 5.92 (d, $J=8.6$ Hz, 1H, minor), 5.81 (m, 1H, major), 5.56 (m, 1H, minor), 5.20 (dq, $J=17.1$, 1.6 Hz, 1H, major), 5.10 (dq, $J=10.3$, 1.3 Hz, 1H, major), 5.01 (dq, $J=17.0$, 1.4 Hz, 1H, minor), 4.97 (dq, $J=10.2$, 1.3 Hz, 1H, minor), 3.62–3.49 (m, 2H, major), 3.40–3.30 (m, 2H, minor), 2.98 (dt, $J=12.1$, 6.8 Hz, 1H, major), 2.82 (dt, $J=12.6$, 6.9 Hz, 1H, minor), 1.60 (s, 3H, minor), 1.59 (s, 3H, major), 1.44 (s, 3H, major), 1.41 (s, 3H, minor); ^{13}C NMR: δ 159.9 (d, $J_{\text{PC}}=6.5$ Hz, major and minor), 135.7 (d, $J_{\text{PC}}=6.3$ Hz, major), 135.4 (d, $J_{\text{PC}}=6.5$ Hz, minor), 135.1 (major and minor), 129.8, 129.7, 129.6, 129.3 (major and minor), 128.1 (minor), 128.6 (minor), 128.4 (major), 128.0 (major), 125.1 (minor), 125.0 (major), 120.44 (d, $J_{\text{PC}}=4.5$ Hz, minor), 120.42 (d, $J_{\text{PC}}=4.1$ Hz, minor), 116.0 (minor), 116.2 (major), 91.4 (d, $J_{\text{PC}}=8.6$ Hz, major), 91.2 (d, $J_{\text{PC}}=8.2$ Hz, minor), 84.5 (d, $J_{\text{PC}}=4.7$ Hz, major), 82.4 (d, $J_{\text{PC}}=4.8$ Hz, minor), 44.2 (major), 44.0 (minor), 24.4 (major), 23.5 (minor), 20.5 (minor), 19.4 (major); ^{31}P NMR: δ 3.45 (major), 2.39 (minor). ESIMS m/z : 413 ($[\text{M}+\text{Na}]^+$, 100), 803 ($[\text{2M}+\text{Na}]^+$, 65). Anal. Calcd for $\text{C}_{19}\text{H}_{23}\text{N}_2\text{O}_5\text{P}$: C, 58.46; H, 5.94. Found: C, 58.64; H, 6.00.

4.1.7.13. Diethyl 2-(ethyl-2-nitro-1-phenylpropyl) phosphite (63). To a solution of diethylchlorophosphite (0.9 mL, 6.3 mmol) and *N,N*-diisopropylethylamine (1.74 mL, 10 mmol) in THF (10 mL) was added dropwise at -78°C a solution of alcohol **58**²⁰ (975 mg, 5 mmol) in THF (3 mL). The reaction mixture was warmed up to rt and stirred for 1 h. The solid was filtered off and washed

with EtOAc. The filtrate was concentrated to give an oil, which was purified by column chromatography on neutral Al_2O_3 (hexane/EA from 90:10) to afford the phosphite **63** (1.28 g, 80%) as colorless oil. IR (neat): 2980, 1545, 1455, 1025, 924 cm^{-1} ; ^1H NMR: δ 7.36–7.31 (m, 5H), 5.63 (d, $J=8.7$ Hz 1H), 3.77–3.58 (m, 4H), 1.41 (s, 3H), 1.59 (s, 3H), 1.10 (t, $J=7.0$ Hz, 3H), 1.07 (t, $J=7.0$ Hz, 3H); ^{13}C NMR: δ 137.4, 128.9, 128.3, 91.9 (d, $J_{\text{PC}}=3.9$ Hz), 78.8 (d, $J_{\text{PC}}=13.1$ Hz), 59.0 (d, $J_{\text{PC}}=12.2$ Hz), 58.7 (d, $J_{\text{PC}}=10.6$ Hz), 23.6, 19.1, 16.9, 16.8; ^{31}P NMR: δ 140.9. Anal. Calcd for $\text{C}_{14}\text{H}_{22}\text{NO}_5\text{S}$: C, 53.33; H, 7.03. Found: C, 53.60; H, 7.07.

4.1.7.14. *N*-Allyl *O,O*-diethyl *O*-2-(ethyl-2-nitro-1-phenylpropyl) phosphorimidate (64). To a solution of sodium azide (2 equiv) and tetrabutylammonium bromide (0.05 equiv) in water was added allyl bromide. The solution was heated at 50–60 $^\circ\text{C}$ for 2 h with a vigorous stirring. The aqueous layer was washed twice with benzene (C_6H_6 or C_6D_6). The combined organic layers were washed with brine, dried over MgSO_4 , and filtered to afford a solution of allyl azide in benzene (~ 0.5 M in C_6H_6 ; ~ 1.33 M in C_6D_6), free from allyl bromide as determined by GC, which was stored over molecular sieves for 24 h prior to use. The 1.33 M solution of allyl azide in C_6D_6 (3.3 mL, 4.38 mmol) was added to a solution of phosphite **63** (230 mg, 0.73 mmol) in C_6D_6 (5 mL) and the solution was heated at reflux for 4 h. The NMR of the crude reaction mixture indicated quantitative conversion of **63** to **64**. ^1H NMR (C_6D_6): δ 7.26–7.22 (m, 2H), 7.12–7.08 (m, 3H), 6.19 (m, 1H), 6.10 (d, $J=9.0$ Hz 1H), 5.62 (dq, $J=16.9$, 2.4 Hz, 1H), 5.21 (dq, $J=10.0$, 2.4 Hz, 1H), 4.09–3.70 (m, 6H), 1.49 (s, 3H), 1.12 (s, 3H), 1.05 (br t, $J=7.0$ Hz, 3H), 1.01 (dt, $J=7.0$, 1.0 Hz, 3H); ^{13}C NMR (C_6D_6): δ 141.6 (d, $J_{\text{PC}}=15.5$ Hz), 136.4, 128.6, 128.1, 127.9, 111.6, 90.7 (d, $J_{\text{PC}}=8.2$ Hz), 82.1 (d, $J_{\text{PC}}=7.2$ Hz), 62.9 (d, $J_{\text{PC}}=9.2$ Hz), 62.8 (d, $J_{\text{PC}}=7.8$ Hz), 45.6, 23.6, 19.1, 15.8; ^{31}P NMR: (C_6D_6) δ -3.69 .

4.1.7.15. *N*-Allyl sulfamic acid (65). A solution of **60** (229 mg, 0.73 mmol) in benzene (36 mL) was degassed by sparging with nitrogen for 40 min. Bu_3SnH (289 μL , 1.17 mmol) and AIBN (48 mg, 0.31 mmol) were added and the solution was heated at reflux for 6 h. Then, Bu_3SnH (96 μL , 0.39 mmol) and AIBN (18 mg, 0.11 mmol) were added and the solution was heated for 3 h. The solvent was evaporated and CH_2Cl_2 and water were added. The organic layer was concentrated but contained only thin residues. The aqueous layer was evaporated to give a gum (90 mg), which was washed with CH_3CN and hexanes to give **65** (80 mg, $\sim 48\%$) contaminated by some tin residues. ^1H NMR: δ 5.94 (m, 1H), 5.23 (d, $J=17.1$ Hz, 1H), 5.08 (d, $J=10.0$ Hz, 1H), 3.60 (d, $J=5.2$ Hz, 2H); ^{13}C NMR: δ 135.1, 115.1, 46.2; ESIMS m/z : 136 (100).

4.1.7.16. *N*-Allyl *O*-(1,1-dimethyl-2-phenylethyl) *O*-phenyl phosphoramidate (66), *N*-allyl *O*-(2-methyl-1-phenylpropyl) *O*-phenyl phosphoramidate (67), and 7,7-dimethyl-2-phenoxy-8-phenyl-[1,3,2]oxazaphosphocane 2-oxide (68). A solution of **62** (195 mg, 0.5 mmol), AIBN (33 mg, 0.20 mmol), and Bu_3SnH (0.2 mL, 0.75 mmol) in degassed benzene (25 mL) was heated at reflux for 6 h. Then AIBN (8 mg, 0.05 mmol) and Bu_3SnH (50 μL ,

0.18 mmol) were added and the mixture was heated for a further 15 h. The reaction mixture was concentrated and the residue was purified by column chromatography (CH₂Cl₂/EA from 100:0 to 70:30) to afford by order of elution **67** (12 mg, 7%), **66** (73 mg, 42%), and **68** (14 mg, 8%). Compound **66**: white solid. mp 40–41 °C. IR (neat): 3220, 1593, 1545, 1491, 1261, 1212, 1041, 1025, 934 cm⁻¹; ¹H NMR: δ 7.39–7.10 (m, 3H), 5.77 (m, 1H), 5.13 (dq, *J*=17.1, 1.5 Hz, 1H), 5.05 (dq, *J*=11.7, 1.4 Hz, 1H), 3.50 (m, 2H), 2.93–3.05 (m, 2H), 1.54 (s, 3H), 1.52 (s, 3H); ¹³C NMR: δ 151.5 (d, *J*_{PC}=6.9 Hz), 137.2, 131.0 (d, *J*_{PC}=6.9 Hz), 131.0, 129.7, 128.4, 126.8, 124.7, 120.7 (d, *J*_{PC}=4.6 Hz), 115.8, 84.9 (d, *J*_{PC}=7.4 Hz), 49.5 (d, *J*_{PC}=6.4 Hz), 44.3, 28.0, 27.5; ³¹P NMR: δ -0.18. Anal. Calcd for C₁₉H₂₂NO₃P: C, 66.07; H, 7.00. Found: C, 66.19; H, 7.02. Compound **67**: colorless oil. ¹H NMR: δ 7.37–6.97 (m, 20H, two dias), 5.81 (m, 1H, one dias), 5.47 (m, 1H, one dias), 5.23–5.03 (m, 4H, two dias), 4.91 (m, 1H, one dias), 3.58 (m, 2H, one dias), 3.35 (m, 1H, one dias), 3.17 (m, 1H, one dias), 2.17–2.07 (m, 2×1H, two dias), 1.03 (d, *J*=6.8 Hz, 3H, one dias), 0.93 (d, *J*=6.8 Hz, 3H, one dias), 0.83 (d, *J*=6.8 Hz, 3H, one dias), 0.74 (d, *J*=6.8 Hz, 3H, one dias); ¹³C NMR: δ 151.3 (d, *J*_{PC}=6.7 Hz), 151.2 (d, *J*_{PC}=6.6 Hz), 139.9, 139.7, 136.0 (d, *J*_{PC}=6.4 Hz), 135.7 (d, *J*_{PC}=7.0 Hz), 129.8, 129.7, 128.5, 128.3 (2C), 128.1, 124.9, 124.6, 120.8 (d, *J*_{PC}=4.6 Hz), 120.3 (d, *J*_{PC}=4.8 Hz), 116.1, 115.9, 85.7 (d, *J*_{PC}=6.7 Hz), 85.2 (d, *J*_{PC}=5.4 Hz), 44.3, 44.1, 35.2 (d, *J*_{PC}=6.4 Hz), 35.1 (d, *J*_{PC}=6.1 Hz), 18.8 (2C), 18.6, 18.5; ³¹P NMR: δ 3.82, 3.70; HRMS: Calcd for C₁₉H₂₄NO₃NaP [M+Na]⁺ 368.1392. Found 368.1397. Compound **68**: white solid. mp 132 °C; IR (neat): 3222, 2963, 1592, 1491, 1250, 1214, 936 cm⁻¹; ¹H NMR: δ 7.33–7.10 (m, 10H), 5.25 (d, *J*=11.8 Hz, 1H), 3.60 (br s, 1H), 3.15–3.10 (m, 1H), 3.05–2.95 (m, 1H), 2.00–1.93 (m, 1H), 1.90–1.60 (m, 3H), 0.82 (s, 3H), 0.80 (s, 3H); ¹³C NMR: δ 151.4 (d, *J*_{PC}=6.0 Hz), 138.3, 129.8, 128.1, 127.9, 127.8, 124.8, 120.7 (d, *J*_{PC}=4.25 Hz), 84.5 (d, *J*_{PC}=3.6 Hz), 43.8, 41.5, 38.7 (d, *J*_{PC}=3.8 Hz), 26.7, 24.5, 21.1; ³¹P NMR: δ 5.16; HRMS: Calcd for C₁₉H₂₄NO₃P [M+Na]⁺ 368.1392. Found 368.1388.

4.1.7.17. N-Allyl diethyl phosphoramidate (69), N-allyl O-ethyl O-(2-methyl-2-nitro-1-phenylpropyl) phosphoramidate (70), and N-allyl O-ethyl ester O-(2-methyl-1-phenylpropyl) phosphoramidate (71). The phosphorimidate **64** was prepared by reaction of **63** (450 mg, 1.4 mmol) and a 0.5 N solution of allyl azide in C₆H₆ (11.2 mL, 5.6 mmol) as described above. Benzene (60 mL) was added to the solution of **64** and the resulting solution was degassed for 30 min. Then AIBN (92 mg, 0.56 mmol) and Bu₃SnH (1.48 mL, 5.6 mmol) were added and the mixture heated at reflux for 10 h. The reaction mixture was concentrated and the residue was purified by column chromatography (CH₂Cl₂/EA from 100:0 to 50:50) to afford by order of elution **70** (30 mg, 6%), **71** (22 mg, 5%), and **69** (120 mg, 40%). Compound **69**: IR (neat): 3227, 3086, 2980, 1645, 1445, 1233, 1034, 965 cm⁻¹; ¹H NMR: δ 5.85 (m, 1H), 5.20 (dq, *J*=17.0, 1.6 Hz, 1H), 5.08 (dq, *J*=10.4, 1.6 Hz, 1H), 4.09–3.99 (m, 4H), 3.51 (m, 2H), 1.30 (t, *J*=7.0 Hz, 6H); ¹³C NMR: δ 136.3 (d, *J*_{PC}=6.1 Hz), 115.6, 62.5 (d, *J*_{PC}=5.1 Hz), 44.0, 16.4 (d, *J*_{PC}=7.0 Hz); ³¹P NMR: δ 9.40; HRMS: Calcd for C₇H₁₆NO₃NaP [M+Na]⁺

216.0766. Found 216.0758. **70**: ¹H NMR: δ 7.38–7.35 (m, 10H, two dias), 5.85 (d, *J*=8.6 Hz, 1H, one dias), 5.81 (d, *J*=8.5 Hz, 1H, one dias), 5.82 (m, 1H, one dias), 5.61 (m, 1H, one dias), 5.19 (dq, *J*=17.0, 1.7 Hz, 1H, one dias), 5.10 (dq, *J*=10.1, 1.5 Hz, 1H, one dias), 5.03 (dq, *J*=17.2, 1.4 Hz, 1H, one dias), 4.98 (dq, *J*=10.4, 1.5 Hz, 1H, one dias), 4.05–3.80 (m, 4H, two dias), 3.52–3.38 (m, 2H, two dias), 3.38–3.20 (m, 2H, two dias), 1.64 (s, 3H, one dias), 1.62 (s, 3H, one dias), 1.45 (s, 3H, one dias), 1.44 (s, 3H, one dias), 1.26 (t, *J*=7.0 Hz, 3H, one dias), 1.12 (t, *J*=7.0 Hz, 3H, one dias); ¹³C NMR: δ 136.1 (d, *J*_{PC}=6.4 Hz), 135.9 (d, *J*_{PC}=6.7 Hz), 135.6, 135.5, 129.5, 129.4, 128.6, 128.5, 128.2, 128.1, 115.9, 115.7, 91.4 (d, *J*_{PC}=8.6 Hz), 91.3 (d, *J*_{PC}=8.3 Hz), 82.1 (d, *J*_{PC}=4.9 Hz), 82.0 (d, *J*_{PC}=5.0 Hz), 63.2 (d, *J*_{PC}=5.4 Hz), 63.0 (d, *J*_{PC}=5.4 Hz), 44.0, 43.9, 24.1, 23.9, 19.6, 19.4, 16.3, 16.2; ³¹P NMR: δ 8.44, 7.46; HRMS: Calcd for C₁₅H₂₃N₂O₅NaP [M+Na]⁺ 365.1243. Found 365.1238. Compound **71**: slightly yellow oil. ¹H NMR: δ 7.33–7.25 (m, 10H, two dias), 5.84 (m, 1H, one dias), 5.50 (m, 1H, one dias), 5.18 (dq, *J*=17.2, 1.6 Hz, 1H, one dias), 5.07 (dq, *J*=10.3, 1.3 Hz, 1H, one dias), 4.99–4.88 (m, 4H, two dias), 4.08 (m, 2H, one dias), 3.81 (m, 2H, one dias), 3.48 (m, 2H, one dias), 3.17 (m, 1H, one dias), 3.08 (m, 1H, one dias), 2.16–2.05 (m, 2H, two dias), 1.31 (t, *J*=7.1 Hz, 3H, one dias), 1.09 (t, *J*=7.1 Hz, 3H, one dias), 1.05 (d, *J*=6.7 Hz, 3H, one dias), 1.01 (d, *J*=6.6 Hz, 3H, one dias), 0.79 (d, *J*=6.7 Hz, 3H, one dias), 0.78 (d, *J*=6.7 Hz, 3H, one dias); ¹³C NMR: δ 140.2, 136.5 (d, *J*_{PC}=7.0 Hz), 136.1 (d, *J*_{PC}=7.0 Hz), 128.4, 128.2, 128.0, 127.4, 127.3, 115.7, 115.5, 84.8 (d, *J*_{PC}=6.3 Hz), 84.4 (d, *J*_{PC}=5.2 Hz), 62.6 (d, *J*_{PC}=5.2 Hz), 62.5 (d, *J*_{PC}=5.3 Hz), 44.1, 43.9, 35.2 (d, *J*_{PC}=7.1 Hz), 35.1 (d, *J*_{PC}=7.1 Hz), 19.0, 18.8, 18.6, 16.5 (d, *J*_{PC}=7.1 Hz, one dias), 16.2 (d, *J*_{PC}=7.1 Hz, one dias); ³¹P NMR: δ 8.75, 8.63; HRMS: Calcd for C₁₅H₂₄NO₃NaP [M+Na]⁺ 320.1392. Found 320.1403.

Acknowledgements

We thank the Ministère des Affaires Étrangères, France, for a Lavoisier Fellowship in support of F.B., and the NSF (CHE 9986200) for partial support of this work.

References and notes

- (a) Crich, D.; Ranganathan, K. *J. Am. Chem. Soc.* **2002**, *124*, 12422–12423; (b) Crich, D.; Ranganathan, K. *J. Am. Chem. Soc.* **2005**, *127*, 9924–9929.
- Preliminary communication: Crich, D.; Shirai, M.; Rumthao, S. *Org. Lett.* **2003**, *5*, 3767–3769.
- (a) Choi, S.-Y.; Crich, D.; Horner, J. H.; Huang, X.; Newcomb, M.; Whitted, P. O. *Tetrahedron* **1999**, *59*, 3317–3326; (b) Whitted, P. O.; Horner, J. H.; Newcomb, M.; Huang, X.; Crich, D. *Org. Lett.* **1999**, *1*, 153–156; (c) Newcomb, M.; Horner, J. H.; Whitted, P. O.; Crich, D.; Huang, X.; Yao, Q.; Zipse, H. *J. Am. Chem. Soc.* **1999**, *121*, 10685–10694; (d) Newcomb, M.; Miranda, N.; Huang, X.; Crich, D. *J. Am. Chem. Soc.* **2000**, *122*, 6128–6129; (e) Bales, B. C.; Horner, J. H.; Huang, X.; Newcomb, M.; Crich, D.; Greenberg, M. M. *J. Am. Chem. Soc.* **2001**, *123*, 3623–3629; (f) Horner, J. H.; Newcomb, M. *J. Am. Chem. Soc.* **2001**, *123*, 4364–4365; (g) Horner, J. H.;

- Taxil, E.; Newcomb, M. *J. Am. Chem. Soc.* **2002**, *124*, 5402–5410; (h) Taxil, E.; Bagnol, L.; Horner, J. H.; Newcomb, M. *Org. Lett.* **2003**, *5*, 827–830; (i) Bagnol, L.; Horner, J. H.; Newcomb, M. *Org. Lett.* **2003**, *5*, 5055–5058; (j) Horner, J. H.; Bagnol, L.; Newcomb, M. *J. Am. Chem. Soc.* **2004**, *126*, 14979–14987; (k) Crich, D.; Jiao, X.-Y. *J. Am. Chem. Soc.* **1996**, *118*, 6666–6670.
- (a) Giese, B. *Top. Curr. Chem.* **2004**, *236*, 27–44; (b) Newcomb, M.; Miranda, N.; Sannigrahi, M.; Huang, X.; Crich, D. *J. Am. Chem. Soc.* **2001**, *123*, 6445–6446.
 - (a) Crich, D.; Yao, Q.; Filzen, G. F. *J. Am. Chem. Soc.* **1995**, *117*, 11455–11470; (b) Crich, D.; Escalante, J.; Jiao, X.-Y. *J. Chem. Soc., Perkin Trans. 2* **1997**, 627–630; (c) Crich, D.; Yao, Q. *Tetrahedron Lett.* **1993**, *34*, 5677–5680.
 - Crich, D.; Yao, Q. *J. Am. Chem. Soc.* **1994**, *116*, 2631–2632.
 - For reviews covering the earlier work see: (a) Beckwith, A. L. J.; Crich, D.; Duggan, P. J.; Yao, Q. *Chem. Rev.* **1997**, *97*, 3273–3312; (b) Crich, D. In *Radicals in Organic Synthesis*; Renaud, P., Sibi, M., Eds.; Wiley-VCH: Weinheim, 2001; Vol. 2, pp 188–206.
 - (a) Zipse, H. *Adv. Phys. Org. Chem.* **2003**, *38*, 111–130; (b) Wang, Y.; Grimme, S.; Zipse, H. *J. Phys. Chem. A* **2004**, *108*, 2324–2331.
 - (a) Crich, D.; Huang, X.; Newcomb, M. *Org. Lett.* **1999**, *1*, 225–228; (b) Crich, D.; Huang, X.; Newcomb, M. *J. Org. Chem.* **2000**, *65*, 523–529; (c) Crich, D.; Ranganathan, K.; Huang, X. *Org. Lett.* **2001**, *3*, 1917–1919; (d) Crich, D.; Ranganathan, K.; Neelamkavil, S.; Huang, X. *J. Am. Chem. Soc.* **2003**, *125*, 7942–7947; (e) Crich, D.; Neelamkavil, S. *Org. Lett.* **2002**, *4*, 2573–2575.
 - Crich, D.; Ranganathan, K.; Rumthao, S.; Shirai, M. *J. Org. Chem.* **2003**, *68*, 2034–2037.
 - (a) Jung, M. E. *Synlett* **1999**, 843–846; (b) Jung, M. E.; Piizzi, G. *Chem. Rev.* **2005**, *105*, 1735–1766.
 - Crich, D.; Hao, X. *J. Org. Chem.* **1997**, *62*, 5982–5988.
 - (a) Corey, E. J.; Helal, C. J. *Angew. Chem., Int. Ed.* **1998**, *37*, 1987–2012; (b) Wallbaum, S.; Martens, J. *Tetrahedron: Asymmetry* **2003**, *3*, 1475–1504.
 - Andres, C.; Duque-Soladana, J. P.; Iglesias, J. M.; Pedrosa, R. *Tetrahedron Lett.* **1999**, *40*, 2421–2424.
 - We note that the ee of **57** calculated from its specific rotation is considerably higher than that determined by chiral chromatography, illustrating the oft-stated dangers of ee measurements by comparison of rotations.
 - (a) Johnston, L. J.; Schepp, N. P. *J. Am. Chem. Soc.* **1993**, *115*, 6564–6571; (b) Johnston, L. J.; Schepp, N. P. *Advances in Electron Transfer Chemistry*; JAI: New York, NY, 1996; Vol. 5, pp 41–102.
 - (a) Beckwith, A. L. J. *Tetrahedron* **1981**, *37*, 3073–3100; (b) Beckwith, A. L. J.; Schiesser, C. H. *Tetrahedron* **1985**, *41*, 3925–3941; (c) Spellmeyer, D. C.; Houk, K. N. *J. Org. Chem.* **1987**, *52*, 959–974; (d) Curran, D. P.; Porter, N. A.; Giese, B. *Stereochemistry of Radical Reactions*; VCH: Weinheim, 1996.
 - Contact radical cation/anion pairs are thought to undergo solvation with rate constants of 10^8 – 10^9 s⁻¹ in the more polar dichloromethane at room temperature. See Ref. 3j and Arnold, B. R.; Noukakis, D.; Farid, S.; Goodman, J. L.; Gould, I. R. *J. Am. Chem. Soc.* **1995**, *117*, 4399–4400.
 - Crich, D.; Sartillo-Piscil, F.; Quintero-Cortes, L.; Wink, D. J. *J. Org. Chem.* **2002**, *67*, 3360–3364.
 - Marquardt, F.-H.; Edwards, S. *J. Org. Chem.* **1972**, *37*, 1861–1863.
 - (a) Picard, J. A.; O'Brien, P. M.; Sliskovic, D. R.; Anderson, M. K.; Bousley, R. F.; Hamelhele, K. L.; Krause, B. R.; Stanfield, R. L. *J. Med. Chem.* **1996**, *39*, 1243–1252; (b) Fiandor, J.; Garcia-Lopez, M. T.; De las Heras, F. G.; Mendez-Castrillon, P. P.; Gil-Fernandez, C.; Perez, S.; Vilas, P.; Perez, C.; Gancedo, A. G. *Nucleosides Nucleotides* **1989**, *8*, 257–271.
 - Gololobov, Y. G.; Kasukhin, L. F. *Tetrahedron* **1992**, *48*, 1353–1406.
 - (a) Bellan, J.; Sanchez, M.; Marre-Mazieres, M. R.; Murillo Beltran, A. *Bull. Soc. Chim. Fr.* **1985**, 491–495; (b) Gajda, T.; Koziara, A.; Osowska-Pacewicka, K.; Zawadzki, S.; Zwierzak, A. *Synth. Commun.* **1992**, *22*, 1929–1938; (c) Koziara, A.; Zwierzak, A. *Tetrahedron Lett.* **1987**, *28*, 6513–6516; (d) Koziara, A.; Zwierzak, A. *Synthesis* **1992**, 1063–1065; (e) Willeit, A.; Mueller, E. P.; Peringer, P. *Helv. Chim. Acta* **1983**, *66*, 2467–2480; (f) Chen, B.; Mapp, A. K. *J. Am. Chem. Soc.* **2004**, *126*, 5364–5365; (g) Chen, B.; Mapp, A. K. *J. Am. Chem. Soc.* **2005**, *127*, 6712–6718.
 - A search of Chemical Abstracts revealed no examples of 1,3,2-azoxaphosphocanes.
 - Srikrishna, A. In *Radicals in Organic Synthesis*; Renaud, P., Sibi, M. P., Eds.; Wiley-VCH: Weinheim, 2001; Vol. 2, pp 151–187.
 - The prototypical 7-octenyl radical cyclizes in the 7-*exo* and 8-*endo* modes with rate constants of $<7 \times 10^1$ and 1.2×10^2 s⁻¹, respectively, at 25 °C (Ref. 17b).
 - In acetonitrile the rate constants for the rearrangement of the 1,1-dimethyl-2-diethylphosphatoxy-2-phenylethyl and the 1,1-dimethyl-2-diphenylphosphatoxy-2-phenylethyl radicals differ by a factor of 300 (Ref. 3a).
 - Zipse, H. *Acc. Chem. Res.* **1999**, *32*, 571–578.
 - Freeman, P. K.; Tafesh, A. M.; Clapp, G. E. *J. Org. Chem.* **1989**, *54*, 782–789.

Distannane mediated reaction of *N*-acyliminium ion pools with alkyl halides. A chain mechanism involving radical addition followed by electron transfer

Tomokazu Maruyama, Seiji Suga* and Jun-ichi Yoshida*

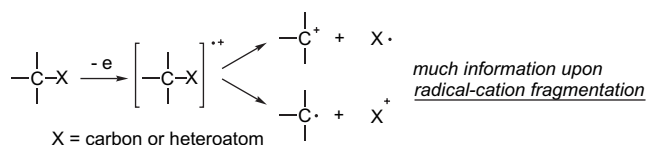
Department of Synthetic Chemistry and Biological Chemistry, Graduate School of Engineering, Kyoto University, Kyoto 615-8510, Japan

Received 18 January 2006; accepted 23 March 2006
Available online 6 May 2006

Abstract—Hexabutyldistannane was found to be an effective mediator allowing the reaction of *N*-acyliminium ion pools with alkyl halides. A chain mechanism involving the addition of an alkyl radical generated from an alkyl halide to an *N*-acyliminium ion followed by the one-electron reduction of the resulting radical-cation by distannane was proposed.
© 2006 Elsevier Ltd. All rights reserved.

1. Introduction

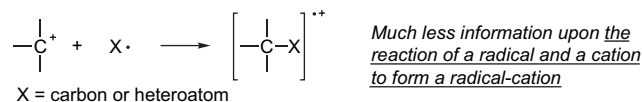
Radical-cations serve as key intermediates in a variety of electron transfer driven transformations in organic synthesis. For example, one-electron oxidation of organic compounds gives radical-cations, which undergo follow-up reactions. Fragmentation of radical-cations to give either a carbocation or a neutral carbon radical as shown in Scheme 1 is one of the most feasible pathways. Extensive studies have been carried out on fragmentation reactions of radical-cations, which are generated in chemical,¹ electrochemical,² and photochemical³ electron transfer. Schmittel's classification⁴ of reactivity patterns of radical-cations is very useful to understand electron transfer driven reactions.⁵



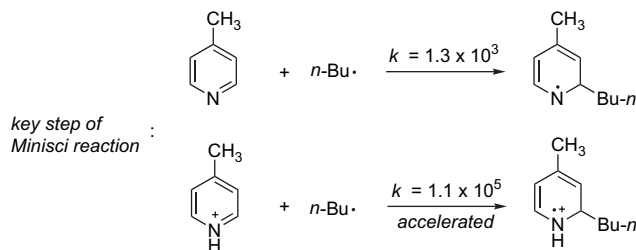
Scheme 1.

Much less information, by contrast, is available for the reverse process: the reaction of a radical and a cation to form a radical-cation (Scheme 2). The Minisci reaction, which involves the addition of nucleophilic radicals, such as alkyl,

benzyl, and phenyl radicals, to protonated heteroaromatic rings, serves as an example of the process.^{6,7} In this reaction, the rates of the addition to protonated heteroaromatic compounds are much higher than that of the addition to the unprotonated compounds. For example, the addition of an *n*-butyl radical to the protonated picoline is 100 times faster than that to neutral picoline, indicating significant polar effects in the transition state (Scheme 3).⁷



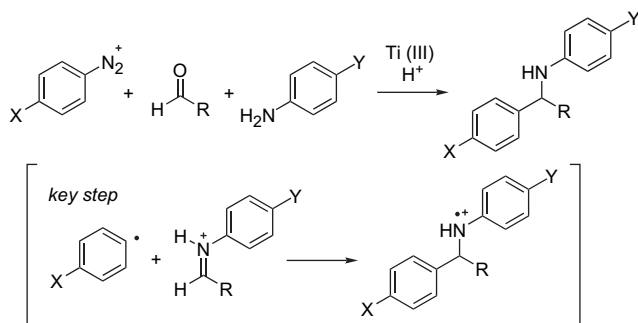
Scheme 2.



Scheme 3.

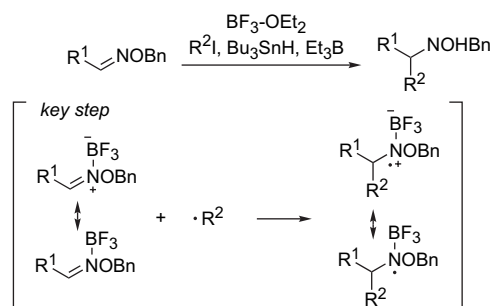
In the arylative amination of aldehydes promoted by titanium trichloride, a mechanism involving the addition of an aryl radical to the cationic carbon of the protonated imine intermediate has been suggested (Scheme 4).⁸

* Corresponding authors. Tel.: +81 75 383 2726; fax: +81 75 383 2727; e-mail: yoshida@sbchem.kyoto-u.ac.jp



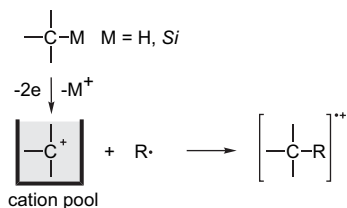
Scheme 4.

It has also been reported that alkyl radical addition to C=N bond is remarkably accelerated by the Lewis acid such as $\text{BF}_3 \cdot \text{OEt}_2$ (Scheme 5).⁹ Lewis acid was suggested to lower the LUMO energy of the radical acceptor and decrease the electron density at the iminyl carbon atom. Similar reactions are possible using imines having an electron-deficient substituent.



Scheme 5.

These observations in the literature indicate the importance of electrophilic character of radical acceptors in radical addition and prompted us to investigate the radical addition to *N*-acyliminium ions, which are generated and accumulated by the ‘cation pools’ method¹⁰ (Scheme 6). In a preliminary communication we have reported that the reaction does take place in the presence of distannane.¹¹ A chain mechanism involving the addition of an alkyl radical generated from an alkyl iodide to an *N*-acyliminium ion followed by the one-electron reduction of the resulting radical-cation by distannane has been proposed. In this paper we report full details of this study.

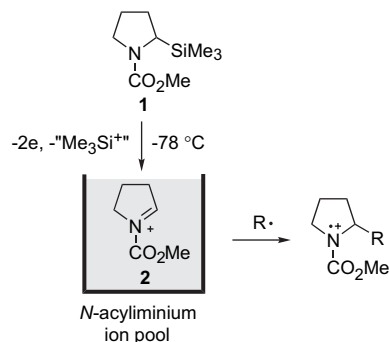


Scheme 6.

2. Result and discussion

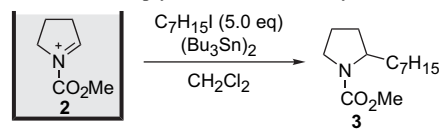
We began our study with surveying appropriate conditions to generate alkyl radicals, which could react with the cation

pools. *N*-Acyliminium ion **2**, generated from *N*-methoxycarbonyl-2-trimethylsilylpyrrolidine **1** by low temperature electrochemical oxidation and accumulated in a solution (cation pool), was utilized as a carbocation component (Scheme 7).



Scheme 7.

The triethylborane/ O_2 system,¹² which could be widely utilized to generate alkyl radicals from alkyl halides at low temperatures, was unsuccessful; however, we found that the hexabutyldistannane ($\text{Bu}_3\text{SnSnBu}_3$)/ $h\nu$ system was quite successful. Thus, heptyl iodide reacted with **2** in the presence of $\text{Bu}_3\text{SnSnBu}_3$ under UV irradiation at -20°C to afford the corresponding heptylated compound **3** (Table 1, entries 1 and 2). It was surprising that the reaction proceeded even in the dark (entries 3–15), although photo irradiation was well-known to enhance the homolytic cleavage of Sn–Sn bond.¹³ A stoichiometric amount of $\text{Bu}_3\text{SnSnBu}_3$ was necessary to complete the reaction, because the reactions using 0.5 and 0.1 equiv of $\text{Bu}_3\text{SnSnBu}_3$ led to the formation of **3** in 50 and 10% yields, respectively (entries 8 and 9). The reaction rates strongly depended on temperature. The reaction almost completed around 60 min at -20°C

Table 1. The addition of heptyl radical to the *N*-acyliminium ion **2**

Entry	Temperature (°C)	Time (min)	Condition	(Bu_3Sn) ₂ (equiv)	Yield (%)
1	-20	60	$h\nu$	5.0	64 ^a
2	-20	60	$h\nu$	2.5	66 ^a
3	-20	60	Dark	2.5	77
4	-20	60	Dark	1.5	77
5	-20	60	Dark	1.5	86 ^b
6	-20	60	Dark	1.0	72
7	-20	60	Dark	0.5	37
8	-20	180	Dark	0.5	50
9	-20	180	Dark	0.1	10
10	-20	5	Dark	1.5	16
11	-20	30	Dark	1.5	45
12	0	60	Dark	1.5	82
13	-78	60	Dark	1.5	9
14	-20	60	Dark	1.5	82 ^c
15	-20	60	Dark	1.5	8 ^d

^a Isolated yield.

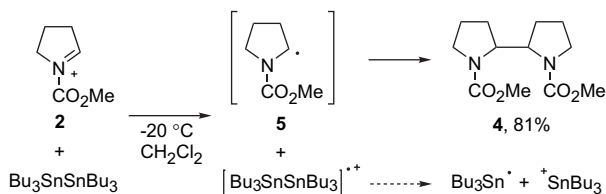
^b Slow addition of distannane.

^c 2,2,6,6-Tetramethyl-1-piperidinyloxy (TEMPO) (0.1 equiv) was added.

^d TEMPO (1.0 equiv) was added.

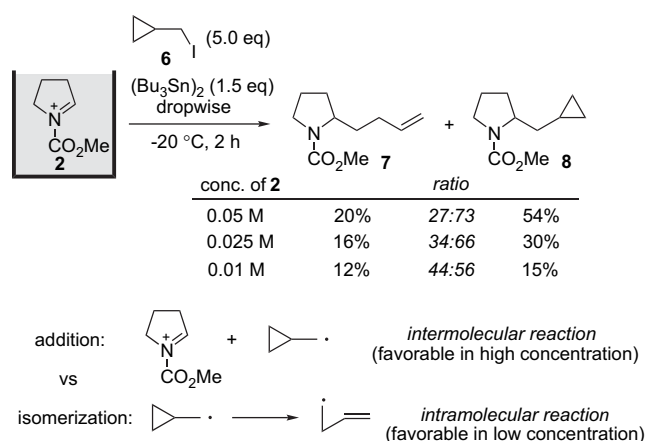
(entries 4, 10, and 11), but only 9% of **3** was obtained at $-78\text{ }^{\circ}\text{C}$ (entry 13).

To obtain a deeper insight into the mechanism, the reaction of **2** with $\text{Bu}_3\text{SnSnBu}_3$ in the absence of alkyl halides was examined at $-20\text{ }^{\circ}\text{C}$. The dimeric product **4** was obtained in 81% yield (a mixture of *dl* and *meso*) probably via one-electron reduction of **2** by $\text{Bu}_3\text{SnSnBu}_3$ to form radical intermediate **5** (Scheme 8).^{14,15} The radical-cation of $\text{Bu}_3\text{SnSnBu}_3$ thus formed may undergo Sn–Sn bond cleavage to give a tributylstannyl radical.



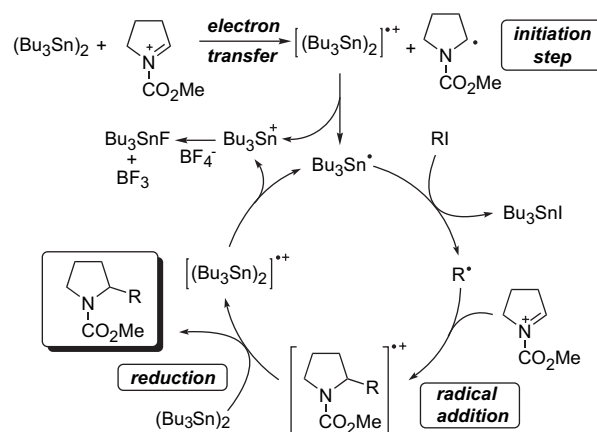
Scheme 8.

The reaction with cyclopropylmethyl iodide **6** was also examined, because the ring opening of cyclopropylmethyl radical is often used as a radical clock (Scheme 9).¹⁶ The product having the cyclopropyl ring (**8**) was obtained together with the ring-opened product (**7**). Formation of the product containing cyclopropyl ring indicated that the rate of radical addition to *N*-acyliminium ion **2** is comparable to that of ring opening.¹⁷ It is also worth mentioning that the product ratio depends upon the concentration of **2**. At lower concentration of **2**, the relative rate of the isomerization compared to the addition increases, and therefore, the amount of **7** increased with the expense of **8**.



Scheme 9.

On the basis of the above observations, we propose a mechanism described in Scheme 10. The reaction is initiated by one-electron transfer from $\text{Bu}_3\text{SnSnBu}_3$ to *N*-acyliminium ion **2** to generate the radical-cation of $\text{Bu}_3\text{SnSnBu}_3$. Cleavage of the Sn–Sn bond leads to the formation of a tributylstannyl radical, together with a tributylstannyl cation, which may react with tetrafluoroborate (electrolyte in electrolysis, see Section 4) to give tributylstannyl fluoride. The tributylstannyl radical abstracts iodine atom from an alkyl iodide to give an alkyl radical. The alkyl radical adds to



Scheme 10.

N-acyliminium ion **2** to generate the radical-cation, which undergoes the electron transfer reaction with $\text{Bu}_3\text{SnSnBu}_3$ to give the final product together with the radical-cation of $\text{Bu}_3\text{SnSnBu}_3$. This electron transfer regenerates the radical-cation of $\text{Bu}_3\text{SnSnBu}_3$. It is important to note that the reduction of the radical-cation by $\text{Bu}_3\text{SnSnBu}_3$ is faster than the reduction of cation **2** by $\text{Bu}_3\text{SnSnBu}_3$. This consideration is supported by the DFT calculations.¹⁸ The DFT calculations using *N*-(methoxycarbonyl)dimethylamine as a model compound indicate that the ionization energy of the radical to cation is ca. 6 eV, whereas the ionization energy of the neutral molecule to radical-cation is 8.44 eV (Fig. 1). It is also noteworthy that the slow addition of $\text{Bu}_3\text{SnSnBu}_3$ increased the yield of the product (Table 1, entry 5). Moreover, the addition of a catalytic amount of TEMPO (0.1 equiv) as a radical inhibitor did not affect the yield of **3**, but the addition of a stoichiometric amount of TEMPO (1.0 equiv) decreased the yield significantly (8%) (Table 1, entries 14 and 15). These results suggested the participation of $\text{Bu}_3\text{SnSnBu}_3$ in the initiation step of the reaction, and the radical initiation process took place spontaneously in situ.

Next, we investigated the scope of the present method using other organic halides and cation pools (Table 2). The reaction with an alkyl bromide was rather slow, and

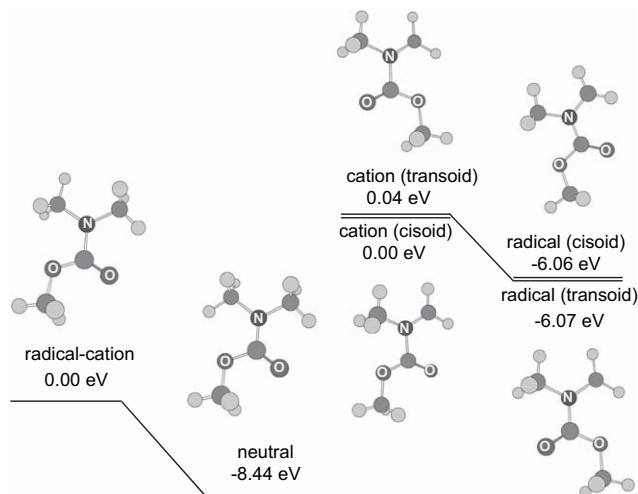
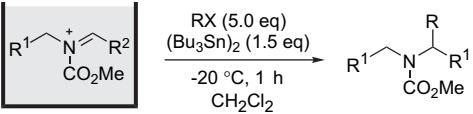
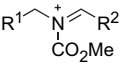
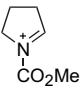
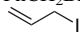
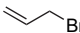
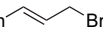
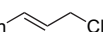
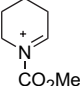
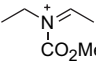


Figure 1. DFT calculations of the radical-cation, neutral molecule, cation, and radical of a model compound.

Table 2. Reactions of organic halides with *N*-acyliminium ion pools in the presence of Bu₃SnSnBu₃

		Yield (%)	
	RX	Normal addition	Slow addition
			C ₇ H ₁₅ I
	C ₇ H ₁₅ Br	20	39
	C ₇ H ₁₅ Cl	1	
	ClC ₇ H ₁₄ I		81
	<i>c</i> -C ₆ H ₁₁ I	60	74
	<i>iso</i> -C ₃ H ₇ I	43	73
	<i>tert</i> -C ₄ H ₉ I	19	
	PhCH ₂ Br	69	77
		3	
		4	
	Ph- 	Complex mixture	
	Ph- 	Complex mixture	
	C ₇ H ₁₅ I		35
	C ₇ H ₁₅ I	31	57

the reaction with an alkyl chloride was unsuccessful. The reaction with 1-chloro-6-iodoheptane gave rise to the formation of the corresponding chloroheptylated compound in 81% yield. The slow addition of the distannane was quite effective for the improvement in the yields of the product in the reaction with secondary and tertiary alkyl iodides. Benzyl bromide smoothly reacted with the cation, whereas the reactions using allylic halides were ineffective. The reaction also works for other cyclic and acyclic *N*-acyliminium ions.

3. Conclusion

In summary, we found that Bu₃SnSnBu₃ markedly promoted the reactions of alkyl halides with *N*-acyliminium ions. A chain mechanism involving the addition of an alkyl radical to an *N*-acyliminium ion followed by electron transfer reduction of thus formed radical-cation has been suggested. The present observations shed light on a new aspect of the chemistry of radical-cations. It is also noteworthy that the present reaction opens a new possibility for radical-cation crossover-mediated carbon–carbon bond formation.¹⁹

4. Experimental

4.1. General remarks

¹H and ¹³C NMR spectra were recorded on Varian GEMINI-2000 (¹H 300 MHz and ¹³C 75 MHz), Varian MERCURY-plus-400 (¹H 400 MHz and ¹³C 100 MHz), JEOL A-500

(¹H 500 MHz and ¹³C 125 MHz), and JEOL ECA-600 (¹H 600 MHz and ¹³C 150 MHz) spectrometers in CDCl₃. EI and CI mass spectra were recorded on JMS-SX102A spectrometer. FAB mass spectra were recorded on JMS-HX110A spectrometer. IR spectra were measured with a SHIMADZU FTIR 1600 spectrometer. GC analysis was performed on a gas chromatograph (SHIMADZU GC-14B) equipped with a flame ionization detector using a fused silica capillary. Gel permeation chromatography (GPC) was carried out by Japan Analytical Industry's LC-908 equipped with JAIGEL-1H and 2H using CHCl₃ as an eluent. Thin-layer chromatography (TLC) was carried out by using Merck precoated silica gel F₂₅₄ plates (thickness 0.25 mm).

4.2. Materials

Dichloromethane was washed with water and distilled from P₂O₅, then removal of a trace amount of acid was carried out by distillation from dried K₂CO₃, and distillate was stored over 4 Å molecular sieves. Trifluoromethanesulfonic acid (TfOH) was purchased from Nacalai and was used without purification. Tetrabutylammonium tetrafluoroborate (Bu₄NBF₄) was purchased from TCI and dried with P₂O₅ under vacuum. All reactions were carried out under Ar atmosphere unless otherwise noted.

4.3. Reactions

4.3.1. Generation of *N*-acyliminium ion pool (2). The anodic oxidation was carried out in an H-type divided cell (4G glass filter) equipped with a carbon felt anode (Nippon Carbon JF-20-P7, ca. 320 mg, dried at 250 °C/1 mmHg for 1 h before use) and a platinum plate cathode (40×20 mm). In the anodic chamber was placed a solution of **1** (563.8 mg, 2.8 mmol) in 0.3 M Bu₄NBF₄/CH₂Cl₂ (56 mL). In the cathodic chamber were placed 0.3 M Bu₄NBF₄/CH₂Cl₂ (56 mL) and trifluoromethanesulfonic acid (0.62 mL, 7.0 mmol). The constant current electrolysis (20 mA) was carried out at –78 °C with magnetic stirring until 2.5 F/mol of electricity was consumed.

4.3.2. Methyl 2-heptylpyrrolidinecarboxylate (3). **Typical procedure.** The electrolysis of **1** was carried out as described above. To the cation pool **2** generated from **1** (56.4 mg, 0.28 mmol) was added 1-iodoheptane (0.20 mL, 1.25 mmol), and hexabutylstannane (0.19 mL, 0.375 mmol) at –20 °C, and the reaction mixture was stirred for 1 h.

Triethylamine were added to the solution at –20 °C, and the resulting mixture was warmed up to room temperature. Solvent was removed under reduced pressure. DBU (1.2 mL, 0.90 mmol) and diethyl ether (10 mL) were added to the residue, and thus obtained solution was quickly filtered through a short column (10 cm) of silica gel. The silica gel was washed with ether (150 mL). The combined solution was concentrated by rotary evaporator, and the crude product thus obtained was purified using flash chromatography (hexane/EtOAc 9:1) and GPC to obtain the title compound (49 mg, 77% by GC analysis): ¹H NMR (400 MHz, CDCl₃) δ 0.88 (t, *J*=6.8 Hz, 3H), 1.20–1.36 (m, 11H), 1.63–1.71 (m, 2H), 1.76–1.97 (m, 3H), 3.30–3.49 (m, 2H), 3.67 (s, 3H), 3.73–3.86 (m, 1H); ¹³C NMR (100 MHz, CDCl₃) δ 14.2, 22.8, 23.6, 26.3, 29.4, 29.7, 30.2, 31.9, 34.2, 46.4, 52.1, 57.7, 155.4; IR (neat) 2926.4,

1705.3 cm^{-1} ; LRMS (CI) m/e 228 (M^+H); HRMS (CI) calcd for $\text{C}_{13}\text{H}_{26}\text{NO}_2$ (M^+H): 228.1964, found: 228.1965.

4.3.3. Methyl 2-cyclohexylpyrrolidinecarboxylate. Typical procedure for slow addition of hexabutylstannane.

The electrolysis of **1** was carried out as described above. To the cation pool **2** generated from **1** (56.4 mg, 0.28 mmol) was added 1-iodocyclohexane (0.16 mL, 1.25 mmol) at -20°C . Then, hexabutylstannane (0.19 mL, 0.375 mmol) was added dropwise over a period of 30 min at the same temperature. Then the reaction mixture was stirred for 1.0 h at -20°C . Triethylamine was added to the solution at -20°C , and the resulting mixture was warmed up to room temperature. Solvent was removed under reduced pressure. DBU (1.2 mL, 0.90 mmol) and diethyl ether (10 mL) were added to the residue, and thus obtained solution was quickly filtered through a short column (10 cm) of silica gel. The silica gel was washed with ether (150 mL). The combined solution was concentrated by rotary evaporator, and the crude product thus obtained was purified by flash chromatography (hexane/EtOAc 9:1) and GPC to obtain the title compound (33.6 mg, 0.159 mmol, 60% yield): ^1H NMR (400 MHz, CDCl_3) δ 0.87–1.09 (m, 2H), 1.09–1.30 (m, 3H), 1.54–1.70 (m, 4H), 1.70–1.90 (m, 6H), 3.21–3.31 (m, 1H), 3.40–3.83 (m, 2H), 3.69 (s, 3H); ^{13}C NMR (100 MHz, CDCl_3) δ 23.6 and 24.4, 26.2, 26.4, 26.6, 27.3 and 27.7, 30.0, 40.6 and 41.3, 46.7, 52.1, 61.8 and 62.4, 156.0; IR (neat) 2926.4, 1703.4 cm^{-1} ; LRMS (CI) m/e 212 (M^+H); HRMS (CI) calcd for $\text{C}_{12}\text{H}_{22}\text{NO}_2$ (M^+H): 212.1651, found: 212.1656.

4.3.4. Methyl 2-(4-chlorobutyl)pyrrolidinecarboxylate.

Prepared from cation pool **2** generated from **1** (50.3 mg, 0.25 mmol), hexabutylstannane (0.19 mL, 0.375 mmol), and 1-chloro-4-iodobutane (0.15 mL, 1.25 mmol), and then purified by flash chromatography (hexane/EtOAc 9:1) to obtain the title compound (44.6 mg, 0.203 mmol, 81% yield): ^1H NMR (400 MHz, CDCl_3) δ 1.13–2.03 (m, 10H), 3.21–3.50 (m, 2H), 3.53 (t, $J=6.4$ Hz, 2H), 3.66 (s, 3H), 3.71–3.89 (m, 1H); ^{13}C NMR (100 MHz, CDCl_3) δ 23.1 and 24.0, 23.5, 30.0 and 30.6, 32.5, 33.2 and 33.8, 45.0, 46.3 and 46.6, 52.1, 57.0 and 57.7, 155.4; IR (neat) 2955.4, 2872.4, 1701.4 cm^{-1} ; LRMS (CI) m/e 220 (M^+H); HRMS (CI) calcd for $\text{C}_{10}\text{H}_{18}\text{ClNO}_2$ (M^+H): 220.1104, found: 220.1100.

4.3.5. Methyl 2-isopropylpyrrolidinecarboxylate.

Prepared from cation pool **2** generated from **1** (56.4 mg, 0.28 mmol), hexabutylstannane (0.19 mL, 0.375 mmol), and *iso*-propyl iodide (0.12 mL, 1.25 mmol), and then purified by flash chromatography (hexane/EtOAc 9:1) and GPC to obtain the title compound (20.6 mg, 0.120 mmol, 43% yield): ^1H NMR (400 MHz, CDCl_3) δ 0.77–0.94 (m, 6H), 1.69–1.94 (m, 4H), 2.00–2.30 (m, 1H), 3.20–3.30 (m, 1H), 3.54–3.80 (m, 2H), 3.64 (s, 3H); ^{13}C NMR (100 MHz, CDCl_3) δ 17.2, 19.9, 24.8, 26.0, 30.4, 47.4, 52.4, 63.3, 156.2; IR (neat) 2961.1, 1703.4 cm^{-1} ; LRMS (CI) m/e 172 (M^+H); HRMS (CI) calcd for $\text{C}_9\text{H}_{18}\text{NO}_2$ (M^+H): 172.1338, found: 172.1337.

4.3.6. Methyl 2-benzylpyrrolidinecarboxylate. Prepared from cation pool **2** generated from **1** (56.4 mg, 0.28 mmol), hexabutylstannane (0.19 mL, 0.375 mmol), and benzyl

bromide (0.15 mL, 1.25 mmol), and then purified by flash chromatography (hexane/EtOAc 9:1) and GPC to obtain the title compound (42.4 mg, 0.190 mmol, 69% yield): ^1H NMR (400 MHz, CDCl_3) δ 1.69–1.89 (m, 4H), 2.58 (dd, $J=13.2$, 9.6 Hz, 1H), 2.96–3.09 (m, 0.5H), 3.16–3.26 (m, 0.5H), 3.31–3.50 (m, 2H), 3.732 (s, 3H), 3.99–4.14 (m, 1H), 7.12–7.30 (m, 5H); ^{13}C NMR (100 MHz, CDCl_3) δ 22.8 and 23.6, 29.0 and 29.9, 39.6 and 40.6, 46.6, 52.2, 58.6 and 59.3, 126.0, 128.2, 129.3, 138.8, 155.4; IR (neat) 2953.4, 1699.5, 702.2 cm^{-1} ; LRMS (CI) m/e 220 (M^+H); HRMS (CI) calcd for $\text{C}_{13}\text{H}_{18}\text{NO}_2$ (M^+H): 220.1338, found: 220.1337.

4.3.7. Methyl ethyl(1-methyloctyl)aminocarboxylate.

The electrolysis of diethylamine carboxylate (52.5 mg, 0.40 mmol) was carried out as described above. To the cation pool **2** thus generated in the anodic chamber, were added 1-iodoheptane (0.33 mL, 2.0 mmol) and hexabutylstannane (0.30 mL, 0.60 mmol) at -20°C and the reaction mixture was stirred for 1 h. Triethylamine was added to the stirred solution at -20°C . Then the mixture was warmed up to room temperature. Solvent was removed under reduced pressure and the residue was quickly filtered through a short column (10 cm) of silica gel to remove Bu_4NBF_4 . The silica gel was washed with ether (150 mL). Then, the crude product thus obtained was purified using flash chromatography (hexane/EtOAc 9:1) and GPC to obtain the title compound (28.6 mg, 0.125 mmol, 31% yield): ^1H NMR (400 MHz, CDCl_3) δ 0.87 (t, $J=6.8$ Hz, 3H), 1.00–1.19 (m, 6H), 1.19–1.57 (m, 13H), 3.00–3.29 (m, 2H), 3.69 (s, 3H), 3.91–4.21 (m, 1H); ^{13}C NMR (100 MHz, CDCl_3) δ 14.5, 15.4 and 16.1, 19.6 and 20.0, 23.1, 27.1, 29.6, 30.0, 32.2, 35.3, 37.4 and 38.2, 52.3, 52.5, 156.9; IR (neat) 2928.3, 1703.4 cm^{-1} ; LRMS (CI) m/e 230 (M^+H); HRMS (CI) calcd for $\text{C}_{13}\text{H}_{28}\text{NO}_2$ (M^+H): 230.2120, found: 230.2119.

4.3.8. Methyl 2-(3-butenyl)pyrrolidinecarboxylate (7).

Prepared from cation pool **2** generated from **1** (56.4 mg, 0.28 mmol), hexabutylstannane (0.19 mL, 0.375 mmol), and cyclopropylmethyl iodide (227.5 mg, 1.25 mmol), and then purified by flash chromatography (hexane/EtOAc 9:1) and GPC to obtain the title compound (5.5 mg, 0.030 mmol, 11% yield): ^1H NMR (400 MHz, CDCl_3) δ 1.30–2.11 (m, 8H), 3.28–3.47 (m, 2H), 3.74–3.88 (m, 1H), 4.88–5.11 (m, 2H), 5.72–5.88 (m, 1H); ^{13}C NMR (100 MHz, CDCl_3) δ 22.9 and 23.8, 29.8 and 30.4, 33.0 and 33.5, 46.2, 52.0, 56.8 and 57.4, 114.5, 138.2, 155.6; IR (neat) 2953.9, 1701.4, 733.0 cm^{-1} ; LRMS (EI) m/e 183 (M^+); HRMS (EI) calcd for $\text{C}_{10}\text{H}_{17}\text{NO}_2$ (M^+): 183.1259, found: 183.1256.

4.3.9. Methyl 2-(cyclopropylmethyl)pyrrolidinecarboxylate (8).

Prepared from cation pool **2** generated from **1** (56.4 mg, 0.28 mmol), hexabutylstannane (0.19 mL, 0.375 mmol), and cyclopropylmethyl iodide (227.5 mg, 1.25 mmol), and then purified by flash chromatography (hexane/EtOAc 9:1) and GPC to obtain the title compound (22.0 mg, 0.12 mmol, 42% yield): ^1H NMR (400 MHz, CDCl_3) δ 0.01–0.16 (m, 2H), 0.37–0.50 (m, 2H), 0.54–0.67 (m, 1H), 1.33–1.46 and 1.49–1.59 (m, 2H), 1.77–2.03 (m, 4H), 3.29–3.51 (m, 2H), 3.67 (s, 3H), 3.80–3.99 (m, 1H); ^{13}C NMR (100 MHz, CDCl_3) δ 4.3, 5.2, 8.3, 23.5 and 24.3, 30.2 and 30.9, 38.7 and 39.6, 46.6, 52.4, 58.0 and

58.5, 155.8; IR (neat) 2955.3, 1703.4 cm^{-1} ; LRMS (CI) *m/e* 184 (M^+H); HRMS (CI) calcd for $\text{C}_{10}\text{H}_{18}\text{NO}_2$ (M^+H): 184.1338, found: 184.1339.

4.3.10. Methyl 2-heptylpiperidinecarboxylate. Prepared from cation pool generated from methyl piperidinecarboxylate (60.3 mg, 0.28 mmol), 1-iodoheptane (0.20 mL, 1.25 mmol), and hexabutyl-distannane (0.19 mL, 0.375 mmol), and then purified by flash chromatography (hexane/EtOAc 9:1) and GPC to obtain the title compound (23.7 mg, 0.098 mmol, 35% yield): ^1H NMR (400 MHz, CDCl_3) δ 0.88 (t, $J=6.8$ Hz, 3H), 1.14–1.33 (m, 10H), 1.33–1.71 (m, 8H), 2.74–2.87 (m, 1H), 3.67 (s, 3H), 3.90–4.06 (m, 1H), 4.14–4.27 (m, 1H); ^{13}C NMR (120 MHz, CDCl_3) δ 14.1, 18.9, 22.6, 25.6, 26.2, 28.3, 29.3, 29.5, 29.5, 31.8, 40.0, 50.7, 52.3, 156.3; IR (neat) 2930.2, 2856.9, 1701.4 cm^{-1} ; LRMS (CI) *m/e* 242 (M^+H); HRMS (CI) calcd for $\text{C}_{14}\text{H}_{28}\text{NO}_2$ (M^+H): 242.2115, found: 242.2120.

4.3.11. *N,N'*-Dimethoxycarbonyl-2,2'-bipyrrolidine (4).

This compound was obtained by the reaction of **2** and $\text{Bu}_3\text{SnSnBu}_3$ in the absence of an alkyl halide. The electrolysis of **1** was carried out as described above. To the cation pool **2** (0.056 M, 5.0 mL, 0.28 mmol) was added hexabutyl-distannane (0.19 mL, 0.375 mmol) at -20°C and the reaction mixture was stirred for 5 h at the same temperature. Triethylamine (0.25 mL) was added to stirred solution at -20°C and the resulting mixture was warmed to room temperature. Solvent was removed under reduced pressure and the residue was quickly filtered through a short column (10 cm) of silica gel to remove Bu_4NBF_4 . The silica gel was washed with ether (150 mL). Then, the crude product thus obtained was purified using flash chromatography (hexane/EtOAc 9:1) and GPC to obtain the title compound (29.3 mg, 0.114 mmol, 82% yield), which was identified by comparison of its ^1H NMR spectrum with that of an authentic sample reported previously.¹⁴

4.3.12. DFT calculations. The DFT calculations were carried out with model compounds (methyl dimethylamine carboxylate, the radical-cation, radical, and cation derived from it at B3LYP/6-31G(d) level using the Gaussian 98W and 2003W.¹⁸ Geometries were fully optimized. All the optimized geometries were local minima according to the vibration analysis.

Acknowledgements

This work was partially supported by the Grant-in-Aid for Scientific Research, Japan. We also thank Professor Michael Schmittel of Siegen University for helpful discussion.

References and notes

- (a) Narasaka, K.; Okauchi, T.; Arai, N. *Chem. Lett.* **1992**, 1229; (b) Chen, C.; Mariano, P. S. *J. Org. Chem.* **2000**, *65*, 3252; (c) Saitoh, T.; Ichikawa, J. *J. Am. Chem. Soc.* **2005**, *127*, 9696.
- (a) Yoshida, J.; Nishiwaki, K. *J. Chem. Soc., Dalton Trans.* **1998**, 2589; (b) Moeller, K. D. *Tetrahedron* **2000**, *56*, 9527 and references cited therein.
- (a) Brumfield, M. A.; Quillen, S. L.; Yoon, U. C.; Mariano, P. S. *J. Am. Chem. Soc.* **1984**, *106*, 6855; (b) Pandey, G.; Kumaraswamy, G.; Bhalerao, U. T. *Tetrahedron Lett.* **1989**, *30*, 6059; (c) Popielarz, R.; Arnold, D. R. *J. Am. Chem. Soc.* **1990**, *112*, 3068; (d) Mikami, T.; Harada, M.; Narasaka, K. *Chem. Lett.* **1999**, 425; (e) Jonas, M.; Blechert, S.; Steckhan, E. *J. Org. Chem.* **2001**, *66*, 6896; (f) Seiders, J. R., II; Wang, L.; Floreancig, P. E. *J. Am. Chem. Soc.* **2003**, *125*, 2406; (g) Liu, H.; Shuangyi Wan, S.; Floreancig, P. E. *J. Org. Chem.* **2005**, *70*, 3814 and references cited therein.
- Schmittel, M.; Burghart, A. *Angew. Chem., Int. Ed.* **1997**, *36*, 2550; See also: Baciocchi, E.; Bietti, M.; Lanzalunga, O. *Acc. Chem. Res.* **2000**, *33*, 243.
- For mechanistic studies of radical-cation fragmentation reactions see: (a) Hammerum, S.; Audier, H. E. *J. Chem. Soc., Chem. Commun.* **1988**, 860; (b) Arnold, D. R.; Lamont, L. J. *Can. J. Chem.* **1989**, *67*, 2119; (c) Horner, J. H.; Martinez, F. N.; Musa, O. M.; Newcomb, M.; Shahin, H. E. *J. Am. Chem. Soc.* **1995**, *117*, 11124; (d) Burton, R. D.; Bartberger, M. D.; Zhang, Y.; Eyler, J. R.; Schanze, K. S. *J. Am. Chem. Soc.* **1996**, *118*, 5655; (e) Baciocchi, E.; Bietti, M.; Putignani, L.; Steenken, S. *J. Am. Chem. Soc.* **1996**, *118*, 5952; (f) Su, Z.; Mariano, P. S.; Falvey, D. E.; Yoon, U. C.; Oh, S. W. *J. Am. Chem. Soc.* **1998**, *120*, 10676; (g) Gould, I. R.; Lenhard, J. R.; Muentner, A. A.; Godleski, S. A.; Farid, S. *J. Am. Chem. Soc.* **2000**, *122*, 11934.
- (a) Minisci, F.; Bernardi, R.; Bertini, F.; Galli, R.; Perchinnmo, M. *Tetrahedron* **1971**, *27*, 3575; (b) Minisci, F. *Synthesis* **1973**, 1; (c) Minisci, F.; Fontana, F.; Pianese, G.; Yan, Y. M. *J. Org. Chem.* **1993**, *58*, 4207; (d) Minisci, F.; Vismara, E.; Fontana, F.; Morini, G.; Serravalle, M. *J. Org. Chem.* **1986**, *51*, 4411 and references cited therein.
- Minisci, F.; Vismara, E.; Fontana, F. *Heterocycles* **1989**, *28*, 489.
- (a) Clerici, A.; Porta, O. *Tetrahedron Lett.* **1990**, *31*, 2069; (b) Clerici, A.; Porta, O. *Gazz. Chim. Ital.* **1992**, *122*, 165; (c) Cannella, R.; Clerici, A.; Pastori, N.; Regolini, E.; Porta, O. *Org. Lett.* **2005**, *7*, 645.
- (a) Miyabe, H.; Ueda, M.; Nishimura, A.; Naito, T. *Org. Lett.* **2002**, *4*, 131; (b) Miyabe, H.; Ueda, M.; Naito, T. *Synlett* **2004**, 1140; (c) Miyabe, H.; Yamaoka, Y.; Takemoto, Y. *J. Org. Chem.* **2005**, *70*, 3324.
- (a) Yoshida, J.; Suga, S.; Suzuki, S.; Kinomura, N.; Yamamoto, A.; Fujiwara, K. *J. Am. Chem. Soc.* **1999**, *121*, 9546; (b) Suga, S.; Suzuki, S.; Yamamoto, A.; Yoshida, J. *J. Am. Chem. Soc.* **2000**, *122*, 10244; (c) Suga, S.; Okajima, M.; Yoshida, J. *Tetrahedron Lett.* **2001**, *42*, 2173; (d) Suga, S.; Okajima, M.; Fujiwara, K.; Yoshida, J. *J. Am. Chem. Soc.* **2001**, *123*, 7941; (e) Yoshida, J.; Suga, S. *Chem.—Eur. J.* **2002**, *8*, 2650; (f) Suga, S.; Watanabe, M.; Yoshida, J. *J. Am. Chem. Soc.* **2002**, *124*, 14824; (g) Suga, S.; Nagaki, A.; Yoshida, J. *Chem. Commun.* **2003**, 354; (h) Suga, S.; Nagaki, A.; Tsutsui, Y.; Yoshida, J. *Org. Lett.* **2003**, *5*, 945; (i) Suga, S.; Kageyama, Y.; Babu, G.; Itami, K.; Yoshida, J. *Org. Lett.* **2004**, *6*, 2709; (j) Suzuki, S.; Matsumoto, K.; Kawamura, K.; Suga, S.; Yoshida, J. *Org. Lett.* **2004**, *6*, 3755; (k) Suga, S.; Nishida, T.; Yamada, D.; Nagaki, A.; Yoshida, J. *J. Am. Chem. Soc.* **2004**, *126*, 14338; (l) Nagaki, A.; Kawamura, K.; Suga, S.; Ando, T.; Sawamoto, M.; Yoshida, J. *J. Am. Chem. Soc.* **2004**, *126*, 14702; (m) Okajima, M.; Suga, S.; Itami, K.; Yoshida, J. *J. Am. Chem. Soc.* **2005**, *127*, 6930; (n) Suga, S.; Tsutsui, Y.; Nagaki, A.; Yoshida, J. *Bull. Chem. Soc. Jpn.* **2005**, *78*, 1206; (o) Nagaki, A.; Togai, M.; Suga, S.; Aoki, N.; Mae, K.; Yoshida, J. *J. Am. Chem. Soc.* **2005**, *127*, 11666.

11. Maruyama, T.; Suga, S.; Yoshida, J. *J. Am. Chem. Soc.* **2005**, *127*, 7324.
12. Nozaki, K.; Oshima, K.; Utimoto, K. *J. Am. Chem. Soc.* **1987**, *109*, 2547.
13. (a) Junggebauer, J.; Neumann, W. P. *Tetrahedron* **1997**, *53*, 1301; (b) Studer, A.; Steen, H. *Chem.—Eur. J.* **1999**, *5*, 759.
14. (a) Suga, S.; Suzuki, S.; Yoshida, J. *J. Am. Chem. Soc.* **2002**, *124*, 30; (b) Suga, S.; Suzuki, S.; Maruyama, T.; Yoshida, J. *Bull. Chem. Soc. Jpn.* **2004**, *77*, 1545.
15. It has been reported that 10-methylacridinium ion reacts with distannane via electron transfer mediated radical chain mechanism to yield the dimeric product. Fukuzumi, S.; Kitano, T.; Mochida, K. *J. Am. Chem. Soc.* **1990**, *112*, 3246; See also: Krusic, P. J.; Stoklosa, H.; Manzer, L. E.; Meakin, P. *J. Am. Chem. Soc.* **1975**, *97*, 667.
16. The rate constant of the ring opening is reported to be $1.3 \times 10^8 \text{ s}^{-1}$: Maillard, B.; Forrest, D.; Ingold, K. U. *J. Am. Chem. Soc.* **1976**, *98*, 7024.
17. The rate constant of the addition of a primary alkyl radical to protonated pyridine derivatives is reported to be 10^4 – $10^6 \text{ M}^{-1} \text{ s}^{-1}$. See: Citterio, A.; Minisci, F.; Franchi, V. *J. Org. Chem.* **1980**, *45*, 4752. See also Ref. 7.
18. Frisch, M. J.; Trucks, G. W.; Schlegel, H. B.; Scuseria, G. E.; Robb, M. A.; Cheeseman, J. R.; Montgomery, J. A., Jr.; Vreven, T.; Kudin, K. N.; Burant, J. C.; Millam, J. M.; Iyengar, S. S.; Tomasi, J.; Barone, V.; Mennucci, B.; Cossi, M.; Scalmani, G.; Rega, N.; Petersson, G. A.; Nakatsuji, H.; Hada, M.; Ehara, M.; Toyota, K.; Fukuda, R.; Hasegawa, J.; Ishida, M.; Nakajima, T.; Honda, Y.; Kitao, O.; Nakai, H.; Klene, M.; Li, X.; Knox, J. E.; Hratchian, H. P.; Cross, J. B.; Adamo, C.; Jaramillo, J.; Gomperts, R.; Stratmann, R. E.; Yazyev, O.; Austin, A. J.; Cammi, R.; Pomelli, C.; Ochterski, J. W.; Ayala, P. Y.; Morokuma, K.; Voth, G. A.; Salvador, P.; Dannenberg, J. J.; Zakrzewski, V. G.; Dapprich, S.; Daniels, A. D.; Strain, M. C.; Farkas, O.; Malick, D. K.; Rabuck, A. D.; Raghavachari, K.; Foresman, J. B.; Ortiz, J. V.; Cui, Q.; Baboul, A. G.; Clifford, S.; Cioslowski, J.; Stefanov, B. B.; Liu, G.; Liashenko, A.; Piskorz, P.; Komaromi, I.; Martin, R. L.; Fox, D. J.; Keith, T.; Al-Laham, M. A.; Peng, C. Y.; Nanayakkara, A.; Challacombe, M.; Gill, P. M. W.; Johnson, B.; Chen, W.; Wong, M. W.; Gonzalez, C.; Pople, J. A. *Gaussian 03, Revision B.05*; Gaussian: Pittsburgh, PA, 2003.
19. For example: (a) Crich, D.; Ranganathan, K.; Neelamkavil, S.; Huang, X. *J. Am. Chem. Soc.* **2003**, *125*, 7942; (b) Crich, D.; Ranganathan, K. *J. Am. Chem. Soc.* **2002**, *124*, 12422; (c) Newcomb, M.; Miranda, N.; Sannigrahi, M.; Huang, X.; Crich, D. *J. Am. Chem. Soc.* **2001**, *123*, 6445.

Organolithiums by reductive lithiation: the catalytic aromatic method versus the use of preformed aromatic radical-anions. Naphthalene can behave as a catalyst or an inhibitor[☆]

Ao Yang, Heather Butela, Kai Deng, Mary Dosch Doubleday and Theodore Cohen^{*}

Department of Chemistry, University of Pittsburgh, Pittsburgh, PA 15260, USA

Received 24 January 2006; accepted 16 March 2006

Available online 2 May 2006

Abstract—Two common modes, using aromatic radical-anions for reductive lithiation, the replacement of a C–heteroatom bond with a C–Li bond, have been compared with regard to yield and the mildness of reaction conditions required. It was found that the use of preformed radical-anions generally resulted in higher yields and milder reaction conditions than the ‘catalytic’ method in which catalytic amounts of the aromatic compound are used and the radical-anion is generated and used in situ. The one apparent exception is *N*-phenylaziridine, but it is shown that in this case the aromatic compound, naphthalene, is actually an *inhibitor* rather than a *catalyst*. Rational mechanistic explanations are given. © 2006 Elsevier Ltd. All rights reserved.

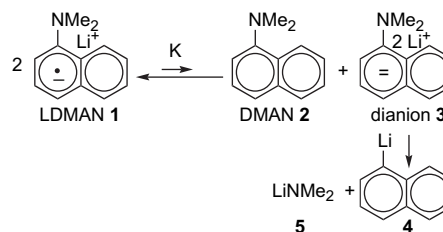
1. Introduction

Since its introduction in 1978,^{2,3} reductive lithiation of phenyl thioethers using aromatic radical-anions has been demonstrated to be one of the most versatile methods known for generating organolithiums.^{4,5} A number of other leaving groups, such as halides,⁶ sulfones,⁷ sulfates,⁸ nitriles,⁹ selenides,¹⁰ allylic and benzylic ethers,^{11,12} sulfides,¹³ amines,¹³ and acetals,¹⁴ have also been used but they have been considerably less versatile than the phenylthio group.¹⁵ An important advantage of reductive lithiation is that unlike the most conventional method of organolithium preparation, removal of an electrophile such as H⁺, I⁺, R₃Sn⁺, etc. by another organolithium, it is often the case that the less stable the organolithium, the greater the ease of its generation by reductive lithiation. The reason is that the mechanism involves the transfer of an electron from the aromatic radical-anion to the substrate followed by a homolytic cleavage of the bond between the organic moiety and the leaving group.¹⁶ Since this step is rate determining, the rate of the reaction is determined largely by the stability of the intermediate radical, rather than that of the carbanion, to which the radical is rapidly reduced. Thus, it is an extremely general method of organolithium production especially since phenyl thioethers are available by a wide variety of synthetic methods, many of

them connective. Another considerable advantage is that the aromatic and the thiophenol are recoverable and thus a stoichiometric amount of lithium metal is the only reagent that is destroyed, making this the most economical method available since lithium is far less expensive than any organic form of lithium.

In the earliest reports of the reductive lithiation of phenyl thioethers,² a stoichiometric quantity of lithium naphthalenide was used but in several cases, a sub-stoichiometric quantity of naphthalene was used along with a stoichiometric quantity of lithium metal. The latter conditions were successful in reducing the amount of naphthalene that had to be removed from the desired product but the reductive lithiations required higher temperatures and longer reaction times.

In 1980, a report from this laboratory indicated a solution to the problem of removal of the aromatic hydrocarbon.¹⁷ When lithium 1-(dimethylamino)naphthalenide (LDMAN **1**, Scheme 1) was used as the reducing agent, the basic aromatic



Scheme 1.

[☆] See Ref. 1.

Keywords: Reductive lithiation; Aromatic catalysis; Radical-anions; Dianions; Organolithium.

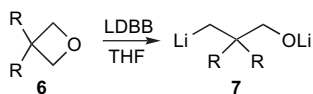
^{*} Corresponding author. Tel.: +44 412 624 8220; fax: +44 412 624 8356; e-mail: cohen@pitt.edu

byproduct **2** could be removed and recovered by washing the reaction mixture with dilute acid. An additional advantage of the use of LDMAN is that it can be used in solvents other than THF, the solvent universally used in synthetic procedures involving aromatic lithium radical-anions.¹⁸

Because LDMAN **1** decomposes to 1-lithionaphthalene **4** above $-45\text{ }^{\circ}\text{C}$,¹⁹ a ‘catalytic method’ was devised, which allowed reactions with LDMAN to be performed with good results at higher temperatures.¹⁷ Because of the great instability of aryl radicals, it was thought that the decomposition of LDMAN at this low temperature was probably not due to the homolytic cleavage of the bond between the ring carbon atom and the heteroatom, the usual mode in radical-anion decompositions.²⁰ It was postulated instead that the aromatic dianion **3** was generated in THF in an unfavorable equilibrium²¹ with the radical-anion **1** and was decomposing directly to the relatively stable naphthyl anion and the dimethylamido anion **5** (Scheme 1).

Since DMAN **2** and Li metal react over a period of hours to produce LDMAN while most reductive lithiations are extremely rapid, it was reasoned that DMAN would act as a conduit for electrons to the substrate undergoing reductive lithiation and that the concentration of the radical-anion **1** would be extremely low until the reductive lithiation is complete. Thus, the equilibrium in Scheme 1 would be driven even further to the left, resulting in a negligible concentration of the unstable dianion **3** and consequently in a very slow decomposition of LDMAN. This reasoning is apparently correct as evidenced by the fact that the green-black color of LDMAN only became evident when all of the substrate thioether had reacted and by the ability, using the catalytic method, of performing reductive lithiations above $-45\text{ }^{\circ}\text{C}$.¹⁷

The success of the next published use of the catalytic method was more mixed. During a study in this laboratory of the reductive lithiation, using lithium 4,4'-di-*tert*-butylbiphenylide (LDBB), one of the most common aromatic radical-anions,²² of oxetanes **6** to produce organolithiums **7** bearing an oxyanionic group (Scheme 2), the catalytic aromatic method, as expected from the above results and discussion, took far longer than the method using preformed aromatic radical-anion at the same temperature.²³ However, the result led to just as favorable an outcome with **6** (R=Me) but with **6** (R=H), the production of **7** (R=H) was far less efficient, giving a lower yield of dianion than when preformed aromatic radical-anion was used and leading to the production of considerable 1-propanol. Undoubtedly, the propanol resulted when the intermediate anion **7** (R=H), during the long reaction time required, removed a proton from the 2-position of the sterically unhindered oxetane, a known type of proton loss for oxetanes.²⁴ The steric hindrance provided by the methyl groups of **6** (R=Me) apparently saved it from this fate.



Scheme 2.

More recently, Yus and his co-workers in Spain introduced the use of the catalytic aromatic method, in a mode somewhat different than that used previously, for the reductive lithiation of some primary alkyl chlorides and two alkyl phenyl sulfides.²⁵ In their work,^{26–28} a solution of the substrate to be reduced in THF is mixed with 1–5 mol % of the aromatic compound, usually naphthalene or 4,4'-di-*tert*-butylbiphenyl (DBB), and a large excess of lithium powder, usually a 4–7-fold molar excess. In their extensive and impressive publications on this topic, they have demonstrated that a large variety of organic compounds can be reductively lithiated, and that this method eases the separation of the aromatic byproduct from the reaction product.^{25–28}

In a number of these papers, the claim is made that this version of the catalytic aromatic method (which we abbreviate CA), in which the radical-anion is continually generated and rapidly destroyed by electron transfer to the substrate, is far more powerful than the use of a stoichiometric amount of preformed aromatic radical-anion (PAR).^{26,29–32} For example, “above all, the catalytic version is far more reactive, so it is possible to perform new lithiation reactions, which do not work when a lithiation-arene is used as lithiation agent”^{29a} and “in the catalytic version, yields are better, reaction times are far shorter, the reactions are very clean.”^{26a}

This assertion seemed unlikely to us based on the experimental results enumerated above and some other results from our laboratory, heretofore only reported in a thesis (see below). The theoretical basis also appears inconsistent with our experience that radical-anion formation is virtually always slower than the reductive lithiation, as mentioned above. Thus, in most cases the rate-determining step for the reductive lithiation would be the transfer of an electron from the surface of the metal to the aromatic catalyst. The net result would be that, as found in the published work described above, the process of reductive lithiation would be slower at any given temperature than the process using preformed radical-anion. As again indicated above, such longer reaction times can in some cases translate into destruction of some organolithium compounds. Of course, damage is minimized in the Yus protocol in which the radical-anion formation is accelerated by supplying the lithium as a powder instead of larger chunks with less surface area and by the use of a very large excess of lithium. Nonetheless, the rate-determining step is still the electron transfer to the aromatic catalyst as evidenced by the fact that, as in the use of the catalytic method with LDMAN mentioned above,¹⁷ the color of the radical-anion does not appear until all of the reduction substrate has been consumed.^{25,29,33}

The mechanistic explanation suggested³⁰ to account for the purported superiority of the CA method is that there is a greater concentration of aromatic dianion during reduction by the CA method than that by the PAR method and that the dianion is expected to be a more powerful reducing agent. However, it seems to us that there should be a far lower concentration of aromatic dianion in the CA method than in the PAR method for the reasons in our earlier paper¹⁷ that are outlined in the discussion above pertaining to Scheme 1.

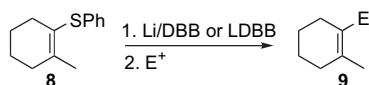
For example, in that scheme, the concentration of dianion **3** is given by the expression: $[3]=K[1]^2/[2]$ where **1** is the radical-anion and **2** is the neutral aromatic. Thus, in the case of preformed aromatic radical-anion, the concentration of dianion is at the maximum since virtually all of the aromatic compound is in the form of the radical-anion and the concentration of neutral aromatic is negligible. On the other hand, in the CA method, the concentration of dianion is minimal since the rapid transfer of an electron from the slowly formed radical-anion to the substrate maintains a negligible concentration of radical-anion and virtually all of the aromatic compound is in the neutral form; this is clearly indicated by the fact that the color of the radical-anion appears only after the substrate has been consumed.^{25,29,33}

Presumably, these claims of the greater power of the CA method are at least partly responsible for the choice that most groups now make to adopt it in new work as indicated in recent reviews of Yus.^{26,34} On the other hand, if this superiority is found to be unsubstantiated, the choice as to which of the two modes of reductive lithiation is appropriate in a given case should be made on other grounds. The present study was performed to directly compare the PAR and CA methods by conducting reactions using both methods to determine the relative advantages of each.

2. Results and discussion

2.1. Reductive lithiation of 2-methyl-1-(phenylthio)cyclohexene

In work that we had performed 15 years ago, but was heretofore only reported in a thesis because its significance was not obvious at the time,¹ evidence for a decreased yield using the catalytic method rather than PAR method was found in the reductive lithiation of 2-methyl-1-(phenylthio)cyclohexene **8** for 8 h at $-78\text{ }^\circ\text{C}$ (Scheme 3), followed by quenching with various electrophiles. The use of a slightly greater than stoichiometric amount of LDBB gave yields of 80%, 71%, and 71%, respectively, of products **9** when the vinyl lithium was quenched with cyclohexanecarboxaldehyde, *n*-hexyl iodide, and allyl bromide. When the same reaction was performed using a slight excess of lithium and only 20% of the stoichiometric amount of DBB, the yields were 54%, 50%, and 52%, respectively. Thus, in this case as in those described in Section 1, preformed aromatic radical-anion gave better yields than the use of the same quantity of Li but a considerably sub-stoichiometric quantity of the aromatic hydrocarbon.

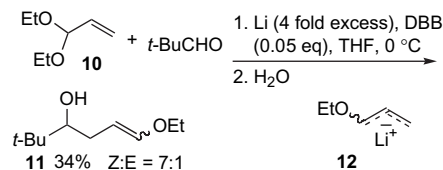


Scheme 3.

2.2. Reductive lithiation of acrolein diethyl acetal

In 1994, a report³² appeared in which acrolein diethyl acetal **10** was reductively lithiated via the CA method at $0\text{ }^\circ\text{C}$ in

the presence of various carbonyl compounds that captured the resulting allylic lithioether **12** (the Barbier method³⁵) to give 34–40% yields of alcohols. Scheme 4 shows one example. Significantly, it was stated that no reduction occurred at $-40\text{ }^\circ\text{C}$ and that if the carbonyl compound were added after the reductive lithiation, the yields were greatly reduced due to decomposition of the allyl anionic intermediate.



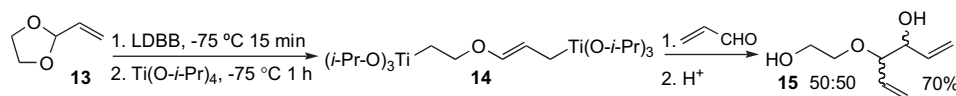
Scheme 4.

This caught our attention for two cogent reasons. First, a previous publication from our laboratory had reported the reductive lithiation of an analogous acrolein acetal **13** at $-75\text{ }^\circ\text{C}$ using the PRA method to deliver a far higher yield of trapped product **15** (Scheme 5).¹² Second, the anions of allyl ethers such as **12** are known to undergo the Wittig rearrangement, the probable cause of the reported³² instability of **12**, at temperatures as low as $-25\text{ }^\circ\text{C}$,³⁶ thus making it imperative to work at a lower temperature; a comparison of Schemes 4 and 5 made it appear that this would be possible only by using the PAR method, as discussed above.

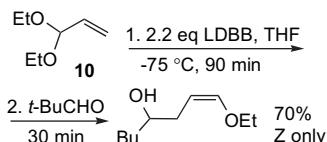
Thus, the substrate **10** was subjected to the PAR conditions. It was found (Scheme 6) that the reductive cleavage occurred smoothly at $-50\text{ }^\circ\text{C}$ to provide the anion **12**, which was trapped with the same aldehyde to provide a 70% yield of **11** with higher stereoselectivity than that reported using the CA method under the required Barbier conditions and higher temperature.³⁷ Attempts to cleave **10** with Li powder in the absence of DBB failed, indicating as expected that the aromatic hydrocarbon indeed acts as a catalyst in this reductive lithiation. This case is an excellent demonstration that in cases in which the carbanion being produced by reductive lithiation is unstable, the use of preformed aromatic radical-anion is preferable to the catalytic method even with a large excess of lithium powder (compare Schemes 4 and 6). It seems likely that a more recent reductive lithiation of a related acetal of acrolein³⁸ using the CA method could have also benefited by the use of a stoichiometric quantity of preformed LDBB.

2.3. Reductive lithiation of 6-chloro-6-methyl-1-heptene

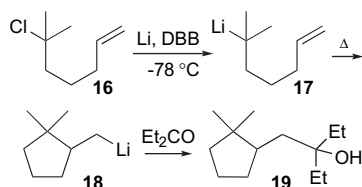
In 2002, a report appeared that the reductive lithiation of 6-chloro-6-methyl-1-heptene **16** using the CA method at $-78\text{ }^\circ\text{C}$ gave an anion that cyclized at higher temperatures but that the cyclization product could be trapped by 2-pentanone only under very special conditions, namely Barbier mode at $0\text{ }^\circ\text{C}$ (76% yield) or in a two-step process at $-30\text{ }^\circ\text{C}$ (75% yield).³⁹ The anion **17** was reported to be unstable at $-78\text{ }^\circ\text{C}$ (Scheme 7).



Scheme 5.

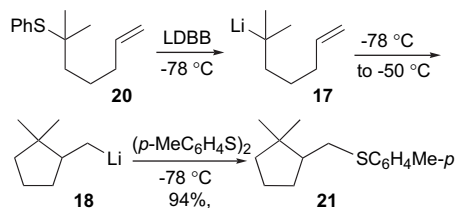


Scheme 6.



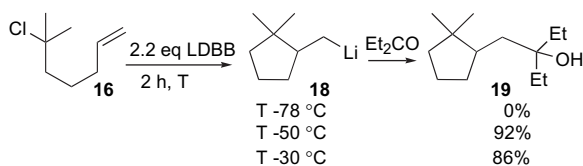
Scheme 7.

This report surprised us since we had performed a reductive lithiation of the phenylthio analogue **20** of **16** at $-78\text{ }^\circ\text{C}$ and found that the reductive lithiation and cyclization, after warming **17** to $-50\text{ }^\circ\text{C}$, occurred smoothly under the usual PAR conditions to provide a 94% yield of trapped product **21**⁴⁰ (Scheme 8).



Scheme 8.

In order to make a direct comparison with the published CA method, the tertiary alkyl chloride **16** was treated with LDBB at three temperatures and the cyclized organolithium **18** was treated with 3-pentanone to provide the alcohol **19**. From the results in Scheme 9, it is clear that the reductive lithiation product **17** of **16** does not cyclize rapidly at $-78\text{ }^\circ\text{C}$ but that it cyclizes smoothly at $-50\text{ }^\circ\text{C}$ to give an excellent yield of trapped product. In order to test the possibility that higher temperatures would cause destruction of the intermediate organolithiums, the experiment was repeated at $-30\text{ }^\circ\text{C}$ and the yield was found to drop slightly, indicating that lower temperatures are preferred for reductive lithiations. These are generally better attainable by the PAR mode as discussed



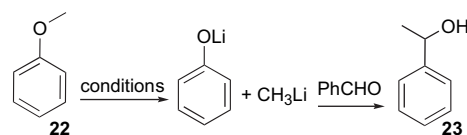
Scheme 9.

above. Once again, the importance of the presence of DBB was tested by performing the reductive lithiation at $-30\text{ }^\circ\text{C}$ without DBB and the yield merely fell to 53%, thus indicating that in this particular case, the catalyst is not absolutely essential.

Unfortunately, this apparent comparison of the CA and PAR methods became somewhat less meaningful when a more recent paper⁴¹ by the Spanish group revealed that the structure **16** in their preliminary communication,³⁹ was in error and that the real compound used was 6-chloro-6-ethyl-1-octene (terminal ethyl groups rather than methyls). Nevertheless, the results in Scheme 9 do indicate that tertiary organolithiums can be readily generated by reductive lithiation of the chloride using the PAR method, just as had occurred with the corresponding phenyl thioether at very low temperatures and that this carbanion cyclizes at $-50\text{ }^\circ\text{C}$ to give an excellent yield of cyclized organolithium. It is also clear (Scheme 8) that the tertiary carbanion is not unstable at $-78\text{ }^\circ\text{C}$ as the corresponding tertiary carbanion from CA reductive lithiation of 6-chloro-6-ethyl-1-octene is reported to be.^{39,41} It seems likely that the latter carbanion does not necessarily remove a proton from the THF at that temperature as suggested, but that the hindered carbanion abstracts an α -proton from the trapping agent, 3-pentanone, instead; the alternative reaction of the carbanion with the carbonyl group would yield a very highly congested di-tertiary C–C bond.

2.4. Reductive cleavage of anisole

A report of the reductive cleavage of anisole **22** at the alkyl C–O bond at room temperature using CA conditions (14-molecular equiv of Li and 0.05 equiv of DBB) yielded 80% of **23**, the product of capture of the methyl lithium by benzaldehyde (Scheme 10).⁴² This paper indicated that the PAR conditions were somewhat inferior but the conditions of the comparison were somewhat nebulous, particularly because room temperature was apparently used and we have found that LDBB is unstable above $0\text{ }^\circ\text{C}$.⁴³



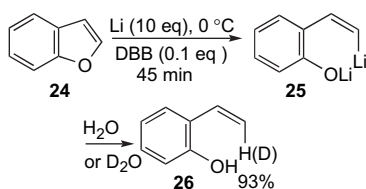
Scheme 10.

We therefore, undertook a comparison of the two methods at $0\text{ }^\circ\text{C}$ for 2 h. The results were striking. The CA method (same conditions as above but at $0\text{ }^\circ\text{C}$) yielded 30% of **23** while the PAR method provided 87% of **23**. Using 14 equiv of Li but no DBB gave no product. Thus, the reaction is clearly faster using preformed stoichiometric LDBB than using the catalytic method even with the use of a large excess

of the metal. This is consistent with our preconceived notions as indicated in Section 1.

2.5. Reductive cleavage of 2,3-benzofuran

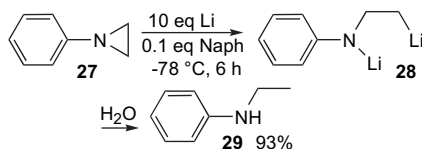
The reductive lithiation of 2,3-benzofuran **24** with an excess of lithium in the presence of DBB was reported to give the result shown in Scheme 11.⁴⁴ Other electrophiles were also used. It occurred to us that the LUMO of **24** may be lower in energy than that of DBB and that the electron transfer might occur directly from the metal to **24**, thus obviating the requirement for the purported catalyst, DBB. Indeed, when the reported conditions were duplicated, but in the absence of DBB, a 91% yield of **26** was generated. It is thus doubtful that DBB serves as a catalyst when the CA method is attempted.



Scheme 11.

2.6. Reductive cleavage of *N*-phenylaziridine

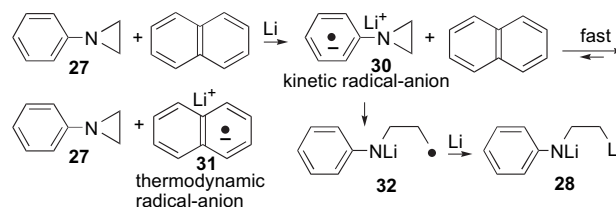
In some of the papers in which the claim is made that the catalytic method is more powerful than the stoichiometric method, there is a reference to a report of the reductive cleavage of *N*-phenylaziridine by the CA method as shown in Scheme 12.⁴⁵ Other electrophiles were used as well. There is a statement in that paper that aziridines do not undergo reductive opening by lithioarenes at low temperature. Since the type of aziridine and the reaction conditions were not included in the paper, we decided to directly compare the CA and PAR methods as applied to the reductive cleavage of *N*-phenylaziridine **27**. To our initial surprise, lithium naphthalenide (LN) did not cause the cleavage of **27** at the temperature and in the time reported in Scheme 12; only the starting material was recovered. A repetition of the literature procedure (Scheme 12)⁴⁵ did indeed produce the reported result. This result appeared to support the claim that the CA method is more powerful than the PAR method. However, for the reasons stated in Section 1, it seemed highly unlikely that the method using naphthalene as a catalyst could lead to a faster reductive cleavage than the use of preformed lithium naphthalenide.



Scheme 12.

A possible alternative explanation for these experimental results is illustrated in Scheme 13. The transfer of an electron from the surface of the lithium occurs more rapidly to the *N*-phenylaziridine **27** than to the naphthalene but in the pres-

ence of the latter, the resulting radical-anion **30** can rapidly transfer an electron to the naphthalene to generate the more thermodynamically stable naphthalenide radical-anion **31**. In other words, the radical-anion **30** is the kinetic product of electron transfer from the lithium but the naphthalenide ion **31** is the thermodynamic radical-anion as indicated by the inequality of the arrows leading from **30** and naphthalene to **27** and **31**. Since **30** is the immediate precursor of the ring-opened product **32**, its concentration is directly proportional to the rate of ring cleavage. The higher the concentration of naphthalene, the lower is the rate of ring cleavage. By behaving as a sink for electrons, naphthalene reduces the concentration of **30**, and thus inhibits the reductive ring opening. If this reasoning is correct, the aziridine should open at -78 °C even in the absence of the naphthalene 'catalyst.' In fact, naphthalene in this specific case should behave as an inhibitor rather than a catalyst.



Scheme 13.

This hypothesis was tested first by attempting the cleavage of **27** with lithium in the absence of naphthalene. The result was quantitative ring opening within the 6 h test period at -78 °C (entry 2, Table 1). Thus, as predicted, naphthalene is not required and, in fact, the yield in its absence was somewhat higher than the 90% in the presence of 0.1 equiv of naphthalene (entry 3). In order to test the prediction that naphthalene is an inhibitor, reductive cleavages were performed with the usual 5-fold excess (10 equiv) of lithium with 1.0 equiv and 10 equiv of naphthalene. As seen in entries 2–5, the larger the quantity of naphthalene the lower the yield. Thus, naphthalene is indeed an inhibitor. The inability of LN to reductively cleave *N*-phenylaziridine is understandable on the basis of the unfavorable position of the equilibrium in which an electron is transferred from the naphthalenide ion **31** to **27** (Scheme 13).

The reason that *N*-phenylaziridine accepts an electron more rapidly from lithium than naphthalene does is not known but this finding is consistent with our experience that 1-(*N,N*-dimethylamino)naphthalene forms a lithium radical-anion at -45 °C somewhat faster⁴⁶ than naphthalene does² at room temperature. One can speculate that the amino group complexes with a lithium cation on the surface of the metal

Table 1. Reductive cleavage of *N*-phenylaziridine^a

Entry	Reagents	Yield%
1	2.2 equiv LN	0
2	10 equiv Li	100
3	10 equiv Li, 0.1 equiv Np	90
4	10 equiv Li, 1.0 equiv Np	76
5	10 equiv Li, 10.1 equiv Np	16

^a All reactions were performed at -78 °C for 6 h in THF.

thus increasing the electrophilicity of the ring while at the same time increasing the electron donating power of the metal surface, leading to a more rapid transfer of an electron to the pi system of the aromatic. Further studies of this phenomenon and its practical applications are now underway in this laboratory.

3. Conclusions

Yus and his group have made an important contribution to the practice of reductive lithiation using lithium radical-anions as a method of cleavage of bonds between carbon and various heteroatoms to produce organolithiums by developing the version, abbreviated in this paper as the CA method, in which a large excess of finely divided lithium is used in the presence of a catalytic amount of naphthalene or 4,4'-di-*tert*-butylbiphenyl. In extensive publications, they have demonstrated the wide generality of this procedure that can significantly ease the problem of separating the aromatic byproduct of the reductive lithiation from the cleavage product. Another advantage that has to our knowledge only been used once¹⁷ in a different version in which a stoichiometric amount of lithium is used along with a catalytic amount of aromatic in order to maintain a low concentration of the aromatic dianion, when this species can do damage; this is discussed in Section 1.

In the present work, we have demonstrated a major disadvantage of the CA method that should be weighed against its advantages in deciding whether to use that method or the PAR method, involving a stoichiometric quantity of preformed aromatic radical-anion, for performing reductive lithiations. The disadvantage of the CA method is that at any given temperature, the catalytic method is slower than that using a stoichiometric amount of preformed aromatic radical-anion. This is illustrated in all of the cases compared above but most vividly by the large decrease in yield in the reductive cleavage of anisole in going from the PAR to the CA method in experiments with the same limited duration. In some cases this lower rate may not be a highly significant disadvantage, particularly when the organolithium being produced is stable under the reaction conditions and some of the reductive lithiations that the Yus group have performed proceed in good yields. However, in cases in which the organolithium is not entirely stable to the reaction conditions, significant decreases in yield are observed in going from the PAR to the CA method. Examples are the reductive lithiation of acrolein acetals to produce allylic α -lithioethers that are capable of undergoing the Wittig rearrangement and of tertiary alkyl chlorides that can undergo elimination in the presence of the tertiary organolithium products.

Furthermore, some compounds previously believed to undergo catalytic reductive lithiation, such as 2,3-benzofuran **24**, pick up an electron and cleave as fast in the absence as in the presence of the aromatic catalyst. This is not surprising as the radical-anion derived from this substrate has extensive delocalization, probably greater than that in the LDBB that would be the intermediate radical-anion if the catalytic process was indeed occurring.

A far more surprising and significant result is that the reductive cleavage of *N*-phenylaziridine **27** not only does not

require naphthalene as a catalyst but the naphthalene is actually an inhibitor of the reductive lithiation. Apparently, this substrate forms a radical-anion **30** by reaction with lithium more rapidly than naphthalene does but the radical-anion **31** from naphthalene is more thermodynamically stable than that of **30** from *N*-phenylaziridine. Thus, the aromatic compound can behave as a catalyst, an unnecessary additive or an inhibitor, depending on the specific substrate.

Finally, one other disadvantage of the CA method should be mentioned. Lithium metal is the most expensive ingredient used in reductive lithiations since the aromatic compound can easily be recovered and recycled. The large excess of lithium used could become an economic liability as well as something of a safety hazard, especially in an industrial setting. The expense is especially onerous considering that the cost of lithium powder from Aldrich is almost six times the cost of the ribbon that we ordinarily use to make preformed radical-anion.

4. Experimental

4.1. General

All reactions were performed under an argon atmosphere in oven-dried (110 °C) flasks and standard precautions against moisture were taken. A dry ice/acetone bath was used to obtain a temperature of –78 °C. An ice bath was used to obtain 0 °C. Silica gel 60 (40–60 μ m, Sorbent Technologies) was used for flash column chromatography. Thin-layer chromatography was performed on glass supported 250- μ m silica GF plates (Analtech). Visualization of TLC plates was accomplished with one or more of the following: 254 nm UV light, aqueous KMnO₄ (1%) with NaOH (0.1%) and K₂CO₃ (6%). Commercial solvents and reagents were used as received with the following exceptions. Tetrahydrofuran (THF) and diethyl ether were distilled over sodium benzophenone ketyl. Most reagents were commercially available from Sigma-Aldrich or Acros. Lithium dispersion was commercially available from Alfa, 30% in paraffin. ¹H and ¹³C NMR spectra were recorded on Bruker DPX-300 spectrometer operating at 300 MHz for ¹H and 75 MHz for ¹³C at 22 °C unless otherwise noted. Chemical shift data are reported in units of δ (ppm) using CHCl₃ as the internal standard: δ =7.27 for ¹H NMR spectra and δ =77.09 for ¹³C NMR spectra unless indicated otherwise. Multiplicities are given as s (singlet), d (doublet), t (triplet), q (quartet), m (multiplet), and br (broad). Coupling constants, *J*, are reported in Hertz.

4.1.1. Reductive lithiation of 1-phenylthio-2-methylcyclohex-1-ene (**8**).

4.1.1.1. Reductive lithiation of 1-phenylthio-2-methylcyclohex-1-ene (8**) with preformed LDBB.** To a solution of LDBB⁴⁷ (5.25 mL of a 0.40 M solution in THF, 2.1 mmol) at –78 °C, 1-phenylthio-2-methylcyclohex-1-ene (**8**, 0.204 g, 1.00 mmol) in THF (2 mL) was slowly added via syringe pump over a 0.50 h period. The deep blue-green reaction mixture was stirred at –78 °C for 8 h during which time the color slowly changed to red. Cyclohexanecarboxaldehyde (0.133 mL, 0.123 g, 1.10 mmol) (or 1-iodohexane or allyl bromide) in THF (2 mL) was added dropwise until the mixture turned yellow. The reaction was quenched at –78 °C with brine and was allowed to warm to room

temperature. The reaction mixture was extracted with ether (3×20 mL) and the combined extract was washed with 10% NaOH (3×10 mL, or at least until all of the thiophenol was removed) and brine. The organic layer was dried over MgSO₄ and the solvent was removed by rotary evaporation. Radial chromatography (4 mm rotor) with hexane was used to recover DBB from the reaction mixture, followed by 20% ethyl acetate in hexane to give the desired product.

9a: E⁺=cyclohexanecarboxaldehyde, 80%, ¹H NMR (CDCl₃) δ 4.23 (d, *J*=9.2 Hz, 1H), 2.07–2.17 (m, 2H), 1.97 (m, 1H), 1.70–1.87 (m, 2H), 0.75–1.64 (m, 18H). ¹³C NMR (CDCl₃) δ 130.9, 130.0, 75.4, 41.1, 32.4, 30.3, 29.0, 26.6, 26.2, 26.0, 23.1, 22.8, 19.2. MS *m/e* exact mass calculated for C₁₄H₂₄O 208.1827, found 208.1827. IR (thin film) 3378 (s), 2924 (s), 2851 (s), 1449 (s), 1273 (m), 1261 (m), 1076 (m), 999 (m) cm⁻¹.

9b: E⁺=iodohexane, 71%, ¹H NMR (CDCl₃) δ 1.96–2.03 (m, 6H), 1.64 (s, 3H), 1.60–1.62 (m, 4H), 1.31–1.32 (m, 8H), 0.93 (t, *J*=6.4 Hz, 3H). ¹³C NMR (CDCl₃) δ 130.4, 125.7, 33.6, 32.0, 29.7, 29.6, 28.4, 23.7, 23.5, 22.8, 19.1, 14.2. MS *m/e* exact mass calculated for C₁₃H₂₄ 180.1878, found 180.1876. IR (thin film) 2924 (s), 1459 (s), 1354 (s), 1141(w) cm⁻¹.

9c: E⁺=allyl bromide, 71%, ¹H NMR (CDCl₃) δ 5.69–5.82 (m, 1H), 4.93–5.02 (m, 2H), 2.73 (d, *J*=6.28 Hz, 2H), 1.81–1.93 (m, 4H), 1.61 (s, 3H), 1.54–1.59 (m, 4H). MS exact mass calculated for C₁₀H₁₆ 136.1252, found 136.1252. IR (thin film) 3078 (w), 2926 (s), 1638 (m), 1438 (m), 992 (m), 909 (m) cm⁻¹.

4.1.1.2. Reductive lithiation of (8) with lithium in the presence of a deficiency of DBB. To a mixture of DBB (100 mg, 0.40 mmol) and lithium powder (21 mg, 2.4 mmol) in 2 mL of THF at –78 °C, 1-phenylthio-2-methylcyclohex-1-ene (**1**, 0.204 g, 1.00 mmol) in THF (2 mL) were slowly added via syringe pump over a 2 h period. The reaction mixture was stirred for an additional 6 h. Cyclohexanecarboxaldehyde (0.133 mL, 0.123 g, 1.10 mmol) (or iodohexane or allyl bromide) in THF (2 mL) was added dropwise and worked-up as described in the procedure above.

9a: 54%; **9b:** 50%; **9c:** 52%.

4.1.2. Reductive lithiation of acrolein diethyl acetal (**10**).

4.1.2.1. Reductive lithiation of 10 with preformed LDBB. To a stirred solution of LDBB (4.00 mmol) under argon at –78 °C, acrolein diethyl acetal (**10**, 0.31 mL, 2.1 mmol) was added dropwise over a period of 5 min. Since no new spot except starting material was observed on TLC for the reaction at –78 °C, the reaction mixture was allowed to warm to –50 °C, where it was stirred for 90 min. Pivalaldehyde (180 mg, 0.23 mL, 2.1 mmol) was then added dropwise to the reaction flask and the mixture was allowed to stir at –50 °C for an additional 30 min. Ice-water (10 mL) was added to quench the reaction. The resulting mixture was extracted with ether (3×20 mL), and the combined extract was dried over anhydrous MgSO₄, filtered, and concentrated by solvent removal by rotary evaporation. Column chromatography, with 10% ethyl acetate in hexanes, afforded the pure product Z-1-ethoxy-5,5-dimethylhex-1-ene-4-ol **11**

(0.27 g, 70%). ¹H NMR (CDCl₃): δ 6.20 (dt, *J*=6.0, 1.5 Hz, 1H), 4.55 (ddd, *J*=6.9, 6.3, 6.0 Hz, 1H), 3.90 (q, *J*=7.0 Hz, 2H), 3.31 (1H, m), 2.28 (2H, m), 2.02 (1H, br s), 1.34 (t, *J*=7.0 Hz, 3H), 1.0 (9H, s). ¹³C NMR (CDCl₃) δ 146.5, 103.4, 78.9, 67.3, 34.4, 26.3, 25.2, 14.9. These spectral data are consistent with those reported in the literature.³²

4.1.2.2. Reductive lithiation of 10 with lithium in the absence of DBB. Li (dispersion, 460 mg, 20.0 mmol) was washed with three 10.0 mL portions of hexane in a 100 mL three-necked flask under argon. THF (10.0 mL) and acrolein dimethyl acetal (**10**, 260 mg, 2.00 mmol) were added under argon at 0 °C. After being stirred for 90 min at that temperature, the mixture was cooled to –78 °C and pivalaldehyde (180 mg, 0.23 mL, 2.10 mmol) was added dropwise to the reaction flask and the mixture was allowed to stir at –50 °C for an additional 30 min. Ice-water (20.0 mL) was slowly added to quench the reaction. The resulting mixture was extracted with ether (3×20 mL) and the organic layer was dried over anhydrous MgSO₄ and concentrated by solvent removal. The residue was starting material acrolein diethyl acetal by crude NMR analysis.

4.1.3. Reductive lithiation of 6-chloro-6-methyl-1-heptene⁴⁸ (**16**).

4.1.3.1. Reductive lithiation of 16 with preformed LDBB. To a stirred solution of LDBB (4.0 mmol) under argon at –78 °C, 6-chloro-6-methyl-1-heptene (**16**, 0.27 g, 1.9 mmol) was added dropwise over a period of 5 min. The reaction mixture was allowed to warm to –50 °C, where it was stirred for 120 min. 3-Pentanone (180 mg, 2.1 mmol) was added dropwise to the reaction flask and the mixture was allowed to stir at –50 °C for an additional 30 min. Sodium bicarbonate was added to quench the reaction and the reaction vessel was allowed to warm to room temperature. The resulting mixture was extracted with ether (3×20 mL), and the combined extract was dried over anhydrous MgSO₄, filtered, and concentrated by solvent removal using rotary evaporation. Column chromatography, with 5% ethyl acetate in hexanes as eluent, afforded pure 3-(2,2-dimethylcyclopentylmethyl)-pentan-3-ol **19** (0.34 g, 92%). ¹H NMR (CDCl₃) δ 2.0 (m, 1H), 1.30 (m, 12H), 0.96 (s, 3H), 0.85 (2t, *J*=7.2 Hz, 6H), 0.71 (s, 3H); ¹³C NMR (CDCl₃) δ 74.87, 44.20, 41.59, 41.03, 38.64, 31.95, 31.59, 30.87, 27.36, 21.34, 20.92, 8.03, 7.63. This compound was reported by Yus,⁴¹ but no spectral data were provided.

Under the same conditions but at –30 °C, 0.32 g (86%) of **19** was obtained.

4.1.3.2. Reductive lithiation of 16 with lithium in the absence of DBB. Li (dispersion, 460 mg, 20.0 mmol) was washed with three 10.0 mL portions of hexane in a 100 mL three-necked flask under argon. THF (10.0 mL) and 6-chloro-6-methyl-1-heptene (**16**, 293 mg, 2.00 mmol) were added under argon at –30 °C. After 2 h stirring at the same temperature, the mixture was cooled to –78 °C and 3-pentanone (180 mg, 2.10 mmol) was added dropwise to the reaction flask and the mixture was allowed to stir at –78 °C for an additional 30 min. Ice-water (20 mL) was added slowly to quench the reaction and the reaction mixture was allowed to warm to room temperature. The resulting mixture was extracted with ether (3×20 mL) and the organic layer was

dried over anhydrous MgSO_4 , filtered, and concentrated. The residue was purified by column chromatography (5% ethyl acetate in hexanes) to afford **19** (0.21 g, 53%).

4.1.4. Reductive lithiation of anisole (**22**).

4.1.4.1. Reductive lithiation of **22 with preformed LDBB.** A solution of freshly prepared LDBB (4.40 mmol) in 10.0 mL of THF was cooled to 0 °C prior to the slow addition of anisole (**22**, 216 mg, 2.00 mmol) under argon over a period of 5 min. The reaction mixture was stirred at the same temperature for 2 h and was then cooled to –40 °C and the reaction was quenched by dropwise addition of benzaldehyde (223 mg, 2.10 mmol). After the reaction mixture had been further stirred for 30 min at –40 °C, the temperature was allowed to rise to room temperature over a period of ca. 3 h and ice-water (20 mL) was added slowly. The resulting mixture was extracted with ether (3×20 mL), and the organic layer was dried over anhydrous MgSO_4 and concentrated by solvent removal. The residue was purified by column chromatography (10% ethyl acetate in hexanes), affording 1-phenylethanol **23** (212 mg, 87%). ^1H NMR (CDCl_3) δ 7.30 (m, 5H), 4.5 (q, $J=6.5$ Hz, 1H), δ 2.10 (s, 1H), 1.47 (d, $J=6.5$ Hz, 3H); ^{13}C NMR (CDCl_3) δ 145.75, 128.44, 127.41, 125.34, 70.33, 25.09. These NMR data compared well with those in Ref. 42.

4.1.4.2. Reductive lithiation of **22 with lithium in the presence of DBB.** Li (dispersion, 644 mg, 28.0 mmol) was washed with three 10 mL portions of hexane in a 100 mL three-necked flask under argon. THF (10.0 mL), DBB (53.2 mg, 0.20 mmol), and anisole (**22**, 216 mg, 2.00 mmol) were added under argon at 0 °C. The reaction mixture was stirred at that temperature for 2 h before it was cooled to –40 °C and quenched by dropwise addition of benzaldehyde (223 mg, 2.10 mmol). After the reaction mixture had been further stirred for 30 min at –40 °C, the temperature was allowed to rise to room temperature over a period of ca. 3 h and ice-water (20 mL) was added slowly. The resulting mixture was extracted with ether (3×20 mL), and the organic layer was dried over anhydrous MgSO_4 and concentrated by solvent removal. The residue was purified by column chromatography (10% ethyl acetate in hexanes), affording 1-phenylethanol **23** (73.0 mg, 30%).

4.1.4.3. Reductive lithiation of **22 with lithium in the absence of DBB.** Under otherwise identical conditions but with no DBB, no 1-phenylethanol **23** was obtained.

4.1.5. Reductive lithiation of 2,3-benzofuran (**24**).

4.1.5.1. Reductive lithiation of **24 with lithium dispersion.** Li (dispersion, 460 mg, 20.0 mmol) was washed with three 10.0 mL portions of hexane in a 100 mL three-necked flask under argon. THF (10.0 mL) and 2,3-benzofuran (**24**, 236 mg, 0.22 mL, 2.00 mmol) were added under argon at 0 °C. After being stirred for 45 min at that temperature, the reaction mixture was cooled to –30 °C and ice-water (20 mL) was added slowly to the resulting mixture. After 15 min, the reaction mixture was neutralized with 1.0 M hydrochloric acid (5 mL). The resulting mixture was extracted with ether (3×20.0 mL), and the organic layer was dried over anhydrous MgSO_4 and concentrated by solvent removal. The residue was purified by column chromatography (10% ethyl acetate in hexanes), affording 2-vinylphenol **26** (218 mg,

91%). ^1H NMR (CDCl_3) δ 7.38 (dd, $J=7.7$, 1.7 Hz, 1H), 7.14 (td, $J=7.7$, 1.1 Hz, 1H), 6.92 (m, 2H), 6.78 (dd, $J=7.7$, 1.1 Hz, 1H), 5.74 (dd, $J=17.7$, 1.4 Hz, 1H), 5.36 (dd, $J=13.2$, 1.4 Hz, 1H), 5.01 (s, 1H); ^{13}C NMR (CDCl_3) δ 152.58, 131.31, 128.84, 127.21, 124.79, 120.94, 115.81. These NMR data compared well with those in Ref. 44.

When the above reaction was quenched with D_2O (0.5 mL), after the same workup procedure, 220 mg of deuterated **26** was obtained; yield 92% (30% cis- and 70% trans-isomer), ^1H NMR (CDCl_3) δ 7.40 (dd, $J=7.7$, 1.7 Hz, 1H), 7.16 (td, $J=7.7$, 1.1 Hz, 1H), 6.97 (m, 2H), 6.79 (dd, $J=7.7$, 1.1 Hz, 1H), 5.75–5.69 (d, $J=17.7$ Hz, 0.7H), 5.35–5.51 (d, $J=11.2$ Hz, 0.3H), 5.019 (s, 1H); ^{13}C NMR (CDCl_3) δ 152.78, 131.40, 128.86, 127.35, 124.84, 120.93, 115.85, 115.52, 115.20.

4.1.6. Reductive lithiation of *N*-phenylaziridine^{49,50} (**27**).

4.1.6.1. General procedure for reductive lithiation of *N*-phenylaziridine (27**) by the PAR method.** A solution of freshly prepared lithium naphthalenide (4.40 mmol) in 10 mL of THF was cooled to –78 °C prior to the slow addition of *N*-phenylaziridine (**27**, 238 mg, 2.00 mmol) under argon. The reaction mixture was stirred at that temperature for 6 h and the reaction was quenched by slow addition of ice-water (20 mL). The resulting mixture was extracted with ether (5×20 mL) and the organic layer was dried over anhydrous Na_2SO_4 and concentrated by solvent removal. The residue was purified by column chromatography (5% ethyl acetate in hexanes), affording only starting material **27** and no **29**.

4.1.6.2. General procedure for reductive lithiation of *N*-phenylaziridine (27**) by the CA method.** Li (dispersion, 460 mg, 20.0 mmol) was washed with four 10 mL portions of hexane in a 100 mL three-necked flask under argon. THF (10 mL) was added and the reaction mixture was cooled to –78 °C. *N*-Phenylaziridine (**27**, 238 mg, 2.00 mmol) and naphthalene (0.05 equiv) were added under argon at the same temperature. After the mixture had been stirred for another 6 h at –78 °C, the reaction was quenched by adding ice-water (20 mL) slowly. The resulting mixture was extracted with ether (5×20 mL) and the organic layer was dried over anhydrous Na_2SO_4 and concentrated by solvent removal. The residue was purified by column chromatography (5% ethyl acetate in hexanes), affording *N*-ethylani-line **29**.

N-Ethylaniline **29**: ^1H NMR (CDCl_3) δ 7.36 (m, 2H), 6.88 (m, 1H), 6.79 (m, 2H), 3.37 (s, 1H), 3.11 (q, $J=7.1$ Hz, 2H), 1.21 (t, $J=7.1$ Hz, 3H); ^{13}C NMR (CDCl_3) δ 148.38, 129.15, 117.12, 112.66, 38.37, 14.82. The spectral data are consistent with those reported by Aldrich.

Acknowledgements

This material is based upon work supported by the National Science Foundation under Grant No. 0102289 and the Camille and Henry Dreyfus Foundation under Senior Scientist Mentor Award SI-01-007. We are grateful to Dr. Fu-Tyan Lin for help in NMR spectroscopy and Dr. Kasi Somayajula for help with the mass spectra.

References and notes

1. Taken in part from the Ph.D. thesis of Mary Dosch Doubleday, University of Pittsburgh, 1991.
2. (a) Screttas, C. G.; Micha-Screttas, M. *J. Org. Chem.* **1978**, *43*, 1064–1071; (b) Screttas, C. G.; Micha-Screttas, M. *J. Org. Chem.* **1979**, *44*, 713–719.
3. (a) Cohen, T.; Daniewski, W. M.; Weisenfeld, R. B. *Tetrahedron Lett.* **1978**, 4665–4668; (b) Cohen, T.; Weisenfeld, R. B. *J. Org. Chem.* **1979**, *44*, 3601–3603.
4. Reviews: (a) Cohen, T.; Bhupathy, M. *Acc. Chem. Res.* **1989**, *22*, 152–161; (b) Cohen, T. *Heteroatom Chemistry*; Block, E., Ed.; VCH: New York, NY, 1990; Chapter 7, pp 129–142.
5. (a) Recent uses of reductive lithiation of phenyl thioethers: Screttas, C. G.; Heropoulos, G. A.; Micha-Screttas, M.; Steele, B. R. *Tetrahedron Lett.* **2005**, *46*, 4357–4360; (b) Tang, T.; Ruan, Y. P.; Ye, J. L.; Huang, P. Q. *Synlett* **2005**, 231–234; (c) de Vicente, J.; Betzemeier, B.; Rychnovsky, S. D. *Org. Lett.* **2005**, *7*, 1853–1856; (d) Wang, L.; Floreancig, P. E. *Org. Lett.* **2004**, *6*, 569–572; (e) Cooksey, J.; Gunn, A.; Kocienski, P. J.; Kuhl, A.; Uppal, S.; Christopher, J. A.; Bell, R. *Org. Biomol. Chem.* **2004**, *2*, 1719–1731; (f) Streiff, S.; Ribeiro, N.; Desaubry, L. *J. Org. Chem.* **2004**, *69*, 7592–7598.
6. (a) Sargent, G. D.; Browne, M. W. *J. Am. Chem. Soc.* **1967**, *89*, 2788–2790; (b) Screttas, C. G. *J. Chem. Soc., Chem. Commun.* **1972**, 752–753; (c) Wilson, S. E. *Tetrahedron Lett.* **1975**, 4651–4654; (d) Caine, D.; Frobese, A. S. *Tetrahedron Lett.* **1978**, 883–886; (e) Barluenga, J.; Flórez, J.; Yus, M. *J. Chem. Soc., Perkin Trans. 1* **1983**, 3019–3026; (f) Beau, J.-M.; Prandi, J. *Tetrahedron Lett.* **1989**, *30*, 4517–4520; (g) Ramón, D. J.; Yus, M. *Tetrahedron Lett.* **1990**, *31*, 3763–3766; (h) Rawson, D. J.; Meyers, A. I. *Tetrahedron Lett.* **1991**, *32*, 2095–2098; (i) Wittman, V.; Kessler, H. *Angew. Chem., Int. Ed. Engl.* **1993**, *32*, 1091–1093; (j) Oku, A.; Ose, Y.; Kamada, T.; Yoshida, T. *Chem. Lett.* **1993**, 573–576; (k) Vlaar, C. P.; Klumpp, G. W. *Angew. Chem., Int. Ed. Engl.* **1993**, *32*, 574–576; (l) Barluenga, J.; Montserrat, J. M.; Flórez, J. *J. Org. Chem.* **1993**, *58*, 5976–5980; (m) Kondo, Y.; Murata, N.; Sakamoto, T. *Heterocycles* **1994**, *37*, 1467–1468; (n) Lesimple, P.; Beau, J.-M. *Bioorg. Med. Chem.* **1994**, *2*, 1319–1330; (o) Tamao, K.; Kawachi, A. *Organometallics* **1995**, *14*, 3108–3111; (p) Yanagisawa, A.; Ogasawara, K.; Yasue, K.; Yamamoto, H. *J. Chem. Soc., Chem. Commun.* **1996**, 367–368; (q) Ley, S. V.; Mio, S. *Synlett* **1996**, 789–790; (r) Grieco, P. A.; Dai, Y. *J. Am. Chem. Soc.* **1998**, *120*, 5128–5129; (s) Schultz, D. A.; Boal, A. K.; Farmer, G. T. *J. Org. Chem.* **1998**, *63*, 9462–9469.
7. (a) Beau, J.-M.; Sinay, P. *Tetrahedron Lett.* **1985**, *26*, 6185–6188, 6189–6192, 6193–6196; (b) Yu, J.; Cho, H.-S.; Falck, J. R. *J. Org. Chem.* **1993**, *58*, 5892–5894; (c) Yu, J.; Cho, H.-S.; Chandrasekhar, S.; Falck, J. R. *Tetrahedron Lett.* **1994**, *35*, 5437–5440; (d) Norcross, R. D.; von Matt, P.; Kolb, H. C.; Bellus, D. *Tetrahedron* **1997**, *53*, 10289–10312.
8. (a) Guijarro, D.; Mancheno, B.; Yus, M. *Tetrahedron Lett.* **1992**, *33*, 5597–5600; (b) Guijarro, D.; Guillena, G.; Mancheno, B.; Yus, M. *Tetrahedron* **1994**, *50*, 3427–3436.
9. (a) Guijarro, D.; Yus, M. *Tetrahedron* **1994**, *50*, 3447–3452; (b) Ribeiro, C. M. R.; Demelo, S. J.; Bonin, M.; Quirion, J. C.; Husson, H. P. *Tetrahedron Lett.* **1994**, *35*, 7227–7230; (c) Wolckenhauer, S. A.; Rychnovsky, S. D. *Tetrahedron* **2005**, *61*, 3371–3381 and citations therein; (d) Zeller, E.; Sajus, H.; Grierson, D. S. *Synlett* **1991**, 44–46; (e) Buckmelter, A. J.; Powers, J. P.; Rychnovsky, S. D. *J. Am. Chem. Soc.* **1998**, *120*, 5589–5590.
10. (a) Agawa, T.; Ohshiro, Y. *Synthesis* **1980**, 933–935; (b) Hoffmann, R.; Bruckner, R. *Chem. Ber.* **1992**, *125*, 1957–1963; (c) Krief, A.; Hobe, M.; Badaoui, E.; Bousbaa, J.; Dumont, W.; Nazih, A. *Synlett* **1993**, 707–709; (d) Krief, A.; Nazih, A.; Hobe, M. *Tetrahedron Lett.* **1995**, *36*, 8111–8114; (e) Krief, A.; Nazih, A. *Tetrahedron Lett.* **1995**, *36*, 8115–8118.
11. (a) Eisch, J. J.; Jacobs, A. M. *J. Org. Chem.* **1963**, *28*, 2145–2146; (b) Lansbury, P. T.; Caridi, F. J. *J. Chem. Soc., Chem. Commun.* **1970**, 714–715; (c) Ireland, R. E.; Smith, M. G. *J. Am. Chem. Soc.* **1988**, *110*, 854–860; (d) Saá, J. M.; Ballesster, P.; Deyá, P. M.; Capó, M.; Garcías, X. *J. Org. Chem.* **1996**, *61*, 1035–1046; (e) Azzena, U.; Demartis, S.; Melloni, G. *J. Org. Chem.* **1996**, 4913–4919; (f) Azzena, U.; Demartis, S.; Pilo, L.; Piras, E. *Tetrahedron* **2000**, *56*, 8375–8382.
12. Mudryk, B.; Cohen, T. *J. Am. Chem. Soc.* **1991**, *113*, 1866–1867.
13. Block, E.; Guo, C.; Thiruvazhi, M.; Toscano, P. J. *J. Am. Chem. Soc.* **1994**, *116*, 9403–9404.
14. Azzena, U.; Melloni, G.; Pisano, L.; Sechi, B. *Tetrahedron Lett.* **1994**, *35*, 6759–6762.
15. The superior versatility of compounds containing the phenylthio group as substrates for reductive lithiation arises from their almost unique ease of construction, particularly by methods involving C–C bond formation but also by the ability of the phenylthio group to enter a molecule as a nucleophile, electrophile, or radical. In addition, the substrates are almost always able to withstand the powerful nucleophiles/bases that are present in the reductive lithiation conditions. For example, alkyl halides, sulfates, sulfonates, etc. are subject to ready nucleophilic substitution, but most seriously to base induced elimination, thus limiting their use largely to the preparation of primary alkyl-lithiums unless an aryl or vinyl group is present to increase the rate of the reductive lithiation and favor it over competing processes.
16. Kulkarni, V.; Cohen, T. *Tetrahedron* **1997**, *53*, 12089–12100.
17. Cohen, T.; Matz, J. R. *Synth. Commun.* **1980**, *10*, 311–317.
18. Cohen, T.; Kreethadumrongdat, T.; Liu, X.; Kulkarni, V. *J. Am. Chem. Soc.* **2001**, *123*, 3478–3483.
19. Various aryl-substituted *N,N*-dimethylanilines also decompose to aryllithiums but at far higher temperatures. (a) Azzena, U.; Dessanti, F.; Melloni, G.; Pisano, L. *Tetrahedron Lett.* **1999**, *40*, 8291–8293; (b) Azzena, U.; Cattari, M.; Melloni, G.; Pisano, L. *Synthesis* **2003**, 2811–2814; See also Azzena, U.; Dessanti, F.; Melloni, G.; Pisano, L. *Arkivoc* **2002**, Part V, 181–188.
20. Another possible indication that homolytic cleavage of the aryl N–C bond was not occurring is the absence of cleavage of the methyl C–N bond, both in the case of LDMAN and of the reductive cleavage reactions of aryl-substituted *N,N*-dimethylanilines.¹⁹ Such a cleavage mode would produce a more stable methyl radical as well as a more stable conjugated amide anion. However, the mechanism of such cleavages is influenced by other factors as well such as the rate of transfer of the electron from the π^* to the two possible σ^* C–N orbitals: Maercker, A. *Angew. Chem., Int. Ed. Engl.* **1987**, *26*, 972–989.
21. (a) Levin, G.; Szwarc, M. *J. Am. Chem. Soc.* **1976**, *98*, 4211–4216; (b) Levin, G.; Holloway, B. E.; Szwarc, M. *J. Am. Chem. Soc.* **1976**, *98*, 5706–5609.
22. Freeman, P. K.; Hutchinson, L. L. *J. Org. Chem.* **1980**, *45*, 1924–1930.
23. Mudryk, B.; Cohen, T. *J. Org. Chem.* **1989**, *54*, 5657–5659.

24. Schakel, M.; Vrieling, J. J.; Klumpp, G. W. *Tetrahedron Lett.* **1987**, 28, 5747–5750.
25. Yus, M.; Ramón, D. J. *J. Chem. Soc., Chem. Commun.* **1991**, 398–400.
26. Reviews: (a) Yus, M. *Chem. Soc. Rev.* **1996**, 155–161; (b) Ramón, D. J.; Yus, M. *Eur. J. Org. Chem.* **2000**, 225–237; (c) Yus, M. *The Chemistry of Organolithium Compounds*; Rappoport, Z., Marek, I., Eds.; Wiley: Chichester, UK, 2004; Chapter 11.
27. Some more recent papers: (a) Alonso, F.; Dacunha, B.; Melendez, J.; Yus, M. *Tetrahedron* **2005**, 61, 3437–3450; (b) Gómez, C.; Maciá, B.; Yus, M. *Arkivoc* **2005**, 10–20; (c) Yus, M.; Gomis, J. *Tetrahedron* **2003**, 59, 4967–4971.
28. Yus, M.; Ortiz, R.; Huerta, F. F. *Tetrahedron* **2003**, 59, 8525–8542.
29. (a) Foubelo, F.; Yus, M. *Tetrahedron Lett.* **2000**, 41, 5047–5051; (b) Gómez, C.; Ruiz, S.; Yus, M. *Tetrahedron* **1999**, 55, 7017–7026.
30. (a) Yus, M.; Herrera, R. P.; Guijarro, A. *Tetrahedron Lett.* **2001**, 42, 3455–3458; (b) Yus, M.; Herrera, R. P.; Guijarro, A. *Chem.—Eur. J.* **2002**, 8, 2574–2584.
31. Foubelo, F.; Moreno, B.; Soler, T.; Yus, M. *Tetrahedron* **2005**, 61, 9082–9096.
32. Gil, J. F.; Ramon, D. J.; Yus, M. *Tetrahedron* **1994**, 50, 3437–3446.
33. Huerta, F. F.; Gómez, C.; Yus, M. *Tetrahedron* **1996**, 52, 8333–8340.
34. At least one other group has mentioned this assertion in explanation of their use of the CA method: Manteca, I.; Etxarri, B.; Ardeo, A.; Arrasate, S.; Osante, I.; Sotomayor, N.; Lete, E. *Tetrahedron* **1998**, 54, 12361–12378.
35. Blomberg, C. *The Barbier Reaction and Related One-step Processes*; Springer: New York, NY, 1993.
36. (a) Dimmel, D. R.; Huang, S. *J. Org. Chem.* **1973**, 38, 2756–2757; (b) Schlosser, M.; Strunk, S. *Tetrahedron* **1989**, 45, 2649–2664.
37. It is known that alkyllithiums such as **12** tend to exist at equilibrium in the cis configuration. Evans, D. A.; Andrews, G. C.; Buckwalter, B. *J. Am. Chem. Soc.* **1974**, 96, 5560–5561.
38. Shin, J.; Gerasimov, O.; Thompson, D. H. *J. Org. Chem.* **2002**, 67, 6503–6508.
39. Yus, M.; Ortiz, R.; Huerta, F. F. *Tetrahedron Lett.* **2002**, 43, 2957–2960.
40. Deng, K.; Bensari, A.; Cohen, T. *J. Am. Chem. Soc.* **2002**, 124, 12106–12107. This paper had not been published at the time when the Yus report³⁹ appeared but the work had been completed.
41. Yus, M.; Ortiz, R.; Huerta, F. F. *Tetrahedron* **2003**, 59, 8525–8542.
42. Bachki, A.; Foubelo, F.; Yus, M. *Tetrahedron Lett.* **1998**, 39, 7759–7762.
43. Strohmman, C.; Schildbach, D. *The Chemistry of Organolithium Compounds*; Rappoport, Z., Marek, I., Eds.; Wiley: New York, NY, 2004; Chapter 15.
44. Yus, M.; Foubelo, F. *Eur. J. Org. Chem.* **2001**, 2809–2813.
45. Almena, J.; Foubelo, F.; Yus, M. *J. Org. Chem.* **1994**, 59, 3210–3215.
46. Cohen, T.; Sherbine, J. P.; Hutchins, R. R.; Lin, M. T. *Organomet. Synth.* **1986**, 3, 361–368.
47. Cohen, T.; Doubleday, M. D. *J. Org. Chem.* **1990**, 55, 4784–4786; Mudryk, B.; Cohen, T. *Org. Synth.* **1995**, 72, 173–179.
48. Vogel, A. I. *Vogel's Textbook of Practical Organic Chemistry*, 5th ed.; Wiley: New York, NY, 1989; p 556.
49. Bird, R.; Knipe, A. C.; Stirling, C. J. M. *J. Chem. Soc., Perkin Trans. 2* **1973**, 1215–1220.
50. Heine, H. W.; Kapur, B. L.; Mitch, C. S. *J. Am. Chem. Soc.* **1954**, 76, 1173.

Anodic cyclization reactions: probing the chemistry of *N,O*-ketene acetal derived radical cations

Yung-tzung Huang and Kevin D. Moeller*

Department of Chemistry, Washington University in St. Louis, St. Louis, MO 63130, USA

Received 27 June 2005; accepted 21 September 2005

Available online 4 May 2006

Abstract—The chemical reactivity of radical cations derived from *N,O*-ketene acetals has been examined and compared with the reactivity of radical cations derived from both ketene dithioacetals and enol ethers. Synthetically, the *N,O*-ketene acetal radical cations lead to more efficient cyclization reactions than either the ketene dithioacetal or enol ether derived radical cations. Cyclic voltammetry experiments using allylsilane trapping groups show that the efficiency of these cyclizations is not due to the *N,O*-ketene acetal radical cations being more reactive but rather more stable to decomposition. Finally, cyclizations using chiral oxizolidinones were examined.

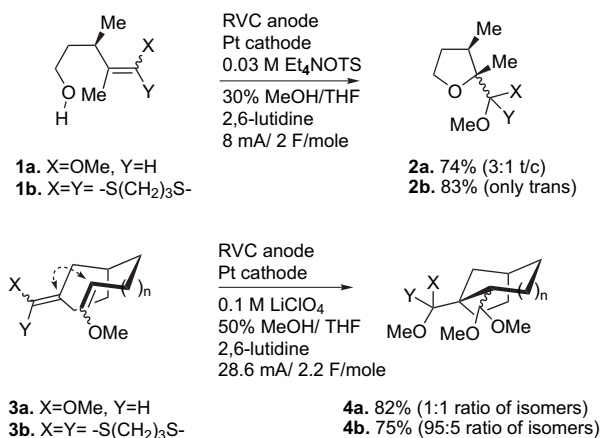
© 2006 Elsevier Ltd. All rights reserved.

1. Introduction

Intramolecular anodic olefin coupling reactions using ketene dithioacetal initiating groups often afford high levels of stereoselectivity.^{1–4} Consider the reactions illustrated in Scheme 1. In both examples, the reaction originating from oxidation of the ketene dithioacetal was far more selective than the analogous reaction originating from oxidation of the enol ether. While the stereochemistry of reactions originating from enol ether oxidation can often be rationalized by kinetic considerations,⁵ the same cannot be said for reactions originating

from ketene dithioacetal oxidation. For example, the difference in stereoselectivity obtained for the oxidation of **3a** and **3b** is most consistent with the oxidation of **3b** leading to a reaction controlled by thermodynamics. This hints that the enol ether and ketene dithioacetal reactions might be governed by different mechanistic concerns suggests that while the reactions look very similar, the radical cation intermediates might be quite different.

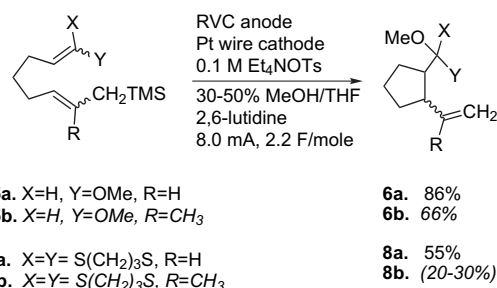
It did not take long to identify other significant differences between enol ether and ketene dithioacetal derived cyclizations. Enol ethers undergo efficient oxidative cyclizations with less reactive allylsilane trapping groups while ketene dithioacetals do not (Scheme 2).⁶ This is especially true for cyclizations utilizing trisubstituted allylsilane trapping groups. The oxidation of **7b** led to a product that was so messy that the cyclic product (**8b**) could not be isolated in pure form. These observations led to a working model for the cyclizations that treated the radical cation derived from oxidation of a ketene dithioacetal as being less reactive than the radical cation derived from oxidation of an enol ether.



Scheme 1.

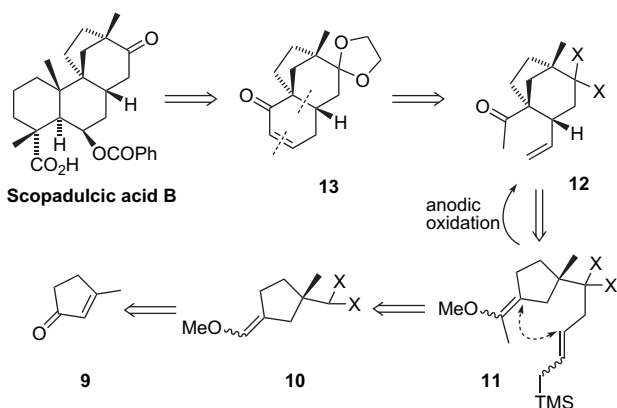
Keywords: Anodic electrochemistry; Oxidative cyclizations; Radical cations; Ketene acetals.

* Corresponding author. Tel.: +1 314 935 4270; fax: +1 314 935 4481; e-mail: moeller@wustl.edu



Scheme 2.

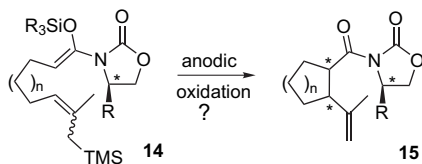
The suggestion that the reactivity of a radical cation can be altered by varying the substituents bound to it is very intriguing. If a change from a methoxy substituent to two thioether groups caused the radical cation to be less reactive, then possibly other changes would lead to a more reactive radical cation. Such a discovery would be extremely useful. Consider the retrosynthetic analysis of scopadulcic acid B illustrated in Scheme 3.⁷ The key step in this proposed synthesis would involve an anodic cyclization of **11** to form the bridged bicyclic intermediate **12**. A hydroboration/oxidation sequence would then convert the olefin to an aldehyde for use in an intramolecular aldol condensation. The strength of the route is that the oxidative cyclization reaction would lead to a product having all of the carbons needed for completing the third ring. However, the proposal is badly flawed in that oxidative cyclization reactions using less reactive allylsilane trapping groups are normally not compatible with the simultaneous formation of six-membered rings and quaternary centers.^{6b,8} But is this always the case? Are there more reactive radical cations that would allow for this transformation? With these questions in mind, we began to expand our exploration of oxidative cyclization reactions by diversifying the nature of the radical cation intermediate.



Scheme 3.

2. *N,O*-Ketene acetal substrates—an initial look

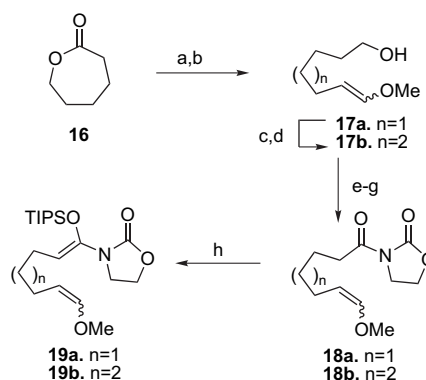
The first question that needed to be addressed was whether the lower efficiency of the dithioetene acetal derived cyclizations with allylsilane trapping groups was representative of all ketene acetal groups or specifically a result of the dithiane moiety. For this reason, we decided to build an oxazolidone based ketene acetal substrate (Scheme 4). Oxazolidinone ketene acetals were selected for this effort because they are stable and can be isolated by chromatography. This enabled the use of clean substrates for the electrolysis reactions. In addition, oxazolidinone ketene acetals possessing a stereogenic atom have been utilized in



Scheme 4.

asymmetric alkylation and aldol reactions. Their availability suggested the possibility of studying asymmetric oxidative cyclization reactions (Scheme 4).

Initially, the very reactive enol ether trapping group was selected for the cyclizations.⁹ This was done in order to probe the compatibility of the *N,O*-ketene acetal groups with the anodic oxidations using substrates that had the best possible chance for cyclization. The substrates were synthesized as outlined in Scheme 5. Both five- and six-membered ring precursors were made by nearly identical routes. The only difference was that the six-membered ring precursor required a one carbon chain extension. The yields in the scheme for steps e–h are given for the synthesis of the five-membered ring substrate. Yields for the six-membered ring substrate are included in Section 7.



Scheme 5. Reagents: (a) Dibal-H, THF/CH₂Cl₂ (1:1), –78 °C–0 °C, 15 min; (b) Ph₃PCH₂OMeCl, *s*-BuLi, THF, –78 °C–rt, 12 h, 90% (two steps); (c) 4 N HCl/acetone (1:1), 0 °C–rt, 1 h; (d) Ph₃PCH₂OMeCl, *s*-BuLi, THF, –78 °C–rt, 3 h, 70% (two steps); (e) PDC, DMF, 0 °C–rt, 12 h, 44%; (f) Et₃N, Pivaloyl chloride, THF, –20 °C, 2 h; (g) LiCl, 2-Oxazolidinone, –20 °C–rt, 6 h, 62% (two steps) and (h) i. LDA, THF, –78 °C, 1 h, ii. TIPSOTf, –78 °C–rt, 5 h, 87%.

The electrolyses of **19a** and **19b** were conducted in an undivided cell using constant current conditions (8 mA/2.2 F/mol), a reticulated vitreous carbon (RVC) anode and cathode, 2,6-lutidine as a proton scavenger, and a 0.1 M tetraethylammonium tosylate electrolyte solution.¹⁰ The solvent for the reaction was either methanol or a mixture of methanol and THF as indicated in Table 1. The overall process was neutral since acid is generated at the anode and base (from the reduction of methanol) is generated at the cathode. Hence the added proton scavenger played no

Table 1

Substrate	Solvent	Product	Yield (%)	Isomer ratio
19a	MeOH	20a	74	2:1
19a	4:1 MeOH/THF	20a	87	3:2
19b	MeOH	20b	63 ^a	1:2
19b	4:1 MeOH/THF	20b	65	1:2

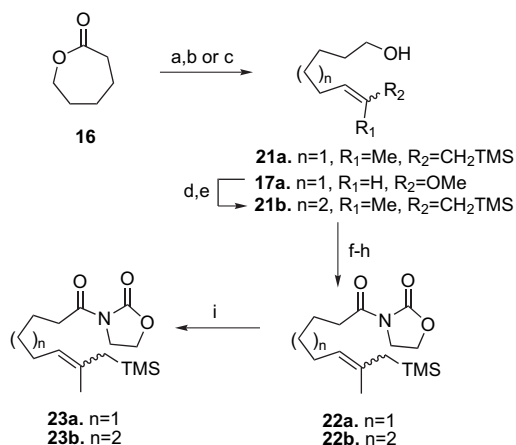
^a 7% recovered starting material.

net role in the reaction. However, due to the acid sensitivity of ketene acetal, the presence of 2,6-lutidine was important for maintaining the neutrality of the reaction in the region immediately surrounding the anode. Using these conditions, both reactions led to good yields of cyclized product. For the oxidation of **19a**, a 74% isolated yield of **20a** was obtained when methanol was used as solvent. The reaction benefited from the use of THF as a cosolvent. An 87% isolated yield of cyclized product was obtained with the addition of 20% THF as a cosolvent. Like previous enol ether–enol ether coupling reactions,⁹ the cyclization did not lead to the formation of products in stereoselective fashion. In this case, the ratio of stereoisomers of the newly formed C–C bond ranged from 2:1 to 3:2. The major isomer was not assigned since the isomers could not be separated and the NMR signals for the methine protons overlap.

The oxidation of **19b** in methanol solvent led to a 63% isolated yield of **20b** in a 1:2 ratio of cis/trans isomers. With the use of the THF cosolvent, a 65% unoptimized yield of product was obtained having the same 1:2 ratio of cis/trans isomers. The poor diastereoselectivity obtained for the cyclization of **20b** was consistent with the stereochemical outcome of earlier anodic cyclizations using enol ether derived radical cations and enol ether trapping groups.⁹

3. *N,O*-Ketene acetal radical cations and allylsilane trapping groups

With the oxidations of **19a** and **19b** leading to good yields of cyclic product, it was time to determine if a radical cation derived from an *N,O*-ketene acetal would be reactive enough to cyclize with a less efficient allylsilane trapping group. To this end, cyclization substrates **23a** and **23b** were synthesized as outlined in Scheme 6. These syntheses paralleled the syntheses of **19a** and **19b**. The ylide used for generating the trisubstituted allylsilane was prepared in situ from ethyltriphenylphosphonium bromide according to the known literature procedure.¹¹ As in the earlier synthesis of **19b**, the



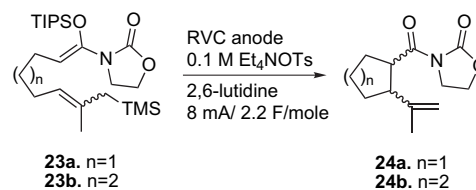
Scheme 6. Reagents: (a) Dibal-H, THF/CH₂Cl₂ (1:1), –78 °C–0 °C, 15 min; (b) Ph₃PC(CH₃)CH₂TMS, *s*-BuLi, THF, –78 °C–rt, 65% (two steps); (c) Ph₃PCH₂OMeCl, *s*-BuLi, THF, –78 °C–rt, 12 h, 90% (two steps); (d) 4 N HCl/acetone (1:1), 0 °C–rt, 1 h; (e) Ph₃PC(CH₃)CH₂TMS, *s*-BuLi, THF, –78 °C–rt, 12 h, 58% (two steps); (f) PDC, DMF, 0 °C–rt, 12 h, 49%; (g) Et₃N, Pivaloyl chloride, THF, –20 °C, 2 h; (h) LiCl, 2-Oxazolidinone, –20 °C–rt, 6 h, 91% (two steps) and (i) i. LDA, THF, –78 °C, 1 h, ii. TIPSOTf, –78 °C–rt, 5 h, 83%.

six-membered ring substrate was made by doing a one carbon chain extension of the aldehyde generated from Dibal-H reduction of the ϵ -caprolactone. The yields given in Scheme 6 for steps f–i are for the five-membered ring substrate. Yields for the six-membered ring case are again given in the Section 7.

Once synthesized, the allylsilane substrates were electrolyzed using the same conditions described above (Table 2). From the start, it was obvious that cyclization reactions originating from the oxidation of *N,O*-ketene acetals proceed far better than do cyclizations originating from the oxidation of a ketene dithioacetal. Electrolysis of **23a** in 4:1 MeOH/THF led to a 70% isolated yield of cyclized product **24a**. The use of dichloromethane as the cosolvent led to a 74% yield of cyclized product along with 7% recovered starting material. Surprisingly, cyclized product was formed even in the absence of a cosolvent. This was a surprise because enol ether–allylsilane coupling reactions require a cosolvent.^{6a} Without it, they predominately form products derived from methanol trapping of the radical cation prior to cyclization. The fact that the *N,O*-ketene acetal reactions do not require a cosolvent suggests that *N,O*-ketene acetal derived radical cations undergo the cyclizations more efficiently than not only ketene dithioacetal radical cations but also the more reactive enol ether radical cations. While it was not clear that the differences observed were really due to changes in radical cation reactivity (*vide infra*), it was clear that the conclusions made with respect to ketene dithioacetal radical cations cannot be universally applied to all ketene acetal substrates.

While the oxidation of **23a** led nicely to cyclized products, it was not stereoselective. In each case, a 3:2 ratio of cis and trans-products was obtained. This ratio was consistent with the mixtures observed for enol ether–allylsilane coupling reactions leading to five-membered rings (substrates **5a** and **5b** in Scheme 2).^{6a} In both cases, one would expect a reaction controlled by thermodynamics to place the groups on the ring trans to each other. Hence, the formation of a stereochemical mixture was most consistent with the reactions being controlled by kinetics and the result of five-membered ring transition states not having well defined

Table 2



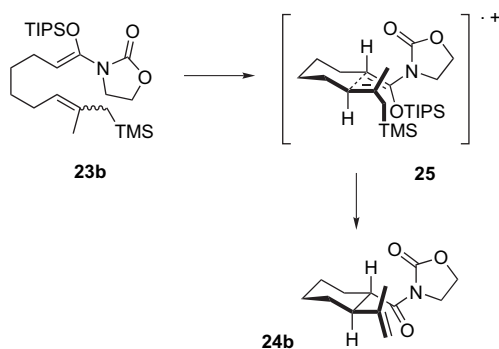
Substrate	Solvent	Product	Yield (%)	Isomer ratio
23a	MeOH	24a	51	3:2
23a	4:1 MeOH/THF	24a	70	3:2
23a	1:4 MeOH/CH ₂ Cl ₂	24a	74 ^a	3:2
23b	MeOH	24b	54	trans
23b	4:1 MeOH/THF	24b	71	trans
23b	1:4 MeOH/CH ₂ Cl ₂	24b	54 ^b	trans
23c ^c	4:1 MeOH/THF	24b	60	trans

^a 7% recovered starting material.

^b 10 F/mol.

^c TBS enol ether.

pseudoaxial and pseudoaxial positions. The oxidation of **23b** supported the suggestion that cyclizations originating from the radical cation of an *N,O*-ketene acetal was under kinetic control. Cyclizations leading to six-membered rings have well defined pseudoaxial and pseudoaxial positions in their transition states. Since both allylsilane⁵ and ketene acetal^{4a} groups are known to prefer pseudoaxial positions in anodic cyclizations, a kinetically controlled reaction resulting from the oxidation of **23b** was expected to afford predominately trans-product (Scheme 7). This was the case. Electrolysis of **23b** using 4:1 MeOH/THF as solvent led to a 71% isolated yield of the trans six-membered ring product (Table 2). Only a small amount (<5%) of a second cyclized product (assumed to be the cis-isomer) was observed in the ¹H NMR spectrum of the crude reaction material. The stereochemistry of the major product was assigned using the coupling patterns observed in the ¹H NMR spectrum for the ring methine protons. Both protons show the triplet of doublets pattern consistent with the protons being axial and trans to each other.



Scheme 7.

The oxidation of **23b** using dichloromethane as the cosolvent led to a much less efficient cyclization (10 F/mol of charge was needed to obtain 54% of the cyclized product). However, the cyclization still proceeded without the use of a cosolvent in spite of the slower six-membered ring formation. With methanol as solvent, the oxidation led to a 57% isolated yield of the trans-product.

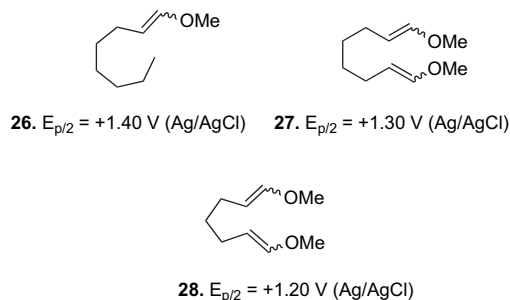
Finally, the compatibility of the anodic oxidation with the less stable TBS enol ether was examined. The oxidation of **23c** in 4:1 MeOH/THF (all other conditions the same) led to a 60% isolated yield of the trans material. In this reaction, a significant amount of imide byproduct from methanolysis of the ketene acetal was observed.

At this point it was clear that radical cations derived from the *N,O*-ketene acetals lead to more efficient cyclizations than either radical cations derived from enol ethers or radical cations derived from ketene dithioacetals. Our working model suggested that this results from the *N,O*-ketene acetals being more reactive than their ketene dithioacetal and enol ether counterparts. But was this really true?

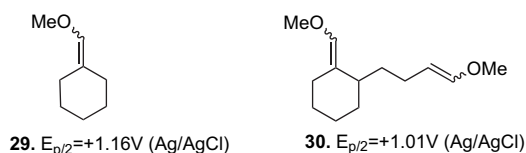
4. Cyclic voltammetry—measuring relative rates

A number of years ago,⁹ we observed that the potential measured by cyclic voltammetry for a bis enol ether substrate

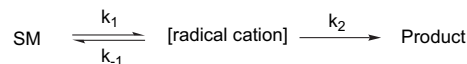
was dependent upon the length of the tether connecting the olefins. Substrates expected to give rise to faster cyclizations afforded lower potentials.¹² For example, a bis methoxyenol ether substrate leading to six-membered ring formation (**27**) had an oxidation potential 100 mV lower than that of a mono methoxyenol ether (**26**) whereas an analogous bis methoxyenol ether substrate leading to five-membered ring formation (**28**) had an oxidation potential 200 mV lower than that of a mono methoxyenol ether (Scheme 8). A five-membered ring precursor (**30**) showed a drop in potential of about 150 mV relative to its corresponding mono enol ether (**29**) even when the reaction required the formation of a quaternary carbon (Scheme 9). These observations are consistent with an oxidation reaction that is followed by a cyclization fast enough to influence the concentration of the radical cation at the electrode surface (Scheme 9). In this scenario, the oxidation reaction (k_1) leads to a radical cation that undergoes either the transfer of an electron back to the electrode (k_{-1}) or cyclization (k_2). If one assumes a steady state concentration of the radical cation, then solving for this concentration and plugging the resulting expression into the Nernst equation affords an equation relating the observed potential to the rate of cyclization. Since E^0 in this equation is positive and everything following the minus sign is positive, a faster cyclization will lead to a lower value for E_{obs} . Hence, the value measured for E_{obs} provides a method for measuring the relative rates of various cyclizations.



Scheme 8.



A shift in potential?



Using steady state kinetics,...

$$[\text{radical cation}] = \frac{k_1[\text{SM}]}{(k_{-1} + k_2)}$$

...and then the Nernst equation

$$E_{obs} = E^0 - RT/nF \ln \frac{[\text{SM}]}{[\text{radical cation}]} = E^0 - RT/nF \ln \frac{(k_{-1} + k_2)}{k_1}$$

Scheme 9.

An alternative explanation for the drop in potentials that invokes an associative electron transfer where oxidation and

cyclization occur in a concerted fashion can be viewed as a limiting example of this general scheme. In this case, the more the overlap between the olefins during the electron-transfer step, the lower is the oxidation potential observed. Of course, the extent of overlap between the olefins during the electron-transfer step is directly related to the rate of cyclization. Therefore, the value of E_{obs} would again provide a method for measuring the relative rates of various cyclizations.

With this in mind, we undertook a CV study of the ketene acetal based substrates in order to determine the relative reactivity of the radical cation intermediates towards allylsilane trapping groups. In order to establish a baseline for these studies, the shifts in potential associated with the coupling of an enol ether to an allylsilane trapping group were examined (Table 3). The parent enol ether **31** was measured to have a potential ($E_{\text{p}/2}$) of +1.44 V versus Ag/AgCl¹³ using a Pt anode, a sweep rate of 25 mV/s, and a 0.1 M LiClO₄ in acetonitrile electrolyte solution. A substrate concentration of 0.025 M was used. All of the potentials listed in Table 3 were obtained using identical conditions. For the six-membered ring enol ether/allylsilane precursor (**32b**), a drop in potential of 100 mV relative to the parent enol ether **31** was observed. For the five-membered ring precursor (**32a**) an additional 80 mV drop in potential (a 180 mV drop for the substrate relative to the parent enol ether **31**) was observed. The smaller drop in potential for the six-membered ring precursor **32b** confirmed that the cyclization derived from this substrate proceeds more slowly than the cyclization originating from the five-membered ring precursor **32a**.

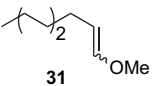
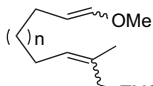
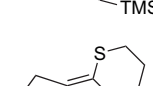
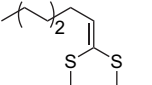
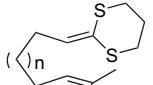

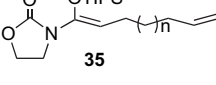
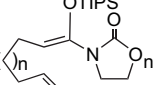
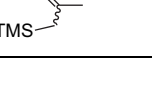
Next, attention was turned towards the cyclizations originating from oxidation of a ketene dithioacetal. In this case, the potential measured for the six-membered ring cyclization substrate (**34b**) was only 30 mV lower than the potential measured for the parent ketene dithioacetal **33**. The five-membered ring substrate (**34a**) had a potential only 50 mV lower than the parent ketene dithioacetal **33**. Clearly, these cyclizations were slower than the cyclizations resulting

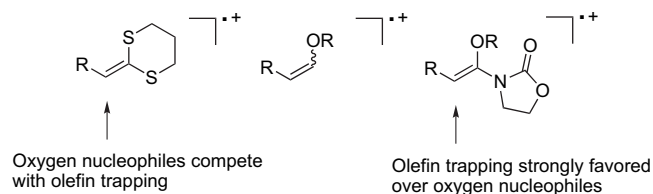
from oxidation of enol ethers **32a** and **32b**, an observation that was consistent with our working model for the reactions. Following these measurements, attention was turned to the *N,O*-ketene acetal derived cyclizations. Surprisingly, the drop in potential measured for substrates **23a** and **23b** was not significantly different than the drop in potential measured for the ketene dithioacetal substrates **34a** and **34b**. For **23b**, a 40 mV drop in potential was measured relative to **35**, while for **23a** an 80 mV drop in potential relative to **35** was observed. In neither case was the drop in potential close to what was observed for the enol ether derived radical cations. This result indicated that the most efficient (*N,O*-ketene acetal) and least efficient (ketene dithioacetal) cyclization reactions from a yield perspective proceeded roughly at the same rate, whereas, the cyclization with an intermediate efficiency (enol ether) proceeded much faster than either of the others. Clearly, our working model for the cyclizations was not correct. The yield of the electrolyses did not depend solely on the rate of the cyclization reaction.

So what does control the yield of an anodic olefin coupling reaction? Typically, when the reactions give a low yield of the desired cyclic product they form products that are derived from either trapping of the initially formed radical cation with solvent, proton elimination from the uncyclized radical cation, or polymerization. Hence, the yield of cyclic product obtained depends on a partitioning between intramolecular trapping of the initially formed radical cation versus solvent trapping, elimination, and polymerization. If higher yielding cyclizations are not faster with respect to the intramolecular reaction, then the radical cation intermediates involved must be more stable with respect to the decomposition reactions. In other words, switching from the ketene dithioacetal to the *N,O*-ketene acetal did not lead to a more reactive radical cation, but rather a more stable one.

It is tempting to speculate that the differences in cyclization efficiency observed for the reactions above result from the ability of the substituents on the radical cation to stabilize a cation (Scheme 10). It is known that enol ether radical cations react with allyl- and vinylsilanes in a ‘radical-like’ fashion meaning that the reaction leads to a radical at the terminating end of the cyclization.¹⁴ At the same time, two of the three decomposition pathways (methanol trapping and elimination) are clearly ‘cation-like’ processes and the third leads to a polymethoxylated polymer that may also be ‘cation-like’ in origin. Do substituents on the radical cation that stabilize a cation reduce the rate of decomposition and afford more time for the ‘radical-type’ cyclization that leads to the desired product? Efforts are underway to begin addressing this question with more electron-rich ketene acetal derivatives.

Table 3

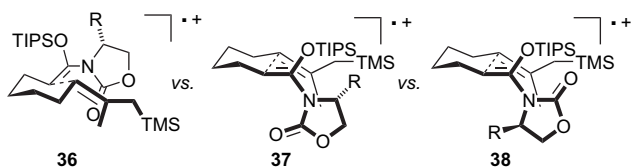
Ag/AgCl reference electrode Pt anode, 25 mV/s 0.1 M LiClO ₄ in CH ₃ CN 0.025 M [substrate]	Potential V ($E_{\text{p}/2}$)	Potential V ($E_{\text{p}/2}$)
	+1.44	
		32a n=1 +1.26
		32b n=2 +1.34
	+1.15	
		34a n=1 +1.10
		34b n=2 +1.12
	+1.15	
		23a n=1 +1.07
		23b n=2 +1.11



Scheme 10.

5. Chiral auxiliaries

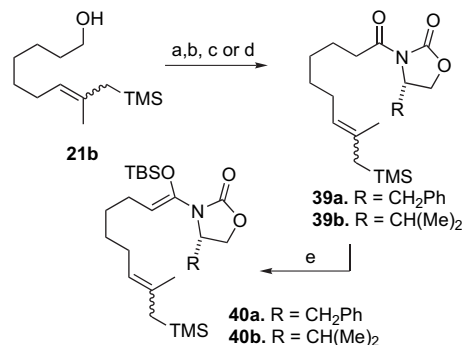
The degree of stereoselectivity obtained for the cyclization originating from **23b** provided an excellent opportunity to probe the potential for asymmetric anodic olefin coupling reactions. Two key, contradictory literature precedents formed the backdrop for this effort. First, Evans and co-workers demonstrated that chiral oxazolidinones are very useful auxiliaries for inducing asymmetry into both aldol and alkylation reactions using silyl based *N,O*-ketene acetal derivatives directly analogous to substrates **23a** and **23b**.^{15,16} In these reactions, the chiral auxiliaries adopt a conformation that minimizes the dipole of the substrate in the transition state leading to product. Second, Sibi and co-workers have shown that chiral oxazolidinone groups are not useful auxiliaries for inducing asymmetry into radical reactions that originate from a radical on the carbon alpha to the imide carbonyl.^{17,18} In these cases, rotation around the bond connecting the nitrogen of the chiral oxazolidinone to the carbonyl of the substrate interferes with the auxiliaries ability to place the sterically bulky directing group on a single face of the substrate. For a radical cation initiated cyclization, the problem can be summarized using the transition state structures as illustrated in Scheme 11. Transition state **36** represents the preferred transition state (relative to **37**) if the radical cation cyclization behaves in a fashion analogous to the aldol and alkylation reactions studied by Evans. In this picture, the large allylsilane group would approach the face of the radical cation opposite to the sterically bulky substituent on the oxazolidinone. Transition states **36** and **38** represent the two preferred transition states if the radical cation cyclization behaves in a fashion analogous to the radical reactions studied by Sibi. In this case, rotation around the bond connecting the nitrogen of the oxazolidinone and C1 of the substrate leads to two conformations that place the bulky R group of the chiral oxazolidinone on opposite faces of the radical cation. Approach of the allylsilane moiety away from the R group would then lead to a mixture of diastereomers.



Scheme 11.

To test which of these two scenarios best describes the radical cation cyclizations, electrolysis substrates **40a** and **40b** were prepared (Scheme 12). The syntheses began with the formation of imides **39a** and **39b** in a fashion identical to that used in Scheme 7. However, formation of the ketene acetal moiety needed for the oxidation proved to be more challenging. With the extra steric bulk of the chiral auxiliary, efforts to synthesize the triisopropylsilyl ketene acetal were not successful. In each case, the starting imide was recovered without silylation. Fortunately, using the same reaction conditions, the less hindered *tert*-butyldimethylsilyl ketene acetal could be made in a 57% isolated yield (along with 39% of the recovered starting material) when the benzyl substituted oxazolidinone was used (**40a**) and an 88% isolated yield

when the isopropyl substituted oxazolidinone was used (**40b**). The TBS based ketene acetals were significantly less stable to the electrolysis conditions than ones possessing the TIPS group. However, they did allow us to assess the utility of the chiral auxiliaries for effecting asymmetric anodic olefin coupling reactions.

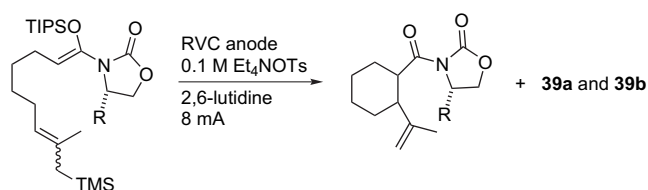


Scheme 12. Reagents: (a) PDC, DMF, 0 °C, 12 h, 65%; (b) Et₃N, Pivaloyl chloride, THF, –20 °C, 2 h; (c) LiCl, (4*S*,5*R*)-(–)-4-Methyl-5-phenyl-2-oxazolidinone, –20 °C–rt, 6 h, 94%; (d) LiCl, (5*S*)-(–)-4-Isopropyl-2-oxazolidinone, –20 °C–rt, 6 h, 85% and (e) i. LDA, THF, –78 °C, 30–90 min. ii. TBSOTf, –78 °C–rt, 6–8 h, 57% (with 39% **39a**) for **40a**, 88% for **40b**.

The oxidation of **40a** was conducted using the same constant current electrolysis conditions as described earlier (Table 4). Unfortunately, only poor yields of the cyclized product could be obtained. In the best case, a 20% yield of product **41a** was obtained. For this product, only the two *trans*-diastereomers were observed. These diastereomers were separated, characterized, and then their experimental ratio (2:1) determined by integration of the proton NMR spectrum taken for the crude reaction product. Efforts to optimize the yield for the reaction were halted when it became clear that the chiral auxiliary was not effective for inducing asymmetry into the oxidative cyclization.

The oxidation of **40a** suggested that the chiral auxiliary rotated and that the radical cation behaved in a fashion analogous to the radical chemistry of Sibi and co-workers rather

Table 4



40a. R = CH₂Ph
40b. R = CH(Me)₂

41a. R = CH₂Ph (*trans* product)
41b. R = CH(Me)₂ (*trans* product)

Substrate	Solvent	# (F/mol)	Recovered 40 (%)	41	39	Diast. ratio
40a	4:1 MeOH/THF	2.2	0	20	45	2:1
40a	MeOH	2.2	0	15	53	2:1
40a	1:4 MeOH/CH ₂ Cl ₂	2.2	37	6	10	2:1
40b	4:1 MeOH/THF	2.2	10	20	20	1:1.5
40b	4:1 MeOH/CH ₃ CN	2.2	27	20	13	2:1
40b	1:1 MeOH/CH ₃ CN	2.2	11	26	8	2:1
40b	1:4 MeOH/CH ₂ Cl ₂	2.2	26	25	8	1:1.5
40b	1:4 MeOH/CH ₂ Cl ₂	4.7	<8	42	6	1:1.5
40b	1:1 MeOH/CH ₂ Cl ₂	3.0	<5	40	7	2:1

than the alkylation chemistry of Evans and co-workers. But what if the poor selectivity obtained from **40a** was simply a result of the benzyl group being too small to be effective? The use of the larger isopropyl group in **40b** was studied in order to address this issue. If the poor diastereoselectivity obtained from the oxidation of **40a** was due to the benzyl group being too small, then the use of the larger isopropyl group in **40b** should improve the diastereoselectivity. However, if the poor diastereoselectivity obtained from the oxidation of **40a** was due to rotation of the chiral auxiliary, then the use of the larger inducing group would not help. The electrolyses of **40b** is summarized in Table 4. While alterations in the solvent used and amount of current employed helped to improve the yield of the cyclizations, the diastereoselectivity of the reaction remained poor in all cases.

In the end, neither the benzyl nor the isopropyl directing group induces a significant degree of asymmetry into the process, a result consistent with rotation of the chiral auxiliary and the radical cation cyclizations being analogous to the corresponding radical reactions.

6. Conclusions

Our work with *N,O*-ketene acetal derived radical cations has led to two major findings. First, the use of an *N,O*-ketene acetal initiating group for anodic olefin coupling reactions leads to more efficient carbon–carbon bond formation than the use of either an enol ether or a ketene dithioacetal initiating group. The higher yield of cyclic product in these reactions is not due to the cyclizations being faster but rather the radical cation intermediates being more stable to decomposition. Knowing that a change in the substituents on a radical cation can dramatically improve the yield of subsequent cyclization, current efforts are aimed at identifying ketene acetal groups that will allow for the simultaneous formation of both quaternary carbons and six-membered rings.¹⁹

Second, the experiment using chiral oxazolidinones demonstrated that the radical cation cyclizations are analogous to asymmetric radical reactions in that rotation of the chiral auxiliary precludes useful levels of induction. This observation will be critical for designing future asymmetric anodic olefin coupling reactions that would appear to require the use of either a Lewis acid to stop rotation of the auxiliary¹⁸ or a *C*₂-symmetric chiral auxiliary.

7. Experimental

7.1. 7-Methoxy-hept-6-en-1-ol (**17a**)

To a flame-dried 500-mL round-bottom flask under an argon atmosphere were added ϵ -caprolactone (5.597 g, 48.5 mmol) and 300 mL of anhydrous solvent (CH₂Cl₂/THF=1:1). The reaction was cooled to -78 °C and 1 M DIBAL solution in toluene (50 mL, 50 mmol) was added dropwise. The reaction was stirred at -78 °C for 15 min. The reaction was then allowed to warm to room temperature, quenched with 200 mL of ether and 60 mL of H₂O, and stirred until it became a translucent white gel. The solution was further diluted with 200 mL of ether, Celite 545 added, and then stirred until

the solution became clear. The resulting mixture was filtered and concentrated in vacuo. The crude product was diluted with 200 mL of ether and dried using anhydrous MgSO₄. It was then filtered and concentrated in vacuo the second time. The crude product was then taken up in 60 mL of anhydrous THF and used directly in the following steps. (The hemiacetal should not be left concentrated in order to avoid polymerization).

A flame-dried 500-mL round-bottom flask under an argon atmosphere was charged with a stirred suspension of (methoxymethyl)triphenylphosphonium chloride (34.985 g, 100 mmol) in 220 mL of anhydrous THF. The reaction was cooled to -78 °C, a 1.4 M *sec*-butyllithium solution in cyclohexane (110 mL, 154 mmol) was added dropwise, and the resulting dark brown mixture allowed to warm from -78 °C to room temperature over 3 h. When complete, the reaction was re-cooled to -78 °C and the crude hemiacetal synthesized above in 60 mL of anhydrous THF added via cannula. The mixture was allowed to warm to room temperature and stirred overnight. In the morning, the reaction was quenched with 300 mL of satd NaHCO₃. The aqueous phase was then extracted with ether (6×300 mL) and the combined organic layers dried over MgSO₄, filtered and concentrated in vacuo. At this point 150 mL of 1:3 ether/hexane was added to the crude product and the mixture stirred for 4 h. (This will precipitate most of triphenylphosphine and triphenylphosphine oxide.) The mixture was filtered and concentrated in vacuo for the second time. The crude product was chromatographed through a silica gel column (crude/gel=1/15~20) with 2–3% Et₃N in 1:6 EtOAc/hexane to afford the desired product **17a** (6.488 g, 45 mmol, 93%, over 2 steps) as a yellow oily liquid. The spectral data were as follows: ¹H NMR (CDCl₃/300 MHz) δ 6.28 (dt, *J*=12.6, 1.2 Hz, trans H8, 0.56H), 5.87 (dt, *J*=6.3, 1.4 Hz, cis H8, 0.44H), 4.72 (dt, *J*=12.6, 7.4 Hz, trans H7, 0.61H), 4.34 (td, *J*=7.4, 6 Hz, cis H7, 0.39H), 3.63 and 3.63 (t and t, *J*=6.6 and 6.8 Hz, H2, 2H), 3.58 (s, cis H9, 1.29H), 3.50 (s, trans H9, 1.71H), 2.13–2.02 (m, cis H6, 0.88H), 1.98–1.88 (m, trans H6, 1.12H), 1.70 (br s, H1, 1H), 1.63–1.51 (m, H3, 2H), 1.44–1.30 (m, H4 and H5, 4H); ¹³C NMR (CDCl₃/300 MHz) δ 147.2, 146.3, 106.9, 103.1, 63.1, 63.1, 59.6, 56.0, 32.8, 30.7, 29.7, 27.8, 25.4, 25.3, 23.9; IR (neat/NaCl) 3342, 3033, 2998, 2931, 2856, 1656, 1462, 1391, 1208, 1110, 1054, 933, 736 cm⁻¹; LRMS (EI) 144 ([M]⁺, 4), 97 (10), 72 (100); HRMS (EI) *m/z* calculated for C₈H₁₆O₂ [M]⁺ 144.1150, found 144.1155.

7.2. 3-(7-Methoxy-hept-6-enoyl)-oxazolidin-2-one (**18a**)

To a flame-dried 100-mL round-bottom flask under an argon atmosphere were added **17a** (1.503 g, 10.4 mmol) and 60 mL of anhydrous DMF. The reaction was cooled to 0 °C and the solution was treated with pyridinium dichromate (PDC) (15.806 g, 42.0 mmol). The temperature of mixture was allowed to warm to room temperature and stirred overnight. The reaction was quenched with 600 mL of water, the aqueous layer extracted with ether (10×150 mL), and the combined organic layers were dried over anhydrous MgSO₄, filtered and concentrated in vacuo. The crude product was eluted with 1:4 ether/hexane through a silica gel column (crude/gel=1:25) to afford the acid product (0.722 g, 4.6 mmol, 44%) as a colorless oily liquid.

A solution of the acid synthesized above (0.47 g, 3.0 mmol) and 20 mL of anhydrous THF was placed in a 100-mL round-bottom flask under an argon atmosphere. After cooling the reaction to $-20\text{ }^{\circ}\text{C}$, anhydrous Et_3N (2.0 mL, 14.3 mmol) was added dropwise followed by trimethylacetyl chloride (0.44 mL, 3.5 mmol). The resulting white suspension solution was stirred at $-20\text{ }^{\circ}\text{C}$. After 2 h, oven-dried lithium chloride (0.155 g, 3.6 mmol) and 2-oxazolidone (0.325 g, 3.7 mmol) were added, the reaction allowed to warm slowly to room temperature, and the room temperature solution stirred for 8 h. After this point, the reaction was concentrated to about 10% of its initial volume. The residue was filtered through a pad of silica gel with 3% Et_3N in ether as eluant. After concentration in vacuo, the crude product was chromatographed through a silica gel column (crude/gel=1:30) with 2–3% Et_3N in 1:4 EtOAc/hexane as eluant in order to afford the desired imide **18a** (0.416 g, 1.8 mmol, 62%) as a colorless oily liquid. The spectral data were as follows: ^1H NMR ($\text{CDCl}_3/300\text{ MHz}$) δ 6.29 (d with fine coupling, $J=12.6\text{ Hz}$, trans H8, 0.81H), 5.88 (dt, $J=6.0, 1.4\text{ Hz}$, cis H8, 0.19H), 4.71 (dt, $J=12.6, 7.4\text{ Hz}$, trans H7, 0.79H), 4.42 (t, $J=8.1\text{ Hz}$, H1, 2H), 4.32 (apparent td, $J=7.2, 6.0\text{ Hz}$, cis H7, 0.21H), 4.02 (t, $J=8.1\text{ Hz}$, H2, 2H), 3.57 (s, cis H9, 0.57H), 3.49 (s, trans H9, 2.43H), 2.91 (t, $J=7.5\text{ Hz}$, H3, 2H), 2.13–2.03 (m, cis H6, 0.42H), 2.01–1.91 (m, trans H6, 1.58H), 1.73–1.60 (m, H4, 2H), 1.47–1.36 (m, H5, 2H); ^{13}C NMR ($\text{CDCl}_3/300\text{ MHz}$) δ 173.5, 173.4, 153.6, 147.3, 146.4, 106.3, 102.5, 62.1, 59.5, 55.9, 42.5, 34.9, 30.1, 29.2, 27.4, 23.8, 23.6, 23.5; IR (neat/NaCl) 3540, 3380, 2930, 2855, 1773, 1698, 1457, 1389, 1209, 1039, 937, 760 cm^{-1} ; LRMS (EI) 209 (13), 140 (100); HRMS (EI) m/z calculated for $\text{C}_{11}\text{H}_{17}\text{NO}_4$ $[\text{M}]^+$ 227.1158, found 227.1157.

7.3. 3-(7-Methoxy-1-triisopropylsilyloxy-hepta-1,6-dienyl)-oxazolidin-2-one (19a)

Into a flamed-dried 50-mL round-bottom flask under an argon atmosphere were placed freshly distilled diisopropyl amine (0.23 mL, 1.6 mmol) and 5 mL of anhydrous THF. The reaction was cooled to $-0\text{ }^{\circ}\text{C}$, 1.6 M *n*-butyllithium (1 mL, 1.6 mmol) was added dropwise, and then the mixture stirred for 30 min. The reaction was then cooled to $-78\text{ }^{\circ}\text{C}$, a solution of imide **18a** (0.299 g, 1.3 mmol) in 5 mL of anhydrous THF was added via a cannula, and the resulting solution stirred for 20 min. While the reaction was still at $-78\text{ }^{\circ}\text{C}$, triisopropylsilyl trifluoromethanesulfonate (0.42 mL, 1.6 mmol) was added. This mixture was allowed to slowly warm to room temperature and stirred for 5 h. The reaction mixture was concentrated to 10% of its original volume and the residue was filtered through a pad of silica gel with 3% Et_3N in ether as eluant. After concentration in vacuo, the crude product was chromatographed through a silica gel column (crude/gel=1:25) using 2–3% Et_3N in 2:3 ether/hexane as eluant in order to afford the desired ketene acetal **19a** (0.438 g, 1.1 mmol, 87%) as a colorless oily liquid. The spectral data were as follows: ^1H NMR ($\text{CDCl}_3/300\text{ MHz}$) δ 6.27 (d with fine coupling, $J=12.6\text{ Hz}$, trans H8, 0.78H), 5.86 (dt, $J=6.0, 1.5\text{ Hz}$, cis H8, 0.22H), 4.69 (dt, $J=13.5, 7.2\text{ Hz}$, trans H7, 0.78H), 4.66 (t, $J=7.2\text{ Hz}$, H3, 0.22H), 4.65 (t, H3, $J=7.2\text{ Hz}$, 0.78H), 4.31 (dd of H1 with cis H7 buried, $J=8.8, 7.1\text{ Hz}$, 2.22H), 3.77 (dd, $J=8.8, 7.1\text{ Hz}$, H2, 2H), 3.56 (s, cis H9, 0.66H), 3.49 (s, trans H9, 2.34H),

2.16–2.02 (m of H4 with cis H6 buried, 2.44H), 1.94 (dtd, $J=7.4, 7.2, 1.1\text{ Hz}$, trans H6, 1.56H), 1.41 (p, $J=7.4\text{ Hz}$, H5, 2H), 1.25–1.07 (m of H11 with d of H10 at 1.11, $J=5.4\text{ Hz}$, 21H); ^{13}C NMR ($\text{CDCl}_3/300\text{ MHz}$) δ 156.0, 147.4, 146.5, 140.1, 106.6, 105.0, 104.8, 102.7, 61.8, 59.6, 56.0, 46.6, 30.6, 29.7, 27.6, 25.3, 25.0, 23.8, 18.0, 13.2; IR (neat/NaCl) 3518, 3055, 2944, 2868, 1770, 1681, 1463, 1398, 1268, 1210, 1109, 1040, 933, 883, 685 cm^{-1} ; LRMS (EI) 383 (M^+ , 2), 368 ($[\text{M}-\text{CH}_3]^+$, 10), 340 ($[\text{M}-\text{C}(\text{CH}_3)_2]^+$, 100), 244 (92), 200 (40); HRMS (EI) m/z calculated for $\text{C}_{20}\text{H}_{37}\text{NO}_4\text{Si}$ $[\text{M}]^+$ 383.2492, found 383.2489.

7.4. 3-(2-Dimethoxymethyl-cyclopentanecarbonyl)-oxazolidin-2-one (20a)

Under an argon atmosphere, a solution of oven-dried tetraethylammonium tosylate (0.453 g, 1.5 mmol), ketene acetal **19a** (0.094 g, 0.25 mmol), and 2,6-lutidine (0.22 mL, 1.5 mmol) in 15 mL of anhydrous solution (THF/MeOH=1:4) was placed in a flame-dried 25-mL three-necked round-bottom flask equipped with a reticulated vitreous carbon (RVC) anode and a RVC cathode. The reaction was electrolyzed at a constant current of 8 mA until 2.2 F/mol of charge was passed. The solution was concentrated to 10% of its original volume and then diluted with 80 mL of pure ether to precipitate tetraethylammonium tosylate. The reaction was then dried over sodium sulfate for 2–3 h, filtered and concentrated in vacuo. The crude product was chromatographed through a silica gel column (crude/gel=1:30) using 2–3% Et_3N in 3:1 ether/hexane as eluant in order to afford the desired product **20a** (0.055 g, 0.21 mmol, 87%) as a colorless oily liquid. The spectral data were as follows: ^1H NMR ($\text{CDCl}_3/300\text{ MHz}$) δ 4.34 (t, $J=7.8\text{ Hz}$, H1, 0.7H), 4.33 (t, $J=7.8\text{ Hz}$, H1, 1.3H), 4.21 (d, $J=9.3\text{ Hz}$, H8, 0.65H), 4.15 (d, $J=7.8\text{ Hz}$, H8, 0.35H), 4.05–3.81 (m of H2 with H3 buried, 3H), 3.23 (s, H9, 1.05H), 3.21 (s, H9, 1.05H), 3.19 (s, H9, 1.95H), 3.14 (s, H9, 1.95H), 2.79–2.61 (m, H7, 1H), 2.12–1.40 (m, H4, H5 and H6, 6H); ^{13}C NMR ($\text{CDCl}_3/300\text{ MHz}$) δ 176.5, 175.0, 153.5, 153.5, 107.4, 104.3, 61.9, 61.8, 54.3, 53.4, 52.2, 51.5, 46.1, 44.6, 44.3, 43.7, 43.0, 42.9, 31.9, 29.3, 28.2, 28.0, 25.3, 24.4; IR (neat/NaCl) 3535, 3372, 2956, 2831, 1770, 1694, 1524, 1480, 1454, 1385, 1223, 1045, 973, 926, 761, 706 cm^{-1} ; LRMS (EI) 226 (43), 166 (63), 138 (100); HRMS (FAB) m/z calculated for $\text{C}_{12}\text{H}_{19}\text{NO}_5$ $[\text{M}+\text{Li}]^+$ 264.1423, found 264.1424.

7.5. 8-Methoxy-oct-7-en-1-ol (17b)

At $0\text{ }^{\circ}\text{C}$, 240 mL of 1 N HCl/acetone (1:1) was added to a 500-mL round-bottom flask containing enol ether **17a** (8.694 g, 60.3 mmol). The reaction was allowed to warm to room temperature and stirred for 1 h (TLC). The reaction was recooled to $0\text{ }^{\circ}\text{C}$ and the pH of the reaction was adjusted to 6–8 using 10% NaOH and satd NaHCO_3 . After excess NaCl was added, the reaction was extracted with ether ($6\times 200\text{ mL}$). The combined organic layers were dried over anhydrous MgSO_4 , filtered and concentrated in vacuo. The crude aldehyde was used directly in the following step without purification. This crude aldehyde should be diluted with solvent (CH_2Cl_2 or ether) or it will polymerize during storage.

To a flamed-dried 1000-mL round-bottom flask under an argon atmosphere was added a stirred suspension of (methoxymethyl)triphenylphosphonium chloride (42.667 g, 120.7 mmol) in 400 mL of anhydrous THF. The mixture was cooled to $-78\text{ }^{\circ}\text{C}$, 1.4 M *sec*-butyllithium solution in cyclohexane (115 mL, 161 mmol) was added dropwise, and the resulting dark brown mixture allowed to warm from $-78\text{ }^{\circ}\text{C}$ to room temperature over 3 h. The reaction was recooled to $-78\text{ }^{\circ}\text{C}$ and the crude aldehyde synthesized above in 60 mL of anhydrous THF added via a cannula. The mixture was allowed to warm to room temperature and stirred overnight. The reaction was quenched with 450 mL of satd NaHCO_3 . The aqueous phase was extracted with ether (6 \times 300 mL). The combined organic layers were dried over MgSO_4 and concentrated in vacuo. At this point the crude reaction mixture was taken up in 150 mL of 1:3 ether/hexane and allowed to stand for 4 h. This procedure precipitates most of the Ph_3PO . The mixture was filtered and concentrated in vacuo for the second time. The crude product was chromatographed through a silica gel column (crude/gel=1:15~20) with 2–3% Et_3N in 1:8 EtOAc/hexane as eluant in order to afford the desired product **17b** (6.658 g, 42.1 mmol, 70%, over 2 steps) as a yellow oily liquid. The spectral data were as follows: ^1H NMR ($\text{CDCl}_3/300\text{ MHz}$) δ 6.28 (dt, $J=12.6, 1.5\text{ Hz}$, trans H9, 0.56H), 5.87 (dt, $J=6.3, 1.4\text{ Hz}$, cis H9, 0.44H), 4.72 (dt, $J=12.6, 7.4\text{ Hz}$, trans H8, 0.58H), 4.34 (td, $J=7.4, 1.4\text{ Hz}$, cis H7, 0.43H), 3.63 and 3.63 (t and t, $J=6.6$ and 6.8 Hz , H2, 2H), 3.58 (s, cis H10, 0.43H), 3.50 (s, trans H9, 0.57H), 2.15–2.02 (br s, H1, 1H), 2.12–2.0 (m, cis H7, H), 1.97–1.87 (m, trans H7, 0.9H), 1.63–1.51 (m, H3, 1.1H), 1.63–1.49 (m, H3, 2H), 1.41–1.28 (m, H4, H5 and H6, 6H); ^{13}C NMR ($\text{CDCl}_3/300\text{ MHz}$) δ 147.0, 146.1, 107.1, 103.2, 63.0, 63.0, 59.6, 56.0, 32.8, 30.8, 29.8, 29.1, 28.9, 27.7, 25.7, 25.7, 23.8; IR (neat/ NaCl) 3343, 3033, 2997, 2929, 2855, 1656, 1463, 1390, 1208, 1108, 1056, 934, 737 cm^{-1} ; LRMS (EI) 158 ($[\text{M}]^+$, 20), 143 (100), 125 (80); HRMS (EI) m/z calculated for $\text{C}_9\text{H}_{18}\text{NO}_2$ $[\text{M}]^+$ 158.1307, found 158.1318.

7.6. 3-(8-Methoxy-oct-7-enoyl)-oxazolidin-2-one (18b)

The acid substrate was prepared using the same method for the synthesis of imide **18a** as described above using **17b** (3.083 g, 19.5 mmol), 200 mL of anhydrous DMF, and PDC (29.932 g, 78.0 mmol). The crude product was chromatographed through a silica gel column (crude/gel=1:25) using 1:2 ether/hexane as eluant in order to afford the acid product (1.47 g, 8.5 mmol, 44%) as a colorless oily liquid.

The coupling reaction was accomplished using the same method as described above for the synthesis of imide **18a**. In this experiment was used the acid made above (1.11 g, 6.4 mmol) in 65 mL of anhydrous THF, anhydrous Et_3N (3.6 mL, 25.8 mmol), trimethylacetyl chloride (0.8 mL, 6.4 mmol), oven-dried lithium chloride (0.2649 g, 6.4 mmol) and 2-oxazolidone (0.574 g, 6.5 mmol). The crude product was chromatographed through a silica gel column (crude/gel=1:30) using 2–3% Et_3N in 3:4 ether/hexane as eluant in order to afford the desired imide **18b** (1.003 g, 4.2 mmol, 65%) as a colorless oily liquid. The spectral data were as follows: ^1H NMR ($\text{CDCl}_3/300\text{ MHz}$) δ 6.27 (d with fine coupling, $J=12.6\text{ Hz}$, trans H9, 0.80H), 5.87 (dt, $J=6.3, 1.2\text{ Hz}$, cis H9, 0.20H), 4.71 (dt, $J=12.6,$

7.2 Hz, trans H8, 0.75H), 4.41 (t, $J=8.1\text{ Hz}$, H1, 2H), 4.32 (apparent td, $J=7.5, 6.3\text{ Hz}$, cis H8, 0.25H), 4.02 (t, $J=8.1\text{ Hz}$, H2, 2H), 3.57 (s, cis H10, 0.58H), 3.50 (s, trans H10, 2.42H), 2.91 (t, $J=7.5\text{ Hz}$, H3, 2H), 2.11–2.01 (m, cis H7, 0.4H), 1.98–1.87 (m, trans H7, 1.60H), 1.73–1.59 (m, H4, 2H), 1.44–1.32 (m, H5 and H6, 4H); ^{13}C NMR ($\text{CDCl}_3/300\text{ MHz}$) δ 173.7, 173.7, 153.7, 147.2, 146.3, 106.8, 103.0, 62.2, 59.6, 56.0, 42.7, 35.2, 30.6, 29.6, 28.8, 28.6, 27.6, 24.2, 24.2, 23.8; IR (neat/ NaCl) 3538, 2993, 2930, 2855, 1781, 1700, 1655, 1388, 1208, 1115, 1040, 935, 761 cm^{-1} ; LRMS (EI) 242 ($[\text{M}+\text{H}]^+$ (22), 209 (17), 176 (19), 154 (96), 142 (37), 129 (61), 112 (100); HRMS (EI) m/z calculated for $\text{C}_{12}\text{H}_{19}\text{NO}_4$ $[\text{M}+\text{H}]^+$ 242.1392, found 242.1401.

7.7. 3-(8-Methoxy-1-triisopropylsilyloxy-octa-1,7-dienyl)-oxazolidin-2-one (19b)

The triisopropylsilyl enol ether was prepared using the method described as above for the synthesis of ketene acetal **19a**. In this case, the reaction utilized freshly distilled diisopropyl amine (0.82 mL, 5.9 mmol) and 40 mL anhydrous THF in 100-mL round-bottom flask along with 2.5 M *n*-butyllithium (2.1 mL, 5.3 mmol), a solution of imide **18b** (1.003 g, 4.2 mmol) in 20 mL of anhydrous THF, and triisopropylsilyl trifluoromethanesulfonate (1.4 mL, 5.1 mmol). The crude product was chromatographed through a silica gel column (crude/gel=1:25) using 2–3% Et_3N in 4:5 ether/hexane as eluant in order to afford the desired ketene acetal **19b** (1.314 g, 3.3 mmol, 80%) as a colorless oily liquid. The spectral data were as follows: ^1H NMR ($\text{CDCl}_3/300\text{ MHz}$) δ 6.26 (d, $J=12.6\text{ Hz}$, trans H9, 0.82H), 5.85 (apparent d, $J=6.3\text{ Hz}$, cis H9, 0.18H), 4.70 (dt, $J=12.6, 7.4\text{ Hz}$, trans H8, 0.82H), 4.64 (t, $J=7.4\text{ Hz}$, H3, 1H), 4.30 (dd of H1 with cis H8 buried, $J=8.5, 7.6\text{ Hz}$, 2.18H), 3.77 (dd, $J=8.5, 7.6\text{ Hz}$, H2, 2H), 3.56 (s, cis H10, 0.54H), 3.48 (s, trans H10, 2.46H), 2.16–1.99 (m of H4 with cis H7 buried, 2.36H), 1.96–1.84 (m, trans H7, 1.64H), 1.50–1.28 (m, H5 and H6, 4H), 1.25–1.07 (m of H12 with d of H11 at 1.10, $J=6.0\text{ Hz}$, 21H); ^{13}C NMR ($\text{CDCl}_3/300\text{ MHz}$) δ 156.0, 147.2, 146.2, 140.0, 107.0, 105.1, 105.0, 103.1, 61.8, 59.6, 56.0, 46.6, 30.7, 29.7, 29.2, 28.9, 27.7, 25.5, 25.5, 23.8, 18.0, 13.2; IR (neat/ NaCl) 3517, 3055, 2944, 2867, 1767, 1678, 1655, 1464, 1399, 1277, 1209, 1131, 1040, 883, 686 cm^{-1} ; LRMS (EI) 397 (M^+ , 2), 382 ($[\text{M}-\text{CH}_3]^+$, 12), 354 ($[\text{M}-\text{C}(\text{CH}_3)_2]^+$, 100), 244 (97), 200 (89), 128 (68); HRMS (EI) m/z calculated for $\text{C}_{21}\text{H}_{39}\text{NO}_4\text{Si}$ $[\text{M}]^+$ 397.2648, found 397.2765 for $[\text{M}]^+$ and 382.2424 for $[\text{M}-\text{CH}_3]^+$.

7.8. 3-(2-Dimethoxymethyl-cyclohexanecarbonyl)-oxazolidin-2-one (20b)

The cyclization was conducted using the same procedure described above for the synthesis of **20a**. This experiment utilized oven-dried tetraethylammonium tosylate (0.607 g, 2.0 mmol), ketene acetal **19b** (0.096 g, 0.02 mmol), 20 mL 1:4 THF/MeOH, 2,6-lutidine (0.22 mL, mmol), an RVC anode and cathode, a constant current of 8 mA, and 2.2 F/mol of charge. The crude product was chromatographed through a silica gel column (crude/gel=1:30) using 2–3% Et_3N in 3:5 EtOAc/hexane as eluant in order to afford the desired product **20b** (0.041 g, 0.015 mmol, 63%) as a colorless

oily liquid. The spectral data were as follows: ^1H NMR ($\text{CDCl}_3/300\text{ MHz}$) δ 4.51–4.33 (m of H1 with cis H9 buried, 2.27H), 4.13 (d, $J=7.2\text{ Hz}$, trans H9, 0.73H), 4.09–4.89 (m, H2, 2H), 3.85–3.61 (m, cis and trans H3, 1H), 3.29 (s, cis H10, 0.81H), 3.24 (s, trans H10, 2.19H), 3.23 (s, cis H10, 0.81H), 3.20 (s, trans H10, 2.19H), 2.26–2.04 (m, H8, 1H), 1.98–0.94 (m, H4, H5, H6 and H7, 8H); ^{13}C NMR ($\text{CDCl}_3/300\text{ MHz}$) δ 177.1, 175.3, 153.8, 153.3, 107.5, 104.4, 61.9, 54.2, 53.9, 53.0, 52.6, 51.8, 43.2, 43.0, 41.8, 41.7, 40.3, 39.9, 30.3, 29.8, 27.1, 26.1, 25.6, 25.4, 25.3, 25.0, 23.7, 23.5; IR (neat/NaCl) 3585, 3534, 3373, 2930, 2857, 1789, 1770, 1728, 1694, 1480, 1454, 1385, 1325, 1262, 1223, 1046, 985, 943, 761, 705 cm^{-1} ; LRMS (EI) 240 ($[\text{M}-\text{OCH}_3]^+$, 19), 208 (9), 185 (23), 180 (40), 152 (59), 125 (59), 93 (53), 81 (44), 75 (100); HRMS (EI) m/z calculated for $\text{C}_{13}\text{H}_{21}\text{NO}_5$ [M^+] 271.1420, found 240.1231 for $[\text{M}-\text{OCH}_3]^+$.

7.9. 7-Methyl-8-trimethylsilylanyl-oct-6-en-1-ol (21a)

The hemiacetal from the reduction of ϵ -caprolactone was prepared using the same method as for the synthesis of enol ether (17a) as described above.

A flamed-dried 500-mL round-bottom flask under an argon atmosphere was charged with a suspension of (ethyl)triphenylphosphonium bromide (18.567 g, 49.5 mmol) in 150 mL of anhydrous THF. The mixture was cooled to $-78\text{ }^\circ\text{C}$, a 1.4 M *sec*-butyllithium solution in cyclohexane (37 mL, 51.8 mmol) was added dropwise, and the resulting dark brown mixture allowed to warm from $-78\text{ }^\circ\text{C}$ to room temperature over a period of 3 h. The reaction was recooled to $-78\text{ }^\circ\text{C}$, iodomethyl-trimethylsilane (7.2 mL, 50.2 mmol) was added dropwise, and the mixture was allowed to warm to room temperature. After 3 h, the mixture became a cloudy red-brown solution. To this mixture was added a 1.6 M *n*-butyllithium in hexane (32 mL, 51.2 mmol) in a dropwise fashion. The resulting dark brown mixture was allowed to warm from $-78\text{ }^\circ\text{C}$ to room temperature over a period of 3 h. The reaction was recooled to $-78\text{ }^\circ\text{C}$ and then the crude hemiacetal (2.4 g, 20.7 mmol) in 40 mL of anhydrous THF added via a cannula. The mixture was allowed to warm to room temperature and stirred overnight. The reaction was then quenched with 300 mL of satd NaHCO_3 . The layers were separated and the aqueous phase was extracted with ether ($6 \times 300\text{ mL}$). The combined organic layers were dried over anhydrous MgSO_4 , filtered and concentrated in vacuo. The crude product was then taken up in 150 mL of 1:3 ether/hexane and allowed to stand for 4 h in order to precipitate most of the triphenylphosphine and triphenylphosphine oxide present in the crude. This mixture was filtered and concentrated in vacuo for the second time. The crude product was chromatographed through a silica gel column (crude/gel=1:25) using 2–3% Et_3N in 1:2 ether/hexane in order to afford the desired product 21a (2.793 g, 13.0 mmol, 63%) as a colorless oily liquid. The spectral data were as follows: ^1H NMR ($\text{CDCl}_3/300\text{ MHz}$) δ 5.03–4.89 (m, H7, 1H), 3.63 and 3.62 (t and t, $J=6.3$ and 6.3 Hz , H2, 2H), 2.03–1.85 (m, H6, 2H), 1.68–1.64 (m, allylic coupling, H8, 1.65H), 1.59–1.56 (m, allylic coupling, H8, 1.35H), 1.65–1.51 (m, H1 and H3, 3H), 1.49 (s, H9, 1.26H), 1.45 (s, H9, 0.74H), 1.41–1.38 (m, H4 and H5, 4H), 0.02 (s, H10, 5.35H), -0.01 (s, H10, 3.65H); ^{13}C NMR ($\text{CDCl}_3/300\text{ MHz}$)

δ 133.2, 132.9, 122.7, 122.3, 63.2, 63.2, 33.0, 33.0, 30.1, 30.0, 30.0, 28.7, 28.3, 26.4, 25.8, 25.5, 23.4, 18.8, -0.5 , -1.1 ; IR (neat/NaCl) 3337, 2931, 2857, 1659, 1436, 1416, 1376, 1248, 1162, 1055, 840, 755, 693 cm^{-1} ; LRMS (EI) 214 ($[\text{M}]^+$, 100), 199 (8), 143 (47), 129 (88); HRMS (EI) m/z calculated for $\text{C}_{12}\text{H}_{26}\text{OSi}$ [$\text{M}]^+$ 214.1753, found 214.1747.

7.10. 3-(7-Methyl-8-trimethylsilylanyl-oct-6-enoyl)-oxazolidin-2-one (22a)

The acid substrate was prepared using the same method as described above during the synthesis of imide 18a. In this case, the experiment used 21a (3.236 g, 15.1 mmol), 100 mL of anhydrous DMF in a 250 mL flamed-dried round-bottom flask, and PDC (22.32 g, 59.3 mmol). The crude product was chromatographed through a silica gel column (crude/gel=1:25) using 1:2 ether/hexane as eluant in order to afford the acid product (1.6805 g, 7.4 mmol, 49%) as a colorless oily liquid.

The coupling reaction was also performed using the same method as described earlier for the synthesis of imide 18a. In this experiment, the acid made in the preceding paragraph (1.384 g, 6.1 mmol), 65 mL of anhydrous THF in flamed-dried 100-mL round-bottom flask, Et_3N (3.4 mL, 24.3 mmol), trimethylacetyl chloride (0.75 mL, 6.1 mmol), oven-dried lithium chloride (0.258 g, 6.2 mmol), and 2-oxazolidone (0.548 g, 6.2 mmol) were used. The crude product was chromatographed through a silica gel column (crude/gel=1:30) with 2–3% Et_3N in 1:1 ether/hexane as eluant in order to afford the desired imide 22a (1.634 g, 5.5 mmol, 91%) as a colorless oily liquid. The spectral data were as follows: ^1H NMR ($\text{CDCl}_3/300\text{ MHz}$) δ 5.01–4.88 (m, H7, 1H), 4.94 (t, $J=8.0\text{ Hz}$, H1, 2H), 4.00 (t, $J=8.0\text{ Hz}$, H2, 2H), 2.90 (t, $J=7.8\text{ Hz}$, H3, 2H), 2.04–1.87 (m, H6, 2H), 1.71–1.59 (m, H4, 2H), 1.67–1.62 (m, allylic coupling, H8, 2.18H), 1.53–1.55 (m, allylic coupling, H8, 0.82H), 1.48 (s, H9, 1.38H), 1.44 (s, H9, 0.62H), 1.45–1.31 (m, H5, 2H), 0.01 (s, H10, 5.78H), -0.02 (s, H10, 3.22H); ^{13}C NMR ($\text{CDCl}_3/300\text{ MHz}$) δ 173.7, 153.7, 133.4, 133.1, 122.2, 121.9, 62.2, 42.7, 35.2, 35.2, 30.0, 29.8, 29.6, 28.4, 28.1, 26.4, 24.2, 24.1, 23.4, 18.8, -0.5 , -1.1 ; IR (neat/NaCl) 3546, 3384, 2951, 1782, 1700, 1478, 1387, 1246, 1110, 1040, 953, 851, 760, 695 cm^{-1} ; LRMS (EI) 297 ($[\text{M}]^+$, 2), 195 (8), 160 (100); HRMS (EI) m/z calculated for $\text{C}_{15}\text{H}_{27}\text{NO}_3\text{Si}$ [$\text{M}]^+$ 297.1760, found 297.1765.

7.11. 3-(7-Methyl-1-triisopropylsilylanyl-oxy-8-trimethylsilylanyl-octa-1,6-dienyl)-oxazolidin-2-one (23a)

The TIPS silyl enol ether was prepared using the same method as described earlier for the synthesis of ketene acetal 19a. This experiment used freshly distilled diisopropyl amine (0.65 mL, 4.6 mmol) and 20 mL of anhydrous THF in a 100-mL round-bottom flask, a 1.6 M *n*-butyllithium in hexane solution (2.9 mL, 4.6 mmol), imide 22a (1.234 g, 4.2 mmol), 16 mL of anhydrous THF, and triisopropylsilyl trifluoromethanesulfonate (1.3 mL, 4.7 mmol) in a 50-mL pear-bottom flask. The crude product was chromatographed through a silica gel column (crude/gel=1:25) with 2–3% Et_3N in 1:2 ether/hexane as eluant in order to afford the desired ketene acetal 23a (1.567 g, 3.5 mmol, 83%) as a

colorless oily liquid. The spectral data were as follows: ^1H NMR ($\text{CDCl}_3/300\text{ MHz}$) δ 5.00–4.88 (m, H7, 1H), 4.65 and 4.64 (t and t, $J=7.2$ and 7.2 Hz, H3, 1H), 4.29 (dd, $J=8.7$, 7.2 Hz, H1, 2H), 3.75 (dd, $J=8.7$, 7.2 Hz, H2, 2H), 2.09 (dt, $J=7.5$, 7.5 Hz, H4, 2H), 2.02–1.84 (m, H6, 2H), 1.64 (m, allylic coupling, H8, 2.04H), 1.56 (s, H8, 0.96H), 1.48 (s, H9, 1.36H), 1.43 (s, H9, 0.64H), 1.37 (p, $J=7.5$ Hz, H5, 2H), 1.10 (m of H12 with d of H11 at 1.06, $J=5.7$ Hz, 2H), 0.00 (s, H10, 6.12H), -0.03 (s, H10, 2.88H); ^{13}C NMR ($\text{CDCl}_3/300\text{ MHz}$) δ 155.9, 140.0, 133.3, 133.0, 122.4, 122.1, 105.0, 61.8, 46.6, 30.1, 30.0, 29.8, 28.4, 28.2, 26.4, 25.4, 25.4, 23.3, 18.0, 13.2, -0.6 , -1.1 ; IR (neat/ NaCl) 3519, 2946, 2867, 1770, 1681, 1464, 1398, 1248, 1054, 883, 856, 687 cm^{-1} ; LRMS (EI) 453 (M^+ , 5), 410 ($[\text{M}-\text{CH}(\text{CH}_3)_2]^+$, 67), 366 (14), 244 (100), 210 (36), 200 (51), 128 (59); HRMS (EI) m/z calculated for $\text{C}_{24}\text{H}_{47}\text{NO}_3\text{Si}_2$ [M^+] 453.3095, found 453.3097.

7.12. 3-(2-Isopropenyl-cyclopentanecarbonyl)-oxazolidin-2-one (24a)

The anodic cyclization was conducted using the same procedure as described above for the synthesis of **20a**. The experiment used oven-dried tetraethylammonium tosylate (0.517 g, 1.7 mmol), ketene acetal **23a** (0.225 g, 0.05 mmol), 17 mL 1:4 THF/MeOH, 2,6-lutidine (0.36 mL, 3.1 mmol), an RVC anode and cathode, a constant current of 8 mA, and 2.2 F/mol of charge. The crude product was chromatographed through a silica gel column (crude/gel=1:35) with 2–3% Et_3N in 1:1 ether/hexane as eluant in order to afford the desired product **24a** (0.083 g, 0.037 mmol, 75%) as white solid, and 0.016 g of starting material **23a** was recovered (0.03 mmol, 7%). The spectral data were as follows: *Isomer 1*: ^1H NMR ($\text{CDCl}_3/300\text{ MHz}$) δ 4.72 and 4.70 (s and s, H9, 2H), 4.41–4.16 (m, H1 and H3, 3H), 4.05–3.81 (m, H2, 2H), 3.01 (dt, approx. $J=8.3$, 8.3 Hz, H7, 1H), 2.13–1.97, 1.95–1.76 and 1.64–1.52 (m, H4, H5 and H6, 6H), 1.67 (s, H8, 3H); ^{13}C NMR ($\text{CDCl}_3/300\text{ MHz}$) δ 175.0, 153.5, 146.2, 111.7, 62.0, 50.0, 46.8, 43.0, 30.4, 29.1, 24.7, 22.1; IR (neat/ NaCl) 3508, 3363, 3083, 2957, 2868, 1778, 1690, 1644, 1477, 1388, 1362, 1249, 1226, 1107, 1038, 914, 894, 699 cm^{-1} ; LRMS (EI) 223 (M^+ , 9), 182 (69), 136 (100), 121 (49), 108 (53), 93 (69), 88 (69); HRMS (EI) m/z calculated for $\text{C}_{12}\text{H}_{17}\text{NO}_3$ [M^+] 223.1208, found 223.1199. *Isomer 2*: ^1H NMR ($\text{CDCl}_3/300\text{ MHz}$) δ 4.71 and 4.68 (s and s, H9, 2H), 4.38 (t, $J=8.3$ Hz, H1, 2H), 4.00 (t of H2 with H3 buried, $J=8.3$ Hz, 3H), 3.00 (dt, $J=9.8$, 8.9 Hz, H7, 1H), 2.28–2.10, 2.01–1.87 and 1.83–1.46 (m of H4, H5 and H6 with s of H8 at 1.70, 9H); ^{13}C NMR ($\text{CDCl}_3/300\text{ MHz}$) δ 176.4, 153.4, 146.7, 110.3, 62.0, 50.8, 46.5, 43.0, 31.7, 31.2, 24.9, 20.6; IR (neat/ NaCl) 3538, 3075, 2979, 2953, 2871, 1795, 1772, 1682, 1645, 1485, 1386, 1362, 1223, 1041, 899, 757 cm^{-1} ; LRMS (EI) 223 (M^+ , 16), 136 (100), 121 (100), 109 (80), 108 (73), 93 (100), 88 (66); HRMS (EI) m/z calculated for $\text{C}_{12}\text{H}_{17}\text{NO}_3$ [M^+] 223.1208, found 223.1212.

7.13. 8-Methyl-9-trimethylsilyl-non-7-en-1-ol (21b)

The aldehyde from the hydrolysis of enol ether **17a** was prepared using the same method for the synthesis of **17b** as described above. This experiment used enol ether **17a** (3.671 g, 25.5 mmol) and 300 mL of 4 N HCl/acetone (1:1) in a

500-mL round-bottom flask. The crude aldehyde was used directly in the following step without purification. The aldehyde was diluted with solvent (CH_2Cl_2 or ether) in order to avoid polymerization.

The allylsilane alcohol **21b** was prepared using the same method as described earlier for the synthesis of **21a** using ethyltriphenylphosphonium bromide (23.538 g, 62.8 mmol) and 250 mL of anhydrous THF in a 500 mL flame-dried round-bottom flask, a 1.4 M *sec*-butyllithium solution in cyclohexane (48 mL, 67.2 mmol), iodomethyl-trimethylsilane (9.4 mL, 62.7 mmol), a 1.6 M *n*-butyllithium solution in hexane (41 mL, 65.6 mmol), and the crude aldehyde synthesized above in 40 mL of anhydrous THF. The crude product was chromatographed through a silica gel column (crude/gel=1:25) using 2–3% Et_3N in 1:1.5 ether/hexane as eluant in order to afford the desired product **21b** (3.433 g, 15 mmol, 59%, over 2 steps) as an almost colorless oily liquid. The spectral data were as follows: ^1H NMR ($\text{CDCl}_3/300\text{ MHz}$) δ 5.02–4.89 (m, H8, 1H), 3.63 and 3.61 (apparent overlap of t and t, $J=6.3$ and 6.6 Hz, H2, 2H), 2.02–1.83 (m, H7, 2H), 1.68–1.64 (m, allylic coupling, H9, 1.34H), 1.66–1.52 (m, H1 and H3, 3H), 1.59–1.56 (m, allylic coupling, H9, 1.63H), 1.49 (s, H10, 0.46H), 1.45 (s, H10, 0.54H), 1.40–1.25 (m, H4, H5 and H6, 6H), 0.02 (s, H11, 4.15H), -0.01 (s, H11, 4.85H); ^{13}C NMR ($\text{CDCl}_3/300\text{ MHz}$) δ 133.0, 132.7, 122.8, 122.5, 63.1, 33.0, 32.9, 30.3, 30.1, 30.0, 29.5, 29.2, 28.7, 28.2, 26.4, 25.9, 25.9, 23.3, 18.8, -0.5 , -1.1 ; IR (neat/ NaCl) 3326, 2929, 2855, 1658, 1437, 1416, 1376, 1248, 1162, 1056, 856, 756, 694 cm^{-1} ; LRMS (EI) 228 ($[\text{M}]^+$, 84), 143 (100), 129 (73); HRMS (EI) m/z calculated for $\text{C}_{13}\text{H}_{28}\text{OSi}$ [$\text{M}]^+$ 228.1909, found 228.1922.

7.14. 3-(8-Methyl-9-trimethylsilyl-non-7-enoyl)-oxazolidin-2-one (22b)

The acid intermediate was prepared using the same method as described for the synthesis of acid **18a**. This experiment used **21b** (2.175 g, 9.5 mmol), 50 mL of anhydrous DMF, and PDC (12.434 g, 33 mmol). The reaction was quenched with 500 mL of water, the layers separated, and the aqueous layer extracted with ether (12×150 mL). The combined organic layers were dried over anhydrous MgSO_4 , filtered and concentrated in vacuo. The crude product was chromatographed through a silica gel column (crude/gel=1:25) using 1:6 EtOAc/hexane as eluant to afford the acid product (1.484 g, 6.1 mmol, 64%) as an almost colorless oily liquid.

The imide intermediate was prepared using the procedure as described earlier for the synthesis of imide **18a**. This experiment used 0.146 g (6.0 mmol) of the acid synthesized in the preceding paragraph in 20 mL of anhydrous THF, anhydrous Et_3N (0.4 mL, 2.9 mmol), trimethylacetyl chloride (0.08 mL, 6.4 mmol), oven-dried lithium chloride (0.03 g, 7.2 mmol), and 2-oxazolidone (0.06 g, 6.7 mmol). The crude product was chromatographed through a silica gel column (crude/gel=1:30) using 2–3% Et_3N in 3:4 ether/hexane as eluant in order to afford the desired imide **22b** (0.171 g, 5.8 mmol, 96%) as a colorless oily liquid. The spectral data were as follows: ^1H NMR ($\text{CDCl}_3/300\text{ MHz}$) δ 5.01–4.87 (m, H8, 1H), 4.40 (t, $J=8.1$ Hz, H1, 2H), 4.00 (t, $J=8.0$ Hz, H2, 2H), 2.90 (apparent t, $J=7.5$ Hz, H3, 2H),

2.02–1.82 (m, H7, 2H), 1.72–1.58 (m, H4, 2H), 1.67–1.62 (m, allylic coupling, H9, 1.50H), 1.58–1.55 (m, allylic coupling, H9, 1.50H), 1.48 (s, H10, 1H), 1.44 (s, H10, 1H), 1.42–1.29 (m, H5 and H6, 4H), 0.01 (s, H11, 4.50H), –0.02 (s, H11, 4.50H); ^{13}C NMR ($\text{CDCl}_3/300\text{ MHz}$) δ 173.7, 153.7, 133.1, 132.8, 122.6, 122.3, 62.2, 42.7, 35.3, 35.3, 30.0, 30.0, 29.9, 29.1, 28.9, 28.5, 28.1, 26.4, 24.4, 24.4, 23.3, 18.8, –0.5, –1.1; IR (neat/ NaCl) 3545, 3385m, 2952, 2929, 2855, 1782, 1700, 1479, 1387, 1247, 1224, 1040, 857, 760, 696 cm^{-1} ; LRMS (EI) 311 ($[\text{M}]^+$, 5), 160 (100), 144 (11); HRMS (EI) m/z calculated for $\text{C}_{16}\text{H}_{29}\text{NO}_3\text{Si}$ $[\text{M}]^+$ 311.1917, found 311.1929.

7.15. 3-(8-Methyl-1-triisopropylsilyloxy-9-trimethylsilyl-nona-1,7-dienyl)-oxazolidin-2-one (23b)

The triisopropylsilyl enol ether was prepared using the same method as described earlier for the synthesis of ketene acetal **19a**. This experiment used freshly distilled diisopropyl amine (0.33 mL, 2.4 mmol) in 15 mL of anhydrous THF, a 1.6 M *n*-butyllithium (1.5 mL, 2.4 mmol) in hexane solution, imide **22b** (0.669 g, 2.1 mmol) in 10 mL anhydrous THF, and triisopropylsilyl trifluoromethanesulfonate (1.3 mL, 4.7 mmol). The crude product was chromatographed through a silica gel column (crude/gel=1:25) using 2–3% Et_3N in 1:2 ether/hexane as eluant in order to afford the desired ketene acetal **23b** (0.814 g, 1.7 mmol, 81%) as an almost colorless oily liquid. The spectral data were as follows: ^1H NMR ($\text{CDCl}_3/300\text{ MHz}$) δ 4.99–4.87 (m, H8, 1H), 4.63 (t, $J=7.2\text{ Hz}$, H3, 1H), 4.29 (dd, $J=8.4, 7.1\text{ Hz}$, H1, 2H), 3.75 (dd, $J=8.4, 7.1\text{ Hz}$, H2, 2H), 2.08 (dt, $J=7.2, 7.0\text{ Hz}$, H4, 2H), 1.99–1.83 (m, H7, 2H), 1.64 (m, allylic coupling, H9, 1.5H), 1.55 (s, H9, 1.5H), 1.47 (s, H10, 1H), 1.43 (s, H10, 1H), 1.40–1.26 (m, H5 and H6, 4H), 1.23–1.06 (m of H13 with d of H12 at 1.09, $J=6\text{ Hz}$, 21H), 0.00 (s, H11, 4.5H), –0.03 (s, H11, 4.5H); ^{13}C NMR ($\text{CDCl}_3/300\text{ MHz}$) δ 155.9, 139.9, 132.9, 132.6, 122.7, 122.4, 105.1, 105.1, 61.8, 46.6, 30.0, 29.9, 29.4, 29.1, 28.5, 28.1, 26.4, 25.6, 25.5, 23.3, 17.9, 13.1, –0.6, –1.1; IR (neat/ NaCl) 2946, 2868, 1769, 1680, 1464, 1399, 1368, 1279, 1248, 1061, 1040, 883, 856, 687 cm^{-1} ; LRMS (EI) 467 (M^+ , 11), 452 ($[\text{M}-\text{CH}_3]^+$, 5), 424 ($[\text{M}-\text{CH}(\text{CH}_3)_2]^+$, 52), 244 (100), 200 (56), 128.1 (37); HRMS (EI) m/z calculated for $\text{C}_{25}\text{H}_{49}\text{NO}_3\text{Si}_2$ $[\text{M}]^+$ 467.3251, found 467.3256.

7.16. 3-(2-Isopropenyl-cyclohexanecarbonyl)-oxazolidin-2-one (24b)

The anodic cyclization was conducted using the same procedure as described for the synthesis of **20a**. This experiment used oven-dried tetraethylammonium tosylate (0.459 g, 1.5 mmol), ketene acetal **23b** (0.091 g, 0.19 mmol), 15 mL of 1:4 THF/MeOH, 2,6-lutidine (0.16 mL, 1.4 mmol), an RVC anode and cathode, a constant current of 8 mA, and 2.2 F/mol of charge. The crude product was chromatographed through a silica gel column (crude/gel=1:35) using 2–3% Et_3N in 1:1 ether/hexane as eluant in order to afford the desired product **24b** (0.033 g, 0.14 mmol, 71%) as white solid. The spectral data were as follows: ^1H NMR ($\text{CDCl}_3/300\text{ MHz}$) δ 4.66 and 4.66 (s and s, H10, 2H), 4.40–4.32 (apparent t, $J=8.1\text{ Hz}$, H1, 2H), 3.96 (t, $J=8.1\text{ Hz}$, H2, 2H), 3.88 (td, $J=11.2, 3.6\text{ Hz}$, H3, 1H), 2.38 (td, $J=11.2, 3.2\text{ Hz}$, H8, 1H), 2.02–1.94 and 1.86–1.73 (m, H4 and H7, 4H), 1.71 (s,

H9, 3H), 1.46–1.13 (m, H5 and H6, 4H); ^{13}C NMR ($\text{CDCl}_3/300\text{ MHz}$) δ 176.3, 153.5, 149.3, 109.8, 61.9, 47.0, 45.1, 42.8, 31.9, 30.5, 26.2, 25.7, 21.5; IR (neat/ NaCl) 3080, 2938, 2912, 2850, 1788, 1766, 1689, 1648, 1475, 1437, 1384, 1360, 1270, 1193, 1038, 942, 909, 759 cm^{-1} ; LRMS (EI) 237 (2), 150 (100), 135 (28); HRMS (EI) m/z calculated for $\text{C}_{13}\text{H}_{19}\text{NO}_3$ $[\text{M}]^+$ 237.1365, found 237.1362.

7.17. 3-[1-(*tert*-Butyl-dimethyl-silyloxy)-8-methyl-9-trimethylsilyl-nona-1,7-dienyl]-oxazolidin-2-one (23c)

The *tert*-butyldimethylsilyl enol ether was prepared using the same method as described above for the synthesis of ketene acetal **19a**. In this experiment, freshly distilled diisopropyl amine (0.22 mL, 1.6 mmol) in 20 mL anhydrous THF was used along with a 2.5 M solution of *n*-butyllithium in hexane (0.63 mL, 1.6 mmol), imide **22b** (0.457 g, 1.5 mmol) in 10 mL of anhydrous THF, and *tert*-butyldimethylsilyl trifluoromethanesulfonate (0.38 mL, 1.6 mmol). The crude product was chromatographed through a silica gel column (crude/gel=1:25) using 2–3% Et_3N in 1:2 ether/hexane as eluant in order to afford the desired product **23c** (0.347 g, 0.8 mmol, 56%) as an almost colorless oily liquid. The spectral data were as follows: ^1H NMR ($\text{CDCl}_3/300\text{ MHz}$) δ 5.02–4.89 (m, H8, 1H), 4.75 (t, $J=7.2\text{ Hz}$, H3, 0.35H), 4.75 (t, $J=7.2\text{ Hz}$, H3, 0.65H), 4.32 (dd, $J=8.7, 7.4\text{ Hz}$, H1, 2H), 3.74 (dd, $J=8.7, 7.4\text{ Hz}$, H2, 2H), 2.07 (dt, $J=7.2, 7.2, \text{H4}$, 2H), 2.02–1.84 (m, H7, 2H), 1.67 (m, allylic coupling, H9, 1.05H), 1.58 (m, allylic coupling, H9, 1.95H), 1.50 (s, H10, 0.7H), 1.46 (s, H10, 1.3H), 1.43–1.23 (m, H5 and H6, 4H), 0.97 (s, H13, 9H), 0.18 (s, H12, 6H), 0.023 (s, H11, 3.15H), 0.002 (s, H11, 5.85H); ^{13}C NMR ($\text{CDCl}_3/300\text{ MHz}$) δ 155.9, 139.1, 133.1, 132.8, 122.8, 122.5, 106.7, 106.7, 61.9, 45.6, 30.1, 30.0, 23.0, 29.5, 29.2, 28.6, 28.2, 26.5, 25.8, 25.6, 25.5, 23.4, 18.8, 18.2, 14.3, –0.5, –1.0, –4.5; IR (neat/ NaCl) 2954, 2930, 2857, 1766, 1683, 1472, 1402, 1249, 1041, 841, 783 cm^{-1} ; LRMS (EI) 425 ($[\text{M}]^+$, 1), 410 ($[\text{M}-\text{CH}_3]^+$, 12), 368 ($[\text{M}-\text{C}(\text{CH}_3)_2]^+$, 42), 202 (100), 160 (90); HRMS (EI) m/z calculated for $\text{C}_{22}\text{H}_{43}\text{NO}_3\text{Si}_2$ $[\text{M}]^+$ 425.2782, found 425.2773.

7.18. (S)-(–)-4-Benzyl-3-(8-methyl-9-trimethylsilyl-nona-1,7-dienyl)-oxazolidin-2-one (39a)

The imide intermediate **39a** was prepared using the procedure as described earlier for the synthesis of imides **18a** and **22b**. This experiment used the acid derived from **21b** (see above) in 90 mL of anhydrous THF, anhydrous Et_3N (5.0 mL, 35.9 mmol), trimethylacetyl chloride (1.1 mL, 8.8 mmol), oven-dried lithium chloride (0.345 g, 8.4 mmol), and (S)-(–)-4-benzyl-2-oxazolidinone (1.491 g, 8.3 mmol). The crude product was chromatographed through a silica gel column (crude/gel=1:30) with 2–3% Et_3N in 1:4 ether/hexane as eluant in order to afford the desired imide **39a** (2.729 g, 6.8 mmol, 82%) as a colorless oily liquid. The spectral data were as follows: ^1H NMR ($\text{CDCl}_3/300\text{ MHz}$) δ 7.35–7.15 (m, H4, H4', H5, H5', H6, 5H), 5.01–4.88 (m, H12, 1H), 4.69–4.59 (m, H2, 1H), 4.21–4.10 (m, H1 and H1', 2H), 3.27 (dd, $J=13.2, 3.2\text{ Hz}$, H3, 1H), 3.02–2.80 (m, H7, 2H), 2.74 (dd, $J=13.2, 9.6\text{ Hz}$, H3', 1H), 2.03–1.83 (m, H11, 2H), 1.72–1.60 (m, H8, 2H), 1.68–1.61 and 1.58–1.54 (m and m, allylic coupling, H13, 3H), 1.48 and 1.43 (s and s, H14, 2H), 1.42–1.26 (m, H9 and H10, 4H), 0.00 and

0.03 (s and s, H15, 9H); ^{13}C NMR ($\text{CDCl}_3/300\text{ MHz}$) δ 173.4, 153.5, 135.5, 133.0, 132.8, 129.5, 129.0, 127.4, 122.6, 122.3, 66.2, 55.2, 38.0, 35.6, 30.0, 29.9, 29.8, 29.0, 28.9, 28.5, 28.1, 26.4, 24.4, 24.3, 23.3, 18.7, -0.6 , -1.1 ; IR (neat/ NaCl) 3550, 3385, 2930, 2856, 1790, 1770, 1704, 1704, 1698, 1604, 1454, 1385, 1246, 1210, 1107, 1029, 875, 701 cm^{-1} ; LRMS (EI) 401 ($[\text{M}]^+$, 10), 250 (100), 73 (59); HRMS (EI) m/z calculated for $\text{C}_{23}\text{H}_{35}\text{NO}_3\text{Si}$ $[\text{M}]^+$ 401.2386, found 401.2381.

7.19. (S)-(-)-4-Benzyl-3-[1-(tert-butyl-dimethyl-silanyloxy)-8-methyl-9-trimethylsilanyl-nona-1,7-dienyl]-oxazolidin-2-one (40a)

The *tert*-butyldimethylsilyl enol ether **40a** was prepared using the same method initially as described above for the synthesis of ketene acetal **19a** above. In this experiment, freshly distilled diisopropyl amine (0.18 mL, 1.3 mmol) in 20 mL anhydrous THF was used along with a 1.6 M *n*-butyllithium (0.86 mL, 1.4 mmol), imide **39a** (0.461 g, 1.2 mmol) in 20 mL of anhydrous THF, and *tert*-butyldimethylsilyl trifluoromethanesulfonate (0.35 mL, 1.5 mmol). The crude product was chromatographed through a silica gel column (crude/gel=1:25) using 2–3% Et_3N in 1:4 ether/hexane as eluant in order to afford the desired ketene acetal **40a** (0.335 g, 0.65 mmol, 57%) as a colorless oily liquid and starting material **40a** (\sim 0.18 g, 0.45 mmol, 39%). The spectral data were as follows: ^1H NMR ($\text{CDCl}_3/300\text{ MHz}$) δ 7.36–7.12 (m, H4, H4', H5, H5', H6, 5H), 5.04–4.90 (m, H12, 1H), 4.86 (dd, $J=6.3$, 6.3 Hz, H7, 1H), 4.24–4.10 (m, H1 and H1', 2H), 4.08–3.97 (m, H2, 1H), 3.2 (dd, $J=13.5$, 3.3 Hz, H3, 1H), 2.61 (dd, $J=13.5$, 9.6 Hz, H3', 1H), 2.32–1.85 (m, H8 and H11, 4H), 1.69–1.63 (m, allylic coupling, H13, 1.59H), 1.61–1.56 (m, allylic coupling, H13, 1.41H), 1.48 and 1.43 (s and s, H14, 2H), 1.48–1.30 (m, H9 and H10, 4H), 1.00 (s, H17, 9H), 0.23 and 0.17 (s and s, H16 and H16', 6H), 0.0 and -0.02 (s and s, H15, 9H); ^{13}C NMR ($\text{CDCl}_3/300\text{ MHz}$) δ 155.5, 137.2, 135.8, 132.9, 132.7, 129.5, 129.0, 127.2, 122.6, 122.3, 109.9, 66.7, 56.3, 38.3, 38.2, 30.0, 29.9, 29.8, 29.3, 29.1, 28.4, 28.0, 26.3, 25.7, 25.6, 25.5, 23.3, 18.7, 18.1, -0.6 , -1.1 , -4.4 , -4.7 ; IR (neat/ NaCl) 3520, 3087, 3063, 3068, 2928, 2857, 1770, 1682, 1644, 1585, 1497, 1454, 1393, 1248, 1122, 1090, 1043, 838, 699 cm^{-1} ; LRMS (EI) 401 ($[\text{M}]^+$, 10), 250 (100), 73 (59); HRMS (EI) m/z calculated for $\text{C}_{23}\text{H}_{35}\text{NO}_3\text{Si}$ $[\text{M}]^+$ 401.2386, found 401.2381.

7.20. (S)-(-)-4-Benzyl-3-(2-isopropenyl-cyclohexane-carbonyl)-oxazolidin-2-one (41a)

The anodic cyclization was conducted using the same procedure as described for the synthesis of **20a**. This experiment used oven-dried tetraethylammonium tosylate (0.458 g, 1.5 mmol), ketene acetal **40a** (0.0959 g, 0.19 mmol), 15 mL MeOH, 2,6-lutidine (0.14 mL, 1.2 mmol), an RVC anode and cathode, a constant current of 8 mA, and 2.2 F/mol of charge. The crude product was chromatographed (crude/gel=1:30) through a silica gel column using 2–3% Et_3N in 1:4 ether/hexane as eluant in order to afford the desired product **41a** (0.008 g, 0.0023 mmol, 13%) as a colorless oil and imide **39a** (0.039 g, 0.1 mmol, 53%). A second chromatography (crude/gel=1:60) was performed to further separate two isomers using 2–3% Et_3N in 1:4

ether/hexane as eluant. The spectral data were as follows: *Isomer 1 (trans)*: ^1H NMR ($\text{CDCl}_3/600\text{ MHz}$) δ 7.35–7.18 (m, H4, H4', H5, H5' and H6, 5H), 4.70–4.67 (m, allylic coupling, H14 and H14, 2H), 4.67–4.61 (m, H2, 1H), 4.17–4.12 (m, H1 and H1', 2H), 3.84 (dt, $J=3.3$, 11.0 Hz, H7, 1H), 3.22 (dd, $J=2.7$, 13.5 Hz, H3, 1H), 2.74 (dd, $J=9.6$, 13.2 Hz, H3', 1H), 2.41 (dt, $J=3.3$, 11.0 Hz, H12, 1H), 2.11–2.05 (m, H9, 1H), 1.88–1.77 (m, H8, H10, and H11, 3H), 1.73 (s, H13, 3H), 1.46–1.30 (m, H8', H9', and H10', 3H), 1.28–1.19 (m, H11', 1H); ^{13}C NMR ($\text{CDCl}_3/600\text{ MHz}$) δ 176.1, 153.4, 149.5, 135.5, 129.7, 129.1, 127.5, 109.8, 66.2, 55.3, 46.8, 45.4, 38.1, 32.0, 30.6, 26.6, 26.3, 25.8, 21.7. *Isomer 2 (trans)*: ^1H NMR ($\text{CDCl}_3/600\text{ MHz}$) δ 7.34–7.19 (m, H4, H4', H5, H5', and H6, 5H), 4.79–4.77 and 4.75–4.72 (m, allylic coupling, H14 and H14', 2H), 4.68–4.63 (m, H2, 1H), 4.16–4.09 (m, H1 and H1', 2H), 3.96 (dt, $J=3.2$, 11.0 Hz, H7, 1H), 3.23 (dd, $J=3.3$, 13.5 Hz, H3, 1H), 2.62 (dd, $J=9.9$, 13.5 Hz, H3', 1H), 2.46 (dt, $J=3.2$, 11.0 Hz, H12, 1H), 2.00–1.95 (m, H8, 1H), 1.87–1.82 (m, H11, 1H), 1.82–1.78 (m, H9 and H10, 2H), 1.77–1.75 (m, allylic coupling, H13, 3H), 1.47–1.23 (m, H8', H9', H10', H11', 4H); ^{13}C NMR ($\text{CDCl}_3/600\text{ MHz}$) δ 176.3, 153.5, 149.0, 135.7, 129.7, 129.1, 127.4, 110.5, 65.9, 44.4, 47.5, 45.0, 38.1, 31.9, 30.6, 26.2, 25.7, 21.5.

7.21. (S)-(-)-4-Isopropyl-3-(8-methyl-9-trimethyl-silanyl-non-7-enoyl)-oxazolidin-2-one (39b)

The imide intermediate **39b** was prepared using the procedure as described earlier for the synthesis of imide **18a** and **22b**. This experiment used the acid derived from alcohol **21b** (0.481 g, 2.0 mmol) in 30 mL of anhydrous THF, anhydrous Et_3N (1.2 mL, 8.6 mmol), trimethylacetyl chloride (0.26 mL, 2.1 mmol), oven-dried lithium chloride (0.095 g, 2.3 mmol), and (S)-(-)-4-benzyl-2-oxazolidinone (0.276 g, 2.1 mmol). The crude product was chromatographed through a silica gel column (crude/gel=1:30) with 2–3% Et_3N in 1:5 ether/hexane as eluant in order to afford the desired imide **39b** (0.599 g, 1.7 mmol, 85%) as a colorless oily liquid. The spectral data were as follows: ^1H NMR ($\text{CDCl}_3/300\text{ MHz}$) δ 5.02–4.88 (m, H10, 1H), 4.47–4.39 (m, H2, 1H), 4.26 (apparent t, $J=9.0$ Hz, H1, 1H), 4.19 (dd, $J=9.0$, 3.3 Hz, H1', 1H), 3.05–2.78 (m, H5, 2H), 2.37 (m, H3, 1H), 2.03–1.82 (m, H9, 2H), 1.72–1.59 (m, H6, 2H), 1.68–1.63 (m, allylic coupling, H11, 1.61H), 1.59–1.56 (m, allylic coupling, H11, 1.39H), 1.49 (s, H12, 1.04H), 1.45 (s, H12, 0.96H), 1.42–1.29 (m, H7 and H8, 4H), 0.91 and 0.87 (d and d, $J=7.2$, 6.9 Hz, H4 and H4', 6H), 0.01 and -0.01 (s and s, H13, 9H); ^{13}C NMR ($\text{CDCl}_3/300\text{ MHz}$) δ 173.2, 154.0, 132.8, 132.5, 122.5, 122.2, 63.3, 58.3, 35.4, 29.8, 29.8, 29.7, 28.9, 28.7, 28.4, 28.3, 28.0, 26.2, 24.5, 24.4, 18.6, 17.9, 14.7, -0.7 , -1.3 ; IR (neat/ NaCl) 2957, 2876, 2856, 1785, 1703, 1386, 1247, 1206, 858 cm^{-1} ; LRMS (EI) 353 ($[\text{M}]^+$, 6), 202 (100), 158 (9); HRMS (EI) m/z calculated for $\text{C}_{19}\text{H}_{35}\text{NO}_3\text{Si}$ $[\text{M}]^+$ 353.2386, found 353.2384.

7.22. 3-[1-(tert-Butyl-dimethyl-silanyloxy)-8-methyl-9-trimethyl-silanyl-nona-1,7-dienyl]-(-)-4-isopropyl-oxazolidin-2-one (40b)

The *tert*-butyldimethylsilyl enol ether **40b** was prepared using the same method as described earlier for the synthesis

of ketene acetal **19a**. In this experiment, freshly distilled diisopropyl amine (0.2 mL, 1.4 mmol) in 30 mL of anhydrous THF was used along with 1.6 M *n*-butyllithium (0.87 mL, 1.4 mmol), imide **39b** (0.363 g, 1.0 mmol) in 20 mL of anhydrous THF, and *tert*-butyldimethylsilyl trifluoromethanesulfonate (0.34 mL, 1.5 mmol). The crude product was chromatographed through a silica gel column (crude/gel=1:25) using 2–3% Et₃N in 1:4 ether/hexane as eluant in order to afford the desired ketene acetal **40b** (0.423 g, 0.9 mmol, 88%) as a colorless oily liquid. The spectral data were as follows: ¹H NMR (CDCl₃/300 MHz) δ 5.02–4.88 (m, H10, 1H), 4.83–4.75 (m, H5, 1H), 4.23 (apparent t, *J*=9.0 Hz, H1, 1H), 4.07 (dd, *J*=9.3, 8.7 Hz, H1', 1H), 3.98–3.90 (m, H2, 1H), 2.22–1.84 (m, H3, H6 and H5, 5H), 1.68–1.63 and 1.59–1.55 (m and m, allylic coupling, H11, 3H), 1.49 and 1.45 (s and s, H12, 2H), 1.43–1.24 (m, H7 and H8, 4H), 0.96 (s, H15, 9H), 0.92 and 0.90 (d and d, *J*=3.3, 3.0 Hz, H4 and H4', 6H), 0.2 and 0.15 (s and s, H14 and H14', 6H), 0.02 and –0.01 (s and s, H13, 9H); ¹³C NMR (CDCl₃/300 MHz) δ 156.1, 137.7, 133.1, 132.8, 122.8, 122.5, 109.6, 63.3, 59.1, 30.0, 29.9, 29.4, 29.2, 28.9, 28.5, 28.1, 26.5, 25.8, 25.6, 25.5, 23.4, 18.8, 18.2, 17.8, 15.2, –0.5, –1.0, –4.3, –4.6; IR (neat/NaCl) 2956, 2930, 2857, 1768, 1683, 1472, 1463, 1401, 1248, 1053, 841, 784 cm^{–1}; LRMS (EI) 467 (M⁺, 11), 452 ([M–CH₃]⁺, 25), 410 (100), 244 (75), 202 (75); HRMS (EI) *m/z* calculated for C₂₅H₄₉NO₃Si₂ [M⁺] 467.3251, found 467.3248.

7.23. 3-(2-Isopropenyl-cyclohexanecarbonyl)-(S)-(-)-4-isopropyl-oxazolidin-2-one (**41b**)

The anodic cyclization was conducted using the same procedure as described for the synthesis of **20a**. This experiment used oven-dried tetraethylammonium tosylate (0.6240 g, 2.1 mmol), ketene acetal **40b** (0.1052 g, 0.23 mmol), 20 mL of a 1:1 CH₂Cl₂/MeOH mixture, 2,6-lutidine (0.2 mL, 1.33 mmol), an RVC anode and cathode, a constant current of 8 mA, and 2.2 F/mol of charge. The crude product was chromatographed through a silica gel column (crude/gel=1:40) using 2–3% Et₃N in 1:6 ether/hexane as eluant in order to afford the desired product **41b** (0.0105 g of *Isomer 1*, 0.038 mmol, 17%, and 0.0159 g of *Isomer 2*, 0.057 mmol, 25%) as colorless oil. The spectral data were as follows: *Isomer 1* (*trans*): ¹H NMR (CDCl₃/300 MHz) δ 4.70–4.65 (m, allylic coupling, H12, 2H), 4.46–4.39 (m, H2, 1H), 4.27–4.15 (m, H1 and H1', 2H), 3.90 (dt, *J*=3.6, 11.1 Hz, H5, 1H), 2.38 (dt, *J*=3.0, 13 Hz, H10, 1H), 2.32 (dq, *J*=1.2, 7.1, 7.1 Hz, H3, 1H), 2.11–2.02 and 1.88–1.76 (m, H6 and H9, 4H), 1.74–1.71 (m, allylic coupling, H11, 3H), 1.52–1.15 (m, H7 and H8, 4H), 0.90 and 0.86 (d and d, *J*=7.2, 6.9 Hz, H4 and H4', 6H); ¹³C NMR (CDCl₃/300 MHz) δ 176.0, 154.0, 149.6, 109.6, 63.5, 58.2, 46.6, 45.6, 32.1, 31.0, 29.9, 28.8, 26.3, 25.9, 21.7, 18.1; IR (neat/NaCl) 3537, 3384, 3076, 2929, 1779, 1698, 1644, 1487, 1447, 1384, 1300, 1203, 1090, 944, 892, 708 cm^{–1}; LRMS (EI) 279 (M⁺, 7), 242 (10), 150 (100); HRMS (EI) *m/z* calculated for C₁₆H₂₅NO₃ [M⁺] 279.1834, found 279.1825. *Isomer 2* (*trans*): ¹H NMR (CDCl₃/300 MHz) δ 4.77–4.73 and 4.70–4.66 (m, allylic coupling, H12, 2H), 4.47–4.40 (m, H2, 1H), 4.26–4.13 (m, H1 and H1', 2H), 3.99 (dt, *J*=3.6, 11.1 Hz, H5, 1H), 2.41 (dt, *J*=3.2, 11.4 Hz, H10, 1H), 2.27 (m, H3, 1H), 2.00–1.90 and

1.86–1.76 (m, H6 and H9, 4H), 1.75–1.72 (m, allylic coupling, H11, 3H), 1.48–1.18 (m, H7 and H8, 4H), 0.88 and 0.82 (d and d, *J*=6.9, 6.8 Hz, H4 and H4', 6H); ¹³C NMR (CDCl₃/300 MHz) δ 176.1, 154.0, 148.9, 110.3, 63.0, 58.6, 31.9, 30.5, 28.5, 27.1, 26.2, 25.6, 21.3, 18.1; IR (neat/NaCl) 3536, 3380, 3074, 2929, 1772, 1700, 1645, 1487, 1448, 1385, 1300, 1259, 1204, 1060, 894, 777, 711 cm^{–1}; LRMS (EI) 279 (M⁺, 4), 200 (12), 186 (100), 150 (71), 100 (32), 73 (57); HRMS (EI) *m/z* calculated for C₁₆H₂₅NO₃ [M⁺] 279.1834, found 279.1839.

Acknowledgements

We thank the National Science Foundation (CHE-9023698) for their generous support of our work. We also gratefully acknowledge the Washington University High Resolution NMR facility, partially supported by NIH grants RR02004, RR05018, and RR07155, and the Washington University Mass Spectrometry Resource Center, partially supported by NIHRR00954, for their assistance.

References and notes

- For a review of anodic cyclization reactions see: Moeller, K. D. *Tetrahedron* **2000**, *56*, 9527.
- For alternative approaches to the oxidation of ketene acetal derivatives see: (a) Snider, B. B.; Shi, B.; Quickley, C. A. *Tetrahedron* **2000**, *56*, 10127; (b) Ryter, K.; Livinghouse, T. *J. Am. Chem. Soc.* **1998**, *120*, 2658.
- For a review on the use of ketene dithioacetals in synthesis see: Kolb, M. *Synthesis* **1990**, 171.
- (a) For the stereochemical consequences of anodic cyclizations utilizing ketene dithioacetal groups see: Sun, Y.; Liu, B.; Kao, J.; d'Avignon, D. A.; Moeller, K. D. *Org. Lett.* **2001**, *3*, 1729; (b) For a total synthesis using a ketene dithioacetal oxidation see: Liu, B.; Duan, S.; Sutterer, A. C.; Moeller, K. D. *J. Am. Chem. Soc.* **2002**, *124*, 10101.
- For an example using an allylsilane terminating group see: Frey, D. A.; Reddy, S. H. K.; Moeller, K. D. *J. Org. Chem.* **1999**, *64*, 2805.
- (a) Hudson, C. M.; Marzabadi, M. R.; Moeller, K. D.; New, D. G. *J. Am. Chem. Soc.* **1991**, *113*, 7372; (b) Tinao-Wooldridge, L. V.; Moeller, K. D.; Hudson, C. M. *J. Org. Chem.* **1994**, *59*, 2381.
- For previous syntheses of scopadulcic acid B see: (a) Ziegler, F. E.; Wallace, O. B. *J. Org. Chem.* **1995**, *60*, 3626; (b) Overman, L. E.; Ricca, D. J.; Tran, V. D. *J. Am. Chem. Soc.* **1993**, *115*, 2042; For other related synthetic efforts see: (c) Robichaud, A. J.; Meyers, A. I. *J. Org. Chem.* **1991**, *56*, 2607; (d) Abelman, M. M.; Overman, L. E. *J. Am. Chem. Soc.* **1988**, *110*, 2328; (e) Kucera, D. J.; O'Connor, S. J.; Overman, L. E. *J. Org. Chem.* **1993**, *58*, 5304.
- Reddy, S. H. K.; Chiba, K.; Sun, Y.; Moeller, K. D. *Tetrahedron* **2001**, *57*, 5183.
- For the initial study using enol ether trapping groups see: Moeller, K. D.; Tinao, L. V. *J. Am. Chem. Soc.* **1992**, *113*, 1033.
- The oxidations were conducted using a Model 630 coulometer, a Model 410 potentiostatic controller, and a Model 420A power supply purchased from The Electrosynthesis Co., Inc. For a simple setup to try electrochemical reactions using a battery

- as a power supply see: Frey, D. A.; Wu, N.; Moeller, K. D. *Tetrahedron Lett.* **1996**, *37*, 8317.
- (a) Seyfreh, D.; Worsthorn, K. R.; Mammarella, R. E. *J. Org. Chem.* **1977**, *42*, 3104; (b) Flemming, I.; Paterson, I. *Synthesis* **1979**, 445.
 - For more recent examples of potential shifts being used to measure relative rates of cyclization see Ref. 8 as well as Sperry, J. B.; Wright, D. L. *J. Am. Chem. Soc.* **2005**, *127*, 8034.
 - A model RE-5B Ag/AgCl reference electrode from BAS was used. The electrode uses a AgCl coated Ag wire immersed in 3 M NaCl. The reference electrodes were calibrated using the ferrocene/ferrocium cation redox cycle.
 - For allylsilanes see Ref. 5. For vinylsilanes see Hudson, C. M.; Moeller, K. D. *J. Am. Chem. Soc.* **1994**, *116*, 3347.
 - For reviews see: (a) Moon, K. B.; Williams, S. F.; Masumunes, S. *The Aldol Reaction: Group III Enolates; Comprehensive Organic Synthesis*; Trost, B. M., Ed.; Pergamon: New York, NY, 1991; Vol. 2, Chapter 1.7, pp 239–275; (b) Caine, D. *Alkylation of Enols and Enolates; Comprehensive Organic Synthesis*; Trost, B. M., Ed.; Pergamon: New York, NY, 1991; Vol. 3; See in particular page 35–54; (c) Evans, D. A.; Nelson, J. V.; Taber, T. R. *Top. Stereochem.* **1982**, *12*, 1–115; (d) Evans, D. A. *Stereoselective Alkylation Reactions of Chiral Metal Enolates; Asymmetric Synthesis*; Morison, J. D., Ed.; 1984; Vol. 3, pp 1–110; (e) Ager, D. J.; Prakash, I.; Schaad, D. R. *Chem. Rev.* **1996**, *96*, 835–875; (f) Evans, D. A.; Ennis, M. D.; Mathre, D. J. *J. Am. Chem. Soc.* **1982**, *104*, 1737; (g) Evans, S. A.; Wu, L. D.; Wiener, J. J. M.; Johnson, J. S.; Ripin, D. H. B.; Tedrow, J. S. *J. Org. Chem.* **1999**, *64*, 6411; (h) Bull, S. D.; Davies, S. G.; Jones, S.; Sanganee, H. J. *J. Chem. Soc., Perkin Trans. 1* **1999**, 387; (i) Gibson, C. L.; Gillon, K.; Cook, S. *Tetrahedron Lett.* **1998**, *39*, 6733; (j) de Parrodi, C. A.; Clara-Sosa, A.; Pérez, L.; Quintero, L.; Marañón, B.; Toscano, R. A.; Aviña, J. A.; Rojas-Lima, S.; Juaristi, E. *Tetrahedron: Asymmetry* **2001**, *12*, 69; (k) Abdel-Magid, A.; Pridgen, L. N.; Eggleston, D. S.; Lantos, I. *J. Am. Chem. Soc.* **1986**, *108*, 4595–4602.
 - For examples with no added Lewis Acid to chelate the enolate oxygen and oxazolidinone carbonyl see: Heathcock, C. H. *The Aldol Addition Reaction. Asymmetric Synthesis*; Morison, J. D., Ed.; 1984; Vol. 3, pp 110–212.
 - Mukund, P. S.; Jianguo, J. *Angew. Chem. Int. Ed.* **1996**, *35*, 190–912.
 - High de's for the radical reactions can be obtained when a Lewis Acid is added to complex the carbonyl alpha to the radical and the carbonyl of the oxazolidinone. The complexation stops rotation of the chiral auxiliary. (a) Mukund, P. S.; Rheault, T. R. *J. Am. Chem. Soc.* **2000**, *122*, 8873; (b) Mukund, P. S.; Jasperse, C. P.; Jianguo, J. *J. Am. Chem. Soc.* **1995**, *117*, 10779; (c) Mukund, P. S.; Porter, N. A. *Acc. Chem. Res.* **1999**, *32*, 163; (d) Mukund, P. S.; Jianguo, J.; Sausker, J. B.; Jasperse, C. P. *J. Am. Chem. Soc.* **1999**, *121*, 7517; (e) Mukund, P. S.; Jianguo, J. *J. Am. Chem. Soc.* **1996**, *118*, 3063; (f) Mukund, P. S.; Jianguo, J. *J. Org. Chem.* **1996**, *61*, 6090.
 - The use of an oxazolidine based ketene acetal proved difficult because of problems encountered during the synthesis of the required tetrasubstituted ketene acetal substrate. With substituted oxazolidinones and a substituent on the carbon alpha to the imide, the yield of silyl enol ether formation was very low. When no substituent was placed on the oxazolidinone, attempts to generate the enolate led to deprotonation and decomposition of the oxazolidinone.

Annulated heterocycles through a radical-cation cyclization: synthetic and mechanistic studies

Jeffrey B. Sperry and Dennis L. Wright*

Burke Laboratories, Department of Chemistry, Dartmouth College, Hanover, NH 03755, United States

Received 17 August 2005; accepted 8 October 2005

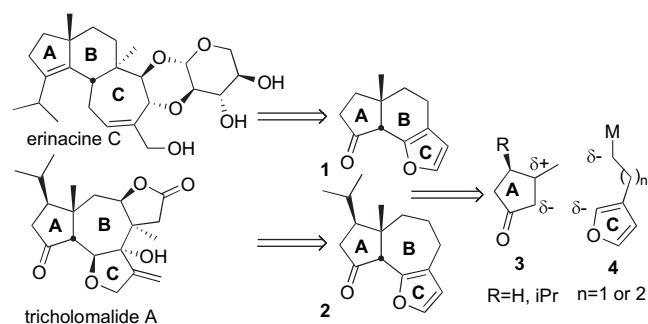
Available online 17 April 2006

Abstract—The wide range of chemical transformations possible with furans and thiophenes, especially reactions leading to dearomatization of the nucleus, make them highly versatile synthons for complex molecule construction. As part of a program to exploit this intrinsic reactivity, we have developed a convenient method to prepare annulated versions of these heterocycles. The strategy is based on a two-step annulation involving the initial conjugate addition of a heteroaryl organometallic to an enone with trapping of the enolate as the silyl enolether. Anodic oxidation of this molecule leads to the initial formation of a radical-cation that is trapped in a heteroaryl-terminated cyclization to give the annulated products.

© 2006 Published by Elsevier Ltd.

1. Introduction

Over the past several years, we have worked on the development of methodology for the synthesis of annulated furans and thiophenes based on the formation and trapping of an intermediate radical-cation generated by electrochemical oxidation at the anode. Our interest in a method of this type has been driven by the recognition that π -excessive heterocycles such as furan and thiophene can serve as versatile precursors to a wide array of non-aromatic functionality.¹ Much of the inspiration for this work has been from erinacine C² and tricholomalide A³, two terpenoid metabolites of fungal origin that act as inducers of nerve growth factor (NGF) expression (Scheme 1).



Scheme 1. Retrosynthetic analysis of terpenoid NGF inducers.

* Corresponding author. Tel.: +1 603 6466481; fax: +1 603 6463946; e-mail: dwright@dartmouth.edu

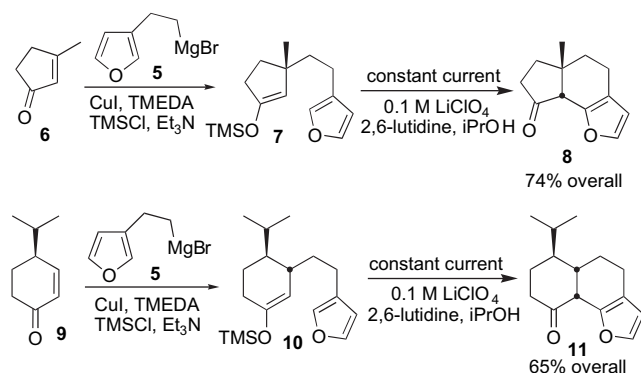
Inducers of NGF have potential for the treatment of neurodegenerative disorders such as Alzheimer's disease and amyotrophic lateral sclerosis.⁴

Retrosynthetic analysis of both structures can lead to a common angular furan framework **1** and **2** where the furan can serve as a precursor to both the carbocyclic seven-membered ring of erinacine C via a [4+3] cycloaddition as well as the furanoid ring of tricholomalide A through adjustment of oxidation states. The initial approach taken to intermediate **1** involved a vinyl furan Diels–Alder reaction between 3-methylcyclopentenone and 3-vinyl furan. Unfortunately, this process was completely ineffective and prompted us to develop new strategies for the construction of annulated furans such as **1** and **2**. We formulated a direct route to such angular-fused heterocycles that would involve the stepwise coupling of simple enone building blocks **3** with alkyl metal derivatives **4** containing a pendant furan. Addition of reagents such as **4** in a conjugate fashion to the enone would form one of the new bonds of the B-ring. The second stage of this annulation protocol was less obvious as it required the polarity reversal of one of the electron-rich carbons either at the silyl enolether or at the C2-position of the furan. Radical-cation chemistry seemed particularly well-suited to trigger the second step of the annulation as removal of one electron from either of the electron-rich π -systems could be followed by nucleophilic attack of the other group to close the central carbocyclic system. In this report, we give a full account of this annulation strategy and an update of the current scope and limitations of this methodology.

2. Results and discussion

2.1. Six-membered ring annulations with furan

The first efforts centered upon the preparation of six-membered ring systems as would be needed for an approach to the erinacines⁵ (Scheme 2).



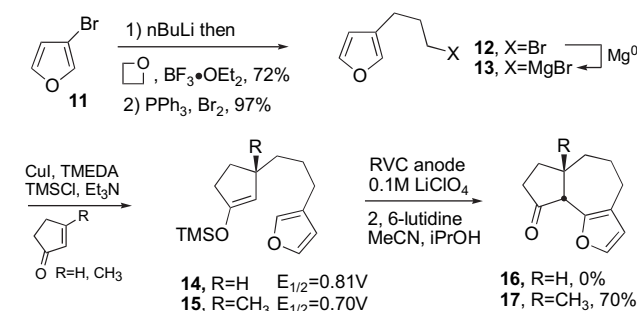
Scheme 2. Six-membered ring annulations.

The requisite furylethyl bromide could be easily prepared by lithiation of 3-bromofuran followed by addition to ethyleneoxide and conversion of the resultant alcohol to the bromide.⁶ Formation of the Grignard reagent **5** under standard conditions was followed by a copper-catalyzed addition to 3-methylcyclopentenone **6** in the presence of trimethylsilyl chloride to give the enolether **7**. The second stage of the annulation would involve the generation of a radical-cation intermediate through a one-electron oxidation of **7**. We initially examined a variety of chemical oxidants including chromium and vanadium reagents but were unable to effect the desired cyclization reaction. Instead, cleavage of the silyl enolether to the corresponding ketone dominated. The seminal work of Moeller⁷ on the electrochemical oxidation of electron-rich alkenes inspired us to examine this non-chemical method for generation of the required radical-cation. Gratifyingly, it was found that oxidation of **7** under electrochemical conditions provided high yields of a cyclized product (all annulation yields are reported as the overall yield for the two steps from the enone) as a single diastereomer **8**. The initially formed product is not the furan **8** but an acetal intermediate derived from addition of isopropanol to the intermediate oxocarbenium ion. Brief acid treatment upon work-up converts this intermediate to the furan. A detailed study on the closure of six-membered rings revealed that the reaction was effective, highly diastereoselective, and tolerant to a wide range of functional groups such as ketals, olefins, and carbamates.⁸ A related example of the enolether **10** derived from cryptone shows how three contiguous stereogenic centers are set and that groups in the allylic position of the enone **9** can effectively direct the addition of the cuprate. As in other cases, the radical-cation initiated cyclization reaction proceeds under complete kinetic control, yielding only the *cis*-descalin isomer **11**.

2.2. Seven- and five-membered ring annulations with furan

With the successful application of this method to the annulation of six-membered rings, our attention turned to the

extension of the process to seven- and five-membered ring annulations. The required furylpropyl bromide **12** needed for the seven-membered ring annulation was conveniently prepared from 3-bromofuran **11** by reaction of the derived organolithium species with trimethyleneoxide⁹ followed by bromination (Scheme 3).



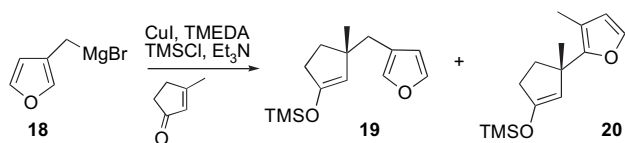
Scheme 3. Seven-membered ring annulations.

Addition of this reagent to cyclopentenone and 3-methylcyclopentenone gave the corresponding silyl enolethers **14** and **15**. A surprising trend emerged during the study of these substrates.¹⁰ Electrochemical oxidation of **14** gave only polymeric materials that precipitated onto the surface of the electrode and caused the consumption of excessive amounts of current. In contrast, electro-oxidation of **15** proceeded smoothly, giving the desired adduct **17** as the exclusive *cis*-isomer. Slightly better yields could be realized with the use of RVC electrodes in place of graphite, likely due to passivation of the graphite anode. No appreciable difference in yields for six-membered cyclizations between graphite and RVC have been observed.

A more detailed investigation revealed that not only a variety of groups could be used in place of methyl but also in the absence of this quaternary center, the reaction would not proceed. We currently favor a model whereby the full substitution at this center helps to pre-organize the substrate for ring closure, an effect related to the well-known *gem*-dialkyl effect. In the absence of this effect, trapping by the furyl terminator is too slow and the initially generated radical-cation suffers decomposition through bimolecular reactions. This model is based on the substantially different oxidation potential of the two substrate of approximately 100 mV. The oxidation potential is directly related to the energy of activation for the reaction¹¹ and indicates a more favorable and faster reaction when the additional substitution is present. The pre-organization induced by the alkyl substituent decreases the potential for formation of the radical-cation. Current efforts are focused on incorporating additional control elements into the substrate and enhancing the nucleophilicity of the furan terminator to enhance the rates of cyclization in the absence of this pre-organizing effect.

Five-membered ring closures have thus far proved elusive, owing not to difficulty in the electrochemical cyclization but in the preparation of the required silyl enolether substrates (Scheme 4).

Addition of a furylmethyl Grignard reagent **18** to a typical enone reproducibly gives mixtures of two regioisomeric silyl

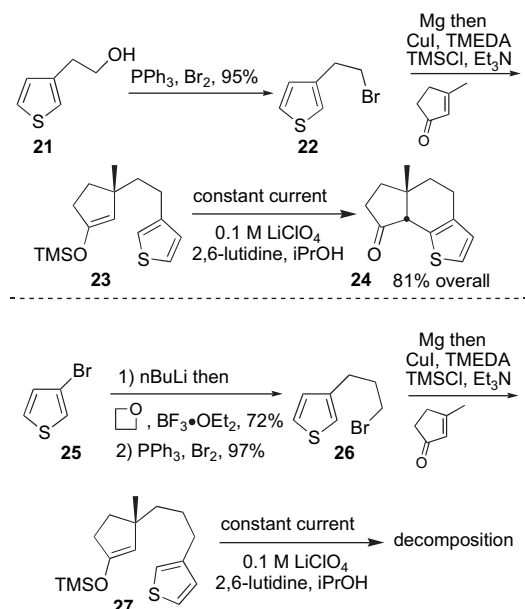


Scheme 4. Attempted application to five-membered rings.

enoleters **19** and **20** in approximately equal ratios. The undesired product **20** apparently arises from addition of the allylic metal at the C2-position of the furan followed by a subsequent isomerization. The distribution of the products has thus far been shown not to be effected by additives, solvent or copper source. Other methods for accessing enoleters such as **19** are currently under investigation.

2.3. Thiophene-based ring annulations

With the successful application of furan terminators to both six- and seven-membered ring annulations, attention was turned to studying the possibility of thiophenes in the annulation (Scheme 5). These adducts would provide access to post-annulation chemistry complimentary to the furans such as Raney nickel desulfurization and access to cyclohexadienes and arenes through Diels–Alder reaction of the derived *S,S*-dioxides.¹² The required thiophene fragment **22** was easily prepared by bromination of commercially available thiophene-3-ethanol while **26** was prepared by reaction of 3-lithiothiophene with trimethyleneoxide and bromination.



Scheme 5. Thiophene-based annulations.

Addition of the Grignard reagent derived from **22** to 3-methylcyclopentenone gave **23** that smoothly cyclized to the annulated thiophene **24** in excellent overall yield. The reaction generally mimicked that observed for the related furan except that the thiophene ring was regenerated immediately rather than being trapped by alcohol to produce a thioacetal intermediate. In contrast to furan, the seven-membered ring

system failed to undergo ring closure, even with the presence of the methyl group that was necessary for a successful furan terminated cyclization. Attempted cyclization of **27** under electrochemical conditions (graphite or RVC) failed to produce any of the desired annulated thiophene. As in the case of other failed reactions, polymeric materials could be observed as coating the electrodes.

2.4. Mechanistic studies

During the course of the synthetic investigations, it was also possible to study various aspects of the mechanism of the key electrochemical step. Two major yet convergent pathways presented themselves that differ primarily to the initial site of oxidation, the silyl enoether or the furan. Unlike chemical oxidation, electrochemical processes can be directly studied by voltammetry to gain insight into the underlying mechanism (Fig. 1).

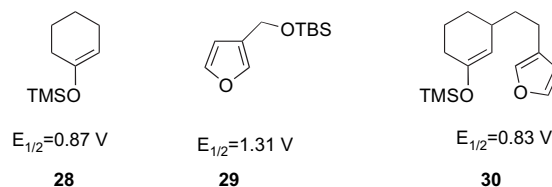
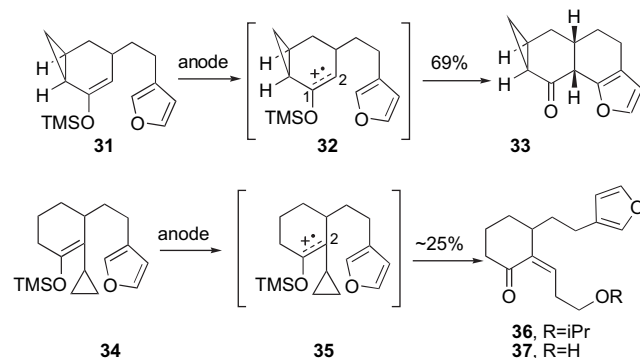


Figure 1. Oxidation potentials of model substrates.

Voltammetry of simple model systems **28** and **29** indicated that, in general, silyl enoleters had a significantly lower oxidation potential than a monoalkyl furan.⁸ Moreover, the oxidation potential of intermediate **30** showed two oxidation potentials with the lowest one closely corresponding to the model silyl enoether, thus suggesting this site as the primary position of electron loss. In an attempt to verify the site, two mechanistic probe molecules **31** and **34** were synthesized⁸ by typical cuprate chemistry that contained cyclopropanes adjacent to the two carbons of the silyl enoether (Scheme 6).

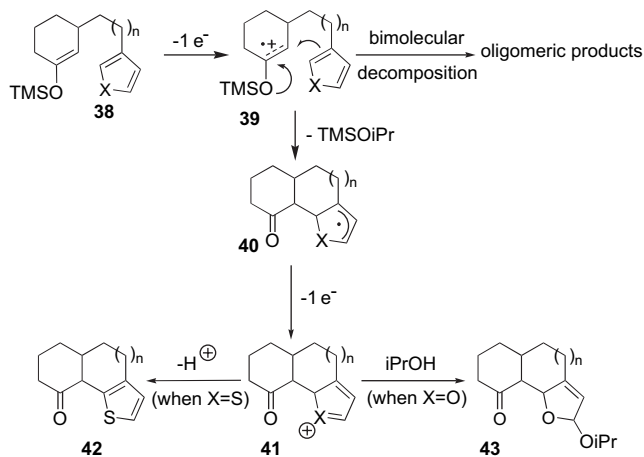


Scheme 6. Mechanistic probe molecules.

It was expected that electrochemical oxidation would generate a cyclopropyl carbinyl radical-cation **32/35** that would undergo rapid ring opening. Surprisingly, oxidation of **31** produce a high yield of the annulated product **33** with no evidence of cyclopropyl cleavage. In contrast, attempted ring closure of **34** led directly to the ring opened products **36** and **37**. These contrasting results suggest that the radical or cation localized at C1 is highly stabilized by the siloxy

group and perhaps that loss of the silyl group to generate an α -carbonyl radical is rapid. If the loss of the silyl group is rapid, then the lifetime of the initial radical-cation may be very short.

Based on these studies, we have developed a working mechanistic model for the electrochemical closure of furans and thiophenes (Scheme 7).

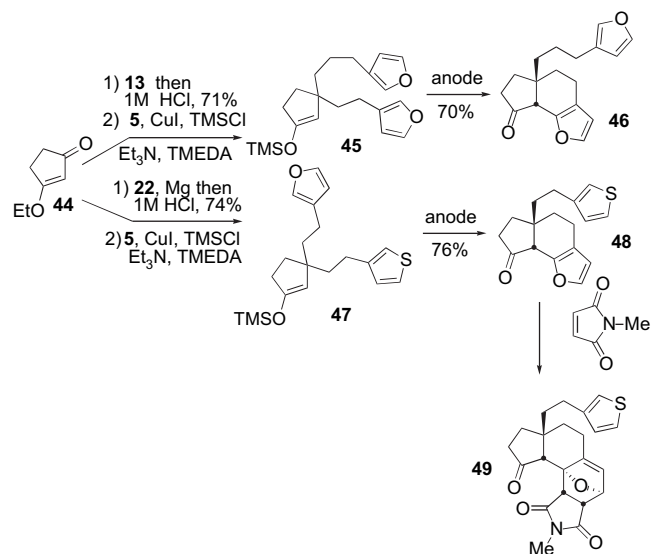


Scheme 7. Proposed mechanism for oxidative ring closure.

Loss of the first electron from the generic substrate **38** is believed to occur from the silyl enoether to produce radical-cation **39**. Rapid loss of the trimethylsilyl group as suggested by probe **31** generates an α -carbonyl radical. The furyl trap could cyclize on the radical (before or after loss of TMS) prior to a second oxidation. Attack of the heterocycle on the initial radical could lead directly to delocalized radical **40** that suffers a second electron loss to generate carbenium ion **41**. Nucleophilic trapping by an alcohol scavenger (furan case) or proton loss (thiophene case) neutralizes the final cation, giving initial products **42** and **43**. Several variations on this model are possible relating to the timing of the loss of the second electron. For example, a second oxidation to a highly reactive α -carbonyl cation could precede cyclization and attack of the heterocycle would directly give the carbenium ion **41**.

The interesting differences between six- and seven-membered ring closures is also rationalized by a mechanism that involves a highly unstable intermediate such that ring closure on the radical-cation intermediate **39** must be sufficiently fast to compete with decomposition pathways that likely involve bimolecular processes or even polymerization. The seven-membered closure illustrates this fine line as the kinetically slower cyclization competes poorly in the absence of pre-organization. Likewise, the failure of the thiophene seven-membered ring closure can be attributed to the decreased nucleophilicity of the heterocycle. To examine the potential of kinetic differences in the radical-cation cyclization, two competition substrates have been prepared and examined for competing cyclizations (Scheme 8).

Addition of heteroaryl substituted Grignard reagents to the vinylogous ester **44** followed by hydrolysis gave substituted enones that undergo a second addition to yield substrates **45**



Scheme 8. Competitive cyclizations.

and **47**. The bis-furan **45** sets up a direct competition between a six- and seven-membered ring closure with the sole product **46** arising from cyclization of the smaller ring.¹⁰ This complete selectivity is consistent with attack of the furan on the radical-cation derived from oxidation of the silyl enoether. Primary oxidation of the furan would not be expected to show significant selectivity and products arising from both closures would be observed. At this time, the possibility of initial oxidation at the heterocycle followed by rapid electron transfer from the silyl enoether cannot be ruled out. The second competition probed the difference between the two heterocycles. Again, the reaction was completely selective with the only product observed being that of closure of the furan, consistent with the greater nucleophilicity of this heterocycle. The assignment of the adduct **48** was easily made by a subsequent Diels–Alder reaction¹³ to give **49** (tentative assignment of stereochemistry). It is noteworthy that although thiophene closes slower than furan, the yields of the six-membered thiophene closure are higher than the furan. This seems to relate primarily to the sensitivity of the furan adduct, which undergoes some oxidation at the bridgehead position. The thiophene seems not to suffer from this problem.

3. Conclusions

The generation of radical-cation reactive intermediates by electrochemical oxidation forms the basis of a selective, high-yielding, and mild method for the formation of angularly fused heterocycles. Through this method, we have been able to develop routes for six-membered annulations involving both furans and thiophenes and seven-membered ring cyclizations involving furans. Mechanistic studies involving voltammetry, probe molecules, and competition reactions strongly point to a mechanism that involves primary oxidation of the silyl enoether. The radical-cation cyclization is extremely sensitive to structural effects and features that slow the rate of ring closure result in the formation of oligomeric products to the complete exclusion of the cyclic product. Several challenges for the methodology remain including the development of a five-membered ring annulation

and annulation of seven-membered ring systems in the absence of geminal disubstitution. Current efforts are also focused on the synthesis of erinacine C and tricholomalide A.

4. Experimental

4.1. General experimental

All reactions were carried out in flame-dried glassware under an atmosphere of argon unless otherwise noted. Tetrahydrofuran was freshly distilled from Na/benzophenone and dichloromethane from calcium hydride. Mixtures of TMSCl and Et₃N refer to the supernatant liquid from a centrifuged 1:1 (v/v) solution made in a flame-dried distillation receiver under argon. These solutions can be kept up to 3 days in a –20 °C freezer. All commercially available enones were distilled prior to use and kept in a freezer under an atmosphere of argon. Copper(I) iodide was either purchased at 99.999% purity (Aldrich) or purified by Soxhlet extraction with CH₂Cl₂. NMR spectra were either obtained on a Varian 300 or a Varian Inova 500 in CDCl₃ with residual chloroform as the internal standard. Elemental analyses were performed by Atlantic Microlab, Inc., and high-resolution mass spectrometry was performed by the Washington University Resource for Biomedical and Bio-organic Mass Spectrometry.

4.2. Synthesis of heteroaryl ethyl and propyl bromides

4.2.1. General trimethyleneoxide opening conditions. To a solution of either 3-bromofuran or 3-bromothiophene (137 mmol) in 137 mL of THF was added *n*-BuLi (137.5 mmol, 55 mL in hexanes) dropwise at –78 °C. After 45 min, trimethyleneoxide (137 mmol, 8.0 g) was added via syringe. Immediately following, BF₃·OEt₂ (137 mmol, 17.2 mL) was added dropwise over 30 min, keeping the reaction temperature below –70 °C. The mixture was stirred for 5 h at –78 °C and quenched by the dropwise addition of saturated sodium bicarbonate. The mixture was allowed to warm slowly overnight and the aqueous layer extracted three times with ethyl acetate. The combined organic layers were washed with water, brine, and dried over sodium sulfate. The product was concentrated in vacuo and vacuum distilled (bulb-to-bulb, ~0.1 mmHg) to provide the desired alcohol.

4.2.1.1. 3-Furan-3-yl-propan-1-ol. Isolated as a colorless oil (12.5 g, 99 mmol, 72%). IR (thin film) λ_{max} (cm⁻¹): 3359, 2936, 2862, 1502, 1449, 1382, 1157; ¹H NMR (500 MHz, CDCl₃): δ 7.35 (d, *J*=1.2 Hz, 1H), 7.23 (m, 1H), 6.28 (d, *J*=1.3 Hz, 1H), 3.54 (t, *J*=7.6 Hz, 2H), 2.52 (t, *J*=6.3 Hz, 2H), 1.82 (m, 2H), 1.29 (br s, 1H); ¹³C NMR (125 MHz, CDCl₃): δ 143.1, 139.1, 124.7, 111.2, 33.0, 32.1, 21.2. HRMS: Anal. Calcd for C₇H₁₀O₂: 126.0681; found: 126.0688.

4.2.1.2. 3-Thiophen-3-yl-propan-1-ol. Isolated as a colorless oil (13.6 g, 95 mmol, 69%). IR (thin film) λ_{max} (cm⁻¹): 3366, 3011, 2982, 1455; ¹H NMR (500 MHz, CDCl₃): δ 7.20 (dd, *J*=1.2 Hz, 1H), 7.23 (m, 1H), 6.28 (d, *J*=1.3 Hz, 1H), 3.54 (t, *J*=7.6 Hz, 2H), 2.62 (t, *J*=6.9 Hz, 2H), 1.80 (m, 2H), 1.34 (br s, 1H); ¹³C NMR (125 MHz, CDCl₃): δ 143.3, 127.5, 125.3, 123.8, 34.6, 33.4, 22.2. EI-HRMS: Anal. Calcd for C₇H₁₀OS (M⁺): 142.0452; found: 142.0463.

4.2.2. General bromination conditions. To a solution of triphenylphosphine (12.85 g, 49 mmol) in 80 mL of dichloromethane was added bromine (2.51 mL, 49 mmol) via syringe at 0 °C. The suspension was allowed to stir for 10 min and 2,6-lutidine (7 mL, 60 mmol) was added dropwise. After 15 min, a solution of the alcohol (44.6 mmol) in 20 mL of dichloromethane was added slowly via syringe. The now homogeneous solution was stirred for 5 h at 0 °C and monitored by TLC until complete. *It is imperative that excess bromine need not be added to the reaction mixture due to over-bromination of the heterocyclic ring.* Once complete, the solvent was removed in vacuo (25 °C water bath) and the slurry treated with 300 mL of pentane. The resulting slurry was passed through a plug of 6 cm Celite and 6 cm silica gel to remove the triphenylphosphine oxide. Once all of the bromide had passed through the plug, the pentane (total pentane volume=1.5 L) was removed to provide the desired bromide as colorless oils. Typical yields ranged from 90–97%. *Caution: these bromides are volatile and are serious lachrymators.*

4.2.2.1. 3-(3-Bromo-propyl)-furan, 12. Isolated as a colorless oil (8.14 g, 43.3 mmol, 97%). IR (thin film) λ_{max} (cm⁻¹): 3132, 2936, 2854, 1572, 1501, 1435, 1258; ¹H NMR (500 MHz, CDCl₃): λ 7.39 (d, *J*=1.5 Hz, 1H), 7.28 (m, 1H), 6.30 (d, *J*=1.6 Hz, 1H), 3.43 (t, *J*=6.6 Hz, 2H), 2.62 (t, *J*=7.3 Hz, 2H), 2.11 (m, 2H); ¹³C NMR (125 MHz, CDCl₃): λ 143.3, 139.5, 123.4, 111.1, 33.4, 33.0, 23.3. EI-HRMS *m/z* calcd for C₇H₉BrO (M⁺): 187.9837; found: 187.9845.

4.2.2.2. 3-(2-Bromo-ethyl)-thiophene, 22. Isolated as a colorless oil (8.05 g, 42.4 mmol, 95%). IR (thin film) λ_{max} (cm⁻¹): 3100, 2962, 1423, 1411, 1270, 1210; ¹H NMR (500 MHz, CDCl₃): δ 7.32 (dd, *J*=4.9, 2.9 Hz, 1H), 7.10 (m, 1H), 7.00 (dd, *J*=4.9, 1.2 Hz, 1H), 3.60 (t, *J*=7.6 Hz, 2H), 3.24 (t, *J*=7.6 Hz, 2H); ¹³C (125 MHz, CDCl₃): δ 139.4, 128.1, 126.1, 122.1, 34.1, 32.6. EI-HRMS *m/z* calcd for C₆H₇BrS (M⁺): 189.9452; found: 189.9455.

4.2.2.3. 3-(3-Bromo-propyl)-thiophene, 26. Isolated as a colorless oil (8.28 g, 40.6 mmol, 91%). IR (thin film) λ_{max} (cm⁻¹): 3105, 3069, 2935, 2848, 1732, 1437, 1254; ¹H NMR (500 MHz, CDCl₃): δ 7.19 (dd, *J*=5.2, 1.2 Hz, 1H), 6.98 (dd, *J*=5.9, 5.1 Hz, 1H), 6.88–6.89 (m, 1H), 3.48 (t, *J*=7.4 Hz, 2H), 3.06 (t, *J*=7.5 Hz, 2H), 2.25 (pentet, *J*=7.4 Hz, 2H); ¹³C (125 MHz, CDCl₃): δ 143.3, 127.2, 125.2, 123.8, 34.6, 33.0, 28.3. EI-HRMS *m/z* calcd for C₇H₉BrS (M⁺): 203.9608; found: 203.9611.

4.3. Synthesis of enones from 44

4.3.1. 3-(3-Furan-3-yl-propyl)-cyclopent-2-one. To a degassed solution of bromide (12) (5 mmol, 945 mg) in THF (5 mL) was added magnesium turnings (5 mmol, 122 mg). The reaction was allowed to stir for 2 h, then cooled to 0 °C. A solution of 3-ethoxy-2-cyclopenten-1-one 44 (4 mmol, 504 mg) in 5 mL of THF was then added dropwise and the bright orange solution was stirred for 2 h at 0 °C and 2 h at 25 °C. The reaction was quenched by adding 20 mL of 1 M HCl and stirred for 4 h. The aqueous layer was extracted twice with 50 mL of EtOAc. The combined organic layers were washed with 20 mL of saturated NaHCO₃, 20 mL of

water, and 20 mL of brine. After drying over sodium sulfate and concentrating, the crude enone was subjected to flash silica gel chromatography (5:1 Hex/EtOAc → 1:1 Hex/EtOAc) to provide the enone as a pale-yellow oil (2.84 mmol, 504 mg, 71%) which solidified in a $-20\text{ }^{\circ}\text{C}$ freezer. IR (neat) λ_{max} (cm^{-1}) 2930, 1667, 1622, 1251; ^1H NMR (500 MHz) δ 7.37 (dd, $J=2.9, 1.7$ Hz, 1H), 7.23 (s, 1H), 6.27 (d, $J=2.8$ Hz, 1H), 5.96 (s, 1H), 2.57 (m, 2H), 2.49 (t, $J=7.6$ Hz, 2H), 2.44 (t, $J=7.6$ Hz, 2H), 2.40 (m, 2H), 1.86 (pentet, $J=7.6$ Hz, 2H); ^{13}C NMR (125 MHz) δ 210.3, 182.7, 143.2, 139.2, 129.8, 124.3, 111.0, 35.5, 33.1, 31.8, 27.5, 24.6; EI-HRMS m/z calcd for $\text{C}_{12}\text{H}_{14}\text{O}_2$ (M^+): 190.0994; found 190.0996.

4.3.2. 3-(2-Thiophen-3-yl-ethyl)-cyclopent-2-enone. To a degassed solution of bromide (**22**) (23.7 mmol, 4.5 g) in THF (24 mL) was added magnesium turnings (23.7 mmol, 492 mg). The reaction was allowed to stir for 2 h, then cooled to $0\text{ }^{\circ}\text{C}$. A solution of 3-ethoxy-2-cyclopenten-1-one **44** (15.8 mmol, 2.0 g) in 10 mL of THF was then added dropwise and the bright orange solution was stirred for 2 h at $0\text{ }^{\circ}\text{C}$ and 2 h at $25\text{ }^{\circ}\text{C}$. The reaction was quenched by adding 60 mL of 1 M HCl and stirred for 4 h. The aqueous layer was extracted twice with 100 mL of EtOAc. The combined organic layers were washed with 50 mL of saturated NaHCO_3 , 50 mL of water, and 50 mL of brine. After drying over sodium sulfate and concentrating, the crude enone was subjected to flash silica gel chromatography (5:1 Hex/EtOAc → 1:1 Hex/EtOAc) to provide the enone as a white solid (3.37 g, 17.5 mmol, 74%). Isolated as a white solid (mp $91.5\text{--}93\text{ }^{\circ}\text{C}$). IR (neat) λ_{max} (cm^{-1}) 2930, 1667, 1622, 1251; ^1H NMR (500 MHz): δ 7.29 (dd, $J=4.9, 2.8$ Hz, 1H), 6.99 (m, 1H), 6.97 (dd, $J=4.9, 1.5$ Hz, 1H), 6.00 (m, 1H), 2.96 (t, $J=7.3$ Hz, 2H), 2.77 (t, $J=8.1$ Hz, 2H), 2.61 (m, 2H), 2.42 (m, 2H); ^{13}C NMR (125 MHz): δ 210.2, 181.9, 141.1, 130.1, 128.0, 126.1, 120.8, 35.5, 34.4, 31.9, 27.9. Anal. Calcd for $\text{C}_{11}\text{H}_{12}\text{OS}$: C, 68.71; H, 6.29; O, 8.32; S, 16.68; found: C, 68.94; H, 6.47; O, 8.23; S, 16.57.

4.4. General cuprate conditions

A solution of the bromide (6 mmol) in 6 mL of THF was degassed by sonication for 10 min. Magnesium turnings (previously washed with 1 M HCl, water, acetone, and diethyl ether) (144 mg, 6 mmol) were added and stirred for 2.5 h or until mostly dissolved. The dark solution was cooled to $0\text{ }^{\circ}\text{C}$ and CuI (1.2 mmol, 228 mg) was added. The black slurry was stirred for 20 min then cooled to $-78\text{ }^{\circ}\text{C}$. A 1:1 solution of $\text{Et}_3\text{N/TMSCl}$ (6 mL) was added dropwise followed by TMEDA (0.98 mL, 6 mmol). After 10 min, a solution of the desired enone (4.6 mmol) in 3 mL of THF was added dropwise at $-78\text{ }^{\circ}\text{C}$. If done correctly, the slurry will turn yellow upon addition of enone. The mixture was allowed to stir for 4 h and allowed to warm to room temperature over 1 h. The now black solution was placed into a $-20\text{ }^{\circ}\text{C}$ freezer overnight. The reaction was quenched by pouring the mixture into ice-cold saturated ammonium chloride (30 mL) and pentane (60 mL) in a separatory funnel. The organic layer was washed with saturated sodium bicarbonate and brine and dried over sodium sulfate. The crude enolether was concentrated in vacuo and taken forward without further purification.

4.5. General electrolysis conditions

Electrolyses were carried out with either a custom-made electrode system consisting of alternating carbon (anode) and stainless steel (cathode) electrodes, or with reticulated vitreous carbon (RVC) fixed onto a carbon rod serving as the anode and another carbon rod serving as the cathode. No attempts were made to exclude air from the prior example, but the latter requires degassing by sonication for reproducible yields. All solvents were purchased at the highest purity and used without further purification. Lithium perchlorate and 2,6-lutidine were also used without further purification. RVC was purchased from Electrolytica, Inc.

4.5.1. Electrolysis with carbon/stainless steel electrodes.

To the crude enolether generated from the cuprate addition (4.6 mmol) was added a 4:1 $\text{CH}_3\text{CN}/i\text{-PrOH}$ (230 mL) and 2,6-lutidine (18.4 mmol, 2.14 mL). Lithium perchlorate (2.48 g, 23 mmol) was then added and allowed to dissolve. An electrode system consisting of alternating carbon and stainless steel plates (five stainless steel and four carbon) was submerged and connected to the potentiostat so that the stainless steel plates acted as the cathode and the carbon plates as the anode. In order to determine the surface area of the electrode (anode), the carbon plates were measured to the depth of the solution and the width of the plate and multiplied by four. The potentiostat was then activated and the current necessary for a current density = $1\text{ mA}/\text{cm}^2$ was dialed in and locked. The reaction was checked by TLC once 2.2 F/mol were consumed and, if complete, the current was stopped. If the reaction was not yet complete, then the reaction was closely monitored by TLC until completion (usually every 10 min). The reaction was worked up by concentrating the reaction solution and partitioning the crude product between ether (100 mL) and 1 M HCl (60 mL). The aqueous layer was extracted three times and the combined organic layers washed again with 1 M HCl, water, saturated sodium bicarbonate, brine, and dried over sodium sulfate. After concentrating, the product was purified by flash chromatography (typical gradient elution conditions were 20:1 hexanes/ethyl acetate → 10:1 hexanes/ethyl acetate). *It is imperative that the silica gel be degassed before chromatography to obtain reported yields* (for procedure, see Ref. 8).

4.5.2. Electrolysis with RVC/carbon electrodes.

To the crude enolether generated from the cuprate addition (4.6 mmol) was added a 4:1 $\text{CH}_3\text{CN}/i\text{-PrOH}$ (230 mL) and 2,6-lutidine (18.4 mmol, 2.14 mL). Lithium perchlorate (2.48 g, 23 mmol) was then added and allowed to dissolve. An electrode system consisting of two carbon rods (diameter = 7 mm, serving as the cathode) and one carbon rod with an approximately 1 cm^3 piece of RVC (serving as the anode) attached at the end was submerged and purged with argon. After 5 min, the solution was degassed by sonication for 15 min. The carbon rods were connected to the potentiostat accordingly, via alligator clips. The optimized current must be determined through several experimental trials and is dependent upon scale and substrate. On this scale (4.6 mmol), 8 mA was passed until 2.3 F/mol were consumed. The reaction was worked up by concentrating the reaction solution and partitioning the crude product between ether (100 mL) and 1 M HCl (60 mL). The aqueous layer was extracted

three times and the combined organic layers washed again with 1 M HCl, water, saturated sodium bicarbonate, brine, and dried over sodium sulfate. After concentrating, the product was purified by flash chromatography (typical gradient elution conditions were 20:1 hexanes/ethyl acetate → 10:1 hexanes/ethyl acetate). *Again, It is imperative that the silica gel be degassed before chromatography to obtain reported yields.*

4.5.2.1. *cis*-5a-Methyl-4,5,5a,6,7,8a-hexahydro-1-oxa-as-indacen-8-one, 8. Isolated as a white solid (mp 42–43 °C, 74%); IR (KBr pellet) λ_{\max} (cm⁻¹) 2959, 2862, 1742, 1625, 1550, 1050; ¹H NMR (300 MHz): δ 7.35 (dd, *J*=1.9 Hz, 1H), 6.21 (*J*=1.9 Hz, 1H), 3.00 (s, 1H), 2.51 (m, 2H), 2.41 (m, 2H), 2.00 (m, 1H), 1.81 (m, 1H), 1.62 (m, 2H), 1.19 (s, 3H); ¹³C NMR (125 MHz): δ 215.1, 144.7, 142.6, 116.7, 110.0, 54.9, 40.2, 35.5, 33.1, 31.7, 25.5, 19.0. Anal. Calcd for C₁₂H₁₄O₂: C, 75.76; H, 7.42; found: C, 75.64; H, 7.51.

4.5.2.2. *cis*-6-Isopropyl-4,5a,6,7,8,9a-hexahydro-5H-naphtho[1,2-b]furan-9-one, 11. Isolated as a colorless oil that solidified in a –20 °C freezer, (65%). IR (neat) λ_{\max} (cm⁻¹): 2927, 1717, 1634, 1511; ¹H NMR (500 MHz, CDCl₃) δ 7.40 (dd, *J*=2.0, 0.9 Hz, 1H), 6.21 (d, *J*=2.0 Hz, 1H), 3.59 (d, *J*=11.2 Hz, 1H), 2.43–2.60 (m, 4H), 2.10–2.23 (m, 3H), 1.87 (qd, *J*=11.5, 2.2 Hz, 1H), 1.78 (tt, *J*=11.5, 3.4 Hz, 1H), 1.54–1.63 (m, 1H), 1.39 (dddd, *J*=30.5, 24.4, 11.7, 5.6 Hz, 1H), 1.03 (d, *J*=6.9 Hz, 3H), 0.80 (d, *J*=7.1 Hz, 3H); ¹³C NMR: δ 208.9, 146.8, 142.6, 119.4, 110.1, 52.9, 46.5, 46.1, 41.4, 27.4, 26.8, 26.5, 22.1, 21.7, 15.0. EI-HRMS *m/z* calcd for C₁₅H₂₀O₂ (M⁺): 232.1463; found: 232.1465.

4.5.2.3. *cis*-6a-Methyl-5,6,6a,7,8,9a-hexahydro-4H-azulenol[4,5-b]furan-9-one, 17. Isolated as a colorless oil, which solidified in a –20 °C freezer, (61% carbon/stainless steel, 70% RVC/carbon) IR (neat) λ_{\max} (cm⁻¹) 2930, 1715, 1631, 1505, 1251, 1107; ¹H NMR (500 MHz) δ 7.28 (d, *J*=1.7 Hz, 1H), 6.18 (d, *J*=1.7 Hz, 1H), 3.37 (s, 1H), 2.49–2.55 (m, 1H), 2.43 (ddd, *J*=8.7, 2.7, 1.0 Hz, 1H), 2.41 (dd, *J*=10.6, 8.4 Hz, 1H), 2.31–2.36 (m, 1H), 1.84–1.99 (m, 2H), 1.70–1.72 (m, 4H), 1.27 (s, 3H); ¹³C NMR (125 MHz) δ 215.4, 145.3, 141.3, 121.9, 113.4, 62.0, 40.2, 39.3, 37.6, 35.1, 26.1, 25.9, 22.5. EI-HRMS *m/z* calcd for C₁₃H₁₆O₂ (M⁺): 204.1150; found: 204.1137.

4.5.2.4. *cis*-5a-Methyl-4,5,5a,6,7,8a-hexahydro-1-thia-as-indacen-8-one, 24. Isolated as a white solid (mp 70.1–70.8 °C, 81%). IR (neat) λ_{\max} (cm⁻¹): 2922, 2855, 17,454, 1454, 1433, 1381; ¹H NMR (500 MHz, CDCl₃): δ 7.19 (dd, *J*=5.1, 0.5 Hz, 1H), 6.80 (dd, *J*=5.1, 0.5 Hz, 1H), 3.04 (s, 1H), 2.68–2.71 (m, 2H), 2.39–2.47 (m, 2H), 2.02 (ddd, *J*=17.5, 8.7, 4.4 Hz, 1H), 2.01 (dt, *J*=13.1, 9.5 Hz, 1H), 1.60–1.72 (m, 2H), 1.24 (s, 3H); ¹³C NMR (125 MHz): δ 215.8, 134.3, 129.4, 126.6, 124.2, 56.5, 39.4, 35.2, 33.5, 31.2, 25.4, 22.4. Anal. Calcd for C₁₂H₁₄OS: C, 69.86; H, 6.84; O, 7.76; S, 15.54; found: C, 69.83; H, 6.85; O, 7.78; S, 15.46.

4.5.2.5. *cis*-5a-(3-Furan-3-yl-propyl)-4,5,5a,6,7,8a-hexahydro-1-oxa-as-indacen-8-one, 46. Isolated as a viscous colorless oil. IR (neat) λ_{\max} (cm⁻¹) 2933, 1717, 1630,

1505, 1107; ¹H NMR (500 MHz) δ 7.35–7.36 (m, 2H), 7.21–7.22 (m, 1H), 6.27 (s, 1H), 6.22 (d, *J*=1.6 Hz, 1H), 3.03 (s, 1H), 2.39–2.47 (m, 6H), 1.97 (ddd, *J*=13.2, 7.9, 5.1 Hz, 1H), 1.83–1.89 (m, 1H), 1.75 (dt, *J*=13.7, 4.4 Hz, 1H), 1.57–1.69 (m, 4H) 1.37–1.44 (m, 1H); ¹³C NMR (125 MHz) δ 215.4, 145.2, 143.1, 142.9, 139.1, 124.9, 116.9, 111.0, 110.2, 55.0, 43.4, 37.4, 35.5, 31.0, 28.7, 25.5, 24.5, 19.0. EI-HRMS *m/z* calcd for C₁₈H₂₀O₃ (M⁺): 284.1412; found: 284.1412.

4.5.2.6. *cis*-5a-(2-Thiophen-3-yl-ethyl)-4,5,5a,6,7,8a-hexahydro-1-oxa-as-indacen-8-one, 48. Isolated as a viscous, pale-yellow oil (1.00 g, 3.5 mmol, 76%), which solidified in a –20 °C freezer. IR (thin film) λ_{\max} (cm⁻¹): 3104, 2920, 2856, 1745, 1502, 1453; ¹H NMR (500 MHz): δ 7.37 (dd, *J*=1.9, 0.7 Hz, 1H), 7.26–7.27 (m, 1H), 6.94–6.95 (m, 2H), 6.24 (d, *J*=1.7 Hz, 1H), 3.10 (s, 1H), 2.71–2.75 (m, 2H), 2.52–2.64 (m, 2H), 2.44–2.48 (m, 2H), 1.93–2.07 (m, 3H), 1.85 (dt, *J*=13.9, 4.7 Hz, 1H), 1.64–1.76 (m, 2H), 1.17–1.28 (m, 1H); ¹³C NMR (125 MHz): δ 215.1, 145.2, 143.0, 142.4, 128.3, 125.9, 120.2, 116.9, 110.3, 55.1, 43.5, 38.6, 35.6, 31.1, 28.6, 24.9, 19.1. EI-HRMS *m/z* calcd for C₁₇H₁₈O₂S: 286.1028; found: 286.1040.

Acknowledgements

We are grateful to the National Science Foundation for support of this work.

References and notes

- Wright, D. L. *Prog. Heterocycl. Chem.* **2005**, x, 1.
- Kawagishi, H.; Shimada, A.; Shirai, R.; Okamoto, K.; Ojima, F.; Sakamoto, H.; Ishiguro, Y.; Furukawa, S. *Tetrahedron Lett.* **1994**, 35, 1569.
- Tsukamoto, S.; Macabalang, A. D.; Nakatani, K.; Obara, Y.; Nakahata, N.; Ohta, T. *J. Nat. Prod.* **2003**, 66, 1578.
- Carswell, S. *Exp. Neurol.* **1993**, 124, 36.
- Wright, D. L.; Whitehead, C. R.; Sessions, E. H.; Ghiviriga, I.; Frey, D. A. *Org. Lett.* **1999**, 1, 1535.
- Whitehead, C. R.; Sessions, E. H.; Ghiviriga, I.; Wright, D. L. *Org. Lett.* **2002**, 4, 3763.
- (a) Moeller, K. D.; New, D. G. *Tetrahedron Lett.* **1994**, 35, 2857; (b) New, D. G.; Tesfai, Z.; Moeller, K. D. *J. Org. Chem.* **1996**, 61, 1578; For an excellent review see: Moeller, K. D. *Tetrahedron* **2000**, 56, 9527; For application in total synthesis see: (c) Mihelcic, J.; Moeller, K. D. *J. Am. Chem. Soc.* **2003**, 125, 36; (d) Mihelcic, J.; Moeller, K. D. *J. Am. Chem. Soc.* **2004**, 126, 9106.
- Sperry, J. B.; Whitehead, C. R.; Ghiviriga, I.; Walczak, R. M.; Wright, D. L. *J. Org. Chem.* **2004**, 69, 3726.
- Clayden, J.; Kenworthy, M. N. *Org. Lett.* **2002**, 4, 787.
- Sperry, J. B.; Wright, D. L. *J. Am. Chem. Soc.* **2005**, 127, 8034.
- (a) Zuman, P. *Prog. Phys. Org. Chem.* **1967**, 5, 81; (b) Moeller, K. D.; Tino, L. V. *J. Am. Chem. Soc.* **1992**, 114, 1033.
- Nakayama, J.; Sugihara, Y. *Top. Curr. Chem.* **1999**, 205, 131.
- For related cases of Diels–Alder reactions on annulated furans see: Sperry, J. B.; Constanzo, J. R.; Jasinski, J.; Butcher, R. J.; Wright, D. L. *Tetrahedron Lett.* **2005**, 46, 2789.

A computational study of solution effects on the disproportionation of electrochemically generated polycyclic aromatic hydrocarbon radical anions. Thermodynamics and structure

Albert J. Fry*

Chemistry Department, Wesleyan University, Middletown, CT 06459, USA

Accepted 15 October 2005

Available online 27 April 2006

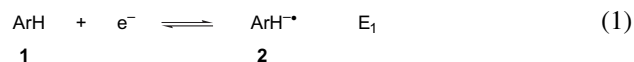
Abstract—Density functional quantum chemical methods are used to predict the thermodynamics of disproportionation of electrochemically generated polycyclic aromatic hydrocarbon radical anions (**2**) into the corresponding neutral species (**1**) and dianions (**3**). The computations reveal the overwhelming influence of solvation effects upon the disproportionation equilibrium. By comparison, the effect of ion pairing between **3** and the cation of the supporting electrolyte (R_4N^+) is modest but real. The computational results can be combined with a variety of entropy effects to calculate the spacing ΔE between the first and second reduction potentials of **1** within 100–150 mV. The highly asymmetric structures of the ion pairs between **3** and R_4N^+ show little evidence for steric hindrance to ion pairing, yet the computations do show that the strength of the ion pairs does appear to diminish with increasing size of the R group. The strength of the ion pairs with small cations appears to arise out of the large charge-to-size ratio in such cations.

© 2006 Elsevier Ltd. All rights reserved.

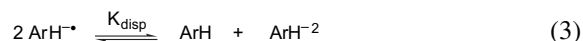
1. Introduction

The most fundamental process in electrochemical reduction of organic substrates, and indeed most reduction and oxidation processes in organic chemistry in general, is injection of an electron into the LUMO orbital of an organic substrate. For most substances, especially those containing heteroatoms, the initial electron transfer is quickly followed by a rapid chemical reaction, indeed often by a cascade of coupled chemical processes initiated by the electron transfer. This makes it quite difficult to study the nature and characteristics of the initial step itself. It has been recognized for many years that reductions of polycyclic aromatic hydrocarbons (PAH's) in aprotic media offer the best opportunity to study such processes: (a) PAH's contain no heteroatoms; (b) electron transfer to the PAH affords long-lived anion radicals, which can be studied by a variety of spectroscopic methods, and (c) a wide variety of PAH's are available, which permits, inter alia, studies of the correlation of redox potentials and electrochemical reactivity with structure.¹ Many such substances also undergo further addition of a second electron at more negative potential to afford a dianion. Dianions are much more reactive toward trace electrophilic impurities in the solvent than the corresponding radical anions, but reversible behavior can be observed in highly

purified media,^{2–5} permitting acquisition of thermodynamically valid data. A particularly significant property of the PAH in such media is the difference in ΔE (in volts) between the first and second reduction potentials (E_1 and E_2 , respectively) of the hydrocarbon. It is readily shown that ΔE is a measure of K_{disp} , the equilibrium constant for disproportionation of the arene radical anion (**2**) into the neutral (**1**) and dianion (**3**) species (Scheme 1). The three species are interrelated via the disproportionation equilibrium (Eq. 3); thus, the study of processes involving the dianion can be used to obtain information about the properties of the radical anion itself. Ion pairing can be accommodated within this schema by incorporating an additional equation (Eq. 4) representing formation of the ion pair between the dianion and the cation of the supporting electrolyte (Scheme 2).



Subtracting Eq 1 from Eq 2, one has:



$$\Delta G_{\text{disp}} = -nF\Delta E = -nF(E_2 - E_1) = -RT \ln K_{\text{disp}}$$

Scheme 1.

Keywords: Radical anions; Ion pairing; Polycyclic aromatic hydrocarbons; Density functional computations; Electrochemically generated dianions.

* Tel.: +1 860 685 2622; fax: +1 860 685 2211; e-mail: afry@wesleyan.edu



Scheme 2.

We pointed out a number of years ago that it ought to be possible to obtain an estimate of ΔE and thus, K_{disp} by computation of the energies of species 1–3.⁶ We found in fact, however, that estimates of ΔE using energies computed by a semi-empirical quantum mechanical method differed by almost an order of magnitude from the experimentally measured values; the theoretical values lie in the range of 4–5 V in contrast to the typical experimental values of 0.5–0.7 V.⁶ While appreciating that part of the discrepancy might have been due to the relatively primitive computational method available at that time, we suggested it to be much more likely that the principal contributors are solvation and ion pairing effects, which were not included in the computations. Because of the high degree of charge on the dianion 3, it should be stabilized substantially more than either 1 or 2 by these effects. Both effects would have the effect of displacing E_2 to more positive potentials and thus reducing ΔE to the experimental value. This interpretation is now generally accepted. Several laboratories have made further inroads into understanding the significance of the value of ΔE for several systems. Evans and Hu assumed a series of PAH's to be approximately spherical and estimated the spherical radius of each PAH.⁷ They then estimated the corresponding values of ΔG_{disp} from Born theory, considering the hydrocarbons simply as structureless chargeable spheres. Values of ΔG_{disp} for a series of PAH's calculated from the corresponding enthalpies of 1–3 by the AM1 semi-empirical method agreed closely with those calculated from Born theory, suggesting that (in vacuum) ΔE is 'almost entirely electrostatic in origin'.⁷ Kubota et al. reached similar conclusions, again using Born theory to estimate the solvation energies.⁸ Both groups were aware of the fact that ion pairing and solvation act in the same way upon ΔE . However, a problem arises when one wishes to dissect the discrepancy between theory and experiment further into the individual contributions of solvation and ion pairing. No experimental method can do so. Even the magnitude of this discrepancy is not known with certainty for *any* PAH because of the rather low accuracy of the semi-empirical methods that have been generally applied to this problem. Development of sufficiently fast computers in recent years has permitted the use of an ab initio theory with rather large basis sets in structure calculations even for molecules as large as these. This, together with the development of DFT (density functional) theory, which permits inclusion of electron correlation into the calculations at reasonable computational cost, has permitted the application of quantum chemical methods to relatively large molecular systems with excellent accuracy.⁹ In addition and of critical importance to studies such as these, the development of good methods for computing solvation energies within the ab initio framework permits the extension of computational methods to experimental situations in solution. The polarized continuum model (PCM), for example, though grounded in Born theory, discards the assumption of a molecule as a sphere (ill-founded in the case of PAH's)

in favor of a more realistic model consisting of a series of spheres centered on each nonhydrogen atom.¹⁰ We recently reported¹¹ a study in which ΔE 's for reduction of the PAH's anthracene (4) and perylene (5) in dimethylformamide (DMF) in the presence of tetraethylammonium ion were computed to surprisingly good accuracy (100–200 mV) by a DFT method, including estimation of solvation energies by the PCM procedure. The calculations showed that at least 98% of the difference between the computed (essentially gas phase) and experimental values of ΔE is due to differential solvation effects favoring the dianion 2. A corollary of this result is that ion pairing plays a very modest role in such systems. Still, it is known that ΔE is sensitive to the size of the electrolyte cation, suggesting that ion pairing does make a real contribution in these systems.^{2,6,12,13} A number of investigators, including our group, have found that the value of ΔE for any particular hydrocarbon depends on the nature of the cation of the supporting electrolyte.^{2,6} The data of Jensen and Parker for the reduction of 4 and 5 in the presence of a series of tetraalkylammonium ions illustrate the phenomenon clearly (Table 1).² A regular pattern can be noted in which ΔE is relatively large for Me_4N^+ ion, reaches a minimum for Et_4N^+ , and increases again as the size of R increases. The effect of increased ΔE for large tetraalkylammonium ions has been observed with hydrocarbons other than PAH's, including cyclooctatetraene⁶ and a series of 15,16-dialkyl-15,16-dihydropyrenes.^{14,15} The increase has been interpreted by all commentators on this effect as arising from steric hindrance to ion pairing of R_4N^+ to the hydrocarbon dianion (3) as R increases in size. It was not possible in our previous work to address the dependence of ΔE upon electrolyte size for electrolytes larger than tetraethylammonium because the calculations on ion pairing of cations larger than Et_4N^+ to large arene dianions such as 4 or 5 would have been impractical with our previous resources. However, recent acquisition of a multiprocessor parallel computer in this laboratory has now permitted an attack on such problems. We report herein the results of such a study. The present study has two aims: (a) to define more closely the thermodynamics, both enthalpy and entropy, of ion pairing and solvation interactions between the larger tetraalkylammonium ions and arene dianions and (b) to develop a clearer picture of the structure of such ion pairs through DFT computations. The computational results provide a number of new insights into the phenomena that operate in these systems.

Table 1. Experimental first and second voltammetric reduction potentials of some polycyclic aromatic hydrocarbons (0.001 M) in dimethylformamide solution containing various tetraalkylammonium supporting electrolytes (0.1 M)

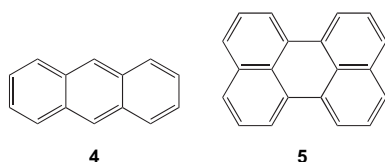
Arene	Electrolyte cation	$-E_1$ (V) ^{a,b}	$-E_2$ (V) ^{a,b}	ΔE (V) ^c
4	Me_4N^+	1.920	2.650	0.730
4	Et_4N^+	1.915	2.585	0.670
4	Pr_4N^+	1.910	2.650	0.740
4	Bu_4N^+	1.905	2.655	0.750
5	Me_4N^+	1.620	2.230	0.610
5	Et_4N^+	1.635	2.180	0.545
5	Pr_4N^+	1.625	2.205	0.580
5	Bu_4N^+	1.610	2.205	0.595

^a Potential versus SCE.

^b See Ref. 2.

^c $\Delta E = -(E_2 - E_1)$.

Jensen and Parker ascribed the relatively large value of ΔE with Me_4N^+ ion to the incursion of solvent-separated ion pairs with this species.² It is possible, however, that the small Me_4N^+ ion is itself solvated, i.e., surrounded by a shell of solvent molecules that prevent it from approaching the dianion closely. This ‘specific solvation’ effect, which would not be accounted for in the standard PCM method, would also have a tendency to increase ΔE . We have deferred a computational decision between these alternatives at this time; it can be expected to be computationally demanding because of the need to include specific solvent molecules into the calculation. This issue is currently under investigation in this laboratory and will be reported on separately when the calculations are complete.



2. Results and discussion

2.1. Radical anion disproportionation equilibria

Computed values for the disproportionation equilibrium for the three hydrocarbons both in the presence and absence of solvent are given in Table 2. The energies of species 1–3 for compounds 4 and 5 have been reported previously.¹¹ We found earlier¹¹ that ΔH for the disproportionation reaction (Eq. 3) is almost +100 kcal/mol in the gas phase for anthracene (4) and pyrene (5) (column 3 of Table 2). This corresponds to a peak spacing ΔE_p of about 4 V in the gas phase. However, as column 6 of the table shows, solvation effects have a major effect on the equilibrium, such that in solution ΔG is computed to be not more than 20 kcal/mol, or less than 1 V. The data in columns 3 and 6 represent what may be considered as the ‘intrinsic’ (in the absence of ion pairing) disproportionation free energies of the two radical anions in the gas phase and in a polar organic solvent, respectively. For comparison purposes, the corresponding computed data for benzene, naphthalene, and chrysene are shown as well, although for the first two of these substances ΔE cannot be determined experimentally because E_2 for them is at too negative a potential to be measured in typical

Table 3. Computed solvation energies of arene species in acetonitrile^a

Arene	No. of carbon atoms	Neutral (kcal/mol)	Anion radical (kcal/mol)	Dianion (kcal/mol)	Dianion solvation energy/carbon atom (kcal/mol)
Benzene	6	−4.1	−50.0	−159.0	−26.5
Naphthalene	10	−5.7	−49.7	−163.3	−16.3
Anthracene	14	−7.3	−47.2	−162.9	−11.6
Chrysene	18	−8.8	−46.1	−154.3	−8.6
Perylene	20	−8.9	−45.7	−152.3	−7.6

^a Solvation energies were computed at the B3LYP/6-311+G* level using the Gaussian 03 PCM parameters for acetonitrile.

organic media (We were unable to obtain good voltammetric data for chrysene in acetonitrile at or below room temperature because of its poor solubility in this solvent). It can be seen that ΔG_{disp} becomes less endothermic as the size of the arene increases. The effect of solvation in mitigating the gas phase ΔG_{disp} arises through differential solvation effects, as seen in Table 3, which shows the dramatically larger solvation energies of the arene dianions in acetonitrile compared to the corresponding neutral species (1) and radical anions (2). The solvation energies of the latter are also less sensitive to the size of the hydrocarbon than the dianion solvation energy. The solvation energy of 4^{−2} is somewhat greater than that of 5^{−2}. To some extent, this may be due to the charge, which is more evenly distributed in the latter species, whereas most of the charge in anthracene dianion is concentrated at the 9 and 10 positions. At least as important as this and probably more so, however, is simply the fact that anthracene is smaller, and with a larger solvation energy per carbon than 5 for the dianions. The solvation energy per carbon atom, which is a direct measure of the charge-to-size ratio, is very large for the smallest dianion, benzene (last column of Table 3); this represents the organic analogue of a phenomenon well known for a number of series of inorganic ions, e.g., the alkali metal (lithium) and halide (fluoride) ions, in which the smallest ion in the series has the highest solvation energy. Although the solvation energies of the neutral hydrocarbons increase with increasing molecular size, those of the monoanions and dianions decrease, though the changes for all species begin to level out for hydrocarbons of 18–20 carbon atoms.

2.2. Entropy effects

The energies computed for species 1–3 in the absence of solvation are enthalpies. Those computed in solution by

Table 2. Thermodynamics of arene radical anion disproportionation in both the absence and presence of solvent

Arene	Number of carbon atoms	$-\Delta H_{\text{disp, unsolv}}^a$ (kcal/mol)	$\Delta E_{\text{unsolv, calcd}}^b$ (V)	ΔG_{solv}^c (kcal/mol)	$-\Delta G_{\text{disp, solv}}^d$ (kcal/mol)	$\Delta E_{\text{solv, calcd}}^{e,f}$ (V)
Benzene	6	69.5	3.016	−44.9	24.6	1.065
Naphthalene	10	92.5	4.010	−69.7	22.8	0.990
Anthracene	14	96.9	4.204	−76.7	20.2	0.876
Chrysene	18	87.4	3.788	−70.9	16.5	0.717
Perylene	20	86.3	3.742	−70.4	15.9	0.694

^a $\Delta H_{\text{disp, unsolv}} = 2 \times H_2 - H_1 - H_3$.

^b $\Delta E_{\text{unsolv, calcd}} = \Delta H_{\text{disp, unsolv}} / 23.06$ kcal/volt.

^c $\Delta G_{\text{solv, calcd}} = \Delta H_{\text{disp, solv}} - \Delta G_{\text{disp, unsolv}}$.

^d $\Delta G_{\text{disp, solv}} = 2 \times G_2 - G_1 - G_3$.

^e $\Delta E_{\text{solv, calcd}} = -\Delta G_{\text{disp, solv}} / 23.06$ kcal/volt.

^f Includes an entropy of mixing term of $RT \ln 2$, or 0.017 V at 284 K.

the PCM method, however, are free energies.¹⁰ However, there are other entropy terms that must also be included in these computations to obtain the final ΔG_{disp} . Thus, Eq. 3 represents an encounter between two radical anions in which one transfers an electron to the other. In this encounter, either radical anion can be the electron donor, whereas the reverse reaction can occur in only one sense (transfer of an electron from **3** to **1**). This confers a kinetic advantage on the forward reaction that acts close to the ΔE gap by increasing the equilibrium constant for disproportionation (Eq. 3). This entropy of mixing contribution ΔS is thus $R \ln 2$. At 284 K (the temperature at which the data of Jensen and Parker were measured²) (Table 1), the corresponding contribution to ΔG_{disp} is -0.39 kcal favoring disproportionation.

Turning to the ion pairing equilibrium (Eq. 4), three more ΔS terms must be included. All of them involve entropy of mixing contributions to the equilibrium free energy. First, the tetraalkylammonium ion can ion pair to either face of **3**. Second, dianion **3** can pair to either face of the *pseudoplanar* R_4N^+ cation. The surprising fact that the lowest energy geometry of all tetra-*n*-alkylammonium ions larger than tetramethyl is approximately planar (D_{2h} symmetry), not tetrahedral, was first pointed out by Alder et al.¹⁶ Figure 1 shows a skeletal model of the Bu_4N^+ cation, which illustrates key features of this geometry. Including the nitrogen atom, one pair of butyl groups forms a continuous 9-atom chain. The other pair of butyl groups forms a second 9-atom chain perpendicular to that containing the first and lying in a plane parallel to it. A space filling model (Fig. 2) shows that upon formation of the ion pair, each chain presents two rows of four hydrogen atoms each to the approaching PAH dianion (We will see later that it is more appropriate to think of the eight methylene hydrogen atoms in this way than as four methylene pairs). The



Figure 1. Skeletal model of the tetrabutylammonium ion, illustrating its quasi-planar geometry.

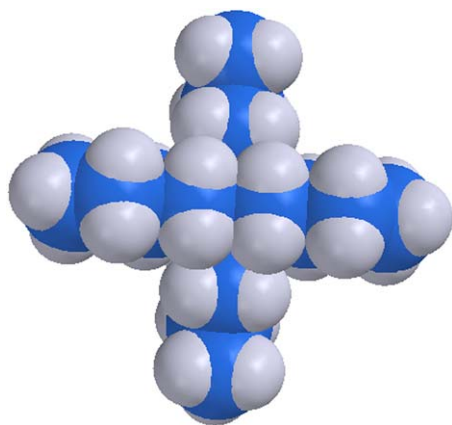


Figure 2. Space filling model of the tetrabutylammonium ion. The molecule has been rotated 90° around an axis running from left to right and passing through the nitrogen atom.

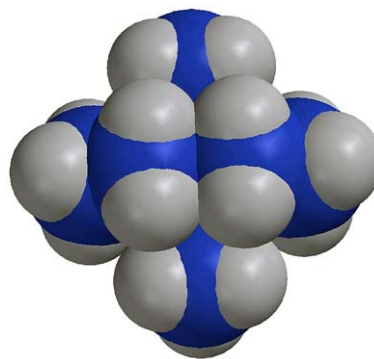
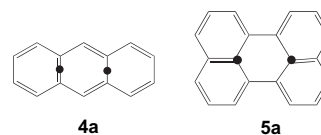


Figure 3. Space filling model of the tetraethylammonium ion.

Pr_4N^+ cation also exhibits this feature. On the other hand, the Et_4N^+ cation presents two rows of only two hydrogen atoms each (Fig. 3). We will address the significance of this difference in Sections 2.4 and 2.5. Finally, inspection of the structures of the ion pairs reveals the fact that each of the three arene dianions studied here has two binding sites *on each face* (see Section 2.3). These three entropic phenomena collectively provide a factor of $3R \ln 2$ favoring ion pair formation (1.17 kcal/mol at 284 K) that must then be added to the $\Delta G_{\text{ion-pair}}$ computed from the solution free energies of the three species in Eq. 4. The ion pairing constants for Et_4N^+ to **4**⁻² and **5**⁻² are larger by a factor of 2, and the resulting ΔE values are smaller, than reported earlier¹¹ because of the fact that **4** and **5** exhibit multiple binding sites on each face, which had not been discovered in our earlier work.



2.3. Thermodynamics of ion pairing

The computed solution free energies of the various tetraalkylammonium ions and their ion pairs with the dianions of **4** and **5** are given in Table 4. The energies were also computed for anthracene in the gas phase to permit estimates of the inherent tendency of these species to associate. The data in Table 4 can then be used to obtain values for the voltammetric peak spacing ΔE (Scheme 1) for various combinations of arene and electrolyte cation (Table 5). These values are

Table 4. Energies (in hartrees)^{a,b} of tetraalkylammonium ions and their ion pairs with anthracene and perylene dianions

R_4N^+	–Energy of R_4N^+	–Energy of $R_4N^+/4^{-2}$	–Energy of $R_4N^+/5^{-2}$
Et_4N^+ (unsolvated)	371.501977	911.274291	—
Et_4N^+ (solvated)	371.5718067	911.364662	1141.313867
Pr_4N^+ (unsolvated)	528.792260	1068.557105	—
Pr_4N^+ (solvated)	528.858704	1068.647892	1298.594973
Bu_4N^+ (unsolvated)	686.082714	1225.845391	—
Bu_4N^+ (solvated)	686.147838	1225.934919	1455.881960

^a One hartree=627.5 kcal/mol.

^b Energies were computed at the DFT B3LYP/6-311+G* level using the Gaussian 03 PCM parameters for acetonitrile.

Table 5. Computed values of ΔE for various combinations of arene and electrolyte cation

Arene	Cation	$\Delta G_{\text{ion-pair}}^{\text{a}}$ (kcal/mol)	$K_{\text{ion-pair}}$	$\Delta E_{\text{p, calcd}}^{\text{b}}$ (mV)	$\Delta E_{\text{p, exp}}^{\text{c}}$ (mV)	Difference (mV)
4	Et ₄ N ⁺	−2.51	85	820	670	150
4	Pr ₄ N ⁺	+0.21	1.4	873	740	133
4	Bu ₄ N ⁺	+1.11	0.14	875	750	125
5	Et ₄ N ⁺	−2.58	96	629	545	84
5	Pr ₄ N ⁺	+1.06	0.15	674	580	94
5	Bu ₄ N ⁺	+2.40	0.014	687	595	92

^a These values are obtained by adding $3RT \ln 2$ (−1.71 kcal/mol at 284 K) to the computed ΔG for ion pair formation from the free energies of the various species.

^b Computed value of peak spacing by voltammetric simulation.

^c Experimental peak spacing (see Ref. 2).

obtained by using the computed intrinsic disproportionation free energy (in volts) of the arene radical anion in solution (the last column of Table 2), the ion pairing equilibrium constant $K_{\text{ion-pair}}$, and the respective voltammetric concentrations of the arene (1 mM) and the supporting electrolyte (0.1 M) as input into a standard voltammetric simulation program.¹⁷ The computations exhibit the expected electrolyte effect, that is, an increase in ΔE with increasing supporting electrolyte size. This increase arises directly from the lower values of $K_{\text{ion-pair}}$ for the larger cations. The reasons for this decrease are given in Section 2.5. We have previously presented dramatic graphical evidence for the effect of solvation and ion pairing on voltammetric peak spacings; see Figure 1 of Ref. 10.

The data in Table 1 show clearly that ion pairing of the radical anions **2** with the R₄N⁺ counter-ions apparently does not occur to any significant extent in polar media. The first reduction potentials (E_1) of **4** and **5** are essentially identical within an experimental error of ± 10 mV. If ion pairing was involved, E_1 would become more negative with increasing size of the R₄N⁺ ion, as observed for E_2 . The fact that ion pairing is not significant with PAH radical anions in polar solvents is unsurprising, as we have previously pointed out.¹¹

2.4. Structure of tetraalkylammonium ion/arene dianion ion pairs

One of the most surprising results that arise from these computations is the structure of the ion pairs. One might expect that since both the electrolyte cation and dianion are symmetric species, they would form symmetric ion pairs. This

turns out to be far from the case. For example, a reasonable a priori assumption would be that the nitrogen atom of the tetraalkylammonium ion should be located directly above the geometric center of the arene ring. Of the six ion pairs represented in Table 4, there are none in which this is so. With both hydrocarbons that we have examined, the nitrogen atom is located as shown in structures **4a** and **5a**, where the black dots represent the point on the dianion nearest to the nitrogen atom in the ion pair. It can be seen that in each case there are two symmetrically equivalent positions involved in ion pairing. The entropic consequences of this fact on ΔE_{p} have already been discussed in Section 2.2.

Undoubtedly the most surprising geometrical feature of these ion pairs is the fact that the symmetry plane of the *quasi-planar*¹⁶ tetraalkylammonium ions is never even approximately parallel to that of the arene dianion. The ion pair between the anthracene dianion and tetrabutylammonium ion exemplifies this point. A side view of the ion pair (Fig. 4a) indicates that the lower chain (closest to the anthracene ring) of the cation is aligned roughly along the long axis of the arene ring. This is more or less as expected, since it places the hydrogen atoms of the lower four methylene groups, which carry a partial positive charge, in close contact with the negatively charged arene ring. However, an end view along the short axis of the anthracene ring (Figs. 4b and 5) indicates that the upper chain of the cation is tipped such that one of its two butyl groups is much closer to the ring than the other. The tip angle of the upper chain with respect to the plane of the anthracene ring is 35°, a very substantial deviation from coplanarity. The corresponding Et₄N⁺ is tipped much less strongly, only 13° (Fig. 6). Every one of the six ion pairs we have examined presents this same

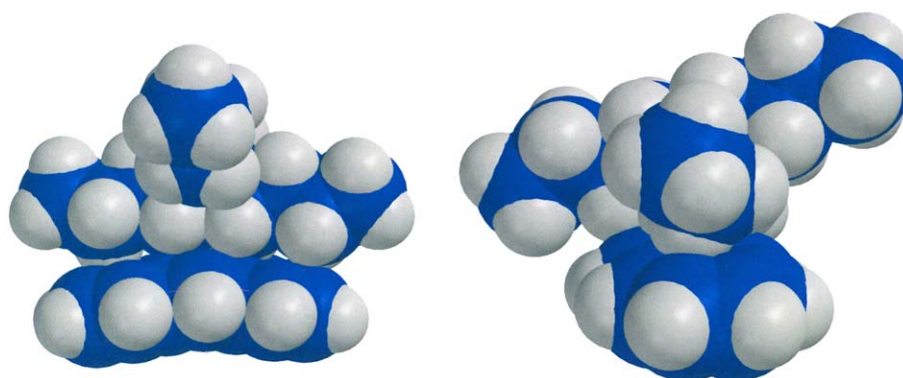


Figure 4. Space filling models of the ion pair between anthracene dianion and tetrabutylammonium ion. (a) [Left-hand structure] side view; (b) [right-hand structure] end view.

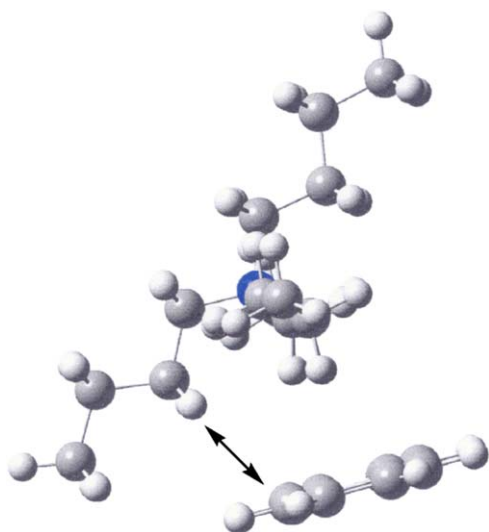


Figure 5. Ball-and-stick model of the ion pair between anthracene dianion and tetrabutylammonium ion. The arrow indicates the interaction between a methylene group and the dianion.

‘tipped’ feature, which strongly suggests that there is some inherent advantage to it. Closer examination of Figures 4b and 5 suggests an explanation. It will be recalled from Figure 2 that each chain presents two parallel rows of four hydrogen atoms to an approaching arene dianion. The same is true for tetra-*n*-propylammonium ion, while tetraethylammonium presents only two pairs of methylene hydrogen atoms to the dianion (Fig. 3). If one were to rotate the left-hand butyl group in Figure 5 clockwise so that the two chains are equidistant from the anthracene ring and lie in a plane parallel to it, all eight hydrogen atoms of the lower chain would then be equidistant from the ring. The advantage of the tipped geometry, however, is that it not only brings one of the two lower chains of four hydrogen atoms into close contact with the ring (the C–H bond in each of the four is perpendicular to the ring) but *it simultaneously places one of the lower methylene groups of the upper chain (see arrow on the left side of Fig. 5) in closer contact with the charged ring.* There appears to be an advantage to this orientation, which directs six carbon–hydrogen atoms more or less directly at the dianion ring, over the symmetrical arrangement, in

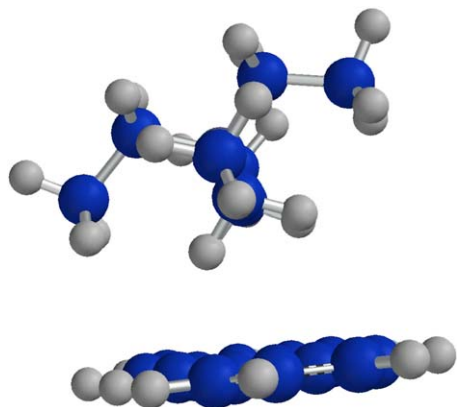


Figure 6. Ball-and-stick model of the ion pair between anthracene dianion and tetraethylammonium ion.

which eight C–H bonds are directed only obliquely at the ring.

The desirability of directing the maximum number of hydrogen atoms directly at the arene ring can also be seen in the computed structure of the anthracene dianion/ NMe_4^+ ion pair (Fig. 7); steric considerations would have suggested an orientation of the cation with only one methyl group in close contact with the ring; this would however require that the three hydrogen atoms of that methyl group would have to be oriented obliquely with respect to the ring. Instead, the preferred orientation of the tetramethylammonium ion is such that the *three* methyl groups are in closer proximity to the ring, with each contributing one hydrogen atom perpendicular to the ring. Furthermore, unlike the others, in this ion pair the nitrogen atom is located directly above the geometric center of the anthracene nucleus; this suggests that the off-center orientation observed with the other ion pairs is associated with their ability to contribute additional hydrogen atoms to the dianion.

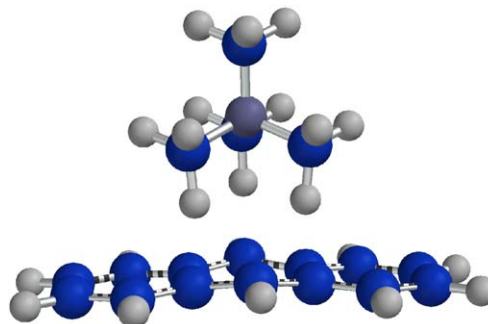


Figure 7. Ball-and-stick model of the ion pair between anthracene dianion and tetramethylammonium ion.

Finally, recall the fact that the tip angle of the upper chain in the $\text{Et}_4\text{N}^+/\text{4}^{-2}$ ion pair is much less than those of the Pr_4N^+ and Bu_4N^+ ions. The Et_4N^+ ion (if tipped as greatly as the other two ions) could still expose only a total of four hydrogen atoms to the anthracene ring (two from the bottom chain and two from the top chain). It appears to be more favorable for it to present all four of the methylene hydrogen atoms of the lower chain more obliquely rather than orienting two of them perpendicularly, though a small degree of tip remains (Figs. 6 and 8).

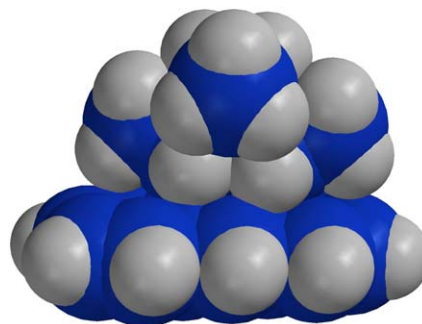


Figure 8. Space filling model of the ion pair between anthracene dianion and tetraethylammonium ion.

Table 6. Free energies of association between tetraalkylammonium ions and anthracene dianion in the gas phase and in solution

R_4N^+	ΔG_{solv}^a for 4^{-2} (kcal/mol)	ΔG_{solv}^a for R_4N^+ (kcal/mol)	ΔG_{solv}^a for $4^{-2}/R_4N^+$ (kcal/mol)	ΔG_{solv} for ion pairing (kcal/mol)	$\Delta G_{\text{ion-pair}}$ in gas phase (kcal/mol)	$\Delta G_{\text{ion-pair}}$ in solution ^b (kcal/mol)
Et_4N^+	−169.8	−43.8	−56.7	+156.9	−158.2	−1.3 ^b
Pr_4N^+	−169.8	−41.7	−56.2	+154.8	−153.5	+1.4 ^b
Bu_4N^+	−169.8	−40.9	−56.2	+154.5	−152.2	+2.3 ^b

^a Solvation energies are the difference between the solution and gas phase computed energies of the species.

^b An entropy of mixing correction of $3R\ln 2$ (−1.17 kcal/mol at 284 K) must be added to these values to obtain the overall $\Delta G_{\text{ion-pair}}$ values (column 3 of Table 5).

2.5. Origin of the ‘steric’ effect

The increase in ΔE with increasing size of the electrolyte cation has been interpreted as arising from increasing steric hindrance to ion pairing as the cation becomes larger.^{2,6} Yet we have seen in the preceding section that, far from a simple steric repulsion effect, the Pr_4N^+ and Bu_4N^+ ions actually orient themselves in a fashion such that they *maximize* their contact with the anthracene ring. Examination of the data in Table 6 suggests that other considerations come into play as well. In the gas phase $\Delta G_{\text{ion-pair}}$ for the interaction between 4^{-2} and Et_4N^+ is more negative than for Pr_4N^+ and Bu_4N^+ by 4.7 and 6.0 kcal/mol, respectively (Table 6, column 6). In solution, however, the magnitude of this effect is reduced (Table 6, column 7). This is because the solvation energies of the three ion pairs are almost identical, whereas the solvation energies of the tetraalkylammonium ions increase with decreasing size. This effect opposes the gas phase ion pairing size dependency and hence $\Delta G_{\text{ion-pair}}$ for Et_4N^+ in solution is favored by the two larger ions by only 2.7 and 3.6 kcal, respectively, compared to the gas phase values of 4.7 and 6.0 kcal/mol.

Finally, it is not clear that even in the gas phase the preference for ion pairing to Et_4N^+ ion represents a steric effect. Space filling models of the $Bu_4N^+/4^{-2}$ and $Et_4N^+/4^{-2}$ ion pairs (Figs. 4 and 7) show that the Bu_4N^+ cation offers no more steric barrier to close approach to the dianion than does $Et_4N^+/4^{-2}$. We have seen that the Pr_4N^+ and Bu_4N^+ ions even appear to benefit by the larger number of hydrogen atoms in close contact with the negatively charged ring compared to Et_4N^+ . However, the latter effect is very likely outweighed by the larger charge-to-size ratio of the tetraethylammonium ion, which will result in it having a stronger affinity for coordination to dianions. There is evidence that this is so: the distance of the central nitrogen atom from carbons 9 and 10 of the anthracene ring in the ion pair is 4.3 Å for the Et_4N^+ ion and 4.8 Å for Bu_4N^+ . The butyl groups in Bu_4N^+ may themselves provide an electrostatic solvation-like stabilizing effect to the central nitrogen atom in the gas phase, which would cause the Bu_4N^+ ion to require less electrostatic stabilization from the dianion and thus permit it to move further away from the latter. The larger tip angle of the upper chain permits two of its methylene protons to remain in contact with the dianion even though the nitrogen atom is further away from the ring.

3. Conclusions

Solvation and ion pairing greatly influence the disproportionation energies of polycyclic aromatic hydrocarbon

radical anions into the corresponding dianions and neutral species. The difference between ΔG for disproportionation (98% or more) arises from differential solvation of the three species involved in the disproportionation. Ion pairing between tetraalkylammonium counter-ions and the arene dianions makes a small but real contribution. The tendency to form ion pairs decreases with increasing size of the cation. It is not clear, however that this is a steric effect, since space filling models suggest that large tetraalkylammonium ions form ion pairs in which they are in almost close contact with the dianion as smaller cations. The highly unsymmetric ‘tipped’ structure of the ion pairs suggests that there is even an energetic advantage to ion pairs from larger cations. Rather than steric hindrance to ion pairing with large cations, it is suggested that ion pairing to small cations is favored because of their greater charge-to-size ratio, which calls for more electrostatic stabilization by the dianion.

4. Computations

The energies of species 1–3 were computed at the DFT B3LYP/6-311+G* level using the Gaussian 03 suite of programs.¹⁸ The reasons for the choice of this computational method have been described previously.¹¹ Solvation energies of the individual constituents were computed by the PCM (polarized continuum model)¹⁰ as implemented in Gaussian. The energies of the tetraalkylammonium ions (R_4N^+ ; R=Et, Pr, and Bu) and their corresponding ion pairs with each of the three hydrocarbon dianions were also computed in order to obtain values for the equilibrium constants ($K_{\text{ion-pair}}$) for ion pairing. The corresponding computed values for the potential peak spacings of ΔE were obtained by a final digital simulation to account for the differing concentrations of the arene and electrolyte.^{11,17} Computations were carried out on a computer (Puget Custom Computers, Seattle, WA) equipped with four parallel 64-bit AMD Opteron[®] processors sharing 4 GB of RAM.

Acknowledgements

Financial support for this research was provided by the National Science Foundation through grants CHE-0100727 and CHE-0411699. Additional support was provided by Wesleyan University.

References and notes

- Fry, A. J.; Fox, P. C. *Tetrahedron* **1986**, *42*, 5255.
- Jensen, B. S.; Parker, V. D. *J. Am. Chem. Soc.* **1975**, *97*, 5211.

3. Heinze, J.; Mortensen, J.; Mullen, K.; Schenk, R. *J. Chem. Soc., Chem. Commun.* **1987**, 701.
4. Heinze, J. *Angew. Chem., Int. Ed. Engl.* **1984**, 23, 831.
5. Kiesele, H. *Anal. Chem.* **1981**, 53, 1952.
6. Fry, A. J.; Hutchins, C. S.; Chung, L. L. *J. Am. Chem. Soc.* **1975**, 97, 591.
7. Evans, D. H.; Hu, K. *J. Chem. Soc., Faraday Trans.* **1996**, 92, 3983.
8. Kubota, T.; Kano, K.; Uno, B.; Konse, T. *Bull. Chem. Soc. Jpn.* **1987**, 60, 3865.
9. Foresman, J. B.; Frisch, A. *Exploring Chemistry with Electronic Structure Methods*, 2nd ed.; Gaussian: Pittsburgh, PA, 1996; p 147.
10. Tomasi, J.; Persico, M. *Chem. Rev.* **1994**, 94, 2027.
11. Fry, A. J. *Electrochem. Commun.* **2005**, 7, 602.
12. Heinze, J. *Organic Electrochemistry*, 4th ed.; Lund, H., Hammerich, O., Eds.; Dekker: New York, NY, 2001; p 293.
13. Fry, A. J. *Topics in Organic Electrochemistry*; Fry, A. J., Britton, W. E., Eds.; Plenum: New York, NY, 1986.
14. Fry, A. J.; Simon, J.; Tashiro, M.; Yamato, T.; Mitchell, R. H.; Dingle, T. W.; Williams, R. V.; Mahedevan, R. *Acta Chem. Scand.* **1983**, 37B, 445.
15. Fry, A. J.; Chung, L. L.; Boekelheide, V. *Tetrahedron Lett.* **1974**, 445.
16. Alder, R. W.; Allen, P. R.; Anderson, K. R.; Butts, C. P.; Khosravi, E.; Martin, A.; Maunder, C. M.; Orpen, A. G.; Pourcain, C. P. S. *J. Chem. Soc., Perkin Trans. 2* **1998**, 2083.
17. *Digitim 3.0*, 2004 Bioanalytical Systems: West Lafayette, IN.
18. Frisch, M. J.; Trucks, G. W.; Schlegel, H. B.; Scuseria, G. E.; Robb, M. A.; Cheeseman, J. R.; Montgomery, J. A., Jr.; Vreven, T.; Kudin, K. N.; Burant, J. C.; Millam, J. M.; Iyengar, S. S.; Tomasi, J.; Barone, V.; Mennucci, B.; Cossi, M.; Scalmani, G.; Rega, N.; Petersson, G. A.; Nakatsuji, H.; Hada, M.; Ehara, M.; Toyota, K.; Fukuda, R.; Hasegawa, J.; Ishida, M.; Naka-jima, T.; Honda, Y.; Kitao, O.; Nakai, H.; Klene, M.; Li, X.; Knox, J. E.; Hratchian, H. P.; Cross, J. B.; Bakken, V.; Adamo, C.; Jaramillo, J.; Gomperts, R.; Stratmann, R. E.; Yazyev, O.; Austin, A. J.; Cammi, R.; Pomelli, C.; Ochterski, J. W.; Ayala, P. Y.; Morokuma, K.; Voth, G. A.; Salvador, P.; Dannenberg, J. J.; Zakrzewski, V. G.; Dapprich, S.; Daniels, A. D.; Strain, M. C.; Farkas, O.; Malick, D. K.; Rabuck, A. D.; Raghavachari, K.; Foresman, J. B.; Ortiz, J. V.; Cui, Q.; Baboul, A. G.; Clifford, S.; Cioslowski, J.; Stefanov, B. B.; Liu, G.; Liashenko, A.; Piskorz, P.; Komaromi, I.; Martin, R. L.; Fox, D. J.; Keith, T.; Al-Laham, M. A.; Peng, C. Y.; Nanayakkara, A.; Challacombe, M.; Gill, P. M. W.; Johnson, B.; Chen, W.; Wong, M. W.; Gonzalez, C.; Pople, J. A. *Gaussian 03, Revision C.02*; Gaussian: Wallingford, CT, 2004.

C–S bond cleavage in the sensitized photooxygenation of *tert*-alkyl phenyl sulfides. The role of superoxide anion

Enrico Baciocchi,^{a,*} Tiziana Del Giacco,^{b,*} Paolo Giombolini^b and Osvaldo Lanzalunga^{a,*}

^aDipartimento di Chimica, Università degli Studi di Roma 'La Sapienza' and Istituto CNR di Metodologie Chimiche (IMC-CNR), Sezione Meccanismi di Reazione, P.le A. Moro, 5 I-00185 Rome, Italy

^bDipartimento di Chimica and Centro di Eccellenza Materiali Innovativi Nanostrutturati (CEMIN), Università di Perugia, Via Elce di Sotto 8, 06123 Perugia, Italy

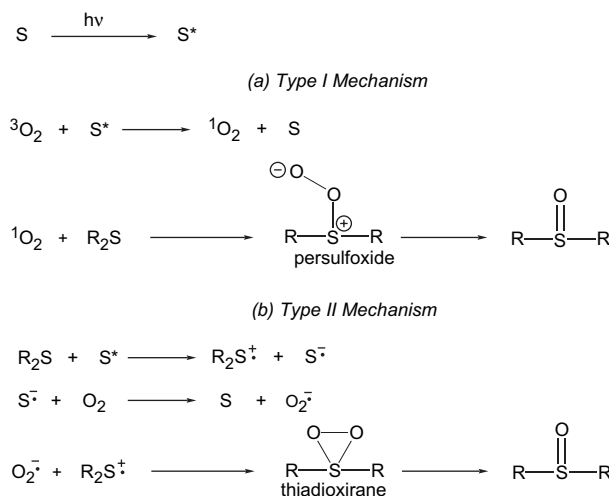
Received 2 September 2005; accepted 26 September 2005

Available online 18 May 2006

Abstract—The *N*-methylquinolinium tetrafluoroborate (NMQ⁺)-photosensitized oxidation of *tert*-alkyl phenyl sulfides **1a–c** (**1a**, *tert*-alkyl=*tert*-butyl; **1b**, *tert*-alkyl=2-phenyl-2-propyl; **1c**, *tert*-alkyl=1,1-diphenylethyl) and benzyl phenyl sulfide (**2**) were investigated in CH₃CN by nanosecond laser flash photolysis (LFP) and steady-state irradiation either under nitrogen or in the presence of O₂. By laser irradiation, the formation of sulfide radical cations **1a⁺–c⁺** in the monomeric form ($\lambda_{\text{max}}=520$ nm) and of **2⁺** in both the monomeric ($\lambda_{\text{max}}=520$ nm) and dimeric form ($\lambda_{\text{max}}=780$ nm) were observed within the laser pulse. In both cases, the radical cations decayed by second-order kinetics without any apparent formation of transients attributable to C–S bond rupture. In line with these results, very small amounts of photoproducts were obtained under nitrogen thus suggesting that the sulfide radical cations mainly undergo a back electron transfer process with the reduced *N*-methylquinolinium (NMQ[•]). A different situation was found in the presence of O₂ since steady-state photolysis produced substantial amounts of C–S bond cleavage products (alcohols, alkenes, and ketones from **1a–c** and benzaldehyde from **2**), in contrast with LFP experiments. Formation of products was, however, significantly reduced in the presence of benzoquinone, a trap for O₂^{•-} generated by NMQ[•] and O₂. For the *tert*-alkyl phenyl sulfides, **1a–c**, these results have been interpreted by suggesting that C–S bond cleavage products in the presence of oxygen mostly derive from the decomposition of a thiadioxirane **6** formed by the reaction of the sulfide radical cation with O₂^{•-}. In this cleavage a sulfinate and a carbocation formed. The former is oxidized to sulfonate, whereas the carbocation can react with adventitious water to form the alcohol (and the alkene therefrom) and with O₂^{•-} to produce the ketone. For **2** (a sulfide with α -CH bonds) probably a different mechanism holds, benzaldehyde coming from the α -phenylthio carbon radical formed from deprotonation by O₂^{•-} of **2⁺**. © 2006 Elsevier Ltd. All rights reserved.

1. Introduction

The sensitized photooxygenation of organic sulfides is receiving continuous attention for the important biological implications as well as the possible practical applications in organic synthesis.^{1–14} Two different mechanisms have been suggested for this process.^{15,16} The Type I mechanism involves the intervention of ¹O₂ generated by the reaction of the excited sensitizer with ³O₂ (henceforth simply indicated as O₂), whereas in the Type II mechanism the excited sensitizer abstracts an electron from the substrate forming a radical cation that then reacts with O₂^{•-} formed by O₂ and the reduced form of the sensitizer. Recent work has presented evidence indicating that the two mechanisms involve different intermediates, namely a persulfoxide in the Type I mechanism and a thiadioxirane in the Type II mechanism (Scheme 1).^{15,16}

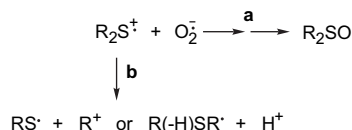


Scheme 1.

In both mechanisms, sulfoxides are generally the main products. However, variable amounts of C–S bond cleavage products can also be obtained, depending on the substrate

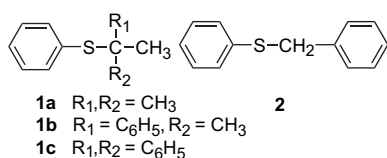
* Corresponding authors. Tel.: +39 0649913711; fax: +39 06490421; e-mail: enrico.baciocchi@uniroma1.it

structure. The formation of these products has been discussed in some detail for the Type I mechanism, where they are suggested to be derived by additional pathways available to the persulfoxide intermediate.^{10,11} In the electron transfer mechanism the fragmentation products are attributed to possible reactions of the sulfide radical cation involving the cleavage of a C–S or an α -C–H bond, in competition with the reaction with $O_2^{\cdot-}$ leading to sulfoxide (Scheme 2).^{13,17}



Scheme 2.

In view of the importance of sulfides photooxygenation, it is certainly of interest to get more information on this problem. Thus, we have carried out a detailed investigation of the photochemical oxygenation of *tert*-alkyl phenyl sulfides **1a–c** sensitized by *N*-methylquinolinium tetrafluoroborate (NMQ⁺) in CH₃CN. These reactions, that exclusively lead to fragmentation products, have been studied by nanosecond laser flash photolysis (LFP) and steady-state photolysis and the transient species produced, their decay pathways, and the final photoproducts have been identified. The results of this study, reported herewith, have led to the important conclusion that the main pathway for the formation of fragmentation products is not the direct C–S bond cleavage in the radical cation, but the reaction of the sulfide radical cation with the superoxide anion generated in the reaction of NMQ⁺ with oxygen. For comparison purposes, the photolysis of benzyl phenyl sulfide (**2**) has also been investigated. Fragmentation products are formed in this case too, but the mechanism is probably different than that proposed for the *tert*-alkyl phenyl sulfides.



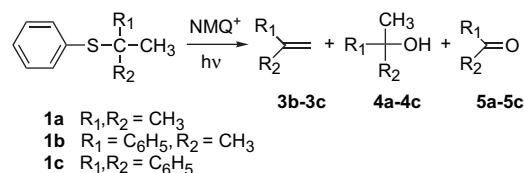
2. Results

2.1. Steady-state photolysis

The steady-state photooxidations sensitized by NMQ⁺ were carried out in air-saturated CH₃CN or for comparison purpose under N₂. No reaction was observed in the absence of the sensitizer. The reaction products were identified by GC–MS and ¹H NMR (comparison with authentic specimens, see Section 5).

Photolysis in the presence of O₂. Under air, quite efficient photochemical processes were observed with **1a–c**. Fragmentation products were obtained exclusively in the photoirradiation of *tert*-alkyl phenyl sulfides **1a–c** with quantum yields (Φ) between 0.3 and 0.5 for the products coming

from the alkyl moiety. Benzenesulfonate is the main product derived from the sulfide moiety even though a small amount of diphenyl disulfide was detected. No quantum yields were determined for the sulfur containing products. Alcohols, alkenes, and ketones were the products formed from **1b** and **1c** as described in Scheme 3, where only the products derived from the alkyl moiety are indicated. The corresponding alcohol and ketone were also formed with **1a**. In this case, *N*-*tert*-butylacetamide was also produced, whereas the alkene was not observed.



Scheme 3.

A further notation, however, was that with **1b** and **1c**, the alcohol is progressively converted into alkene as the reaction proceeds, as shown, for example, from the data in Table 1 for the photolysis of **1b**.

Table 1. Quantum yields of the photoproducts formed in the oxidation of 2-phenyl-2-propyl phenyl sulfide (**1b**) photosensitized by NMQ⁺ in air-saturated CH₃CN^a

T (min)	$\Phi(3b)$	$\Phi(4b)$	$\Phi(5b)$	$\Phi(3b)+\Phi(4b)$
60	0.018	0.17	0.10	0.188
90	0.13	0.060	0.086	0.190
120	0.16	0.057	0.096	0.217

^a [sulfide]=0.01 M. [NMQ⁺]=3.4 × 10⁻³ M.

Accordingly, it can be seen that whereas the overall quantum yield is substantially independent of irradiation time, those of the alkene **3b** and the alcohol **4b** increase and decrease, respectively, by increasing the irradiation time. However, the sum $\Phi(3b)+\Phi(4b)$ remains almost constant. Most likely, alcohol is the primary product and there is a substantial and increasing conversion of the alcohol into the alkene, probably promoted by H⁺ formed during the photolysis. Thus, in Table 2, where the results for all *tert*-alkyl phenyl sulfides are depicted, we report the Φ value for the ketone and the overall quantum yield, $\Phi(3)+\Phi(4)$, of alkene and alcohol for **1b** and **1c**. In the same Table the results of the steady-state photolysis of benzyl phenyl sulfide that leads to benzyl phenyl sulfoxide and a fragmentation product, benzaldehyde, are also reported. The possible role of $O_2^{\cdot-}$, that forms in the reaction with NMQ⁺ (Scheme 1b, S=NMQ⁺), was investigated by performing the photolysis in the presence of benzoquinone, a well known trap for $O_2^{\cdot-}$.¹⁸ A very significant drop in the product quantum yields was observed, particularly with **1a** and **1b** (Table 2).

When the above reactions were carried out *in the absence of oxygen* (flushing the solutions with N₂ before irradiation) no products were observed with the NMQ⁺/**1a** and NMQ⁺/**2** systems and a substantial decrease (about one order of magnitude) in quantum yields was observed with the sulfides **1b** and **1c**. Under these conditions, diphenyl disulfide was also

Table 2. Quantum yields of the photoproducts formed in the oxidation of *tert*-alkyl phenyl sulfides (**1a–c**) and benzyl phenyl sulfide (**2**) photosensitized by NMQ⁺ in CH₃CN^a

Substrate		Quantum yields ^b		
		Φ_{TOT}	$\Phi(3)+\Phi(4)$	$\Phi(5)$
1a	Air	0.36	0.085 ^c	0.21
	Air ^d	— ^e	— ^e	— ^e
	N ₂	— ^e	— ^e	— ^e
1b	Air	0.29	0.19	0.10
	Air ^d	0.015	0.007	0.008
	N ₂	0.038	0.038	—
1c	Air	0.44	0.31	0.13
	Air ^d	0.13	0.087	0.043
	N ₂	0.058	0.058	— ^e
2	Air	0.14	$\Phi(\text{PhCH}_2\text{SOPh})$	$\Phi(\text{PhCHO})$
	Air ^d	— ^e	0.03	0.11
	Air ^d	— ^e	— ^e	— ^e
	N ₂	— ^e	— ^e	— ^e

^a [sulfide]= 1.0×10^{-2} M, [NMQ⁺]= 1.0×10^{-2} M under nitrogen and [NMQ⁺]= 3.4×10^{-3} M in air-saturated condition. Quantum yields are determined after 1 h irradiation.

^b Quantum yields of all the products from the alkyl moiety. The error is $\pm 10\%$.

^c *N*-*tert*-butylacetamide ($\Phi=0.065$) is also formed.

^d In the presence of 1.2×10^{-3} M *p*-benzoquinone.

^e Under the detection limit ($\Phi < 0.001$).

formed, whereas no formation of the ketone **5** was observed. These results are also displayed in Table 2.

Finally, since excited NMQ⁺ can also react with O₂ to form ¹O₂,¹⁵ we tested the reactivity of our sulfides toward ¹O₂. Thus, the photolysis of **1b** was carried out in the presence of Rose Bengal in O₂-saturated CH₃CN.¹⁹ No detectable amounts of photoproducts were obtained after 30 min of irradiation.

2.2. Fluorescence quenching

Fluorescence quenching experiments were carried out in air-saturated CH₃CN to determine the efficiency by which substrates **1a–c** and **2** quench the lowest excited singlet state of NMQ⁺. The fluorescence intensity of NMQ⁺ was recorded by steady-state experiments in the absence (*I*⁰) and in the presence (*I*) of increasing concentrations of the substrates **1a–c** and **2**. The second-order rate constants for NMQ⁺ fluorescence quenching (*k*_q) were calculated from the slopes of the linear Stern–Volmer plots (*I*⁰/*I* vs [**1a–c**, **2**]) divided by the lifetime of ¹NMQ⁺* (20 ns)²⁰ (Fig. S1 and Table S1 in the Supplementary data). The Stern–Volmer plots show that all the substrates quench the emission of NMQ⁺ with rate constants, which are close to the diffusion limit (1.5 – 1.8×10^{10} M⁻¹ s⁻¹).²¹

2.3. Laser flash photolysis studies

The laser photolysis experiments ($\lambda_{\text{exc}}=355$ nm) were carried out in CH₃CN under N₂- and O₂-saturated conditions in the presence of 1 M toluene, which was used as cosensitizer to reduce the efficiency of the back electron transfer process and, consequently, to increase the concentration of the transient formed within the laser pulse.²² By laser photolysis of the NMQ⁺/toluene/**1a–c** systems in N₂-saturated solutions, similar time-resolved absorption spectra were

observed. Two absorption bands were detected just after the laser pulse in the 400 and 520 nm regions (time-resolved absorption spectra for the NMQ⁺/toluene/**1a** system are reported in Fig. 1a, time-resolved absorption spectra for the NMQ⁺/toluene/**1b** and NMQ⁺/toluene/**1c** systems are reported in Figs. S2 and S3 in the Supplementary data). These bands were assigned to NMQ^{*} ($\lambda_{\text{max}}=400$ and 550 nm)²³ and the sulfide radical cations in the monomeric form ($\lambda_{\text{max}}=520$ nm).²⁴

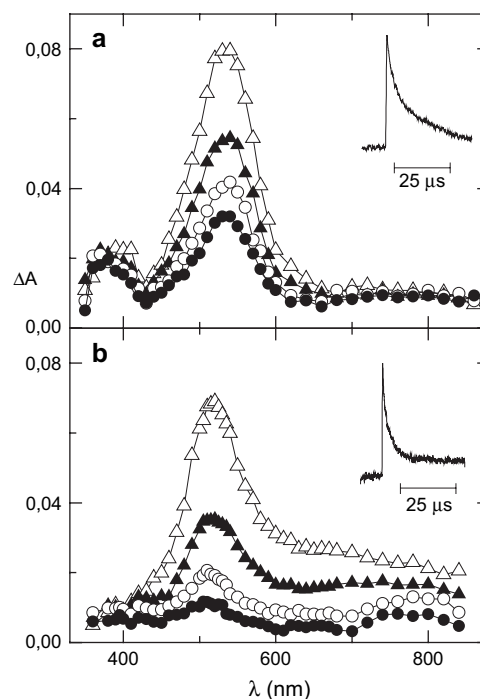


Figure 1. Time-resolved absorption spectra of the NMQ⁺ (3.4×10^{-3} M)/toluene (1 M)/(CH₃)₃CSPH (1.0×10^{-2} M) system in CH₃CN: (a) N₂-saturated, recorded 0.2 (Δ), 4.8 (▲), 10 (○) and 16 (●) μs after the laser pulse; inset: decay kinetics recorded at 520 nm. $\lambda_{\text{exc}}=355$ nm. (b) O₂-saturated, recorded 0.08 (Δ), 2.0 (▲), 4.0 (○), 6.1 (●) μs after the laser pulse; inset: decay kinetics recorded at 520 nm. $\lambda_{\text{exc}}=355$ nm.

Laser photolysis of the NMQ⁺/toluene/**2** system under N₂ showed an additional broad absorption band at 780 nm that was assigned to the dimer sulfide radical cation (Fig. 2a).²⁵ Very reasonably, the dimer was not observed with **1a–c** due to the steric hindrance of the *tert*-alkyl group.²⁶

The time-evolution of the absorption spectra shows that the decay of the two signals recorded at ca. 400 and 520 nm is not accompanied by the buildup of any transient, which can be assigned to products of C–S bond cleavage, i.e., the phenylthiyl radical PhS^{*} ($\lambda_{\text{max}}=450$ – 490 nm)²⁷ and, in the case of **1c**⁺, the 1,1-diphenylethyl cation ($\lambda_{\text{max}}=420$ nm).²⁸ Moreover, in the LFP experiment with the NMQ⁺/toluene/**2** system, analysis of the spectral evolution did not show the growth of the absorption of PhSCH^{*}Ph ($\lambda_{\text{max}}=350$ nm),²¹ i.e., the product of benzylic C–H deprotonation of **2**⁺. In O₂-saturated solutions, an identical situation was observed, apart from the fact that the time-resolved absorption spectra are modified by the fast decay of NMQ^{*}, that is efficiently quenched by molecular oxygen;¹⁵ thus, the shoulder at ca. 400 nm disappears and the only recorded transient concerns

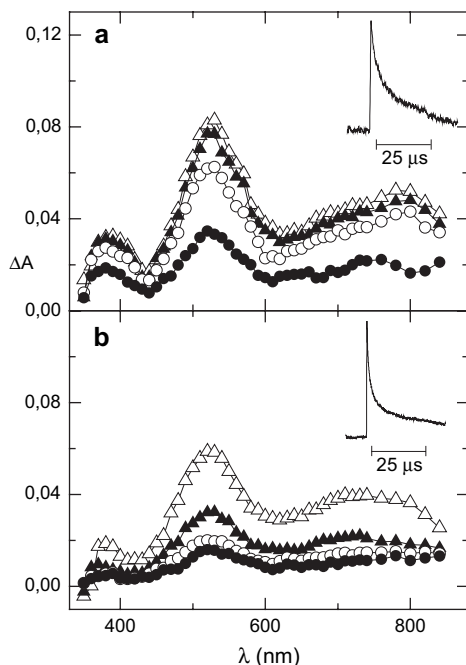


Figure 2. Time-resolved absorption spectra of the NMQ^+ (3.4×10^{-3} M)/toluene (1 M)/ PhCH_2SPh (1.0×10^{-2} M) system in CH_3CN : (a) N_2 -saturated, recorded 0.08 (Δ), 0.32 (\blacktriangle), 1.0 (\circ) and 5.8 (\bullet) μs after the laser pulse; (b) O_2 -saturated, recorded 0.08 (Δ), 0.94 (\blacktriangle), 3.0 (\circ), 6.0 (\bullet) μs after the laser pulse. Inset: decay kinetics recorded at 530 nm. $\lambda_{\text{exc}}=355$ nm.

the sulfide radical cation (time-resolved absorption spectra are reported in Fig. 1b and Fig. 2b for the NMQ^+ /toluene/**1a** and NMQ^+ /toluene/**2** systems and in Figures S2 and S3 in the Supplementary data for the NMQ^+ /toluene/**1b** and NMQ^+ /toluene/**1c** systems). The decay rate of radical cations **1a-c**^{•+} and **2**^{•+} was determined by following the absorption decay at 520 nm. Under nitrogen and oxygen the decay kinetics followed second-order laws, (see insets in Figs. 1 and 2 for the decay of **1a**^{•+} and **2**^{•+}, respectively) and the decay rate constants (k_2) divided by the extinction coefficient (ϵ), for all the radical cations, measured at 25 °C are reported in Table 3.

It can be observed that the decay rate constants are not significantly influenced by the structure of the sulfide and that the values under oxygen are higher than those observed under nitrogen.

Time-resolved spectra recorded by laser flash photolysis of the NMQ^+ /**1b** system in the presence of BQ (9.7×10^{-4} M) in O_2 -saturated CH_3CN (see Fig. S4 in the Supplementary data) showed the characteristic absorption band of $\text{BQ}^{\cdot-}$ ($\lambda_{\text{max}}=520$ nm)²⁹ thus confirming the electron transfer process from $\text{O}_2^{\cdot-}$ to BQ.

Table 3. Decay rate constants of **1a-c**^{•+} and **2**^{•+} formed by laser photolysis of the NMQ^+ (3.4×10^{-3} M)/toluene (1 M)/**1a-c**, **2** (1.0×10^{-2} M) systems in N_2 - and O_2 -saturated CH_3CN ($\lambda_{\text{exc}}=355$ nm)

Sulfide	k_2/ϵ (10^6 s ⁻¹ cm)	
	N_2	O_2
1a	4.0	12
1b	2.7	12
1c	5.0	16
2	4.0	15

3. Discussion

3.1. *tert*-Alkyl phenyl sulfides

The observation that sulfides **1a-c** quench the fluorescence emission of NMQ^+ with rates close to the diffusion limit indicates that NMQ^+ acts as an electron transfer sensitizer. The high efficiency is certainly related to the reduction potential of $^1\text{NMQ}^{+\bullet}$ (2.7 V vs SCE)²² that is much higher than those of the *tert*-alkyl phenyl sulfide radical cations **1a**^{•+}–**1c**^{•+} (ca. 1.6 V vs SCE).¹⁷ Any possible contribution of $^1\text{O}_2$ to the photooxidation has been shown to be negligible.

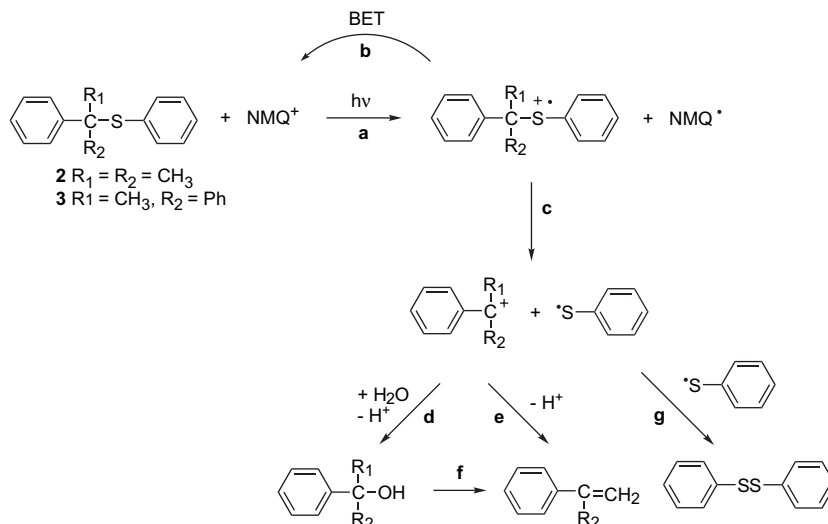
The ET mechanism from the sulfides to $^1\text{NMQ}^{+\bullet}$ is also supported by the observation, in the laser flash photolysis experiments of the NMQ^+ /toluene/**1a-c** systems in N_2 -saturated solutions, of absorption bands that have been assigned to NMQ^{\cdot} ($\lambda_{\text{max}}=400$ and 550 nm) and the sulfide radical cations ($\lambda_{\text{max}}=520$ nm). Under oxygen, the only recorded transient is the sulfide radical cation ($\lambda_{\text{max}}=520$ nm) since NMQ^{\cdot} is converted to NMQ^+ .

However, both under oxygen and nitrogen the decay of the radical cation is not accompanied by the buildup of any transient. Particularly, the transients expected for a direct C–S bond cleavage in the radical cation (phenylthiyl radical in all cases and the tertiary carbocation from **1c**^{•+}) were not observed. Since second-order kinetics were followed and the rates are faster under oxygen, the decays are reasonably attributed to back electron transfer, under nitrogen, and to a reaction with $\text{O}_2^{\cdot-}$, under oxygen.

The results of steady-state photoirradiations under nitrogen (formation of small amounts of photoproducts with sulfides **1b** and **1c**, and no reaction at all with **1a**) were in substantial agreement with those of the laser photolysis study. The low efficiency observed is fully consistent with a process dominated by back electron transfer in the geminate radical/radical cation pair (Scheme 4, path b).

The structure of photoproducts formed (alkenes **3b** and **3c** and alcohols **4b** and **4c**, from **1b** and **1c**, respectively) suggests that at least for **1b**^{•+} and **1c**^{•+} a pathway involving the cleavage of the C–S bond, leading to the tertiary benzylic cations and the phenylthiyl radical (Scheme 4, path c) can also operate, albeit as a minor route (not revealable in LFP experiments). The benzylic cations can react with adventitious water to form the alcohols **4** or lose a proton to produce the alkenes **3** (paths d and e in Scheme 4). However, alkenes **3** seem to be formed primarily by acid induced dehydration of the alcohol (Scheme 4, path f, see Section 2). In both cases, dimerization of the phenylthiyl radical leads to diphenyl disulfide. With **1a**^{•+}, C–S bond cleavage is probably slower (a less stable carbocation is formed) than with **1b**^{•+} and **1c**^{•+} and cannot compete at all with back electron transfer. Thus, no products are observed in the steady-state photolysis.

However, as shown by the data in Table 2, the efficiency of photolysis of the sulfides **1a-c** significantly increases in the presence of oxygen (under air). From **1a**, the alcohol **4a** and *tert*-butylacetamide are formed together with acetone (**5a**). The ketones **5b** and **5c**, the alkenes **3b** and **3c**, and the



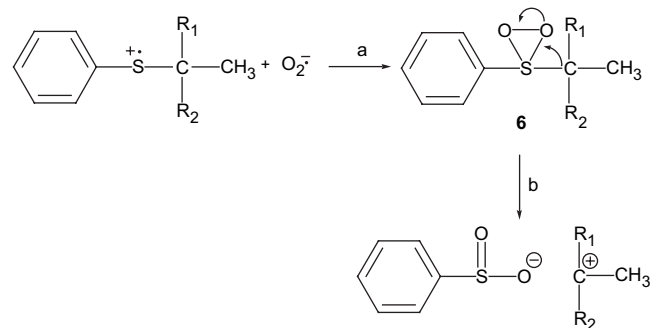
Scheme 4.

alcohols **4b** and **4c**, are formed from **1b** and **1c**, respectively. In all cases, benzenesulfonate is the main product coming from the phenyl sulfide moiety even though small amounts of diphenyl disulfide are observed.

Clearly, the presence of O_2 promotes a fragmentation process that is much more important than that coming from the direct C–S bond cleavage in the radical cation mentioned above. A possible proposal is that the fragmentation products in the presence of oxygen mostly derive from the decomposition of an intermediate formed by the reaction of the radical cation with the superoxide anion generated by NMQ^\bullet and O_2 . As already mentioned, the reaction of sulfide radical cations with O_2^- is the key step in the electron transfer photoinduced sulfoxidations of sulfides and it is reasonable to suggest that it can play a fundamental role also in the fragmentation reactions investigated. This suggestion is supported by the following. First, as already observed, the presence of oxygen strongly increases the efficiency of the photolysis, producing quantum yields of fragmentation products much higher than those found in the presence of nitrogen. Second, a reaction of O_2^- with the radical cation is indicated by the results of time-resolved experiments. Accordingly, as already noted, the second-order decay of the radical cation in the presence of O_2 is ca. 3–4 times faster than in the presence of nitrogen, being probably determined by the reaction of the radical cation with O_2^- , and there is no effect of the sulfide structure on the reactivity. Third and still more significant, in the presence of benzoquinone that can trap O_2^- , a substantial drop of the quantum yield in the photolysis of **1a–c** under air was observed.³⁰

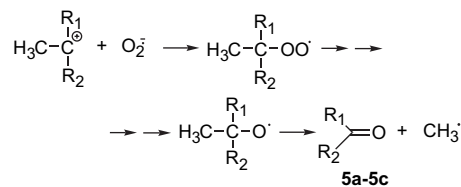
With convincing evidence in hand that the reaction of the sulfide radical cations of **1a–c** with O_2^- is en route to fragmentation products, we can try to envisage a reasonable mechanistic scheme. In previous work¹⁵ we have reported evidence indicating that in electron transfer photooxygenations, the reaction of the sulfide radical cation with O_2^- leads to a thiadioxirane **6** (Scheme 5, path a). Usually, the thiadioxirane is expected to react with another sulfide molecule to form the sulfoxide. However, it is not unreasonable to suggest that with the sterically crowded sulfides **1a–c**,

such a bimolecular reaction can become very difficult and the thiadioxirane (that probably is in a vibrationally excited state due to the very large exergonicity of its formation) may instead undergo C–S bond cleavage, presumably concerted with the opening of the three-member ring, leading to a quite stable tertiary carbocation and phenylsulfinate (Scheme 5, path b).³¹ The phenylsulfinate should be oxidized to the sulfonate under the reaction conditions.³² The alcohols (and alkenes) are formed from the carbocations as shown in Scheme 4. With **1a**, also *N*-*tert*-butylacetamide is formed,³³ whereas the alkene is not observed.



Scheme 5.

The formation of ketones **5**, that are a significant fraction of the products mixture obtained under air, may be justified by the possible reaction of the carbocation with O_2^- . An alkylperoxyl radical is formed that can be converted into ketone as shown in Scheme 6. Indeed, by generating the cumylperoxyl radical in the photolysis of cumene in the presence



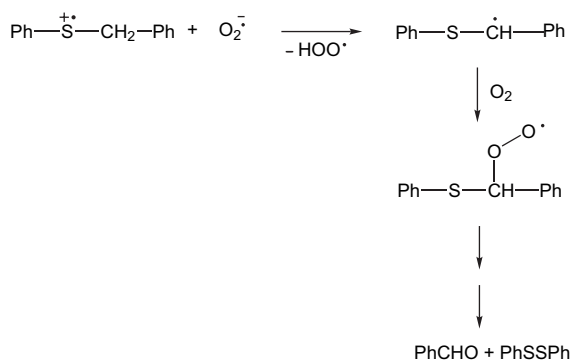
Scheme 6.

of di-*tert*-butyl peroxide and oxygen, benzophenone **5b** was obtained as the main product accompanied by small amounts of **3b** and **4b** (Section 5).³⁴

3.2. Benzyl phenyl sulfide

The behaviors of sulfide (**2**) were similar to that of the *tert*-alkyl phenyl sulfides, discussed above. Thus, laser photolysis experiments showed the formation of the sulfide radical cation (in this case the dimeric form was also observed) that, however, decayed without the apparent formation of any transient. The decay rate followed second-order kinetics with a $k_2\epsilon$ value very close to that found with the radical cations of *tert*-alkyl phenyl sulfides. In this case too the decay rate was faster under oxygen than under nitrogen (Table 3). As with *tert*-alkyl phenyl sulfides, steady-state photolysis of **2** sensitized by NMQ⁺ led to significant amounts of products (benzyl phenyl sulfoxide and benzaldehyde) only in the presence of oxygen. However, when the photolysis was run in the presence of benzoquinone the yield of products dropped almost to zero in the presence of oxygen.

It seems clear that with **2**, the reaction of the sulfide radical cation with O₂⁻ also plays a key role in product formation. When O₂⁻ attacks sulfur, thiadioxirane forms leading to sulf-oxide by reaction with another molecule of sulfide, as previously suggested for electron transfer sulfoxxygenations.¹⁵ In this case, the sulfide is not sterically congested, thus this reaction predominates with respect to the C–S bond cleavage reactions observed with **1a–c**.³⁵ However, since α -CH bonds are present in **2**⁺, O₂⁻ can also perform a deprotonation process forming an α -phenylthio carbon radical that can lead to benzaldehyde and diphenyl disulfides by reaction with O₂, as shown in Scheme 7. The possibility that in electron transfer sulfoxxygenations of sulfides with α -CH bonds, C–S bond cleavage products would derive from deprotonation of the sulfide radical cation had already been proposed,¹³ but the key role played by O₂⁻ in this respect had not been hitherto demonstrated.



Scheme 7.

4. Conclusions

The results of LFP and steady-state photolysis experiments have allowed us to reach the important conclusion that the C–S bond cleavage products formed in the photooxygenation of *tert*-alkyl phenyl sulfides sensitized by NMQ⁺ mainly derive from the sterically congested thiadioxirane formed by

the reaction of the sulfide radical cation with O₂⁻. The mesolytic rupture of the C–S bond in the intermediate radical cation plays a minor role. A different situation holds with benzyl phenyl sulfide **2** (a primary alkyl sulfide with α -CH bonds) where the fragmentation product, benzaldehyde, is suggested to come from deprotonation of **2**⁺ by O₂⁻ in competition with the formation of thiadioxirane. The latter species is much less congested than that formed from *tert*-alkyl phenyl sulfides and can therefore react, as expected, with another sulfide molecule to give benzyl phenyl sulfoxide that accordingly is among the reaction products.

5. Experimental

5.1. Starting materials

Commercial benzyl phenyl sulfide (**2**) was further purified by recrystallization from EtOH/H₂O. *tert*-Butyl phenyl sulfide (**1a**) was prepared by acid catalyzed reaction of thiophenol with *tert*-butanol.³⁶ 2-Phenyl-2-propyl phenyl sulfide (**1b**) and 1,1-diphenylethyl phenyl sulfide (**1c**) were prepared by acid catalyzed addition of thiophenol on α -methylstyrene and 1,1-diphenylethylene, respectively.³⁷ CH₃CN (spectrophotometric grade) and toluene were used as received. *N*-Methylquinolinium tetrafluoroborate was prepared according to a literature procedure.³⁸

5.2. Quantum yields

A 2 ml solution of NMQ⁺ (4×10^{-4} M) in CH₃CN and **1a–c** and **2** (1.0×10^{-2} M) in CH₃CN (CD₃CN in the case of **1a**) was placed in a quartz cuvette and irradiated at 313 nm, selected with a Balzer interference filter by a high pressure Hg lamp. The substrate conversion to photoproduct was held below 10% to avoid secondary reactions. The photoproducts were quantified by GC and ¹H NMR. Bibenzyl was used as an internal standard. The products from sulfide **1a** were analyzed exclusively by ¹H NMR, because of their high volatility. Water soluble photoproducts were identified by ¹H NMR after evaporation of the solvent CH₃CN and addition of D₂O. All products formed were identified by comparison with authentic specimens. *tert*-Butyl acetamide, acetophenone, benzophenone, 2-phenyl-2-propanol, α -methylstyrene, 1,1-diphenylethanol, 1,1-diphenylethylene, *tert*-butanol, acetone, benzaldehyde, diphenyl disulfide, sodium benzenesulfonate were commercial products. Benzyl phenyl sulfoxide was prepared by oxidation of benzyl phenyl sulfide with NaO₄.³⁹ The light intensity (ca. 1×10^{15} photons s⁻¹) was measured by potassium ferric oxalate actinometry.⁴⁰

5.3. Steady-state photooxidation of cumene

By irradiation of *tert*-butyl peroxide (0.16 M) at 313 nm in the presence of cumene (1.0×10^{-2} M) in O₂-saturated CH₃CN, acetophenone (3.4%), α -methylstyrene (1.0%), and 1,1-diphenylethanol (0.8%) formed after 7 h.

5.4. Fluorescence quenching

Measurements were carried out on a Spleg Fluorolog F112AF spectrofluorometer. Relative emission intensities

at 390 nm (NMQ⁺ emission maximum) were measured by irradiating at 315 nm (NMQ⁺ absorption maximum) a solution containing NMQ⁺ (1.0×10^{-5} M) and the substrates **1a–c** and **2** at different concentrations (from 0 to 7.0×10^{-3} M) in CH₃CN at 22 °C. The error estimated on the Stern–Volmer constants (K_{SV}) was $\pm 5\%$.

5.5. Laser flash photolysis

The excitation wavelength of 355 nm from a Nd:YAG laser (Continuum, third harmonic) was used in nanosecond flash photolysis experiments (pulse width ca. 7 ns and energy <3 mJ per pulse). The transient spectra were obtained by a point-to-point technique, monitoring the absorbance changes (ΔA) after the flash at intervals of 5–10 nm over the spectral range 350–850 nm, averaging at least 10 decays at each wavelength. The lifetime values (the time at which the initial signal is reduced to $1/e$, experimental error $\pm 10\%$) are reported for transients showing first-order decay kinetics. The k_2/ϵ values are reported for the transients showing second-order kinetics. A 2 ml solution containing the substrate (1.0×10^{-2} M), NMQ⁺ (4×10^{-4} M) and the cosensitizer (1 M toluene) was flashed in a quartz photolysis cell while nitrogen or oxygen was bubbling through them. All measurements were carried out at 22 ± 2 °C. The experimental error was $\pm 10\%$.

Acknowledgements

MIUR, University 'la Sapienza' of Rome and University of Perugia are thanked for the financial support.

Supplementary data

Supplementary data associated with this article can be found in the online version, at doi:10.1016/j.tet.2005.09.154.

References and notes

- Eriksen, J.; Foote, C. S.; Parker, T. L. *J. Am. Chem. Soc.* **1977**, *99*, 6455–6456.
- Ando, W.; Kabe, Y.; Shohei, K.; Takyu, C.; Yamagishi, A.; Inaba, H. *J. Am. Chem. Soc.* **1980**, *102*, 4526–4528.
- Marciniak, B.; Hug, G. L.; Rozwadowski, J.; Bobrowski, K. *J. Am. Chem. Soc.* **1995**, *117*, 127–134.
- Miller, B.; Williams, T. D.; Schöneich, C. *J. Am. Chem. Soc.* **1996**, *118*, 11014–11025.
- Bobrowski, K.; Hug, G. L.; Marciniak, B.; Miller, B.; Schöneich, C. *J. Am. Chem. Soc.* **1997**, *119*, 8000–8011.
- Tung, C.-H.; Guan, J.-Q. *J. Am. Chem. Soc.* **1998**, *120*, 11874–11879.
- Bonesi, S. M.; Mella, M.; d'Alessandro, N.; Aloisi, G. G.; Vanossi, M.; Albini, A. *J. Org. Chem.* **1998**, *63*, 9946–9955.
- Toutchkine, A.; Clennan, E. L. *J. Org. Chem.* **1999**, *64*, 5620–5625.
- Bonesi, S. M.; Albini, A. *J. Org. Chem.* **2000**, *65*, 4532–4536.
- Toutchkine, A.; Aebischer, D.; Clennan, E. L. *J. Am. Chem. Soc.* **2001**, *123*, 4966–4973.
- Clennan, E. L. *Acc. Chem. Res.* **2001**, *34*, 875–884.
- Clennan, E. L.; Zhou, W.; Chan, J. *J. Org. Chem.* **2002**, *67*, 9368–9378.
- Lacombe, S.; Cardy, H.; Simon, M.; Khoukh, A.; Soumillion, J. P.; Ayadim, M. *Photochem. Photobiol. Sci.* **2002**, *1*, 347–354.
- Zen, J. M.; Liou, S. L.; Kumar, A. S.; Hsia, M. S. *Angew. Chem., Int. Ed.* **2003**, *42*, 577–579.
- Baciocchi, E.; Del Giacco, T.; Elisei, F.; Gerini, M. F.; Guerra, M.; Lapi, A.; Liberali, P. *J. Am. Chem. Soc.* **2003**, *125*, 16444–16454.
- Che, Y.; Ma, W.; Ren, Y.; Chen, C.; Zhang, X.; Zhao, J.; Zang, L. *J. Phys. Chem. B* **2005**, *109*, 8270–8276.
- Baciocchi, E.; Crescenzi, C.; Lanzalunga, O. *Tetrahedron* **1997**, *53*, 4469–4478.
- Manring, L. E.; Kramer, M. K.; Foote, C. S. *Tetrahedron Lett.* **1984**, *25*, 2523–2526.
- Bonesi, S. M.; Fagnoni, M.; Albini, A. *J. Org. Chem.* **2004**, *69*, 928–935.
- Fukuzumi, S.; Fujita, M.; Noura, S.; Ohkubo, K.; Suenobu, T.; Araki, Y.; Ito, O. *J. Phys. Chem. A* **2001**, *105*, 1857–1868.
- Baciocchi, E.; Del Giacco, T.; Elisei, F.; Gerini, M. F.; Lapi, A.; Liberali, P.; Uzzoli, P. *J. Org. Chem.* **2004**, *69*, 8323–8330.
- Dockery, K. P.; Dinnocenzo, J. P.; Farid, S.; Goodman, J. L.; Gould, I. R.; Todd, W. P. *J. Am. Chem. Soc.* **1997**, *119*, 1876–1883.
- Bockman, T. M.; Kochi, J. K. *J. Am. Chem. Soc.* **1989**, *111*, 4669–4683.
- Jonsson, M.; Lind, J.; Merényi, G.; Eriksen, T. E. *J. Chem. Soc., Perkin Trans. 2* **1995**, 67–70; Ioele, M.; Steenken, S.; Baciocchi, E. *J. Phys. Chem. A* **1997**, *101*, 2979–2987; Mohan, H.; Mittal, J. P. *J. Phys. Chem. A* **1997**, *101*, 10012–10017.
- Yokoi, H.; Hatta, A.; Ishiguro, K.; Sawaki, Y. *J. Am. Chem. Soc.* **1998**, *120*, 12728–12733.
- Asmus, K.-D. *Acc. Chem. Res.* **1979**, *12*, 436–442.
- Armstrong, D. A.; Sun, Q.; Schuler, R. H. *J. Phys. Chem.* **1996**, *100*, 9892–9899.
- Cozens, F. L.; Kanagasabapathy, V. M.; McClelland, R. A.; Steenken, S. *Can. J. Chem.* **1999**, *77*, 2069–2082.
- Fukuzumi, S.; Nakanishi, J.; Maruta, J.; Yorise, J.; Suenobu, T.; Itoh, S.; Arakawa, R.; Kadish, K. M. *J. Am. Chem. Soc.* **1998**, *120*, 6673–6680.
- The effect of benzoquinone also shows that the higher quantum yields in the presence of oxygen are not due to a suppression of the BET process by the reaction of NMQ⁺ with O₂. This possibility is also made unlikely by the fact that no transients were observed in the laser photolysis experiments in the presence of O₂.
- Theoretical calculations (B3LYP/6-31G* level) have shown that such a C–S bond cleavage, in CH₃CN as solvent, is exothermic by 11 kcal mol⁻¹. We are very grateful to Dr. M. F. Gerini for performing this calculation.
- Oae, S.; Takata, T.; Kim, H. K. *Tetrahedron* **1981**, *37*, 37–44.
- tert*-Butyl cation is less stable and less selective than the cations from **1a** and **1b**, therefore it can also react with the solvent that is a weaker nucleophile than water.
- It might be suggested that the C–S bond breaking in the thia-dioxirane is homolytic forming a benzenesulfonyl radical and a carbon radical. Reaction of the carbon radical with oxygen should lead to the observed reaction products. However, the formation of *N-tert*-butylacetamide is a clear indication that a carbocation is also formed and supports the heterolytic

- cleavage. Moreover, in this case the ketone would be the main reaction product, which is not observed.
35. In the photooxygenation of **2** sensitized by 9,10-dicyanoanthracene we have also observed the formation of benzyl derivatives.¹⁷ However, those experiments were carried out at a significantly higher temperature, ≥ 40 °C.
 36. Cutress, N. C.; Grindley, T. B.; Katritzky, A. R.; Topsom, R. D. *J. Chem. Soc., Perkin Trans. 2* **1974**, 263–268.
 37. Screttas, C. G.; Micha-Screttas, M. *J. Org. Chem.* **1979**, *44*, 713–719.
 38. Donovan, P. F.; Conley, D. A. *J. Chem. Eng. Data* **1966**, *11*, 614–615.
 39. Johnson, C. R.; Leonard, N. J. *J. Org. Chem.* **1962**, *27*, 282–284.
 40. Bunce, N. J. *Handbook of Organic Photochemistry*; Scaiano, J. C., Ed.; Academic: New York, NY, 1999; Vol. 1, p 243.

Externally sensitized mesolytic fragmentations in dithiane–ketone adducts

Tiffany P. Gustafson, Alexei N. Kurchan and Andrei G. Kutateladze*

Department of Chemistry and Biochemistry, University of Denver, Denver, CO 80208-2436, USA

Received 11 September 2005; accepted 12 November 2005

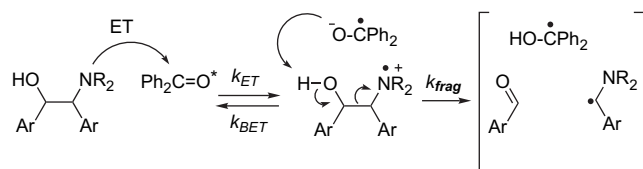
Available online 17 April 2006

Abstract—The apparent activation enthalpies, ΔH^\ddagger , for externally sensitized mesolytic fragmentations in benzophenone–dithiane adducts were obtained in variable temperature photolyses and compared with DFT activation barriers calculated for β -scission in the corresponding oxygen-centered radicals. The results of these experimental and theoretical studies further support the mechanism in which deprotonation of the hydroxy-group, in the transient cation radical, is coupled with intramolecular electron transfer furnishing the O-centered radical, which subsequently fragments. The quantum yields of fragmentation increase for higher alkyl substituted dithiane adducts. © 2006 Elsevier Ltd. All rights reserved.

1. Introduction

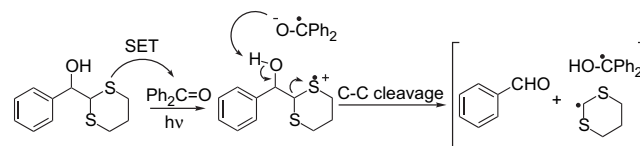
Heteroatom-centered cation radicals, $C_\beta-C_\alpha-X^{+\cdot}$, which are readily generated by photoinduced electron transfer (ET), are subject to mesolytic fragmentation. It is well known that removal of one electron from the heteroatom's lone pair in the ground state significantly reduces the bond order of the geminal bonds, which either increases the acidity of the alpha-proton ($H-C_\alpha$) or causes the $C_\alpha-C_\beta$ bond to cleave. In our previous work we utilized this increased acidity of the alpha-proton and developed an efficient electrochemical deprotection for carboxylates in general, and amino acids in particular, based on esters of hydroxymethyldithiane.¹ In this paper we will focus primarily on photoinduced C–C bond fragmentations in adducts of dithianes with ketones.

ET-induced fragmentations in vicinal amino alcohols and diols have been extensively studied.² The accepted mechanistic rationale includes photoinduced electron transfer to an ET-sensitizer, e.g., benzophenone, followed by a mesolytic cleavage of the generated cation radical, assisted by the benzophenone anion radical deprotonating the vicinal hydroxy group. It was noted that the C–C bond cleavage step is reminiscent of the Grob fragmentation in closed shell systems.³

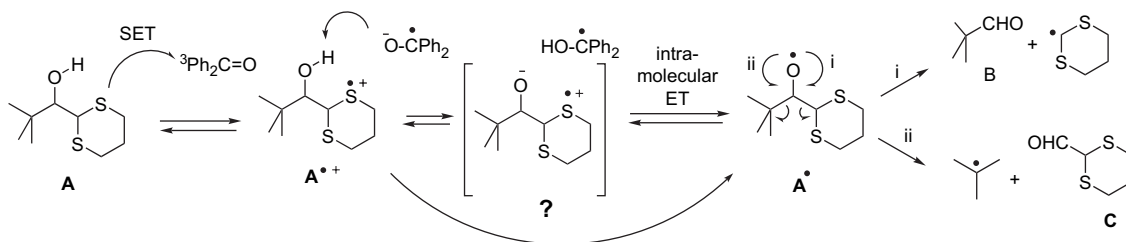


* Corresponding author. E-mail: akutatel@du.edu

One of the early examples by Whitten and Ci involved thioindigo-sensitized fragmentation in the *threo*- and *erythro*-2-morpholino-1,2-diphenylethanol.^{3a} Assuming that the only temperature-dependent process in the reaction of the geminate ion radical pair is k_{frag} , they determined the Arrhenius activation energy for the *threo*- and *erythro* diastereomers to be 4.9 and 2.8 kcal/mol, respectively. This demonstrates a strong conformational dependence of the cleavage and shows that the activation barrier is very low.

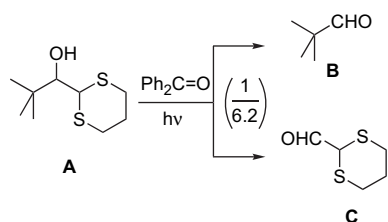


Similar reactions of sulfido-alcohols are also known. For example, Gravel et al. utilized the C–C cleavage in β -phenylthioalkanol as a synthetic method for indirect cleavage of olefins⁴ and also in carbohydrate synthesis.⁵ Some time ago we found that dithianes are particularly suitable for this chemistry: their adducts are readily synthesized and they cleave efficiently upon photoinduced fragmentation. The mechanism of cleavage in dithiane adducts was investigated by utilizing classical physical organic methods such as the Hammett substituent effect, the kinetic isotope effect,⁶ and laser flash photolysis studies.⁷ Our initial mechanistic findings were in keeping with the universally recognized 'Grob-like' mechanism, until we tested the photoinduced fragmentation in the *tert*-butyl derivative **A**, which in addition to the expected pivalaldehyde **B** ('normal' cleavage) produced dithiane-2-carboxaldehyde **C** as a major product in 1:6.2 ratio.⁸ It became clear that the quasi-Grob electron

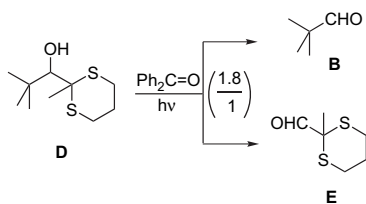


Scheme 1.

pushing rationale needed refinement because adduct **A** was primarily cleaving the wrong bond.



Further experimental and computational investigation suggested that deprotonation of the hydroxy group in the initially generated cation radical does not result in the formation of a charge separated ‘Grob-like’ precursor $^-\text{O}-\text{C}-\text{C}-\text{S}^+-\text{R}$, but rather produces a neutral oxygen-centered radical (or a species behaving as one) via intramolecular electron transfer. The O-centered radical undergoes subsequent fragmentation in either direction and the partitioning correlates with stability of the produced radicals, Scheme 1.⁹ When methylthiane derivative **D** was used in place of **A**, the ratio of **B**:**C**=1:6.2 was inverted to become **B**:**E**=1.8:1, all in keeping with relative stability of *tert*-butyl, dithian-2-yl, and 2-methyldithian-2-yl radicals. We also compared the



results of the fragmentation in methylene chloride and acetonitrile, which constitutes almost an order of magnitude difference in the dielectric constant, and did not see any difference in the partitioning within experimental error. All these results seem to indicate that the charge separated species does not exist, or at best it is in fast equilibrium with the alkoxy radical (Scheme 1).

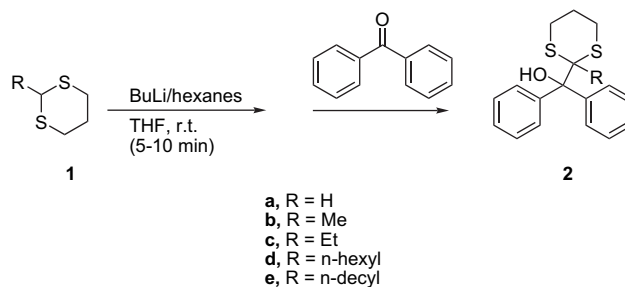
The case of *tert*-butyl derivatives, such as **A** and **D**, is unique in a sense that it allowed us to discover this new channel in the mechanism of fragmentation simply by product analysis. For dithiane adducts of aromatic aldehydes and ketones the barrier for the aryl radical departure is prohibitively high, i.e., it is the dithiane radical, which is *always* departing. Therefore, it is much more difficult to ascertain whether or not the original Grob-like mechanism for cleavage competes with the anomalous O-centered radical mechanism (or either one of them is operating exclusively) in the case of aromatic adducts. Because of the presence of sulfur it is synthetically

challenging, if not impossible, to generate the O-radical **A**[•] from an alternative precursor, for example, a peroxide, and study the effect of substituents on the rate of its degradation.

In this paper we report our experimental and computational study of the mechanism of photoinduced cleavage in adducts of 2-alkyl substituted dithianes with benzophenone, which is intended to further refine the mechanism of fragmentation. Benzophenone-sensitized mesolytic fragmentations, in adducts of the sensitizer itself, result in generation of more benzophenone and, as such, constitute its amplification. Hence, our particular interest in this system, which we plan to utilize in various photochemical applications.

2. Results and discussion

Benzophenone adducts **2a–e** of unsubstituted (**1a**), 2-methyl- (**1b**), 2-ethyl- (**1c**), 2-hexyl (**1d**), and 2-decyl (**1e**) dithiane were synthesized according to a modified Corey–Seebach procedure¹⁰ (Scheme 2) and their photoinduced fragmentation was studied over a temperature range from -40 to $+40$ °C in acetonitrile upon benzophenone sensitization. The driving force for the oxidative electron transfer from the dithiane moiety to the triplet state of benzophenone in acetonitrile is rather large: the one electron reduction potential of triplet benzophenone is -1.68 V (vs SCE in acetonitrile),¹¹ whereas various 2-substituted dithianes oxidize in the range of $+0.73$ to $+1.18$ V in the same solvent.¹² During the course of a laser flash photolysis study⁷ we found that the rate of initial electron transfer quenching of triplet benzophenone with dithiane–benzophenone adduct in dry acetonitrile was near the diffusion limit, $8.4 \pm 0.7 \times 10^8 \text{ M}^{-1} \text{ s}^{-1}$. In 10% aqueous acetonitrile the quenching rate was even higher, $1.31 \pm 0.06 \times 10^9 \text{ M}^{-1} \text{ s}^{-1}$. In the present study we have determined the dependence of the quantum efficiency of fragmentation on temperature and compared the experimental (apparent) activation enthalpy with the calculated activation barrier for the β -scission in the corresponding



Scheme 2.

Table 1. Quantum efficiencies and dithiane recovery rates at +20 °C for adducts **2b–e**

Adduct	ϕ	Dithiane recovery (%)
Methyl- (2b)	0.20	32.8
Ethyl- (2c)	0.23	35.3
Hexyl- (2d)	0.25	41.0
Decyl- (2e)	0.27	47.8

O-centered radicals. The computations were run at the DFT, B3LYP/6-31G(d), level using Gaussian 03, revision C.02.¹³

Photolyses were carried out in a carousel Rayonet photo-reactor with a Pyrex heat exchange jacket cooled by ethanol circulating through a FTS Systems Multi-Cool refrigeration unit. The quantum yield determinations were done using the classic benzophenone—benzhydrol actinometer system as a standard.¹⁴ Having benzophenone as a common sensitizer, in both the photoinduced fragmentation under study and the actinometer system, significantly improves the accuracy of quantum yield determinations. In addition to the overall quantum yield of adduct disappearance another important parameter is the percent recovery of the corresponding dithiane. Both the Grob-like and the O-centered radical mechanisms have a dithian-2-yl radical as the immediate fragmentation product. Its fate depends on multiple factors, including the reactivity of such a radical towards oxygen, dimerization, disproportionation etc. The recovery of dithiane in turn depends on all of the above and also on the rate of its degradation as a result of secondary photooxidation by benzophenone. We found that more substituted dithianes showed better recovery, which is in agreement with the overall trends in reactivity of the dithian-2-yl radicals (i.e., unsubstituted dithianyl radicals react/degrade faster) and of the final products—dithianes (i.e., less substituted dithianes undergo benzophenone-sensitized oxidative photodegradation faster). The quantum efficiency of cleavage also steadily

Table 2. Quantum yields of fragmentation and % dithiane recovery as a function of temperature

T (°C)	Ethyl adduct 2c		Methyl adduct 2b	
	ϕ	Dithiane recovery (%)	ϕ	Dithiane recovery (%)
–40	0.04	0.7	0.01	1.5
–20	0.13	6.2	0.05	4.3
0	0.18	17.8	0.10	6.2
20	0.21	14.8	0.15	8.7
40	0.32	37.6	0.25	12.5

increases for adducts of dithianes substituted with longer alkyl chains (Table 1).

The adduct of the parent compound, unsubstituted dithiane, showed poor efficiency of cleavage. This deficiency is not due to the impediment of the initial electron transfer: our previous LFP experiments show that the initial electron transfer quenching rate increases with the decreased substitution.⁷ It is difficult to argue definitively about the partitioning of the initially formed dithiane cation radical—benzophenone anion radical pair (i.e., the partition between the back electron transfer and the productive deprotonation of the adduct by the anion radical leading to fragmentation). However, following Whitten's assumption^{3a} that the only temperature-dependent process in a reaction of the geminate radical ion pair is fragmentation, we obtained the enthalpy of activation by plotting the data shown in Table 2 as $\ln(\phi/T)$ versus $1/T$ for the reaction of **2b** and **2c** (Fig. 1).

The activation enthalpies, ΔH^\ddagger , are obtained from the slopes: 4.7 kcal/mol for the methyl derivative **2b** and 1.5 kcal/mol for the ethyl derivative **2c** (Fig. 1a). These values are very similar to the activation energies obtained by Whitten for the thioindigo-sensitized fragmentation in vicinal amino alcohols.^{3a}

We suggest that the effect of substitution at position 2 of dithiane reflects largely the acceleration of the fragmentation in the deprotonated species, the oxygen-centered radical. Walling and Padwa¹⁵ studied the substitution effect in decomposition of hypochlorites of alkyl dimethylcarbinols, $R-C(Me)_2-O-Cl$, by comparing the differences in activation energies for decomposition and hydrogen abstraction. They reported that while the difference was 10 kcal/mol for *tert*-butoxy radical (i.e., $R=Me$), it decreased to 1.7 for $R=i-Pr$, 0.7 for $R=benzyl$, and was negligibly small for $R=t-Bu$. The absolute value for the activation energy of fragmentation in *tert*-butoxy radical is 11–13 kcal/mol.¹⁶ Assuming that the rate of hydrogen abstraction does not change much, introduction of the *tert*-butyl group in place of methyl should lower the activation energy of fragmentation in these alkoxy radicals by about 10 kcal/mol, to approx. 1–3 kcal/mol. 2-Methyl-1,3-dithian-2-yl and 2-ethyl-1,3-dithian-2-yl are very stable (and bulky) radicals. Judging by our previous observations of the competitive cleavage, the 2-methyldithianyl radical is more stable than *tert*-butyl, which in turn is more stable than the unsubstituted dithiane-2-yl radical.⁸ Summarizing these arguments, it is

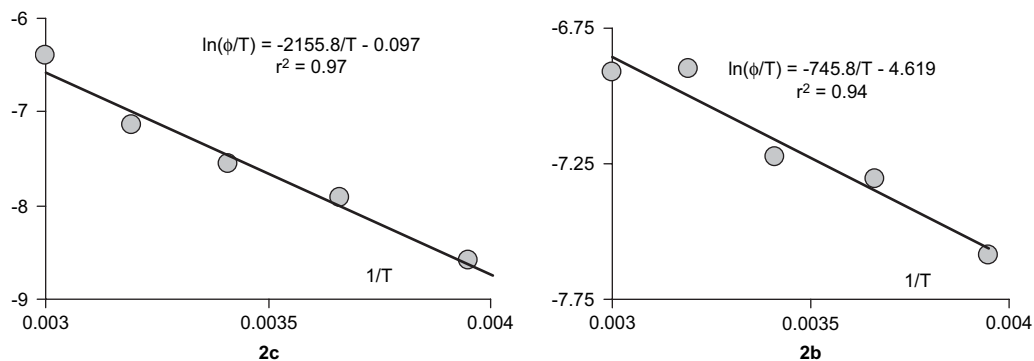
**Figure 1.** $1/T$ dependence of fragmentation quantum yields for ethyl (**2c**) and methyl (**2b**) adducts.

Table 3

	SS (kcal/mol)	TS (kcal/mol)	ΔH^\ddagger (kcal/mol)
<i>Ethyl-derivative 2c• (O-radical)</i>			
aEaO-2c•	5.4	10.2	4.77
aEgO-2c•	4.5	22.6	18.15
eEaO-2c•	1.1	^a —	—
eEgO-2c•	0.0	1.7	1.70
<i>Methyl derivative 2b• (O-radical)</i>			
aMaO-2b•	3.4	8.5	5.05
aMgO-2b•	2.8	5.1	2.24
eMaO-2b•	0.9	^a —	—
eMgO-2b•	0.0	1.7	1.72

^a Computations did not converge.

not unreasonable to assume that the apparent ΔH^\ddagger of 4.7 and 1.5 kcal/mol, obtained in this study, correspond to fragmentation in the oxygen-centered radicals, expelling methylthianyl and ethylthianyl radicals, respectively.

To support this hypothesis we carried out DFT computations at a B3LYP/6-31G(d) level, using the whole untruncated structures of the methyl- and ethyldithiane adducts of benzophenone (**2b** and **2c**). The initial geometries of the respective oxygen-centered radicals (**2b•** and **2c•**) were generated with Chem3D and pre-optimized at the AM1 level. Vibrational analysis of the DFT optimized geometries show no imaginary frequencies for the computed minima (ground states) and only one imaginary frequency for the transition states corresponding to the reaction coordinate (i.e., C–C stretch). Given the importance of conformational considerations, we scanned the conformational space and analyzed the relative energies of the starting alkoxy radicals and their respective fragmentation transition states for the four major conformers: (i) equatorial 2-alkyl with the CO bond in *anti* conformation to this alkyl, denoted eMaO, i.e., equatorial Methyl anti Oxygen (the oxygen is *anti* to the methyl group), and eEaO for Ethyl; (ii) equatorial 2-alkyl—*gauche* CO bond, eMgO/eEgO; (iii) axial 2-alkyl—*anti* CO bond; aMaO/aEaO; (iv) axial 2-alkyl—*gauche* CO bond, aMgO/aEgO. The other two sets of the *gauche* conformers are enantiomers of eMgO/eEgO and aMgO/aEgO. The relative energies of the starting oxy-radicals and their respective transition states are listed in Table 3 with the calculated ΔH^\ddagger summarized in the third column.

Strikingly, the lowest energy conformations for both methyl and ethyl derivatives had the smaller alkyl substituent in the

Table 4. DFT relative energies for the conformers of alcohols **2a–c**

Conformers	Rel energy (kcal/mol)
aMaO-2b	3.15
aMgO-2b	3.45
eMaO-2b	2.90
eMgO-2b	0.00
aEaO-2c	5.52
aEgO-2c	1.91
eEaO-2c	3.18
eEgO-2c	0.00
aHaO-2a	0.01
aHgO-2a	0.00
eHaO-2a	3.31
eHgO-2a	2.80

equatorial position, whereas the bulky benzhydryl group was axial, with oxy-radical being *gauche* to methyl/ethyl (i.e., *anti* to one of sulfur atoms). The transition state geometries were obtained at the same B3LYP/6-31G(d) level of theory. The electronic energies for all the species in Table 3 are zpe-corrected. As follows from the table, the eMgO/eEgO conformers have the lowest energies both at the minima and the transition states (see also Fig. 2). This is also in keeping with the computed conformational energies of the parent alcohols that showed at least a 2 kcal/mol preference for the eRgO conformers (Table 4).

On the contrary, for the C-2 unsubstituted dithiane adduct it was the axial-H (i.e., the equatorial benzhydryl) conformers aHaO and aHgO that were expectedly more stable by approx. 3 kcal/mol.

NMR spectroscopic study of the parent alcohols supported the DFT findings. The initial analysis of the 1D proton NMR spectra of the three adducts shows systematic upfield shift of the dithiane's H₂C⁽³⁾ and H₂C⁽⁵⁾ protons upon introduction of the methyl and then ethyl group. The downfield multiplet corresponds to two axial H₂C⁽³⁾ and H₂C⁽⁵⁾ protons and the upfield—equatorials (Fig. 3).

Low temperature NMR data show dramatic differences in conformational behavior of the substituted (**2b** and **2c**) versus unsubstituted (**2a**) derivatives. The temperature-dependent changes in one-dimensional ¹H NMR spectra are shown in Figure 4. Below –40 °C the multiplets for both axial and equatorial protons H₂C⁽³⁾ and H₂C⁽⁵⁾ in the Me- and Et-derivatives split into two sets. It appears that the

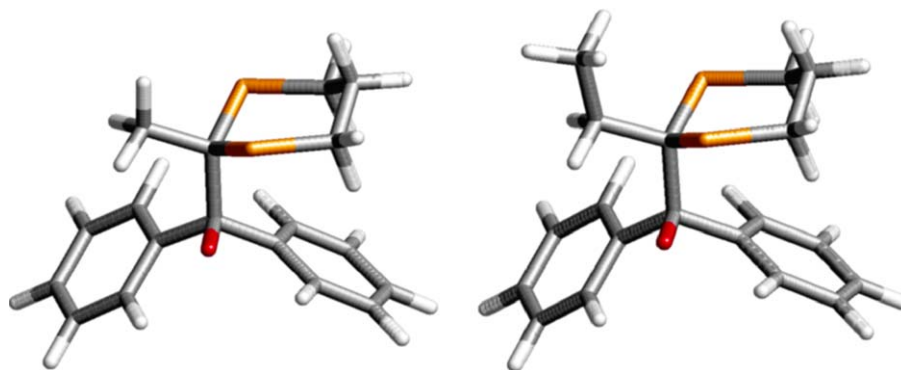


Figure 2. The lowest energy conformers of the respective O-centered radicals: eMgO-2b• (left) and eEgO-2c• (right).

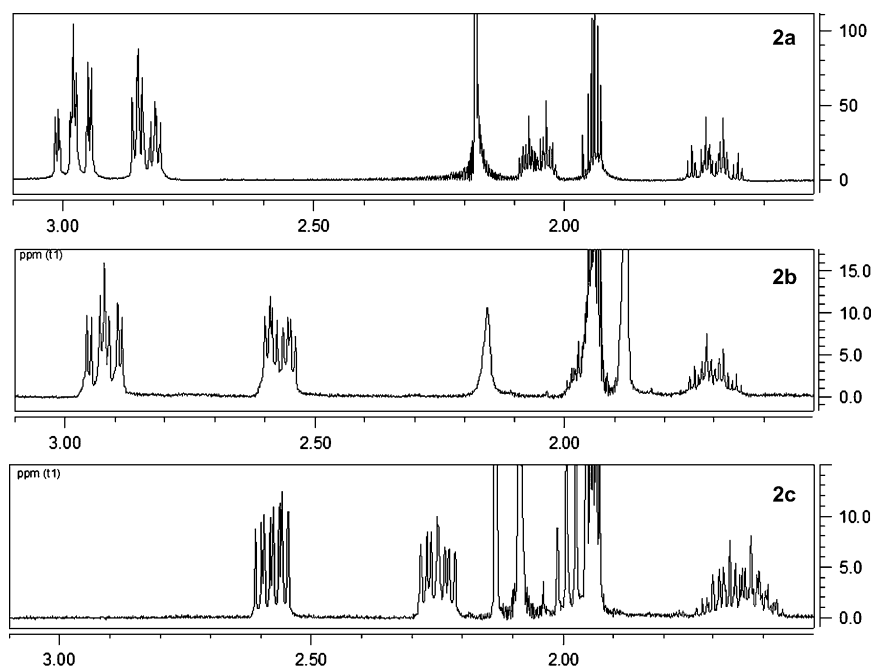


Figure 3. 1D proton NMR spectra of 2a–c.

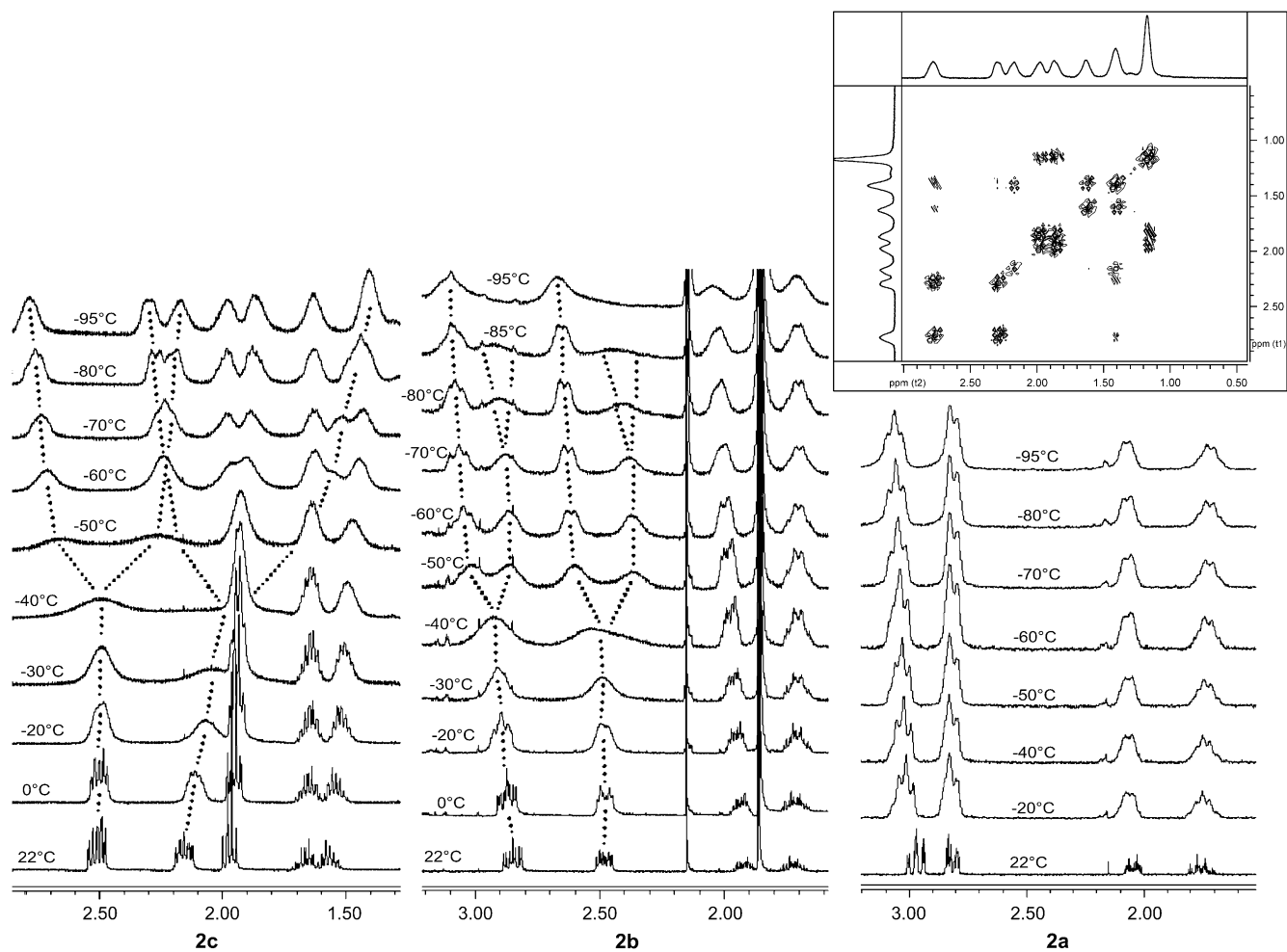


Figure 4. VT NMR data for 2a–c. The inset shows low temperature COSY spectrum for 2c at -95°C .

rotation of the benzhydryl group is stopped at this temperature and that the most stable isomer is unsymmetrical.

On the contrary, NMR spectrum of unsubstituted **2a** shows negligible temperature-dependent changes, which could indicate that the most stable conformer is symmetric (i.e., *anti*). An alternative interpretation is that the rotation of the benzhydryl group is not stopped even at $-95\text{ }^{\circ}\text{C}$ in unsubstituted **2a**.

Equal integrated intensities of the split signals of the equatorial and axial protons indirectly confirm that they belong to the same conformer, not to two frozen populations of conformers, e.g., chair-to-chair, or chair–twist conformers of dithiane, in which case they would be expected to have different integrated values. For more definitive assignment, we ran a COSY experiment of **2c** at $-95\text{ }^{\circ}\text{C}$, which unambiguously showed strong cross-peaks for the respective split pairs of signals. We therefore conclude, that below $-40\text{ }^{\circ}\text{C}$ both equatorial protons $\text{H}_{\text{eq}}\text{-C}^{(3)}$ and $\text{H}_{\text{eq}}\text{-C}^{(5)}$ of the dithiane ring are not equivalent and separate into two signals. The same is true for the pair of axial protons $\text{H}_{\text{ax}}\text{-C}^{(3)}$ and $\text{H}_{\text{ax}}\text{-C}^{(5)}$. These data can only be explained in terms of asymmetric conformation of the frozen benzhydryl group, which is in keeping with our computational finding that the asymmetric eRgO conformers are the most stable. The low temperature data for the Me derivative **2b** in Figure 4 show some additional line broadening for each of the upfield (right) signals of the split peaks, indicating that another degree of freedom is being frozen at $-60\text{ }^{\circ}\text{C}$ and below. We do not have an immediate explanation for this behavior—there can be a number of conformational processes that can cause the observed coalescence of signals at this temperature.

In conclusion, the measured apparent enthalpies of activation for photoinduced fragmentation in the alkyl dithiane–benzophenone adducts are in keeping with the kinetic barriers computed at the B3LYP/6-31G(d) level of theory for the mechanism involving formation of an alkoxy radical and its subsequent fragmentation. The findings do not rule out the charge separated Grob-like mechanism, but rather provide new evidence to support an alternative nonpolar mechanism. As to the design and development of the dithiane-based photolabile latches: utilization of higher alkyls at position 2 of dithiane increases both the quantum yield of fragmentation and recovery of dithiane, attesting to the potential of longer alkyl chains as a promising alternative for the molecular design of efficient photolabile tethers.

3. Experimental

3.1. General

Common solvents were purchased from Pharmco and used as is, except for THF, which was refluxed over and distilled from potassium benzophenone ketyl prior to use. *n*-BuLi (as a 1.6 M solution in hexane), 1,3-dithiane, 2-methyl-1,3-dithiane, benzophenone, and benzhydryl were purchased from Aldrich. 1,3-Dithiol was purchased from Acros. Propional, decanal, and heptanal were purchased from Alfa Aesar. All reagents were used without purification. ^1H NMR spectra were recorded at $25\text{ }^{\circ}\text{C}$ on a Varian Mercury 400 MHz

instrument in CDCl_3 with TMS as an internal standard (unless noted otherwise). Low temperature NMR was carried out in CD_3OD using a Varian Mercury VT system. Temperature was controlled using dry nitrogen flow through a liquid nitrogen Dewar. Column chromatography was performed on silica gel, 70–230 mesh ASTM, using ethyl acetate–hexane mixtures as eluent. Photoreactions were carried out in the carousel Rayonet photoreactor outfitted with a jacketed Pyrex reaction vessel connected to a FTS Systems Multi-Cool refrigeration unit with a peristaltic pump, using ethanol as a coolant.

Ab initio computations were performed on a Linux workstation using Gaussian 03, Revision C.02.¹³ Input geometries were created and pre-optimized using a force field geometry optimization as implemented in Chem3D (Cambridgesoft). The geometries were further pre-optimized at the AM1 level. Full geometry optimizations were performed using density functional theory (DFT) at the B3LYP/6-31G(d) level of theory (the Becke three-parameter hybrid functional combined with Lee, Yang, and Parr correlation functional¹⁷).

3.2. General method for dithiane preparation

1,3-Propanedithiol (0.07 mol) and the appropriate aldehyde (0.06 mol) were dissolved in 250 mL CH_2Cl_2 . $\text{BF}_3\cdot\text{Et}_2\text{O}$ (0.26 mol) was added to the solution. The reaction mixture was then stirred overnight at room temperature. The mixture was washed with NaOH (5% aq soln) and water. The organic layer was dried over anhydrous NaSO_4 and the solvent was removed by rotary evaporator and the resulting product was distilled under vacuum.

3.2.1. 2-Ethyl-1,3-dithiane (1c). Yield 8.7 g, 59 mmol, 86%; bp $38\text{ }^{\circ}\text{C}/63\text{ mTorr}$; ^1H NMR (CDCl_3 , 400 MHz): δ 4.0 (t, 1H, $J=6.8\text{ Hz}$), 2.80–2.92 (m, 4H), 2.09–2.16 (m, 1H), 1.84–1.92 (m, 1H), 1.77–1.92 (m, 2H), 1.09 (t, 3H).

3.2.2. 2-Hexyl-1,3-dithiane (1d). Yield 5.4 g, 26 mmol, 54%; bp $125\text{ }^{\circ}\text{C}/72\text{ mTorr}$; ^1H NMR (CDCl_3 , 400 MHz): δ 4.03 (t, 1H, $J=6.9\text{ Hz}$), 2.76–2.90 (m, 4H), 2.06–2.13 (m, 1H), 1.83–1.92 (m, 1H), 1.68–1.74 (m, 2H), 1.44–1.52 (m, 2H), 1.22–1.35 (m, 6H), 0.87 (t, 3H).

3.2.3. 2-Decyl-1,3-dithiane (1e). Yield 12.56 g, 48 mmol, 63%; bp $142\text{ }^{\circ}\text{C}/69\text{ mTorr}$; ^1H NMR (CDCl_3 , 400 MHz): δ 4.07 (t, 1H, $J=6.9\text{ Hz}$), 2.81–2.94 (m, 4H), 2.10–2.17 (m, 1H), 1.85–1.94 (m, 1H), 1.73–1.79 (m, 2H), 1.48–1.55 (m, 2H), 1.25–1.33 (m, 14H), 0.90 (t, 3H).

3.3. General method for adduct preparation

A generic method by Corey and Seebach was modified and used to prepare the desired dithiane–benzophenone adducts.¹⁰ Dithiane (5.1 mmol) was dissolved in freshly distilled THF (30 mL) and placed under nitrogen. *n*-Butyllithium (4.3 mL, 6.8 mmol) was added at room temperature upon stirring and the resulting mixture was stirred for 10 more minutes. Benzophenone (3.4 mmol) was dissolved in freshly distilled THF (10 mL) and added to the anion mixture with stirring. The reaction was left overnight. The reaction mixture was quenched with a saturated solution of ammonium chloride and the aqueous layer was extracted

twice with ethyl acetate. The combined organic layer was dried over anhydrous sodium sulfate. The solvent was removed with a rotary evaporator, and the residue was purified by column chromatography (silica gel, ethyl acetate–hexane) or recrystallization (methanol).

3.3.1. (2-Methyl-[1,3]-dithian-2-yl)-diphenyl-methanol (2b). Yield 0.80 g, 2.7 mmol, 80%; ^1H NMR (CDCl_3 , 400 MHz): δ 7.85–7.87 (m, 4H), 7.21–7.30 (m, 6H), 2.82 (ddd, 2H, $J=3.5, 10.5, 14.6$ Hz), 2.53 (ddd, 2H, $J=3.9, 5.7, 14.7$ Hz), 1.80–1.97 (m, 2H), 1.894 (s, 3H).

3.3.2. (2-Ethyl-[1,3]-dithian-2-yl)-diphenyl-methanol (2c). Yield 0.94 g, 2.8 mmol, 93%; ^1H NMR (CDCl_3 , 400 MHz): δ 7.93–7.96 (m, 4H), 7.28–7.33 (m, 4H), 7.22–7.26 (m, 2H), 2.52 (ddd, 2H, $J=4.8, 7.0, 14.2$ Hz), 2.25 (ddd, 2H, $J=4.8, 8.1, 13.0$ Hz), 1.97–2.04 (m, 2H), 1.67–1.73 (m, 2H), 1.12–1.16 (m, 3H).

3.3.3. (2-Hexyl-[1,3]-dithian-2-yl)-diphenyl-methanol (2d). Yield 0.61 g, 1.6 mmol, 49%; ^1H NMR (CDCl_3 , 400 MHz): δ 7.91–7.94 (d, 4H), 7.20–7.31 (m, 6H), 2.49 (td, 1H, $J=4.8, 10.3$ Hz), 2.22 (ddd, 1H, $J=5.9, 8.0, 14.1$ Hz), 1.91–1.96 (m, 2H), 1.60–1.73 (m, 4H), 1.10–1.31 (m, 6H), 0.81–0.85 (t, 3H).

3.3.4. (2-Decyl-[1,3]-dithian-2-yl)-diphenyl-methanol (2e). Yield 0.62 g, 1.4 mmol, 52%; ^1H NMR (CDCl_3 , 400 MHz): δ 7.92–7.94 (dd, 4H), 7.20–7.33 (m, 6H), 2.49 (td, 2H, $J=5.4, 14.1$ Hz), 2.23 (ddd, 1H, $J=5.7, 8.2, 13.9$ Hz), 1.91–1.96 (m, 2H), 1.60–1.77 (m, 6H), 1.10–1.34 (m, 12H), 0.81–0.85 (t, 3H).

Acknowledgements

Support for this research by the National Science Foundation (CHE-314344) is gratefully acknowledged.

References and notes

- Barnhurst, L. A.; Wan, Y.; Kutateladze, A. G. *Org. Lett.* **2000**, *2*, 799.
- For review see: Gaillard, E. R.; Whitten, D. G. *Acc. Chem. Res.* **1996**, *29*, 292.
- (a) Ci, X.; Whitten, D. G. *J. Am. Chem. Soc.* **1987**, *109*, 7215; (b) Ci, X.; Whitten, D. G. *J. Am. Chem. Soc.* **1989**, *111*, 3459.
- Gravel, D.; Farmer, L.; Ayotte, C. *Tetrahedron Lett.* **1990**, *31*, 63.
- Gravel, D.; Farmer, L.; Denis, R. C.; Schultz, E. *Tetrahedron Lett.* **1994**, *35*, 8981.
- McHale, W. A.; Kutateladze, A. G. *J. Org. Chem.* **1998**, *63*, 9924.
- Vath, P.; Falvey, D. E.; Barnhurst, L. A.; Kutateladze, A. G. *J. Org. Chem.* **2001**, *66*, 2886.
- Li, Z.; Kutateladze, A. G. *J. Org. Chem.* **2003**, *68*, 8236.
- β -Alkylthio-ethoxy radicals were implicated in the dissociation of hydroxyl radical adducts of (alkylthio)ethanol derivatives: Schöneich, C.; Bobrowski, K. *J. Am. Chem. Soc.* **1993**, *115*, 6538.
- Seebach, D.; Corey, E. J. *J. Org. Chem.* **1975**, *30*, 231.
- Roth, H. D.; Lamola, A. A. *J. Am. Chem. Soc.* **1974**, *96*, 6270.
- Glass, R. S.; Petsom, A.; Wilson, G. S. *J. Org. Chem.* **1986**, *51*, 4337.
- Frisch, M. J.; Trucks, G. W.; Schlegel, H. B.; Scuseria, G. E.; Robb, M. A.; Cheeseman, J. R.; Montgomery, J. A., Jr.; Vreven, T.; Kudin, K. N.; Burant, J. C.; Millam, J. M.; Iyengar, S. S.; Tomasi, J.; Barone, V.; Mennucci, B.; Cossi, M.; Scalmani, G.; Rega, N.; Petersson, G. A.; Nakatsuji, H.; Hada, M.; Ehara, M.; Toyota, K.; Fukuda, R.; Hasegawa, J.; Ishida, M.; Nakajima, T.; Honda, Y.; Kitao, O.; Nakai, H.; Klene, M.; Li, X.; Knox, J. E.; Hratchian, H. P.; Cross, J. B.; Adamo, C.; Jaramillo, J.; Gomperts, R.; Stratmann, R. E.; Yazyev, O.; Austin, A. J.; Cammi, R.; Pomelli, C.; Ochterski, J. W.; Ayala, P. Y.; Morokuma, K.; Voth, G. A.; Salvador, P.; Dannenberg, J. J.; Zakrzewski, V. G.; Dapprich, S.; Daniels, A. D.; Strain, M. C.; Farkas, O.; Malick, D. K.; Rabuck, A. D.; Raghavachari, K.; Foresman, J. B.; Ortiz, J. V.; Cui, Q.; Baboul, A. G.; Clifford, S.; Cioslowski, J.; Stefanov, B. B.; Liu, G.; Liashenko, A.; Piskorz, P.; Komaromi, I.; Martin, R. L.; Fox, D. J.; Keith, T.; Al-Laham, M. A.; Peng, C. Y.; Nanayakkara, A.; Challacombe, M.; Gill, P. M. W.; Johnson, B.; Chen, W.; Wong, M. W.; Gonzalez, C.; Pople, J. A. *Gaussian 03, Revision C.02*; Gaussian: Wallingford, CT, 2004.
- Moore, W. M.; Hammond, G. S.; Foss, R. P. *J. Am. Chem. Soc.* **1961**, *83*, 2789.
- Walling, C.; Padwa, A. *J. Am. Chem. Soc.* **1963**, *85*, 1593.
- Gray, P.; Williams, A. *Chem. Rev.* **1959**, *59*, 239.
- (a) Becke, A. D. *Phys. Rev. A* **1988**, *38*, 3098; (b) Lee, C.; Yang, W.; Parr, R. G. *Phys. Rev. B* **1988**, *37*, 785.



ELSEVIER

Photoinduced electron-transfer systems consisting of electron-donating pyrenes or anthracenes and benzimidazolines for reductive transformation of carbonyl compounds

Eietsu Hasegawa,^{a,*} Shinya Takizawa,^a Takayuki Seida,^a Akira Yamaguchi,^a Naoto Yamaguchi,^a Naoki Chiba,^a Tomoya Takahashi,^a Hiroshi Ikeda^b and Kimio Akiyama^c

^aDepartment of Chemistry, Faculty of Science, Niigata University, Ikarashi, Niigata 950-2181, Japan

^bDepartment of Chemistry, Graduate School of Science, Tohoku University, Sendai 980-8578, Japan

^cInstitute of Multidisciplinary Research for Advanced Materials, Tohoku University, Sendai 980-8577, Japan

Received 26 December 2005; accepted 18 February 2006

Available online 2 May 2006

Abstract—Photoinduced electron-transfer reactions of several ketone substrates were studied to evaluate the utilities of 1,6-bis(dimethylamino)pyrene (BDMAP), 1,6-dimethoxy pyrene (DMP), 9,10-bis(dimethylamino)anthracene (BDMAA), and 9,10-dimethoxyanthracene (DMA) as electron-donating sensitizers cooperating with 2-aryl-1,3-dimethylbenzimidazolines. BDMAP and DMP generally led higher conversion of ketones and better yield of reduction products compared to BDMAA and DMA.

© 2006 Elsevier Ltd. All rights reserved.

1. Introduction

Electron transfer is a fundamental reaction process, which is operating in reduction and oxidation (redox) reactions in chemical and biological systems.¹ Single electron transfer (SET) of neutral organic molecules generates radical ions that undergo various transformations.² Whereas using redox reagents as well as electrochemical procedures are traditional ways to generate these reactive species, photoinduced electron-transfer (PET) is an alternative method.¹ Without a doubt, PET chemistry of organic molecules has been a central topic in organic photochemistry over the past several decades.³ Significant progress has been accomplished in understanding PET reaction mechanisms and application of PET reactions to organic synthesis. Reactivity of radical cations generated by PET processes between electron-donating substrates and electron-accepting sensitizers has been extensively investigated.³ On the other hand, reactivity of radical anions has been less explored in PET reactions,⁴ which must be in part ascribed to the fact that practical electron-donating sensitizers are few as compared to electron-accepting sensitizers such as aromatic nitriles, quinones, and cationic salts.

In the course of our research program focused on reaction mechanism and synthetic application of carbonyl radical

anions (ketyl radicals) in PET reactions,⁵ we needed to find effective PET conditions to generate such radical anions. Especially, to promote reactions of substrates not efficiently absorbing light filtered by Pyrex™ of which ordinary photo-reaction vessels are made, electron-donating sensitizers absorbing light of longer wavelength were desired. Related to this purpose, we have also found that some benzimidazolines act as effective electron- and proton-donors to promote PET reduction of various carbonyl compounds in which their radical anions are generated.⁶ In this context, we became interested in developing electron-donating sensitizers cooperating with benzimidazolines for PET-promoted reductions of carbonyl compounds.

For this objective, we chose dimethylamino- or methoxy-substituted pyrenes or anthracenes,⁷ namely 1,6-bis(dimethylamino)pyrene (BDMAP), 1,6-dimethoxy pyrene

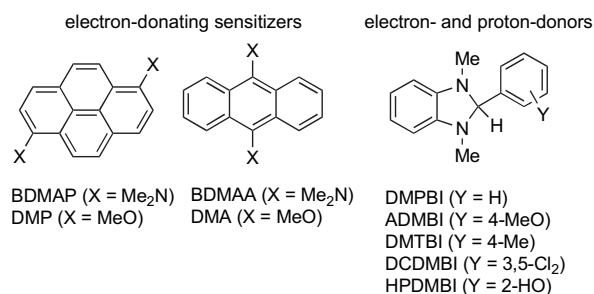


Chart 1.

* Corresponding author. Tel./fax: +81 25 262 6159; e-mail: chase@chem.sc.niigata-u.ac.jp

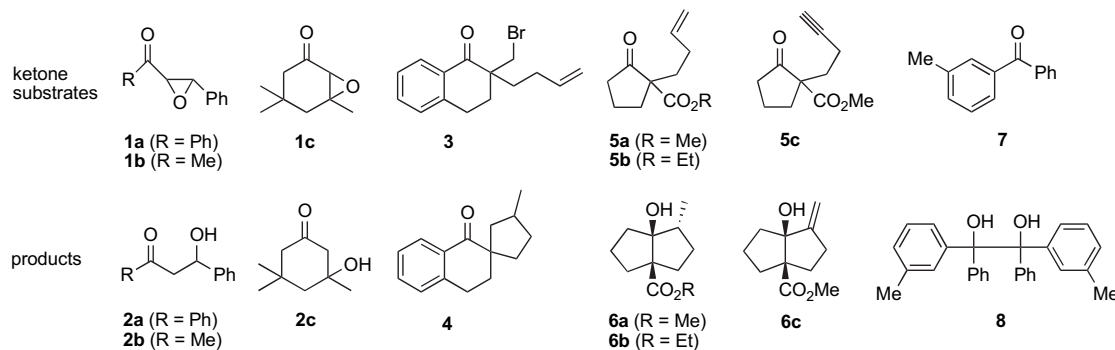


Chart 2.

(DMP), 9,10-bis(dimethylamino)anthracene (BDMAA), and 9,10-dimethoxyanthracene (DMA),⁸ and five 2-aryl-1,3-dimethylbenzimidazolines (DMBIs), which are shown in Chart 1. Carbonyl substrates, epoxy ketones **1**, α -bromomethyltetralone **3**, carbon–carbon multiple bond tethered ketones **5**, and 3-methylbenzophenone **7**, and the corresponding PET reaction products **2**, **4**, **6**, and **8** are represented in Chart 2. In the reactions, unimolecular or bimolecular rearrangements of ketyl radicals of these substrates are expected to proceed, i.e., C α –O bond cleavage of the ketyl radicals of **1**,¹⁰ C β –Br bond cleavage of the ketyl radical of **3**,^{6c} intramolecular ketyl radical addition to C–C multiple bonds for **5**,¹¹ and dimerization of ketyl radical of **7**.^{6g} We also conducted PET reactions using above four sensitizers with *N,N*-diethyl-*N*-trimethylsilylmethylamine (TMSA),¹² and using Ru(bpy)₃Cl₂, well-known PET sensitizer,¹³ with DMBI. In this paper, we report the results obtained and discuss the features and the utilities of these PET systems.

2. Results and discussion

2.1. Fundamental properties of sensitizers and benzimidazolines, and basic concept of PET systems

Selected photophysical and electrochemical data of the sensitizers are summarized in Table 1. These pyrenes and anthracenes can absorb the light of longer wavelength than both ketone substrates and DMBIs studied. As shown in Figure 1, cyclic voltammograms of BDMAP and DMP demonstrate reversible redox processes (differences of redox peak potentials are 56 mV and 66 mV, respectively), while those of BDMAA and DMA do not.

Table 1. Photophysical and electrochemical data of sensitizers^a

Sensitizer	λ_{\max} (log ϵ) (nm)	λ_{end} (nm)	$\lambda_{\max}^{\text{F}}$ (nm)	τ (ns)	E_{ex} (kcal/mol) ^b	$E_{1/2}^{\text{ox}}$ in V vs SCE	$E^{\text{ox}*}$ in V vs SCE
BDMAP	373 (4.35)	450	450	5.3 ^c	64 (2.8)	+0.43 ^d	–2.4
DMP	335 (4.38), 351 (4.57), 376 (4.16), 397(4.24)	420	402, 423	7.0 ^e	72 (3.1)	+0.85 ^d	–2.2
BDMAA	397 (3.76)	490	— ^f	— ^f	ca. 60 (2.6) ^{f,g}	+0.24	ca. –2.4
DMA	361 (3.79), 381 (3.95), 402 (3.87)	430	436	14.3 ^h	70 (3.0)	+0.98	–2.0

^a Measured in MeCN. λ_{\max} , Absorption maximum; λ_{end} , end absorption; $\lambda_{\max}^{\text{F}}$, fluorescence maximum; τ , lifetime; E_{ex} , excitation energy; $E_{1/2}^{\text{ox}}$, Half-wave oxidation potential of ground state and $E^{\text{ox}*}$, oxidation potential of the excited state that is obtained by the equation $E_{1/2}^{\text{ox}} - E_{\text{ex}}$.

^b Values in parentheses are reported in eV.

^c In 5% aqueous THF (Ref. 7d).

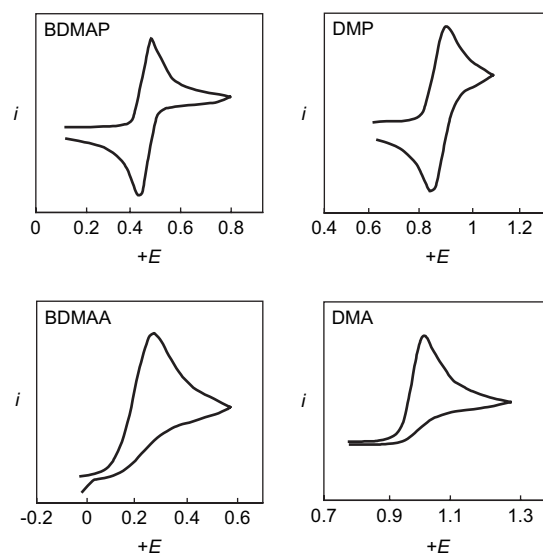
^d Standard potential.

^e The lifetime in DMF was 6.5 ns (this work).

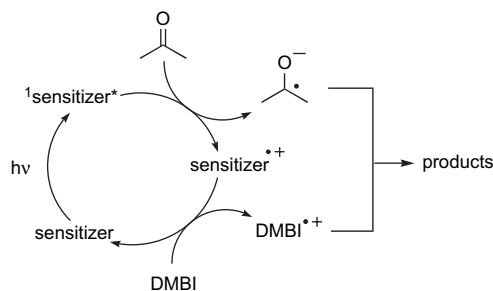
^f BDMAA was non-fluorescent.

^g Estimated from the absorption spectrum.

^h In heptane (Ref. 9b).

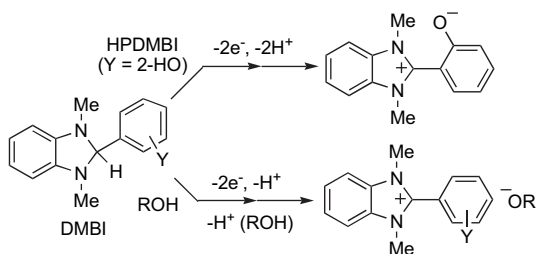
Figure 1. Cyclic voltammograms of sensitizers (E in V vs SCE).

Expected PET reaction pathways are presented in Scheme 1. Selective photoexcitation of a sensitizer produces its singlet excited state (¹sensitizer*). The excited sensitizer donates single electron to a ketone within its lifetime to produce a radical cation of the sensitizer (sensitizer^{•+}) and a radical anion of the ketone. Feasibility of this initial SET step is evaluated using the equation $\Delta G = E_{1/2}^{\text{ox}} - E_{\text{ex}} - E_{1/2}^{\text{red}} + C$, in which $E_{1/2}^{\text{ox}}$ and E_{ex} are a half-wave oxidation potential of the ground state and an excitation energy of a sensitizer, respectively, $E_{1/2}^{\text{red}}$ is a half-wave reduction potential of ketone substrate studied,¹⁴ and C is the coulomb term that depends



Scheme 1.

on the polarity of solvent used; the value for MeCN was reported to be -0.06 eV.¹⁵ Formed sensitizer^{•+}, except for BDMAA^{•+}, is exoergonically reduced by DMBIs to its ground state because $E_{1/2}^{\text{ox}}$ of DMBIs ($E_{1/2}^{\text{ox}}$ in V vs SCE: +0.33, +0.28, +0.29, +0.40, and +0.30 for DMPBI, ADMBI, DMTBI, DCDMBI, and HPDMBI, respectively) are lower than that of each sensitizer. Then, a radical cation of DMBI (DMBI^{•+}) and a radical anion of the ketone react with each other. For an effective sensitization (Scheme 1), a radical ion pair generated from a sensitizer and a ketone should smoothly dissociate. Therefore, a polar solvent is recommended to be used because such dissociation proceeds more efficiently in polar solvents than in nonpolar solvents.^{16,17} Also noted that, in these PET reactions, HPDMBI is expected to act as a two-electron- and two-proton-donor,^{6f,g} while other DMBIs are expected to perform as two-electron- and one-proton-donors that require addition of appropriate proton-donors (ROH) for reduction of ketones (Scheme 2).⁶



Scheme 2.

2.2. C α -O bond cleavage of α,β -epoxy ketones 1

The first examples of PET reactions of α,β -epoxy ketones with amines were independently reported by Cossy^{10a} and us.^{10b} At that moment, triethylamine was used as an electron- and proton-donor, and yields of the expected β -hydroxy ketones were moderate. Furthermore, it was found that β -diketones were major products instead of the desired β -hydroxy ketones in the reactions of 1,3-diaryl-2,3-epoxy-1-propanones (chalcone epoxides) with triethylamine.^{10b} A breakthrough to solve this problem was a discovery of DMBIs, which act as effective electron- and proton-donors to give β -hydroxy ketones.⁶

First, we conducted PET reactions of epoxy ketones **1** to compare DMP, BDMAA, and DMA with previously examined BDMAP.⁶ Whereas reactions of **1a** with ADMBI in DMF–AcOH afforded **2a** (86% for BDMAP, 85% for DMP, 68% for BDMAA, 62% for DMA based on the conversions of **1a**), some conversions from **1a** to **2a** were also

Table 2. PET reactions of **1b** with DMBI^a

Exp	Sensitizer	DMBI	Additive	Conv. of 1b ^b (%)	Yield of 2b ^{b,c} (%)
1	BDMAP	ADMBI	AcOH	64	80
2	DMP	ADMBI	AcOH	67 ^d	84
3	BDMAA	ADMBI	AcOH	57	— ^e
4	DMA	ADMBI	AcOH	54	64
5	BDMAP	HPDMBI	—	41	93
6	DMP	HPDMBI	—	30	86
7	BDMAA	HPDMBI	—	15	92
8	DMA	HPDMBI	—	30	90

^a Compound **1b** (0.40 mmol), sensitizer (0.05 equiv vs **1b**), DMBI (1.2 equiv vs **1b**), AcOH (5.0 equiv vs **1b**), DMF (4 mL), $\lambda > 340$ nm for 1 h.

^b Determined on the basis of isolated compounds.

^c Based on the conversion of **1b**.

^d Determined with ¹H NMR.

^e Detected with ¹H NMR but not isolated.

observed without irradiation in the cases of BDMAP and BDMAA. Therefore, we concluded that **1a** is too reactive to evaluate these sensitizers. Then, we conducted PET reactions of **1b** under two different sensitization conditions, using sensitizer–ADMBI–AcOH^{6d} and sensitizer–HPDMBI (Table 2).^{6f} In most of the cases, **2b** was obtained in good yields based on the conversion of **1b**. However, in the case of BDMAA with ADMBI and AcOH, **2b** could not be isolated although **1b** was consumed (exp 3). Because the decomposition of **2b** was suspected during irradiation, **2b** was subjected to the same reaction condition using BDMAA. However, **2b** was quantitatively recovered. Although this unique behavior of BDMAA could not be rationalized at the moment, combination of ADMBI and AcOH seems not to be tolerated with BDMAA (also see exp 3 in Table 6). In the reactions using HPDMBI, the conversion of **1b** in the case of BDMAA was lower than those of other sensitizers (compare exp 7 to exps 5, 6, and 8). This must be in part ascribed to endoergonic electron transfer between BDMAA^{•+} and DMBIs (Scheme 1).

We then studied substituent effects of the phenyl group of DMBI on PET reaction of **1c** with BDMAP under the conditions same as experiment 1 in Table 2. Plots of the conversion of **1c** versus $E_{1/2}^{\text{ox}}$ of DMBIs are presented in Figure 2. The conversion of **1c** decreased as $E_{1/2}^{\text{ox}}$ increases, being consistent with the expected SET between BDMAP^{•+} and DMBI (Scheme 1).

A set of Ru(bpy)₃Cl₂ and amines is a well-known sensitization system for reductive transformation of organic compounds,^{13d–h} and Ru(bpy)₃Cl₂ is considered to have some advantages compared with organic sensitizers, for example, photoexcitation using longer wavelength of light is possible, and separation of Ru(bpy)₃Cl₂ is more easily performed. Then, we examined PET reaction of **1b** using Ru(bpy)₃Cl₂ with ADMBI and AcOH or with HPDMBI (Table 3). In this sensitization system, Ru(I) is an expected reducing agent. Based on the standard potential of Ru(I) ($E = -1.30 \sim -1.33$ V vs SCE),^{13a–c,18} reducing ability of Ru(I) must be

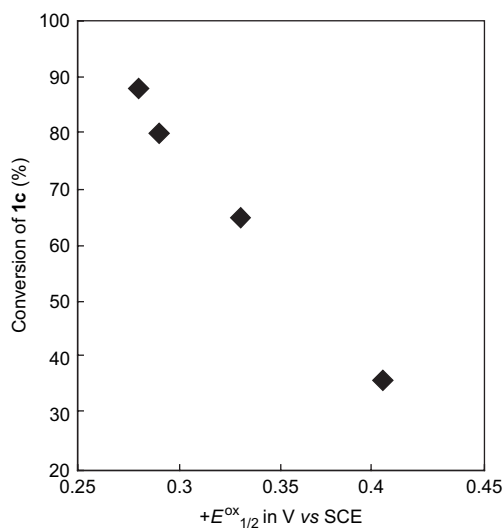
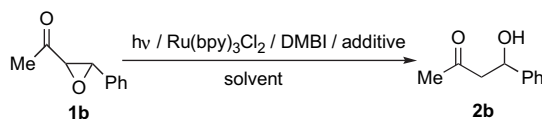


Figure 2. Plots of conversion of **1c** versus oxidation potentials of DMBIs in PET reaction of **1c** using BDMAP and DMBIs with AcOH in DMF.

Table 3. PET reactions of **1b** with Ru(bpy)₃Cl₂ and DMBI^a



Exp	DMBI	Solv	Additive	Conv. of 1b ^b (%)	Yield of 2b ^{b,c} (%)
1	ADMBI	DMF	AcOH	71	41
2	HPDMBI	DMF	—	45	70
3	HPDMBI	MeCN	—	41	75
4	HPDMBI	THF	—	25	71
5	HPDMBI	MeOH	—	36	72

^a Compound **1b** (0.40 mmol), Ru(bpy)₃Cl₂ (0.01 equiv vs **1b**), DMBI (1.2 equiv vs **1b**), AcOH (5.0 equiv vs **1b**), solvent (4 mL), λ>390 nm for 3 h.

^b Determined with ¹H NMR.

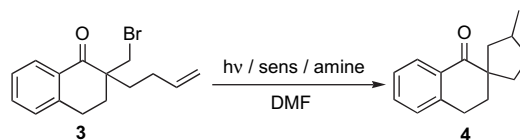
^c Based on the conversion of **1b**.

weaker than those of the excited states of above electron-donating pyrenes and anthracenes (see $E^{\text{ox}*}$ in Table 1). As anticipated, although the reactions of **1b** proceeded, yields of **2b** were relatively low as compared to those reported in Table 2.

2.3. C_β–Br bond cleavage of α-bromomethyltetralone **3**

Next, we conducted PET reactions of 2-bromomethyl-2-(3-butenyl)-1-tetralone **3** with ADMBI or TMSA (Table 4). Although yields of the expected spiro-cyclization product **4** were good in all cases, the conversions of **3** in the reactions with BDMAP or DMP were greater than those with BDMAA or DMA. This tendency was more significant in the reactions with TMSA. SET steps between ADMBI and sensitizers⁺⁺, except for BDMAA⁺⁺, are exoergonic as described above. On the other hand, calculated free energy changes for SET between TMSA ($E_{1/2}^{\text{ox}}=+0.49$ V vs SCE) and sensitizers⁺⁺ suggest that SET with DMP⁺⁺ is exoergonic ($\Delta G=-8.3$ kcal/mol) while SET with BDMAP⁺⁺ is slightly endoergonic ($\Delta G=+1.4$ kcal/mol). However, the conversions of **3** were not significantly different from each other (greater than 50% in both cases). This phenomena would

Table 4. PET reactions of **3** with ADMBI or TMSA^a



Exp	Sensitizer	Amine	Conv. of 3 ^b (%)	Yield of 4 ^{b,c} (%)
1	BDMAP	ADMBI	83	57
2	DMP	ADMBI	70	54
3	BDMAA	ADMBI	42	53
4	DMA	ADMBI	56	59
5	BDMAP	TMSA	68	67
6	DMP	TMSA	53	59
7	BDMAA	TMSA	19	69
8	DMA	TMSA	27	46

^a Compound **3** (0.50 mmol), sensitizer (0.05 equiv vs **3**), ADMBI (1.2 equiv vs **3**), TMSA (5.0 equiv vs **3**), DMF (5 mL), λ>360 nm for 5 h.

^b Determined with ¹H NMR.

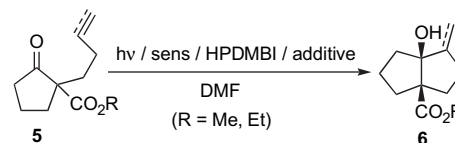
^c Based on the conversion of **3**.

be ascribed to an efficient and irreversible fragmentation of TMSA⁺⁺.^{4a,19}

2.4. Intramolecular ketone–olefin or –acetylene coupling of C–C multiple bond tethered ketones **5**

Cossy and co-workers reported that PET-promoted intramolecular coupling reactions of ketone carbonyls with C–C multiple bonds.¹¹ However, the light of shorter wavelength (254 nm) was usually used, and highly toxic hexamethylphosphorotriamide (HMPA) was in some cases required to obtain cyclization products in better yields. Therefore, we became interested in testing applicability of our PET methods to these synthetically relevant transformations. Then, we conducted reactions of **5a** with HPDMBI using four sensitizers. The results presented in Table 5 clearly indicate that both the conversion of **5a** and the yield of **6a** were essentially same regardless of the sensitizer (exps 1–4). Similar cyclization reactions of **5b** and **5c** were achieved by BDMAP with HPDMBI to produce **6b** and **6c**, respectively. Notably, addition of Mg(ClO₄)₂ significantly increased the

Table 5. PET reactions of **5** with HPDMBI^a



Exp	5	Sensitizer	Additive	Conv. of 5 ^b (%)	Yield of 6 ^{b,c} (%)
1	5a	BDMAP	—	71	59
2	5a	DMP	—	72	62
3	5a	BDMAA	—	75	55
4	5a	DMA	—	78	60
5	5b	BDMAP	—	68	71
6	5b	BDMAP	Mg(ClO ₄) ₂	93	88
7	5c	BDMAP	—	58	86

^a Compound **5** (0.40 mmol), sensitizer (0.05 equiv vs **5a**; 0.1 equiv vs **5b** and **5c**), HPDMBI (1.2 equiv vs **5**), Mg(ClO₄)₂ (1.2 equiv vs **5b**), DMF (4 mL for exps 1–4; 2 mL for exps 5–7), λ>340 nm for 22 h for exps 1–5 and 7; for 16 h for exp 6.

^b Determined with ¹H NMR.

^c Based on the conversion of **5**.

conversion of **5b** and the yield of **6b** for the shorter reaction time (compare exp 6 to exp 5). This phenomenon would be rationalized by the assumption that back-electron transfer from $5^{\cdot-}$ to BDMAP^{+} is suppressed through ion-pair exchange with $\text{Mg}(\text{ClO}_4)_2$, and therefore the reaction is accelerated.²⁰

2.5. Pinacol coupling of 3-methylbenzophenone **7**

We recently found that 3-methylbenzophenone **7** was a suitable substrate to probe the mechanism of PET reactions with DMBIs.^{6g} Thus, we decided to examine the PET reaction of **7** using the sensitizers with ADMBI and AcOH, or with HPDMBI (Table 6). Whereas benzpinacol **8** was obtained almost quantitatively in the case of DMP with ADMBI and AcOH (exp 2), BDMAA did not work at all (exp 3). Both BDMAP and DMA were similarly effective (exps 1 and 4). In the cases of HPDMBI, both the conversion of **7** and the yield of **8** were greater in the reactions with BDMAP and DMP than in those with BDMAA and DMA. It should also be noted that selective formation of **8** rather than benzhydryl is similar to the product selectivity observed in the PET reactions of **7** with DMPBI and AcOH or with HPDMBI without sensitizers.^{6g} In the latter case, specific interactions of radical ion pairs are involved. Therefore, observed product selectivity in this work is consistent with the proposed reaction pathways in which reaction between independently generated $7^{\cdot-}$ and DMBI^{+} proceeds (Scheme 1).

Table 6. PET reactions of **7** with DMBI^a

Exp	Sensitizer	DMBI	Additive	Conv. of 7 ^b (%)	Yield of 8 ^{b,c} (%)
1	BDMAP	ADMBI	AcOH	78	86
2	DMP	ADMBI	AcOH	100	100
3	BDMAA	ADMBI	AcOH	6	0
4 ^d	DMA	ADMBI	AcOH	64	79
5	BDMAP	HPDMBI	—	34	100
6	DMP	HPDMBI	—	57	92
7	BDMAA	HPDMBI	—	17	53
8 ^d	DMA	HPDMBI	—	22	77

^a Compound **7** (0.20 mmol), sensitizer (0.05 equiv vs **7**), DMBI (1.2 equiv vs **7**), AcOH (6.6 equiv vs **7**), DMF (2 mL), $\lambda > 360$ nm for 4 h.

^b Determined with ¹H NMR.

^c Based on the conversion of **7**.

^d Benzhydryl was also obtained: 13% for exp 4 and 6% for exp 8.

3. Conclusion

We have studied PET reactions of several ketone substrates using electron-donating pyrenes or anthracenes as sensitizers with benzimidazolines as electron- and proton-donors (reducing reagents). Differences in effectiveness of these sensitizers were observed depending on the substrates and conditions. Among properties to be required for an effective sensitizer is the stability of its radical cation. Based on the cyclic voltammetry of sensitizers (Fig. 1), radical cations of the pyrenes must be more stable than those of the anthracenes in the sensitization cycle in Scheme 1, which is compatible with some of the results described above. Therefore, we would like to conclude that BDMAP and DMP are more reliable

sensitizers than BDMAA and DMA. As a result, we recommend both BDMAP and DMP as visible light absorbing and electron-donating sensitizers for PET reactions. Another notable point is that DMP, unprecedented PET sensitizer, acted reasonably well in above examples. We will further explore the PET reactions of DMP and other alkoxy substituted pyrenes. The results and discussion described in this paper will hopefully provide useful information for any individual who is interested in PET chemistry to perform reductive transformation of organic compounds.

4. Experimental

4.1. General

NMR spectra were recorded in CDCl_3 with Me_4Si as an internal standard at 200 and 270 MHz for ¹H NMR, and 50 MHz for ¹³C NMR. Uncorrected melting points are reported. Absorption and fluorescence spectra were measured in MeCN. The fluorescence lifetime was determined by time-correlated single photon counting technique based on picoseconds laser pulse excitation. Oxidation and reduction potentials in MeCN were measured with cyclic voltammetry using platinum electrodes as working and counter electrodes, $\text{Ag}/0.01 \text{ M AgNO}_3$ as a reference electrode, and 0.1 M Et_4NClO_4 as a supporting electrolyte at the scan rate of 100 mV/s. Sample solutions were purged with N_2 before measurements. Ferrocene was used as a reference.²¹ Standard Potentials of ferrocene/ferrocenium couple were measured to be +0.066 V and +0.439 V versus Ag/AgNO_3 and SCE, respectively. Then, peak potentials of sensitizers, DMBIs, and ketone substrates were converted to those against SCE. Half-wave potentials were obtained from these peak potentials by subtracting or adding 0.029 V.²² Photo-reactions were conducted in a Pyrex test tube (1.5 cm diameter) immersed in a water bath at room temperature with either a 500 W Xe lamp or 500 W Xe–Hg lamp as a light source. Column chromatography was performed with silica-gel (Wakogel C-200). Preparative TLC was performed on 20 cm × 20 cm plates coated with silica-gel (Wakogel B-5F). Anhydrous DMF was purchased and used for the photoreactions. MeCN was distilled over P_2O_5 and subsequently with K_2CO_3 . THF was distilled over sodium–benzophenone under N_2 . Other reagents and solvents were purchased and used without further purification. DMPBI,^{23a} ADMBI,^{6g} HPDMBI,^{6g} DMTBI,^{23b} and DCDMBI^{23b} were prepared by the previously reported methods.^{6g} BDMAP,^{9a} DMP,^{9a} BDMAA,^{9c} DMA^{9a,24} were prepared by the slight modifications of the literature procedures (see below). Substrates (**1a**,^{10b} **1b**,²⁵ **1c**,²⁵ **5a**,¹¹ **5b**,¹¹ **5c**,¹¹ and **7**^{6g}) and photoproducts (**2a**,^{10b} **2b**,²⁵ **2c**,²⁵ **6a**,¹¹ **6b**,¹¹ **6c**,¹¹ and **8**^{6g}) are known compounds. Preparation of **3** and spectral data of **3** and **4** are described below because their characterizations have not been completed.^{6c}

4.2. Preparations of sensitizers

4.2.1. Preparation of BDMAP.^{9a} 1,6-Diaminopyrene was prepared by the reaction of pyrene with HNO_3 , followed by the reduction of 1,6-dinitropyrene with $\text{Na}_2\text{S} \cdot 9\text{H}_2\text{O}$. Then, an aqueous MeOH solution ($\text{H}_2\text{O} + \text{MeOH} = 21 \text{ mL} + 86 \text{ mL}$) of 1,6-diaminopyrene (1.9 g, 8.3 mmol),

CaCO₃ (1.8 g, 18 mmol), and MeI (20.7 mL, 0.33 mol) was heated at 55 °C for 29 h. After addition of MeI (20.0 mL, 0.32 mol), the mixture was heated for another 36 h. Precipitated yellow solid obtained after cooling was heated with NaOEt (19.7 g, 0.29 mol) at 90 °C for 48 h. After concentration and addition of H₂O, extraction with C₆H₆ was performed. The extract was treated with H₂O, satd aqueous NaCl, and dried over anhydrous MgSO₄, and then concentrated. Silica-gel column chromatography (CH₂Cl₂) gave yellow solid that was recrystallized twice from EtOH to give BDMAP (709 mg, 2.5 mmol, 30%) as yellow plates: mp 163.2–164.5 °C (lit.^{9a} 164–165 °C).

4.2.2. Preparations of DMP and DMA.²⁶ Pyrene (4.3 g, 21 mmol) and K₂Cr₂O₇ (6.2 g, 21 mmol) in 8 M H₂SO₄ (44 mL) were heated at 90 °C for 1 h and subsequently at 120 °C for 3 h. The mixture was poured into H₂O and the precipitated red-brown solid was filtered. The solid was subjected to silica-gel column separation (AcOH) to give a mixture of 1,6-pyrenedione and 1,8-pyrenedione (1.2 g, 5.2 mmol, 25%).²⁷ A part of the mixture (250 mg, 1.08 mmol), Na₂S₂O₄ (1.13 g, 6.48 mmol), and *n*-Bu₄NBr (35 mg, 0.11 mmol) in aqueous THF (H₂O+THF=4.7 mL+2.7 mL) were stirred at room temperature for 1 h. KOH (1.39 g, 24.8 mmol) in H₂O (3.6 mL) was added, and Me₂SO₄ (2.1 mL, 22.7 mmol) was slowly added in an ice-water bath. After the resulting mixture was stirred at room temperature for 22 h, addition of H₂O was followed by extraction with CH₂Cl₂. The extract was treated with H₂O and dried over anhydrous MgSO₄, and then concentrated. Silica-gel column chromatography (CH₂Cl₂) gave a mixture of 1,6-dimethoxypyrene and 1,8-dimethoxypyrene. The mixture was subjected to fractional recrystallization three times from C₆H₅Cl, and then DMP (52.7 mg, 0.20 mmol, 19%) was obtained as yellow needles: mp 250–252 °C (lit.^{9a} 244–245 °C). DMA was prepared from anthraquinone (624 mg, 3.00 mmol) in the similar manner to DMP (see above). Successive recrystallization of the crude product from EtOH gave DMA (466 mg, 1.95 mmol, 65%) as pale yellow plates: mp 204–207 °C (lit.²⁴ 198–199 °C).

4.2.3. Preparation of BDMAA.^{9c} 9,10-Diaminoanthracene was obtained by the reaction of anthraquinone (6.0 g, 29 mmol) with formamide, followed by a treatment with KOH. To the crude 9,10-diaminoanthracene were added MeOH (8 mL), MeI (8.0 mL, 129 mmol), and subsequently Na₂CO₃ (3.2 g, 30 mmol) in H₂O (8 mL). After the resulting mixture was stirred under N₂ for 16 h at room temperature and heated at 60 °C for 24 h, addition of H₂O was followed by extraction with CHCl₃. The extract was treated with H₂O, satd aqueous NaHCO₃, and dried over anhydrous MgSO₄, and then concentrated. Silica-gel column chromatography (CHCl₃/*n*-C₆H₁₄=2/1) gave yellow solids, which were recrystallized twice from EtOH to give BDMAA (552 mg, 2.09 mmol, 19% from anthraquinone) as yellow plates: mp 197–200 °C.

4.3. Preparation of 2-bromomethyl-2-(3-butenyl)-1-tetralone 3

To the mixture of NaH (ca. 66% in oil, 604 mg, 16.6 mmol) and HMPA (2.9 mL, 16.6 mmol) in THF (23 mL) was slowly added a THF solution (7 mL) of 2-(3-butenyl)-1-

tetralone (1.66 g, 8.31 mmol) that was obtained through the sequence of NaH promoted reaction of 4-bromo-1-butene with ethyl 1-tetralone-2-carboxylate²⁸ and NaOH promoted hydrolytic decarboxylation, and stirred for 1 h under N₂. Then, CH₂Br₂ (2.9 mL, 41.6 mmol) was added and the resulting mixture was heated at 75 °C for 22 h. After addition of H₂O, extraction with Et₂O was performed. The extract was treated with satd aqueous Na₂S₂O₃, satd aqueous NaHCO₃, satd aqueous NaCl, and dried over anhydrous MgSO₄, and then concentrated. Silica-gel column chromatography (C₆H₆/*n*-C₆H₁₄=1/1) and subsequent distillation gave **3** (924 mg, 3.15 mmol, 38%) as colorless oil: bp 105–110 °C (0.45 mmHg); IR (Neat) 1681 cm⁻¹; ¹H NMR (270 MHz) δ 1.73–2.37 (m, 6H), 2.93–3.15 (m, 2H), 3.66 (d, *J*=10.4 Hz, 1H), 3.76 (d, *J*=10.4 Hz, 1H), 4.91–5.04 (m, 2H), 5.66–5.81 (m, 1H), 7.22–7.34 (m, 2H), 7.45–7.51 (m, 1H), 8.02–8.05 (m, 1H) ppm; ¹³C NMR (50 MHz) δ 24.9, 27.9, 31.1, 32.5, 39.1, 48.5, 115.1, 126.8, 128.1, 128.8, 131.3, 133.6, 137.6, 142.9, 198.4 ppm. HRMS (ESI) calcd for C₁₅H₁₇O⁷⁹BrNa⁺: 315.0361, found: 315.0355; C₁₅H₁₇O⁸¹BrNa⁺: 317.0341, found: 317.0335.

4.4. General procedure of PET reactions

A solution of a ketone substrate (0.20–0.50 mmol) and DMBI (0.24–0.60 mmol) or TMSA (2.50 mmol) with a sensitizer (generally 1.0–4.0×10⁻² mmol and 4.0×10⁻³ mmol for Ru(bpy)₃Cl₂) in DMF (2–5 mL) or other solvents (MeCN, THF, MeOH 4 mL) in the presence or absence of AcOH (1.32–2.00 mmol) or Mg(ClO₄)₂ (0.48 mmol) was purged with N₂ for 5 min prior to irradiation. This solution was irradiated with the light (λ>340 and 360 nm for pyrenes and anthracenes, and 390 nm for Ru(bpy)₃Cl₂) using a cut-off glass-filter for an appropriate irradiation time. While a photolysate without additive was concentrated, a photolysate containing AcOH or Mg(ClO₄)₂ was subjected to the extraction with EtOAc or C₆H₆. The extract was treated with satd aqueous NaHCO₃, satd aqueous NaCl, and dried over anhydrous MgSO₄, and then concentrated. For the reactions of **7**, the resulting residue was directly analyzed with ¹H NMR using triphenylmethane as an internal standard. For other reactions, the residues were subjected to silica-gel TLC or column separation for the reactions of **1**, **3** or **5** using appropriate mixed solvents (EtOAc/*n*-C₆H₁₄ for **1**, C₆H₆/*n*-C₆H₁₄ for **3**, EtOAc/C₆H₆ for **5**) to give the starting ketones and the products. Photoproducts were identified by analyses with their NMR and IR spectra. Product **4** (3/1 mixture of two diastereomers): colorless oil; IR (Neat) 1678 cm⁻¹; ¹H NMR (270 MHz) δ 1.00 (d, *J*=6.5 Hz, 3H, major isomer), 1.07 (d, *J*=6.8 Hz, 3H, minor isomer), 1.12–2.28 (m, 9H), 2.91–3.06 (m, 2H), 7.18–7.31 (m, 2H), 7.40–7.46 (m, 1H), 8.02–8.05 (m, 1H) ppm; ¹³C NMR (50 MHz) δ 19.8, 20.2, 26.3, 26.7, 34.2, 34.3, 34.4, 34.5, 35.4, 35.7, 36.5, 42.6, 44.6, 53.4, 126.4, 127.9, 128.5, 131.5, 132.8, 143.5, 202.2 ppm. Anal. Calcd for C₁₅H₁₈O: C, 84.07; H, 8.47; found: C, 83.91; H, 8.63.

Acknowledgements

E.H. and H.I. thank the Ministry of Education, Culture, Sports, Science, and Technology of Japan for financial support in the form of Grants-in-Aid for Scientific Research C (No. 15550028) and for Scientific Research in Priority

Areas (Area No. 417), respectively. E.H. thanks financial support from the Uchida Energy Science Promotion Foundation. H.I. gratefully acknowledges financial support from the Izumi Science and Technology Foundation and the Shorai Foundation. We thank Dr. D. D. M. Wayner (National Research Council of Canada) for his valuable comments on electrochemistry. We also thank Professor K. Okada (Osaka City University) for his donation of Ru(bpy)₃Cl₂. Generous assistance provided by Professors T. Horaguchi (Niigata University), M. Ueda (Tohoku University), and S. Tero-Kubota (Tohoku University) is also acknowledged.

References and notes

- (a) Ebersson, L. *Electron Transfer Reactions in Organic Chemistry*; Springer: Berlin, 1987; (b) *Advances in Electron Transfer Chemistry*; Mariano, P. S., Ed.; JAI: Greenwich, CT, 1991–1999; Vols. 1–6; (c) *Electron Transfer in Chemistry*; Balzani, V., Ed.; Wiley-VCH: Weinheim, 2001; Vols. 1–5.
- (a) Schmittel, M.; Burghart, A. *Angew. Chem., Int. Ed.* **1997**, *36*, 2550–2589; (b) Berger, D. J.; Tanko, J. M. *The Chemistry of Double-Bonded Functional Groups*; Patai, S., Ed.; Wiley: New York, NY, 1997; pp 1281–1354; (c) Schmittel, M.; Ghorai, M. K. *Electron Transfer in Chemistry*; Balzani, V., Ed.; Wiley-VCH: Weinheim, 2001; Vol. 2, pp 5–54.
- (a) *Photoinduced Electron Transfer*; Fox, M. A., Chanon, M., Eds.; Elsevier: Amsterdam, 1988; Parts A–D; (b) Kavarnos, G. J. *Fundamental of Photoinduced Electron Transfer*; VCH: New York, NY, 1993; (c) *CRC Handbook of Organic Photochemistry and Photobiology*, 1st ed.; Horspool, W. M., Song, P. S., Eds.; CRC: Boca Raton, FL, 1994, and 2nd ed.; Horspool, W. M., Lenci, F., Eds.; CRC: Boca Raton, FL, 2003.
- Representative reviews for PET-promoted reductions of carbonyl compounds with amine donors. (a) Yoon, U. C.; Marinao, P. S.; Givens, R. S.; Atwater, B. W., III. *Advances in Electron Transfer Chemistry*; Mariano, P. S., Ed.; JAI: Greenwich, CT, 1994; Vol. 4, pp 117–205; (b) Cossy, J.; Pete, J. P. *Advances in Electron Transfer Chemistry*; Mariano, P. S., Ed.; JAI: Greenwich, CT, 1996; Vol. 5, pp 141–195.
- Hasegawa, E. *J. Photoscience* **2003**, *10*, 61–69.
- (a) Hasegawa, E.; Kato, T.; Kitazume, T.; Yanagi, K.; Hasegawa, K.; Horaguchi, T. *Tetrahedron Lett.* **1996**, *37*, 7079–7082; (b) Hasegawa, E.; Tamura, Y.; Tosaka, E. *Chem. Commun.* **1997**, 1895–1896; (c) Hasegawa, E.; Yoneoka, A.; Suzuki, K.; Kato, T.; Kitazume, T.; Yanagi, K. *Tetrahedron* **1999**, *55*, 12957–12968; (d) Hasegawa, E.; Chiba, N.; Nakajima, A.; Suzuki, K.; Yoneoka, A.; Iwaya, K. *Synthesis* **2001**, 1248–1252; (e) Hasegawa, E.; Takizawa, S.; Iwaya, K.; Kurokawa, M.; Chiba, N.; Yamamichi, K. *Chem. Commun.* **2002**, 1966–1967; (f) Hasegawa, E.; Chiba, N.; Takahashi, T.; Takizawa, S.; Kitayama, T.; Suzuki, T. *Chem. Lett.* **2004**, *33*, 18–19; (g) Hasegawa, E.; Seida, T.; Chiba, T.; Takahashi, T.; Ikeda, H. *J. Org. Chem.* **2005**, *70*, 9632–9635.
- Representative examples for PET reactions using dimethylamino- or methoxy-substituted arenes as sensitizers. (a) Lee, J. A.; Israel, S. H. *J. Org. Chem.* **1983**, *48*, 4557–4563; (b) Hamada, T.; Nishida, A.; Yonemitsu, O. *J. Am. Chem. Soc.* **1986**, *108*, 140–145; (c) Nishida, A.; Hamada, T.; Yonemitsu, O. *J. Org. Chem.* **1988**, *53*, 3386–3387; (d) Okada, K.; Okamoto, K.; Oda, M. *J. Am. Chem. Soc.* **1988**, *110*, 8736–8738; (e) Pandey, G.; Rao, K. S. S. P.; Rao, K. V. N. *J. Org. Chem.* **1996**, *61*, 6799–6804; (f) Banerjee, A.; Falvey, D. E. *J. Org. Chem.* **1997**, *62*, 6245–6251; (g) Pandey, G.; Hajira, S.; Ghorai, M. K.; Kumar, K. R. *J. Am. Chem. Soc.* **1997**, *119*, 8777–8787; (h) Pandey, G.; Rao, K. S. S. P.; Rao, K. V. N. *J. Org. Chem.* **2000**, *65*, 4309–4314.
- Although these pyrenes and anthracenes are previously known (Ref. 9) and both BDMAP (Refs. 6,7d) and DMA (Ref. 7a,h) have been used for some PET reactions, PET reactions of DMP and BDMAA have not been reported. In addition, no systematic study on the utilities of these four compounds as sensitizers for PET reactions has been conducted.
- (a) Zweig, A.; Maurer, A. H.; Roberts, B. G. *J. Org. Chem.* **1967**, *32*, 1322–1329; (b) Dreeskamp, H.; Pabst, J. *Chem. Phys. Lett.* **1979**, *61*, 262–265; (c) Chung, Y.; Duerr, B. F.; McKelvey, T. A.; Najappan, P.; Czarnik, A. W. *J. Org. Chem.* **1989**, *54*, 1018–1032.
- (a) Cossy, J.; Aclinou, P.; Bellosta, V.; Furet, N.; Baranne-Lafont, J.; Sparfel, D.; Souchaud, C. *Tetrahedron Lett.* **1991**, *32*, 1315–1316; (b) Hasegawa, E.; Ishiyama, K.; Horaguchi, T.; Shimizu, T. *J. Org. Chem.* **1991**, *56*, 1631–1635; (c) Cossy, J.; Bouzide, A.; Ibhi, S.; Aclinou, P. *Tetrahedron* **1991**, *47*, 7775–7782; (d) Kirschberg, T.; Mattay, J. *J. Org. Chem.* **1996**, *61*, 8885–8896; (e) Hasegawa, E.; Ishiyama, K.; Fujita, T.; Kato, T.; Abe, T. *J. Org. Chem.* **1997**, *62*, 2396–2400; (f) Zhang, J.; Jin, M.-Z.; Zhang, W.; Yang, L.; Liu, Z.-L. *Tetrahedron Lett.* **2002**, *43*, 9687–9689; (g) Recent review: Hasegawa, E.; Kamata, M. *CRC Handbook of Organic Photochemistry and Photobiology*, 2nd ed.; Horspool, W. M., Lenci, F., Eds.; CRC: Boca Raton, FL, 2003; Chapter 53, pp 1–17.
- Belotti, D.; Cossy, J.; Pete, J. P.; Portella, C. *J. Org. Chem.* **1986**, *51*, 4196–4200.
- (a) Hasegawa, E.; Xu, W.; Mariano, P. S.; Yoon, U. C.; Kim, J. U. *J. Am. Chem. Soc.* **1988**, *110*, 8099–8111; (b) Hasegawa, E.; Brumfield, M. A.; Yoon, U. C.; Mariano, P. S. *J. Org. Chem.* **1988**, *53*, 5435–5442.
- Representative examples for PET reactions using Ru(bpy)₃Cl₂ with amines. (a) DeLaive, P. J.; Lee, J. T.; Sprinschinik, H. W.; Abruna, H.; Meyer, T. J.; Whitten, D. G. *J. Am. Chem. Soc.* **1977**, *99*, 7094–7097; (b) Ballardini, R.; Varani, G.; Indelli, M. T.; Scandola, F.; Balzani, V. *J. Am. Chem. Soc.* **1978**, *100*, 7219–7223; (c) Bock, C. R.; Connor, J. A.; Gutierrez, A. R.; Meyer, T. J.; Whitten, D. G.; Sullivan, B. P.; Nagle, J. K. *J. Am. Chem. Soc.* **1979**, *101*, 4815–4824; (d) Pac, C.; Miyauchi, Y.; Ishitani, O.; Ihama, M.; Yasuda, M.; Sakurai, H. *J. Org. Chem.* **1984**, *49*, 26–34; (e) Ishitani, O.; Yanagida, S.; Takamuku, S.; Pac, C. *J. Org. Chem.* **1987**, *52*, 2790–2796; (f) Willner, I.; Tsfania, T.; Eichen, Y. *J. Org. Chem.* **1990**, *55*, 2656–2662; (g) Fukuzumi, S.; Mochizuki, S.; Tanaka, T. *J. Phys. Chem.* **1990**, *94*, 722–726; (h) Okada, K.; Okubo, K.; Morita, N.; Oda, M. *Chem. Lett.* **1993**, 2021–2024.
- Reduction potentials ($E_{1/2}^{\text{red}}$ in V vs SCE) of some representative substrates are –1.59 V for **1a**, –1.82 V for **3**, and –1.78 V for **7**, respectively. In the cases of **1b**, **1c**, and **5a**, the reduction peaks were not observed below –2.3 V.
- (a) Rehm, D.; Weller, A. *Isr. J. Chem.* **1970**, *8*, 259–271; (b) Weller, A. *Z. Phys. Chem. Neue Folge* **1982**, *133*, 93–98.
- In principle, a polar solvent accelerates initial PET processes (Refs. 3,15,17), and is desirable for a PET reaction involving sensitization. However, if a reaction requires a chemical process within a radical ion pair, e.g., proton transfer from a radical cation to a radical anion (Ref. 17), nonpolar solvents are in some cases more favorable to lead better yields of products

- as compared to polar solvents (Ref. 10e). Therefore, a choice of a suitable solvent for each case is important for preparative PET reactions.
17. Devadoss, C.; Fessenden, R. W. *J. Phys. Chem.* **1991**, *95*, 7253–7260.
 18. Tokel-Takvoryan, N. E.; Hemingway, R. E.; Bard, A. J. *J. Am. Chem. Soc.* **1973**, *95*, 6582–6589.
 19. (a) Zhang, X.; Ye, S. R.; Hong, S.; Freccero, M.; Albini, A.; Falvey, D. E.; Mariano, P. S. *J. Am. Chem. Soc.* **1994**, *116*, 4211–4220; (b) Su, Z.; Mariano, P. S.; Falvey, D. E.; Yoon, U. C.; Oh, S. W. *J. Am. Chem. Soc.* **1998**, *120*, 10676–10686.
 20. Representative examples of inorganic salt effects on PET reactions. (a) Simon, J. D.; Peters, K. S. *J. Am. Chem. Soc.* **1983**, *105*, 4875–4882; (b) Mizuno, K.; Ichinose, N.; Otsuji, Y. *Chem. Lett.* **1985**, 455–458; (c) Review: Loupy, A.; Tchoubar, B.; Astruc, D. *Chem. Rev.* **1992**, *92*, 1141–1165.
 21. (a) Gritzne, G.; Kuta, J. *Pure Appl. Chem.* **1984**, *56*, 461–466; (b) Workentin, M. S.; Parker, V. D.; Morkin, T. L.; Wayner, D. D. M. *J. Phys. Chem. A* **1998**, *102*, 6503–6512.
 22. Mann, C. K.; Barnes, K. K. *Electrochemical Reactions in Nonaqueous Systems*; Marcel Dekker: New York, NY, 1970.
 23. (a) Chikashita, H.; Itoh, K. *Bull. Chem. Soc. Jpn.* **1986**, *59*, 1747–1752; (b) Lee, I.-S. H.; Jeoung, E. H.; Kreevoy, M. *J. Am. Chem. Soc.* **1997**, *119*, 2722–2728.
 24. Meek, J. S.; Monroe, P. A.; Bouboulis, C. J. *J. Org. Chem.* **1963**, *28*, 2572–2577.
 25. Hasegawa, E.; Ishiyama, K.; Kato, T.; Horaguchi, T.; Shimizu, T.; Tanaka, S.; Yamashita, Y. *J. Org. Chem.* **1992**, *57*, 5352–5359.
 26. Kraus, G. A.; Man, T. O. *Synth. Commun.* **1986**, *16*, 1037–1042.
 27. Fatiadi, A. J. *J. Chromatogr.* **1965**, *20*, 319–324.
 28. Bowman, W. R.; Westlake, P. J. *Tetrahedron* **1992**, *48*, 4027–4038.

Facile ring opening of siloxy cyclopropanes by photoinduced electron transfer. A new way to β -keto radicals

Heiko Rinderhagen, Prashant A. Waske and Jochen Mattay*

Organische Chemie I, Fakultät für Chemie, Universität Bielefeld, Postfach 100131, 33501 Bielefeld, Germany

Received 6 December 2005; accepted 12 February 2006

Available online 17 April 2006

Abstract—Siloxy cyclopropanes undergo ring opening and fragmentation of formal silyl cations under formation of β -keto radicals. These reactive intermediates can be used in inter- and intramolecular addition reactions leading to complex ring systems if more than one unsaturated side chain is present in the starting material. Beside some synthetic examples mainly the mechanism will be discussed focusing on the structure of the primarily formed radical cations, the regioselectivity of cyclopropane cleavage (*endo* vs *exo* ring opening), leaving of the silyl group, and termination by H-transfer.

© 2006 Elsevier Ltd. All rights reserved.

1. Introduction

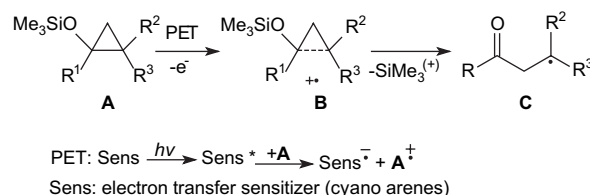
Single Electron Transfer (SET)¹ and especially Photoinduced Electron Transfer (PET)² has become a powerful tool in organic synthesis³ after fundamental research, which started already in 1960s, e.g., by Marcus,⁴ Weller,⁵ and others.⁶ Early highlights of synthetic applications are related to the work of Arnold,⁷ Mariano,⁸ Schuster,^{9a} Steckhan,^{9b} and many other groups¹⁰ including ourselves.¹¹

The very simple but even most powerful concept behind this methodology is based on the weakening of bonds by oxidation/reduction under formation of radical cations/radical anions leading to an increased reactivity of the molecules.¹² Examples of synthetic applications cover addition,¹³ cycloaddition,¹⁴ fragmentation,¹⁵ substitutions,¹⁶ and other reactions.¹⁷ Often the details of the mechanisms involved in these reactions are not yet completely known although the primary and initiating step is always PET. Especially in fragmentation and addition reactions radical species may also be involved.¹⁸

In this report we will focus on a new method of generating β -keto radicals from siloxy cyclopropanes by oxidative PET (Scheme 1). The primary step is oxidation of the starting material under cleavage of the cyclopropane **A** leading to a distonic radical cation **B**, which finally forms the β -keto radical **C**.

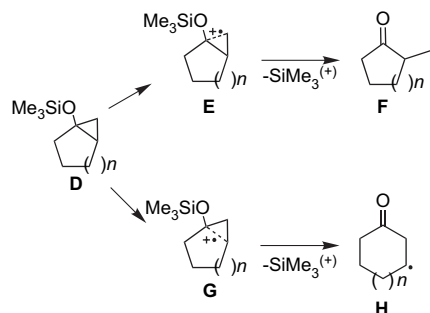
Keywords: Siloxy cyclopropanes; Photoinduced electron transfer; Radical cations; Radicals; Radical cascade reactions; Reaction mechanism.

* Corresponding author. Tel.: +49 521 1062072; fax: +49 521 1066417; e-mail: mattay@uni-bielefeld.de



Scheme 1. Cleavage and fragmentation of siloxy cyclopropanes **A** to radical cations **B** and β -keto radicals **C**.

Both the radical cation **B** and the β -keto radical **C** are very useful intermediates especially in intramolecular addition reactions to π -systems leading to new cyclized products. We have made use of this method for synthesizing polycyclic compounds.¹⁹ Beside some exemplary reactions we will discuss in more detail the mechanism involved especially regarding bicyclic siloxy cyclopropanes (Scheme 2).

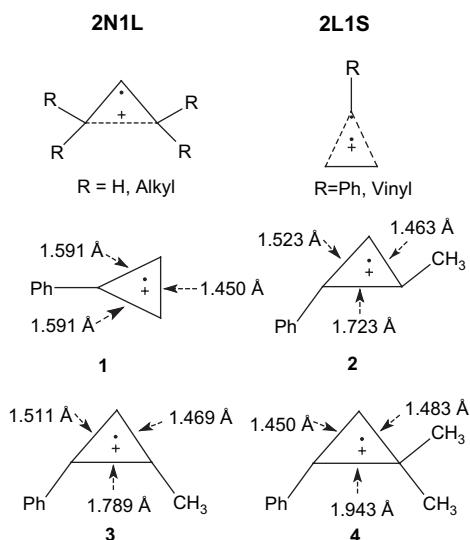


Scheme 2. *exo*- and *endo*-cleavage of bicyclic siloxy cyclopropanes.

Important questions concern the structure of siloxy cyclopropane radical cations in comparison with unsubstituted or alkyl-substituted cyclopropane radical cations, the regioselectivity of *endo*- versus *exo*-cleavage of bicyclic cyclopropanes **D** yielding **E** and **G**, and the factors controlling the fragmentation of **D** to the β -keto radicals **F** and **H**.

2. Structure of siloxy cyclopropane radical cations

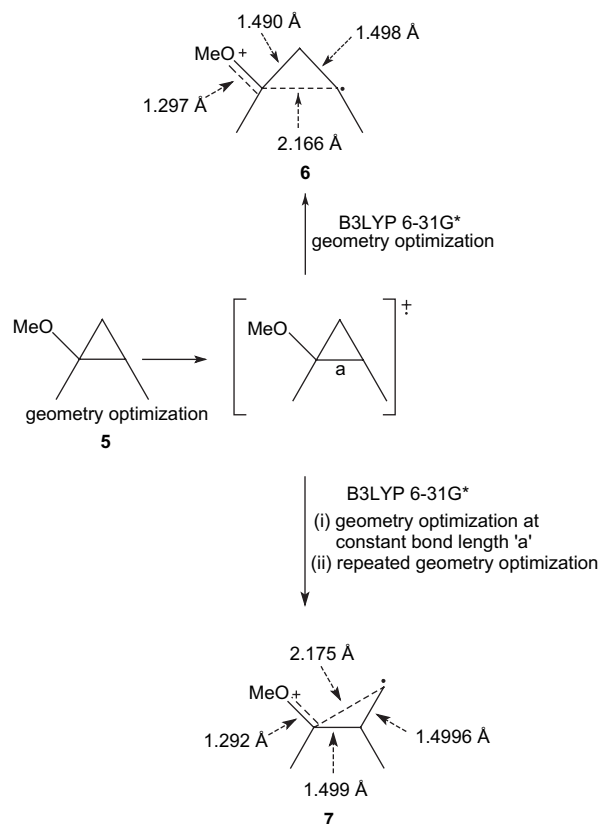
Upon ionization, cyclopropane derivatives can form two types of radical cations depending on the substitution pattern (Scheme 3, top).^{20,21} The **2N1L** type (2 normal, 1 long) shows a long one electron-two center bond in the range of 1.85–1.95 Å. The calculated bond lengths of the radical cations **2–4** indeed confirm this classification (Scheme 3, bottom). On the contrary, aryl- and vinyl-substituted cyclopropanes prefer the **2L1S** type (2 long, 1 short) as shown for 1-phenylcyclopropane **1** (Scheme 3).



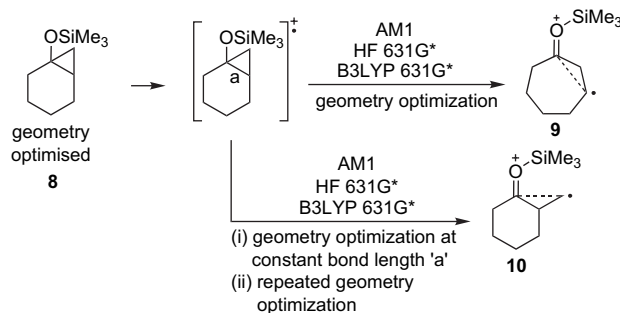
Scheme 3. Types of cyclopropane radical cations according to Hudson and structural details of selected examples (for Refs. 20 and 21 see text).

Following this classification for siloxy cyclopropanes of the type **D** should give radical cations of the type **2N1L** after oxidation. Scheme 4 shows the results of an ab initio calculation of the model compound 1-methoxy-1,2-dimethylcyclopropane **5**. Note, that the elongated C–C bonds of **6** and **7** are even longer (ca. 2.17 Å) compared to **2–4** (ca. 1.72–1.94 Å). However, the results considering only the energetics show that it is not possible to differentiate between the two ways of cleavage leading to **6** and **7**, respectively.

Even similar calculations on the radical cations **9** and **10** generated from the bicyclic siloxy cyclopropane **8** upon oxidation (cf. Scheme 2, **D**, $n=2$) do not allow a differentiation between *endo*- versus *exo*-cleavage (Scheme 5). Both semiempirical and ab initio methods lead to extremely elongated *endo*- and *exo*-bonds (ca. 2.4–2.5 Å).²² Only a calculation of the transition states and the complete potential hypersurface clearly verify the preferred cleavage of the *endocyclic* bond under formation of **9**. Details of this theoretical analysis including matrix isolation studies on the reactive intermediates will be published separately.²³



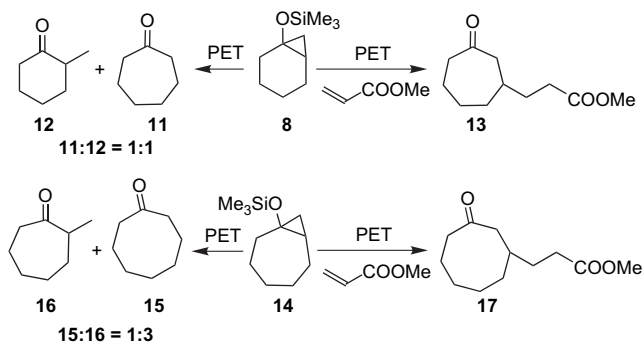
Scheme 4. Structural details of radical cations of 1-methoxy-1,2-dimethylcyclopropane.



Scheme 5. Quantum chemical calculations on the structure of radical cations **9** and **10**.

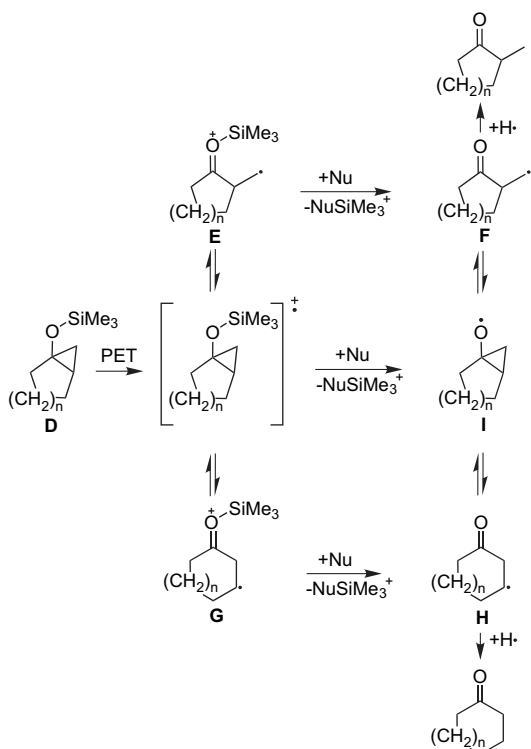
3. Experimental studies on *endo*- versus *exo*-cleavage of bicyclic siloxy cyclopropanes of structure **D**

Irradiation of bicyclic siloxy cyclopropanes **D** leads to the ring opening of the three-membered ring under ring enlargement (*endo*-cleavage) or under preservation of the ring (*exo*-cleavage) depending on the ring size (Scheme 6). However, in presence of methyl acrylate as scavenger only the ring enlarged addition products are formed (e.g., **8** → **13** and **14** → **17**). This observation strongly indicates that the primary step after oxidation is ring opening of the *endocyclic* bond of **8** and **14**.



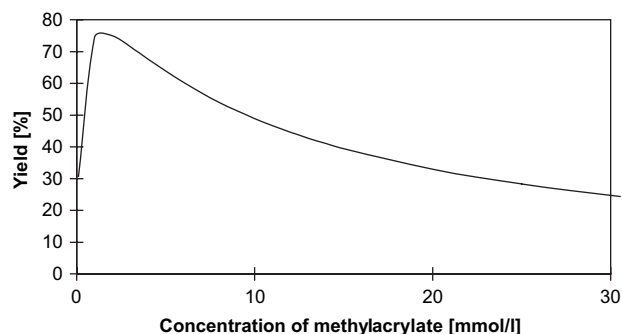
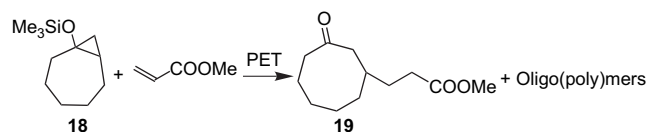
Scheme 6. PET reactions of bicyclic siloxy cyclopropanes in the absence and presence of methyl acrylate as scavenger.

The ring opening may already occur at the level of the radical cation of the **D** (leading to **G**) or at the level of the oxy radical **I** generated after fragmentation of the trimethylsilyl cation (leading to **H**). These results also show that the possible equilibrium between ring-preserved and ring-opened intermediates (**E** ↔ **G** and **F** ↔ **H**) is slow compared to the fast scavenging reactions in the presence of the methyl acrylate (Scheme 7).



Scheme 7. Equilibrium between ring-opened and ring-preserved intermediates (radical cations **E** and **G** structures are presented with already broken C–C bond, cf. Scheme 2).

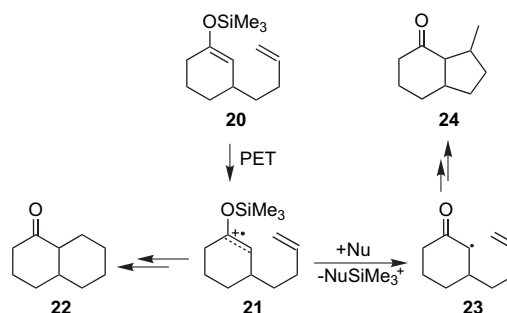
Further studies on the kinetics of **18** as model compound in the presence of methyl acrylate confirm these findings and furthermore, show that the termination step (H-abstraction) is relatively slow (Scheme 8). A detailed analysis is reported elsewhere.^{22,24}



Scheme 8. Yield of the trapping product **19** in dependence on the methyl acrylate concentration.

4. Fragmentation of the trimethylsilyl group

One important question concerns the timing of loss of the silyl group. Recent studies on the PET reactions of silyl enol ethers have shown that this cleavage is strongly influenced by nucleophiles such as alcohols or even the solvents (most often acetonitrile whose nucleophilicity can be increased by high pressure).^{18,24} Silyl enol ethers give nondistonic radical cations on PET-oxidation, whereas siloxy cyclopropane radical cations undergo C–C bond cleavage activationless according to quantum chemical calculations.^{22,25} Therefore, we assume that the loss of the silyl group takes place only at the stage of the distonic radical cations **E** and **G**. Using silyl enol ethers the course of the reaction, i.e., radical cation versus radical reaction pathway, can be controlled by timing the cleavage of the silyl group. For example, in solvent mixtures of high nucleophilicity loss of the silyl group leads to the corresponding α -keto radical **23**, which preferentially undergoes 5-*exo* cyclization to **24** if a suitable unsaturated side chain is present.^{18,24} However, in the absence of nucleophiles 6-*endo* is the preferred cyclization mode leading to **22** (Scheme 9).



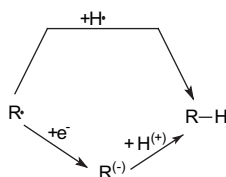
Scheme 9. Radical cations versus radical cyclization pathways in PET reactions of the silyl enol ethers.

In the case of siloxy cyclopropanes this dependency on the reaction medium is not as pronounced as for silyl enol

ethers.^{19a,22} This might be taken as an indication for the higher reactivity of the distonic radical cations compared to nondistonic ones.

5. Termination by H-transfer

An often discussed question is related to the mechanism of the final step of PET-induced cyclizations of unsaturated silyl enol ethers and siloxy cyclopropanes. In all examples studied by us this termination is based on H-transfer to the final radical intermediate of the cascade fragmentation addition process (cf. Schemes 6–9). Two mechanisms can be discussed, i.e., a formal H-atom transfer (e.g., from the solvent) and a two-step process via electron and proton transfer (Scheme 10). The reduction of the radical R^{\cdot} may occur by electron transfer from the radical anion of the sensitizer (cf. Scheme 1).



Scheme 10. Possible H-saturation pathways.

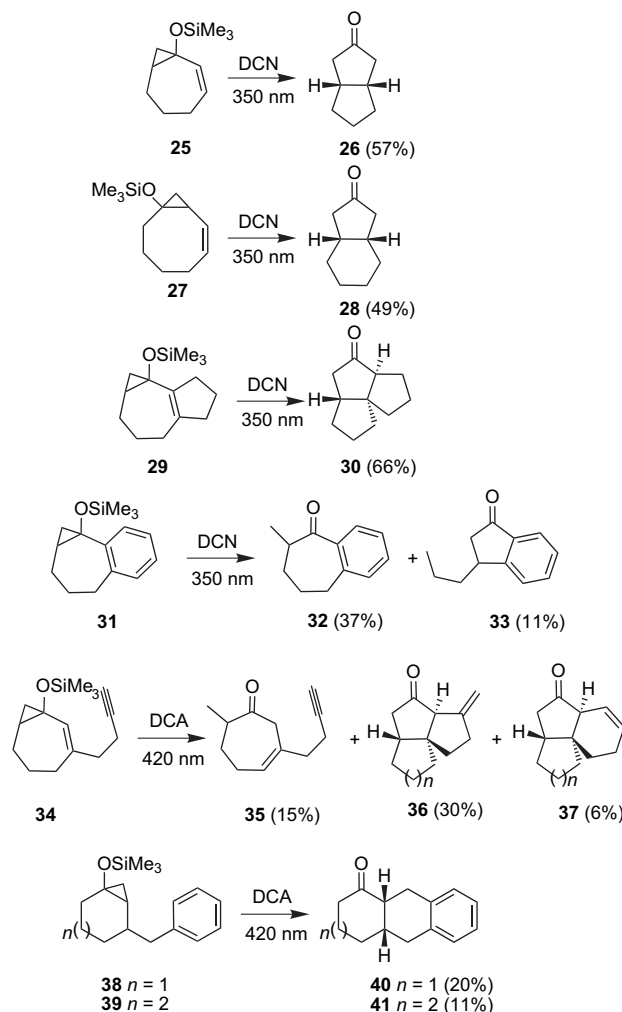
We have shown by a comprehensive study using deuterated solvents that both acetonitrile and water are sources for this saturation. In addition, kinetic isotope effects of H-transfer from acetonitrile influence the ratio of direct and two-step H-transfer as well. These effects are even stronger for secondary radicals.

In summary, both H-atom transfer from the solvent and return electron transfer followed by protonation from water are responsible for the final saturation process.

6. Synthetic examples of radical cationic/radical cascade cyclizations

As shown above siloxy cyclopropanes are useful starting materials for generation of β -keto radicals. These radicals can be used in further cyclization reactions leading to new rearranged products or even in radical cascade reactions involving two cyclization steps. Examples are shown in Scheme 11 and were taken from recent reports.¹⁹ The primary step after PET-oxidation is cleavage of the *endocyclic* C–C-bond of the cyclopropane followed by transannular cyclization (e.g., **25** \rightarrow **26**, **27** \rightarrow **28**, and **29** \rightarrow **30**).

The PET reaction of **31** is somewhat more complicated. Compound **32** is probably formed via a cyclopropyloxy radical rearrangement, whereas the formation of **33** requires first transannular addition of the β -keto radical to the benzene ring followed by second C–C bond cleavage.^{19a} This latter example already indicates some limitations of the method regarding aryl substituents. However, examples **38** \rightarrow **40** and **39** \rightarrow **41** show that this protocol is still applicable to arene systems in moderate yields.^{19b} Example **34** \rightarrow **36**



Scheme 11. Examples of radical cationic/radical cascade cyclization reactions (DCA=9,10-dicyanoanthracene; DCN=1,4-dicyanonaphthalene).

and **37** demonstrate that even more complicated condensed ring systems are accessible by this method.^{19b}

Acknowledgements

Our studies on PET reactions have been supported by Deutsche Forschungsgemeinschaft DFG (Bonn) and the Volkswagenstiftung (Hannover). We are very grateful to these funding agencies. In particular we are very grateful to Thomas Bally (Fribourg) for fruitful discussions and critical reading of the manuscript.

References and notes

- (a) Organic Molecules. In *Electron Transfer in Chemistry*; Balzani, V., Mattay, J., Eds.; Wiley-VCH: New York, NY, 2001; Vol. 2.1; (b) Linker, T.; Schmittel, M. *Radikale und Radikationen in der Organischen Synthese*; Wiley-VCH: Weinheim, 1998; (c) *Electron Transfer in Chemistry I and II. In Topics in Current Chemistry*; Mattay, J., Ed.; Springer: Berlin, 1994 and 1996; Vols. 169 and 177.
- (a) Kavarnos, G. J. *Fundamentals of Photoinduced Electron Transfer*; VCH: New York, NY, 1993; (b) Photoinduced

- Electron Transfer I–V. In *Topics in Current Chemistry*; Mattay, J., Ed.; Springer: Berlin, 1990–1993; Vols. 156, 158, 159, 163, and 168.
- Mattay, J. *Synthesis* **1989**, 233–252.
 - (a) Marcus, R. A. *Annu. Rev. Phys. Chem.* **1964**, *15*, 155–196; (b) Marcus, R. A.; Sutin, N. *Biochim. Biophys. Acta* **1985**, *811*, 265–322; (c) Marcus, R. A. *Angew. Chem., Int. Ed. Engl.* **1993**, *29*, 1111–1121; (d) Marcus, R. A. *Pure Appl. Chem.* **1997**, *69*, 13–29.
 - (a) Rehm, D.; Weller, A. *Ber. Bunsen-Ges. Phys. Chem.* **1969**, *73*, 834–839; (b) Rehm, D.; Weller, A. *Isr. J. Chem.* **1970**, *8*, 259–271; (c) Weller, A. *Z. Phys. Chem. (München)* **1982**, *133*, 93–98.
 - A historical review on the scope of Photoinduced Electron Transfer has been published by Roth, H. D. *Top. Curr. Chem.* **1990**, *156*, 1–19.
 - (a) Neunteufel, R. A.; Arnold, D. R. *J. Am. Chem. Soc.* **1973**, *95*, 4080–4081; (b) Maroulis, A. J.; Shigemitsu, Y.; Arnold, D. R. *J. Am. Chem. Soc.* **1978**, *100*, 535–541.
 - Mariano, P. S. *Photoinduced Electron Transfer*; Fox, M. A., Chanon, M., Eds.; Elsevier: Amsterdam, 1988; Part C, Chapter 4.6.
 - (a) Calhoun, G. C.; Schuster, G. B. *J. Am. Chem. Soc.* **1984**, *106*, 6870–6871; (b) Gieseler, A.; Steckhan, E.; Wiest, O.; Knoch, F. *J. Org. Chem.* **1991**, *56*, 1405–1411.
 - An early review on PET was published by Mattes, S. L.; Farid, S. *Organic Photochemistry*, Padwa, A., Ed.; M. Dekker: New York, NY, 1983; Vol. 6, Chapter 4.
 - (a) Mattay, J.; Gersdorf, J.; Leismann, H.; Steenken, S. *Angew. Chem., Int. Ed. Engl.* **1987**, *23*, 249–250; (b) Mattay, J.; Runsink, J.; Rumbach, T.; Ly, C.; Gersdorf, J. *J. Am. Chem. Soc.* **1985**, *107*, 2557–2558; (c) Mattay, J.; Gersdorf, J.; Mertes, J. *Chem. Commun.* **1985**, 1088–1090.
 - (a) Mattay, J. *Angew. Chem., Int. Ed. Engl.* **1987**, *26*, 825–845; (b) Mattay, J.; Vondenhof, M. *Top. Curr. Chem.* **1991**, *159*, 219–255.
 - Lewis, F. D. *Acc. Chem. Res.* **1986**, *19*, 401–405.
 - (a) Müller, F.; Mattay, J. *Chem. Rev.* **1993**, *93*, 99–117; (b) Bauld, N. L. *Tetrahedron* **1989**, *45*, 5307–5363.
 - (a) Albrecht, E.; Averdung, J.; Bischof, E. C.; Heidbreder, A.; Kirschberg, T.; Müller, F.; Mattay, J. *J. Photochem. Photobiol. A: Chem.* **1994**, *82*, 219–233; (b) Cossy, J. *Pure Appl. Chem.* **1992**, *64*, 1883–1888.
 - (a) Albin, A.; Fagnoni, M. Molecular and Supramolecular Photochemistry. In *Synthetic Organic Photochemistry*; Griesbeck, A. G., Mattay, J., Eds.; M. Dekker: New York, NY, 2005; Vol. 12, Chapter 15; (b) Rossi, R. A. Molecular and Supramolecular Photochemistry. In *Synthetic Organic Photochemistry*; Griesbeck, A. G., Mattay, J., Eds.; M. Dekker: New York, NY, 2005; Vol. 12, Chapter 16.
 - More examples are reviewed in Refs. 1–3, 10, and 12.
 - Hintz, S.; Mattay, J.; Eldik, R. V.; Fu, W.-F. *Eur. J. Org. Chem.* **1998**, 1583–1596.
 - (a) Rinderhagen, H.; Mattay, J. *Chem.—Eur. J.* **2004**, *10*, 851–874; (b) Waske, P. A.; Mattay, J. *Tetrahedron* **2005**, *61*, 10321–10330.
 - Hudson, C. E.; Giam, C. S.; McAdoo, D. J. *J. Org. Chem.* **1993**, *58*, 2017–2019.
 - (a) Jespersen, K. K.; Roth, H. D. *J. Am. Chem. Soc.* **1992**, *114*, 8388–8394; (b) Herbertz, T.; Roth, H. D. *J. Am. Chem. Soc.* **1998**, *120*, 11904–11911; (c) Dinnocenzo, J. P.; Zuilhof, H.; Liebermann, D. R.; Simpson, T. R.; McKechney, M. W. *J. Am. Chem. Soc.* **1997**, *119*, 994–1004.
 - Rinderhagen, H. Ph. D. Thesis, University of Bielefeld, 2002.
 - A full paper covering both theoretical and spectroscopic details of siloxy cyclopropane radical cations will be published separately. Rinderhagen, H.; Waske, P. A.; Bally, T.; Mattay, J., in preparation.
 - Ackermann, L.; Heidbreder, A.; Wurche, F.; Klärner, F.-G.; Mattay, J. *J. Chem. Soc., Perkin Trans. 2* **1999**, 863–870.
 - Rinderhagen, H.; Grota, J.; Mattay, J. *J. Inf. Recording* **2000**, *25*, 229–233.